SRI CHANDRASEKHARENDRA SARASWATHI VISWA MAHA VIDYALAYA

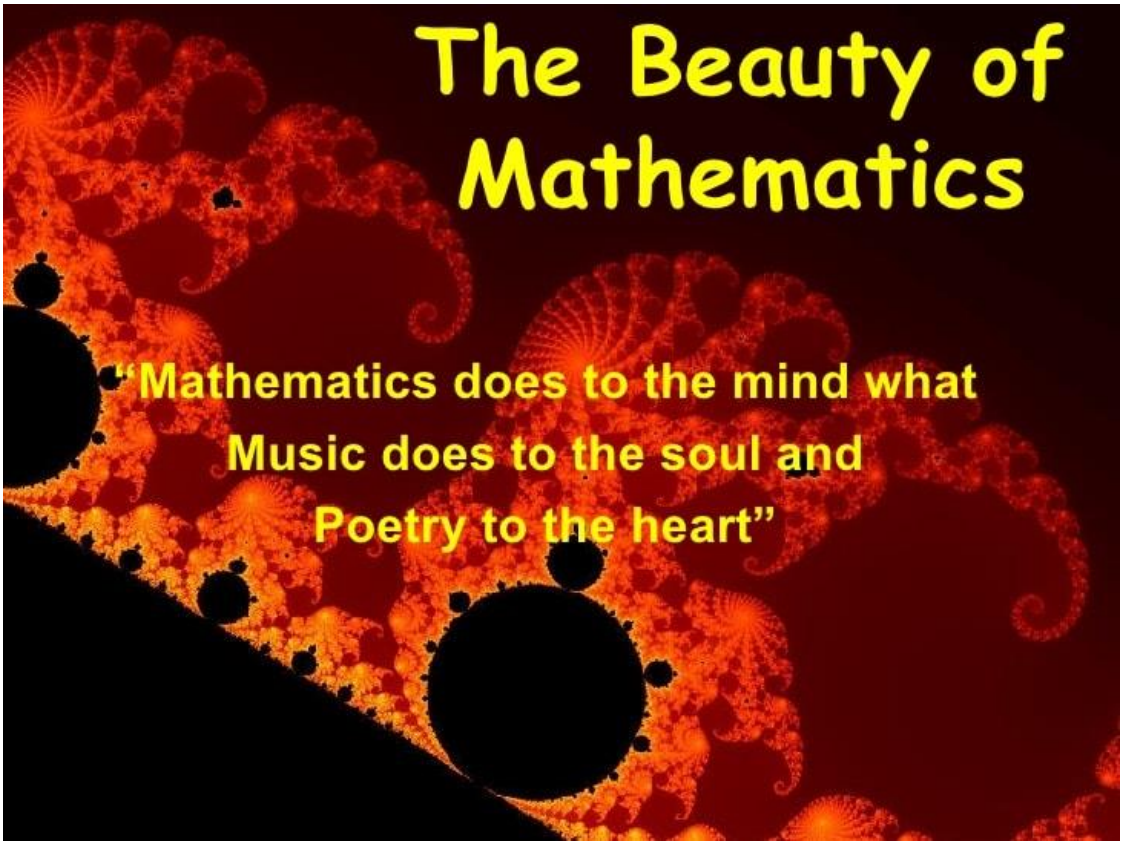
(University U/S 3 of UGC Act 1956)

Accredited with "A" Grade by NAAC

RESEARCH COMPENDIUM

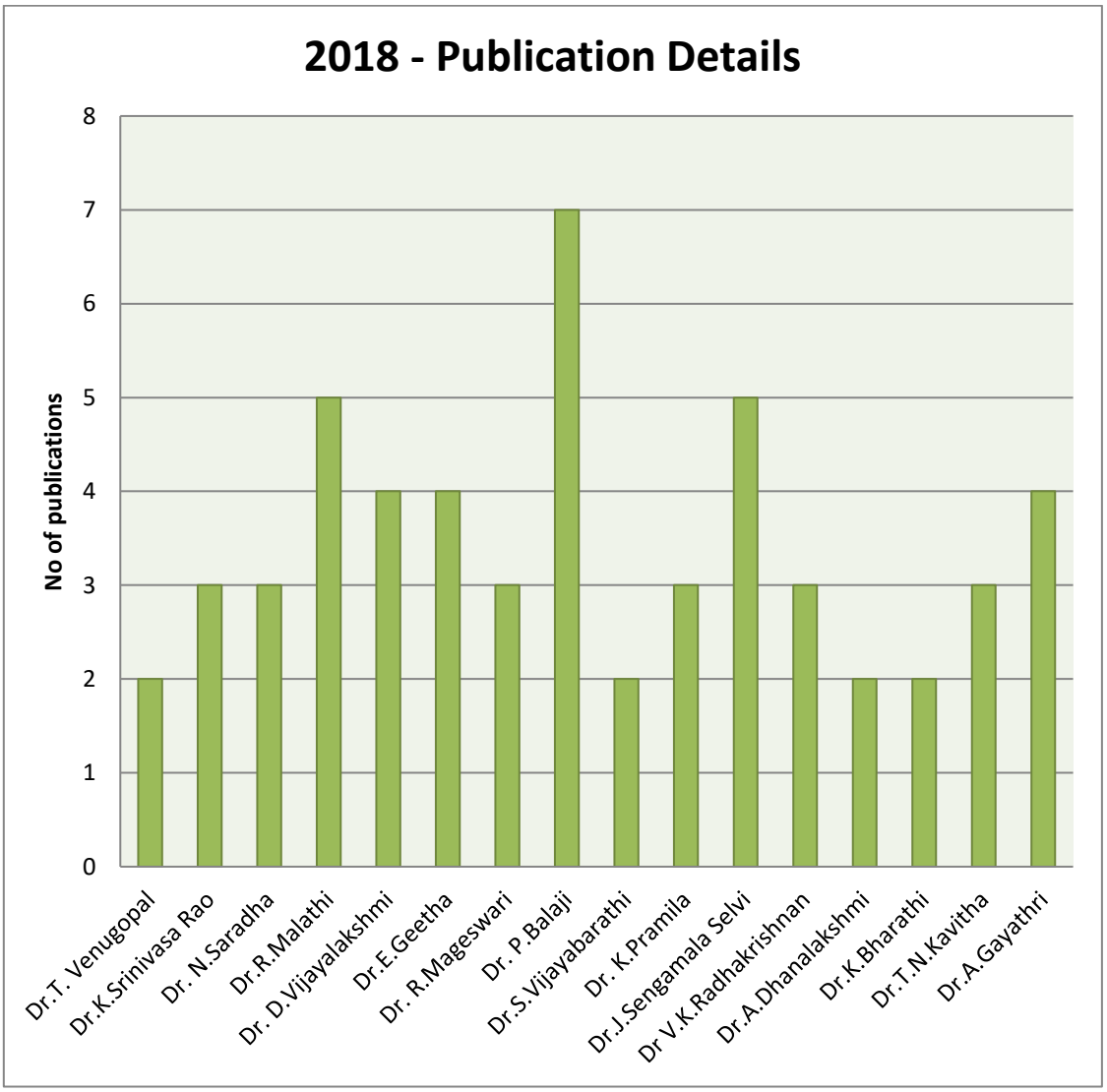
DEPARTMENT OF MATHEMATICS

2018





Department Publication - 2018			
Sl.no	**Name of the Faculty**	**Designation**	**No. of Publications**
1.	**Dr.T. Venugopal**	**Prof. of Mathematics, COE & Director Research and Publication**	**2**
2.	**Dr.K.Srinivasa Rao**	**Prof. of Mathematics & HOD**	**3**
3.	**Dr. N.Saradha**	**Assistant Professor of Mathematics**	**3**
4.	**Dr.R.Malathi**	**Assistant Professor of Mathematics**	**5**
5.	**Dr. D.Vijayalakshmi**	**Assistant Professor of Mathematics**	**4**
6.	**Dr.E.Geetha**	**Assistant Professor of Mathematics**	**4**
7.	**Dr. R.Mageswari**	**Assistant Professor of Mathematics**	**3**
8.	**Dr.P.Nagarajan**	**Assistant Professor of Mathematics**	**-**
9.	**Dr. P.Balaji**	**Assistant Professor of Mathematics**	**7**
10.	**Dr.S.Vijayabarathi**	**Assistant Professor of Mathematics**	**2**
11.	**Dr. K.Pramila**	**Assistant Professor of Mathematics**	**3**
12.	**Dr.J.Sengamala Selvi**	**Assistant Professor of Mathematics**	**5**
13.	**Dr. V.K.Radhakrishnan**	**Assistant Professor of Mathematics**	**3**
14.	**Dr.A.Dhanalakshmi**	**Assistant Professor of Mathematics**	**2**
15.	**Dr. K.Bharathi**	**Assistant Professor of Mathematics**	**2**
16.	**Dr.T.N.Kavitha**	**Assistant Professor of Mathematics**	**3**
17.	**Dr.A.Gayathri**	**Assistant Professor of Mathematics**	**4**


2018 - Publication Details
No of publications
0
1
2
3
4
5
6
7
8
Dr.T. Venugopal
Dr.K.Srinivasa Rao
Dr. N.Saradha
Dr.R.Malathi
Dr. D.Vijayalakshmi
Dr.E.Geetha
Dr. R.Mageswari
Dr. P.Balaji
Dr.S.Vijayabarathi
Dr. K.Pramila
Dr.J.Sengamala Selvi
Dr V.K.Radhakrishnan
Dr.A.Dhanalakshmi
Dr.K.Bharathi
Dr.T.N.Kavitha
Dr.A.Gayathri

CONTENT

S.No	Publication Details	Page No
1.	***T.Venugopal, S.Indirapriyadarshini***, Optimal Distribution of Vegetables from a Group of Dealers to Different Whole Sale Customers on a Typical Day, International Research Journal of Mathematical Sciences,Vol.7, Issue 1, 2018.	1
2.	***A.Gayathri, T.Venugopal,*** A Numerical study of comparative analysis of Experimental and Theoretical viscosities of Binary mixtures of few polymer systems, Mathematical Sciences International Research Journal, Vol 7, Issue 1, PP 350-354, ISBN: 2278-8697, 2018.	9
3.	***N.Saradha, V. Swaminathan, P.Anjali***, Triple Connected Complementary Tree Equitable Domination, International Research Journal of Mathematical Sciences, Vol.7, Issue 1, PP 340-343. ISSN: 2278-8697, 2018.	14
4.	***N.Saradha, V. Swaminathan, S.Arumugam***, Global Triple Connected Complementary Acyclic Domination, International Research Journal of Mathematical Sciences, Vol.7, Issue 1, PP 78-80, ISSN: 2278-8697, 2018.	18
5.	***N. Saradha,V. Swaminathan, K.Amudhavalli***,. Strong efficient triple connected domination , International Research Journal of Mathematical Sciences,Vol.7, Issue 1, PP 316-.319, ISSN: 2278-8697, 2018.	21

6.	***R.Malathi & Babu.N***, Perfect Edge Domination and Efficient Edge Domination in Graphs, International Research Journal of Mathematical Sciences,Vol.7, Issue 1, PP 299-304, ISSN: 2278-8697, 2018.	25
7.	***R.Malathi & Balamurugan.D***, Connected Domatic Number of a Graph, Mathematical Sciences International Research Journal, Vol.7, Issue 1, PP 295-298, ISSN: 2278-8697, 2018.	31
8.	***R.Malathi & Bangarappa.G***, Unique Minimum Edge Domination in Trees, Mathematical Sciences International Research Journal, Vol.7, Issue 1, PP 292-294, ISSN: 2278-8697, 2018.	35
9.	***Vijayalakshmi. D, Hemalatha .S***, Protein Similarity/ Dissimilarity study using Moment Vector by Non – Homologous method. Mathematical Sciences International Research Journal, Vol 7, Spl issue, ISSN 2278 – 8697, PP 81-85, 2018.	38
10.	***Vijayalakshmi. D, Anandraj. T,*** Comparative Analysis of Methods for Protein Similarity and Dissimilarity using Graphical Representation. Mathematical Sciences International Research Journal, Vol. 7, Spl. issue , ISSN 2278 – 8697, PP 1-7, 2018.	43
11.	***Vijayalakshmi. D, Geethanjali. P***, Similarity/ Dissimilarity study of Protein in Non homologous way using Root Mean Square, Mathematical Sciences International Research Journal ,Vol 7, Spl issue ISSN 2278 – 8697, PP 73-77, 2018.	50

12.	***Vijayalakshmi. D, Shakila.B,*** Measurement of Similarity/ Dissimilarity study of Protein using polarity of Amino acids, Mathematical Sciences International Research Journal, Vol 7, Spl issue, ISSN 2278 – 8697, PP 53-57, 2018.	55
13.	***E.Geetha, M.Anushalini, R.Muthucumaraswamy***, Impact of Thermal radiation on an unsteady copper-water nanofluid flow past over an infinite vertical plate with variable temperature, International Research Journal of Mathematical Sciences, Vol.7, Issue 1, PP 8 – 16, ISSN 2278 – 8697, 2018.	60
14.	***E.Geetha***, Effects of thermal radiation of an unsteady convectiveAl2O3 nanofluid flow past on vertical plate in a porous medium, International Research Journal of Mathematical Sciences, Vol.7, Issue 1, , PP 56 - 64, ISSN 2278 – 8697, 2018.	69
15.	***E.Geetha***, Effects of Heat transfer of an unsteady nanofluid flow past over an isothermal vertical plate in the presence of thermal radiation, International Research Journal of Mathematical Sciences, Vol.7, Issue 1, PP 65 - 72, ISSN 2278 – 8697, 2018.	78
16.	***E.Geetha, A.Janagiraman***, Magneto Hydrodynamic effects on a transient Al2O3 nanofluid past over an vertical plate, International Research Journal of Mathematical Sciences, Vol.7, Issue 1, PP 148 - 156, ISSN 2278 – 8697, 2018.	86

17.	***Mageswari. R, Meena.V***, Finding Residues Residing at the Protein Core and Protein Surface Using Graph Theoretical Techniques, International Research journal of Mathematical Sciences, Vol.7,Issue 1, PP 192-195, ISSN: 2278-8697, 2018.	95
18.	***Mageswari. R, M.Kalpana***, Finding Graph of the Protein from its Contact Map, International Research journal of Mathematical Sciences, Vol.7, Issue 1, PP 196- 200, ISSN: 2278-8697, 2018.	99
19.	***Mageswari. R***, Similarity / Dissimilarity of Protein Structures Through Strength of Nodes, International journal of Mathematical Sciences, PP 219-224, ISSN: 2278-8697, 2018.	104
20.	***P.Balaji D.Dinakar*** , Analysis of Marked Graph of Cases of Deadlock Using Sign Incidence Matrix and Their Conversion into Digraphs, International Research Journal of Mathematical Sciences, Vol.7, Issue 1, PP 252-257, ISSN 2278 – 8697, 2018.	110
21.	***P.Balaji G Balamurugan*** , Analysis of Marked Graph of Cases of Assembling Plan using Sign Incidence Matrix and its Conversion into Digraphs, International Research Journal of Mathematical Sciences, Vol.7, Issue 1, PP 258-263, ISSN 2278 – 8697, 2018.	116
22.	***P.Balaji I Davidraj***, Analysis of Marked Graph with Equivalent Critical Place using Sign Incidence Matrix and its Conversion into Digraphs, International Research Journal of Mathematical Sciences, Vol.7, Issue 1, PP 264-270, ISSN 2278 – 8697,	122

	2018.	
23.	***P.Balaji M Devarajulu*** , Digraphs of the Marked graphs of a Machine that Process One Job at a Time and Basic Schema of Production State, International Research Journal of Mathematical Sciences, Vol.7, Issue 1, PP 271-274, ISSN 2278 – 8697, 2018 .	129
24.	***P.Balaji , M Dinesh***, Analysis of Digraphs of NON_Deadlock Free FMS and Machining Station with Four Machines and Two Robots, International Research Journal of Mathematical Sciences, Vol.7, Issue 1, PP 275-278, ISSN 2278 – 8697, 2018.	133
25.	***P.Balaji , S.Arumugam***, Analysis of Marked Graph of Cases of Several Dependant Critical Places using Sign Incidence Matrix And Its Conversion Into Digraphs, International Research Journal of Mathematical Sciences, Vol.7, Issue 1, PP 279-285, ISSN 2278 – 8697, 2018.	137
26.	***P.Balaji,V.Elumalai***, Analysis of Digraph of Flexible Manufacturing Cell With Four Machines and Three, International Research Journal of Mathematical Sciences, Vol.7, Issue 1, PP 286-291, ISSN 2278 – 8697, 2018.	144
27.	***Vijayabarathi.S***, Annihilator ideals of Pre A*-algebra, International Research Journal of Mathematical Sciences, Vol.7, Issue 1, PP 372-376, ISSN 2278 – 8697, 2018.	150
28.	***Vijayabarathi.S***, Laplace expansion in Rhotrix, International Journal of Mathematical Archive, Vol. 9(4), PP 45-48, 2018.	155

29.	***K.Pramila***, "Solving Integer Programming Problems Using MATLAB", International Research Journal of Mathematical Sciences, Vol. 7 Issue 1, PP.123-130, ISSN 2278 – 8697, 2018.	159
30.	***K.Pramila, P.SebastiSuganya***, Cost Effective and Very Cost Effective Bipartition of Few Families of Graph, International Research Journal of Mathematical Sciences , Vol. 7 Issue 1, PP 100-106, ISSN 2278 – 8697, 2018.	167
31.	***K.Pramila, D.Ramya***, Application of Graph Theory in Traffic Control Problem, International Research Journal of Mathematical Sciences, Vol 7 Issue 1, PP 241-245, ISSN 2278 – 8697, 2018.	174
32.	***J.Sengamalaselvi, T. Latha, T.Venugopal*** , Optic Math of linear programming problem and Graphical method using the open source software, International Research Journal of Mathematical Sciences, Vol. 7, Issue 1, PP 137-142, ISSN 2278-8697, 2018.	179
33.	***J.Sengamalaselvi, V.Nalini, T.Venugopal***, Visual Math of Secondary Mathematics Education in the Area of Geometry using Geogebra, International Research Journal of Mathematical Sciences, Vol 7, Issue 1, PP 143-147, ISSN 2278-8697, 2018.	185
34.	***J.Sengamalaselvi, K.Murugasen***, An Analytical Method for finding Critical path in a Fuzzy project Network, International Research Journal of Mathematical Sciences, Vol. 7, Issue 1, PP 131-136, ISSN	190

	2278-8697, 2018.	
35.	***J.Sengamalaselvi***, Visual Graph of Higher Secondary Mathematics Education using the Open Source Software, International Journal of Engineering Sciences and Technology, Vol. 7, Issue 6, PP 406 - 411 , ISSN 2277- 9655, 2018.	196
36.	***V.K. Radhakrishnan***, Exhibiting Railway Junctions as Steiner Points, International Research Journal of Mathematical Sciences, Vol. 7, Issue 1, PP 44-47 , ISSN 2278-8697,2018 .	202
37.	***V.K. Radhakrishnan, J. Senthilkumar***, Object Oriented Approach to Travelling Salesman Problem International Research Journal of Mathematical Sciences, Vol. 7, Issue 1, PP 237-240 ,ISSN 2278-8697, 2018.	206
38.	***V.K. Radhakrishnan, B. Shanmugam***, Nurse Scheduling Problem using Linear Programming Problem for Day-wise Schedule in Journal of Statistics and Mathematical Engineering, Vol. 4, Issue 1, PP 1-7, 2018.	210
39.	***Dhanalakshmi.A, Sivakumar. C***, Kekule Indices of Circumcoronene, Mathematicsl Science international research journal, Vol. 7, Issue 1, PP 107-111, ISSN 2278-8697, 2018.	217
40.	***Dhanalakshmi.A, Thamarai Lakshmi.S***, Computational Method Of An Incompressible Viscous Couettee Flow By Means Of Crank Nicolson Technique And Thomas Algorithm, Mathematical Science international Research Journal, Vol. 7, Issue 1, PP 112-118, ISSN 2278-8697, 2018.	322

41.	***K.Bharathi, C.Vijaylakshmi***, Evolutionary Analysis for Optimization Model with the Design of Job Shop Scheduling, Journal of Advanced Research in Dynamical & Control Systems, Vol. 10, 03-Special Issue, PP 1119-1123, ISSN 1943-023X, 2018.	229
42.	***K.Bharathi, C.Vijaylakshmi***, Design and Review of Optimization using Evolutionary, Mathematical Sciences International Research Journal, ISSN: 2278 - 8697 (printed version), Vol. 7, Issue 1, PP 157-160, ISSN 2278-8697, 2018.	234
43.	***T. N. Kavitha, A. Jayalakshmi***, Some Relations on a Right Near Idempotent Semigroup, Mathematical Sciences International Research Journal, Vol. 7, Issue 1, PP 335-340,ISSN 2278-8697, 2018.	238
44.	***M.Uma Priya, T. N. Kavitha***, Application of Neuro- Fuzzy Controller in Finding the Quality of Jaggery, Mathematical Sciences International Research Journal, Vol. 7, Issue 1, PP 344-349, ISSN 2278-8697, 2018.	243
45.	***T.N. Kavitha, A. Jayalakshmi***, A Special Case of near Idempotent Semigroup, Journal of Global Research and Mathematical Archives, Vol. 5, Issue 5, PP 335-340, 2018, ISSN 2320- 5822, 2018.	249
46.	***A.Gayathri***, A study on higher order triangular sum numbers of polyhedral and graceful graphs, Mathematical Sciences International Research Journal, Vol. 7, issue -1, PP 48-55, ISBN: 2278-8697, 2018.	255

47.	***D.Tabhita, K.Srinivasa Rao, Dr.P.Vijaya Vani***, A study on Class of lattice ordered recursively enumerable and recursive languages, IMRF Journals, vol 7, issue 5, 2018 ,ISSN: 2278-8697	263
48.	***A.Kanchana, K.Srinivasa Rao***, Software Approach to Minimize Boolean Function as 'n' Distinct Functions, Jour of Adv Research in Dynamical & Control Systems, Vol. 10, No. 7, 2018	272
49.	***A.Kanchana, K. Srinivasa Rao***, Reducing the Variables in Boolean Function Using Fuzzy Cognitive Map to Create a Circuit, International Journal of Pure and Applied Mathematics Volume 119 No. 9 2018, 89-100 ISSN: 1311-8080 (printed version); ISSN: 1314-3395 (on-line version).	280
50.	***A.R.Shoba, Hemanath S, R.Malathi***, Condition for Double Line Graph – Using FUZZY GRAPH, International Journal of AdvancedResearch in Science, Engineering and Technology Vol. 5, Issue 10 , October 2018 , ISSN: 2350-0328.	291
51.	***A.R.Shoba and R.Malathi***, Condition for Complete Graph – Using Fuzzy Graph, Journal of Environmental Science, Computer Science and Engineering & Technology , JECET, September 2018 - November 2018; Section C; Vol.7. No.4, 315-320. E-ISSN: 2278–179X	296
52.	***Dr.J.Sengamala Selvi***, Visual Graph of Higher Secondary Mathematics Education using the open source Software, International Journal of Engineering Sciences and Technology, 2018, PP: 406-411	302

	ISSN:2277- 9655.	
53.	***Dr.A.Gayathri, T Venugopal, R Padmanaban,K Venkatramanan and R Vijayalakshmi*** A comparative study of experimental and theoretical refractive index of binary liquid mixtures using mathematical methods, IOP Conf. Series: Materials Science and Engineering, 2018 PP: 112-116 ISSN:1757-899X	308
54.	***R Padmanaban, A Gayathri and K Venkatramanan***, A study on Thermodynamic, Acoustic and Elastic properties of aqueous solutions of Hydroxyethyl Cellulose, IOP Conf. Series: Materials Science and Engineering, 2018 PP: 38-44 ISSN:1757-899X	311
55.	***Dr.A.Gayathri, T.Venugopal, K.Venkatramanan***, A Comparative Study of Experimental and Theoretical Ultrasonic Velocity of Binary Liquid Mixtures Using Mathematical Methods, International Journal of Engineering & Technology, 2018 PP:602-604.	317

OPTIMAL DISTRIBUTION OF VEGETABLES FROM A GROUP OF DEALERS TO DIFFERENT WHOLE SALE CUSTOMERS ON A TYPICAL DAY

Dr.T.Venugopal
Professor of Mathematics, SCSVMV, Enathur, Kanchipuram. mail id:drmathtvg@gmail.com
S.Indirapriyadarshini
Research Scholar, SCSVMV, Enathur, Kanchipuram, mail id: sinduooo84@gmail.com

Abstract: This paper is the third in a series of papers on modeling mathematically and optimizing the whole sale vegetable business. In the first paper Monte Carlo Technique was applied to observed data to forecast the demand of vegetables on any day of the year. In the second paper Atypical Restricted Transportation Modeling of Wholesale Vegetable Procurement was solved optimally for transporting 47 kinds of vegetables from 13 cities across India to Arakkonam. In this third paper we consider the optimal distribution of the vegetables from a group of dealers to different whole sale customers viz. Big Hotels, Marriage Halls, Restaurants, Medium Hotels, Messes, Canteens, College Hostels, Lodges., Small Hotels, Fast food stalls, side walk hotels, School hostels, Government Hospitals, Pani puri shops, Cinema theaters and Retail sales on a typical day so as to maximize the total sales amount, taking into account various factors like - varied cost of vegetables to these different customers, the minimum and maximum demand of these customers. Our research is to build a mathematical model for the entire vegetable whole sale business and to optimize from the points of view of Dealer, Retailer and Customer.

Keywords: Vegetable Business, Operation Research, Open Solver.

Introduction of the Problem: The market in Arakkonam contributes to the vegetable needs of varied customers from the common man to large-scale customers. A number of dealers associated with this business procure vegetables from many cities across India. Now in this paper, we consider a group of three wholesale dealers who have to distribute the procured vegetables from big customers to small customers so as to maximize sales. The point to be noted is that the selling price each vegetable varies according to the nature of the customer, for instance hotels. We have constraints on the demand of vegetables for varied customers like minimum and maximum. Supply can also vary despite orders placed due to various factors. Hence the problem on hand is to distribute the procured vegetables considering supply, demand selling price so as to maximum sales.

Solving Procedures: This problem is solved using transportation algorithm. The tables of (i)Maximum Demand/ Supply of Vegetables(in Kgs) on a typical day in Arakkonam Town (ii) Minimum Demand/ Supply of Vegetables(in Kgs) on a typical day in Arakkonam Town (iii) Selling Price of Vegetables (in Rs) on a typical day in Arakkonam Town (iv)Solution by open solver.

Table 1: Maximum Demand/ Supply of Vegetables (in Kgs) on a typical day in Arakkonam Town

Customers	Big Hotels	Marriage Halls	Restaurants	medium Hotels	Mess	Canteen	Colleges Hostels	Lodges	Small Hotels	Fast food stall	side walk hotels	Schools hostels	Government Hospitals	pani puri shop	Cinema theaters	Retail sales	Demand	supply
VEG	**1**	**2**	**3**	**4**	**5**	**6**	**7**	**8**	**9**	**10**	**11**	**12**	**13**	**14**	**15**	**16**		
POT	150	150	100	35	25	20	10	8	10	2	6	5	2	5	5	17	550	600
TOM	200	200	80	60	50	40	30	25	25	10	9	9	5	0	4	53	800	850
SON	60	60	5	4	3	3	2	2	2	0	0.5	0.5	0	0	0	18	160	170
BON	220	200	150	100	20	20	10	10	10	8	5	5	5	6	6	75	850	800
GBL	45	45	0	10	8	8	3	2	2	0	2	1	1	0	0	13	140	135
DRM	25	22	0	15	10	8	1	1	1	0	1	1	1	0	0	14	100	110
CAB	12	10	15	6	3	3	2	2	2	3	0	1	1	0	1.5	13.5	75	100
SNG	25	0	0	15	5	3	2	0	1	0	0	1	1	0	0	7	60	70
BNS	30	30	30	15	10	5	5	3	3	6	0	1	1	0	1	20	160	160
CFR	25	20	35	15	5	3	5	5	0	4	0	0	0	4	0	29	150	165
YAM	25	0	0	25	20	10	0	0	8	0	0	0	0	0	0	12	100	130
BJL	45	40	0	33	30	20	18	13	15	0	8	5	2	0	0	31	260	240
SPO	0	10	30	0	0	0	0.5	0	0	4	0	0	0	0	0.5	5	50	75
RGG	40	0	0	25	20	15	3	3	2	0	1	1	1	0	0	19	130	120
CRT	30	35	41	23	20	20	14	11	8	12	4	3	1	1.5	1.5	5	230	235
BTG	15	0	10	15	10	8	0	0	5	0	0	0	3	0	0	54	120	140
BOG	30	0	0	22	20	12	10	8	10	0	0	5	5	0	0	28	150	150
BTT	30	35	10	15	10	9	8	5	4	0	0	2	2	0	0	0	130	130
TRP	25	0	0	25	20	10	3	0	6	0	0	3	2	0	0	6	100	125
LFR	50	0	0	40	35	30	20	5	10	0	0	5	4	0	0	51	250	275
ASG	90	50	10	50	35	40	15	10	25	0	0	5	5	0	0	215	550	600
IVG	15	0	0	3	2	1	0	0	1	0	0	0	1	0	0	37	60	90
GIN	15	10	15	7	5	4	0.5	2	0.5	4	1	0.5	0.5	0.5	0.5	34	100	110
RWB	150	110	0	100	15	14	7	5	10	0	3	2	2	0	2	80	500	470
RAD	45	0	0	25	15	10	7	0	6	0	3	3	3	0	0	13	130	135
CBR	10	10	15	0	0	0	1	2	0	2	0	0	0	0	0	10	50	75
CPS	15	10	20	1	0	0	0.5	1	0	1.5	0	0	0	0	0.5	10.5	60	75
CYT	25	10	0	20	15	10	5	0	3	0	2	2	2	0	0	6	100	110
BFR	90	0	0	75	30	25	0	0	12	0	3	2	3	0	0	60	300	320
GMG	10	15	0	1	1	1	0	0	0.5	0	0	0	0	0	0	21.5	50	90
GCH	20	20	25	10	9	8	3	2	2	3	2	1	1	0.5	0.5	13	120	125
BST	60	0	25	20	18	15	7	5	5	0	4	3	4	0	0	94	260	275
FBN	60	50	0	25	20	15	5	0	6	0	3	4	3	0	0	59	250	300
SWC	5	5	20	0	0	0	1	1	0	0	0	0	0	0	0	18	50	90
CRL	9	8	7	6	3	2	1	1	0.5	1.5	0.5	0.5	0.5	0.5	0.5	38.5	80	100

COL	10	9	10	7	6	6	2	3	4	4	2	1	1	1	1	13	80	95
GRN	20	0	0	18	10	9	0	0	5	0	0	5	5	0	0	28	100	120
BTL	0	15	5	0	0	0	0	5	0	0	0	0	0	0	0	35	60	75
CBN	15	0	0	10	5	4	1	0	3	0	0	2	2	0	0	18	60	70
YEL	20	0	0	15	13	12	4	0	3	0	2	1	0	0	0	20	90	110
GAR	100	75	90	50	25	13	5	6	3	5	4	2	3	0	4	115	500	550
MLE	20	10	25	5	2	2	2	3	1	1	0.5	0	0.5	0.5	0.5	27	100	125
SWP	0	0	0	0	0	0	0	0	0	0	0	0	0	0	0	60	60	75
PEA	30	25	30	6	7	6	4	4	5	4	3	2	2	4	5	23	160	165
CCT	200	220	140	90	60	45	15	10	8	0	7	5	8	0	0	92	900	950
BLV	50	100	50	50	25	20	0	0	20	0	0	0	0	0	0	235	550	575
MUS	0	0	20	0	0	0	0	0	0	0	0	0	0	0	0	40	60	75
LMN	15	15	18	2	0	0.5	0.5	0.5	0.5	1	0	0.5	0.5	0.5	0	5.5	60	80



Picture 1: Restaurant

Table 2: Minimum Demand/ Supply of Vegetables (in Kgs) on a typical day in Arakkonam Town

Customers	**Big Hotels**	**Marriage Halls**	**Restaurants**	**medium Hotels**	**Mess**	**Canteen**	**Colleges Hostels**	**Lodges**	**Small Hotels**	**Fast food stall**	**side walk hotels**	**Schools hostels**	**Government Hospitals**	**pani puri shop**	**Cinema theaters**	**Retail sales**
VEG	**1**	**2**	**3**	**4**	**5**	**6**	**7**	**8**	**9**	**10**	**11**	**12**	**13**	**14**	**15**	**16**
POT	450	450	300	105	75	60	30	8	15	5	9	8	3	8	8	26
TOM	600	600	240	180	150	120	90	25	37.5	15	13.5	14	8	0	6	80
SON	180	180	15	12	12	12	10	2	4	0	0.75	1	0	0	0	27
BON	660	600	450	300	60	60	30	10	15	12	7.5	8	8	9	9	113
GBL	135	135	0	30	24	24	24	2	4	0	5	5	5	0	0	20
DRM	75	66	0	45	30	24	10	1	6	0	5	6	6	0	0	24
CAB	50	40	45	18	8	9	8	2	5	7.5	0	4	5	0	8	23

SNG	75	0	0	45	25	9	8	0	6	0	6.5	5	6	0	0	12
BNS	100	90	90	45	30	25	23	3	4.5	9	0	5	5	0	4	25
CFR	75	60	105	45	15	9	15	5	0	6	0	0	0	8	0	45
YAM	75	0	0	75	80	30	0	0	13	0	0	0	0	0	0	18
BJL	135	120	0	99	90	80	24	13	22.5	0	12	8	5	0	0	47
SPO	30	40	90	12	0	24	5	0	1.5	7.5	0	0	0	0	2	8
RGG	120	0	0	75	80	45	9	3	3.5	0	2.5	2	3	0	0	40
CRT	90	120	124	69	80	80	52	11	12	18	6	3	3	3	4	8
BTG	45	0	30	45	30	24	0	0	7.5	0	0	0	5	0	0	76
BOG	90	0	0	88	80	36	30	8	15	0	0	8	8	0	0	42
BTT	90	105	40	45	30	27	24	5	6	0	0	4	5	0	0	0
TRP	75	0	0	75	60	30	9	0	9	0	0	5	5	0	0	9
LFR	150	0	0	120	105	90	80	5	15	0	0	8	4	0	0	77
ASG	270	150	30	150	105	80	45	10	37.5	0	0	8	9	0	0	275
IVG	45	0	0	9	8	5	0	0	3.5	0	0	0	5	0	0	54
GIN	45	30	45	21	15	8	7	2	4.5	6	2	2	2	2	2	29
RWB	450	330	0	300	45	52	21	5	15	0	4.5	4	3	0	3	120
RAD	135	0	0	75	45	30	21	0	9	0	4.5	5	4	0	0	20
CBR	40	45	45	0	0	0	4	2	0	4	0	0	0	0	0	23
CPS	45	30	60	5	0	0	3	1	0	2.5	0	0	0	0	2	17
CYT	75	30	0	60	45	30	15	0	4.5	0	4	5	5	0	0	9
BFR	270	0	0	225	90	75	0	0	18	0	6	4	6	0	0	90
GMT	60	45	0	5	8	9	0	0	3	0	0	0	0	0	0	38
GCH	60	80	75	30	27	24	6	2	4.5	13.5	4	4	4	2	3	20
BST	180	0	75	80	54	45	21	5	7.5	0	6	5	4	0	0	129
FBN	180	150	0	75	80	45	15	0	9	0	4.5	7	14	0	0	90
SWC	15	15	60	0	0	0	8	1	0	0	0	0	0	0	0	27
CRL	27	24	21	18	9	8	6	1	4.5	4.5	2	2	3	2	2	60
COL	40	27	40	21	18	16	8	3	6	7.5	4	3	3	2	3	20
GRN	80	0	0	54	40	27	0	0	7.5	0	0	13	13	0	0	42
BTL	0	45	15	0	0	0	0	5	0	0	0	0	0	0	0	53
CBN	45	0	0	40	15	8	6	0	4.5	0	0	4	4	0	0	27
YEL	60	0	0	45	40	48	12	0	4.5	0	2.5	2	0	0	0	30
GAR	300	225	270	150	75	40	15	6	4.5	7.5	4	4	5	0	7	173
MLE	60	30	75	25	8	8	9	3	1.5	2	3	0	2	3	2	41
SWP	0	0	80	0	0	0	0	0	0	0	0	0	0	0	0	90
PEA	90	75	90	18	21	18	12	4	12.5	8	6	4	4	6	8	35
CCT	600	880	520	270	180	105	45	10	12	0	10.5	8	12	0	0	140
BLV	150	300	150	200	75	80	0	0	40	0	0	0	0	0	0	300
MUS	0	0	90	0	0	0	0	0	0	0	0	0	0	0	0	75
LMN	150	150	160	24	0	12	15	0.5	4.5	6	0	9	14	8	0	27



Picture 2: Hotel

Table 3: Selling Price of Vegetables (in Rs) on a typical day in Arakkonam Town

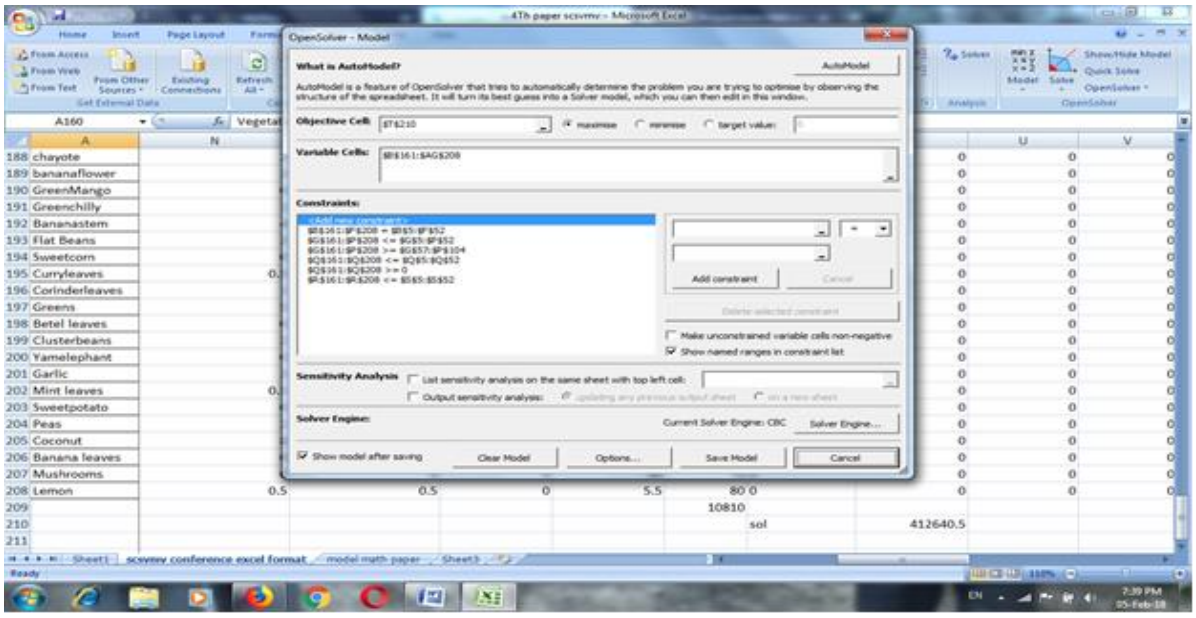
Customers	Big Hotels	Marriage Halls	Restaurents	medium Hotels	Mess	Canteen	Colleges Hostels	Lodges	Small Hotels	Fast food stall	side walk hotels	Schools hostels	Government Hospitals	pani puri shop	Cinema theaters	Retail sales
VEG	**1**	**2**	**3**	**4**	**5**	**6**	**7**	**8**	**9**	**10**	**11**	**12**	**13**	**14**	**15**	**16**
POT	20	25	25	22	22	23	25	25	24	24	24	25	25	25	25	18
TOM	18	23	23	21	21	22	23	23	20	23	20	23	23	23	23	15
SON	70	75	77	70	72	71	77	76	70	76	74	75	75	75	75	66
BON	50	52	54	50	50	52	55	55	52	54	53	54	52	54	54	49
GBL	25	27	26	24	24	26	28	28	25	24	25	26	25	25	25	19
DRM	75	78	77	76	76	75	78	78	76	75	76	73	75	75	76	68
CAB	13	16	15	14	14	15	16	16	15	15	14	15	15	15	16	11
SNG	14	16	15	14	15	16	15	14	14	16	16	14	15	13	17	13
BNS	16	18	18	17	16	16	17	18	16	18	16	15	15	16	17	13
CFR	30	36	35	30	32	34	35	35	33	35	32	32	31	34	32	28
YAM	38	40	39	38	39	38	40	40	39	39	38	39	38	39	38	35
BJL	28	30	30	29	29	30	30	30	29	30	30	30	30	29	30	25
SPO	60	68	67	62	63	61	62	63	64	64	64	62	61	65	61	58
RGG	46	48	47	45	45	47	42	49	47	48	45	45	45	45	46	44
CRT	50	55	54	51	53	53	52	56	52	53	54	52	51	54	53	49
BTG	20	24	23	22	21	23	24	24	25	21	24	23	22	25	26	19
BOG	14	16	15	14	15	16	17	14	15	16	17	14	15	14	15	10
BTT	18	22	21	20	21	23	23	21	21	24	25	26	25	21	23	15
TRP	25	26	25	27	28	26	27	28	23	27	26	24	26	26	28	20
LFR	22	25	24	23	24	24	25	26	24	23	25	24	23	23	25	20
ASG	15	16	17	15	16	17	18	19	15	13	14	14	13	13	13	11
IVG	32	33	34	32	31	32	34	35	33	32	32	31	32	34	32	30
GIN	45	46	45	46	45	46	45	47	45	46	43	44	45	46	43	40
RWB	26	27	26	25	27	28	26	25	26	27	28	29	24	25	25	20
RAD	13	16	15	16	13	12	16	14	13	14	17	15	16	13	14	10
CBR	25	33	32	26	27	28	29	27	26	29	28	26	25	28	27	20
CPS	35	40	38	36	37	38	39	38	37	36	36	37	36	36	37	32
CYT	22	25	24	23	24	25	23	25	24	25	24	23	25	23	24	20
BFR	40	42	41	40	41	42	43	42	41	43	43	42	41	44	42	42
GMG	90	95	94	91	92	93	91	92	93	94	91	91	92	92	91	89
GCH	30	36	35	31	32	33	34	32	32	34	31	32	31	32	31	27
BST	30	36	35	31	32	33	32	34	31	32	33	34	35	31	32	27

FBN	32	35	34	33	32	31	32	31	34	32	34	32	31	33	31	30
SWC	71	79	77	76	76	77	78	79	76	78	78	77	76	73	74	69
CRL	60	65	64	61	62	63	64	61	62	64	62	61	63	63	62	58
COL	80	85	84	81	82	82	83	81	84	85	84	82	84	84	82	75
GRN	35	40	39	38	37	36	35	37	38	36	39	36	37	35	34	30
BTL	60	65	64	61	64	62	64	61	63	63	62	64	62	62	61	58
CBN	35	40	39	36	37	37	38	36	35	34	36	38	39	36	35	30
YEL	35	40	40	36	37	38	36	39	37	39	35	39	37	37	36	33
GAR	120	125	124	121	122	123	124	121	123	124	123	124	123	124	126	115
MLE	90	95	96	91	91	92	93	94	92	93	92	94	91	92	91	93
SWP	55	60	59	56	57	56	58	57	56	58	57	56	56	57	58	50
PEA	70	79	78	71	72	73	74	75	75	71	72	73	74	73	71	74
CCT	33	38	36	34	35	36	37	38	35	34	37	35	36	35	34	30
BLV	50	59	58	51	53	54	53	52	51	53	52	52	51	53	54	53
MUS	220	225	224	223	221	223	221	224	225	224	221	223	224	224	223	200
LMN	50	58	57	51	52	54	53	54	56	52	54	51	53	51	52	45

Table 4: Solution by Open Solver

customers	Big Hotels	Marriage Halls	Restaurants	medium Hotels	Mess	Canteen	Colleges Hostels	Lodges	Small Hotels	Fast food stall	side walk hotels	Schools hostels	Government Hospitals	pani puri shop	Cinema theaters	Retail sales	TOTAL	supply
VEG	**1**	**2**	**3**	**4**	**5**	**6**	**7**	**8**	**9**	**10**	**11**	**12**	**13**	**14**	**15**	**16**		
POT	150	150	100	35	25	20	10	8	10	2	6	5	2	5	5	17	600	0
TOM	200	200	80	60	50	40	30	25	25	10	9	9	5	0	4	53	850	0
SON	60	60	5	4	3	3	2	2	2	0	0.5	0.5	0	0	0	18	170	0
BON	220	200	150	100	20	20	10	10	10	8	5	5	5	6	6	75	800	0
GBL	45	45	0	10	8	8	3	2	2	0	2	1	1	0	0	13	135	0
DRM	25	22	0	15	10	8	1	1	1	0	1	1	1	0	0	14	110	0
CAB	12	10	15	6	3	3	2	2	2	3	0	1	1	0	1.5	13.5	100	0
SNG	25	0	0	15	5	3	2	0	1	0	0	1	1	0	0	7	70	0
BNS	30	30	30	15	10	5	5	3	3	6	0	1	1	0	1	20	160	0
CFR	25	20	35	15	5	3	5	5	0	4	0	0	0	4	0	29	165	0
YAM	25	0	0	25	20	10	0	0	8	0	0	0	0	0	0	12	130	0
BJL	45	40	0	33	30	20	18	13	15	0	8	5	2	0	0	31	240	0
SPO	0	10	30	0	0	0	0.5	0	0	4	0	0	0	0	0.5	5	75	0
RGG	40	0	0	25	20	15	3	3	2	0	1	1	1	0	0	19	120	0
CRT	30	35	41	23	20	20	14	11	8	12	4	3	1	1.5	1.5	5	235	0
BTG	15	0	10	15	10	8	0	0	5	0	0	0	3	0	0	54	140	0
BOG	30	0	0	22	20	12	10	8	10	0	0	5	5	0	0	28	150	0
BTT	30	35	10	15	10	9	8	5	4	0	0	2	2	0	0	0	130	0
TRP	25	0	0	25	20	10	3	0	6	0	0	3	2	0	0	6	125	0
LFR	50	0	0	40	35	30	20	5	10	0	0	5	4	0	0	51	275	0
ASG	90	50	10	50	35	40	15	10	25	0	0	5	5	0	0	215	600	0
IVG	15	0	0	3	2	1	0	0	1	0	0	0	1	0	0	37	90	0
GIN	15	10	15	7	5	4	0.5	2	0.5	4	1	0.5	0.5	0.5	0.5	34	110	0

RWB	150	110	0	100	15	14	7	5	10	0	3	2	2	0	2	80	470	0
RAD	45	0	0	25	15	10	7	0	6	0	3	3	3	0	0	13	135	0
CBR	10	10	15	0	0	0	1	2	0	2	0	0	0	0	0	10	75	0
CPS	15	10	20	1	0	0	0.5	1	0	1.5	0	0	0	0	0.5	10.5	75	0
CYT	25	10	0	20	15	10	5	0	3	0	2	2	2	0	0	6	110	0
BFR	90	0	0	75	30	25	0	0	12	0	3	2	3	0	0	60	320	0
GMG	10	15	0	1	1	1	0	0	0.5	0	0	0	0	0	0	21.5	90	0
GCH	20	20	25	10	9	8	3	2	2	3	2	1	1	0.5	0.5	13	125	0
BST	60	0	25	20	18	15	7	5	5	0	4	3	4	0	0	94	275	0
FBN	60	50	0	25	20	15	5	0	6	0	3	4	3	0	0	59	300	0
SWC	5	5	20	0	0	0	1	1	0	0	0	0	0	0	0	18	90	0
CRL	9	8	7	6	3	2	1	1	0.5	1.5	0.5	0.5	0.5	0.5	0.5	38.5	100	0
COL	10	9	10	7	6	6	2	3	4	4	2	1	1	1	1	13	95	0
GRN	20	0	0	18	10	9	0	0	5	0	0	5	5	0	0	28	120	0
BTL	0	15	5	0	0	0	0	5	0	0	0	0	0	0	0	35	75	0
CBN	15	0	0	10	5	4	1	0	3	0	0	2	2	0	0	18	70	0
YEL	20	0	0	15	13	12	4	0	3	0	2	1	0	0	0	20	110	0
GAR	100	75	90	50	25	13	5	6	3	5	4	2	3	0	4	115	550	0
MLE	20	10	25	5	2	2	2	3	1	1	0.5	0	0.5	0.5	0.5	27	125	0
SWP	0	0	0	0	0	0	0	0	0	0	0	0	0	0	0	60	75	0
PEA	30	25	30	6	7	6	4	4	5	4	3	2	2	4	5	23	165	0
CCT	200	220	140	90	60	45	15	10	8	0	7	5	8	0	0	92	950	0
BLV	50	100	50	50	25	20	0	0	20	0	0	0	0	0	0	235	575	0
MUS	0	0	20	0	0	0	0	0	0	0	0	0	0	0	0	40	75	0
LMN	15	15	18	2	0	0.5	0.5	0.5	0.5	1	0	0.5	0.5	0.5	0	5.5	80	0
Sol: 412640.5																		



Picture 3

Abbreviations of Names of Vegetables: POT: Potatao, TOM: Tomato, SON: Small Onion, BON: Big Onion, GBL: Green Brinjal, DRM: Drumstick, CAB: Cabbage, SNG: Snake Gourd, BNS: Beans, CFR: Cauliflower, YAM: Yam, BJL: Brinjal, SPO: Spring Onion, RGG: Ridge Gourd, CRT: Carrot, BTG: Bitter Gouard, BOG: Bottle Gourd, BTT: Beetroot, TRP: Turnip, LFR: Ladys Finger, ASG: Ash Gourd, IVG: Ivy Gourd, GIN: Ginger, RWB: Raw Banana, RAD: Radish, CBR: Cucumber, CPS: Capsicum, CYT: Chayote, BFR: Banana Flower, GMG: Green Mango, GCH: Green Chilly, BST: Banana Stem, FBN: Flat Beans, SWC: Sweet Corn, CRL: Curry Leaves, COL: Coriander Leaves, GRN: Greens BTL: Betel Leaves CBN: Cluster Beans, YEL: Yam Elephant, GAR: Garlic, MLE: Mint Leaves, SWP: Potato, PEA: Peas, CCT: Coconut, BLV: Banana Leaves, MUS: Mushroom, LMN: Lemon.



Map 1: Location of Arakkonam Town

Conclusion: If a wholesale dealer follows this way of modeling and solving the problem he can maximize his sales on a typical day.

Acknowledgment: The authors thank the authorities of SCSVMV University for having provided the facilities to carry out this research. The second author thanks SCSVMV University for the research fellowship awarded for the tenure of research.

References:

1. Author's names. "Title of Article." Name of Publication volume. issue (year of publication): page numbers. 1. Chukwu, O. Technical evaluation of rice threshers in use in Niger state, Nigeria. M. Eng. Project Report (Unpublished). Department of Agricultural Engineering, UNN, Nsukka, Nige¬ria.1994
2. P.A. Idah, E.S.A. Ajisegiri and M.G. Yisa "Fruits and Veg¬etables Handling and Transportation in Nigeria" AU J.T. 10(3): 175-183 (Jan. 2007)
3. Egharevaba, R.K.A 1995. Post harvest physiology of fruits and vegetables. J. Trop. Postharvest 2: 51-73
4. Fredrick S. Hillier. Mark S. Hillier Introduction to Management Science, A Modeling and Case Studies Approach With Spread¬sheets. 5th Edition April – 1, 2013.
5. Dr.T.Venugopal and S.Indira Priyadarshini " Atypical Restricted Transportation Modeling of Wholesale Vegetable Procurement" IJCRR, Vol 9, issue 10, pp 146-151, may 2017.
6. Dr.T.Venugopal and S.Indira Priyadarshini "Application of Monte Carlo Simulation Technique in Whole Sale Vegetable Purchase by Dealers" (Unpublished). Department of Mathematics, SCSVMV University, Enathur, Kanchipuram.

***

A NUMERICAL STUDY OF COMPARATIVE ANALYSIS OF EXPERIMENTAL AND THEORETICAL VISCOSITIES OF BINARY MIXTURES OF FEW POLYMER SYSTEMS

A.Gayathri
Dept. of Mathematics, SCSVMV (Deemed University), Kanchipuram, India
T.Venugopal
Director (Research & Publication), SCSVMV (Deemed University), Kanchipuram, India

Abstract: The knowledge of thermo physical properties of liquid mixtures is very useful in applied areas of the research design and has a theoretical significance in the liquid state theory. The viscosity of binary mixtures is one of the properties widely used in numerous chemical-engineering correlations regarding the fluid flow, mass and heat transfer calculations. In this paper, the viscosity of binary mixtures of Polyethylene glycol in water and Polypropylene Glycol (PPG 400, PPG 4000) in toluene have been estimated for different concentrations (2%, 4%, 6%, 8% & 10%) and these experimental values are compared with theoretical values obtained by using various mathematical methods like Kendall Monroe, Arrhenius, Hind & Frenkel. The most reliable method that matches with experimental method is identified using Average Percentage Error (APE) and analyzed in the light of molecular interactions occurring in the binary liquid systems. Comparison of evaluated theoretical viscosities with experimental values will reveal the nature of interaction between component molecules in the mixtures. Such theoretical study is useful in defining a comprehensive theoretical model for a specific liquid mixture.

Keywords: Arrhenius, Hind, Kendall Monroe, Frenkal.

1. Introduction: In recent years, there has been a continuous improvement in the experimental investigation of excess thermodynamic properties of liquid mixtures. These have been employed in understanding the nature of molecular interactions in binary liquid mixtures. In chemical industry, knowledge of the thermodynamic properties of non-electrolyte solutions is essential in the design involving chemical separation, heat transfer, mass transfer and fluid flow. The present study involves study about one such property 'Viscosity'. Viscosity data on a material gives manufacturers the ability to predict how the material will behave in the real world [1-4].

Polypropylene glycol is a polymer of propylene glycol. Polypropylene Glycol is used as a primary ingredient in the production of paintballs, tuning reference in mass spectrometry, used as a surfactant, wetting agent, dispersant in leather finishing and used in many formulations for Polyurethanes. During the last two decades, ultrasonic study of
liquid mixtures has gained much importance in assessing the nature of molecular interactions present in the mixtures[5]. In the present study the viscosity of PPG 400 and PPG 4000 in tolune at 303 K. is being measured The experimental viscosity values are compared with theoretical values obtained by using various methods like Kendall Monroe, Arrhenius, Hind & Frenkel. The most suitable method is identified using Average Percentage Error (APE) and discussed in terms of polymer solvent interactions.

2. Methods and Materials: The polymer solutions are obtaining by dissolving PPG 400 and PPG 4000 in toluene to get desired concentrations (2%, 4%, 6%, 8% and 10%). Magnetic stirrer [REMI make] was used for this purpose at a rate of 1000 rpm. The experimental viscosity of the polymer solutions is studied at 303K for different concentrations using Brookfield viscometer [accuracy ±0.01 cP]. The

temperature of viscometer and interferometer are maintained at 303K by circulating water from a thermostat with a thermal stability of ± 0.05 K.

3. Results and Discussion:

3.1 Evaluation of Viscosity: In recent years, measurement of viscosity found extensive application in determining the physicochemical behavior of liquid mixtures. Theoretical evaluation of viscosity gives a better understanding of molecular arrangement in liquids. In the present study, viscosity is determined for PEG in Water and PPG 400 & PPG 4000 in toluene at different concentrations at 303K temperature [6-7]. The experimental viscosity values are compared with theoretical viscosity values by Kendall Monroe, Arrhenius, Hind & Frenkel as given below

Kendall and Monroe derived following equation for analyzing the viscosity of binary mixtures based on zero adjustable parameter.

$\eta_m = (x_1 \eta_1^{\frac{1}{3}} + x_2 \eta_2^{\frac{1}{3}})^3$

Arrhenius equation :

$log\eta_m = x_1 log\eta_1 + x_2 log\eta_2$

Hind equation

$\eta = x_1^2\eta_1 + x_2^2\eta_2 + 2x_1 x_2 \eta_{12}$

Frenkal equation

$ln\eta = x_1^2 ln\eta_1 + x_2^2 ln\eta_2 + 2x_1 x_2 ln\eta_{12}$

where η_{12} is a constant attributed to unlike pair interactions. Its value is obtained from equation

$\eta_{12} = 0.5\eta_1 + 0.5\eta_2$

Where,

ηm viscosity of mixture. Whereas xi , ηi , are mole fraction, viscosity of individual pure liquids[8-10].

The percentage of deviation is calculated by the following equation

$$APD = \frac{100}{N} \sum_{i=1}^{i=N} \left| \frac{(\eta \exp - \eta\ calc)}{\eta\ exp} \right|$$

where exp and calc represent the viscosity of experimental and calculated data, N is the number of experimental data points.

The experimentally measured viscosity and the estimated viscosity from various mathematical models like Kendall Monroe, Arrhenius, Hind & Frenkel for the binary liquid mixture of PEG in water and PPG 400 & PPG 4000 in toluene at five different concentrations at 303K are presented in the Table.

Table

COMPOUND NAME	Conc in % gm/ml	Effective molecular weight	X1 peg 200	X2 water	Density Kg/m3	Refractive Index	Relative Viscosity
PEG 200 + Water	2	0.0183	0.0018	0.9982	1004.9	1.341	1.03
	4	0.0187	0.0036	0.9964	1008.2	1.343	1.09
	6	0.0190	0.0054	0.9946	1011.2	1.346	1.14
	8	0.0193	0.0071	0.9929	1013.7	1.348	1.20
	10	0.0196	0.0089	0.9911	1016.4	1.350	1.26
			Water(Pure)		**995.60**	**1.340**	**0.89**
			PEG 200(Pure)		**1121.8**	**1.459**	**40.6**

PEG 200			Water		
	η1	**40.6**		**η2**	**0.89**
Mole value (X1)	Exp viscosity	Kendall Monroe	Arrhenius	Hind	Frenkel
0.001797	1.03	0.903234	0.896130	0.961350	0.900121
0.003587	1.09	0.915497	0.902280	1.032443	0.910305
0.005371	1.14	0.927826	0.908450	1.103282	0.920553
0.007149	1.2	0.940221	0.914640	1.173868	0.930865
0.00892	1.26	0.952681	0.920850	1.244202	0.941240

COMPOUND NAME	**Conc in % gm/ml**	**Expt Viscosity**	Kendall Monroe	Arrhenius	Hind	Frenkel
PEG 200 + Water	2	1.03	12.30735	12.99707	6.66509	12.60964
	4	1.09	16.00942	17.22199	5.28044	16.48576
	6	1.14	18.61172	20.31137	3.22085	19.24972
	8	1.20	21.64826	23.77996	2.17765	22.42794
	10	1.26	24.39043	26.91664	1.25380	25.29843
APE			**18.59343**	**20.24541**	**3.71957**	**19.21430**

From this table, it is observed that the experimental values of viscosity increases with increase in concentration for both systems. The molecular association is responsible for this increasing trend.

COMPOUND NAME	**Conc in %**	**Effective molecular weight**	**X1 ppg 4000**	**X2 tol**	**Density Kg/m3**	**Molar Volume**	**Relative Viscosity**
PPG 4000 + Toluene	2	0.0923020	0.0053	0.9947	856.37	0.1316	0.85
	4	0.0924657	0.0105	0.9895	859.38	0.1549	0.87
	6	0.0926282	0.0156	0.9844	862.29	0.1777	0.97
	8	0.0927907	0.0207	0.9793	864.39	0.2004	1.12
	10	0.0929529	0.0258	0.9742	867.50	0.2224	1.26
			Toluene		**858.49**		**1.04**
			PPG 4000		**997.79**		**1.06**

PPG 4000			Toluene		
	η1	**1.06**		**η2**	**1.04**
Mole value (X1)	Exp viscosity	Kendall Monroe	Arrhenius	Hind	Frenkel
0.005268	0.85	1.039696	1.040104	1.040105	1.040105
0.01048	0.87	1.039798	1.040208	1.040210	1.040209
0.015638	0.97	1.039900	1.040310	1.040313	1.040311
0.020742	1.12	1.040000	1.040411	1.040415	1.040413
0.025794	1.26	1.040100	1.040511	1.040516	1.040513

COMPOUND NAME	Conc in % gm/ml	Expt Viscosity	Kendall Monroe	Arrhenius	Hind	Frenkel
PPG 4000 + Toluene 303 K	2	0.85	22.3172	22.3652	22.3653	22.3653
	4	0.87	19.5170	19.5641	19.5643	19.5642
	6	0.97	7.2062	7.2484	7.2487	7.2486
	8	1.12	7.1428	7.1062	7.1058	7.1060
	10	1.26	17.4524	17.4198	17.4194	17.4196
APE			**14.7271**	**14.7407**	**14.7407**	**14.7407**

From this table, again it is observed that the experimental values of viscosity increases with increase in concentration for both systems.

PPG 400 in Toluene

COMPOUND NAME	Conc. in %	Effective molecular weight	X1 ppg 400	X2 tol	Density Kg/m3	Mol. Vol. V^E	Viscosity
PPG 400 + toluene 303K	2	0.0938	0.00527	0.99473	857.8700	0.1093	0.8200
	4	0.0954	0.01048	0.98952	860.8800	0.1108	0.8600
	6	0.0970	0.01564	0.98436	864.3900	0.1122	0.8900
	8	0.0985	0.02074	0.97926	866.9000	0.1137	0.9300
	10	0.1001	0.02579	0.97421	868.9100	0.1152	1.0000

For the above given values theoretical viscosity values are as per the following table.

PPG 400			Toluene		
	η_1	1		η_2	1.04
Mole value (X1)	**Exp viscosity**	**Kendall Monroe**	**Arrhenius**	**Hind**	**Frenkel**
0.005268	0.82	1.039381	1.039785	1.039789	1.039787
0.01048	0.86	1.039172	1.039573	1.039581	1.039577
0.015638	0.89	1.038965	1.039362	1.039374	1.039368
0.020742	0.93	1.038761	1.039154	1.039170	1.039162
0.025794	1	1.038558	1.038948	1.038968	1.038958

COMPOUND NAME	Conc in % gm/ml	Expt Viscosity	Kendall Monroe	Arrhenius	Hind	Frenkel
PPG 400 + Toluene	2	0.82	26.7538	44.8031	26.8036	26.8033
	4	0.86	20.8339	34.8805	20.8815	20.8810
	6	0.89	16.7377	27.7823	16.7837	16.7830
	8	0.93	11.6947	18.7370	11.7387	11.7379
	10	1.00	3.8558	3.8948	3.8968	3.8958
APE			**15.98**	**26.02**	**16.02**	**16.02**

Conclusion: The Viscosity is calculated for the binary mixtures of PEG in water and PPG 400 & PPG 4000 in toluene for different concentrations at 303K. The experimental values are compared with the theoretical methods. From these, it may be concluded that Kendall Monroe method is the best suitable method for estimating the viscosity in the systems taken for study. Variation of molecular interaction parameters with concentration suggested the absence of complex formation between the molecules and the effect of concentration is analyzed.

References:

1. Rita Mehra. "Application of Refractive index mixing rules in binary systems of Hexadecane and hepta decane with n-alkanols at different temperatures" Proc. Indian Acad. Sci. (Chem. Sci), vol. 115, pp. 147-154, 2003.
2. Dnyaneshwar Shamrao Wankhede. "Refractive index, molar refraction and comparative refractive index study of propylene carbonate binary liquid mixtures", Acta Chim. Slov, vol. 59, pp. 258-263, 2012.
3. A. Gayathri, T. Venugopal, K.Venkatramanan, "A Comparative analysis of Ultrasound velocity in binary liquidsystems of PPG by mathematical and experimental methods", Physics Procedia, vol. 70, pp. 241-244, 2015.
4. K. Venkatramanan, V. Arumugam, "Viscosity studies on PPG and its blend in toluene", Int.J. Thermophysics, vol. 27(1), pp. 66-78, 2006.
5. Gayathri.A et al, "Mathematical and Experimental Analysis of Ultrasound Velocity and Refractive Index in Binary Mixtures of Pharmaceutically Important Polymer— PEG 600", Recent Trends in Materials Science and Applications, Springer Proceedings in Physics, Vol. 189, pp 709-722, 2017.
6. A.Gayathri, T.Venugopal, "Analysis of speed of acoustic waves in binary liquid systems through mathematical and experimental methods", Indian Journal of Science vol.13, 1-4, 2015.
7. P.Krishnamurthi, P.A. Thenmozhi, "Ultrasonic studies of molecular interaction of octanol and decanol with nonpolar solvents", Journal of Chemical and Pharmaceutical research vol.4, 4677-4681, 2012.
8. J.Thennarasu, G.Meenakshi, "Evaluation of Ultrasonic Velocity and Percentage Deviation of Ternary Mixtures at Different Temperatures", Rasayan Journal of Chemistry vol.4, 904-909, 2011.
9. R.Vadamalar, D.Mani, R.Balakrishnan, "Ultrasonic Study of Binary Liquid Mixtures of Methyl Methacrylate with Alcohols", Research Journal of Chemical Sciences vol.1, 79-82, 2011.
10. N. Siddharthan S. Jayakumar, "Theoretical Evaluation of Sound Velocity, Viscosity and Density of Binary Liquid System" Int. J. Chem.Sci.,vol. 14(4), 2016.

***

TRIPLE CONNECTED COMPLEMENTARY TREE EQUITABLE DOMINATION

N. Saradha
Assistant Professor, SCSVMV, Enathur, Kanchipuram.
V. Swaminathan
Ramanujan Research Center in Mathematics,Saraswathi Narayanan College,Madurai, India
P. J. Anjali
Research Scholar, SCSVMV, Enathur, Kanchipuram

Abstract. A dominating set $S \subseteq V(G)$ is said to be Triple connected complementary tree equitable dominating set if S is a triple connected equitable dominating set and $\langle V-S \rangle$ is a tree. The minimum cardinality taken over all triple connected complementary tree equitable dominating sets is called the triple connected complementary tree equitable domination number of G and is denoted by $\gamma_{tc-cteq}$. In this paper, we introduce the concept of triple connected complementary tree equitable dominating set and we found this number for some standard graphs. Also some results on triple connected complementary tree equitable dominating sets are established.

Keywords: Triple Connected Dominating Set, Equitable Dominating Set, Triple Connected Complementary Equitable Dominating Set.

1. Introduction: A subset S of V is called a dominating set of G if every vertex in V -S is adjacent to at least one vertex in S. The domination number $\gamma(G)$ is the minimum cardinality taken over all dominating sets in G. A dominating set S of a connected graph G is said to be a connected dominating set of G if the induced sub graph $\langle S \rangle$ is connected. The minimum cardinality taken over all connected dominating sets is the connected domination number and is denoted by $\gamma_c(G)$. Many authors have introduced different types of domination parameters by imposing conditions on the dominating set [5]. Recently, the concept of triple connected graphs has been introduced by Paulraj Joseph *et.al* [4] by considering the existence of a path containing any three vertices of G. They have studied the properties of triple connected graphs and established many results on them. A graph G is said to be triple connected if any three vertices of G lie on a path in G. All paths, cycles, complete graphs and wheels are some standard examples of triple connected graphs. G. Mahadevan etal., introduced triple connected domination number of a graph. A subset S of V of a nontrivial connected graph G is said to be triple connected dominating set, if S is a dominating set and the induced sub graph $\langle S \rangle$ is triple connected. The minimum cardinality taken over all triple connected dominating sets is called the triple connected domination number of G and is denoted by $\gamma_{tc}(G)$. A dominating set $S \subseteq V(G)$ is said to be equitable dominating set if for every $v \in V-S$, there exists a vertex $u \in S$ such that $uv \in E(G)$ and $|\deg(u)-\deg(v)| \leq 1$. A dominating set $S \subseteq V(G)$ is said to be triple connected equitable dominating set if S is a equitable dominating set and $\langle S \rangle$ is triple connected In this paper, we introduce the concept of triple connected complementary tree equitable dominating set and we found this number for some standard graphs. Also some results on triple connected complementary tree equitable dominating sets are established.

Theorem1.1[4] A connected graph G is not triple connected if and only if there exists a H-cut with $\omega(G-H) \geq 3$, such that $|V(H) \cap N(C_i)| = 1$ for at least three components C_1, C_2 and C_3 of G-H.

2. Triple Connected Complementary Tree Equitable Domination:

Definition 2.1: A dominating set $S \subseteq V(G)$ is said to be Triple connected complementary tree equitable dominating set if S is a triple connected equitable dominating set and $\langle V - S \rangle$ is a tree. The minimum cardinality taken over all triple connected complementary tree equitable dominating sets is called the triple connected complementary tree equitable domination number of G and is denoted by $\gamma_{tc-cteq}$.

Example 2.2: For the graph G in Figure 2.1, $S = \{v_2, v_3, v_5\}$ forms a $\gamma_{tceq-ct}$ set of G. Hence $\gamma_{tc-cteq}(G) = 3$.

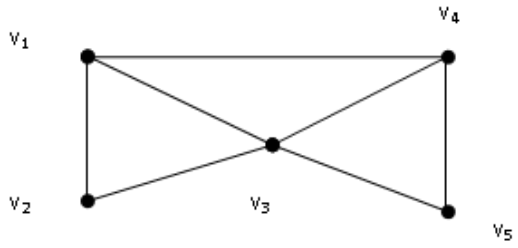


Figure 2.1

Observation 2.3: Triple connected complementary tree equitable dominating set does not for all graph and if exists then $\gamma_{tc-cteq}(G) \geq 3$.

Example 2.4: For K_2, there does not exist a triple connected complementary tree equitable dominating set.

Throughout, this paper we consider only connected graphs for which Triple connected complementary tree equitable dominating set exists.

Observation 2.5: The complement of the triple connected complementary tree equitable dominating set need not be a triple connected complementary tree equitable dominating set.

Example 2.6: For the graph G in Figure 2.2, S = $\{v_2, v_3, v_4\}$ forms a triple connected complementary tree equitable dominating set of G. But the complement V-S = $\{v_1, v_5\}$ is not a triple connected complementary tree equitable dominating set.

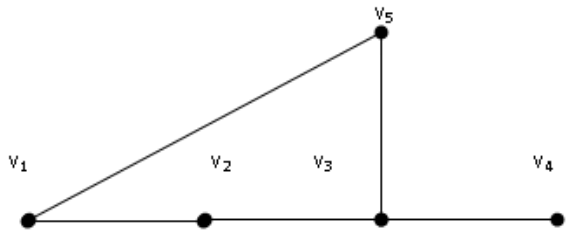


Figure 2.2

Observation 2.8: Every triple connected complementary tree equitable dominating set is a dominating set but not conversely.

Example 2.9: For the graph G in Figure 2.3, S={v_3,v_4,v_5} forms the triple connected complementary tree equitable dominating set as well as the dominating set of G. But S = {v_1,v_2} is a dominating set but not a triple connected complementary tree equitable domination set.

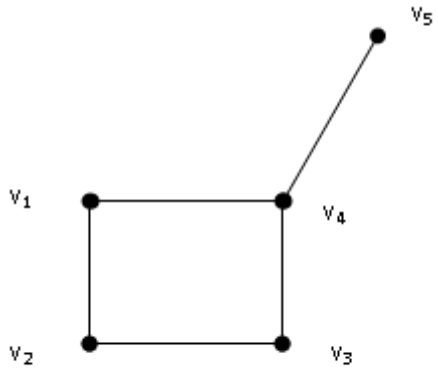


Figure 2.3

Theorem 2.10: If the induced sub graph of each connected dominating set of G has more than two pendent vertices, then G does not contain a triple connected complementary tree equitable dominating set.
Proof: The proof follows from theorem 1.1

Exact Value for Some Standard Graphs:
1. For any cycle of order p ≥ 3,

$$\gamma_{tc-cteq}(C_p) = p \text{ if } p < 5$$
$$= p - 2 \text{ if } p \geq 5$$

2. For any path of order p ≥ 3,

$$\gamma_{tc-cteq}(P_p) = p \text{ if } p = 3$$
$$= p - 1 \text{ if } p = 4$$
$$= p - 2 \text{ if } p \geq 5$$

3. For any complete graph of order p ≥ 3,

$$\gamma_{tc-cteq}(K_p) = p$$

4. For any complete bipartite graph of order p ≥ 4,

$$\gamma_{tc-cteq}(K_{m,n}) = p \text{ where } m + n = p$$

5. For any wheel graph of order p ≥ 3,

$$\gamma_{tc-cteq}(W_p) = p$$

Theorem 2.11: For any connected graph G with p ≥ 3, we have $3 \leq \gamma_{tc-cteq}(G) \leq n$ and the bounds are sharp.
Proof: The lower and upper bound follows from definition 2.1.

References:

1. K. D. Dharmalingam and V. Swaminathan, Degree equitable domination on graph, Kragujevac Journal of Mathematics, Vol-35, NO. 1, (2011), pages 191 -197.
2. F.Harary, Graph Theory, Addison –Wessley, Reading Mass. (1969).
3. T.W. Haynes, S.T. Hedetniemi and P. J. Slater, Fundamentals of domination in graphs, Marcel Dekker Inc. New Yory(1998).
4. Paulraj Joseph J and Arumugam S, Dominatinon and connectivity in graphs, International Journal of Management and Systems, Vol. 8 No. 3, 233-236.
5. Teresa W. Haynes, Stephen T. Hedetniemi, Peter J. Slater, Fundamentals of domination in graphs, Marcel Decker, Inc., New York 1998.
6. J.A. Bondy and U.S.R. Murty, Graph Theory with Applications, The Macmillan Press Ltd, 1976.
7. G. Mahadevan, A. Selvam, J. Paulraj Joseph and T. Subramanian, Triple connected domination number of a graph, International Journal of Mathematical combinatorics, Vol.3(2012), 93-104.

***

GLOBAL TRIPLE CONNECTED COMPLEMENTARY ACYCLIC DOMINATION

N. Saradha
Assistant Professor, SCSVMV, Enathur, Kanchipuram.
V. Swaminathan
Ramanujan Research Center in Mathematics,Saraswathi Narayanan College,Madurai, India
Arumugam
Research Scholar, SCSVMV, Enathur, Kanchipuram

Abstract. A dominating set $S \subseteq V(G)$ is said to be global Triple connected dominating set if S is a global dominating set and $\langle S \rangle$ is a triple connected. The minimum cardinality taken over all global triple connected dominating sets is called the global triple connected domination number of G and is denoted by γ_{gtc}. A dominating set $S \subseteq V(G)$ is said to be global Triple connected complementary acyclic dominating set if S is a global triple connected dominating set and $\langle V - S \rangle$ is acyclic. The minimum cardinality taken over all global triple connected complementary acyclic dominating sets is called the global triple connected complementary acyclic domination number of G and is denoted by γ_{gtc-ca}. In this paper, we introduce the concept of global triple connected complementary acyclic dominating set and we found this number for some standard graphs. Also some results on global triple connected complementary acyclic dominating sets are established.

Keywords: Triple Connected Dominating Set, Global Dominating Set, Global Triple Connected Dominating Set, Global Triple Connected Complementary Acyclic Dominating Set.

1. Introduction: A subset S of V is called a dominating set of G if every vertex in V -S is adjacent to at least one vertex in S. The domination number $\gamma(G)$ is the minimum cardinality taken over all dominating sets in G. A dominating set S of a connected graph G is said to be a connected dominating set of G if the induced sub graph $\langle S \rangle$ is connected. The minimum cardinality taken over all connected dominating sets is the connected domination number and is denoted by $\gamma_c(G)$. Many authors have introduced different types of domination parameters by imposing conditions on the dominating set [4]. Recently, the concept of triple connected graphs has been introduced by Paulraj Joseph *et.al* [3] by considering the existence of a path containing any three vertices of G. They have studied the properties of triple connected graphs and established many results on them. A graph G is said to be triple connected if any three vertices of G lie on a path in G. All paths, cycles, complete graphs and wheels are some standard examples of triple connected graphs. G. Mahadevan etal., introduced triple connected domination number of a graph. A subset S of V of a nontrivial connected graph G is said to be triple connected dominating set, if S is a dominating set and the induced sub graph $\langle S \rangle$ is triple connected. The minimum cardinality taken over all triple connected dominating sets is called the triple connected domination number of G and is denoted by $\gamma_{tc}(G)$. A dominating set $S \subseteq V(G)$ is said to be Global dominating set if for every $v \in V - S$, there exists a vertex $u \in S$ such that v is not adjacent to u. A dominating set $S \subseteq V(G)$ is said to be global triple connected dominating set if S is a global dominating set and $\langle S \rangle$ is triple connected In this paper, we introduce the concept of global triple connected complementary acyclic dominating set and we found this number for some standard graphs. Also some results on global triple connected complementary acyclic dominating sets are established.

Theorem1.1[4] A connected graph G is not triple connected if and only if there exists a H-cut with $\omega(G-H)\geq 3$, such that $|V(H)\cap N(C_i)|=1$ for at least three components C_1, C_2 and C_3 of G-H.

2. Global Triple Connected Complementary Acyclic Domination:

Definition 2.1: A subset S of V of a non trivial graph G is said to be a Global Triple Connected Complementary acyclic dominating set if S is a Global triple connected dominating set and the induced sub graph $\langle V-S\rangle$ is acyclic. The minimum cardinality taken over all global triple connected complementary acyclic dominating sets is called the global triple connected complementary acyclic domination number of G and is denoted by $\gamma_{gtc-ca}(G)$.

Example 2.2: For the graph K4, $S=\{v_1,v_2,v_3,v_4\}$ forms a global triple connected complementary acyclic dominating set.

Example 2.3: Global triple connected complementary acyclic dominating set does not exist for all graphs p

Observation 2.4: Every global triple connected complementary acyclic dominating set is a triple connected dominating set. But every triple connected dominating set is not a global triple connected complementary acyclic dominating set.

Observation 2.5: For any connected graph G with p vertices,
$\gamma(G)\leq\gamma_C(G)\leq\gamma_{gc}(G)\leq\gamma_{gtc}(G)\leq\gamma_{gtc-ca}(G)\leq p$ and this inequalities are strict.

Example 2.6: $\gamma(K_n)=1,\gamma_C(K_n)=2,\gamma_{gc}(K_n)=n,\gamma_{gtc}(K_n)=n,\gamma_{gtc-ca}(K_n)=n$

Theorem 2.7: If the induced sub graph of all connected dominating set of G has more than two pendent vertices then G does not contains a global triple connected complementary acyclic dominating set.

Example 2.8; Global triple connected complementary acyclic domination number for some standard graphs.

1. For any complete graph G with p vertices $\gamma_{gtc-ca}(G\circ K_1)=p$
2. For any path of order $p\geq 3$, $\gamma_{gtc-ca}(P_p)=3$ if $p<5$; $=p-2$ if $p\geq 5$
3. For any cycle of length p for $p\geq 3$, $\gamma_{gtc-ca}(C_p)=3$ if $p<5$; $=p-2$ if $p\geq 5$
4. For the complete bipartite graph $K_{m,n}(m,n\geq 2)$, $\gamma_{gtc-ca}(K_{m,n})=m+n-3$
5. For any star $K_{1,p-1}(p\geq 3)$, $\gamma_{gtc-ca}(K_{1,p-1})=3$
6. For any complete graph Kp $p\geq 3$, $\gamma_{gtc-ca}(K_p)=p$
7. For any wheel Wn , $\gamma_{gtc-ca}(W_p)=3$

Theorem 2.9: For any connected graph G with $p\geq 4$ we have $3\leq\gamma_{gtc-ca}\leq p$ and the bound is sharp.

References:

1. F.Harary, Graph Theory, Addison –Wessley, Reading Mass. (1969).
2. T.W. Haynes, S.T. Hedetniemi and P. J. Slater, Fundamentals of domination in graphs, Marcel Dekker Inc. New Yory(1998).
3. Paulraj Joseph J and Arumugam S, Dominatinon and connectivity in graphs, International Journal of Management and Systems, Vol. 8 No. 3, 233-236.
4. Teresa W. Haynes, Stephen T. Hedetniemi, Peter J. Slater, Fundamentals of domination in graphs, Marcel Decker, Inc., New York 1998.
5. J.A. Bondy and U.S.R. Murty, Graph Theory with Applications, The Macmillan Press Ltd, 1976.
6. G. Mahadevan, A. Selvam, J. Paulraj Joseph and T. Subramanian, Triple connected domination number of a graph, International Journal of Mathematical combinatorics, Vol.3(2012), 93-104.
7. E.Sampathkumar, Global domination number of a graph, Jour. Math. Phy. Sci., Vol. 23, Vol. 5, October 1989.

***

STRONG EFFICIENT TRIPLE CONNECTED DOMINATION

N. Saradha
Department of Mathematics, SCSVMV University, Kanchipuram, Tamilnadu, India
V. Swaminathan
Ramanujan Research Center in Mathematics, Saraswathi Narayanan College, Madurai, Tamilnadu, India
Amudhavalli
Research Scholar, Department of Mathematics, SCSVMV University, Kanchipuram, Tamilnadu, India

Abstract. A subset S of V of a nontrivial connected graph G is said to be an efficient triple connected dominating set, if S is an efficient dominating set and the induced sub graph $\langle S \rangle$ is triple connected. The minimum cardinality taken over all efficient triple connected dominating sets is called the efficient triple connected domination number and is denoted by γ_{etc}. In this paper we introduce new domination parameter, strong efficient triple connected domination number of a graph with real life application. A subset S of V of a nontrivial connected graph G is said to be a strong efficient triple connected dominating set, if S is a strong efficient dominating set and the induced sub graph $\langle S \rangle$ is triple connected. The minimum cardinality taken over all strong efficient triple connected dominating sets is called the strong efficient triple connected domination number of G and is denoted by $\gamma_{setc}(G)$. Any strong efficient triple connected dominating set with γ_{setc} vertices is called a γ_{setc} - set of G. We also determine this number for some standard graphs and obtain bounds for general graph. Its relationship with other graph theoretical parameters are also investigated.

Keywords: Dominating Set, Efficient Dominating Set, Triple Connected Dominating Set, Strong Efficient Triple Connected Dominating Set.

1. Introduction: A subset S of V is called a dominating set of G if every vertex in V -S is adjacent to at least one vertex in S. The domination number $\gamma(G)$ is the minimum cardinality taken over all dominating sets in G. A dominating set S of a connected graph G is said to be a connected dominating set of G if the induced sub graph $\langle S \rangle$ is connected. The minimum cardinality taken over all connected dominating sets is called the connected domination number and is denoted by $\gamma_c(G)$. Many authors have introduced different types of domination parameters by imposing conditions on the dominating set [10]. Recently, the concept of triple connected graphs has been introduced by Paulraj Joseph *et.al* [12] by considering the existence of a path containing any three vertices of G. They have studied the properties of triple connected graphs and established many results on them. A graph G is said to be triple connected if any three vertices of G lie on a path in G. All paths, cycles, complete graphs and wheels are some standard examples of triple connected graphs. A subset S of V of a nontrivial connected graph G is said to be a triple connected dominating set, if S is a dominating set and the induced sub graph $\langle S \rangle$ is triple connected. The minimum cardinality taken over all triple connected dominating sets is called the triple connected domination number of G and is denoted by $\gamma_{tc}(G)$. A subset S of V of a nontrivial graph G is said to be an efficient dominating set, if every vertex is dominated by exactly once. The minimum cardinality taken over all efficient dominating sets is called the efficient domination number and is denoted by $\gamma_e(G)$. A subset S of V of a nontrivial connected graph G is said to be an efficient triple connected dominating set, if S is an efficient dominating set and the induced sub graph

$\langle S \rangle$ is triple connected. The minimum cardinality taken over all efficient triple connected dominating sets is called the efficient triple connected domination number and is denoted by $\gamma_{etc}(G)$. In this paper we introduce new domination parameter, strong efficient triple connected domination number of a graph with real life application.

Theorem 1.1[12]: A connected graph G is not triple connected if and only if there exists a H-cut with $\omega(G-H) \geq 3$, such that $|V(H) \cap N(C_i)| = 1$ for at least three components C_1, C_2 and C_3 of G-H.

2. Strong Efficient Triple Connected Dominating Set:

Definition 2.1.: A subset S of V of a nontrivial connected graph G is said to be a strong efficient triple connected dominating set, if S is a strong efficient dominating set and the induced sub graph $\langle S \rangle$ is triple connected. The minimum cardinality taken over all strong efficient triple connected dominating sets is called the strong efficient triple connected domination number of G and is denoted by $\gamma_{setc}(G)$. Any strong efficient triple connected dominating set with γ_{setc} vertices is called a γ_{setc} - set of G. We also determine this number for some standard graphs and obtain bounds for general graph.

Example 2.2.: For the graph G in Figure 2.1, S={v_1, v_4, v_5, v_6} forms a γ_{setc} of G. Hence $\gamma_{setc}(G) = 4$.

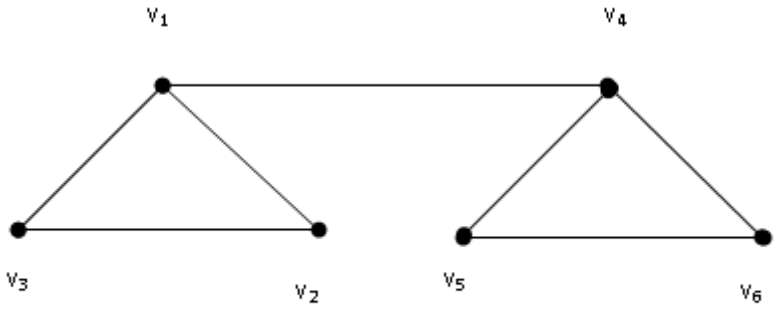


Figure 2.1

Observation 2.3: Strong efficient triple connected dominating set does not exist for all graphs and if exists, then $\gamma_{setc}(G) \geq 3$

Example 2.4: For K_2, there does not exists any strong efficient triple connected dominating set.

Remark 2.5: Throughout this paper we consider only connected graphs for which strong efficient triple connected dominating set exists.

Observation 2.6: The complement of the strong efficient triple connected dominating set need not be a strong efficient triple connected dominating set.

Example 2.7: For the graph G_2 is Figure 2.2, S={v_3, v_5, v_6, v_9} forms a strong efficient triple connected dominating set of G. But the complement V-S={$v_1, v_2, v_4, v_7, v_9, v_{10}$} is not a strong efficient triple connected dominating set.

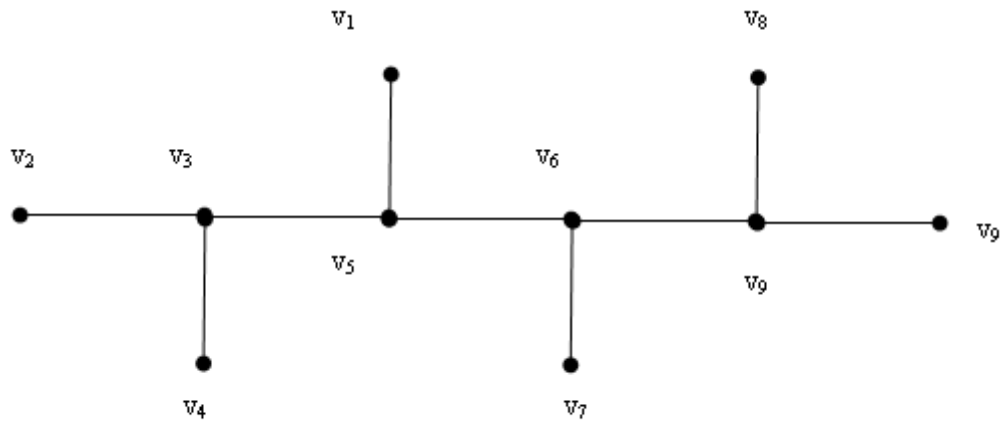


Figure 2.2

Observation 2.8: Every strong efficient triple connected dominating set is a dominating set but not conversely.

Example 2.9: For the graph G in Figure 2.3, S={v_1,v_2,v_3} forms the strong efficient triple connected dominating set as well as the dominating set of G. For the graph in Figure 2.4, S={v_2} is a dominating set but not a strong efficient triple connected dominating set.

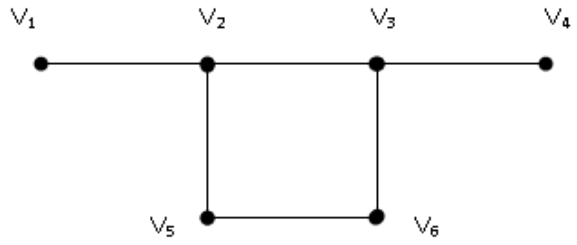


Figure 2.3

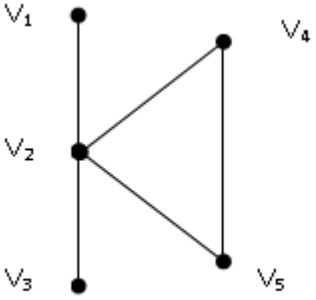


Figure 2.4

Theorem 2.10: If the induced sub graph of each connected dominating set of G has more than two pendent vertices, then G does not contain a strong efficient triple connected dominating set.
Proof: The proof follows from theorem 1.1.

Exact Value for Some Standard Graphs:

1. For any cycle of order p ≥ 3,

$$\gamma_{setc}(C_p) = p \text{ if } p < 5$$

$$= p - 2 \text{ if } p \geq 5$$

2. For any path of order p≥3,

$$\gamma_{setc}(P_p) = \begin{cases} p \text{ if } p = 3 \\ p - 1 \text{ if } p = 4 \\ p - 2 \text{ if } p \geq 5 \end{cases}$$

3. For any complete graph of order $p \geq 3$,

$$\gamma_{setc}(K_p) = p$$

4. For any complete bipartite graph of order $p \geq 4$,
   $\gamma_{setc}(K_{m,n}) = p$ where m+n = p.
5. For any star of order $p \geq 3$,
   $\gamma_{setc}(K_{1,n}) = 3$, where n+1=p
6. For any wheel graph of order $p \geq 3$,
   $\gamma_{setc}(W_p) = p$

Theorem 2.11: For any connected graph G with $p \geq 3$, we have $3 \leq \gamma_{setc}(G) < p$ and the bounds are sharp.

Proof: The lower and upper bound follows from definition 2.1. For C_5 the lower bound is attained and for K_5, the upper bound is attained.

Conclusion: In this paper, we introduced the concept of strong efficient triple connected domination number of G. Also we found this number for some standard graphs.

References:

1. D.W. Bange, A.E. Barkauskas and P.J. Slater, Disjoint dominating sets in trees. Technical Report 78-1087J,Sandia Laboratories, 1978.
2. D.W. Bange, A.E. Barkauskas and P.J. Slater, Efficient dominating sets in graphs, Application of Discrete Mathematics, 189-199, SIAM, Philadephia, 1988.
3. F. Harary, Graph Theory, Addison-Weslay.
4. N. Meena, A, Subramaniyan and V. Swaminathan, Strong Efficient Domination in Graphs, International Journal of Innovative Science, Engineering & Technology, Vol. 1 Issue 4, 172-177, 2014.
5. Meena, Further Results on Sum of Strong Efficient Domination Number and Chromatic Number, International Journal of Innovative Science, Engineering & Technology, Vol. 3 Issue 11,300-304 November 2016.
6. Paulraj Joseph J and Arumugam S, Domination and colouring in graphs, International Journal of Management and Systems, Vol.8 No.1,37-44,1997.
7. Paulraj Joseph J and Arumugam S, Dominatinon and connectivity in graphs, International Journal of Management and Systems, Vol. 8 No. 3, 233-236.
8. Paulraj Joseph J and Mahadevan G, Complementary connected domination number and Chromatic number of a graph, ActascienciaIndica, Vol. XXXI M, No.2, 847-854, 2006.
9. E. Samapthkumar and L. PushpaLatha, Strong weak domination and domination balance in a graph, Discrete Mathematics, 161: 235-242, 1996.
10. Teresa W. Haynes, Stephen T. Hedetniemi, Peter J. Slater, Fundamentals of domination in graphs, Marcel Decker, Inc., New York 1998.
11. J.A. Bondy and U.S.R. Murty, Graph Theory with Applications, The Macmillan Press Ltd, 1976.
12. Paulraj JosephJ., AngelJebitha M.K., Chithra Devi P.and Sudhana G., Triple connected graphs, Indian Journal of Mathematics and Mathematical Sciences,Vol.8, No. 1(2012), 61-75.
13. G. Mahadevan, A. Selvam, J. Paulraj Joseph and T. Subramanian, Triple connected domination number of a graph, International Journal of Mathematical combinatorics, Vol.3(2012), 93-104.

***

PERFECT EDGE DOMINATION AND EFFICIENT EDGE DOMINATION IN GRAPHS

R. Malathi
Asst. Prof. of Mathematics, SCSVMV, Kanchipuram
Babu. N
M.Phil Scholar, SCSVMV, Kanchipuram

Abstract: In this paper, we first show that the perfect edge domination problem on bipartite graphs and the efficient edge domination problem on planar bipartite graphs are NP-complete. Then, we give linear-time algorithms for solving the weighted perfect and efficient edge domination problems on generalized series–parallel graphs using parse trees.

Keywords: Perfect Edge Domination, Efficient Edge Domination and Planar Bipartite Graphs.

NP-Completeness Results:

Problem PED (perfect edge domination)
Instance:
A graph G = (V, E) and a positive integer K ≤ |E|.
Question:
Does G have a perfect edge dominating set of cardinality K or less?

Problem EED (efficient edge domination)
Instance:
A graph G = (V, E).
Question:
Does G have an efficient edge dominating set?

X3C (exact cover by 3-sets)
Instance:
A finite set X with $|X| = 3_n$ and a collection S of 3-element subsets of X with |S| = m.
Question:
Does S contain an exact cover for X, i.e., a subcollection S′ ⊆ S such that every element of X occurs in exactly one member of S′ ?

Problems PED and EED are the decision problems which correspond to the perfect and the efficient edge domination problems, respectively. It is well known that X3C is NP-complete.

Perfect Edge Domination on Bipartite Graphs: By the definition of perfect edge domination, we have the following lemma immediately.

Lemma 1: Given a graph G = (V, E), let D be any perfect edge dominating set of G. For any v ∈ V, if there are at least two edges of D which are incident with v, then all edges incident with v are in D.

Theorem 1: Problem PED is NP-complete for bipartite graphs.

Efficient Edge Domination on Planar Bipartite Graphs: Note that planar bipartite graphs are graphs that are both planar and bipartite.

Theorem 2: Problem EED is NP-complete for planar bipartite graphs.

Perfect Edge Domination on Generalized Series–Parallel Graphs: For a set S of vertices, denote by G \ S the subgraph induced by V \ S. For a generalized series–parallel graph G(u,v), we define $MP_{\alpha\beta}(G)$, where α, β ∈ {0, 1, 2, 3}, to be an arbitrary minimum weighted perfect edge dominating set of

$$\begin{Bmatrix} G & \text{if } \alpha \neq 3 \text{ and } \beta \neq 3, \\ G \setminus \{u\} & \text{if } \alpha = 3 \text{ and } \beta \neq 3, \\ G \setminus \{v\} & \text{if } \alpha \neq 3 \text{ and } \beta = 3, \\ G \setminus \{u, v\} & \text{if } \alpha = 3 \text{ and } \beta = 3, \end{Bmatrix}$$

such that

$$\begin{Bmatrix} \text{no edge in } MP\alpha\beta(G) \text{ is incident with u} & \text{if } \alpha = 0 \\ \text{exactly one edge in } MP\alpha\beta(G) \text{ is incident with u} & \text{if } \alpha = 1, \\ MP\alpha\beta(G) \text{ contains all edges which are incident with u} & \text{if } \alpha = 2, \\ \text{no edge in } MP\alpha\beta(G) \text{ is incident with u or its neighbors} & \text{if } \alpha = 3 \end{Bmatrix}$$

and

$$\begin{Bmatrix} \text{no edge in } MP\alpha\beta(G) \text{ is incident with v} & \text{if } \alpha = 0 \\ \text{exactly one edge in } MP\alpha\beta(G) \text{ is incident with v} & \text{if } \alpha = 1, \\ MP\alpha\beta(G) \text{ contains all edges which are incident with v} & \text{if } \alpha = 2, \\ \text{no edge in } MP\alpha\beta(G) \text{ is incident with u or its neighbors} & \text{if } \alpha = 3 \end{Bmatrix}$$

By the definition, it is not hard to verify that

$$\min\{MP_{\alpha\beta}(G) \mid \alpha, \beta \in \{0, 1, 2\}\}$$

is a minimum weighted perfect edge dominating set of G. For the complete graph $K_2(u, v)$, we initialize $MP_{\alpha\beta}(K_2)$, where α, β ∈ {0, 1, 2, 3}, as follows.

- $MP_{11}(K_2) = MP_{12}(K_2) = MP_{21}(K_2) = MP_{22}(K_2) = \{(u,v)\}$
- $MP_{03}(K_2) = MP_{30}(K_2) = \emptyset$ with weights zero.

Other cases do not exist and are denoted by Φ with weights ∞, where we let S ∪ Φ = Φ for any set S.

Lemma 2: Let $G(u_1, v_2)$ be a generalized series–parallel graph obtained by applying a series-1 composition to generalized series–parallel graphs $G_1(u_1, v_1)$ and $G_2(u_2, v_2)$. Then, for any α, β ∈ {0, 1, 2, 3}, we have

$$MP_{\alpha\beta}(G) = \min \begin{Bmatrix} MP_{00}(G_1) \cup MP_{00}(G_2), \\ MP_{01}(G_1) \cup MP_{30}(G_2), \\ MP_{03}(G_1) \cup MP_{10}(G_2), \\ MP_{02}(G_1) \cup MP_{20}(G_2) \end{Bmatrix}$$

Lemma 3: Let $G(u_1, v_1)$ be a generalized series–parallel graph obtained by applying a series-2 composition to generalized series–parallel graphs $G_1(u_1, v_1)$ and $G_2(u_2, v_2)$. Then, for any α ∈ {0, 1, 2, 3} and β ∈ {0, 2, 3}, we have

(1) $MP_{\alpha\beta}(G) = MP_{\alpha\beta}(G_1) \cup \min\{MP_{\beta 0}(G_2), MP_{\beta 1}(G_2), MP_{\beta 2}(G_2)\}$.

$$MP_{\alpha 1}(G) = \min \begin{Bmatrix} MP_{\alpha 1}(G_1) \cup \min\{MP_{30}(G_2), MP_{31}(G_2), MP_{32}(G_2)\}, \\ MP_{03}(G_1) \cup \min\{MP_{10}(G_2), MP_{11}(G_2), MP_{12}(G_2)\}\} \end{Bmatrix}$$

Lemma 4: Let $G(u_1, v_1)$ be a generalized series–parallel graph obtained by applying a parallel composition to generalized series–parallel graphs $G_1(u_1, v_1)$ and $G_2(u_2, v_2)$. Then, for any $\alpha, \beta \in \{0, 2, 3\}$, we have

1. $MP_{\alpha\beta}(G) = MP_{\alpha\beta}(G_1) \cup MP_{\alpha\beta}(G_2)$.
2. $MP_{\alpha 1}(G) = \min\{MP_{\alpha 1}(G_1) \cup MP_{\alpha 3}(G_2), MP_{\alpha 3}(G_1) \cup MP_{\alpha 1}(G_2)\}$.
3. $MP_{1\beta}(G) = \min\{MP_{1\beta}(G_1) \cup MP_{3\beta}(G_2), MP_{3\beta}(G_1) \cup MP_{1\beta}(G_2)\}$.
4. $$MP_{11}(G) = \min \begin{Bmatrix} MP_{11}(G_1) \cup MP_{33}(G_2), \\ MP_{13}(G_1) \cup MP_{31}(G_2), \\ MP_{31}(G_1) \cup MP_{13}(G_2), \\ MP_{33}(G_1) \cup MP_{11}(G_2) \end{Bmatrix}$$

Algorithm PEDP-GSP computes $MP_{\alpha\beta}(G_i)$, $0 \le \alpha, \beta \le 3$. The details of Algorithm PEDP-GSP are described as follows.

Algorithm PEDP-GSP:
Input: A generalized series–parallel graph G.
Output: A minimum weighted perfect edge dominating set D of G.
Step 1: Construct a parse tree PT(G) of G,
Step 2: for each leave $K_2(u, v)$ of PT(G) **do** /***Initialization** */
$MP_{11}(K_2) = MP_{12}(K_2) = MP_{21}(K_2) = MP_{22}(K_2) = \{(u, v)\}$;
$MP_{03}(K_2) = MP_{30}(K_2) = \emptyset$ and others are Φ;
Mark (u, v);
end for
Step 3:
while all nodes of PT(G) are not marked **do**
Choose an unmarked node i of PT(G) whose children are marked;
Let G_i be the corresponding subgraph of node i;
case 1: Node i is labeled as S_1 **then**
Compute all $MP_{\alpha\beta}(G_i)$ by Lemma 1, where $0 \le \alpha, \beta \le 3$;
end case
case 2: Node i is labeled as S_2 **then**
Compute all $MP_{\alpha\beta}(G_i)$ by Lemma 2, where $0 \le \alpha, \beta \le 3$;
end case
case 3: Node i is labeled as P then
Compute all $MP_{\alpha\beta}(G_i)$ by Lemma 3, where $0 \le \alpha, \beta \le 3$;
end case
Mark i;
end while
Step 4:
$D = \min\{MP_{\alpha\beta}(G_i) \mid \alpha, \beta \in \{0, 1, 2\}\}$.

Theorem 3: Algorithm PEDP-GSP finds a minimum weighted perfect edge dominating set of a generalized series–parallel graph in $O(|V| + |E|)$ time.

Theorem 4: The weighted perfect edge domination problem can be solved in linear time for generalized series–parallel graphs.

Efficient Edge Domination on Generalized Series–Parallel Graphs: Recall that Grinstead et al. had proposed a linear-time algorithm for computing the maximum number of edges that can be efficiently dominated on generalized series–parallel graphs. However, their algorithm cannot be directly applied for computing a minimum weighted efficient edge dominating set on the same graphs. In this subsection, we will present a linear-time algorithm to solve the weighted efficient edge domination problem on generalized series–parallel graphs. Using this algorithm, we will be capable of designing a

linear-time algorithm for chordal graphs in the next section. For a generalized series–parallel graph G(u, v), we define $ME_{\alpha\beta}(G)$, where $\alpha, \beta \in \{0, 1, 3\}$, to be an arbitrary minimum weighted efficient edge dominating set of [3]

$$\begin{cases} G & \text{if } \alpha \neq 3 \text{ and } \beta \neq 3, \\ G \setminus \{u\} & \text{if } \alpha = 3 \text{ and } \beta \neq 3, \\ G \setminus \{v\} & \text{if } \alpha \neq 3 \text{ and } \beta = 3 \\ G \setminus \{u, v\} & \text{if } \alpha = 3 \text{ and } \beta = 3, \end{cases}$$

such that

$$\begin{cases} \text{no edge } ME_{\alpha\beta}(G) \text{ incident with u} & \text{if } \alpha = 0 \\ \text{exactly one edge in } ME_{\alpha\beta}(G) \text{ is incident with u} & \text{if } \alpha = 1 \\ \text{no edge in } ME_{\alpha\beta}(G) \text{ incident with u or any of its neighbours} & \text{if } \alpha = 3 \end{cases}$$

and

$$\begin{cases} \text{no edge } ME_{\alpha\beta}(G) \text{ incident with v} & \text{if } \alpha = 0 \\ \text{exactly one edge in } ME_{\alpha\beta}(G) \text{ is incident with v} & \text{if } \alpha = 1 \\ \text{no edge in } ME_{\alpha\beta}(G) \text{ incident with v or any of its neighbours} & \text{if } \alpha = 3 \end{cases}$$

Clearly, if G has an efficient edge dominating set, then $\min\{ME_{\alpha\beta}(G) \mid \alpha, \beta \in \{0, 1\}\}$ is a minimum weighted efficient edge dominating set in G. For a complete graph $K_2(u, v)$, we initialize $ME_{\alpha\beta}(K_2)$, where $\alpha, \beta \in \{0, 1, 3\}$, as follows.

- $ME_{11}(K_2) = \{(u, v)\}$.
- $ME_{03}(K_2) = ME_{30}(K_2) = \emptyset$ with weights zero.
- $ME_{13}(K_2) = ME_{31}(K_2) = ME_{33}(K_2) = \Phi$ (with weights ∞.

Similar to the proofs discussed at the previous subsection, it is not hard to verify the following three lemmas.

Lemma 5: Let $G(u_1, v_2)$ be a generalized series–parallel graph obtained by applying a series-1 composition to generalized series–parallel graphs $G_1(u_1, v_1)$ and $G_2(u_2, v_2)$. Then, for any $\alpha, \beta \in \{0, 1, 3\}$, we have

$$ME_{\alpha\beta}(G_1) = \min \begin{Bmatrix} ME\alpha_0(G_1) \cup ME_{0\beta}(G_2) \\ ME\alpha_1(G_1) \cup ME_{3\beta}(G_2) \\ ME\alpha_3(G_1) \cup ME_{30}(G_2) \end{Bmatrix}$$

Lemma 6: Let $G(u_1, v_1)$ be a generalized series–parallel graph obtained by applying a series-2 composition to generalized series–parallel graphs $G_1(u_1, v_1)$ and $G_2(u_2, v_2)$. Then, for any $\alpha \in \{0, 1, 3\}$ and $\beta \in \{0, 3\}$, we have

1. $ME_{\alpha\beta}(G) = ME_{\alpha\beta}(G_1) \cup \min\{ME_{\beta 0}(G_2), ME_{\beta 1}(G_2)\}$.
2. $ME_{\alpha 1}(G) = \min \begin{Bmatrix} ME\alpha_1(G_1) \cup ME_{30}(G_2) ME\alpha_1(G_1) \cup ME_{31}(G_2), \\ ME\alpha_3(G_1) \cup ME_{10}(G_2) ME\alpha_3(G_1) \cup ME_{11}(G_2) \end{Bmatrix}$

Lemma 7: Let $G(u_1, v_1)$ be a generalized series–parallel graph obtained by applying a parallel composition to generalized series–parallel graphs $G_1(u_1, v_1)$ and $G_2(u_2, v_2)$. Then, for any $\alpha, \beta \in \{0, 3\}$, we have

1. $ME_{\alpha\beta}(G) = ME_{\alpha\beta}(G_1) \cup ME_{\alpha\beta}(G_2)$.
2. $ME_{\alpha 1}(G) = \min\{ME_{\alpha 1}(G_1) \cup ME_{\alpha 3}(G_2), ME_{\alpha 3}(G_1) \cup ME_{\alpha 1}(G_2)\}$.
3. $ME_{1\beta}(G) = \min\{ME_{1\beta}(G_1) \cup ME_{3\beta}(G_2), ME_{3\beta}(G_1) \cup ME_{1\beta}(G_2)\}$.
4. $ME_{11}(G) = \min \begin{cases} ME_{11}(G_1) \cup ME_{33}(G_2), \\ ME_{13}(G_1) \cup ME_{31}(G_2), \\ ME_{31}(G_1) \cup ME_{13}(G_2), \\ ME_{33}(G_1) \cup ME_{11}(G_2), \end{cases}$

The weighted efficient edge domination problem on generalized series–parallel graphs can be solved using the following Algorithm EEDP-GSP, which is similar to Algorithm PEDP-GSP of the previous subsection and runs in linear time.
Hence, we have the following two theorems immediately.

Theorem 5: Algorithm EEDP-GSP finds a minimum weighted efficient edge dominating set of a generalized series–parallel graph in $O(|V| + |E|)$ time[1].

Theorem 6: The weighted efficient domination problem can be solved in linear time for generalized series–parallel graphs.

Algorithm EEDP-GSP:
Input: A generalized series–parallel graph G.
Output: A minimum weighted efficient edge dominating set D of G.
Step 1:
` Construct a parse tree PT(G) of G,
Step 2:
for each leave $K_2(u, v)$ of PT(G) **do** /* **Initialization** */
$ME_{11}(K_2) = \{(u, v)\}$, $ME_{03}(K_2) = ME_{30}(K_2) = \emptyset$;
$ME_{13}(K_2) = ME_{31}(K_2) = ME_{33}(K_2) = \Phi$;
Mark (u, v);
Step 3:
while all nodes of PT(G) are not marked **do**
Choose an unmarked node i of PT(G) whose children are marked;
Let G_i be the corresponding subgraph of node i;
case 1: Node i is labeled as S_1 **then**
Compute all $ME_{\alpha\beta}(G_i)$ by Lemma 1, where $\alpha, \beta \in \{0, 1, 3\}$;
end case
case 2: Node i is labeled as S_2 **then**
Compute all $ME_{\alpha\beta}(G_i)$ by Lemma 2, where $\alpha, \beta \in \{0, 1, 3\}$;
end case
case 3: Node i is labeled as P **then**
Compute all $ME_{\alpha\beta}(G_i)$ by Lemma 3, where $\alpha, \beta \in \{0, 1, 3\}$;
end case
Mark i,
end while
Step 4:
if $\min\{ME_{\alpha\beta}(G) \mid \alpha, \beta \in \{0, 1\}\} \neq \Phi$ **then**
$D = \min\{ME_{\alpha\beta}(G) \mid \alpha, \beta \in \{0, 1\}\}$;
else G has no efficient edge dominating set.

Conclusion: We showed that the perfect edge domination problem on bipartite graphs and the efficient edge domination problem on planar bipartite graphs are NP-complete. Using the structures of parse trees, we give linear-time algorithms to solve the weighted perfect and efficient edge domination problems on generalized series–parallel graphs.

References:

1. Chin Lung Lua, Ming-Tat Koa , Chuan Yi Tangb, Perfect edge domination and efficient edge domination in graphs, Discrete Applied Mathematics 119 (2002) 227–250
2. Miranca Fischermann and Lutz Volkmann, Unique minimum domination in trees, Australasian Journal of Combinatorics 25(2002), pp.117–124
3. M.H.Muddebihal ans A.R.Sedamkar, Characterizations of Trees with Equal end edge Domination, Independent edge Domination and Connected edge Domination numbers, Subject classification numbers: AMS-05C69, C70.

***

CONNECTED DOMATIC NUMBER OF A GRAPH

R.Malathi
Asst.Prof.of Mathematics, SCSVMV, Kanchipuram, Tamilnadu
Balamurugan.D
M.Phil Scholar, SCSVMV, Kanchipuram, Tamilnadu

Abstract: In this paper, we will discuss about the definitions and basic concepts of graph theory along with some applications. Through, a series of applications, we will also present several different types of dominating sets. We also describe about the bounds for the domination number $\gamma(G)$.We also discuss some properties about the connected domatic number and give some bounds for the parameters. And we will also see the dominating set for connected graph & disconnected graph.

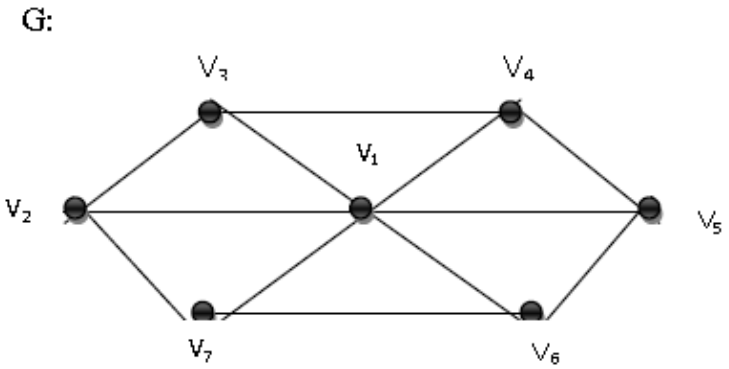
Keywords: Multiple Edges, Complete Bipartite Graph, Domatic Number.

Introduction: In this chapter, we discuss some properties about the connected domatic number and give some bounds for this parameter [2]. Throughout this chapter we consider only finite connected graphs without loops and multiple edges.

The connected domatic number of a graph is well defined only for connected graphs; in a disconnected graph there exists no connected dominating set and thus no connected domatic partition, while in every connected graph there exists at least one connected domatic partition, namely that which consists of one class.

Definition: A connected domatic partition of a graph G is a pertition of V(G), all of whose classes are connected dominating sets of G. The maximum number of classes of a connected domatic partition of G is called the **connected domatic number** of G and is denoted by $d_C(G)$.

Example: The connected domatic number of the following graph G is obtained as follows.



Figure

Here $\{\{v_1\}, \{v_2, v_3, v_4, v_5, v_6, v_7\}\}$ is a maximum connected domatic partition of G. Hence the connected domatic number $d_C(G) = 2$.

Remark: The following results can be easily seen.
i) For any complete graph K_n , $d_C(K_n) = n$.
ii) For any tree T, $d_C(T) = 1$, so that $d_C(K_{1,n-1}) = 1$.

iii) For any path P_n on n vertices,

$d_c(P_n)$ = 2, if n = 2

1, otherwise.

iv) For any cycle C_n of length n,

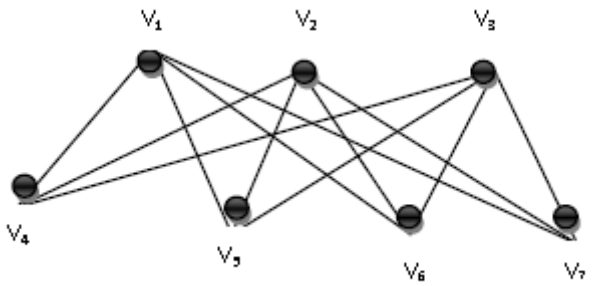
3, if n = 3

$d_c(C_n)$ = 2, if n = 4

1, otherwise.

v) For any complete bipartite graph $K_{r,s}$ $d_c(K_{r,s})$ = min {r, s}, r, s ≥2.

Example: Consider the complete bipartite graph $K_{3,4}$ given in Figure 3.2



Figure

Here {{v_1, v_4}, {v_2, v_5}, {v_3, v6, v_7}} is a maximum connected domatic partition. Hence the connected domatic number $d_c(K_{3,4})$ =3.

Lemma: Let G be a connected graph which is not a complete graph, let R be its vertex cut, let S be its connected dominating set. Then S∩R ≠ ∅.

Proof: Let G' = G – R and let C_1, C_2 … ,C_t be the connected components of the sub graph G' of G. It is clear that t ≥ 2.

Suppose S∩R = ∅. As the sub graph of G induced by S is connected, it is a sub graph of C_i for some i ∈ {1,2 … , t}. Let x ∈ Cj for j ≠i. Then x ∉ S and x has no neighbour in S, which is a contradiction.

Hence S ∩ R ≠ ∅.

Theorem: Let G be a connected graph which is not complete, let $d_c(G)$ be its connected domatic number, let k(G) be its vertex connectivity number. Then $d_c(G) \leq k(G)$.

Proof: Let R be a vertex cut of G of the cardinality k(G) and let {V_1, V_2 …., V_d }be a connected domatic partition of G having d = $d_c(G)$ classes. By Lemma, we have $V_i \cap R \neq \emptyset$ for i = 1,2, …, d. Since V_1, V_2, …, V_d are pair wise disjoint,

the sets $V_1 \cap R$, $V_2 \cap R$,…,$V_d \cap R$ are also pair wise disjoint.

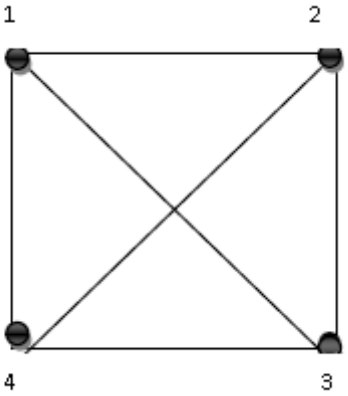
Therefore, d = $d_c(G) \leq R = K(G)$

$d_c(G) \leq k(G)$.

Remark: For complete graph, the above theorem is not true, since $d_c(K_n) = n$ but $k(K_n) = n-1$.

Example: The following graph in Figure illustrates the above result.

K_4:



In the above graph, $d_C(K_4) = \{\{1\},\{2\},\{3\},\{4\}\}$ but $k(K_n)=n-1= 4-1=3$.

Theorem: For an arbitrary positive integer q there exists a graph G such that $d(G) - d_C(G) = q$.

Proof: Let G' be a complete graph with vertices u, v, ... , v_q' Let G'' be a complete graph with vertices u, v'', ...,v_q''. The vertices u, v', ... , v_q',v'', ...,v_q''. are pair wise distinct and the vertex u is common to both G' and G'' Let G be the union of G' and G''. The set {u} is a vertex cut of G, therefore k (G) =1 and by Theorem 3.1, $d_C(G) = 1$. It is clear that $\{\{u\}, \{v', v''\}, ..., \{v_q', v_q''\}\}$ is the maximum domatic partition of G. Therefore the domatic number d(G) = q+1. Hence $d(G) - d_C(G) = q$.

Theorem: Let G be a connected graph and let n_o be the number of vertices of degree n – 1. Then

$$d_c(G) \le \frac{1}{2}(n + n_0)$$

Theorem: Let G be a connected graph with at least three vertices. Let e = uv be an edge of G which is not a bridge. Let G'= G–e. If deg u = deg v = n–1 in G then $d_C(G') \ge d_C(G)-2$, otherwise $d_C(G') \ge d_C(G) - 1$.

Theorem: Let G be a graph. Then $d_C(G) \le \delta(G) + 1$.

Corollary: If the domination number of graph G, $\gamma(G) \ge 2$ then $d_C(G) \le \delta(G)$.

Definition: A graph G is called **connected domatically full** if $d_C(G) = \delta(G)+1$.

Example: Any complete graph is connected domatically full graph.

Theorem: Let G be a graph such that both G and G are connected. Then $d_C(G) = d_C(G) \le n-1$.

Theorem: For any connected graph G with n vertices $\gamma_C(G) + d_C(G) \le n+1$ with equality if and only if G is complete.

Theorem: For any connected graph G with n vertices, $\gamma_C(G) . d_C(G) \le n$.

Definition: A connected graph G is said to be connected domatically critical, if $d_C(G-e) < d_C(G)$ for any edge e in G.

Theorem: Let G be a connected domatically critical graph, let $d_C(G) = d$. Then the vertex set of G is the union of pair wise disjoint sets $V_1, V_2, \ldots, V_d$ such that
i) the sub graph G_i of G induced by V_i is a tree for each i = 1, 2, ..., d.
ii) the sub graph G_{ij} of G with the vertex set $V_i \cup V_j$ and with the edge set consisting of all edges joining a vertex of V_i with a vertex of V_j is a forest, each of whose connected components is a star or a complete graph with two vertices for any i.j from the set {1,2 ... , d} i≠j.

Theorem: Let G be a connected domatically critical graph with $d_C(G) = d$. If G is regular of degree d–1, then G is isomorphic to K_d. If G is regular of degree d, then G_i is K_2 for each $i \in \{1,2 \ldots, d\}$ and G_{ij} consists of two connected components isomorphic to K_2 for any i,j from {1, 2, ..., d), i≠j.

Conclusion: In general, when studying subsets of a given type, we are interested in finding either a smallest or a largest such set in a graph. For instance, one considers such problems as finding the minimum cardinality of a dominating set or a cover or finding the maximum cardinality of an independent set or packing. In this dissertation, we described bounds for the domination number $\gamma(G)$.

References:

1. K.Appel and W. Hankin, "Every planar map is 4-colorable," Bulletin of the AMS, Volume 82 (1976), 711-712.
2. Beck, M. Bleicher and D. Crowe, Excursion into Mathematics, Worth Publishers, 1969 (ISBN 0-87901-004-5
3. N.Biggs, E. Lloyd, and R. Wilson, Graph Theory *1736-1936,* Clarendon Press Oxford, 1976 (ISBN 0-19-853901-0).
4. E.B.Dynkins and V. A. Uspenskii, Multicolor Problems, D.C.Heath and Company, Boston, 1963.
5. L.Euler, "Solutio Problematis Ad geometriam Situs Pertinentis," Commenrarii Academiae Scientiarum Imperialis Petropolitanae 8 (1736), pp. 128-140. O. Ore, The Four Color Problem, Academic Press, New York 1967.
6. K.H.Rosen, Discrete Mathematics and its Applications, Random House, NY, 1988. (ISBN 0-394-36768-5, QA39.2 R654)
7. L.Steen editor, For All Practical Purposes: Introduction to Contemporary Mathematics 3ed. W. H. Freeman and Company, New York 1994. (ISBN 0-7167-2378-6, QA7.F68 1994).

***

UNIQUE MINIMUM EDGE DOMINATION IN TREES

R.Malathi
Asst. Prof. of Mathematics, SCSVMV, Kanchipuram, Tamilnadu
Bangarappa.G
M.Phil Scholar, SCSVMV, Kanchipuram, Tamilnadu

Abstract: For any graph G and any edge e ∈ E(G) we define N′(e) = {f ∈ E(G) | f adjacent to e} and the set N′ [e] = N′ (e) ∪ {e}. If B ⊆ E(G), then N′ (B) = ∪∉e ∈ B N′ (e) and N′ [B] = N′ (B) ∪ B. For a subset F of E(G) and an edge e ∈ F we define the set P′ (e, F) = N′ [e] \N′ [F \{e}],
and we call an edge f ∈ P′ (e, F) a private adjacent edge of e with regard to F. Further, we give a characterization of trees with unique minimum edge dominating sets.

Keywords: Edge dominating set, unique minimum edge dominating set and component.

Introduction:

Lemma: Let G be a connected graph of order at least 3 and let F be a unique minimum edge dominating set of G. Then the set F is independent, and every edge e ∈ F contains at least two non adjacent edges in P′ (e, F).

Proof: Let e ∈ F be arbitrary. Since F is minimal, we have

$$P'(e, F) \neq \emptyset.$$

If P′ (e, F) = {e}, then we can take any edge f adjacent to e and

$$(F \setminus \{e\}) \cup \{f\}$$

Is a minimum edge dominating set of G different from F, which is a contradiction.
If

$$f \in P'(e, F) \setminus \{e\} \neq \emptyset$$

and every edge in P′ (e, F) \ {f} is adjacent to f, then again

$$(F \setminus \{e\}) \cup \{f\}$$

is a minimum edge dominating set of G different from F, which is a contradiction.

Hence, for every edge e ∈ F the set P′ (e, F) contains two non adjacent edges. This also implies that no two edges in F are adjacent.

The next theorem is a characterization of trees with unique minimum edge dominating sets similar to the characterization in Corollary. One part of this theorem says that, for trees, the necessary condition in Lemma is also sufficient. The converse does not hold in general, as we can see with the simple graph G with vertex set

$$V(G) = \{u, v, w, x\},$$

edge set

$$E(G) = \{uv, uw, ux, vw\}$$

and with the two minimum edge dominating sets {uv} and {uw}.

Theorem: Let T be a tree of order at least 3 and let F be a subset of E(T).
Then the following conditions are equivalent:

1. F is the unique minimum edge dominating set of T.
2. F is an edge dominating set of T such that every edge e in F has at least two non adjacent edges in P′ (e, F).
3. F is an independent edge dominating set of T such that every edge e in F has at least two non adjacent edges in P′ (e, F).
4. F is a minimum edge dominating set of T such that γ′ (T –e) > γ′ (T) for every edge E ∈ F.

Proof:

(i) ⇒ (iii):

Follows immediately from Lemma.

(iii) ⇒ (ii):

Obviously.

(ii) ⇒ (i):

Let F be an edge dominating set of T as in (ii).

For any subset B of the edge set of T we define

$$V(B) = \{u, u' \in V(T) \mid uu' \in B\}.$$

Thus, for every edge $e = vw \in F$ there are two edges vv' and ww' with

$$v' \neq w' \text{ and } v, v', w, w' \notin V(F \setminus \{e\}).$$

Hence, no two edges in F are adjacent. Suppose there is a minimum edge dominating set $F' \neq F$ of T.

Then,

$$|F \setminus F'| \geq |F' \setminus F|.$$

Let the set

$$B = (F \setminus F') \cup (F' \setminus F)$$

and

$$H = T[V(B)].$$

Let

$$F_{1'} = \{vw \in F' \setminus F \mid v,w \in V(F \setminus F')\},$$
$$F_{2'} = \{vw \in F' \setminus F \mid |\{v,w\} \cap V(F \setminus F')| = 1\},$$

and

$$F_{3'} = \{vw \in F' \setminus F \mid v,w \notin V(F \setminus F')\}.$$

The set $F' \setminus F$ is the disjoint union of $F_{1'}$, $F_{2'}$ and $F_{3'}$. We get for the vertex set of H

$$|V(H)| = |V(B)| \leq 2|F \setminus F'| + |F_{2'}| + 2|F_{3'}|.$$

By (ii), for every vertex $v \in V(F \setminus F')$ there is an edge $vw \in F \setminus F'$ and an edge $vv' \neq vw$ such that $v, v' \notin V(F \setminus \{e\})$.

Since F′ is an edge dominating set of T, we get that v or v′ is in V (F′).

If

$$v \in (V(F) \setminus V(F')) \subseteq V(F \setminus F'),$$

then

$$v' \in (V(F') \setminus V(F)) \subseteq V(F' \setminus F)$$

and

$$vv' \in E(H) \setminus B.$$

This implies that

$$|E(H) \setminus B| \geq |V(F) \setminus V(F')| \geq 2|F \setminus F'| - 2|F_{1'}| - |F_{2'}|.$$

Hence, we obtain for the cardinality of E(H)

$$\begin{aligned} |E(H)| &= |F \setminus F'| + |F' \setminus F| + |E(H) \setminus B| \\ &\geq 2|F' \setminus F| + (2|F \setminus F'| - 2|F_{1'}| - |F_{2'}|) \\ &= 2(|F_{1'}| + |F_{2'}| + |F_{3'}|) + (2|F \setminus F'| - 2|F1'| - |F_{2'}|) \\ &= |F_{2'}| + 2|F_{3'}| + 2|F \setminus F'| \\ &\geq |V(H)|. \end{aligned}$$

But, since H is a forest, we have

$m(H) = n(H) - \kappa(H) < n(H)$, which is a contradiction.

(i) ⇒ (iv):

Let F be the unique minimum edge dominating set of T,

let

$$e = v_1v_2 \in F$$

be arbitrary, and let T_1 and T_2 be the components of $T - e$ where $v_i \in V(T_i)$ forest $i = 1, 2$.

Further, let F′ be a minimum edge dominating set of $T - e$ and for $i = 1, 2$

let

$$F_i = F \cap E(T_i)$$

and

$$F_{i'} = F' \cap E(T_i).$$

By (i) ⇒ (ii), the edge e is adjacent to at least two edges $v_1w_1 \in E(T_1)$ and $v_2w_2 \in E(T_2)$ that are not adjacent to any other edge in F. Hence, the set F_i is not an edge dominating set of Ti, contrary to $F_{i'}$ for i ∈ {1, 2}.

Thus, we have $F_i \neq F_{i'}$ for i = 1, 2.

Since the set

$$F_{i''} = (F \setminus F_i) \cup F_{i'} \neq F$$

is an edge dominating set of T, we get $|F_i| < |F_{i'}|$.

This yields

$$\gamma'(T - e) = |F'| = |F_{1'}| + |F_{2'}| \geq |F_1| + |F_2| + 2 = |F| + 1 > \gamma'(T).$$

(iv) ⇒ (i):

Let F be a minimum edge dominating set of T such that

$$\gamma'(T - e) > \gamma'(T)$$

for every edge e ∈ F.

Suppose that there is a minimum edge dominating set F′ ≠ F of T. There exists at least one edge e ∈ F \F′ and the set F′ is an edge dominating set of T –e.

Hence,

$$\gamma'(T - e) \leq |F'| = \gamma'(T)$$

for some e ∈ F, which is a contradiction.

Corollary: Let T be a tree of diameter at least 3, let F be a minimum edge dominating set of T, and let e ∈ F arbitrary. Then F is the unique minimum edge dominating set of T if and only if every component of the forest H = T –N_[e] is of order at least 4 and H has the unique minimum edge dominating set F \ {e}.

Proof: Let F be a minimum edge dominating set of T and let e ∈ F be arbitrary.

First, let F be unique.

Hence F fulfils (ii) in Theorem, and this implies that F \ {e} fulfils (ii) for the forest H.

Thus each component of H is of order at least 4. If we use Theorem on these components, then we get that H has the unique minimum edge dominating set F \{e}.

Now, let F \{e} be the unique edge dominating set of H and every component of H be of order at least 4. By Theorem, the set F \{e} fulfils (ii). This implies that F fulfils (ii) for T.

Thus F is unique, by Theorem.

Conclusion: We present a linear time algorithm for finding a minimum edge dominating set of a block graph. Finally we given a characterization of trees with unique minimum distance domination sets, and trees with unique minimum edge domination sets.

References:

1. K.Appel and W. Hankin, "Every planar map is 4-colorable," Bulletin of the AMS, Volume 82 (1976), 711-712.
2. Beck, M. Bleicher and D. Crowe, Excursion into Mathematics, Worth Publishers, 1969 (ISBN 0-87901-004-5
3. N.Biggs, E. Lloyd, and R. Wilson, Graph Theory 1736-1936, Clarendon Press Oxford, 1976 (ISBN 0-19-853901-0).
4. E.B.Dynkins and V.A.Uspenskii, Multicolor Problems, D. C. Heath and Company, Boston, 1963.
5. L.Euler, "Solutio Problematis and geometriam Situs Pertinentis," Commenrarii Academiae Scientiarum Imperialis Petropolitanae 8 (1736), pp. 128-140. O.Ore, The Four Color Problem, Academic Press, New York 1967.
6. K. H. Rosen, Discrete Mathematics and its Applications, Random House, NY, 1988. (ISBN 0-394-36768-5, QA39.2 R654)
7. L.Steen editor, For All Practical Purposes: Introduction to Contemporary Mathematics 3ed. W.H.Freeman and Company, New York 1994. (ISBN 0-7167-2378-6, QA7.F68 1994).

***

PROTEIN SIMILARITY / DISSIMILARITY STUDY USING MOMENT VECTOR BY NON-HOMOLOGOUS METHOD

D. Vijayalakshmi
Assistant Professor, Department of Mathematics
Sri Chandrasekharendra Saraswathi Viswa Mahavidyalaya,Kanchipuram, Tamilnadu
S. Hemalatha
M. Phil Scholar ,Department of Mathematics
Sri Chandrasekharendra Saraswathi Viswa Mahavidyalaya,Kanchipuram, Tamilnadu

Abstract: Similarity / Dissimilarity of protein is measured using moment vector. The moment vector is constructed in a novel way by using physic-chemical properties of amino acids. Moment vector upto four dimensions are constructed. Euclidean distance between the moment vectors of each pair of protein measures the similarity between proteins.

Keywords: Protein Sequence, Sequence Similarity, Moment Vector.

1. Introduction: Development of sequencing techniques have increased the number of biological sequences in the data bases. Extracting the potential information from these sequences proves to be a challenging task. Extracting the information is essential as they determine the barer for the physicology and anatomy study of organisms. This study can be done by homologous method and non-homologous method.

Some non-homologous method Yao [1] studied the protein sequence based on pk_a value of COOH and NH_3^+ of 20 amino acids graphically. Xiao and Wu[2] represented protein in a 2-D graph based on physicochemical properties Liao et al [3] calculated the similarity or dissimilarity using distance formula and also represented protein sequence in a 2-D graph. Randic [4] represented protein in 2-D graph using the physicochemical property to study the similarity. Feng & Zhang [5] represented protein as Z_p-curve using hydrophobicity of amino acids. Bai and Wang [6] studied protein by 2-D graph using nucleotide triplet codons. Based on 3 physicochemical properties Abo el Maaty et al [7] represented protein in a 3-D graphical method. Yao [8] developed a graphical method to study about protein based on the Pk_a values of COOH and NH_3^+ of a amino acids. Also Xiao and Wu [9] studied protein in 2 dimensional graph using the physicochemical properties. In [10], Liao et al measures the similarity and dissimilarities between proteins using distance formula and also developed a new 2-D graphical representation. In this paper we present a novel moment vector using the primary structure of protein sequence. The moment vector of 4 dimension is obtained for each protein similarity/dissimilarity between protein sequences are measured using Euclidean distance between these moment vector of proteins.

2. Moment Vector: The primary structure of protein – the amino acid sequence plays a vital role in this part. PI_a and Kh values of the amino acids are considered as x and y co-ordinates of the amino acids. Then the moment vector of 1 – dimension is calculated using the formula.

$M_1 = X$

$X= \frac{\Sigma(xi-yi)^1}{n^1}$ where n is the number of amino acids in the sequence.

The moment vector (X, Y) of 2-dimension is calculated using the formula

$M_2 = (X, Y)$, $X= \frac{\Sigma(xi-yi)^1}{n^1}$, $Y= \frac{\Sigma(xi-yi)^2}{n^2}$

The moment vector (X,Y,Z) of 3-dimension is calculated using the formula

M_3=(X,Y,Z) $X=\frac{\Sigma(xi-yi)^1}{n^1}$, $Y=\frac{\Sigma(xi-yi)^2}{n^2}$, $Z=\frac{\Sigma(xi-yi)^3}{n^3}$

M_4=(X,Y,Z,S) $X=\frac{\Sigma(xi-yi)^1}{n^1}$, $Y=\frac{\Sigma(xi-yi)^2}{n^2}$, $Z=\frac{\Sigma(xi-yi)^3}{n^3}$, $S=\frac{\Sigma(xi-yi)^4}{n^4}$

The Euclidean distance between moment vectors of each pair of proteins are calculated. This Euclidean distance measures the similarity between protein.

Data Used:

Protein ID	Protein Structure	Protein Description
4fc1		TTCCPSIVARSNFNVCRLPGTPEALCATYTGCIIIPGATCPGDYAN
3ue7		TTCCPSIVARSNXNACRLPGTPEALCATYTGCIIIPGATCPGDYAN
3nir		TTCCPSIVARSNFNVCRLPGTPEALCATYTGCIIIPGATCPGDYAN
2eyb		TTCCPSIVARSNFNVCRLPGTPEALCATYTGCIIIPGATCPGDYAN
2eyc		TTCCPSIVARSNFNVCRLPGTPEALCATYTGCIIIPGATCPGDYAN
2eyd		TTCCPSIVARSNFNVCRLPGTPEALCATYTGCIIIPGATCPGDYAN
1yv8		TTCCPSIVARSNFNVCRLPGTPEALCATYTGCIIIPGATCPGDYAN
1yva		TTCCPSIVARSNFNVCRLPGTPEALCATYTGCIIIPGATCPGDYAN
1cxr		TTCCPSIVARSNFNVCRLPGTSEAICATYTGCIIIPGATCPGDYAN
1cnr		TTCCPSIVARSNFNVCRLPGTPEALCATYTGCIIIPGATCPGDYAN

Moment Vector:

	Protein-1 (4FC1)	Protein-2 (3UE7)	Euclidean distance
One dimension	X= 5.510652	X=5.524783	0.014130435
Two dimension	X= 5.510652	X=5.524783	0.022164611
	Y=0.872683696	Y=0.855607372	
Three dimension	X= 5.510652	X=5.524783	0.024536339
	Y=0.872683696	Y=0.855607372	
	Z=0.170296821	Z=0.159772471	
Four dimension	X= 5.510652	X=5.524783	0.024968447
	Y=0.872683696	Y=0.855607372	
	Z=0.170296821	Z=0.159772471	
	S=0.039524883	Z=0.034899799	

	Protein-1 (4FC1)	Protein-3 (3NIR)	Euclidean distance
One dimension	X= 5.510652	X= 5.510652	0
Two dimension	X= 5.510652	X= 5.510652	0
	Y=0.872683696	Y=0.872683696	
Three dimension	X= 5.510652	X= 5.510652	0
	Y=0.872683696	Y=0.872683696	
	Z=0.170296821	Z=0.170296821	
Four dimension	X= 5.510652	X= 5.510652	0
	Y=0.872683696	Y=0.872683696	
	Z=0.170296821	Z=0.170296821	
	S=0.039524883	S=0.039524883	

	Protein-2 (3UE7)	Protein-3 (3NIR)	Euclidean Distance
One dimension	X=5.524783	X= 5.510652	0.014130435
Two dimension	X=5.524783	X= 5.510652	0.022164611
	Y=0.855607372	Y=0.872683696	
Three dimension	X=5.524783	X= 5.510652	0.024536339
	Y=0.855607372	Y=0.872683696	
	Z=0.159772471	Z=0.170296821	
Four dimension	X=5.524783	X= 5.510652	0.024968447
	Y=0.855607372	Y=0.872683696	
	Z=0.159772471	Z=0.170296821	
	Z=0.034899799	S=0.039524883	

Result:

Table 1: Result using M1

	PRO 2	PRO 3	PRO 4	PRO 5	PRO 6	PRO 7	PRO 8	PRO 9	PRO 10
PRO 1	0.014130435	0	0	0	0	0	0	0.045217391	0
PRO 2		0.014130435	0.014130435	0.014130435	0.014130435	0.014130435	0.014130435	0.059347826	0.014130435
PRO 3			0	0	0	0	0	0.045217391	0
PRO 4				0	0	0	0	0.045217391	0
PRO 5					0	0	0	0.045217391	0
PRO 6						0	0	0.045217391	0
PRO 7							0	0.045217391	0
PRO 8								0.045217391	0
PRO 9									0.045217391

Table 2: Result using M2

	PRO 2	PRO 3	PRO 4	PRO 5	PRO 6	PRO 7	PRO 8	PRO 9	PRO 10
PRO 1	0.022134611	0	0	0	0	0	0	0.046494459	0
PRO 2		0.022134611	0.022134611	0.022134611	0.022134611	0.022134611	0.022134611	0.059677638	0.022134611
PRO 3			0	0	0	0	0	0.046494459	0
PRO 4				0	0	0	0	0.046494459	0
PRO 5					0	0	0	0.046494459	0
PRO 6						0	0	0.046494459	0
PRO 7							0	0.046494459	0
PRO 8								0.046494459	0
PRO 9									0.04649459

Table 3: Result using M3

	PRO 2	PRO 3	PRO 4	PRO 5	PRO 6	PRO 7	PRO 8	PRO 9	PRO 10
PRO 1	0.024536339	0	0	0	0	0	0	0.046553565	0
PRO 2		0.024536339	0.024536339	0.024536339	0.024536339	0.024536339	0.024536339	0.060234645	0.024536339
PRO 3			0	0	0	0	0	0.046553565	0
PRO 4				0	0	0	0	0.046553565	0
PRO 5					0	0	0	0.046553565	0
PRO 6						0	0	0.046553565	0
PRO 7							0	0.046553565	0
PRO 8								0.046553565	0
PRO 9									0.046553565

Table 4: Result using M4

	PRO 2	PRO 3	PRO 4	PRO 5	PRO 6	PRO 7	PRO 8	PRO 9	PRO 10
PRO 1	0.024968447	0	0	0	0	0	0	0.046556042	0
PRO 2		0.024968447	0.024968447	0.024968447	0.024968447	0.024968447	0.024968447	0.060377089	0.024968447
PRO 3			0	0	0	0	0	0.046556042	0
PRO 4				0	0	0	0	0.046556042	0
PRO 5					0	0	0	0.046556042	0
PRO 6						0	0	0.046556042	0
PRO 7							0	0.046556042	0
PRO 8								0.046556042	0
PRO 9									0.046556042

Conclusion: The similarity / dissimilarity of protein is studied using non-homologous moment vector. This is a novel method of constructing moment vector using physicochemical properties of amino acids. This method yields a result close to the results obtained by Blast sequence site. This also shows that as the dimensions of moment vector increase the accuracy of result obtained also increase.

References:

1. Yao YH, Dai Q, Li C, He PA Nan XY, Zhang YZ. Analysis of similarity / Dissimilarity of protein sequences. Proteins 2008;73:864-871.

2. Wu ZC, Xiao X, Chou KC. 2D-MH. A web server for generating graphic representation of protein sequence based on the physicochemical properties of their constituent amino acids. J.Theor, Biol.2010 267:29-34
3. Liao B, Liao B Y, sum XM, Zeng QG. A novel method for similarity analysis and protein subcellular localization prediction. Bioinformatics 2010; 20 : 2678 – 2683.
4. Randic M. 2D – graphical representation of protein based on physicochemical properties of amino acids, chemical Physics Letter 2007; 444 176 – 180
5. Z.P.Feng and C.T. Zhang, "A graphic representation of protein sequence and predicting the subcellulae locations of prokaryotic proteins. "International journal of Biochemistry and cell biology, Vol 34, No 3 . pp. 298 – 207, 2002
6. F. Bai and T. Wang "A 2-D graphical representation of protein sequence based on nucleotide triplet codons". Chemical Physics letters . vol 413 no: 4-6. pp 458-462, 2005
7. M.I. Abo el Maaty M.M.Abo Elkhier and M.A.Abd Elwahaab, "3D graphical representation of protein sequences and their statistical characterization". Physical A : Statistical Mechanics and its applications vol. 389 no 21 PP 4668 – 4676 2010.
8. Yao YH, Dai Q, Lic, He PA, Nan XY, Zhang YZ. Analysis of similarity / dissimilarity of protein sequences. Proteins 2008; 73: 864 – 871.
9. WuZC, Xiao X, Chou KC, 2D – MH; A Web server for generating graphic representation of protein sequences based on the physicochemical properties of their constituent amino acids. J. Theor boil 2010 ; 267 : 29 – 34.
10. Liao B, Liao BY, Sun XM, Zeng QG. A novel method for similarity analysis and protein subcellular localization prediction. Bioinformatics 2010. 26 : 2678 – 2683.

***

COMPARATIVE ANALYSIS OF METHODS FOR PROTEIN SIMILARITY AND DISSIMILARITY STUDY USING GRAPHICAL REPRESENTATION

D. Vijayalakshmi
Assistant Professor, Department of Mathematics
Sri Chandrasekharendra Saraswathi Viswa Mahavidyalaya,Kanchipuram,Tamilnadu
T.Anantharaj
M. Phil Scholar,Department of Mathematics
Sri Chandrasekharendra Saraswathi Viswa Mahavidyalaya,Kanchipuram,Tamilnadu

Abstract: Two different analytical methods of protein similarity/dissimilarity study (i) magic circle approach and (ii) physico-chemical properties of amino acids were compared in this study. Both the methods offer graphical and numerical characterization of individual protein. In the magic circle method protein representation are constructed in the interior of the unit circle and on the circumference the 20 amino acids are positioned at equal distances. In physico-chemical properties based method the graphical representation of proteins is established on 2D map of amino acids. The amino acid map is obtained by constructing the partial order on a selected pair of physico-chemical properties of amino acids. We apply these two approaches on four different cycloviolacin protein sequence data and we find that both methods yields almost same percentage of similar and dissimilar residues in the compared set of proteins.

Introduction: Sequence analysis plays an important role in protein structure prediction.Proteins with similar sequence mostly have similar structures [1]. Usual representation of protein sequence is alphabetic representation which is called as LSR.LSR represents any protein sequence by letter corresponding to the 20 amino acids. The 20 amino acids' letters are A,R,N,C,Q,E,G,I,L,K,M,F,P,S,T,W,Y, and V. As comparing the protein sequences by LSR is difficult many mathematical approaches were proposed to translate protein sequences from letters to 2D graphical representation along with mathematical objects.

Materials and Methods:

Test Data Set: Four different sequence of Cycloviolacin proteins are taken into consideration. The details are in Table1.

Table 1:

Accession no	Organism	Protein name	Sequence length
P82230	***Viola odorata*** (Sweet violet)	CYO1_VIOOD Cycloviolacin-O1	30
P85526	***Viola biflora*** (Yellow wood violet)	CYO2_VIOBI Cycloviolacin-O2	30
P58433	***Viola hederacea*** (Australian violet)	CYH1_VIOHE Cycloviolacin-H1	30
P85234	***Viola hederacea*** (Australian violet)	CYH4_VIOHE Cycloviolacin-H4	30

The protein sequences are as follows

1. CYO1_VIOOD Cycloviolacin-O1 GIPCAESCVYIPCTVTALLGCSCSNRVCYN
2. CYO2_VIOBI Cycloviolacin-O2 GIPCGESCVWIPCISSAIGCSCKSKVCYRN
3. CYH1_VIOHE Cycloviolacin-H1 GIPCGESCVYIPCLTSAIGCSCKSKVCYRN
4. CYH4_VIOHE Cycloviolacin-H4 GIPCAESCVWIPCTVTALLGCSCSNNVCY.

The two methods are applied to each pair of the four sequences and the results are analysed by graphical methods.

Method 1: Magic circle is a circle of unit radius. The 20 amino acids are uniformly distributed on the circumference of the circle. Based on the three letter code the amino acids were arranged alphabetically on the periphery of the circle. The coordinates of the amino acids are given by

$$x_i = \cos\left(\frac{2i\pi}{20}\right); y_i = \sin\left(\frac{2i\pi}{20}\right); i = 0-19$$

The numerical values of amino acids are in the Table2

Table 2

S.No	Amino Acid	Symbol	X	y
1	Alanine	A	1	0
2	Arginine	R	0.95106	0.30902
3	Aspargine	N	0.80902	0.58779
4	Aspartic acid	D	0.58779	0.80902
5	Cysteine	C	0.30902	0.95106
6	Glutamic acid	Q	0	1
7	Glutamine	E	-0.309	0.95106
8	Glycine	G	-0.5878	0.80902
9	Histidine	I	-0.809	0.58779
10	Isoleucine	H	-0.9511	0.30902
11	Leucine	L	-1	0
12	Lysine	K	-0.9511	-0.309
13	Methionine	M	-0.809	-0.5878
14	Phenyalanine	F	-0.5878	-0.809
15	Proline	P	-0.309	-0.9511
16	Serine	S	0	-1
17	Threonine	T	0.30902	-0.9511
18	Tryptophan	W	0.58779	-0.809
19	Tyrosine	Y	0.80902	-0.5878
20	Valine	V	0.95106	-0.309

For a given protein sequence, we start from the origin, moves towards the first amino acid in the sequence at the periphery of the circle and to stophalfway(ie) stopped at the midpoint between the origin and first amino acid co-ordinates.In the next step ,from that point we move towards the second amino acid in the sequence and againto stop half way. Exactly at the midpoint of the previous point obtained and the second amino acid co-ordinates. This process is continued till all the amino acids in the sequence are depicted. The successive points are connected and we get a zigzag curve which represents the protein sequence. This representation of protein preserves all information about protein.

The protein sequence can also be constructed from the complete information on x-y coordinates of amino acids in the sequence. We find the x and y co-ordinate of amino acids in the sequence from the known co-ordinate. We start with the first coordinate (x_1, y_1) .As we start from the origin

$$x_1 = \left(\frac{0 + x_{i,0}}{2} \right), y_1 = \left(\frac{0 + y_{i,0}}{2} \right),$$

where ($x_{i,o}$,$y_{i,o}$) represents the x and y co-ordinate of the first amino acid in the sequence .The second amino acid co-ordinates is obtained by

$$x_2 = \left(\frac{x_1 + x_{i,0}}{2} \right), y_2 = \left(\frac{y_1 + y_{i,0}}{2} \right)$$

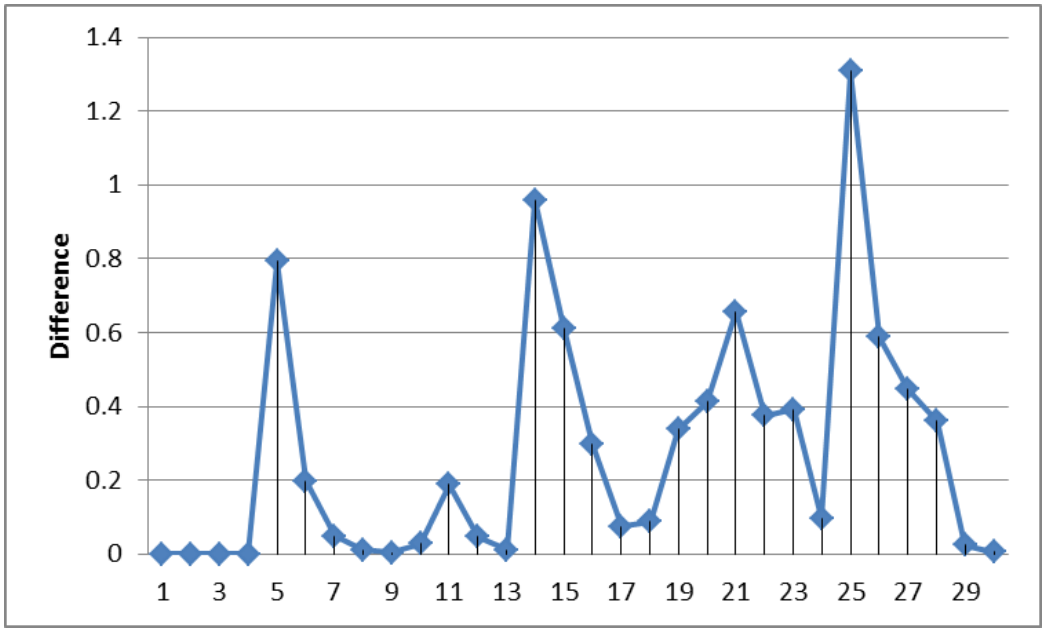
where ($x_{i,o}$,$y_{i,o}$) is the x and y co-ordinate of the second amino acid in the sequence. The process is continued for all the amino acids in the sequence. The (x,y) co-ordinates of the two sequences are obtained by the method mentioned earlier. The similarity between the two sequence is detected by calculating the Euclidean distance of the (x,y) co-ordinates of the corresponding amino acids in both sequences . Then the Euclidean distance is plotted as graph. The peaks in the graph represent dissimilarity and points along the slope shows similarity between two sequences.

Method 1: Magic Circle Method

Sequences CYO1_VIOOD Cycloviolacin-O1 and CYO2_VIOBI Cycloviolacin-O2

Protein-1	x1	y1	Protein-2	x2	y2	Difference
G	-0.2939	0.404509	G	-0.2939	0.404509	0
I	-0.55146	0.496147	I	-0.55146	0.496147	0
P	-0.43024	-0.22746	P	-0.43024	-0.22746	0
C	-0.06061	0.3618	C	-0.06061	0.3618	0
A	0.469695	0.1809	G	-0.3242	0.585409	0.793896
E	0.080337	0.565979	E	-0.31661	0.768233	0.198474
S	0.040169	-0.21701	S	-0.15831	-0.11588	0.049619
C	0.174593	0.367023	C	0.075356	0.417587	0.012405
V	0.562824	0.029002	V	0.513206	0.054283	0.003101
Y	0.685921	-0.27939	W	0.550495	-0.37737	0.027939
I	0.302509	0.154195	I	-0.12926	0.105208	0.188826
P	-0.00326	-0.39843	P	-0.21914	-0.42293	0.047207
C	0.152881	0.276312	C	0.044938	0.264066	0.011802
T	0.230949	-0.33737	I	-0.38204	0.425925	0.958382
V	0.591002	-0.3232	S	-0.19102	-0.28704	0.612867
T	0.45001	-0.63713	S	-0.09551	-0.64352	0.297633
A	0.725005	-0.31856	A	0.452245	-0.32176	0.074408
L	-0.1375	-0.15928	I	-0.17839	0.133013	0.087108
L	-0.56875	-0.07964	G	-0.38309	0.471015	0.337692
G	-0.57827	0.364688	C	-0.03704	0.711036	0.412891
C	-0.13463	0.657872	S	-0.01852	-0.14448	0.657254
S	-0.06731	-0.17106	C	0.14525	0.403287	0.375062
C	0.120852	0.389997	K	-0.40291	0.047134	0.391877
S	0.060426	-0.305	S	-0.20145	-0.47643	0.097969
N	0.434721	0.141392	K	-0.57626	-0.39273	1.307358
R	0.692889	0.225204	V	0.1874	-0.35087	0.587385
V	0.821973	-0.04191	C	0.248208	0.300092	0.446169
C	0.565495	0.454575	Y	0.528613	-0.14385	0.359471
Y	0.687256	-0.06661	R	0.739835	0.082584	0.025023
N	0.748136	0.260589	N	0.774426	0.335184	0.006256

Graphical Representation



Method 2: In this method the amino acids are ordered based on their physico chemical properties. This offers better insights into comparative study of proteins. Two meaningfully related properties of amino acids are considered. The considered properties are either structurally or functionally related to each other. For instance, molecular surface and molecular volume or solubilities in different media are some properties of amino acids related to each other.

Here we consider pKa values for terminal amino acids groups NH_3^+ and COOH which determine the activity of enzymes. The pKa values listed in Table 3.

Amino acid	Symbol	pKaCOOH	pKaNH3
Small Hydrophilic			
Glycine	G	2.34	9.6
Alanine	A	2.34	9.69
Threonine	T	2.63	10.43
Serine	S	2.21	9.15
Proline	P	1.99	10.6
Small Hydrophobic			
Valine	V	2.32	9.62
Leucine	L	2.36	9.6
Isoleucine	I	2.36	9.68
Methionine	M	2.28	9.21
Aromatic			
Phenyalanine	F	1.83	9.13
Tyrosine	Y	2.2	9.11
Tryptophan	W	2.38	9.39
Acids And Their Amides			
Aspartic acid	D	2.09	9.82
Glutamic acid	E	2.19	9.67
Aspargine	N	2.02	8.8
Glutamine	Q	2.17	9.13

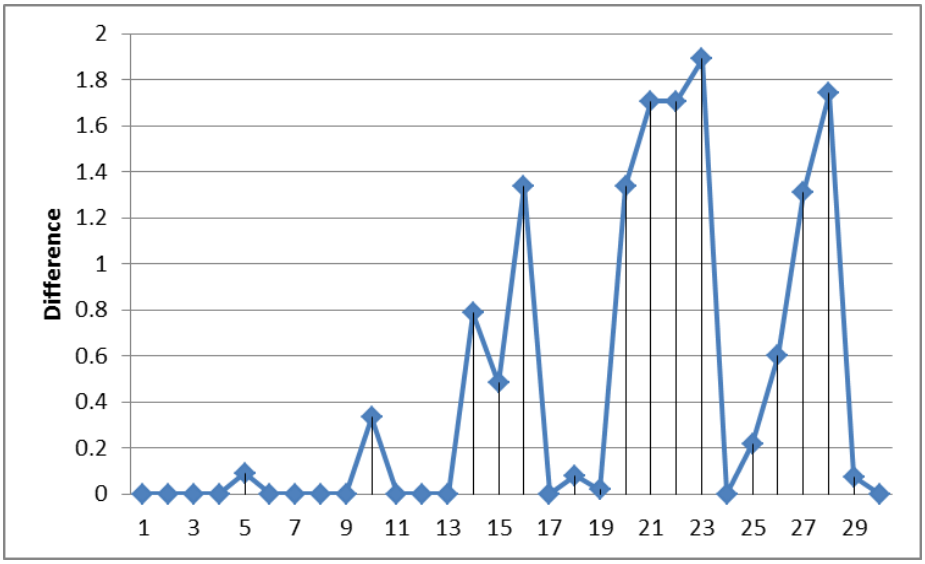
Bases			
Lysine	K	2.18	8.95
Arginine	R	2.17	9.04
Histidine	H	1.82	9.17
Sulphydryl			
Cysteine	C	1.71	10.78

Table 3: The 2-D map of amino acids is obtained by considering the pKa(COOH) values along x-axis and pKa(NH_3^+) values along y-axis. Similarity between two sequence is obtained by calculating the Euclidean distance of (x,y) co-ordinates of corresponding amino acids.The graph based on Euclidean distance is plotted.In the graph the peaks represents the mismatches and the matches of amino acids are along the x-axis.

Method 2: Physico-Chemical Properties Method

Protein-1	X1	Y1	Protein-2	X2	Y2	Difference
G	2.34	9.6	G	2.34	9.6	0
I	2.36	9.68	I	2.36	9.68	0
P	1.99	10.6	P	1.99	10.6	0
C	1.71	10.8	C	1.71	10.78	0
A	2.34	9.69	G	2.34	9.6	0.09
E	2.19	9.67	E	2.19	9.67	0
S	2.21	9.15	S	2.21	9.15	0
C	1.71	10.8	C	1.71	10.78	0
V	2.32	9.62	V	2.32	9.62	0
Y	2.2	9.11	W	2.38	9.39	0.33287
I	2.36	9.68	I	2.36	9.68	0
P	1.99	10.6	P	1.99	10.6	0
C	1.71	10.8	C	1.71	10.78	0
T	2.6	10.4	I	2.36	9.68	0.78746
V	2.32	9.62	S	2.21	9.15	0.4827
T	2.6	10.4	S	2.21	9.15	1.3381
A	2.34	9.69	A	2.34	9.69	0
L	2.36	9.6	I	2.36	9.68	0.08
L	2.36	9.6	G	2.34	9.6	0.02
G	2.34	9.6	C	1.71	10.78	1.33765
C	1.71	10.8	S	2.21	9.15	1.70496
S	2.21	9.15	C	1.71	10.78	1.70496
C	1.71	10.8	K	2.18	8.95	1.88939
S	2.21	9.15	S	2.21	9.15	0
N	2.02	8.8	K	2.18	8.95	0.21932
R	2.17	9.04	V	2.32	9.62	0.59908
V	2.32	9.62	C	1.71	10.78	1.31061
C	1.71	10.8	Y	2.2	9.11	1.7404
Y	2.2	9.11	R	2.17	9.04	0.07616
N	2.02	8.8	N	2.02	8.8	0

Graphical Representation



The two methods listed above were analyzed to evaluate the similarity between each set of sequences. The result obtained is then compared with **BLAST TWO PROTEIN** sequence software.

Results: The Result Obtained Is Shown In Table 4

Table 4

Sequences	Method1		Method2		Blast 2 Proteins
	Mismatches%	Identical%	Mismatches%	Identical%	Identical%
Cycloviolacin-O1 & Cycloviolacin-O2	33.33	66.66	26.66	73.33	66.00
Cycloviolacin-O1 & Cycloviolacin-H1	33.33	66.66	30.00	70.00	69.00
Cycloviolacin-O1 & Cycloviolacin-H4	0.00	100.00	0.00	100.00	93.00
Cycloviolacin-O2 & Cycloviolacin-H1	0.00	100.00	3.33	96.66	90.00
Cycloviolacin-O2 & Cycloviolacin-H4	36.66	63.33	30.00	70.00	69.00
Cycloviolacin-H1 & Cycloviolacin-H4	40.00	60.00	33.33	66.66	66.00

Discussion: The two methods yield almost the same result. On comparing the result with blast two protein sequence software ,the results from the first method is nearer but the results from the second method is more nearer to software result. The graphical alignments of proteins based on the ordering of amino acids with respectto the acid dissociation constants of the side chains clearly indicate that not all mismatches are equal. In the graph of Physico-chemical property method, the mismatches are accompanied by a small or large amplitude .The small amplitude implies the corresponding amino acids in the two sequences are from same group and large amplitude means the amino acids from different groups. Magic circle method clearly shows the dissimilar fragments in protein sequences but the second method along with dissimilarity gives information about degree of dissimilarity. i.e those associated with small amplitudes are less likely to drastically change properties of proteins.

References:

1. Echenique P.(2007) Introduction to protein folding for physicists. Contemporary Physics,48,81-108,
2. Novel 2-D graphical representation of proteins. M.Randic, D.Butina, J.Zupan, J.Chem.Phys.Lett.419(2006)528.
3. 2-D Graphical representation of proteins based on physic-chemical properties of amino acids. M.RandicJ.Chem.Phys.Lett.440(2007)291-295

***

SIMILIARITY / DISSIMILARITY STUDY OF PROTEIN IN NON-HOMOLOGOUS WAY USING ROOT MEAN SQUARE

D. Vijayalakshmi
Assistant Professor, Department of Mathematics
Sri ChandrasekharendraSaraswathiViswaMahavidyalaya,Kanchipuram,Tamilnadu
P. Geethanjali
M. Phil Scholar, Department of Mathematics
Sri ChandrasekharendraSaraswathiViswaMahavidyalaya,Kanchipuram,Tamilnadu

Abstract: We propose a new 2-D representation of protein using three Physico - Chemical prosperities of amino acids. Next to this, using the above information and root mean square value between each pair of protein we measure the similarity between proteins.

Keyword: Similarity study, Physico Chemical Properties, Root Mean Square.

1. Introduction: In protein study, the tasks protein representation and similarity study occupies a major part. Because the way of representation of protein reduces the difficulty in the study of protein to a large extend and the similarity study makes easier the analysis of evolutionary relationships.

We brief some newly implemented idea of protein representation and similarity study in this paragraph.. Yongbin et al [1] introduced a new graphic representation of protein sequence to measure study the similarity – dissimilarity between proteins. A novel method Alignment Diagonal line diagram is proposed to determine similarity between protein by Wang et al [2]. Lakkani [3] developed 2D and 3D amino acid adjacency matrices that helps in similarity analysis. Abo-Elkhier [4], An innovative method of representing protein sequence based on right cone of unit base and length. Ma et al [5] represented protein sequence in 2 Dimension by introducing family of iterated function system. In [6] sun et al represents protein sequence in 2-Dimension using six physicochemical prosperities, that is represented in vector and the distance between the vector measure similarity / dissimilarity Zhu [7] Introduces a feature appearance model based on newly developed 2D representation of Protein. Yao et al [8] introduced a spectrum like representation for protein sequence based on hydrophobicity of amino acids and illustrated a new similarity measure by performing Chi Square value of compatibility test. In [9] Ragor et al proposed a new similarity approach based on the neighborhood of each residues in a protein sequences.

In this paper, the physicochemical properties

Pk_1 – pk_a value of terminal amino acid group COOH

Pk_2 – pk_a value of terminal amino acid group NH_3 and

Abu – Abundance are used to represent the amino acids in 3 Dimension similarity between proteins is measured using Root mean square value.

2. Protein Data Used:

PROTEIN ID	PROTEIN NAME	PROTEIN DESCRIPTION
4FC1	Ultra-high resolution neutron structure of crambin at room-temperature	Direct observation of hydrogen atom dynamics and interactions by ultrahigh resolution neutron protein crystallography.
3UE7	X-ray crystal structure of a novel topological analogue of crambin	Design, total chemical synthesis, and x-ray structure of a protein having a novel linear-loop polypeptide chain topology.
3NIR	Crystal structure of small protein crambin at 0.48 A resolution	Crystal structure of small protein crambin at 0.48 A resolution
2EYB	Water refined solution structure of crambin in ACETONE/WATER	Three-dimensional structure of the water-insoluble protein crambin in dodecylphosphocholine micelles and its minimal solvent-exposed surface.
2EYC	DMSO refined solution structure of crambin in dpc micelles	Three-dimensional structure of the water-insoluble protein crambin in dodecylphosphocholine micelles and its minimal solvent-exposed surface.
2EYD	Water refined solution structure of crambin in dpc micelles	Three-dimensional structure of the water-insoluble protein crambin in dodecylphosphocholine micelles and its minimal solvent-exposed surface.
1YV8	Solution structure of crambin in acetone/water mixed solvent	Three-Dimensional Structure of the Water-Insoluble Protein Crambin in Dodecylphosphocholine Micelles and Its Minimal Solvent-Exposed Surface.
1YVA	NMR solution structure of crambin in DPC micelles	Three-Dimensional Structure of the Water-Insoluble Protein Crambin in Dodecylphosphocholine Micelles and Its Minimal Solvent-Exposed Surface.
1CXR	Automated 2D NOESY assignment and structure calculation of crambin(S22/I25) with self-correcting distance geometry based NOAH/Diamod programs.	Automated 2D NOESY assignment and structure calculation of Crambin(S22/I25) with the self-correcting distance geometry based NOAH/DIAMOD programs.
1CNR	Correlated disorder of the pure PRO22(SLASH)LEU25 form of crambin at 150K refined to 1.05 Angstroms resolution.	Correlated disorder of the pure Pro22/Leu25 form of crambin at 150 K refined to 1.05-A resolution.

The proteins are represented in 3 Dimension and Pk_1 value is considered as x co-ordinate, Pk_2 value is considered as y co-ordinate and Abu value is taken as z co-ordinate for each amino acid. To each pair of protein the root mean square value is found.

PROTEIN I (4FC1)			PROTEIN II (3UE7)			ROOT MEAN SQUARE VALUE
x	y	z	x	y	z	
2.09	9.1	1.5	2.09	9.1	1.5	0.1063
2.09	9.1	1.5	2.09	9.1	1.5	0.1063
1.92	10.7	0.52	1.92	10.7	0.52	0.1063
1.92	10.7	0.52	1.92	10.7	0.52	0.1063
1.95	10.64	1.3	1.95	10.64	1.3	0.1063
2.19	9.21	1.2	2.19	9.21	1.2	0.1063
2.32	9.76	1.7	2.32	9.76	1.7	0.1063
2.39	9.74	2.4	2.39	9.74	2.4	0.1063
2.35	9.87	2.9	2.35	9.87	2.9	0.1063
1.82	8.99	1.7	1.82	8.99	1.7	0.1063
2.19	9.21	1.2	2.19	9.21	1.2	0.1063
2.14	8.72	1.4	2.14	8.72	1.4	0.1063
2.2	9.31	1.1	2.2	9.31	1.1	0.1063
2.14	8.72	1.4	2.14	8.72	1.4	0.1063
2.39	9.74	2.4	2.35	9.87	2.9	0.1063
1.92	10.7	0.52	1.92	10.7	0.52	0.1063
1.82	8.99	1.7	1.82	8.99	1.7	0.1063
2.33	9.74	2.6	2.33	9.74	2.6	0.1063
1.95	10.64	1.3	1.95	10.64	1.3	0.1063
2.35	9.78	3.5	2.35	9.78	3.5	0.1063
2.09	9.1	1.5	2.09	9.1	1.5	0.1063
1.95	10.64	1.3	1.95	10.64	1.3	0.1063
2.1	9.47	1.5	2.1	9.47	1.5	0.1063
2.35	9.87	2.9	2.35	9.87	2.9	0.1063
2.33	9.74	2.6	2.33	9.74	2.6	0.1063
1.92	10.7	0.52	1.92	10.7	0.52	0.1063
2.35	9.87	2.9	2.35	9.87	2.9	0.1063
2.09	9.1	1.5	2.09	9.1	1.5	0.1063
2.2	9.21	0.79	2.2	9.21	0.79	0.1063
2.09	9.1	1.5	2.09	9.1	1.5	0.1063
2.35	9.78	3.5	2.35	9.78	3.5	0.1063
1.92	10.7	0.52	1.92	10.7	0.52	0.1063
2.32	9.76	1.7	2.32	9.76	1.7	0.1063
2.32	9.76	1.7	2.32	9.76	1.7	0.1063
2.32	9.76	1.7	2.32	9.76	1.7	0.1063
1.95	10.64	1.3	1.95	10.64	1.3	0.1063
2.35	9.78	3.5	2.35	9.78	3.5	0.1063
2.35	9.87	2.9	2.35	9.87	2.9	0.1063
2.09	9.1	1.5	2.09	9.1	1.5	0.1063
1.92	10.7	0.52	1.92	10.7	0.52	0.1063
1.95	10.64	1.3	1.95	10.64	1.3	0.1063
2.35	9.78	3.5	2.35	9.78	3.5	0.1063
1.99	9.9	1.4	1.99	9.9	1.4	0.1063
2.2	9.21	0.79	2.2	9.21	0.79	0.1063
2.35	9.87	2.9	2.35	9.87	2.9	0.1063
2.14	8.72	1.4	2.14	8.72	1.4	0.1063

Root mean square = $\sqrt{\frac{\sum\sqrt{(x_1-x_2)^2+(y_1-y_2)^2+(z_1-z_2)^2}}{N}}$

$$= \sqrt{0.52/46}$$

$$= 0.1063$$

Table 1: The Root Mean Value between each pair of Protein

	3UE7	3NIR	2EYB	2EYC	2EYD	1YV8	1YVA	1CXR	1CNR
4FC1	0.1063	0	0	0	0	0	0	0.226	0
3UE7	-	0.1063	0.1063	0.1063	0.1063	0.1063	0.1063	0.2498	0.1063
3NIR	-	-	0	0	0	0	0	0.226	0
2EYB	-	-	-	0	0	0	0	0.226	0
2EYC	-	-	-	-	0	0	0	0.226	0
2EYD	-	-	-	-	-	0	0	0.226	0
1YV8	-	-	-	-	-	-	0	0.226	0
1YVA	-	-	-	-	-	-	-	0.226	0
1CXR	-	-	-	-	-	-	-	-	0.226
1CNR	0.1063	0	0	0	0	0	0	0.226	0

Result: From the table, considering the protein 4FC1 and its corresponding row, we infer the Root mean square value corresponding to proteins 3NIR, 2EYB, 2EYC, 1YC8, 1YVA, 1CNR is zero. This implies these proteins are 100% similar to 4FC1. If we consider 3UE7 and 1CXR the Root mean square value is a bit greater than zero. This infers these proteins are not 100% similar and at the same time they are not dissimilar. On this basis we measure the similarity / dissimilarity based on the ROOT MEAN SQUARE value. If the Root mean square value is zero then the proteins are 100% similar and if the Root mean square value increases the similarity percentage decreases. This fact is proved by the values in the above table. To verify the blast sequence site result is given below:

Blast Sequence Result:

	3UE7	3NIR	2EYB	2EYC	2EYD	1YV8	1YVA	1CXR	1CNR
4FC1	96%	100%	100%	100%	100%	100%	100%	96%	100%
3UE7		96%	96%	96%	96%	96%	96%	91%	91%
3NIR			100%	100%	100%	100%	100%	96%	100%
2EYB				100%	100%	100%	100%	96%	100%
2EYC					100%	100%	100%	96%	100%
2EYD						100%	100%	96%	100%
1YV8							100%	96%	100%
1YVA								96%	100%
1CXR									96%
1CNR	96%	100%	100%	100%	100%	100%	100%	96%	100%

Conclusion: This is a simple method to measure similarity / dissimilarity between proteins. This is a novel method calculating Root Mean Square value in non homologous way. This method yields the accurate result in a easier way in less time.

References:

1. Yongbin zhao, Xiaohong Li, Zhaohui Qi, "Novel 2D Graphic representation of protein sequenc and its application ". Journal of fiber Bio engineering and informatics 7:1 2014 23-33
2. Lei Wang, Hai Peng and Jinhua zheng " ADCD A Novel graphical representation of protein sequences and its application. Computational and Mathematical methods in Medicine. Volume 2014 Article id 959753, 15 pages
3. A.El.Lakkani and S.El-Sherif, "Similarity analysis of protein sequences based on 2D and 3D amino acid adjacency matrices, chemical physics letters vol-590 PP-192-195, 2013
4. MM Abo Elkhier " Similarity / Dissimilarity analysis of protein sequences using the spatial median as descriptor ". Journal of Biophysical chemistry vol-3 PP.142-148, 2012

5. T.Ma, Y.Liu, Q.Dai, Y.Yao and P.-A. He " A graphical representation of protein based on a novel iterated function system " Physica a : Statistical Mechanics and its applications, Vol-403 PP 21-28 2014
6. Dandan sun, Chunrui Xu, Yusen Zhang " A Novel method of 2D graphical representation for proteins and its application". Match commun.Math.comput.chem 75(2016) 431-446
7. Xianyou Zhu " A noval 2D Graphical Representation and its application in the similarities / dissimilarities Analysis of protein sequence. A American Journal of Biochemistry and Biotechnology 2016
8. Yuhua Yao, Shoujiang Yan, Huimin Xu, Jianning Han, Xuying Nan, Ping-an He and Qi Dai, " Similarity / Dissimilarity analysis of protein sequences based on a New spectrum –like graphical representation". Evolutionary bioinformatics 2014. 10 87-96
9. Sergey I. Rogov and Alexei N.Nekrasov. " A numerical measure of amino acid residues similarity based on the analysis of their surroundings in natural protein sequences" Protein Engineering Vol14 No.7. PP 459-463 2001

***

MEASUREMENT OF SIMILARITY/DISSIMILARITY OF PROTEIN USING POLARITY OF AMINO ACIDS

D. Vijayalakshmi
Assistant Professor, Department of Mathematics
Sri Chandrasekharendra Saraswathi Viswa Mahavidyalaya,Kanchipuram, Tamilnadu
A.Shakila
Assistant Professor, Department of Mathematics
Sri Chandrasekharendra Saraswathi Viswa Mahavidyalaya,Kanchipuram, Tamilnadu

Abstract: In this paper a novel 2-D representation of protein is introduced to measure the similarity between them and polarity value of amino acid plays a key role in measuring similarity between proteins. This method provides accurate result when compared with blast sequence results. This proves the efficiency & simplicity of this method.

Keywords: Polarity, Similarity Measure.

Introduction: Similarity/dissimilarity measure of protein occupies a huge space in the study of protein. The key aspect of this study is the representation of protein in a suitable way that yields the required solution in a minimum number of steps. Many researchers state that graphical representation proves to be a best tool in visual comparison of proteins. This graphical representation aims at similarity/dissimilarity study of proteins to a very large extend [4]. Now we see some 2-D representation of protein in brief. Researcher Randic [1-3] analyses protein sequences using graphical representation. Using PK_α values of COOH & NH_3^+ Yao [4] developed a method to study the proteins. Randic [5] using the pka value of NH_3 & COOH proposed a new graphical representation. In [6] Y Zhao et al developed a novel 2-D representation of protein using 4 physicochemical properties. Qi Zh et al [7] proposes a 2-D representation based on Huffman tree. In this paper, we introduce a novel 2-D representation of protein based on polarity. Using these co-ordinates of amino acids we measure similarity between proteins.

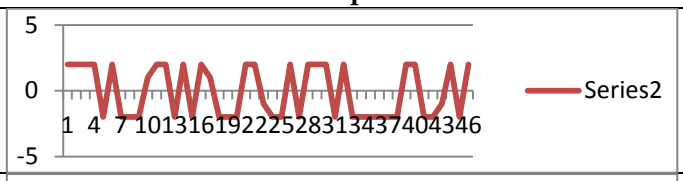
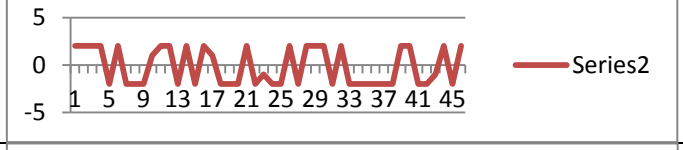
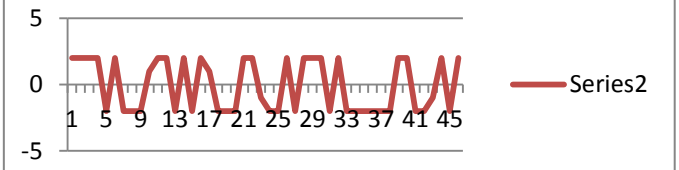
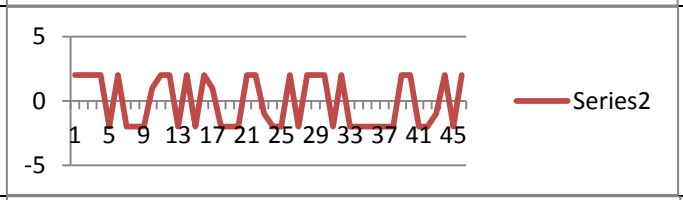
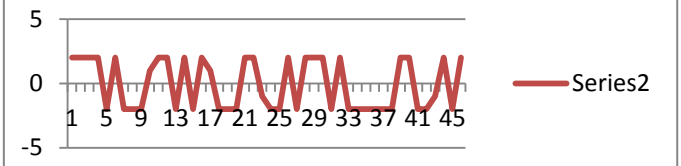
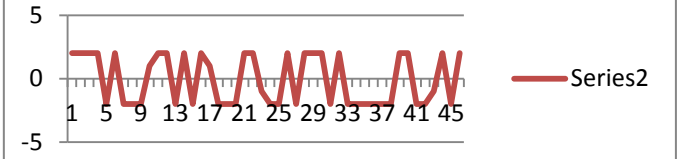
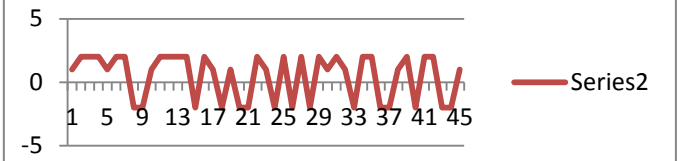
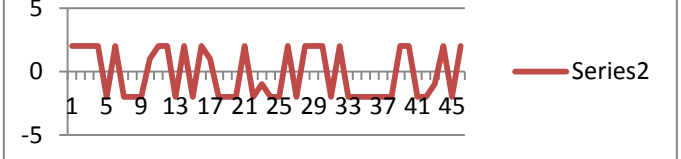
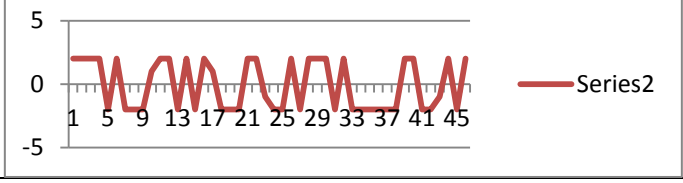
Method: The polarity property of amino acid is very important in characterizing a protein. The solving capacity of protein in aqueous water plays a vital role in identifying its nature. In this part we assign value -2, -1, 1 and 2 to each amino acid based on the polarity property. These values are considered as Y co-ordinates of each amino acid. Their sequential position is considered as their X co-ordinates. Keeping these 2 values the proteins are represented in 2 dimensions. To each protein under consideration we calculate the X & Y values as mentioned above. To measure similarity the Euclidean distance between each pair of protein is determined. Based on this value we narrate the percentage of similarity between proteins.

Table 1: Numerical Values for Amino Acids Based on Polarity

Amino acids	1 Letter	Polarity value	Amino acids	1 Letter	Polarity value
Alanine	A	-2	Leucine	L	-2
Arginine	R	1	Lysine	K	1
Asparagine	N	2	Methionine	M	-2
Aspartic	D	-1	Phenylalanine	F	-2
Cysteine	C	2	Proline	P	-2
Glumatic	E	-1	Serinr	S	2
Glutamine	Q	2	Threonine	T	2
Glycine	G	-2	Tryptophan	W	-2
Histidine	H	1	Tyrosine	Y	2
Isoleucine	I	-2	Valine	V	-2

Data Used:

Table 2

Protein Id	Protein 2-D representation
1jxt	
1ccn	
1jxx	
1cbn	
1jxw	
1jxu	
1wuw	
2fd7	
1jxy	

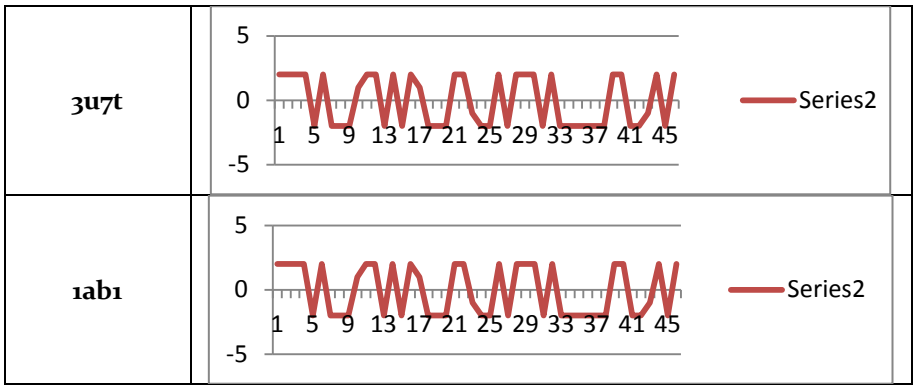


Table 3: Calculation of Euclidean Distance

1jxt			1ccn			1jxt:1ccn
Seq 1	**X_1**	**Y_1**	**Seq 2**	**X_2**	**Y_2**	**Distance**
T	1	2	T	1	2	0
T	2	2	T	2	2	0
C	3	2	C	3	2	0
C	4	2	C	4	2	0
P	5	-2	P	5	-2	0
S	6	2	S	6	2	0
I	7	-2	I	7	-2	0
V	8	-2	V	8	-2	0
A	9	-2	A	9	-2	0
R	10	1	R	10	1	0
S	11	2	S	11	2	0
N	12	2	N	12	2	0
F	13	-2	F	13	-2	0
N	14	2	N	14	2	0
V	15	-2	V	15	-2	0
C	16	2	C	16	2	0
R	17	1	R	17	1	0
L	18	-2	L	18	-2	0
P	19	-2	P	19	-2	0
G	20	-2	G	20	-2	0
T	21	2	T	21	2	0
S	22	2	P	22	-2	4
E	23	-1	E	23	-1	0
A	24	-2	A	24	-2	0
I	25	-2	L	25	-2	0
C	26	2	C	26	2	0
A	27	-2	A	27	-2	0
T	28	2	T	28	2	0
Y	29	2	Y	29	2	0
T	30	2	T	30	2	0
G	31	-2	G	31	-2	0
C	32	2	C	32	2	0
I	33	-2	I	33	-2	0
I	34	-2	I	34	-2	0
I	35	-2	I	35	-2	0
P	36	-2	P	36	-2	0

G	37	-2	G	37	-2	0
A	38	-2	A	38	-2	0
T	39	2	T	39	2	0
C	40	2	C	40	2	0
P	41	-2	P	41	-2	0
G	42	-2	D	42	-2	0
D	43	-1	G	43	-1	0
Y	44	2	Y	44	2	0
A	45	-2	A	45	-2	0
N	46	2	N	46	2	0
						Sum = 4

Table 4: Result

PROTEIN	1ccn	1jxx	1cbn	1jxw	1jxu	1wuw	2fd7	1jxy	3u7t	1ab1
1jxt	4	0	0	0	0	74	4	0	0	0
1ccn		4	4	4	4	78	4	4	4	4
1jxx			0	0	0	74	4	0	0	0
1cbn				0	0	74	4	0	0	0
1jxw					0	74	4	0	0	0
1jxu						74	4	0	0	0
1wuw							78	74	74	74
2fd7								4	4	4
1jxy									0	0
3u7t										0

Discussion: From the row corresponding to 1jxt, we infer the Euclidean distance between proteins 1jxt, 1cbn, 1jxw, 1jxu, 1jxy, 3u7t, 1ab1 are zero. We state that these proteins are 100% similar to each other. Similarly the Euclidean distance between 1jxt & 1ccn is 4. Based on this value we state that the proteins are less than 100% similar for instance we take the proteins are 96% similar. In this way we measure the similarity between proteins (i.e.) if the value of Euclidean distance increases the percentage of similarity between proteins decrease. And this is clear while comparing the results obtained from blast sequence given below.

Table 5:

PROTEIN	1ccn	1jxx	1cbn	1jxw	1jxu	1wuw	2fd7	1jxy	3u7t	1ab1
1jxt	97.83%	100%	100%	100%	100%	54%	100%	100%	100%	100%
1ccn		95%	95%	95%	100%	52%	100%	95%	95%	95%
1jxx			100%	100%	95%	55%	95%	100%	100%	100%
1cbn				100%	95%	55%	95%	100%	100%	100%
1jxw					100%	54%	100%	100%	100%	100%
1jxu						52%	100%	95%	95%	95%
1wuw							55%	54%	55%	55%
2fd7								100%	95%	95%
1jxy									100%	100%
3u7t										100%

Conclusion: This is a simple & novel method in measuring similarity between proteins. Even it is simple it proves its efficiency is measuring similarity. A novel 2-D representation of protein introduced in this part acts a good tool in visual comparison of protein.

Reference:

1. Randic M, Vracko M, Nandy A, basak sc. On 3-D graphical representation of DNA primary sequences and their numerical characterization. J chem. Inf Model 2000 ; 40 : 1235 – 1244.
2. Randic M, Vracko M, lers n, Plavic D. novel 2-D graphical representation of DNA sequences and their numerical characterization Chem Phys Lett 2003 ; 368: 1 – 6.
3. Randic M. Graphical representation of DNA as 2-D map Chem Phys Lett 2004 ; 386 : 468 – 471.
4. Yao Y H, Dai Q, Lic, He PA Nan X Y, Zhang Y Z. analysis of similarity/dissimilarity of protein sequences. Poteins 2008 ; 73 : 864 – 871.
5. Randic M withdrawn 2-D graphical representation of proteins based on physico- chemical properties of amino acids Chem Phys Let 2007 ; 444 : 176 – 180.
6. Yongbin Zhao, Xiaohong Li, Zhaohui Qi. Novel 2-D graphical representation of protein sequence and its application. Journal of fiber Bioengineering and Informatics 7;1(2014) : 23 -33.
7. Qi Z H, Feng J, Qi X Q, Li L. Application of 2-D graphical representation of protein sequence based on Huffman tree method. Comput Biol Med2012; 42 : 556 – 563.

***

IMPACT OF THERMAL RADIATION ON AN UNSTEADY COPPER-WATER NANOFLUID FLOW PAST OVER AN INFINITE VERTICAL PLATE WITH VARIABLE TEMPERATURE

E.Geetha

Assistant Professor, Department of Mathematics, SCSVMV University, Enathur, Kanchipuram.
geethamuthuo6@gmail.com

M.Anushalini

Research scholar, Department of Mathematics, SCSVMV University, Enathur, Kanchipuram.

R.Muthucumaraswamy

Professor, Department of Applied Mathematics, Sri Venkateswara College of Engineering, Sriperumbudur.

Abstract: This paper analyses the thermal radiation with variable temperature effects on the unsteady nanofluid flow past over an infinitely long vertical plate. The nanofluids are used to increase the thermal conductivity. In this study, we have considered the copper (Cu) nanofluid for increasing thermal conductivity. The exact analytical solutions are derived by the method of Laplace Transform. The solutions for temperature and velocity are obtained in terms of complementary error function and the effects of various parameters like prandtl number, radiation parameter, thermal grashof number, size of the nanofluid and time on temperature and velocity of the plate are depicted graphically and discussed in a detailed manner.

Keywords: Nanofluid (Cu), Thermal Radiation, Variable Temperature, Vertical Plate.

1. Introduction: The nanoparticle-fluid suspensions are termed nanofluids, obtained by dispersing nanometer sized particles in a conventional base fluid like water, oil, ethylene glycol etc. Nanoparticles are of great scientific interest as they are effectively a bridge between bulk materials and atomic or molecular structures. Generally, metals like Copper, Aluminium, Gold, Silver are good heat conductors. For this reason, we are considering copper is a nanoparticle for increasing thermal conductivity and water is a base fluid. Copper nanoparticles can be manufactured using numerous methods. The electro deposition method is considered by many as one of the most suitable and easiest. The copper nanoparticle acts as an anti-biotic, anti-microbial and anti-fungal agent when added to plastics, coatings, and textiles; Copper diet supplements with efficient delivery characteristics; High strength metals and alloys; EMI shielding; Heat sinks and highly thermal conductive materials; Efficient catalyst for chemical reactions and for the synthesis of methanol and glycol. Copper nanoparticles application research is ongoing to discover their potential dielectric, magnetic, electrical, optical, imaging, and catalytic, biomedical, bioscience properties.

Thermal radiation effects on an initial unsteady free convective flow past over an infinite vertical plate with mass transfer effects is clearly examined by A.Khan and R.Solangi [1]. Chandrakala.P and Narayana bhaskar.P,[2] analyzed the radiation effects on oscillating vertical plate with uniform heat and mass flux by using Laplace transform technique. Prasad.K.V., Mallikarjun.P, et al[3] investigated mixed convective fully developed flow in a vertical channel in the presence of thermal radiation and viscous dissipation by via Differential transform method. Vijayakumar .A.G.,Vijayakumar varma.S [4] analyzed thermal radiation and mass transfer effects on MHD flow past an impulsively started exponentially accelerated vertical plate with variable temperature and mass diffusion by using Laplace transform method. Suneetha.S, Bhaskar reddy.N, et al [5] explored thermal radiation effects on MHD free convection flow past an impulsively started vertical plate with variable surface temperature and concentration by using

Implicit finite difference method of crank-nicholson type. Chamkha.A.J.,Takhar.H.S.,et al[6] examined radiation effects on free convection flow past a semi-infinite vertical plate with mass transfer by using Implicit finite difference technique.The radiation effects on an unsteady nanofluid flow past over an vertical plate is clearly investigated by researcher [7],[12],[13]. Uwanta .I.J.,Murtala sani[8] numerically solved heat and mass transfer flow past an infinite vertical plate with variable thermal conductivity with the aid of MAPLE package. Venkateswarlu malapati, Padma polarapu, [9] analyzed unsteady MHD free convective heat and mass transfer in a boundary layer flow past a vertical permeable plate with thermal radiation and chemical reaction by using two term Perturbation technique. Rajesh.V.,Mallesh.M.P., et al[10] studied transient MHD nanofluid flow &heat transfer due to a moving vertical plate with thermal radiation and temperature effects using implicit finite difference method. Balamurugan.K.S.,Ramaprasad.J.L.,et al [11]analyzed unsteady MHD free convective flow past a moving vertical plate with time dependent suction and chemical reaction in a slip flow regime by using Perturbation technique. Mohammed Mehdi Rashidi,Behnam Rostami., et al[14] examined free convective heat and mass transfer for MHD fluid flow over a permeable vertical stretching sheet in the presence of radiation & buoyancy forces by homotopy analysis method. K.Javaherdeh, Mehrzad Mirzaei Nejad, et al [15] analyzed natural convection heat & mass transfer in MHD fluid flow past a moving vertical plate with variable temperature and concentration in a porous medium by implicit finite difference process. Nader Y Abd Elazem, Abdelhalim ebald, et al[16] examined numerically ,radiation effect of MHD on Cu-water and Ag-water nanofluids flow over a stretching sheet by using Chebychev collocation method.

From the author's knowledge, the analytical solution for thermal radiation with variable temperature on an unsteady nanofluid flow past over an infinite vertical plate has not been studied. In this study, a free convective flow of a nanofluid on an infinite vertical plate with thermal radiation and variable temperature has been considered. The joined nonlinear partial differential equations are converted into a non dimensional form and the solutions are derived by using the Laplace transform. The water based nanofluid containing nanoparticles Copper (Cu) has been considered in the present work. The governing equations are solved analytically and presented in closed form. The effects on temperature of the plate and the velocity of the plate by the various parameters like thermal radiation parameter, grashof number, Prandtl number, solid volume fraction and time are drawn graphically and discussed in a detailed manner.

2. Mathematical Analysis: The viscous flow of an incompressible nanofluid past an uniformly accelerated vertical infinite plate in the existence of thermal radiation and variable temperature has been considered. Further it is assumed to be an unsteady flow of a viscous incompressible fluid which is initially at rest and surrounds an infinite vertical plate maintaining temperature T_∞.

The x-axis is taken alongside the plate in the vertically upward direction and the y-axis is taken perpendicular to the plate. At time $t' \leq 0$, the plate and fluid are at the same temperature T_∞. At time $t' > 0$, the plate is accelerated with a velocity $\frac{u_0^3}{v_f} t'$ its own plane against gravitational field and the temperature from the plate is raised to T_ω. It is also assumed that a radiative heat flux q_r is applied in the normal direction to the plate. The fluid is a water based nanofluid containing Cu. It is further assumed that the base fluid and the suspended nanoparticles are in thermal equilibrium.

The thermophysical properties of the nanofluids are given in Table 2.1.

Table 2.1: Thermo Physical Properties of Water and Nanoparticles

Physical Properties	Water/ Base Fluid	Cu
$\rho(kg/m^3)$	997.1	8933
$c_\rho(J/kgK)$	4179	385
$K(W/mK)$	0.613	401
$\beta \times 10^5(K^{-1})$	21	1.67
ϕ	0.0	0.05
$\sigma(S/m)$	5.5×10^{-6}	59.6×10^6

Then under usual Boussinesq's approximation the unsteady flow is governed by the following equations:

$$\rho_{nf}\frac{\partial u}{\partial t'} = g(\rho\beta)_{nf}(T - T_\infty) + \mu_{nf}\frac{\partial^2 u}{\partial y^2} \quad (1)$$

$$\left(\rho c_p\right)_{nf}\frac{\partial T}{\partial t'} = K_{nf}\frac{\partial^2 T}{\partial y^2} - \frac{\partial q_r}{\partial y} \quad (2)$$

where u is the velocity components along the x direction, T the temperature of the nano fluid, μ_{nf} the dynamic viscosity of the nano fluid, β_{nf} the thermal expansion coefficient of the nano fluid, ρ_{nf} the density of the nano fluid, K_{nf} the thermal conductivity of the nano fluid, g the acceleration due to gravity, q_r the radiative heat flux and $\left(\rho c_p\right)_{nf}$ the heat capacitance of the nano fluid which are given by

$$\mu_{nf} = \frac{\mu_f}{(1-\phi)^{2.5}},\ \rho_{nf} = (1-\phi)\rho_f + \phi\rho_s$$
$$\left(\rho c_p\right)_{nf} = (1-\phi)\left(\rho c_p\right)_f + \phi\left(\rho c_p\right)_s \quad (3)$$
$$(\rho\beta)_{nf} = (1-\phi)(\rho\beta)_f + \phi(\rho\beta)_s$$

Where ϕ is the solid volume fraction of the nano particle, ρ_f the density of the base fluid, ρ_s the density of the nano particle, μ_f the viscosity of the base fluid, $\left(\rho c_\rho\right)_f$ the heat capacitance of the base fluid and $\left(\rho c_\rho\right)_s$ the heat capacitance of the nanoparticle. It is worth mentioning that the expressions (1) are restricted to spherical nanoparticles, where it does not account for other shapes of nanoparticles. The effective thermal conductivity of the nano fluid given by Hamilton and Crosser model followed by[13],

$$K_{nf} = K_f\left[\frac{K_s + 2K_f - 2\phi(K_f - K_s)}{K_s + 2K_f + \phi(K_f - K_s)}\right] \quad (4)$$

where K_f is the thermal conductivity of the base fluid and K_s is the thermal conductivity of the nanoparticle. In Eqns. (1)–(4), the subscripts *nf*, *f* and *s* denote the thermo physical properties of the nanofluid, base fluid and nanoparticles, respectively.

The initial and boundary conditions of the proposed problem are given by:

$$u = 0, \qquad T = \mathrm{T}_\infty, \qquad for\ all\ y, t' \le 0$$
$$t' > 0: \quad u = \frac{u_0^3}{v_f}t', \quad T = \mathrm{T}_\infty + (\mathrm{T}_\omega - \mathrm{T}_\infty)At' \qquad at\ y = 0 \quad (5)$$
$$u \to 0, \quad T \to \mathrm{T}_\infty \qquad as\ y \to \infty$$

On introducing the following non dimensional quantities are

$$U = \frac{u}{u_0}\ ,\quad t = \frac{t'u_0^2}{v_f}\ ,\quad Y = \frac{yu_0}{u_f} \quad (6)$$
$$\theta = \frac{T - T_\infty}{T_w - T_\infty},\quad A = \frac{u_0^2}{v_f}\ ,\quad Gr = \frac{g v_f \beta(T_w - T_\infty)}{u_0^3}\ ,\quad R = \frac{16a^*\sigma T_\infty^3}{K_f}\left(\frac{v_f^2}{u_0^2}\right)\ , Pr = \frac{\mu c_p}{K_f}$$

The local radiant for the case of an visually thin gray gas is expressed by

$$\frac{\partial q_r}{\partial y} = -4a^*\sigma(T_\infty^4 - T^4) \quad (7)$$

It is assume that the temperature differences within the flow are sufficiently small such that T^4 may be expressed as a linear function of the temperature. This is accomplished by expanding T^4 in a Taylor series about T_∞ and neglecting higher-order terms, thus

$$T^4 \cong 4T_\infty^3 T - 3T_\infty^4 \quad (8)$$

By using equations (6) and (7), equation (2) reduces to

$$\left(\rho c_p\right)_{nf}\frac{\partial T}{\partial t'} = K_{nf}\frac{\partial^2 T}{\partial y^2} + 16a^*\sigma T_\infty^3(T_\infty - T) \quad (9)$$

By using equations (3),(4) and (6), equations (1) and (9) leads to,

$$L_1\frac{\partial U}{\partial t} = L_3\frac{\partial^2 U}{\partial Y^2} + L_2 Gr\,\theta$$
$$L_5\frac{\partial \theta}{\partial t} = L_6\frac{1}{Pr}\frac{\partial^2\theta}{\partial Y^2} - \frac{R}{Pr}\theta \quad (10)$$

Where $L_1 = (1-\phi) + \phi\left(\frac{\rho_s}{\rho_f}\right),\ L_2 = (1-\phi) + \phi\left(\frac{(\rho\beta)_s}{(\rho\beta)_f}\right)$,

$$L_3 = \frac{1}{(1-\phi)^{2.5}}\ , L_5 = (1-\phi) + \phi\left(\frac{(\rho c_p)_s}{(\rho c_p)_f}\right), L_6 = \left[\frac{K_s+2K_f-2\phi(K_f-K_s)}{K_s+2K_f+\phi(K_f-K_s)}\right] \quad (11)$$

Where R is the radiation parameter, Pr is the Prandtl number, Gr is the thermal grashof number, Gr approximates the ratio of the buoyancy force to the viscous force acting. Large R signifies a large radiation effect while R→0 corresponds to zero radiation effect.

The corresponding initial and boundary conditions are,

$$\left.\begin{array}{lll} & U = 0, \quad \theta = 0, & for\ all\ Y, t \le 0 \\ t > 0: & U = gt, \quad \theta = t & at\ Y = 0 \\ & U \to 0, \quad \theta \to 0 & as\ Y \to \infty \end{array}\right\} \quad (12)$$

Where $g = \frac{L_1}{L_3}$

3.Solution Procedure:

The solutions are represented in terms of exponential and complementary error function. The relation connecting error function and its complementary error function is as follows:

$$erfc(x) = 1 - \mathrm{erf}(x) \quad (13)$$

The dimensionless governing equations (10), subject to the initial and boundary conditions (12), are solved by the usual Laplace-transform technique and the solutions are derived as follows:

$$\theta = \frac{t}{2}\left[\exp\left(2\eta\sqrt{abt}\right) erfc\left(\eta\sqrt{a} + \sqrt{bt}\right) + \exp\left(-2\eta\sqrt{abt}\right) erfc\left(\eta\sqrt{a} - \sqrt{bt}\right)\right]$$
$$- \frac{\eta a\sqrt{t}}{2\sqrt{ab}}\left[\exp\left(-2\eta\sqrt{abt}\right) erfc\left(\eta\sqrt{a} - \sqrt{bt}\right) - \exp\left(2\eta\sqrt{abt}\right) erfc\left(\eta\sqrt{a} + \sqrt{bt}\right)\right]$$

$$U = gt\left[(1 + 2\eta^2 g) erfc\left(\eta\sqrt{g}\right) - \frac{2\eta\sqrt{g}}{\sqrt{\pi}}\exp(-\eta^2 g)\right] + \frac{h}{d} erfc\left(\eta\sqrt{g}\right)$$
$$+ \frac{ht}{d}\left[(1 + 2\eta^2 g) erfc\left(\eta\sqrt{g}\right) - \frac{2\eta\sqrt{g}}{\sqrt{\pi}}\exp(-\eta^2 g)\right]$$
$$- \frac{h}{2d^2}\exp(dt)\left[exp\left(2\eta\sqrt{gdt}\right) erfc\left(\eta\sqrt{g} + \sqrt{dt}\right)\right.$$
$$\left. + exp\left(-2\eta\sqrt{gdt}\right) erfc\left(\eta\sqrt{g} - \sqrt{dt}\right)\right]$$
$$- \frac{h}{2d^2}\left[exp\left(2\eta\sqrt{abt}\right) erfc\left(\eta\sqrt{a} + \sqrt{bt}\right) + exp\left(-2\eta\sqrt{abt}\right) erfc\left(\eta\sqrt{a} - \sqrt{bt}\right)\right]$$
$$- \frac{ht}{2d}\left[exp\left(2\eta\sqrt{abt}\right) erfc\left(\eta\sqrt{a} + \sqrt{bt}\right) + exp\left(-2\eta\sqrt{abt}\right) erfc\left(\eta\sqrt{a} - \sqrt{bt}\right)\right]$$
$$- \left(\frac{\eta a\sqrt{t}}{2\sqrt{ab}}\left[\exp\left(-2\eta\sqrt{abt}\right) erfc\left(\eta\sqrt{a} - \sqrt{bt}\right) - \exp\left(2\eta\sqrt{abt}\right) erfc\left(\eta\sqrt{a} + \sqrt{bt}\right)\right]\right)$$
$$+ \frac{h}{2d^2}\exp(dt)\left[exp\left(2\eta\sqrt{a(b+d)t}\right) erfc\left(\eta\sqrt{a} + \sqrt{(b+d)t}\right)\right.$$
$$\left. + exp\left(-2\eta\sqrt{a(b+d)t}\right) erfc\left(\eta\sqrt{a} - \sqrt{(b+d)t}\right)\right]$$

where $a = \frac{L_5 Pr}{L_6}, b = \frac{R}{L_5 Pr}, h = \frac{L_2 Gr}{L_1 - L_3 a}, d = \frac{L_3 ab}{L_1 - L_3 a}, g = \frac{L_1}{L_3}$

4. Results and Discussion: In order to get a clear vision on the physical of the problem, extensive numerical computations are conducted for various values of the thermo physical parameters are designed in graphs. We consider nanofluid containing copper nanoparticles with water as a base fluid. The values of volume fraction of nanoparticles reconsidered to be in the range $0 \le \phi \le 0.2$. The case ϕ = 0 corresponds to the regular fluid.i.e. nanoscale characteristics are eliminated. In this study, we have considered spherical shape nanoparticles with thermal conductivity and variable temperature.

4.1: Consequences of Parameters on Velocity Profiles: In Fig.1, The velocity summary of Copper-water nanofluid with coordinate η for different values of thermal grashof number in graph are shown. When Pr=6.2, ϕ= 0.05, t=0.5 and R=2 are kept at stable, the Fig.1 is explained that the velocity of the

plate U enhances with a rising values of thermal grashof number Gr at the time of cooling. Also, it is explained that velocity of the plate U reduces with a falling values of thermal grashof number Gr at the time of heating.

In Fig.2, the velocity profiles of Copper-Water nanofluid with coordinate η for different values of Pr in graph are exposed. When R=2, ϕ= 0.05, t=0.5 are kept constant, Fig.2 observed at the time of heating, that the velocity of the plate U reduces with an increasing values of Pr. Then, at the time of cooling, Fig.2 explained that the velocity U grows with an increasing values of Pr.

In Fig.3, At the time of heating and At the time of cooling the velocity profiles of Copper-Water nanofluid with coordinate η for different values of nanoparticle size in graph are examined. When Pr=6.2, R=2, t=0.5 are kept constant, Fig.3 explained the velocity of the plate U reduces with an falling values of solid volume fraction at the time of heating. Also shown, the velocity U rises with an falling values of ϕ at the time of cooling.

In Fig.4, At the time of heating and At the time of cooling the velocity profiles of Copper-Water nanofluid with different values of t in graph are shown. When Pr=6.2, R=2, ϕ= 0.05 are kept steady, Fig.4 explained the velocity of the plate U reduces with a falling values of t at time of heating. Also examined, the velocity U enhances with a rising values of t at the time of cooling.

At the time of heating and At the time of cooling, the combination of Copper-Water nanofluid with different values of R in graph Fig.5 are revealed. When Pr=6.2, t=0.5, ϕ= 0.05 are kept stable, Fig.5 examined the velocity of the plate U amplifies with a lessening values of R at the time of cooling. Also exposed the velocity U reduces with lessening values of R at the time of heating.

4.2: Effects of Parameters on Temperature Profiles: Fig.6 exemplifies the variation of temperature of the fluid for different Prandtl number, when t =0.5, R = 2, Gr=4 and ϕ = 0.005 are kept stable .The temperature profile reveals that the fluid temperature reduces as Prandtl number increases. This is due to the fact that a higher Prandtl number fluid has relatively low thermal conductivity, which reduces conduction and it results temperature decreases.

Fig.7 shows the variation of temperature of the fluid for different nanofluid size, when t=0.5, R=2, Gr = 4 and Pr=0.25 are kept constant. It examined that the fluid temperature reduces as nanofluid size increases. Fig.8,9 exposed variation of temperature of the fluid for different time and for different radiation R. It is found that the temperature of Copper – Water nanofluid decreases with rising values of t as well as R.

Because decrease in the values of R for given k_{nf} and T_{∞} means a decrease in the Rosse land radiation absorptive a^*. Since divergence of the radiative heat flux $\frac{\partial q_r}{\partial y}$ increases, a^* reduces which in turn causes o increase the rate of radiative heat transfer to the fluid and hence the fluid temperature enlarges.

Fig.1. Velocity profiles for different values of Gr

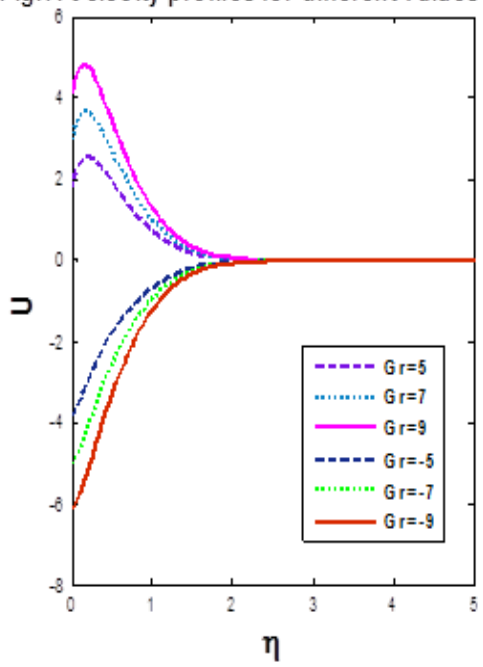


Fig.2. Velocity profiles for different values of Pr

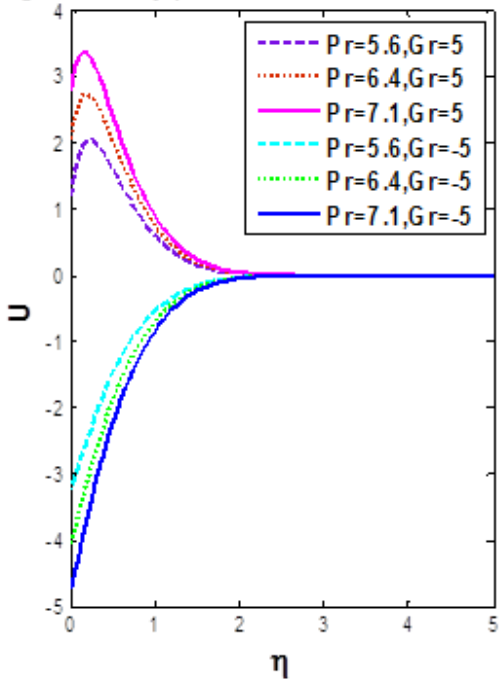


Fig.3. Velocity profiles for different nanofluid size

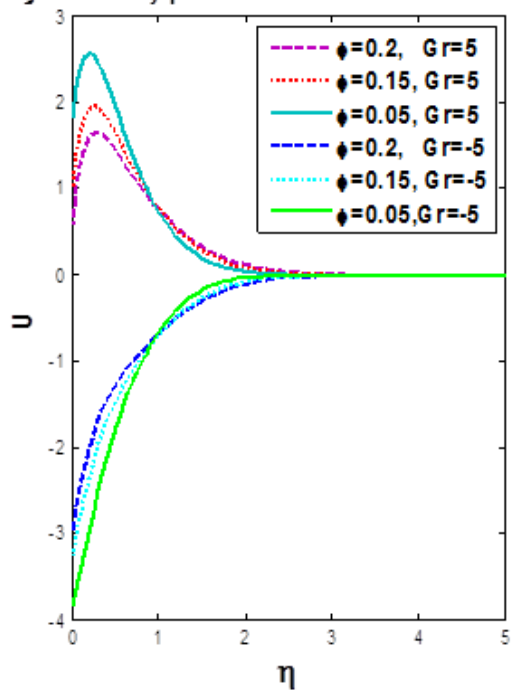


Fig.4. Velocity profiles for different values of t

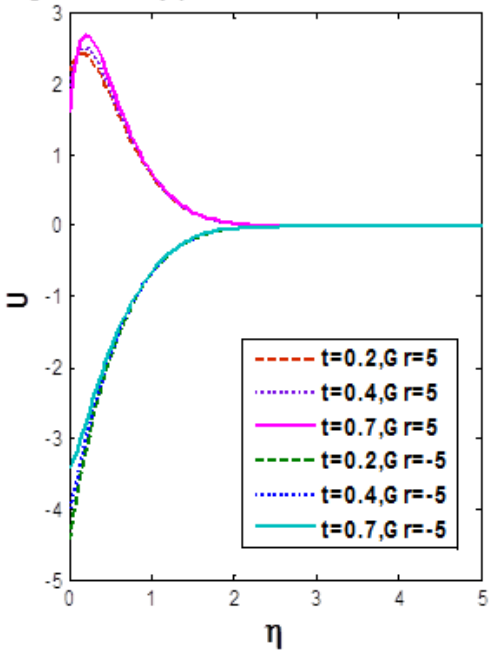


Fig.5. Velocity profiles for different values of R

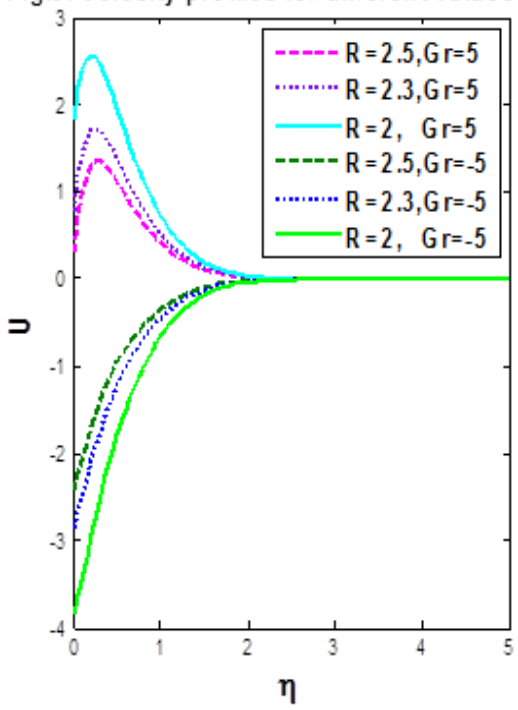


Fig.6. temperature profiles for different Pr

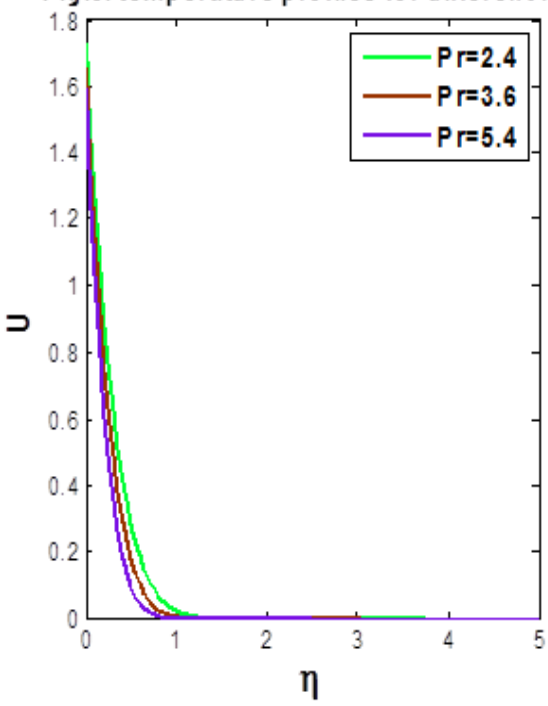


Fig.7. temperature profiles for different Nanofluid size

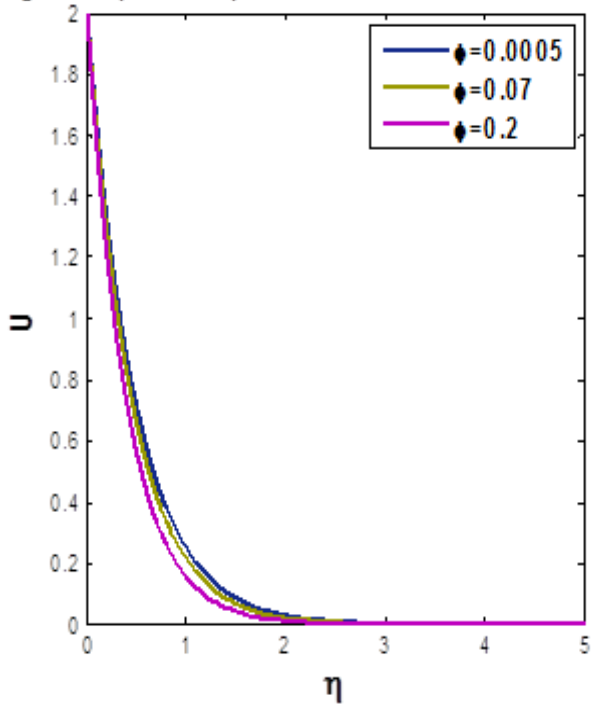
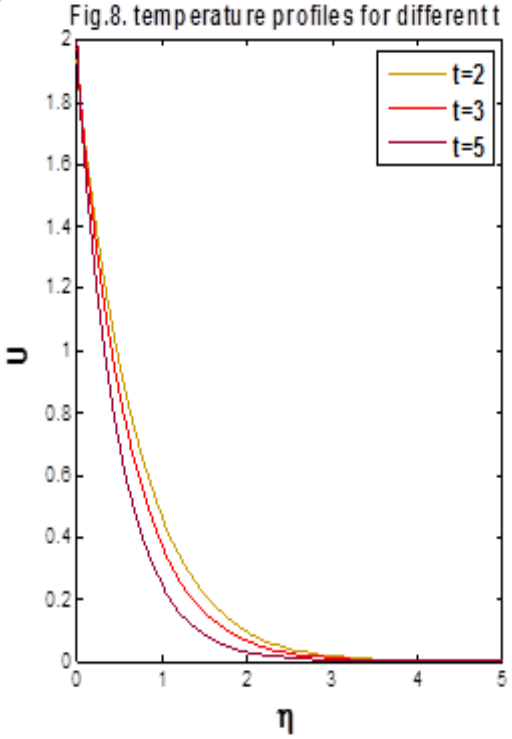
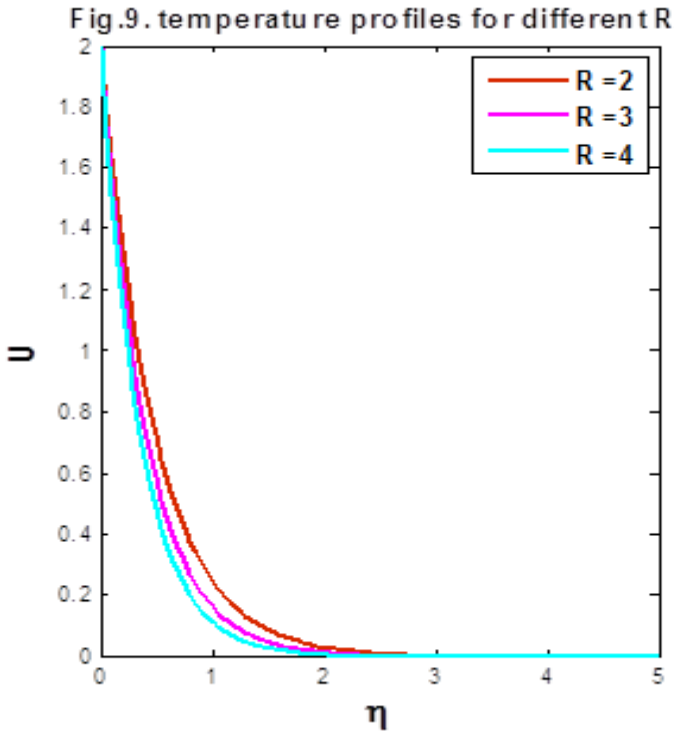


Fig.8. temperature profiles for different t





5. Conclusion: The main aspire of this study is to get the exact solution for the unsteady free convective Copper-Water nanofluid flow past over an infinitely long vertical plate in the rate of thermal radiation with variable temperature. Copper- Water nanofluid is engaged into description and the expression for the temperature of the fluid and the velocity of the plate has been obtained in closed form by using the laplace transform. The effects of the various parameters on velocity and temperature are presented graphically and the most important remarks are studied as follows:

- The temperature of the Copper-Water nanofluid reduces directly with an increases of Prandtl number, Nanofluid size, Radiation and time .
- At the time of cooling, the velocity of the plate enhances with an rising values of thermal grashof number, prandtl number, time and the decreasing values of nanofluid size, radiation. At the time of heating, the velocity of the plate decreases with an decreaing values of Gr, solid volume fraction, time, radiation and the increasing value of Pr.

6. References:

1. A.Khan and R.Solanki., Initial unsteady free convective flow past an infinite vertical plate with radiation and mass transfer effects.Int.J.of Applied Mechanics and Engineering. 2017,22,931-943.
2. Chandrakala.P and Narayana bhaskar.P., Radiation effects on oscillating vertical plate with uniform heat and mass flux.Int.J.of Applied Mechanics and Engineering.2013,18,643-652.
3. Prasad.K.V., Mallikarjun.P, H.Vaidya, Mixed convective fully developed flow in a vertical channel in the presence of thermal radiation and viscous dissipation. Int.J.of Applied Mechanics and Engineering.2017,22,123-144.
4. Vijayakumar.A.G.,Vijayakumarvarma.S, Thermal radiation and mass transfer effects on MHD flow past an impulsively started exponentially accelerated vertical plate with variable temperature and mass diffusion.Int.J.of Mathematics and Analysis.2011,3,33-56.
5. Suneetha.S,Bhakar Reddy.N,Ramachandra Prasad.V.,Thermal radiation effects on MHD free convection flow past an impulsively started vertical plate with variable surface temperature and concentration. Journal of Naval Architecture and Marine Engineering.2008,5.
6. Chamkha.A.J.,Takhar.H.S.,Soundalgekar.V.M.,Radiation effects on free convection flow past a semi-infinite vertical plate with mass transfer. Chemical Engineering Journal.2001,84, 335-342.

7. Geetha.E.,Muthucumaraswamy.R, MHD and thermal radiation effects on linearly accelerated isothermal vertical plate with chemical reaction of first order. Int.Jounal of Innovative Research in Science, Engineering and Technology. 2013,2, issue12.
8. Uwanta.I.J., Murtala Sani, Heat and transfer flow past an infinite vertical plate with variable thermal conductivity. Int.Journal of Applied information systems.2013,6, No.1.
9. Venkateswarlu Malapati, Padma Polarapu.,Unsteady MHD free convective heat and mass transfer in a boundary layer flow past a vertical permeable plate with thermal radiation and chemical reaction. Procedia Engineering. 2015,127,791-799.
10. Rajesh.V, Mallesh.M.P., Sridevi.Ch., Transient MHD nanofluid flow and heat transfer due to a moving vertical plate with thermal radiation and temperature oscillation effects. Procedia Engineering. 2015,127,901-908.
11. Balamurugan.K.S.,Ramaprasad.J.L., Vijayakumarvarma.S, Unsteady MHD free convective flow past a moving vertical plate with time dependent suction and chemical reaction in a slip flow regime. Procedia Engineering. 2015,127,516-523.
12. Geetha.E, Sarala.S,Nirmala.M, Consequences of thermal radiation on an unsteady nanofluid Tio_2 flow past over a vertical plate. Int.Journal of Pure and Applied Mathematics. 2017,116,53-59.
13. Geetha.E,Muthucumaraswamy.R,Kothandapani.M, Effects of thermal radiation on an unsteady nanofluid flow past over an vertical plate. Int.Journal of Pure and Applied Mathematics. 2017.113,38-46.
14. Mohammed Mehdi Rashidi, Behnam Rostami, Navid Freidoonimehr, Saeid Abbasbandy, Free convective heat and mass transfer for MHD fluid flow over a permeable vertical stretching sheet in the presence of the radiation and buoyancy effects. Ain Shams Engineering Journal. 2016,5,901-912.
15. Javaherdeh.K, Mehrzad Mirzaei Nejad, Moslemi.M, Natural convection heat and mass transfer in MHD fluid flow past a moving vertical plate with variable surface temperature and concentration in a porous medium. Engineering and Technology an International Journal. 2015,18,423-431.
16. Nader Y Abd Elazem, Abdelhalm Ebald, Emad H Aly, Radiation effect of MHD on Cu-water and Ag-Water nanofluids flow over a stretching sheet; Numerical study. Applied and Computational Mathematics. 2015,4,4.

***

EFFECTS OF THERMAL RADIATION OF AN UNSTEADY CONVECTIVE $AL_2 O_3$ NANOFLUID FLOW PAST ON VERTICAL PLATE IN A POROUS MEDIUM

E.Geetha
Assistant Professor, Department of Mathematics,
Sri Chandrasekharendra Saraswathi Viswa MahaVidyalaya, Enathur, Kanchipuram.
geethamuthuo6@gmail.com

Abstract: In this paper, we have considered the thermal radiation effects of a transient free convective aluminium oxide nanofluid flow past on a vertical plate with porous medium. Here three different nanofluids Cu, $Al_2 O_3$ and TiO_2 are considered for study, to enhance the thermal conductivity of a fluid. Here the dimensional governing equations like momentum equations, energy equations are converted into the non-dimensional form by using the non-dimensional quantities. The solutions for velocity and temperature of a plate are derived by using analytical technique. The graphs are also plotted for different values of thermal grashof number, time, solid volume fraction, Prandtl number and different nanofluid and the discussed in a detailed manner.

Keywords: Thermal Radiation, Laplace Transform, Porous, Vertical Plate.

1. Introduction: Transport processes through porous media play important roles in diverse applications, such as in geothermal operations, petroleum industries, thermal insulation, design of solid-matrix heat exchangers, chemical catalytic reactors, and many others. The study of convective heat transfer and fluid flow in porous media has received great attention in recent years. The effect of radiation on Darcy's buoyancy induced flow of an optically dense viscous incompressible fluid along a heated inclined flat surface maintained at uniform temperature placed in a saturated porous medium with Rosseland diffusion approximation employing the implicit finite difference method together with Keller box elimination technique by Hossain and Pop[1]. Hsu et al. [2] have studied the natural convection flow over an inclined surface in porous medium, in which the normal component of the buoyancy force had been neglected in the momentum equations and obtained the similarity solutions for the flow , results of which are not valid for the small angles of inclination from the vertical that are not small. Hossain and Takhar [3] have investigated the radiation effect on mixed convection boundary layer flow of an optically dense viscous incompressible fluid along a vertical plate with uniform surface temperature.

A nonsimilar boundary layer analysis has been analysed for the free convection along a vertical plate embedded in a fluid-saturated porous medium in the presence of surface mass transfer and internal heat generation by Bakier et al [4]. Gorla and co-workers [5, 6] investigated the corresponding nonsimilar free convection boundary layer problem due to variations in surface temperature or heat flux. The effects of thermal dispersion and thermal radiation on the non-Darcy natural convection over a vertical flat plate in a fluid saturated porous medium are studied by Mohammadien and El-Amin [7].

Effects of thermal dispersion and lateral mass flux on non-Darcy natural convection over a vertical flat plate in a fluid saturated porous medium was studied by Murthy and Singh [8].

At high temperatures thermal radiation can significantly affect the heat transfer and the temperature distribution in the boundary layer flow of participating fluid. Gorla [9], and Gorla and Pop [10] has investigated the effects of radiation on mixed convection flow over vertical cylinders. Forced convection–radiation interaction heat transfer in boundary-layer over a flat plate submersed in a porous medium was analyzed by Mansour [11].

It is observed that no author has studied on a viscous flow of a natural convective flow of an Al_2O_3 nanofluid over an infinite isothermal vertical plate through a porous medium with radiation effect. Here the coupled nonlinear differential equations are converted into a radiation effect. Here the coupled non linear differential equations are converted into a non dimensional form and it is solved by Laplace transform. Three types of water based nanofluids containing nano particles of copper(cu), aluminum oxide (Al_2O_3) and titanium dioxide (TiO_2)have been considered in the present work. Effects of various parameters like thermal grashof number, time, radiation parameter and Prandtl number on the velocity of the plate and temperature of the fluid are discussed and the graphs are drawn and explained in a detailed manner.

2. Mathematical Analysis: The transient free convective viscous flow of an Al_2O_3 nanofluid through a porous infinite vertical plate with a radiation effect has-been considered. Further it is an unsteady flow of a viscous incompressible fluid which is initially at rest and surrounds an infinite vertical plate maintaining temperature T_∞. The x-axis is taken along the plate in the vertically upward direction and the y-axis is taken perpendicular to the plate. At time $t \leq 0$, the plate and fluid are at the same temperature T_∞. At time $t > 0$, the plate is accelerated with a velocity $u = \frac{u_0^3}{\nu_f} t'$ its own plane against gravitational field and temperature from the plate is raised to T_w. It is also assumed that a radiative heat flux q_r is applied which is normal to the plate .The fluid is a water based nanofluid containing three types nanoparticles Cu, Al_2O_3 and TiO_2. It is further assumed that the base fluid and the suspended nanoparticles are in themal equilibrium. The thermo physical properties of the nanofluids are given in table 1.

Table 1: Thermal Physical Properties of Water and Nano Particles

Physical properties	Water/base fluid	Cu(Copper)	Al_2O_3(Alumina)	TiO_2
$\rho(kg/m^3)$	997.1	8933	3970	4250
c_ρ (J/kgk)	4179	385	765	686.2
K(W/mK)	0.613	401	40	8.9538
$\beta \times 10^5(k^{-1})$	21	1.67	0.85	0.90
0	0.0	0.05	0.15	0.2
σ(S/m)	5.5×10^{-6}	59.6×10^6	35×10^6	2.6×10^6

Then under usual Boussinessq's approximation, the unsteady viscous flow of a nano fluid is governed by the following equations:

$$\rho_{nf} \frac{\partial u}{\partial t'} = g(\rho\beta)_{nf}(T - T_\infty) + \mu_{nf} \frac{\partial^2 u}{\partial y^2} - \frac{\upsilon}{k'} u \quad (1)$$

$$(\rho c_p)_{nf} \frac{\partial T}{\partial t'} = k_{nf} \frac{\partial^2 T}{\partial y^2} - \frac{\partial q_r}{\partial y} \quad (2)$$

Where u is the velocity components along the x-direction ,T the temperature of the nanofluid ,μ_{nf} the dynamic viscosity of the nanofluid, β_{nf} the thermal expansion coefficient of the nanofluid , ρ_{nf} the density of the nano fluid , K_{nf} the thermal conductivity of the nanofluid , g the acceleration due to gravity, q_r the radiative heat flux and $(\rho c_p)_{nf}$ the heat capacitance of the nanofluid which are given by

$$\mu_{nf} = \frac{\mu_f}{(1-\phi)^{2.5}}, \rho_{nf} = (1-\phi)\rho_f + \phi\rho_s$$
$$(\rho c_p)_{nf} = (1-\phi)(\rho c_p)_f + \phi(\rho c_p)_s$$
$$(\rho\beta)_{nf} = (1-\phi)(\rho\beta)_f + \phi(\rho\beta)_s \quad (3)$$

Where Φ is the solid volume fraction of the nano particle, ρ the density of the base fluid ,ρ_s the density of the nanoparticle, μ_f the viscosity of the base fluid, $(\rho c_p)_f$ the heat capacitance of the base fluid and $(\rho c_p)_s$ the heat capacitance of the nanoparticle. It is worth mentioning that the expressions (1) are restricted to spherical nanoparticles, where it does not account for other shapes of nano particles. The effective thermal conductivity of the nanofluid given by Hamilton and crosser model followed by kakae and Pramuanjaroenkij [12], and oztop and Abu-nada [13] is given by

$$k_{nf} = k_f \left[\frac{k_s + 2k_f - 2\phi(k_f - k_s)}{k_s + 2k_f + \phi(k_f - k_s)} \right] \quad (4)$$

Where k_f is the thermal conductivity of the base fluid and k_s the thermal conductivity of the nanoparticle. In Eqs.(1)-(4), the subscripts *nf*, *f* and *s* denote the thermophysical properties of the nano fluid ,basefluid and nano particles, respectively.
The local radiant for the case of an optically thin gray gas is expressed by

$$\frac{\partial q_r}{\partial y} = -4a^* \sigma\left(T_\infty^4 - T^4\right) \quad (5)$$

It is assume that the temperature differences within the flow are sufficiently small such that T^4 may be expressed as a linear function of the temperature .This is accomplished by expanding T^4 in a Taylor series about T_∞ and neglecting higher-order terms, thus

$$T^4 \cong 4T_\infty^3 T - 3T_\infty^4 \quad (6)$$

By using equations (6) and (7) ,equation (2) reduces to

$$(\rho c_p)_{nf} \frac{\partial T}{\partial t'} = k_{nf} \frac{\partial^2 T}{\partial y^2} + 16a^*\sigma T_\infty^3 (T_\infty - T) \quad (7)$$

The initial and boundary conditions of the proposed problem are given by:

$$\begin{aligned} & u = 0, && T = T_\infty && \text{for all} && y, t' \le 0 \\ t' > 0: \quad & u = \frac{u_0^3}{\nu_f} t', && T = T_\omega && \text{at} && y = 0 \\ & u \to 0 && T \to T_\infty && \text{as} && y \to \infty \end{aligned} \quad (8)$$

On introducing the following non dimensional quantities are:

$$U = \frac{u}{u_0}, \quad t = \frac{t' u_0^2}{\nu_f}, \quad Y = \frac{y u_0}{\nu_f}, \quad (9)$$

$$\theta = \frac{T - T_\infty}{T_w - T_\infty},\ Gr = \frac{g\, v_f \beta (T_w - T_\infty)}{u_0^{\,3}},\ R = \frac{16\, a^*\, \sigma T_\infty^{\,3}}{k_f}\left(\frac{v_f^{\,2}}{u_0^{\,2}}\right), \Pr = \frac{\mu c_p}{k_f}$$

By using equations (3), (4) and (9),equations (1) and (7) leads to,

$$L_1 \frac{\partial U}{\partial t} = L_3 \frac{\partial^2 U}{\partial Y^2} + L_2 Gr\theta$$

$$L_5 \frac{\partial \theta}{\partial t} = L_6 \frac{1}{\Pr}\frac{\partial^2 \theta}{\partial Y^2} - \frac{R}{\Pr}\theta \qquad (10)$$

Where $L_1 = (1-\phi) + \phi\left(\frac{\rho_s}{\rho_f}\right), L_2 = (1-\phi) + \phi\left(\frac{(\rho\beta)_s}{(\rho\beta)_f}\right), L_3 = \frac{1}{(1-\phi)^{2.5}}$

$$L_5 = (1-\phi) + \phi\left(\frac{(\rho c_p)_s}{(\rho c_p)_f}\right), L_6 = \left[\frac{k_s + 2k_f - 2\phi(k_f - k_s)}{k_s + 2k_f + \phi(k_f - k_s)}\right] \qquad (11)$$

Where R is the radiation parameter, pr is the Prandtl number, Gr is the thermal grashof number, Gr approximates the ratio of the buoyancy force to the viscous force acting, Large R signifies a large radiation effect while R→o corresponds to zero radiation effect.
The corresponding initial and boundary conditions are,

$$\begin{array}{lllll} & U = 0, & \theta = 0, & for\ all & Y, t \le 0 \\ t > 0: & U = gt, & \theta = 1, & at & Y = 0 \\ & U \to 0, & \theta \to 0, & as & Y \to \infty \end{array} \qquad (12)$$

Where $g = \frac{L_1}{L_3}$

Methods of solutions

Equation (10) is solved subject to the initial and boundary conditions with the help of laplace transform analytically. The exact solutions are expressed in terms of exponential function and complementary error function.

$$\theta = \frac{1}{2}\left[\exp(2\eta\sqrt{abt})\ erfc\left(\eta\sqrt{a} + \sqrt{bt}\right) + \exp(-2\eta\sqrt{abt})\ erfc\left(\eta\sqrt{a} - \sqrt{bt}\right)\right] \qquad (13)$$

$$U = \frac{gt}{2}\begin{bmatrix}\exp(2\eta\sqrt{ht})\ erfc\left(\eta\sqrt{g}+\sqrt{ht}\right)\\ +\exp(-2\eta\sqrt{ht})\ erfc\left(\eta\sqrt{g}-\sqrt{ht}\right)\end{bmatrix}$$
$$-\frac{\eta\sqrt{g}\sqrt{t}}{2\sqrt{h}}\begin{bmatrix}\exp(-2\eta\sqrt{ht})\ erfc\left(\eta\sqrt{g}-\sqrt{ht}\right)\\ +\exp(2\eta\sqrt{ht})\ erfc\left(\eta\sqrt{g}+\sqrt{ht}\right)\end{bmatrix}$$
$$+\frac{c}{2d}\begin{bmatrix}\exp(2\eta\sqrt{ght})\ erfc\left(\eta\sqrt{g}+\sqrt{ht}\right)\\ +\exp(-2\eta\sqrt{ght})\ erfc\left(\eta\sqrt{g}-\sqrt{ht}\right)\end{bmatrix}$$
$$-\frac{c\exp(dt)}{2d}\begin{bmatrix}\exp(2\eta\sqrt{g(h+d)t})\ erfc\left(\eta\sqrt{g}+\sqrt{(h+d)t}\right)\\ +\exp(-2\eta\sqrt{g(h+d)t}\ erfc\left(\eta\sqrt{g}-\sqrt{(h+d)t}\right)\end{bmatrix}$$
$$-\frac{c}{2d}\begin{bmatrix}\exp(2\eta\sqrt{abt})\ erfc\left(\eta\sqrt{a}+\sqrt{bt}\right)\\ +\exp(-2\eta\sqrt{abt})\ erfc\left(\eta\sqrt{a}-\sqrt{bt}\right)\end{bmatrix}$$
$$+\frac{c\exp(dt)}{2d}\begin{bmatrix}\exp(2\eta\sqrt{a(b+d)t})\ erfc\left(\eta\sqrt{a}+\sqrt{(b+d)t}\right)\\ +\exp(-2\eta\sqrt{a(b+d)t})\ erfc\left(\eta\sqrt{a}-\sqrt{(b+d)t}\right)\end{bmatrix} \quad (14)$$

Where $a=\frac{L_5\,\mathrm{Pr}}{L_6}, b=\frac{R}{L_5\,\mathrm{Pr}}, c=\frac{L_2 Gr}{L_1-L_3 a}, d=\frac{L_3 ab}{L_1-L_3 a}, g=\frac{L_1}{L_3}, h=\frac{1}{KL_1}$

3. Results and Discussion: In order to get physical insight in to the problem, the computed values of different parameters like thermal Grashof number, Prandtl number, time, volume solid fraction and radiation parameter on the temperature of the fluid and velocity of the plate are considered and it is depicted in graph. The effects are explained in a detailed manner. By changing the values of various parameters for the above expression, the numerical values are computed until they converge to free stream boundary conditions. We have considered three different types of nanofluids containing Copper (Cu), Aluminum oxide (Al_2O_3) and Titanium oxide (TiO_2) with water as a base fluid. The nanoparticle volume fraction is considered in the range of $0 \le \Phi \le 0.2$. In this study, we have considered spherical nanoparticles with thermal conductivity and dynamic viscosity shown in model I in table 2.

Table 2: Thermal Conductivity and Dynamic Viscosity for Various Shapes of Nanoparticles

Model	Shape Of Nanoparticles	Thermal Conductivity	Dynamic Viscosity
I	Spherical	$\frac{k_{nf}}{k_f}=\frac{k_s+2k_f-2\phi(k_f-k_s)}{k_s+2k_f+\phi(k_f-k_s)}$	$\mu_{nf}=\frac{\mu_f}{(1-\phi)^{2.5}}$
II	Spherical (nanotubes)	$\frac{k_{nf}}{k_f}=\frac{k_s+2k_f-2\phi(k_f-k_s)}{k_s+2k_f+\phi(k_f-k_s)}$	$\mu_{nf}=\mu_f(1+7.3\phi+12.3\phi^2)$
III	Cylindrical	$\frac{k_{nf}}{k_f}=\frac{k_s+\frac{1}{2}k_f-\frac{1}{2}\phi(k_f-k_s)}{k_s+\frac{1}{2}k_f+\phi(k_f-k_s)}$	$\mu_{nf}=\frac{\mu_f}{(1-\phi)^{2.5}}$

IV	Cylindrical(nanotubes)	$\frac{k_{nf}}{k_f} = \frac{k_s + \frac{1}{2}k_f - \frac{1}{2}\phi(k_f - k_s)}{k_s + \frac{1}{2}k_f + \phi(k_f - k_s)}$	$\mu_{nf} = \mu_f(1 + 7.3\phi + 12.3\phi^2)$

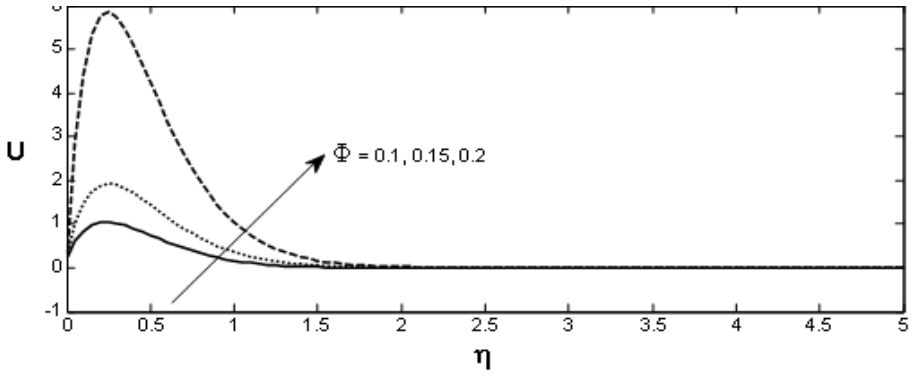


Fig.3.1 Velocity profiles for different values of Φ

Fig.3.1 explains the effect of volume of solid fraction (Φ = 0.1, 0.15, 0.2) parameter of Al_2O_3-water nanoparticles on the velocity profile and it can be easily seen that the velocity profile increases with increasing values of volume solid fraction. It is also revealed that the increase in the value of Φ results in the increase of velocity of the plate.

Fig.3.2 shows that the velocity profile of Al_2O_3-water nanoparticles for various values of Prandtl number (Pr = 0.71, 6.2, 7.1) with coordinate η. The values of different parameters t= 0.2, Gr = 5, ∅ = 0.1 is considered. It is noticed that velocity of the plate increases for the increasing values of Prandtl number.

The effect of radiation parameter (R=0.5, 1, 2) on the velocity profile is considered when Pr=0.71 which correspond to air ,thermal grashof number Gr=5 and time t=0.5. It is noticed that the velocity profile enhances as the value of radiation parameter increases is noticed in Fig.3.3.

The value profile increases sharply and it remains respective maxima, the curve's settle down to the corresponding asymptotic value, is observed in Fig.3.4 and it shows the influence of Al_2O_3-water nanoparticles on the velocity profile for the different time (t=0.1,0.2,0.3). It is also observed that whenever the time increases, the velocity of the plate also increases.

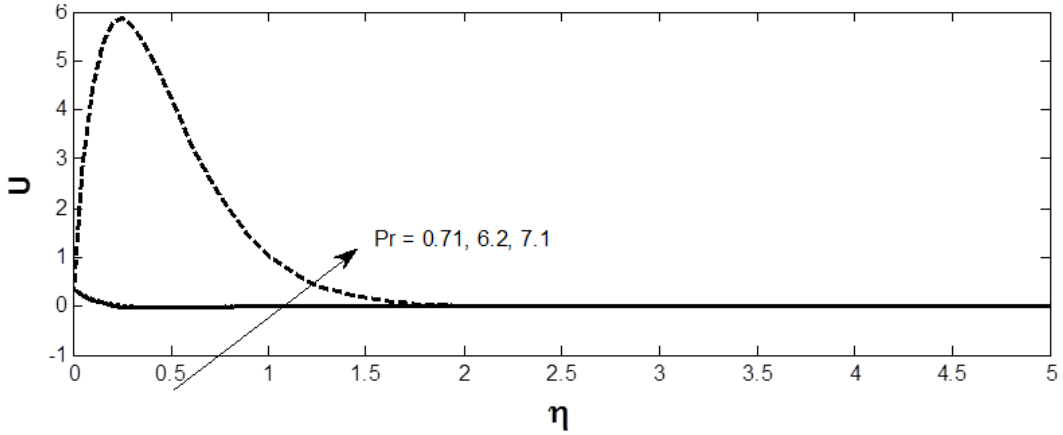


Fig.3.2 Velocity profiles for different values of Pr

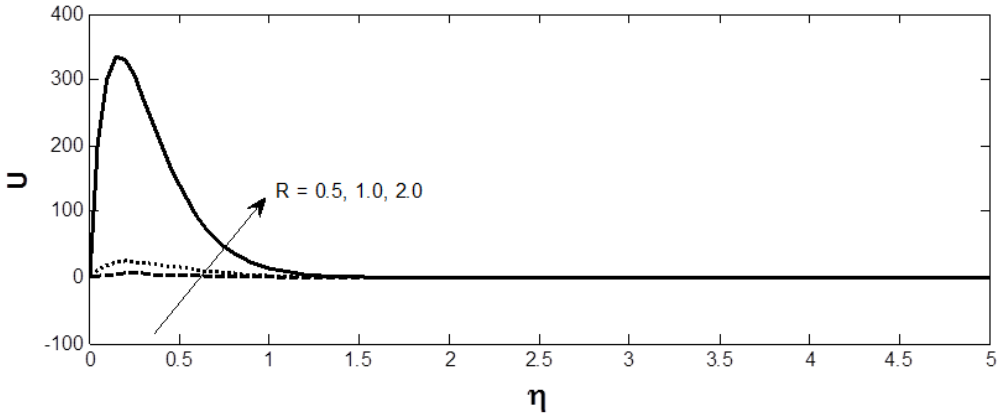


Fig.3.3 Velocity profiles for different values of R

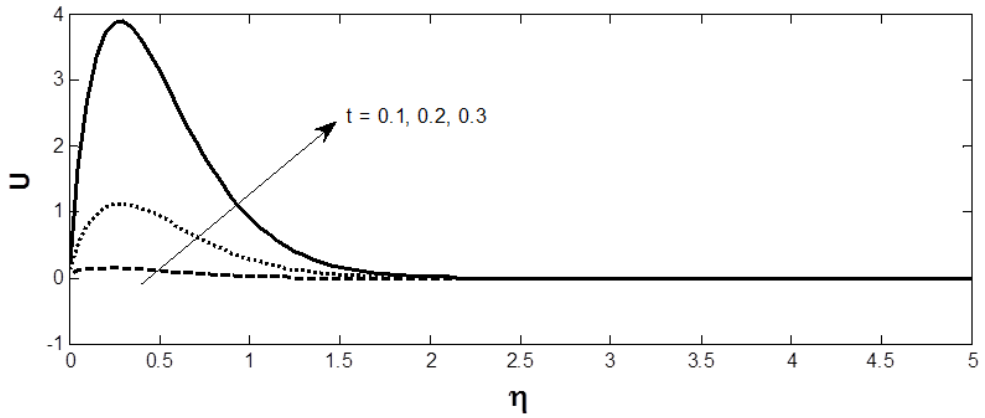


Fig.3.4 Velocity profiles for different values of t

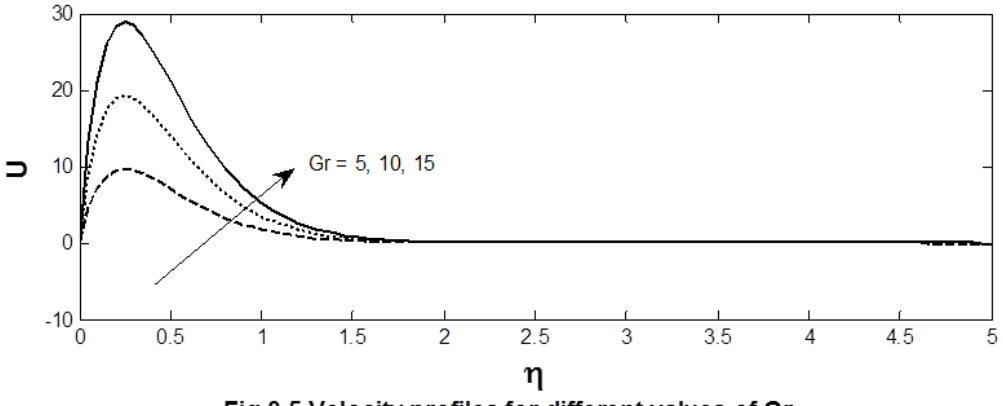


Fig.3.5 Velocity profiles for different values of Gr

The velocity profiles of Al_2O_3-water nanofluid with coordinate η for different values of thermal grashof number, radiation parameter ,time and volume solid fraction when Pr=0.71 are presented in, the effect of thermal grashof number on the velocity profile is shown in Fig.3.5 Thermal grashof number is the ratio

of the buoyancy force due to spatial variation in the fluid density to the viscous force and grashof number (Gr = 5, 10, 15) represents the cooling effect near the plate. It is noticed that the velocity increases with increasing values of thermal grashof number.

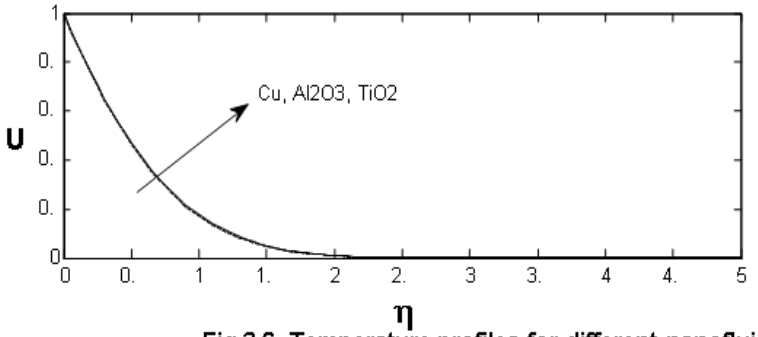


Fig.3.6. Temperature profiles for different nanofluids

Fig.3.6 reveals that the fluid temperature variations for the three types of water based nanofluids Al_2O_3 – water and TiO_2 -water when Pr=0.71 and Gr=5 at t=0.5.Due to higher thermal conductivity of Cu-water nanofluids, the temperature of Cu-water nanofluid is found to be higher than Al_2O_3 –water and TiO_2 – water nanofluids .It is also seen that the thermal boundary layer thickness is more for Al_2O_3 -water than Cu – water and TiO_2 – water nanofluids.

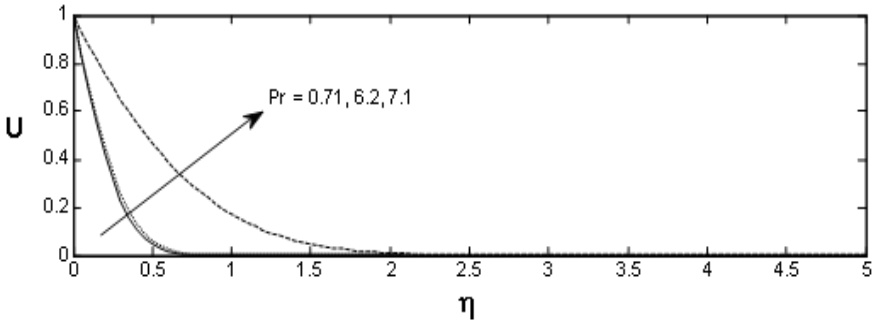


Fig.3.7. Temperature profiles for different values of Pr

In Fig. 3.7. temperature profile for different values of Prandtl number (Pr = 0.71 ,3, 7.1) is presented when R=3,Gr=5 at t=0.5. The size of the thermal boundary layer increases with increasing Prandtl number because the Boussinesq's approximation in the momentum equation consists of assuming that density of the fluid varies with temperature linearly.

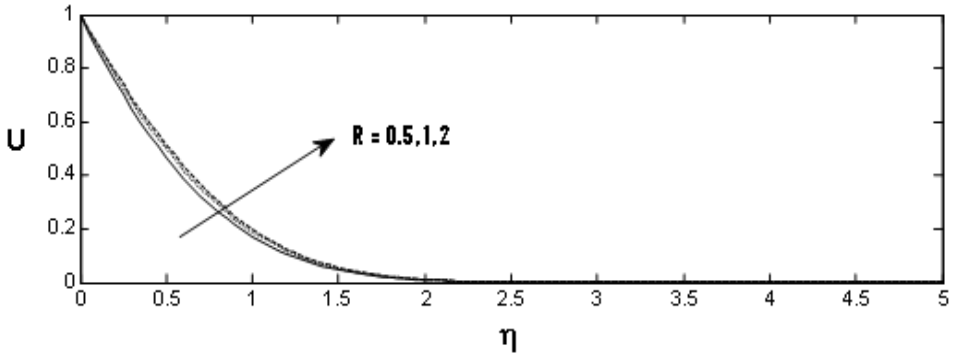


Fig.3.8. Temperature profiles for different values of

Here temperature profile gradually reduces to reach the free stream temperature which is shown in Fig.3.8. It can be seen that the effect of radiation parameter (R=0.5,1,2) on the temperature profile when Pr=0.71,Gr=5 at t=0.5.The increase in radiation parameter means the exhausting of heat energy from the flow region and so the temperature of the fluid increases.

Conclusion: The transient free convective Al_2O_3 nanofluid flow of a isothermal vertical plate in the presence of thermal radiation with porous medium was considered. The coupled governing equations are solved by using laplace transform technique. The effect of various parameters like Thermal grashof number, time Prandtl number, Radiation parameter on the velocity of the plate and temperature of the fluid are discussed in a detailed way and graphs are also depicted and the conclusions are as follows:

1. An increase in the radiation parameter as well as Prandtl number leads to the decrease in the temperature of the fluid.
2. An increase in the volume solid fraction, time, radiation parameter, Prandtl number and thermal grashof number leads to an increase in the velocity of the plate.

References:

1. M. A. Hossain, I. Pop., "Radiation effect on Darcy free convection flow along an inclined surface placed in porous media". Heat and Mass Transfer 32 (1997) 223–227.
2. Hsu, C. T.; Cheng, P.; Homsy, G. M.: "Instability of free convection flow over a horizontal impermeable surface in a porous medium". Int. J. Heat Mass Transfer 21 (1978) 1221–1228.
3. Hossain, M. A.; Takhar, H. S. "Radiation effect on mixed convection along a vertical plate with uniform surface temperature". Heat and Mass Transfer 31 (1996)
4. A. Y. Bakier, M. A. Mansour, R. S. R. Gorla, A. B. Ebiana., "Nonsimilar solutions for free convection from a vertical plate in porous media". Heat and Mass Transfer 33 (1997) 145-148.
5. Gorla, R. S. R.; Zinolabedini, A. "Free convection from a vertical plate with nonuniform surface temperature and embedded in a porous medium". Transactions of ASME, J Energy Resources Technology 109 (1987) 26-30
6. Gorla, R. S. R.; Tornabene, R. "Free convection from a vertical plate with nonuniform surface heat flux and embedded in a porous medium". Transport in Porous Media 3: (1988) 95-106.
7. A. A. Mohammadien and M. F. El-amin., "Thermal Dispersion–Radiation Effects on Non-Darcy Natural Convection in a Fluid Saturated Porous Medium". Transport in Porous Media 40: (2000) 153–163.
8. Murthy, P. V. S. N. and Singh, P. "Thermal dispersion effects on non-Darcy natural convection with lateral mass flux", Heat and Mass Transfer 33 (1997), 1–5.
9. Gorla, R. S. R. "Radiative effect on conjugate forced convection and conductive heat transfer in a circular pin", Int. J. Heat Fluid Flow 9 (1988), 49–51.
10. Gorla, R. S. R. and Pop, I., "Conjugate heat transfer with radiation from vertical circular pin in a non-Newtonian ambient medium", Warme-und Stoffubertragung 28 (1993), 11–15.
11. Mansour, M. A., "Forced convection radiation interaction heat transfer in boundary layer over a flat plate submersed in a porous medium", Appl. Mech. Engng 2 (1997), 405–413.
12. S. Kakac and A. Pramuanjaroenkij, "Review of convective heat transfer enhancement with nanofluids", Int. J. Heat Mass Transfer 52 (2009) 3187–3196.
13. F. Oztop and E. Abu-Nada, "Numerical study of natural convection in partially heated rectangular enclosures filled with nanofluids", Int. J. Heat Fluid Flow 29 (2008) 1326–1336.

***

EFFECTS OF HEAT TRANSFER OF AN UNSTEADY NANOFLUID FLOW PAST OVER AN ISOTHERMAL VERTICAL PLATE IN THE PRESENCE OF THERMAL RADIATION

E.Geetha

Assistant Professor, Department of Mathematics, Sri Chandrasekharendra Saraswathi Viswa MahaVidyalaya, Enathur, Kanchipuram, geethamuthuo6@gmail.com

Abstract: In this paper,heat transfer effects on the unsteady nanofluid flow past on a vertical plate in the presence of thermal radiation with uniform temperature has been studied. The exact analytical solutions are derived for different water-based nanofluids containing Cu, Al $_2O_3$, and TiO_2. The dimensional form of governing equations for momentum and energy equations are considered. The nondimensional governing equations are solved by laplace transform analytically. Solutions for temperature and velocity of the plate are obtained and the effects of various different parameters like Prandtl number, Radiation parameter, Thermal Grashof number and time on velocity of the plate are depicted graphically and discussed.

1. Introduction: Conventional heat transfer fluids, for example oil, water, and ethylene glycol mixtures, are fluids whose heat transfer is poor because of their poor thermal conductivity. Application of these fluids as a cooling tool enhances manufacturing and operating costs. Many attempts have been taken by many researchers to intensify the thermal conductivity of these fluids by suspending nano/micro particles in liquids [3], [9]. Nanofluids are made of ultrafine nanoparticles (100 nm) enervated in a base fluid, which can be water or an organic solvent [10]. Nanofluids are found to exhibit higher conductive, minimum clogging, boiling, and convective heat transfer performances compared to conventional fluids [5], [21], [28]. There are several industrial and engineering applications of nanofluids such as chemical production, solar and power plant cooling, cooling of transformer oil, production of microelectronics, automotive and air conditioning frosting, advanced nuclear systems, nano-drug delivery, micro fluidics, transportation, biomedicine, solid –state lighting and manufacturing [7].

The free convective flow of a nanofluid over a vertical plate under different boundary condition has been investigated by several researchers [1], [2], [4], [13], [15], [17], [18], [19], [22]. Ho et al. [15] studied natural convective flow of a nanofluid under various flow configurations. The recent book by Das et al [11] and more recent review paper by Kakac and Pramuanjaroenkij [16] examined an excellent aggregation of the study done on nanofluids. Oztop and Abu-Nada [23] analyzed the numerical study of free convection in partially heated rectangular enclosures filled with nanofluids using different types of nanoparticles. Mohammed J. Uddin et al [20] examined hydrodynamic Free Convective Boundary Layer Flow of a Nanofluid over a Flat Vertical Plate with Newtonian Heating Boundary Condition. Khan and Pop [18] have proposed the problem of laminar fluid flow over the stretching surface in a nanofluid and they investigated it numerically. Anjali Devi and Julie Andrews [6] studied the streamline boundary layer flow of nanofluid over a flat plate and it was found out that the suspended nanoparticles of the nanofuid enhance the heat transfer capacity of the fluids. The convective flow and heat transfer of an incompressible viscid nanofluid past a semi-infinite vertical stretching sheet in the presence of a magnetic field was examined by Hamad [14].

Tzou [26], [27] presented the thermal instability of nanofluids in natural convection. Recently, Bachok et al. [8] studied the flow in a boundary layer of a nanofluid past a moving surface in a flowing fluid. Polidori et al. [24] studied the free convection heat transfer of Newtonian nanofluids in streamline boundary layers using the integral approach, for the case of γ –Al_2O_3/water nanofluids whose Newtonian behaviour with particle volume fractions was less than 4%. They showed that heat transfer by free

convection is not only representing by the nanofluid's effective thermal conductivity but also that the sensitivity to the viscosity model exerts a major role in the heat transfer behaviour. Yacob [29] demonstrated the mixed convection of fluid flow and heat transfer over a stretching vertical surface immersed in a nanofluid. Srikanth et al [25] investigated theoretically the hydrodynamic flow of a nanofluid past an inclined permeable plate with constant heat source and thermal radiation.

To the authors' knowledge, no study has been communicated on a unsteady natural convective flow of a nanofluid with thermal radiation on a infinite isothermal vertical plate. In this study, a free convective flow of a nanofluid on an infinite vertical plate with thermal radiation has been considered. The coupled nonlinear partial differential equations are converted into a non dimensional form and the solutions are derived by using the Laplace transform. Three types of water based nanofluids containing nanoparticles of copper (Cu), aluminum oxide (Al_2O_3) and titanium dioxide (TiO_2) have been considered in the present work. The governing equations are solved analytically and presented in closed form. The effects on temperature of the plate and the velocity of the plate by the various parameters like thermal radiation parameter, Grashof number, Prandtl number and time are shown graphically and discussed in a detailed manner.

2. Mathematical Analysis: The viscous flow of a incompressible nanofluid past an uniformly accelerated isothermal vertical infinite plate in the presence of thermal radiation has been considered. Further it is an unsteady flow of a viscous incompressible fluid which is initially at rest and surrounds an infinite vertical plate maintaining temperature T_∞ and concentration $C_\infty^{/}$. The *x*-axis is considered along the plate in the vertically upward direction and the *y*-axis is assigned normal to the plate. At time $t^{/} \le 0$, the plate and fluid are at the same temperature T_∞. At time $t^{/} > 0$, the plate is accelerated with a velocity its own plane against gravitational field and the temperature from the plate is raised to T_w and the concentration levels near the plate are also raised to $C_w^{/}$. It is also assumed that a radiative heat flux q_r is applied in the normal direction to the plate. The fluid is a water based nanofluid containing three types' nanoparticles Cu, Al_2O_3 and TiO_2. It is further assumed that the base fluid and the suspended nanoparticles of nanofluids are in thermal equilibrium. The thermophysical properties of the nanofluids are given in Table 1.

Table 1: Thermo Physical Properties of Water and Nanoparticles [12]

Physical properties	Water/Base fluid	Cu(Copper)	Al_2O_3 (Alumina)	TiO_2
ρ (kg / m^3)	997.1	8933	3970	4250
c_ρ (J / kgK)	4179	385	765	686.2
K(W / mK)	0.613	401	40	8.9538
β x 10^5 (K^{-1})	21	1.67	0.85	0.90
ϕ	0.0	0.05	0.15	0.2
σ (S / m)	5.5 x 10^{-6}	59.6 x 10^6	35 x 10^6	2.6 x 10^6

.

Then under usual Boussinesq's approximation the unsteady flow is governed by the following equations:

$$\rho_{nf}\frac{\partial u}{\partial t'} = g(\rho\beta)_{nf}(T - T_\infty) + \mu_{nf}\frac{\partial^2 u}{\partial y^2} \quad (1)$$

$$(\rho c_p)_{nf}\frac{\partial T}{\partial t'} = k_{nf}\frac{\partial^2 T}{\partial y^2} - \frac{\partial q_r}{\partial y} \quad (2)$$

where u is the velocity components along the x-direction, T the temperature of the nanofluid, μ_{nf} the dynamic viscosity of the nanofluid, β_{nf} the thermal expansion coefficient of the nanofluid, ρ_{nf} the

density of the nanofluid, k_{nf} the thermal conductivity of the nanofluid, g the acceleration due to gravity, q_r the radiative heat flux and $(\rho c_p)_{nf}$ the heat capacitance of the nanofluid which are given by

$$\mu_{nf} = \frac{\mu_f}{(1-\phi)^{2.5}}, \rho_{nf} = (1-\phi)\rho_f + \phi\rho_s$$
$$(\rho c_p)_{nf} = (1-\phi)(\rho c_p)_f + \phi(\rho c_p)_s \quad (3)$$
$$(\rho\beta)_{nf} = (1-\phi)(\rho\beta)_f + \phi(\rho\beta)_s$$

where ϕ is the solid volume fraction of the nanoparticle, ρ_f the density of the base fluid, ρ_s the density of the nanoparticle, μ_f the viscosity of the base fluid, $(\rho c_p)_f$ the heat capacitance of the base fluid and $(\rho c_p)_s$ the heat capacitance of the nanoparticle. It is worth mentioning that the expressions (1) are restricted to spherical nanoparticles, where it does not count for other shapes of nanoparticles. The effective thermal conductivity of the nanofluid given by Hamilton and Crosser model followed by Kakac and Pramuanjaroenkij [18], and Oztop and Abu-Nada [19] is given by

$$k_{nf} = k_f \left[\frac{k_s + 2k_f - 2\phi(k_f - k_s)}{k_s + 2k_f + \phi(k_f - k_s)} \right] \quad (4)$$

where k_f is the thermal conductivity of the base fluid and k_s the thermal conductivity of the nanoparticle. In Eqs. (1)–(4), the subscripts nf, f and s denote the thermophysical properties of the nanofluid, base fluid and nanoparticles, respectively.

The initial and boundary conditions of the proposed problem are given by:

$$\begin{array}{lllll} & u = 0, & T = T_\infty, & C' = C'_\infty & \text{for all} \quad y, t' \le 0 \\ t' > 0: & u = \frac{u_0^3}{\nu_f} t', & T = T_\omega, & C' = C'_\omega & \text{at} \quad y = 0 \\ & u \to 0 & T \to T_\infty, & C' \to C'_\infty & \text{as} \quad y \to \infty \end{array} \quad (5)$$

On introducing the following non dimensional quantities are:

$$U = \frac{u}{u_0}, \quad t = \frac{t' u_0^2}{\nu_f}, \quad Y = \frac{y u_0}{\nu_f}, \quad (6)$$

$$\theta = \frac{T - T_\infty}{T_w - T_\infty}, \quad Gr = \frac{g \nu_f \beta (T_w - T_\infty)}{u_0^3}, \quad R = \frac{16 a^* \sigma T_\infty^3}{k_f} \left(\frac{\nu_f^2}{u_0^2} \right), \quad \Pr = \frac{\mu c_p}{k_f}$$

The local radiant for the case of an optically thin gray gas is expressed by

$$\frac{\partial q_r}{\partial y} = -4a^* \sigma \left(T_\infty^4 - T^4 \right) \quad (7)$$

It is assume that the temperature differences within the flow are sufficiently small such that T^4 may be expressed as a linear function of the temperature. This is accomplished by expanding T^4 in a Taylor series about T_∞ and neglecting higher-order terms, thus

$$T^4 \cong 4T_\infty^3\, T - 3T_\infty^4 \tag{8}$$

By using equations (6) and (7), equation (2) reduces to

$$(\rho\, c_p)_{nf}\, \frac{\partial T}{\partial t'} = k_{nf}\, \frac{\partial^2 T}{\partial y^2} + 16a^*\sigma T_\infty^3\, (T_\infty - T) \tag{9}$$

By using equations (3),(4) and (6), equations (1) and (9) leads to,

$$L_1 \frac{\partial U}{\partial t} = L_3 \frac{\partial^2 U}{\partial Y^2} + L_2 Gr\theta$$
$$L_5 \frac{\partial \theta}{\partial t} = L_6 \frac{1}{\mathrm{Pr}} \frac{\partial^2 \theta}{\partial Y^2} - \frac{R}{\mathrm{Pr}}\theta \tag{10}$$

Where $L_1 = (1-\phi) + \phi\left(\frac{\rho_s}{\rho_f}\right), L_2 = (1-\phi) + \phi\left(\frac{(\rho\beta)_s}{(\rho\beta)_f}\right), L_3 = \frac{1}{(1-\phi)^{2.5}}$

$$L_5 = (1-\phi) + \phi\left(\frac{(\rho c_p)_s}{(\rho c_p)_f}\right), L_6 = \left[\frac{k_s + 2k_f - 2\phi(k_f - k_s)}{k_s + 2k_f + \phi(k_f - k_s)}\right] \tag{11}$$

Where R is the radiation parameter, Pr is the Prandtl number, Gr is the thermal Grashof number, Gr approximates the ratio of the buoyancy force to the viscous force acting. Large R signifies a large radiation effect while R→o corresponds to no radiaton effect.

The corresponding initial and boundary conditions are,

$$\begin{array}{lllll} & U = 0, & \theta = 0, & for\ all & Y, t \le 0 \\ t > 0: & U = gt, & \theta = 1, & at & Y = 0 \\ & U \to 0, & \theta \to 0, & as & Y \to \infty \end{array} \tag{12}$$

Where $g = \frac{L_1}{L_3}$

Solution Procedure: The solutions are in terms of exponential and complementary error function. The relation connecting error function and its complementary error function is as follows:

erfc(x) =1- erf(x) (13)

The dimensionless governing equations (10), subject to the initial and boundary conditions (12), are solved by the usual Laplace-transform technique and the solutions are derived as follows:

$$\theta = \frac{1}{2}\left[\exp(2\eta\sqrt{abt})\ erfc\left(\eta\sqrt{a} + \sqrt{bt}\right) + \exp(-2\eta\sqrt{abt})\ erfc\left(\eta\sqrt{a} - \sqrt{bt}\right)\right] \tag{14}$$

$$U = gt\left[(1+2\eta^2 g)erfc(\eta\sqrt{g}) - \frac{2\eta\sqrt{g}}{\sqrt{\pi}}\exp(-\eta^2 g)\right]$$
$$+\frac{c}{d}\left[erfc(\eta\sqrt{g}) - \frac{1}{2}\left[\begin{matrix}\exp(2\eta\sqrt{abt})\ erfc\left(\eta\sqrt{a}+\sqrt{bt}\right)\\ +\exp(-2\eta\sqrt{abt})\ erfc\left(\eta\sqrt{a}-\sqrt{bt}\right)\end{matrix}\right]\right] \qquad (15)$$
$$+\frac{c\exp(dt)}{2d}\left[\begin{matrix}\left[\begin{matrix}\exp(2\eta\sqrt{gdt})\ erfc\left(\eta\sqrt{g}+\sqrt{dt}\right)\\ +\exp(-2\eta\sqrt{gdt})\ erfc\left(\eta\sqrt{g}-\sqrt{dt}\right)\end{matrix}\right]\\ -\left[\begin{matrix}\exp(2\eta\sqrt{a(b+d)t})\ erfc\left(\eta\sqrt{a}+\sqrt{(b+d)t}\right)\\ +\exp(-2\eta\sqrt{a(b+d)t})\ erfc\left(\eta\sqrt{a}-\sqrt{(b+d)t}\right)\end{matrix}\right]\end{matrix}\right]$$

Where $a = \frac{L_5\,\mathrm{Pr}}{L_6}, b = \frac{R}{L_5\,\mathrm{Pr}}, c = \frac{L_2 Gr}{L_1 - L_3 a}, d = \frac{L_3 ab}{L_1 - L_3 a}, g = \frac{L_1}{L_3}$

3. Results and Discussion: The extensive numerical computations are conducted for various values of the thermo physical parameters are depicted in graphs. We consider three different types of nanofluids containing aluminium oxide, copper and titanium oxide nanoparticles with water as a base fluid. The values of volume fraction of nanoparticles considered to be in the range $0 \le \phi \le 0.2$. The case $\phi = 0$ corresponds to the regular fluid .i.e. nanoscale characteristics are eliminated.

Effects of Parameters on Velocity Profiles: Fig.3.1 shows that the effect of solid volume fraction ϕ (0.2, 0.15, 0.1) of nanoparticles on the fluid velocity with Pr = 7.1, Gr = 5, R = 3, t = 0.3. The fluid velocity U increases for decreasing values of ϕ, results that in the increase of the momentum boundary layer thickness. In Fig. 3.2. Velocity profile for different values of Prandtl number (Pr = 2.1, 5.1, 7.1) in presented when Gr = 5, t = 0.2, $\phi = 0.1$, R = 3. Here Velocity profile gradually reduces for increasing values of Prandtl number.

The velocity profiles of Al_2O_3 – Water with coordinate η for different values of radiation parameter (R = 2, 6, 10) with $\phi = 0.1$, t = 0.2, Gr = 5, Pr = 7.1. is kept at constant which is depicted in Fig. 3.3. It explains that the velocity U increases with an increasing values of thermal radiation R.

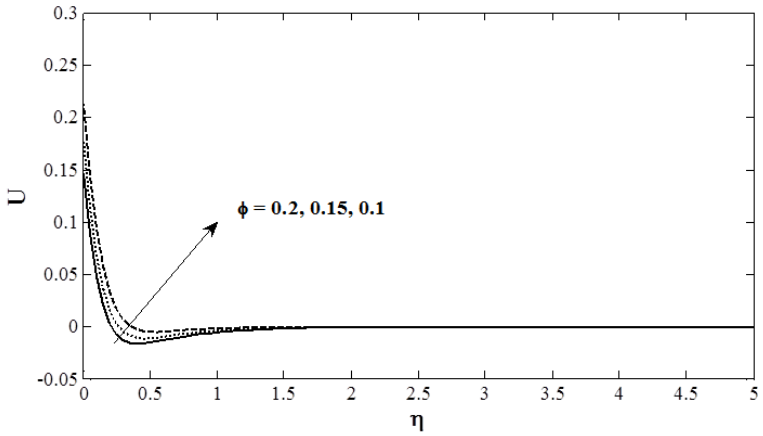


Fig.3.1 Velocity profile for different values of ϕ

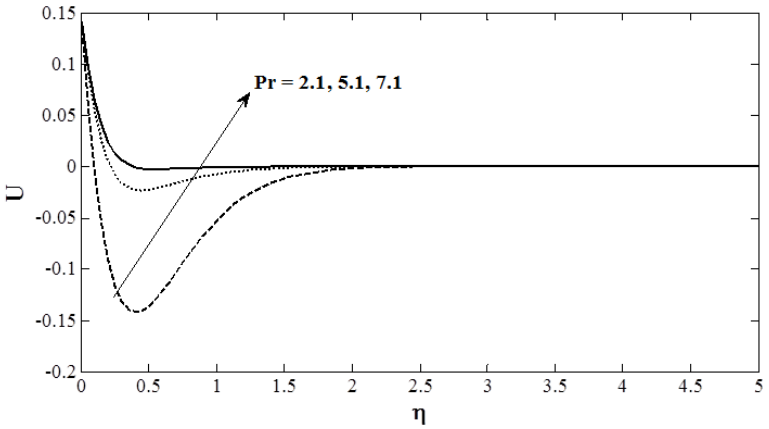


Fig.3.2 Velocity profile for different values of Pr

The velocity profiles of $Al_2 O_3$ – Water with coordinate η for different values of time (t= 0.2, 0.4, 0.6) are depicted in graph which are shown in Fig. 3.4 when $\phi = 0.1$, Pr = 7.1, Gr = 5, R = 3 is kept at constant. Fig.3.4 reveals that the velocity of the plate increases with an increasing value of time.

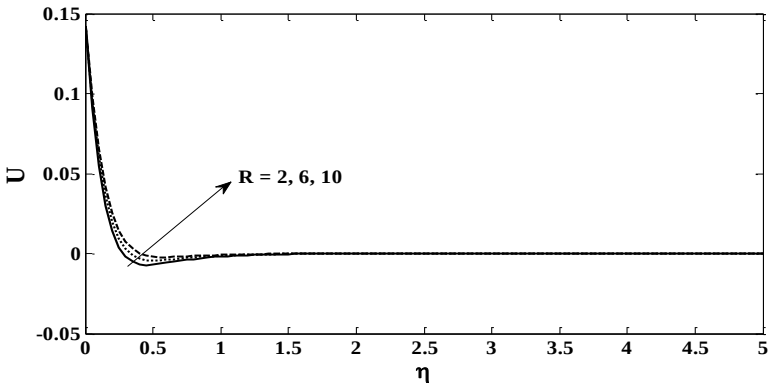


Fig.3.3 Velocity profile for different values of R

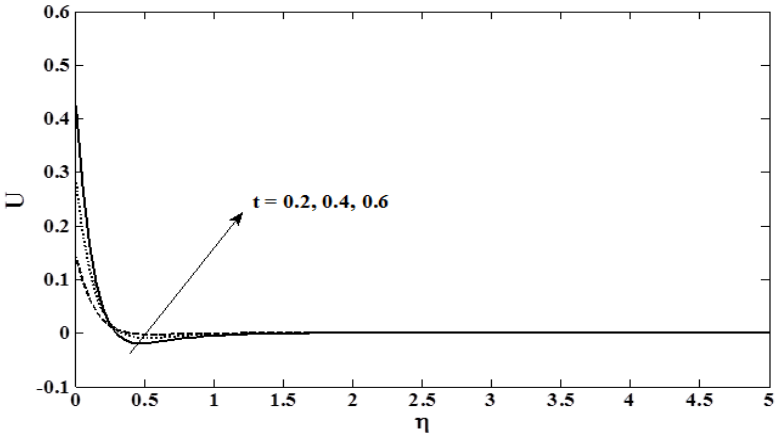


Fig.3.4 Velocity profile for different values of t

The velocity profiles for different types of nanoparticles (Cu, Al_2O_3 and TiO_2) and constant solid volume fraction Pr = 7.1, $\phi = 0.1$, t = 0.2, R = 3 are taken and graph is plotted which is shown in Fig.3.5. It explains that the velocity distributions for Al_2O_3 – water and TiO_2 – water are almost the same as their densities are near to each other, but due to high density of Cu, for Cu – Water the dynamic viscosity enhances more and leads to a thinner boundary layer than other particles.

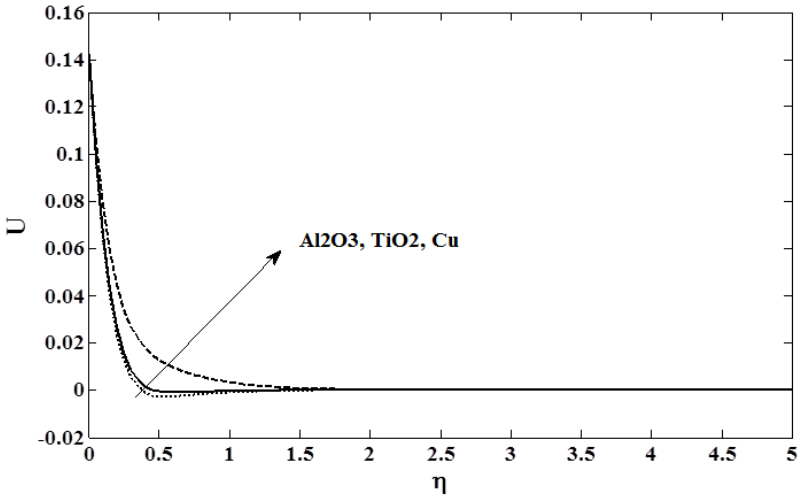


Fig.3.5 Velocity profile for different values of Nano particles

Conclusion: The purpose of this study is to get the exact solution for the unsteady free convective nanofluid flow over a vertical plate in the presence of thermal radiation. Three different types of nanofluids are taken into account and the expression for the temperature of the fluid and the velocity of the plate has been obtained in closed form by using the Laplace transform. The effect of the various parameters on velocity of the plate is depicted graphically and the most important remarks can be concluded as follows:

- An increase in the volume solid fraction, radiation parameter and time leads to an increase in the velocity of the plate but the trend is reversed in the case of radiation parameter.

References:

1. E. Abu-Nada, Effect of nanofluid variable properties on natural convection in enclosures, Int J Therm Sci., **49** (2010), 479–491.
2. E. Abu-Nada, A. Chamkha, Effect of nanofluid variable properties on natural convection in enclosures filled with CuO–EG–water nanofluid, Int J Therm Sci., **49** (2010), 2339–2352.
3. E. Abu-Nada, F. Hakan, Oztop, I. Pop, Buoyancy induced flow in a nanofluid filled enclosure partially exposed to forced convection, Superlattices and Microstructures, **51** (2012), 381–395.
4. S. M. Aminossadati, B. Ghasemi, Natural convection cooling of a localized heat source at the bottom of a nanofluid-filled enclosure, Eur J Mech B/Fluids, **28** (2009), 630–640.
5. A. Akbarinia, M. Abdolzadeh, R. Laur, Critical investigation of heat transfer enhancement using nanofluids in microchannels with slip and non-slip flow regimes, ApplTherm Eng., **31** (2011), 556–565
6. S.P. Anjali Devi ,Julie Andrews, Laminar Boundary Layer Flow of Nanofluid Over A Flat Plate, International Journal of Applied Mathematics and Mechanics, **7** (2011), 52-71.
7. S. P. Anjali Devi and P. Suriyakumar, Hydromagnetic Mixed Convective Nanofluid Slip Flow past an Inclined Stretching Plate in the Presence of Internal Heat Absorption and Suction, Journal of Applied Fluid Mechanics, **9** (2016), 1409-1419.

8. N. Bachok, A. Ishak, I. Pop, Boundary layer flow of nanofluid over a moving surface in a flowing fluid, Int. J. Therm. Sci., **49** (2010), 1663–1668.
9. S. U. S. Choi, Enhancing Thermal Conductivity of Fluids with Nanoparticles, Developments and Applications of Non-Newtonian Flows, FED-231/MD, **66** (1995), 99–105.
10. S.U.S. Choi, Nanofluids: from vision to reality through research, J of Heat Transf., **131** (2009), 1–9.
11. S. K. Das, S.U.S. Choi, W. Yu and T. Pradeep, Nanofluids: Science and Technology, John Wiley and Sons, Inc.,Hoboken, New Jersey, USA, (**2007**).
12. S. Das, R.N. Jana, Natural convective magneto-nanofluid flow and radiative heat transfer past a moving vertical plate, Alexandria Engineering Journal, **54** (2015), 55–64.
13. B. Ghasemi, S.M. Aminossadati, Brownian motion of nanoparticles in a triangular enclosure with natural convection, Int J ThermSci**49** (2010), 931–940.
14. M. A. A. Hamad, Analytical Solution of Natural Convection Flow of a Nanofluid Over a Linearly Stretching Sheet in the Presence of Magnetic Field, International communications in Heat and Mass Transfer, **38** (2011), 487- 492.
15. C.H. Ho, M. W. Chen, Z. W. Li, Numerical simulation of natural convection of nanofluid in a square enclosure: effects due to uncertainties of viscosity and thermal conductivity, Int J Heat Mass Transf, **47** (2008), 4506–4516.
16. S Kakac, A Pramuanjaroenkij, Review of convective heat transfer enhancement with nanofluids, International Journal of Heat and Mass Transfer, **52** (2009), 3187-3196.
17. W.A. Khan, A. Aziz, Natural convection flow of a nanofluid over a vertical plate with uniform surface heat flux, Int J ThermSci, **50** (2011), 1207–1214.
18. W. A. Khan, I. Pop, Boundary Layer Flow of a Nanofluid Past a Stretching Sheet, International Journal of Heat and Mass Transfer, **53** (2010), 2477-2483.
19. A.V. Kuznetsov, D.A. Nield, Natural convective boundary- layer flow of a nanofluid past a vertical plate, Int J ThermSci, **49** (2010), 243–247.
20. Mohammed J. Uddin, Waqar A. Khan, Ahmed I. Ismail, MHD Free Convective Boundary Layer Flow of a Nanofluid past a Flat Vertical Plate with Newtonian Heating Boundary Condition, Plos one, **7** (2012), 494- 499.
21. S. M. S. Murshed, et al, A review of boiling and convective heat transfer with nanofluids, Renewable and Sustainable Energy Reviews, **15** (2011), 2342–2354.
22. E. B. Ogut, Natural convection of water-based nanofluid in an inclined enclosure with a heat source, Int J ThermSci**48** (2009), 2063–2073.
23. H. F. Oztop and E. Abual Nada, Numerical Study of Natural Convection in Partially Heated Rectangular Enclosures Filled With Nanofluids, International Journal of Heat and Fluid Flow, **29** (2008), 1326-1336
24. G. Polidori, S. Fohanno, C.T. Nguyen, A note on heat transfer modelling of Newtonian nanofluids in laminar free convection, Int. J. Therm. Sci., **46** (2007) 739–744.
25. G. V. P. N. Srikanth, G. Srinivas, B. R. K. Reddy, MHD Convective Heat Transfer of a Nanofluid Flow Past an Inclined Permeable Plate With Heat Source and Radiation, International Journal of Physics and Mathematical Sciences, **3** (2013), 89-95.
26. D.Y. Tzou, Thermal instability of nanofluids in natural convection, Int. J. Heat Mass Transfer, **51** (2008), 2967–2979.
27. D.Y. Tzou, Instability of nanofluids in natural convection, ASME J. Heat Transfer, **130** (2008), 1–9.
28. W. Yu, D. M. France, J. L. Routbort, S. U. S. Choi, Review and comparison of nanofluid thermal conductivity and heat transfer enhancements, Heat Transfer Engineering, **29** (2008), 432–460.
29. N. A. Yacob, A. Ishak, R. Nazar, I. Pop, Mixed Convection Flow Adjacent to a Stretching Vertical Sheet in a Nanofluid, Journal of Applied Mathematics, (**2013**), Article ID 696191.

***

MAGNETO HYDRODYNAMIC EFFECTS ON A TRANSIENT Al_2O_3 NANOFLUID PAST OVER AN VERTICAL PLATE

E.Geetha
Assistant professor, Department of Mathematics,
Sri ChandrasekharendraSaraswathiViswaMahaVidyalaya, Enathur, Kanchipuram.
A.Janagiraman
Research Scholar, Department of Mathematics,
Sri ChandrasekharendraSaraswathiViswaMahaVidyalaya, Enathur, Kanchipuram.

Abstract: In this paper, the characteristics of heat transfer with magneto hydrodynamic effects on an unsteady Al_2O_3nanofluid flow over a vertical plate are considered. Three different types of water based nanofluids (Cu, Al_2O_3, TiO_2) are considered to derive the exact solution for the problem. The dimensionless governing equations are solved by laplace transform technique. Solutions for temperature and velocity of the plate are derived and the graphs are also obtained for the different parameters like thermal Grashof number, time, magnetic field parameter, Prandtl number and solid volume fraction. The effects of these parameters on the velocity and temperature of the plate are discussed in a detailed manner.

1. Introduction: In recent years, considerable attention has been devoted to the study of magnetohydrodynamics (MHD) flow and heat. In addition to useful features of MHD flows, such studies can be helpful in prediction of the effects of magnetic intrusions. Magnetohydrodynamics is attracting the attention of the many authors due to its applications in geophysics; it is applied to study the stellar and solar structures, interstellar matter, radio propagation through the ionosphere etc. In engineering in MHD pumps, MHD bearings etc. at high temperatures attained in some engineering devices, gas, for example, can be ionized and so becomes an electrical conductor. The ionized gas or plasma can be made to interact with the magnetic and alter heat transfer and friction characteristic.

The study ofMHDfree convective flow of a viscoelastic(Kuvshinski type) dusty gas through a porous medium induced by the motionof a semi-infinite flat plate under the influence of radiative heat transfer moving withvelocity decreasing exponentially with time was analysed byOm Prakash, Devendra Kumar and Y. K. Dwivedi[1]. The influence of radiation and chemical reaction on MHD thermosolutalnanofluidconvective slip flow over a vertical plate in porous medium in presence of thermophoresis and Brownian motioneffects was studied by Sulochana et al[2].Md. Jashim Uddin et al [3] explained with Scaling Group Transformation for MHD Boundary Layer Slip Flow of a Nanofluid over a Convectively Heated Stretching Sheet with Heat Generation. Farhad Ali et al [4] studied Heat and Mass Transfer with Free Convection MHD Flow Past a Vertical Plate Embedded in a Porous Medium.The effect of local thermal non-equilibrium on transient MHD laminar boundary layerflow of viscous, incompressible nanofluid over a moving surface in a saturated porous media was discussed byMuthtamilselvan et al.[5]. Alam .M.S and Rahman [6] studied And Soret effects on MHD free convective heat and mass transfer flow past a vertical porous plate embedded in a porous medium..Ahmmed et al [7] studied Analytical Study on Unsteady MHD Free Convection and Mass Transfer Flow Past a Vertical Porous Plate. Das .S, Jana .R.N and Chamkha ,A.J [8] analysed Unsteady Free Convection Flow past a Vertical Plate with Heat and Mass Fluxes in the Presence of Thermal Radiation.The magnetic field,radiation and soret effect of a nanofluid flow over a moving vertical plate in porous medium was analysed by Raju et al. [9]. The effects of aligned magnetic field, radiation and rotation on unsteady hydromagnetic freeconvection flow of a viscous incompressible electrically conducting fluid past an impulsively moving verticalplate in a porous medium in presence of heat sources was analysed by Sandeep et al. [10].

Rajesh vemula et al [11] studied the unsteady MHD free convection flow of nanofluid past an exponentially accelerated vertical plate with variable temperature and thermal radiation.Makinde and Ogulu[12] analysed the effect of thermal radiation on the heat and mass transfer flow of a variable viscosity fluid past a vertical porous plate permeated by a transverse magnetic field. Natural convective magneto-nanofluid flow and radiative heat transfer past a moving vertical plate was discussed by Das and Jana [13].

It is noticed that from the above literature survey no authors have been studied the transient incompressible flow of aAl_2O_3nanofluid with magnetohydrodynamic effects on a vertical plate. The coupled dimensional governing equations for momentum and energy without viscous dissipation were considered. By using non-dimensional quantities, these equations are converted into dimensionless form. Here the dimensionless governing equations are solved by laplace transform technique. Al_2O_3 - water combination is analysed for the different parameters like time, thermal grashof number, Magnetic field parameter and solid volume fraction on the velocity and temperature of the plate and the graphs are also drawn and the effects of the above parameters are also discussed in a detailed manner. The graphs are also obtained for the different nanofluids(Cu, Al_2O_3, TiO_2) on the velocity and the temperature profile.

2. Mathematical Analysis: The transient free convective viscous flow of a Al_2O_3 nanofluid through an infinite vertical plate with a magnetohydrodynamic effect has been considered. Further it is an unsteady flow of a viscous incompressible fluid which is initially at rest and surrounds an infinite vertical plate maintaining temperature T_∞. The *x*-axis is considered along the plate in the vertically upward direction and the *y*-axis is assigned normal to the plate. At time $t' \le 0$, the plate and fluid are at the same temperature T_∞. At time $t' > 0$, the plate is accelerated with a velocity its own plane against gravitational field and the temperature from the plate is raised to T_w. The magnetic field B_o is applied normal to the plate. The fluid is a water based nanofluid containing three types' nanoparticles Cu, Al_2O_3 and TiO_2. It is further assumed that the base fluid and the suspended nanoparticles are in thermal equilibrium. The thermophysical properties of the nanofluids are given in Table 1.

Table 1: Thermo Physical Properties of Water and Nanoparticles

Physical properties	Water/Base Fluid	Cu(Copper)	Al_2O_3 (Alumina)	TiO_2
ρ (kg / m^3)	997.1	8933	3970	4250
c_ρ (J / kgK)	4179	385	765	686.2
K(W / mK)	0.613	401	40	8.9538
β x 10^5 (K^{-1})	21	1.67	0.85	0.90
ϕ	0.0	0.05	0.15	0.2
σ (S / m)	5.5 x 10^{-6}	59.6 x 10^6	35 x 10^6	2.6 x 10^6

Then under usual Boussinesq's approximation, the unsteady viscous flow of a nanofluid is governed by the following equations:

$$\rho_{nf}\frac{\partial u}{\partial t'} = g(\rho\beta)_{nf}(T - T_\infty) + \mu_{nf}\frac{\partial^2 u}{\partial y^2} - \sigma B_0^2 u \qquad (1)$$

$$(\rho c_p)_{nf}\frac{\partial T}{\partial t'} = k_{nf}\frac{\partial^2 T}{\partial y^2} \qquad (2)$$

where u is the velocity components along the x-direction, T the temperature of the nanofluid, μ_{nf} the dynamic viscosity of the nanofluid, β_{nf} the thermal expansion coefficient of the nanofluid, ρ_{nf} the

density of the nanofluid, k_{nf} the thermal conductivity of the nanofluid, g the acceleration due to gravity, q_r the radiative heat flux and $(\rho c_p)_{nf}$ the heat capacitance of the nanofluid which are given by

$$\begin{aligned}
&\mu_{nf} = \frac{\mu_f}{(1-\phi)^{2.5}}, \rho_{nf} = (1-\phi)\rho_f + \phi\rho_s \\
&(\rho c_p)_{nf} = (1-\phi)(\rho c_p)_f + \phi(\rho c_p)_s \\
&(\rho\beta)_{nf} = (1-\phi)(\rho\beta)_f + \phi(\rho\beta)_s
\end{aligned} \tag{3}$$

where ϕ is the solid volume fraction of the nanoparticle, ρ_f the density of the base fluid, ρ_s the density of the nanoparticle, μ_f the viscosity of the base fluid, $(\rho c_p)_f$ the heat capacitance of the base fluid and $(\rho c_p)_s$ the heat capacitance of the nanoparticle.

It is worth mentioning that the expressions (1) are restricted to spherical nanoparticles, where it does not count for other shapes of nanoparticles. The effective thermal conductivity of the nanofluid given by Hamilton and Crosser model followed by Kakacand Pramuanjaroenkij [14], and Oztop and Abu-Nada [15] is given by

$$k_{nf} = k_f \left[\frac{k_s + 2k_f - 2\phi(k_f - k_s)}{k_s + 2k_f + \phi(k_f - k_s)} \right] \tag{4}$$

where k_f is the thermal conductivity of the base fluid and k_s the thermal conductivity of the nanoparticle. In Eqs. (1)–(4), the subscripts nf, f and s denote the thermo physical properties of the nanofluid, base fluid and nanoparticles, respectively.

The initial and boundary conditions of the proposed problem are given by:

$$\begin{aligned}
& u = 0, && T = T_\infty && \text{for all} && y, t' \le 0 \\
t' > 0: \quad & u = \frac{{u_0}^3}{\nu_f} t', && T = T_\omega && \text{at} && y = 0 \\
& u \to 0 && T \to T_\infty && \text{as} && y \to \infty
\end{aligned} \tag{5}$$

On introducing the following non dimensional quantities are:

$$U = \frac{u}{u_0}, \quad t = \frac{t' {u_0}^2}{\nu_f}, \quad Y = \frac{y u_0}{\nu_f}, \tag{6}$$

$$\theta = \frac{T - T_\infty}{T_w - T_\infty}, \; Gr = \frac{g \nu_f \beta (T_w - T_\infty)}{{u_0}^3}, \quad M = \frac{\sigma {B_0}^2 V}{\rho {u_0}^2}, \Pr = \frac{\mu c_p}{k_f},$$

By using equations (3), (4) and (6), equations (1) and (2) leads to,

$$L_1\frac{\partial U}{\partial t} = L_3\frac{\partial^2 U}{\partial Y^2} + L_2 Gr\theta - MU$$
$$L_5\frac{\partial \theta}{\partial t} = L_6\frac{1}{\Pr}\frac{\partial^2 \theta}{\partial Y^2} \qquad (7)$$

Where

$$L_1 = (1-\phi) + \phi\left(\frac{\rho_s}{\rho_f}\right), L_2 = (1-\phi) + \phi\left(\frac{(\rho\beta)_s}{(\rho\beta)_f}\right), L_3 = \frac{1}{(1-\phi)^{2.5}}$$

$$L_5 = (1-\phi) + \phi\left(\frac{(\rho c_p)_s}{(\rho c_p)_f}\right), L_6 = \left[\frac{k_s + 2k_f - 2\phi(k_f - k_s)}{k_s + 2k_f + \phi(k_f - k_s)}\right] \qquad (8)$$

Where Pr is the Prandtl number, Gr is the thermal Grashof number, Gr approximates the ratio of the buoyancy force to the viscous force acting.

The corresponding initial and boundary conditions are,

$$\begin{array}{lllll} & U = 0, & \theta = 0, & for\ all & Y, t \le 0 \\ t > 0: & U = gt, & \theta = 1, & at & Y = 0 \\ & U \to 0, & \theta \to 0, & as & Y \to \infty \end{array} \qquad (9)$$

Where $g = \frac{L_1}{L_3}$

Methods of Solutions: Equation (7) is solved subject to the initial and boundary conditions(9) with the help of Laplace transform analytically. The Exact solutions are expressed in terms of exponential function and complementary error function.

$$\theta = erfc(\eta\sqrt{L7})$$
$$U = \frac{gt}{2}[\exp(2\eta\sqrt{dt})erfc(\eta\sqrt{g} + \sqrt{dt}) + \exp(-2\eta\sqrt{dt})erfc(\eta\sqrt{g} - \sqrt{dt})]$$
$$-\frac{c}{b}[erfc(\eta\sqrt{g})] + \frac{c}{b}[erfc(\eta\sqrt{a})]$$
$$+\frac{c(\exp(bt))}{2b}[\exp(2\eta\sqrt{g(d+b)t})erfc(\eta\sqrt{g} + \sqrt{(d+b)t}))$$
$$+\exp(-2\eta\sqrt{g(d+b)t})erfc(\eta\sqrt{g} - \sqrt{(d+b)t})]$$
$$-\frac{c(\exp(bt))}{2b}[\exp(2\eta\sqrt{abt})erfc(\eta\sqrt{a} + \sqrt{bt})$$
$$+\exp(-2\eta\sqrt{abt})erfc(\eta\sqrt{a} - \sqrt{bt})]$$
$$where, a = \frac{L5\Pr}{L6}; c = \frac{GrL2}{L7L3 - L1}; d = \frac{M}{L9}; g = \frac{L1}{L3}; \eta = \frac{1}{2\sqrt{t}}$$

3. Results and Discussion: To get the physical insight into the problem, the computed values of different parameters like thermal Grashof number, Prandtl number, time , volume solid fraction and magnetic field parameter on the temperature and velocity of the plate are considered and the effects are explained in a detailed manner through graph. For that the Prandtl number Pr = 7.1 is considered which corresponds to water, time t = 0.5, thermal Grashof number Gr = 5 which represents cooling of the plate. We have considered three different types of nanofluids containing Copper(Cu), Aluminium oxide(Al_2O_3) and Titanium oxide(TiO_2) with water as a base fluid. The nanoparticle volume fraction is considered in the range of $0 \le \phi \le 0.2$. In this study, we have considered spherical nanoparticles with thermal conductivity and dynamic viscosity [16] shown in model I in Table 2.

Table 3.2: Thermal Conductivity and Dynamic Viscosity for Various Shapes of Nanoparticles

Model	Shape of nanoparticles	Thermal conductivity	Dynamic viscosity
I	Spherical	$\frac{k_{nf}}{k_f} = \frac{k_s + 2k_f - 2\phi(k_f - k_s)}{k_s + 2k_f + \phi(k_f - k_s)}$	$\mu_{nf} = \frac{\mu_f}{(1-\phi)^{2.5}}$
II	Spherical (nanotubes)	$\frac{k_{nf}}{k_f} = \frac{k_s + 2k_f - 2\phi(k_f - k_s)}{k_s + 2k_f + \phi(k_f - k_s)}$	$\mu_{nf} = \mu_f(1 + 7.3\phi + 12.3\phi^2)$
III	Cylindrical	$\frac{k_{nf}}{k_f} = \frac{k_s + \frac{1}{2}k_f - \frac{1}{2}\phi(k_f - k_s)}{k_s + \frac{1}{2}k_f + \phi(k_f - k_s)}$	$\mu_{nf} = \frac{\mu_f}{(1-\phi)^{2.5}}$
IV	Cylindrical (nanotubes)	$\frac{k_{nf}}{k_f} = \frac{k_s + \frac{1}{2}k_f - \frac{1}{2}\phi(k_f - k_s)}{k_s + \frac{1}{2}k_f + \phi(k_f - k_s)}$	$\mu_{nf} = \mu_f(1 + 7.3\phi + 12.3\phi^2)$

Figure 3.1 shows that the effect of thermal grashof number Gr on the velocity of the plate for different values (Gr = 2, 5, 7). Here Prandtl number Pr = 7.1, time t = 0.5, Magnetic field parameter M = 5 and solid volume fraction =0.2 are considered. Since Grashof number is the ratio of the buoyancy force to viscous force. Grashof number Gr decreases, the velocity of the plate increases due to the buoyancy force for the nanofluid Al_2O_3 - water.

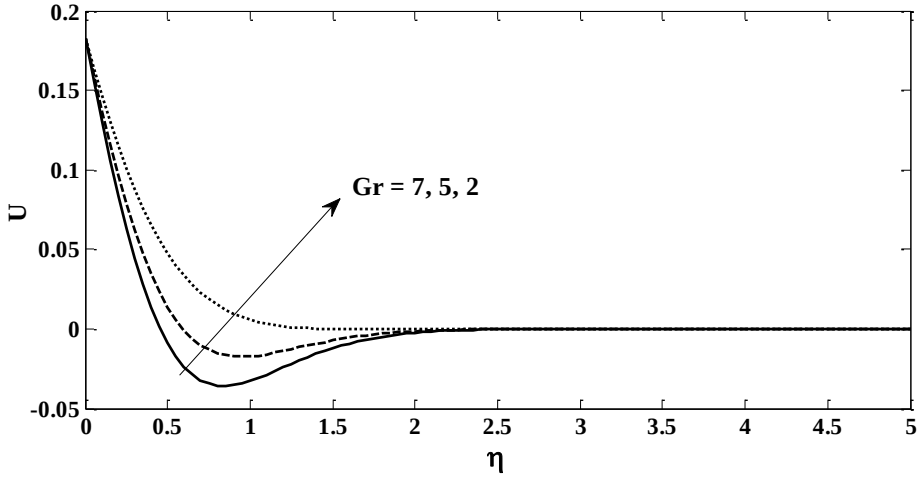


Figure 3.1 Velocity profile for different values of Gr

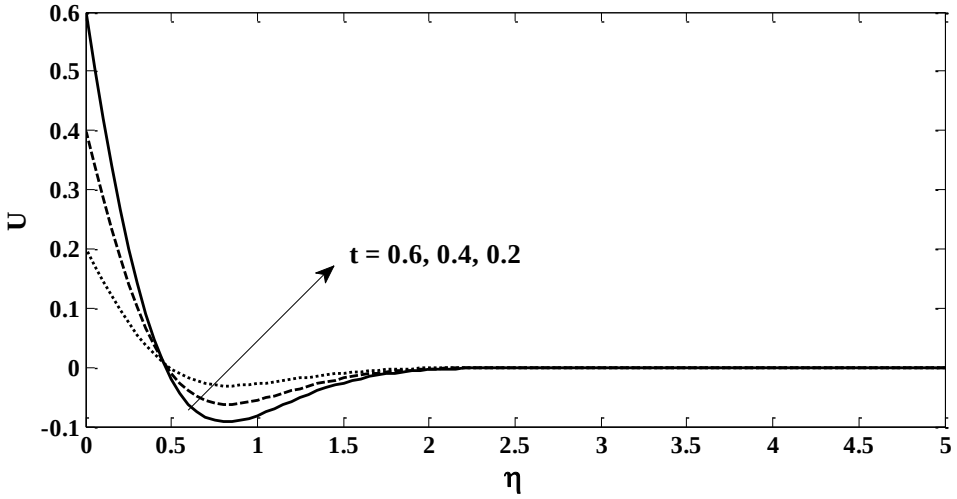


Figure 3.2 Velocity profile for different values of t

Figure 3.2 reveals the effect of time t(t = 0.2, 0.4, 0.6) on the velocity of the plate when Prandtl number Pr = 6.2, Thermal grashof number Gr = 5, Magnetic field parameter M=2 and solid volume fraction ϕ =0.1are taken. This graph shows that the time enhances forthe increasing values of velocity of the plate.

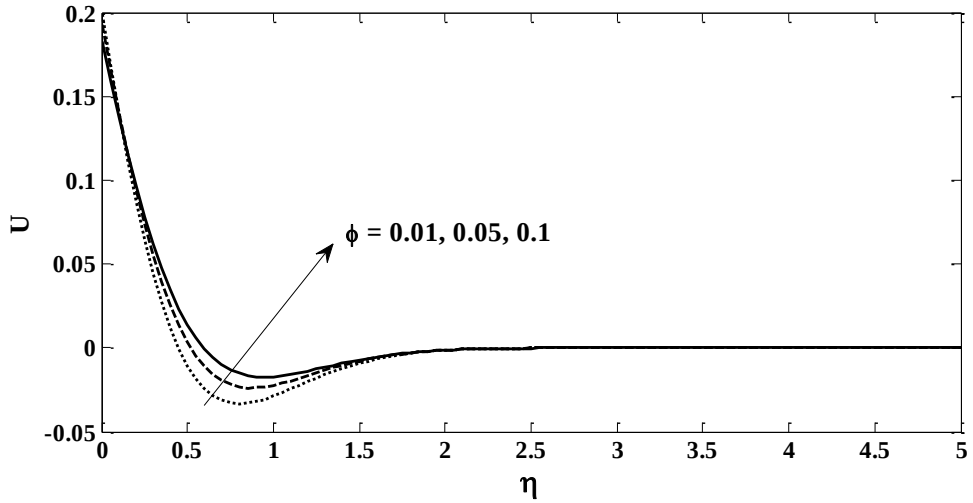


Figure 3.3 Velocity profile for different values of ϕ

In Figure 3.3 shows the effect of the solid volume fraction on the velocity profile for different values (ϕ =0.01, 0.05, 0.1). HerePrandtlnumber Pr = 7.1, Thermal Grashof number Gr = 5, Magnetic field parameter M = 5 and time t = 0.2 are kept at constant. The velocity of the plate increases for the enhancing values of solid volume fraction.The effect of Magnetic field parameter M (M = 2, 4, 5) on the velocity of the plate for the nanofluid Al_2O_3– water is shown in Figure 4. Here Prandtl number Pr = 7.1, time t = 0.2, Thermal grashof number Gr = 5 and solid volume fraction ϕ =0.2 are kept to be constant. Since Lorentz force causes due to the magnetic field and it acts against the plate. Whenever magnetic field parameter increases, the velocity of the plate decreases due to the Lorentz force and it is shown in Figure 3.4.

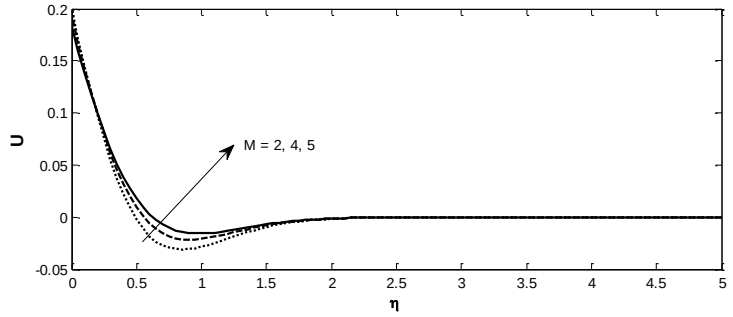


Fig.3.4 Velocity profile for different values of M

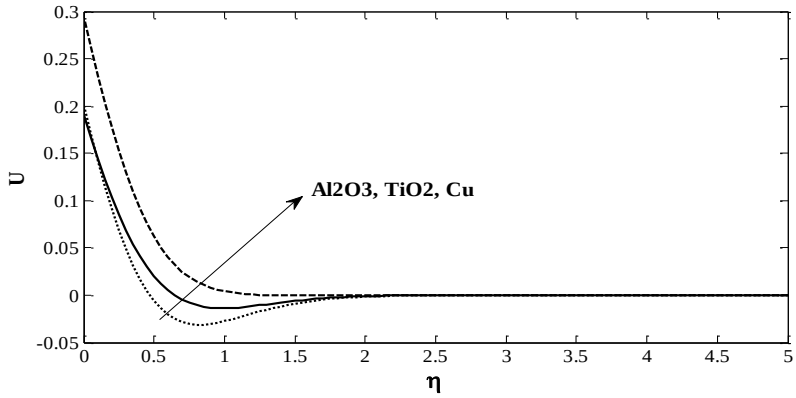


Figure 3.5 Velocity profile for different values of nano particals

Figure 3.5 reveals that the plate velocity variations for the three types of water based nanofluids Cu-Water, Al_2O_3– water and TiO_2-Water when Pr=7.1, M = 5 and Gr=5 at t=0.2. Here the velocity of the plate is found to be similar for Cu and TiO_2 when compared to Al_2O_3 - water.

In Figure3.6 temperature profile for different values of Prandtl number (Pr= 0.71, 6.2, 7.1) is presented when t=0.2. The size of the thermal boundary layer increases with decreasing Prandtl number because the Boussinesq's approximation in the momentum equation consists of assuming that density of the fluid varies with temperature linearly. Here temperature profile gradually reduces to reach the free stream temperature. Figure 3.7 reveals that the plate velocity variations for the three types of water based nanofluids Cu-Water, Al_2O_3– water and TiO_2-Water when Pr = 7.1, and t = 0.5. Due to higher thermal conductivity of Al_2O_3 - water nanofluids, the temperature of Al_2O_3 - water nanofluid is found to be higher than Cu–water and TiO_2–water nanofluids. It is also seen that the thermal boundary layer thickness is more for Al_2O_3– water than Cu–water and TiO_2–water nano fluids.

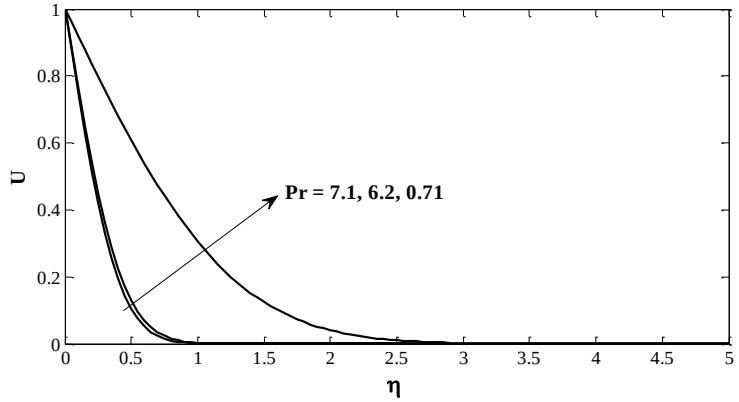


Figure 3.6 temperature profile for different values of Pr

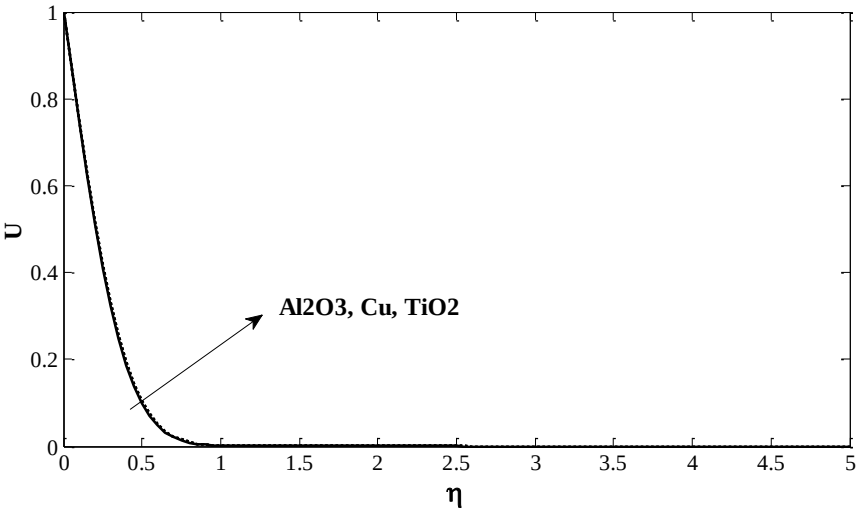


Figure 3.7 Temperature profile for different values of nano particles

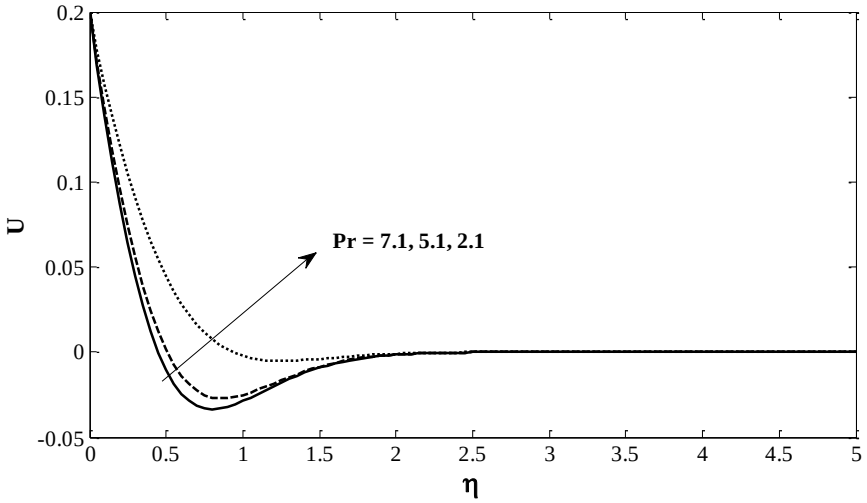


Figure 3.8 Velocity profile for different values of Pr

In Figure 3.8. Velocity profile for different values of Prandtl number (Pr = 2.1, 5.1, 7.1) in presented when t=0.2, ϕ =0.1, Gr=5, Here Velocity profile gradually reduces for increasing values of Prandtl number.

Conclusion: The Unsteady flow of a viscous incompressible Al_2O_3 nanofluid flow over an infinite vertical plate with the effect of Magnetichydrodynamic was considered. Here the dimensional governing equations are converted into a nondimensional form using dimensionless quantities. These dimensionless equations with the nondimensional boundary conditions are solved by Laplace transform technique. The solutions are obtained in terms of exponential and complementary error functions. The graphs are plotted for different values of thermal Grashof number, Prandtl number, time, volume solid fraction and magnetic field parameter on the temperature and velocity of the plate and discussed in a detailed manner. In this study the conclusion is as follows:

a) The velocity of the plate enhances for the increasing values of time and solid fraction fraction but the trend is reversed in the case of thermal Grashof number, magnetic field parameter and Prandtl number.
b) The temperature of the plate increases for the decreasing values of Prandtl number.

References:

1. Om Prakash, DevendraKumar,and Y. K. Dwivedi., MHD free convection flow of a visco-elastic (Kuvshiniskitype) dusty gas through a semi-infinite plate moving withvelocity decreasing exponentially with time and radiativeheat transfer. *AIP ADVANCES***1**, 022132 (2011).
2. C.Sulochana, M.K.Kishor Kumar andN.Sandeep, Radiation and Chemical Reaction Effects on MHD ThermosolutalNanofluid Flow over a Vertical Plate in Porous Medium, *Chemical and Process Engineering Research* ISSN 2224-7467 (Paper) ISSN 2225-0913 (Online) (2015), Vol.34, pp. 28-37.
3. Md. Jashim Uddin, Khan .W.A, and Md. Ismaili.A.I. Scaling Group Transformation for MHD Boundary Layer Slip Flow of a Nanofluid over a Convectively Heated Stretching Sheet with Heat Generation,*Mathematical Problems in Engineering*, (2012), Article ID 934964, pp 1-20.
4. Farhad Ali, Ilyas Khan, SharidanShafie, and NorziehaMusthapa. Heat and Mass Transfer with Free Convection MHD Flow Past a Vertical Plate Embedded in a Porous Medium,*Mathematical Problems in Engineering*, (2013), Article ID 346281, pp 1-13.
5. Muthtamilselvan, M., Prakash, D., and Deog-Hee Hoh.. Effect of thermal non- equilibrium on transienthydromagnetic flow over a moving surface in a nanofluid saturated porous media, *Journal ofMechanical Science and Technology*, (2014), 28(9), 3709- 3718.
6. Alam .M.S and Rahman .M.M ,Dufour. And Soret effects on MHD free convective heat and mass transfer flow past a vertical porous plate embedded in a porous medium, *Journal of Naval Architecture and Marine Engineering* ,10 (2005),pp 1-8.
7. Ahmmed .S.F and Das .M.K, Ali .L.E. Analytical Study on Unsteady MHD Free Convection and Mass Transfer Flow Past a Vertical Porous Plate,*American Journal of Applied Mathematics*, 3,(2015), pp. 64-74.
8. Das .S, Jana .R.N and Chamkha .A.J. Unsteady Free Convection Flow past a Vertical Plate with Heat and Mass Fluxes in the Presence of,Thermal Radiation, *Journal of Applied Fluid Mechanics*, 8, (2015), pp. 845-854.
9. Raju, C S K., JayachandraBabu, M., Sandeep, N., Sugunamma, V., and Ramana Reddy, J.V.. Radiationand Soret Effects of MHD Nanofluid Flow over a Moving Vertical Moving Plate in Porous Medium,*Chemical and Process Engineering Research*, 30,(2015), 9- 23.
10. Sandeep Naramgari., SugunammaVangala., and MohankrishnaPenem. Aligned Magnetic Field,Radiation and Rotation Effects on Unsteady Hydromagnetic Free Convection Flow Past anImpulsively Moving Vertical Plate in a Porous Medium, Hindawi Publishing Corporation *International Journal of Engineering Mathematics.*(2014).
11. Rajesh Vemula, LokenathDebnath and SrideviChakrala,Unsteady MHD Free Convection Flow of Nanofluid Past an Accelerated Vertical Plate with Variable Temperature and Thermal Radiation., *Int. J. Appl. Comput. Math.*,(2016) ,pp 1-17.
12. Makinde .O.D, and Ogulu .A, The effects of thermal radition on the heat and mass transfer flow of a variable viscosity fluid past a vertical porous plate permeated by a transverse magnetic field, *chemical engineering Communications*, 195 (2008),pp 1575-1584.
13. Das .S and Jana .R.N, Natural convective magneto-nanofluid flow and radiative heat transfer past a moving vertical plate, *Alexandria Engineering Journal* ,54 (2015),pp 55–64.
14. Kakac .S and Pramuanjaroenkij .A, Review of convective heat transfer enhancement with nanofluids, *Int. J. Heat Mass Transfer* ,52 (2009),pp 3187–3196.
15. Oztop .F and Abu-Nada .E, Numerical study of natural convection in partially heated rectangular enclosures filled with nanofluids, *Int. J. Heat and Fluid Flow* ,29 (2008),pp 1326–1336.
16. Brinkman .H.C, The viscosity of concentrated suspensions and solution, *J. Chem. Phys*. 20 (1952), pp.571–581.

***

FINDING RESIDUES RESIDING AT THE PROTEIN CORE AND PROTEIN SURFACE USING GRAPH THEORETICAL TECHNIQUES

R.Mageswari
Assistant Professor, Department of Mathematics
Sri Chandrasekharendra Saraswathi Viswa Mahavidyalaya
Kanchipuram - 631 561, Tamilnadu, India
V.Meena
Scholar, Department of Mathematics
Sri Chandrasekharendra Saraswathi Viswa Mahavidyalaya
Kanchipuram - 631 561, Tamilnadu, India

Abstract: Graph of the protein can be obtained from the protein contact map. In this paper, residues residing at the core of the protein with protein id 2WPO can be identified clearly from the minimal connected dominating sets.

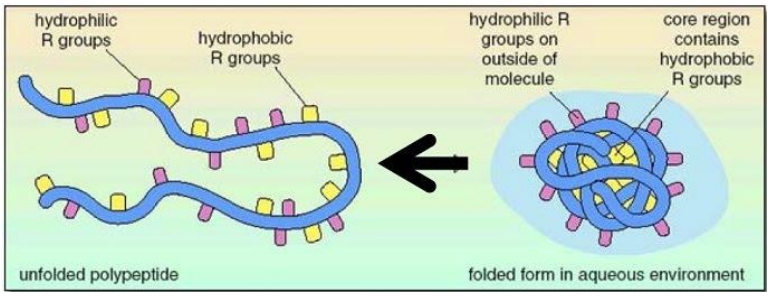


Figure 1: Hydrophobic Core and Hydrophilic Surface of A Protein

Keywords: Contact Map, Residues.

1. Introduction: Amino Acids are organic compounds containing amine (-NH2) and carboxyl (-COOH) functional groups, along with a side chain (R group) specific to each amino acids. There are twenty amino acids. Proteins are large bio molecules or macro molecules consisting of one or more long chains of amino acid residues. There are thousands of different proteins and the characteristic of each type of protein is determined by a different gene.

Proteins make up the cellular structure of organisms and proteins structure determines its biological function. Understanding the structure of protein is significantly useful in understanding its function. Around one lakh protein 3D structures were identified by the experimental methods such as X-ray crystallography, NMR and Electron Microscopy and are available in the Protein Data Bank [1]. But, experimental methods are more expensive, time consuming and the process is also tedious. Hence, mathematical methods are introduced in the analysis of proteins.

Among the different mathematical methods for protein structure identification, graph theoretical methods are easy to estimate. Three dimensional structure of a protein is well determined by its continuous folds. Protein core is occupied by the amino acids with the higher average degree [2-8]. Hydrophobic amino acids reside at the core of the protein to avoid water [9] (Figure 1).

Contact map plays an important role in understanding proteins structure [10]. Using contact map of the protein, the hydrophobic and hydrophilic amino acids are predicted by its total average degree using the HYDCORE algorithm [11]. Also, specific folds [12] in the protein are identified using contact map. In [13],

a new method is introduced to identify the hydrophobic residues from the minimal connected dominating set [14] of the graph of the protein. In this paper, hydrophobic residues of the protein with PDB id 2WPO are obtained using the concept of dominating sets.

2. Preliminaries

2.1 Graph: Let G = <V, E> be a graph in which V denotes the set of vertices, E denotes the set of edges and |V (G)| is the number of vertices of G. Two vertices u and v of G are called adjacent or neighbors if u-v is an edge of G. The degree d(v) of a vertex v is denoted by d(v) and is defined as the number of neighbors of v.

2.2 Connected Graph: A graph G is said to be connected if every pair of its points are connected.

2.3 Dominating Set of a Graph: Let G = (V,X) be a graph. A subset S of V is called a dominating set if every vertex in V-S is adjacent to a vertex in S.

2.4 Minimal Connected Dominating Set: A Minimal Connected Dominating Set is a connected dominating set from which no vertex can be removed without destroying its dominance property.

2.5 Contact Maps: The distance between two residues may be defined by the distance between two alpha carbon (C_α) atoms or between two beta carbon (C_β) atoms or it may be the minimum distance between any pair of atoms belonging to the side chain or to the backbone of two residues. A contact between two given atoms (or residues) exists when a certain distance is below a given threshold.

Let P be a protein with n atoms which are labeled 1,2,3,....n. We define the contact map of the protein as a matrix,

$T = (t_{ij})_{1\le i,,j\le n}$

where $t_{ij} = 1$ if $i \neq j$ and d_{ij} (Euclidean distance between i & j) $\le$ 6Å

= 0 otherwise.

2.6 Graph of the Protein: A protein can be considered as a graph G = <V,E> for which each vertex $v_k \in$ V represents a residue of the protein and each v_i-$v_j \in$ E represents a contact between two residues v_i and v_j. On the other hand, there is an edge v_i-$v_j \in$ E if $t_{ij} = 1$.

3. Methodology: Coordinates of the alpha carbons of the Protein with PDB id 2WPO is taken from the Protein Data Bank and the three dimensional structure of the protein for the required alpha carbons can be seen using the software Molsoft. The distances between the alpha carbons have been noted and the contact map, graph of the protein have been obtained as given below.

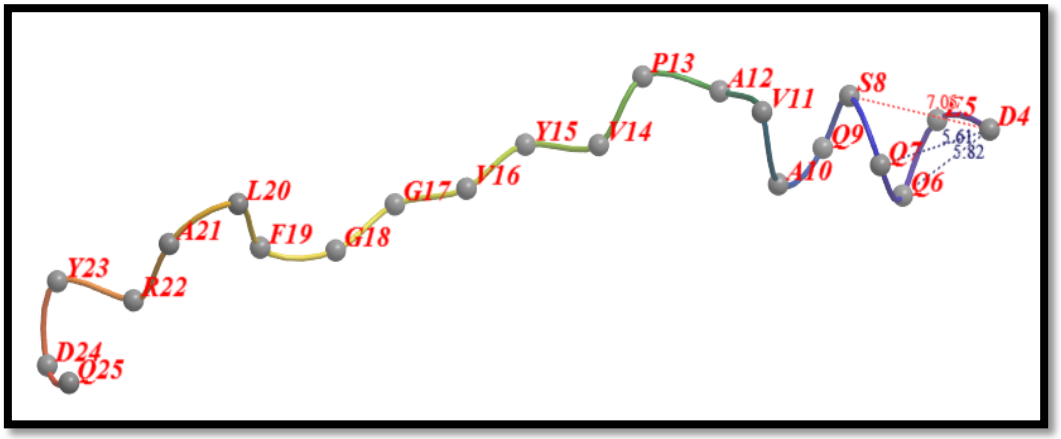


Figure 1: Wire Representation of the Protein 2WPO

Table 1: Residues and its Adjacent Residues with 6 Å

Residue	Vertex Number	Adjacent Residues
D_4	1	E_5,Q_6,Q_7
E_5	2	D_4,Q_6,Q_7,S_8,Q_9
Q_6	3	D_4,E_5,Q_7,S_8,Q_9
Q_7	4	D_4,E_5,Q_6,S_8,Q_9,A_{10}
S_8	5	L_5,Q_6,Q_7,Q_9,A_{10},V_{11}
Q_9	6	E_5,Q_6,Q_7,S_8,A_{10},V_{11},A_{12}
A_{10}	7	Q_7,S_8,Q_9,V_{11},A_{12}
V_{11}	8	S_8,Q_9,A_{10},A_{12}
A_{12}	9	Q_9,A_{10},V_{11},P_{13}
P_{13}	10	A_{12}, V_{14}
V_{14}	11	P_{13},Y_{15}
Y_{15}	12	V_{14},V_{16}
V_{16}	13	Y_{15}, G_{17}
G_{17}	14	V_{16},G_{18}
G_{18}	15	G_{17},F_{19}
F_{19}	16	G_{18}, L_{20}, A_{21}
L_{20}	17	F_{19}, A_{21}
A_{21}	18	F_{19}, L_{20}, R_{22}
R_{22}	19	Q_{21}, Y_{23}, D_{24}, Q_{25}
Y_{23}	20	R_{22}, D_{24}, Q_{25}
D_{24}	21	Y_{23}, R_{22}, Q_{25}
Q_{25}	22	R_{22}, Y_{23}, D_{24}

Contact Map of the protein is obtained as a matrix given below.

$$\begin{pmatrix}
0&1&1&1&0&0&0&0&0&0&0&0&0&0&0&0&0&0&0&0&0&0\\
1&0&1&1&1&1&0&0&0&0&0&0&0&0&0&0&0&0&0&0&0&0\\
1&1&0&1&1&1&0&0&0&0&0&0&0&0&0&0&0&0&0&0&0&0\\
1&1&1&0&1&1&1&0&0&0&0&0&0&0&0&0&0&0&0&0&0&0\\
0&1&1&1&0&1&1&1&0&0&0&0&0&0&0&0&0&0&0&0&0&0\\
0&1&1&1&1&0&1&1&1&0&0&0&0&0&0&0&0&0&0&0&0&0\\
0&0&0&1&1&1&0&1&1&0&0&0&0&0&0&0&0&0&0&0&0&0\\
0&0&0&0&1&1&1&0&1&0&0&0&0&0&0&0&0&0&0&0&0&0\\
0&0&0&0&0&1&1&1&0&1&0&0&0&0&0&0&0&0&0&0&0&0\\
0&0&0&0&0&0&0&0&1&0&1&0&0&0&0&0&0&0&0&0&0&0\\
0&0&0&0&0&0&0&0&0&1&0&1&0&0&0&0&0&0&0&0&0&0\\
0&0&0&0&0&0&0&0&0&0&1&0&1&0&0&0&0&0&0&0&0&0\\
0&0&0&0&0&0&0&0&0&0&0&1&0&1&0&0&0&0&0&0&0&0\\
0&0&0&0&0&0&0&0&0&0&0&0&1&0&1&0&0&0&0&0&0&0\\
0&0&0&0&0&0&0&0&0&0&0&0&0&1&0&1&1&0&0&0&0&0\\
0&0&0&0&0&0&0&0&0&0&0&0&0&0&1&0&1&0&0&0&0&0\\
0&0&0&0&0&0&0&0&0&0&0&0&0&0&0&1&1&0&1&0&0&0\\
0&0&0&0&0&0&0&0&0&0&0&0&0&0&0&0&0&1&0&1&1&1\\
0&0&0&0&0&0&0&0&0&0&0&0&0&0&0&0&0&0&1&0&1&1\\
0&0&0&0&0&0&0&0&0&0&0&0&0&0&0&0&0&0&1&1&0&1\\
0&0&0&0&0&0&0&0&0&0&0&0&0&0&0&0&0&0&1&1&1&0
\end{pmatrix}$$

Using the contact map shown above, the graph of the protein is obtained as below.

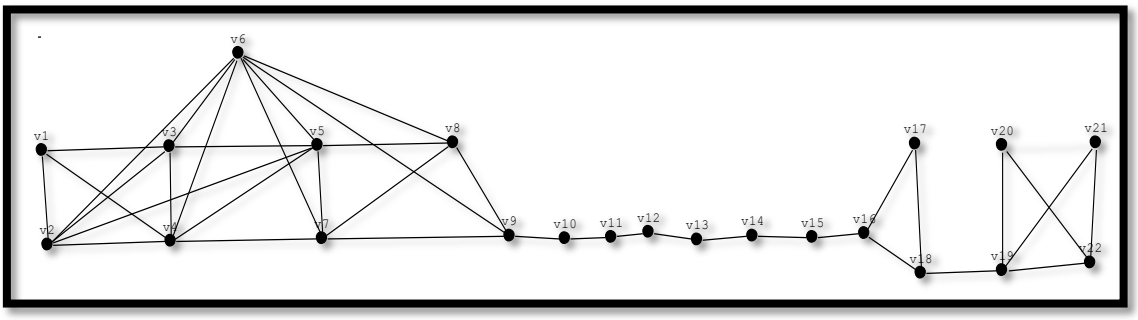


Figure 2: Graph of the Protein 2WPO

The minimal connected dominating sets of the above graph are,
$D_1 = \{ v_4, v_5, v_6, v_7, v_9, v_{10}, v_{11}, v_{12}, v_{13}, v_{14}, v_{15}, v_{16}, v_{17}, v_{18}, v_{19}, v_{20}, v_{21}, v_{22}\}$
$D_2 = \{v_6, v_9, v_{12}, v_{13}, v_{14}, v_{15}, v_{16}, v_{17}, v_{18}, v_{19}, v_{20}, v_{21}, v_{22}\}$
$D_3 = \{v_4, v_5, v_{11}, v_{12}, v_{13}, v_{14}, v_{15}, v_{16}, v_{17}, v_{18}, v_{19}, v_{20}, v_{21}, v_{22}\}$

Conclusion: Residues residing at the core of the protein 2WPO are listed as $v_4, v_5, v_6, v_7, v_9, v_{10}, v_{11}, v_{12}, v_{13}, v_{14}, v_{15}, v_{16}, v_{17}, v_{18}, v_{19}, v_{20}, v_{21}, v_{22}$ and the remaining residues v_1, v_2, v_3 and v_8 are hydrophilic.

References:

1. The Protein Data Bank: Exploring Biomolecular Structure. Nature Education 2010, 39.
2. Cornette J L, Cease K B, Margalit H, Spouge J L, Berzofsky J A, DeLisi C. Hydrophobicity scales and computational techniques for detecting amphipathic structures in proteins. J Mol Biol. 1987, 195, 659–685.
3. Eisenberg D, Schwarz E, Komaromy M, Wall R. Analysis of membrane and surface protein sequences with the hydrophobic moment plot. J Mol Biol. 1984, 179, 125–142.
4. Engelman D M, Steitz T , Goldman A. Identifying nonpolar transbilayer helices in amino acid sequences of membrane proteins. Annu Rev Biophys Biophys Chem.1986, 15, 321–353.
5. Hopp T P, Woods K R. A computer program for predicting protein antigenic determinants. Mol Immunol. 1983, 20, 483–489.
6. Janin J. Surface and inside volumes in globular proteins. Nature. 1979, 277,491–492.
7. Kyte J, Doolittle R F. A simple method for displaying the hydropathic character of a protein. J Mol Biol. 1982,157,105–132.
8. Rose G D, Geselowitz A R, Lesser G J, Lee R H, Zehfus M H. Hydrophobicity of amino acid residues in globular proteins. Science. 1985,229,834–838.
9. Kauzmann W. Some factors in the interpretation of protein denaturation. Adv Prot Chem. 1959,14, 1–63.
10. Mageswari R, Srinnivasa Rao K, Sivakumar K: Protein similarity/dissimilarity using contact map and matching index, *Mathematical Sciences International Research Journal*, 2014,3 672-676.
11. Mahnaz Habibi, Changiz Eslahchi, Mehdi Sadeghi , Hamid Pezashk: The interpretation of protein structures based on graph theory and contact map Open Access Bioinformatics 2010 ,2, 127-137.
12. Dahiyat .B I; Mayo .S L.: Probing the role of packing specificity in protein.. Natl Acad Sci U S A. 1997, 94, 10172–10177.
13. Mageswari.R, SrinivasaRao.K, Sivakumar.K, Prediction of Hydrophobic Core using Contact Map and Minimal Connected Dominating Sets, Indian Journal of Science, 2015, 13(37), 24-28.
14. Narsingh Deo: Graph Theory with Applications to Engineering and Computer Science, Prentice Hall of India Private Limited, New Delhi 2008.

***

FINDING GRAPH OF THE PROTEIN FROM ITS CONTACT MAP

R.Mageswari
Assistant Professor, Department of Mathematics
Sri Chandrasekharendra Saraswathi Viswa Mahavidyalaya
Kanchipuram - 631 561, Tamilnadu, India
B.Kalpana
Scholar, Department of Mathematics
Sri Chandrasekharendra Saraswathi Viswa Mahavidyalaya
Kanchipuram - 631 561, Tamilnadu, India

Abstract: Contact map plays an important role in analyzing protein characteristics. Protein characteristics can be studied from its graph. In this paper, the steps involved in getting the graph of the protein are briefly explained for easy application.

1. Introduction: X-ray crystallography, NMR and Electron Microscopy are the experimental methods available for studying proteins. But, these experimental methods are more expensive. Hence, researchers are trying to study proteins using mathematical concepts. Also, Graph theory is a new branch of mathematics which has more useful applications. From the contact map of the protein, protein graph is obtained.

Using contact map of the protein, specific folds [1] in the protein are identified. [2] Content Based Image Retrieval (CBIR) and image registration techniques are also used to measure the similarity between contact maps. The Contact map overlap [3] measures the similarity between two proteins (in lattice model) based on the pair wise distances of the Cα – atoms of each protein. Similarity is also computed by [4] aligning the proteins to maximize the number of shared contacts in their corresponding contact maps. Similarity & dissimilarity of the protein structure is measured using matching index [5].

2. Preliminaries:

2.1 Alpha Carbon and Beta Carbon: The alpha carbon (α carbon) in organic molecules refers to the first carbon atom that attaches to a functional group. The second carbon atom is called the beta carbon (β-carbon).

2.2 Contact Maps: The distance between two residues (d_{ij}) may be defined by the distance between two carbon alpha (C_α) atoms or between two carbon beta (C_β) atoms or it may be the minimum distance between any pair of atoms belonging to the side chain or to the backbone of two residues. A contact between two given atoms (or residues) exists when a certain distance is below a given threshold.

Let P be a protein with n atoms which are labeled 1,2,3,....n.

We define the contact map of the protein as a matrix,

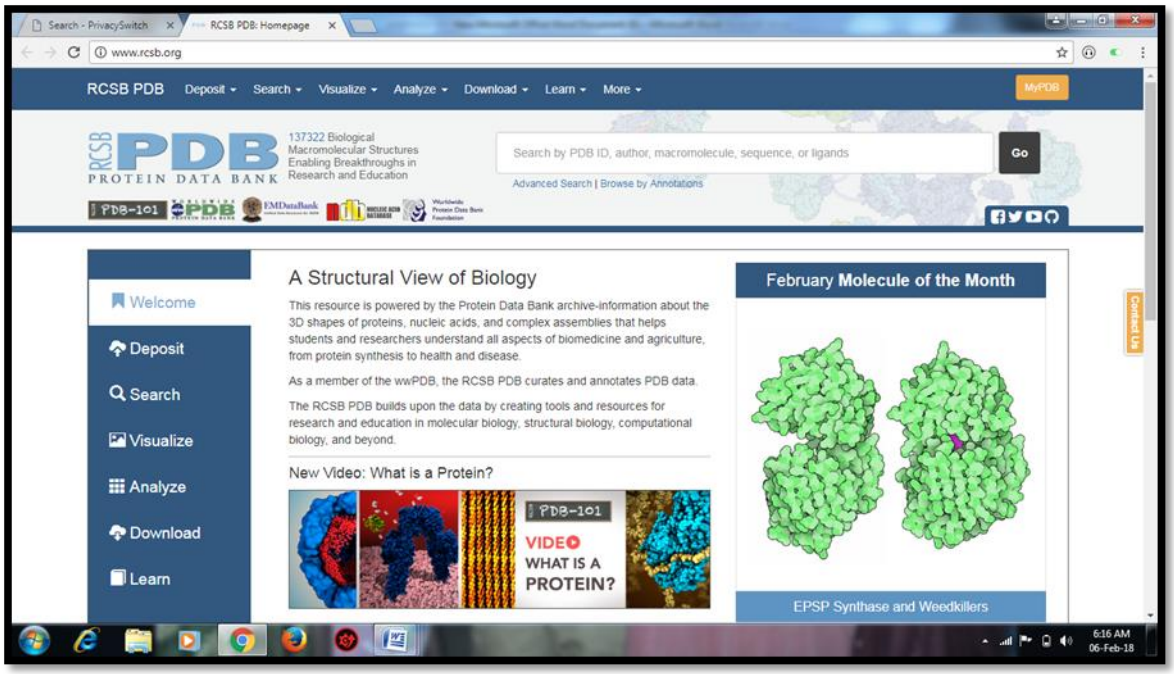
$T = (t_{ij})_{1\le i,,j\le n}$, where $t_{ij} = 1$ if $i \neq j$ & $d_{ij} \le 6$Å,

Zero, otherwise.

2.3 Graph of the Protein: A protein can be considered as a graph G = <V,E> for which each vertex $v_k \in V$ represents a residue of the protein and each $v_i - v_j \in E$ represents a contact between two residues v_i and v_j. On the other hand, there is an edge $v_i - v_j \in E$ if $t_{ij} = 1$.

3. Methodology for Getting the Protein Graph:

Step 1: Protein three dimensional coordinates can be obtained from the Protein Data Bank (PDB) as shown below. This following view is the home page of the PDB site.



By using the PDB id , we can get the atomic coordinates from the PDB as below for the protein id 2WPO.

```
ATOM     1  N   ASP A   4      70.274  15.637  43.233  1.00 29.03           N
ATOM     2  CA  ASP A   4      70.516  14.276  43.764  1.00 30.90           C
ATOM     3  C   ASP A   4      71.940  13.807  43.430  1.00 32.91           C
ATOM     4  O   ASP A   4      72.585  13.162  44.260  1.00 37.55           O
ATOM     5  CB  ASP A   4      69.466  13.306  43.210  1.00 33.23           C
ATOM     6  CG  ASP A   4      69.044  12.233  44.219  1.00 36.65           C
ATOM     7  OD1 ASP A   4      69.920  11.461  44.683  1.00 38.68           O
.....
.....

ATOM   8886  OXT ALA D 256      93.861  21.787  24.324  1.00 22.55      O
ATOM   8887  H   ALA D 256      92.826  24.130  22.985  1.00 22.00      H
```

Step2: By the definition of contact map, to get the contact map of the protein we need only the coordinates of the carbon alphas. For our convenient, we consider only 22 residues (residue 4 – residue 25) and hence 22 carbon alphas.

```
ATOM     2  CA  ASP A   4      70.516  14.276  43.764  1.00 30.90           C

ATOM    10  CA  GLU A   5      73.820  13.718  41.923  1.00 29.27           C

ATOM    20  CA  GLN A   6      75.443  17.096  42.484  1.00 32.35           C

ATOM    32  CA  GLN A   7      75.382  15.841  46.082  1.00 31.71           C

ATOM    44  CA  SER A   8      77.229  12.673  45.207  1.00 33.42           C
```

ATOM 52 CA GLN A 9 79.361 14.892 42.975 1.00 25.83 C

ATOM 64 CA ALA A 10 80.593 16.601 46.216 1.00 27.12 C

ATOM 70 CA VAL A 11 80.705 13.420 48.291 1.00 25.08 C

ATOM 78 CA ALA A 12 83.631 12.353 46.020 1.00 22.92 C

.....

.....

ATOM 175 CA TYR A 23 113.791 20.647 58.017 1.00 18.97 C

ATOM 189 CA ASP A 24 114.459 24.398 57.675 1.00 27.38 C

ATOM 198 CA GLN A 25 112.340 25.324 60.711 1.00 22.90 C

Save this coordinates of the carbon alphas in a notepad.

Step3: The three dimensional structure of a protein can be viewed through the molecular viewer Molsoft. The three dimensional structure of a protein 2WPO is viewed as shown below.

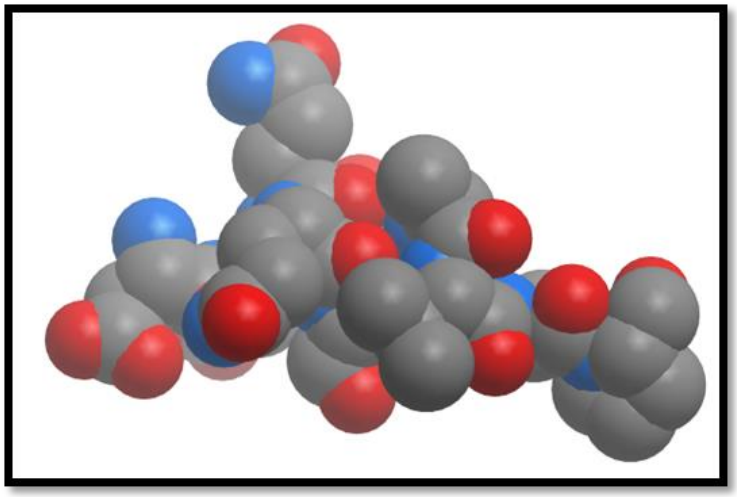


Figure1: Protein 2WPO -3D View (Residue 4 – Residue 13)

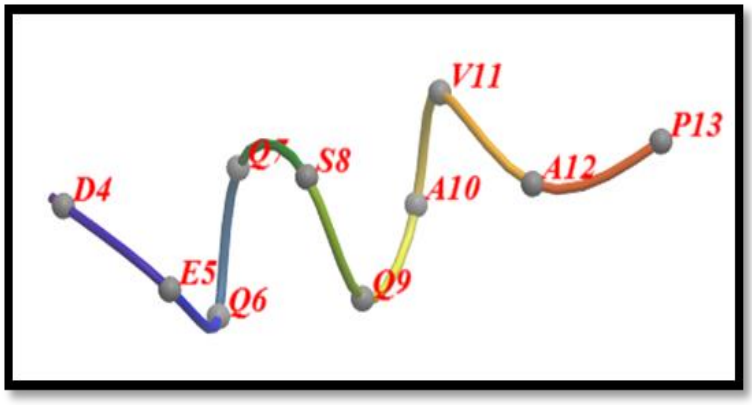


Figure2: Protein 2WPO – Wire Representation (Residue 4 – Residue 13)

The distances between residues are measured using Molsoft and the residues within the distance cutoff 6 are considered as adjacent residues and tabulated as below.

Residue	Vertex Number	Adjacent Residues
D_4	1	E_5,Q_6,Q_7
E_5	2	D_4,Q_6,Q_7,S_8,Q_9
Q_6	3	D_4,E_5,Q_7,S_8,Q_9
Q_7	4	D_4,E_5,Q_6,S_8,Q_9,A_{10}
S_8	5	L_5,Q_6,Q_7,Q_9,A_{10},V_{11}
Q_9	6	E_5,Q_6,Q_7,S_8,A_{10},V_{11},A_{12}
A_{10}	7	Q_7,S_8,Q_9,V_{11},A_{12}
V_{11}	8	S_8,Q_9,A_{10},A_{12}
A_{12}	9	Q_9,A_{10},V_{11},P_{13}
P_{13}	10	A_{12}, V_{14}

Contact map of the protein 2WPO is obtained as a matrix given below.

$$\begin{pmatrix} 0 & 1 & 1 & 1 & 0 & 0 & 0 & 0 & 0 & 0 \\ 1 & 0 & 1 & 1 & 1 & 1 & 0 & 0 & 0 & 0 \\ 1 & 1 & 0 & 1 & 1 & 1 & 0 & 0 & 0 & 0 \\ 1 & 1 & 1 & 0 & 1 & 1 & 1 & 0 & 0 & 0 \\ 0 & 1 & 1 & 1 & 0 & 1 & 1 & 1 & 0 & 0 \\ 0 & 1 & 1 & 1 & 1 & 0 & 1 & 1 & 1 & 0 \\ 0 & 0 & 0 & 1 & 1 & 1 & 0 & 1 & 1 & 0 \\ 0 & 0 & 0 & 0 & 1 & 1 & 1 & 0 & 1 & 0 \\ 0 & 0 & 0 & 0 & 0 & 1 & 1 & 1 & 0 & 1 \\ 0 & 0 & 0 & 0 & 0 & 0 & 0 & 0 & 1 & 0 \end{pmatrix}$$

From this matrix, graph of the respective protein is obtained as below.

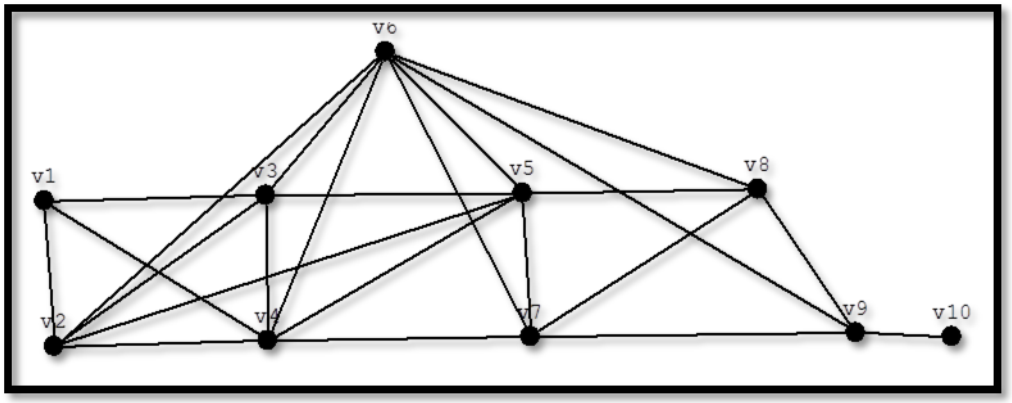


Figure3: Graph of the Protein 2WPO (Residue 4 – Residue 13)

References

1. Pankaj Barah & Som data Sinha, "Analysis of Protein folds using protein contact networks", Pramana Journal of physics, Vol. 71,(2008), pp: 2.

2. Yan, Shenggui Zhang, Fang-Xiang Wu, "Applications of graph theory in protein structure identification", Proteome Science , 9(2011).
3. Fernando Fernandes JR, Carlos Eduardo Lopes, Raquel Melo, Marcelo Santoro, Rodrigo Carceroni, Wagner Meira JR, Arnaldo Araujo, "An Image –Matching Approach to Protein Similarity Analysis", Computer Graphics and Image Processing, (2004) pp: 17-24.
4. Rosni Abdullah, Nu' Aihi Abdul Rashid & Fazilah Othman, "Graph Theory in Protein Sequence Clustering and Tertiary Structural Matching" , AIP Conference Proceedings, Vol. 971, pp:19.
5. Mageswari.R, SrinivasaRao.K, Sivakumar.K, Identifying similarity/dissimilarity between proteins through their contact maps and matching index, Global Journal of Pure and Applied Mathematics, 13(1), (2017), 233-237.

***

SIMILARITY / DISSIMILARITY OF PROTEIN STRUCTURES THROUGH STRENGTH OF NODES

R.Mageswari
Assistant Professor, Department of Mathematics
Sri Chandrasekharendra Saraswathi Viswa Mahavidyalaya
Kanchipuram - 631 561, Tamilnadu, India

Abstract: Graph of the protein is obtained from the protein contact map. Graph theoretical techniques are used to study the protein characteristics. A new method is proposed to find the similarity / dissimilarity between protein structures through its nodes strength.

Keywords: Contact Map, Protein, Node Strength.

1. Introduction: Analyzing and understanding the structure of protein is more useful in understanding its function. A total of 1,00,000 protein structures were identified by the experimental methods such as X-ray crystallography, NMR and Electron Microscopy and are available in the Protein Data Bank (PDB). But, experimental methods are more expensive, time consuming and the process is also tedious. So, mathematical methods are introduced in the analysis of proteins.

Similarity and dissimilarity of protein sequences is found using the Euclidean distance between the [1] spatial median of each protein. Structural similarity is predicted from the [2] structural descriptors derived from the geometric properties of secondary structure elements. Similarity is measured by the [3] compression ratio of the concatenated image using the image and audio compression – based approach. Among the different mathematical methods for protein structure identification, graph theoretic methods are very easy to handle, less expensive and more effective. Contact map plays an important role in understanding proteins' structure. Using contact map of the protein, specific folds [4] in the protein are identified. Similarity is also measured between protein structures from the matching pairs of secondary structure elements by the interaction of each pair between their axial line segments using a [5] fast bipartite graph matching algorithm. Another method to measure similarity is by comparing the centroids of all secondary structures using [6] largest common sub graph detection algorithm.

Similarity of the two proteins can also be measured from the [7] maximum common edge sub graph of the labeled graph of the protein according to its secondary structures, chemical properties & topological relations. [8]Homology modeling based on clique finding, identification of side chain clusters in protein structures upon graph spectrum are introduced to solve protein structure identification problems. [9] Content Based Image Retrieval (CBIR) and image registration techniques are also used to measure the similarity between contact maps. The Contact map overlap [10] measures the similarity between two proteins (in lattice model) based on the pair wise distances of the Cα – atoms of each protein. Another method uses the [11] maximum clique algorithm PLS (Phased Local Search) for finding the structural similarity between two proteins. The bipartite graph matching algorithm [12] in which the reference frames extracted from protein tertiary structure are used to find the feature vectors for matching similarity between two structures, is also used . Similarity is also computed by [13] aligning the proteins to maximize the number of shared contacts in their corresponding contact maps. Similarity & dissimilarity of the protein structure is measured using matching index [14].

In this paper, using graph theoretical concept, similarity & dissimilarity of the protein structure is measured using nodes strength.

2. Preliminaries:

2.1 Node Strength: A node's strength in a weighted network is given by the sum of the weights of its adjacent edges.

$S(v_i) = \sum_{j=1}^{20} a_{ij} w_{ij,}$ *where* a_{ij} is the adjacency matrix and w_{ij} is the weighted matrix of the nodes i and j.

2.2 Contact Map: Let P be a protein with n atoms which are labeled 1,2,3,....n. We define the contact map of the protein as a matrix,

$T = (t_{ij})_{1 \le i,,j \le n}$, where $t_{ij} = 1$ if $i \neq j$ & $d_{ij} \le 6$Å, otherwise zero.

2.3 Graph of the Protein: A protein can be considered as a graph G = <V,E> for which each vertex $v_k \in V$ represents a residue of the protein and each $v_i - v_j \in E$ represents a contact between two residues v_i and v_j. On the other hand, there is an edge $v_i - v_j \in E$ if $t_{ij} = 1$.

3. Similarity/Dissimilarity Checking Through Node Strength: Similarity / Dissimilarity of protein structures can be identified through from the graphs of the protein using the node strengths. We extract the information of a protein from its contact map and measure the similarity & dissimilarity of the protein structures using graph theoretical concepts and node strengths. Protein sequences and tertiary structures (only C_α) of the three proteins with PDB ID 2RM2, 2RR1 and 5JXL are extracted from the database PDB.

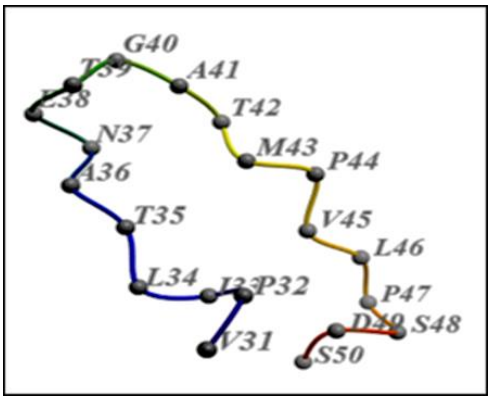


Figure1: 2RM2 -Ball and Stick Representation of Carbon-Alphas (Cα)

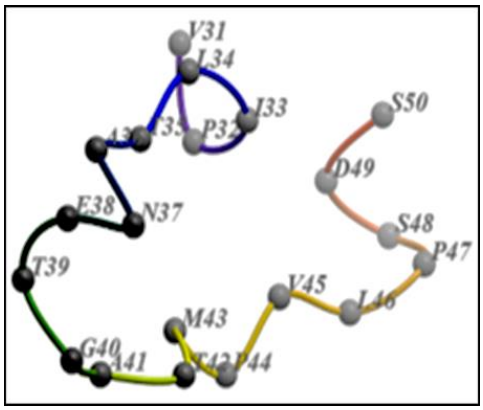


Figure2: 2RR1 (residue 31 – residue50) - Ball and Stick Representation of Carbon-Alphas

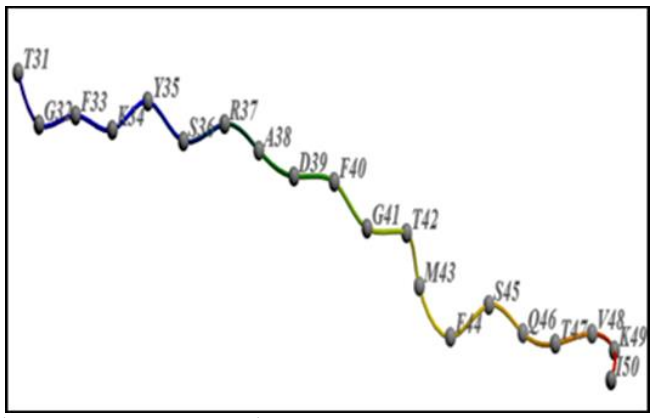


Figure3: 5JXL(residue 31 – residue50)-Ball and Stick Representation of Carbon-Alphas

The contact maps of the above three proteins are found by using the definition above and the graphs are obtained from the contact maps as shown in figure 4,5 and 6.

Consider the graph of 2RM2. Here, v_1 is connected to the vertices 2 and 3. The strength of the node v_1 is calculated as 9.36 using the definition stated above.

The remaining node strengths are calculated in the similar way and tabulated in Table 1.

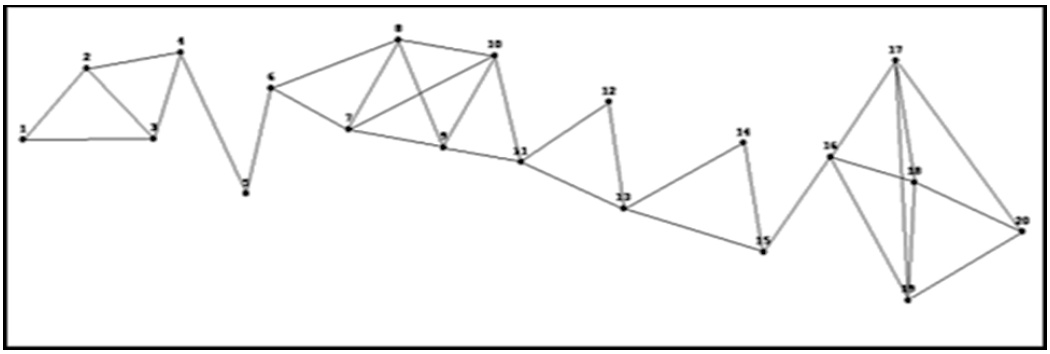


Figure4: Graph of the protein 2RM2

Calculating node strength for the protein 2RM2: Node Strength is obtained using the formula given below.

$S(v_i) = \sum_{j=1}^{20} a_{ij} w_{ij,}$ *where* a_{ij} is the adjacency matrix and w_{ij} is the weighted matrix.

For the vertex 1:
Vertex 1 is adjacent to vertex 2 and vertex 3.
Therefore, its adjacency matrix is,

$$\begin{pmatrix} 0 & 1 & 1 & 0 & 0 & 0 & 0 & 0 & 0 & 0 & 0 & 0 & 0 & 0 & 0 & 0 & 0 & 0 & 0 & 0 \end{pmatrix}$$

Its weighted matrix is,

$$\begin{pmatrix} 0 \\ 3.81 \\ 5.55 \\ 6.12 \\ 8.87 \\ 12.5 \\ 15.1 \\ 17.7 \\ 17.4 \\ 19.1 \\ 16.7 \\ 15.5 \\ 12.3 \\ 13 \\ 10.7 \\ 12.5 \\ 13.4 \\ 12.2 \\ 8.41 \\ 9.22 \end{pmatrix}$$

Therefore, $S(v_1) = 3.81+5.55 = 9.36$.
Similarly, strength of the other nodes are also calculated and listed in the Table:1.

Calculating Node Strength for the Protein 2RR1: Consider the graph of 2RR1.

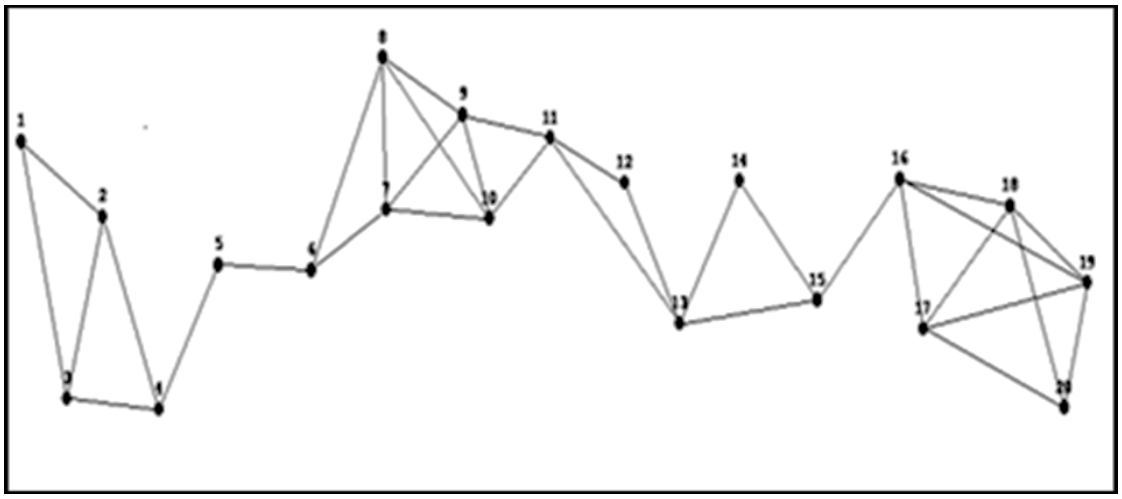


Figure5: Graph of the protein 2RR1

For the vertex 1:
Vertex 1 is adjacent to vertex 2 and vertex 3.
Therefore, $S(v_1) = 3.81+5.55 = 9.36$.
The strengths of all other nodes of the protein 2RR1 are calculated in the similar way and tabulated in Table 1.
Consider the graph of 5JXL.

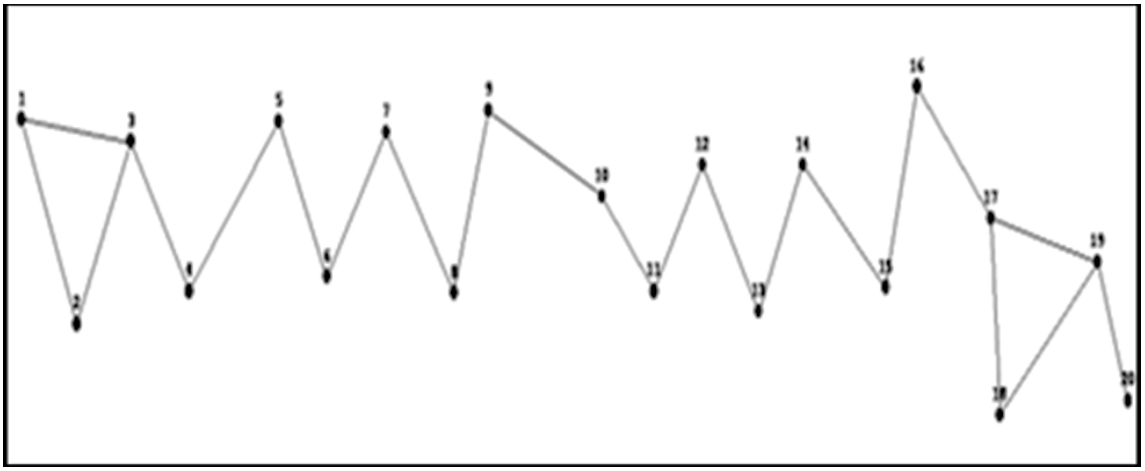


Figure6: Graph of the protein 5JXL

Calculating Strength of Nodes for the Protein 5JXL: For the vertex 1:
Vertex 1 is adjacent to vertex 2 and vertex 3.
Therefore, $S(v_1) = 3.77+5.58 = 9.35$.
The strengths of all other nodes of the protein 5JXL are calculated in the similar way and tabulated in Table 1.

Table 1: Calculation of Correlation Coefficient

S. NO	S_V	2RM2 (X)	2RR1 (Y)	5JXL (Z)	X^2	Y^2	Z^2	XY	YZ	ZX
1	S_{V_1}	9.36	9.36	9.35	87.61	87.61	87.42	87.61	87.52	87.52
2	S_{V_2}	13.42	13.42	7.55	180.01	180.01	57.00	180.01	101.32	101.32
3	S_{V_3}	13.21	13.21	7.58	174.50	174.50	57.46	174.50	100.13	100.13
4	S_{V_4}	13.45	13.45	7.59	180.90	180.90	57.61	180.90	102.09	102.09
5	S_{V_5}	7.64	7.64	7.59	58.37	58.37	57.61	58.37	57.99	57.99
6	S_{V6}	13.04	13.04	7.6	170.04	170.04	57.76	170.04	99.10	99.10
7	S_{V_7}	18.6	18.6	7.6	345.96	345.96	57.76	345.96	141.36	141.36
8	S_{V8}	18.43	18.43	7.61	339.66	339.66	57.91	339.66	140.25	140.25
9	S_{V_9}	18.41	18.41	7.62	338.93	338.93	58.06	338.93	140.28	140.28
10	$S_{V_{10}}$	18.92	18.92	7.66	357.97	357.97	58.68	357.97	144.93	144.93
11	$S_{V_{11}}$	19.14	19.14	7.59	366.34	366.34	57.61	366.34	145.27	145.27
12	$S_{V_{12}}$	7.63	7.63	7.6	58.22	58.22	57.76	58.22	57.99	57.99
13	$S_{V_{13}}$	19.29	19.29	7.61	372.10	372.10	57.91	372.10	146.80	146.80
14	$S_{V_{14}}$	7.6	7.6	7.6	57.76	57.76	57.76	57.76	57.76	57.76
15	$S_{V_{15}}$	13.45	13.45	7.59	180.90	180.90	57.61	180.90	102.09	102.09
16	$S_{V_{16}}$	18.46	18.46	7.6	340.77	340.77	57.76	340.77	140.30	140.30
17	$S_{V_{17}}$	18.91	18.91	13.06	357.59	357.59	170.56.	357.59	246.96	246.96
18	$S_{V_{18}}$	18.36	18.36	7.58	337.09	337.09	57.46	337.09	139.17	139.17
19	$S_{V_{19}}$	18.59	18.59	13.08	345.59	345.59	171.09	345.59	243.16	243.16
20	$S_{V_{20}}$	15.05	15.05	3.8	226.50	226.50	14.44	226.50	57.19	57.19
TOTAL		300.96	300.96	160.86	4876.81	4876.81	1367.23	4876.81	2451.66	2451.66

Calculation of Pearson Coefficient for Correlation:

$$\rho_{XY} = \frac{N\sum(XY)-\sum(X)\sum(Y)}{\sqrt{(N\sum(X^2)-[\sum(X)]^2}\sqrt{(N\sum(Y^2)-[\sum(Y)]^2}}$$

$$= \frac{20\times4876.81-300.96\times300.96}{\sqrt{20\times4876.81-(300.96)^2}\sqrt{20\times4876.81-(300.96)^2}}$$

$$= 1$$

$$\rho_{YZ} = \frac{N\sum(YZ)-\sum(Y)\sum(Z)}{\sqrt{(N\sum(Y^2)-[\sum(Y)]^2}\sqrt{(N\sum(Z^2)-[\sum(Z)]^2}}$$

$$= \frac{20\times2451.66-300.96\times160.86}{\sqrt{20\times4876.81-(300.96)^2}\sqrt{20\times1367.23-(160.86)^2}}$$

$$= 0.19$$

$$\rho_{ZX} = \frac{N\sum(ZX)-\sum(Z)\sum(X)}{\sqrt{(N\sum(Z^2)-[\sum(Z)]^2}\sqrt{(N\sum(X^2)-[\sum(X)]^2}}$$

$$= \frac{20\times2451.66-160.86\times300.96}{\sqrt{20\times1367.23-(160.86)^2}\sqrt{20\times4876.81-(300.96)^2}}$$

$$=.19$$

Conclusion: The correlation between the node strengths of 2RM2 and 2RR1 is found as 1 and it shows that the two proteins are exactly similar. The correlation between 2RR1 and 5JXL is 0.19 and it shows the two proteins are dissimilar.

References

1. Abo-Elkhier, Mervat M, Similarity/dissimilarity analysis of protein sequences using the spatial median as a descriptor, Journal of Biophysical Chemistry, Vol. 3 (2012), pp:142-148.
2. Pooja Jain and Jonathan D.Hirst, "Study of Protein Structural Descriptors Towards Similarity & Classification" , Computational Biophysics to Systems Biology, Vol. 36, (2007), pp:165-167.
3. Morihiro Hayashida and Tatsuya Akutsu, "Image compression – Based approach to measuring the similarity of protein structures", WSPC- Proceedings October 2007 pp:17.
4. Mahnaz Habibi, Changiz Eslahchi, Mehdi Sadeghi , Hamid Pezashk, "The interpretation of protein structures based on graph theory and contact map", Open Access Bioinformatics 2010, pp: 127-137.
5. William R.Taylor, "Protein structure comparison using Bipartite Graph Matching and its application to protein structure classification", Molecular & Cellular Proteomics, 1(4), (2002) pp. 334-339.
6. Stoicho Stoichev, Debrinka Petrova, "Protein Structure Models for Determining Protein Structure Similarity", Comp. Sys. Tech'06.
7. Cheng – Hsien Hsu, Sheng-Lung Peng and Yu-Wei Tsay, "An improved Algorithm for Protein Structural Comparison Based on Graph Theoretical Approach", Journal of Science, 2011, pp: 71-81.
8. Yan Yan, Shenggui Zhang, Fang-Xiang Wu, "Applications of graph theory in protein structure identification", Proteome Science 2011, 9.
9. Fernando Fernandes JR, Carlos Eduardo Lopes, Raquel Melo, Marcelo Santoro, Rodrigo Carceroni, Wagner Meira JR, Arnaldo Araujo, "An Image –Matching Approach to Protein Similarity Analysis", Computer Graphics and Image Processing, 2004 pp: 17-24.
10. Pankaj k.Agarwal, Nabic H.Mustafa and Yusu Wang, "Fast Molecular Shape Matching Using Contact Maps", Journal of Computational Biology, Vol. 14, (2007), pp: 131-143.
11. Wayne Pullan, "Protein Structure Alignment Using Maximum Cliques and Local Search", M.A Orgun and J.Thornton(Eds): AI 2007, 4830, pp: 776-780.
12. Rosni Abdullah, Nu' Aihi Abdul Rashid & Fazilah Othman, "Graph Theory in Protein Sequence Clustering and Tertiary Structural Matching" , AIP Conference Proceedings, Vol. 971, pp:19.
13. B.Carr, W.Hart, E.Burke J.Smith, "Alignment of protein Structures with a Memetic Evolutionary Algorithm", Proceedings of the Genetic and Evolutionary Computation Conference, 2002.
14. Mageswari.R, SrinivasaRao.K, Sivakumar.K, Identifying similarity/dissimilarity between proteins through their contact maps and matching index, Global Journal of Pure and Applied Mathematics, 13(1),(2017), 233-237.

***

ANALYSIS OF MARKED GRAPH OF CASES OF DEADLOCK USING SIGN INCIDENCE MATRIX AND ITS CONVERSION INTO DIGRAPHS

P Balaji
Assistant Professor, Department of Mathematics,
Sri Chandrasekara Saraswathi Viswa Maha Vidyalaya,,Kanchipuram, pbr1002007@yahoo.com
D.Dinakar
M.Phl Scholar, Department of Mathematics,
Sri Chandrasekara Saraswathi Viswa Maha Vidyalaya,, Kanchipuram, dhinadd16041989@gmail.com

Abstract: In this paper a marked graph is taken and analyzed for set of places which are both siphon and trap first. Then the marked graph is converted into digraphs by three methods and the graph theoretic properties are analyzed.

1.1 Introduction: In this paper we take a Petri net model which is also marked graph present in [7].First we analyze it using the algorithm given in[3,4,5].Then we convert them into digraphs by the methods given in [8].The resulting digraphs are analyzed for graph theoretic properties.

1.2 Basic Definitions:

Definition 1.2.1: Petri Net: A Petri Net is a directed bipartite graph composed of four parts, a set of places P, a set of transitions T, an input function I, an output function O.These two functions connects places and transitions. A Petri Net N is denoted by N = {P, T, I, O, M_o} Where M_o is the initial marking (no of tokens present in each place in the beginning). [1][12]

Definition 1.2.2: Siphon and Trap: A subset of places denoted as S in Petri Net N is called a siphon if *S ⊂ S *, i,e every transition having an output place in S has an input place in S.
where
*S denotes the set of input places for all transitions.
S* denotes the set of output places for all transitions.
A non-empty subset of places Q in a Petri Net N is called a trap if Q * ⊂ *Q i,e every transition having an input place in Q has an output place in Q.[3][4][5]

Definition: 1.2.3: A Marked graph is a Petri net C = (P, T, I, O) such that for each $p_i \in P, |I(p_i)| = |\{t_j / p_i \in O(t_j)\}| = 1$ and $|O(p_i)| = |\{t_j / p_i \in I(t_j)\}| = 1$. An example is given in Figure 1.

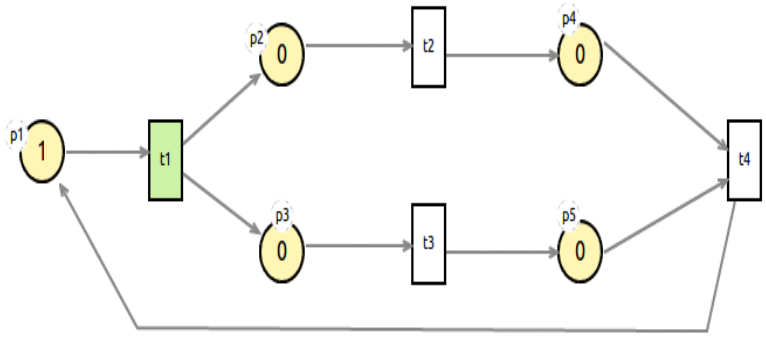


Figure 1: Example for Marked Graph

Enumeration of Siphon and Trap Subsets of Places of Marked Graphs: Here the algorithm is presented to find all subsets of places which are both siphon and trap for marked graphs given in .To apply the Algorithm the sign incidence matrix is required, and that is also defined

Definition 1.2.5: Sign Incidence Matrix: For a Petri net N with n-transitions and m-places, the sign incidence matrix A = [aij] is an n x m matrix whose entry is given as follows. [3,4,5]

a_{ij}= + if place j is an output place of transition i.
a_{ij} = - if it is an input place of transition i.
a_{ij} = ± if it is both input and output places of transition i (I.e. transition i and place j form a self loop)
a_{ij} = o otherwise.

Definition 1.2.6: Addition: The addition denoted by $\oplus$ is a commutative binary operation on the set of four elements.
B = {+,-, o, ±} defined as follows.[3][4][5]
$+\oplus -$ = ±
$x\oplus x$ = x, For every x ε B
$\pm\oplus x$ = ±, For every $x \in B$
$o\oplus x$ = x, For every $x \in B$
]
Theorem: 1.2.7: A subset of k-places Z = {p_1, p_2 ..... p_k) in a marked graph N is both siphon and trap if and only if the addition of k-column vectors of the sign incidence matrix of N, $A_1\oplus A_2\oplus.....\oplus A_k$ contains either zero entry or ± entry where A_j denote the column vector corresponding to place P_j, j = 1,2,....k.[3][4][5]

Definition: 1.2.8: A + entry is said to be neutralized by adding a—entry to get a ± entry.[3][4][5]

1.3 Algorithm for Finding Siphon and Trap using Sign Incidence Matrix
Input: Sign incidence matrix A of order m x n.
Step 1: Select A_j, the first column in the sign incidence matrix A, whose corresponding 'place is denoted as $PLACE_j$.
Set recursion level r to 1
Set $V_{j\,r} = A_j$
Set $PLACE_{jr} = PLACE_j$
Step 2: If V_{jr} has a ± entry at i^{th} row then $PLACE_j$ is a self loop with transition t_j. Go to step 5.
Step 3: If $V_{i\,j}$ has a+ entry in the kth row find a column in A, which contains a - entry at the kth row.
(a) If no such column in A \exists, Go to step 5.
(b) If such A, exists add it to $V_{j\,r}$ to obtain $V_{j(r+1),} = V_{j\,r} \oplus A_s$ containing a ± entry at k^{th} row. Then $PLACE_{j(r+1)} = PLACE_{jr} \cup PLACE_s$.
(c) Repeat this step for all possible neutralizing columns A_s. This gives a new set of $V_{j(r+1)}$'s and $PLACE_{j(r+!)}$'s.
Step 4: Increment r by 1. Repeat step 3 until there are no more + entries in each
$V_{jr} = A_1 \oplus A_2 \oplus ...A_{jr}$ or no neutralizing column can be defined.
Step 5: Any V_{jr} without + entries and without-entries (i.e., all the entries are either zero or ±) represents siphon and trap. i.e., the places in $PLACE_{ir}$ form both siphon and trap.
Step 6: Delete A_j
j=j+1
Go to step 1.
Output: All sets which are both siphon and trap.[3][4][5]

1.4 Basic Definitions of Graph theory

Definition: 1.4.1

A digraph D consists of a non-empty finite set V (D) of elements called vertices, and finite family A (D) of ordered pairs of elements of V (D) called arcs. V (D) is called the vertex set and A (D) the arc family of D. [6]

Definition: 1.4.2

Euler Digraph: In a digraph G a closed directed walk which traverses every edge of G exactly once is called a directed Euler line. A digraph containing a directed Euler line is called Euler digraph.[6]

Theorem: 1.4.3

A digraph G is an Euler digraph if and only if G is connected and is balanced i.e. $d^-(v) = d^+(v)$ for every vertex v in G.[6]

1.5 Methods to Convert Petri Nets into Digraphs: A Petri net can be converted into a digraph in three ways. [8]

Method 1: Here the transitions are changed in to vertices and places in to edges and connections as in the marked graph.

Method 2: Here the transitions are changed into edges and places into vertices.

Method 3: Here both transitions and place are changed in to vertices and arcs between them as edges.[8]

1.6 Enumerating the Set of Places which are both Siphons and Traps for the Marked Graphs: Consider the following marked graph given in [7]

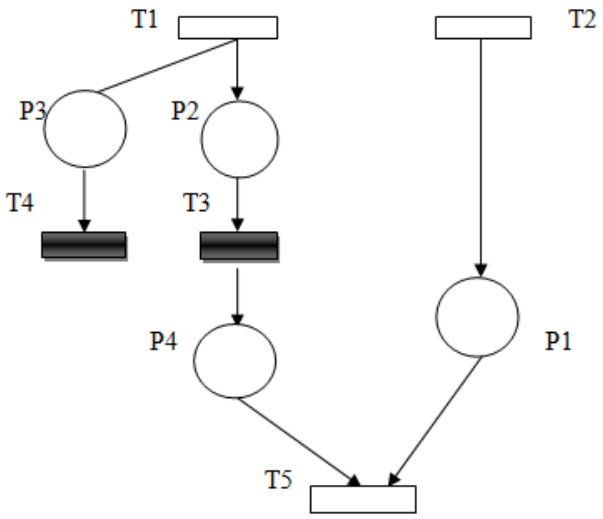


Figure2: Cases of Deadlock

The sign incidence matrix for the above marked graph is given by

$$B = \begin{array}{c} \\ t_1 \\ t_2 \\ t_3 \\ t_4 \\ t_5 \end{array} \begin{array}{c} \begin{array}{cccc} p_1 & p_2 & p_3 & p_4 \end{array} \\ \begin{pmatrix} 0 & + & + & 0 \\ + & 0 & 0 & 0 \\ 0 & - & 0 & + \\ 0 & 0 & 0 & - \\ - & 0 & 0 & - \end{pmatrix} \end{array}$$

Now we apply the algorithm for the above matrix [3][4][5]

$$A_1 = \begin{pmatrix} 0 \\ + \\ 0 \\ 0 \\ - \end{pmatrix}, \qquad Place_1 = \{P_1\}$$

A_1 has x + in 2nd row but there is no (-) in 2nd row.
Naturalizing column -> Nil.

$$A_2 = \begin{pmatrix} + \\ 0 \\ - \\ 0 \\ 0 \end{pmatrix}$$

A_2 has a + in 1st row, But there is no (-) 1st row Naturalizing row -> Nil.

$$A_3 = \begin{pmatrix} + \\ 0 \\ 0 \\ 0 \\ 0 \end{pmatrix}$$

A_3 has a + in 1st row, but there is no (-) in 1st Row Naturalizing column > Nil

$$A_4 = \begin{pmatrix} 0 \\ 0 \\ + \\ - \\ - \end{pmatrix}$$

A_4 has a + in 3rd row. Naturalizing column ->A_2

$$V_{41} = \begin{pmatrix} 0 \\ 0 \\ + \\ - \\ - \end{pmatrix} = A_4$$

$$V_{42}^{(1)} = A_4 + A_2 = \begin{pmatrix} 0 \\ 0 \\ + \\ - \\ - \end{pmatrix} \oplus \begin{pmatrix} + \\ 0 \\ - \\ 0 \\ 0 \end{pmatrix} = \begin{pmatrix} + \\ 0 \\ + \\ - \\ - \end{pmatrix}$$

$V_{42}^{(1)}$ has a + in 1st row But there is no (-) in 1st row. Neutralizing column -> Nil
Result: The marked graph in Figure 1has no set of places which are both siphon and trap.

1.7. Conversion of the Marked Graph in Figure 3.7 in to Digraphs:
METHOD 1[8]:

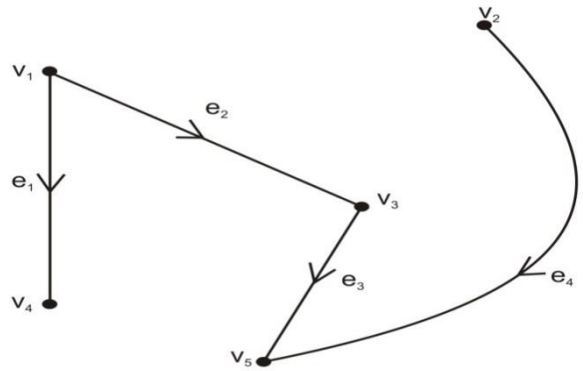


Figure: 3

METHOD 2:

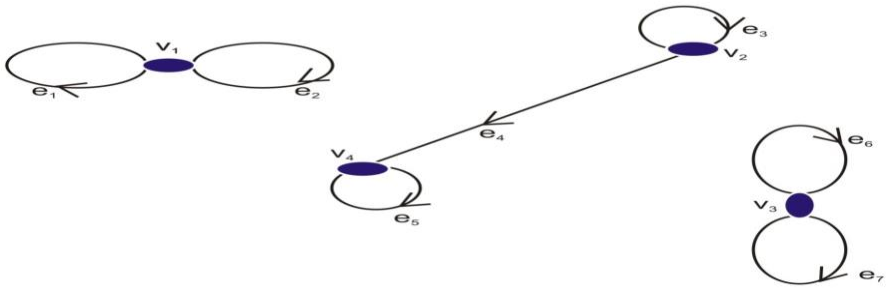


Figure: 4

METHOD - 3

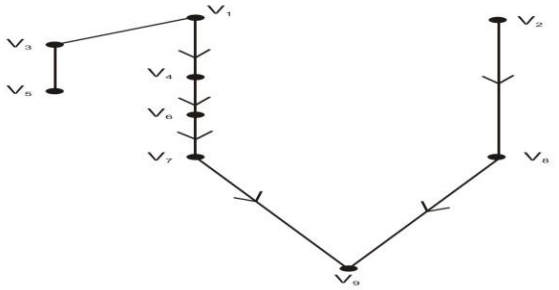


Figure: 5

1.8 Analysis of the Digraphs of the Marked Graph [6]

S. no	Digraph Figure number	Number of vertices	Number of Edges	Directed Euler Graph	Chromatic number	No of Directed Circuits
1	2	5	4	No	2	0
2	3	4	13	No	2	0
3	4	9	8	No	3	0

Conclusion: From the above analysis the marked graph taken does not have any set of places Siphon and trap. Also the converted digraphs are not Euler digraphs. Similar work is done in [9,10,11].

References:

1. J L Peterson, Petri nets, Computing Survey Vol 9, No 3,September 1977, Department of Computer Sciences, The University of Texas, Austin, Texas 78712
2. Murata T:Petrinets: Properties, Analysis and Applications, Proceedings of IEEE,Vol.77, No.4,pp.541-580(1989)
3. Ervin R.Boer and Tadao Murata, Generating Basis Siphons and Traps of Petri Nets using the Sign Incidence Matrix, IEEE Transaction on Circuits and System-I. Fundamental Theory and Application, Vol.41, No.4,April 1994
4. K.Thirusangu and K.Rangarajan, Marked Graphs and Euler Graphs, Microelectron.Reliab., Vol.37, No.2.pp. 225-235,1997
5. K.Thirusangu and K.Rangarajan, Marked Graphs and Hamiltonian Graphs, Microelectron.Reliab., Vol.37, No.8.pp. 1243-1250,1997.
6. Narasing Deo,Graph Theory with applications to Engineering and Computer Science (Prentice Hall India) 2011.
7. Deadlock freeness supervisor for marked graph H.SIOUD,Z.ACHOUR,A.SAVA* and N.REZG Bulletin of the polish Academy of sciences technical sciences, vol.57,No.3,2009.
8. Sunita Kumawat,A Graph Theoretic Approach: Petri Net, International Journal of Mathematical Sciences and Applications,Vol 1,No.3,September 2011.
9. Balaji P & Rangarajan K &.Tamil mozhi M, Marked Graph of an Four Work Station Automated Manufacturing System Sign Incidence Matrix, Applied Mechanics and Materials,Vol 813-814(2015).pp 1121-1125.

   10. Balaji. P & Rangarajan K, Marked Graphs of Basic Stock Control System and Kanban Control System and their Conversion into Digraphs, International journal of Applied Engineering Research, ISSN 0973-4562 Vol. 10 No.80 (2015)
10. Balaji P & Rangarajan K, Analysis of Marked graph of Basic control systems and kanban control systems using sign incidence matrix, Journal of Chemicals and Pharmaceutical sciences, Special issue-9, Article no 38, April 2015.

***

ANALYSIS OF MARKED GRAPH OF CASES OF AN ASSEMBLING PLAN USING SIGN INCIDENCE MATRIX AND ITS CONVERSION INTO DIGRAPHS

P Balaji
Assistant Professor, Department of Mathematics,
Sri Chandrasekara Saraswathi Viswa Maha Vidyalaya,,Kanchipuram
pbr1002007@yahoo.com
I G Balamurugan
M.Phil Scholar, Department of Mathematics,
Sri Chandrasekara Saraswathi Viswa Maha Vidyalaya,, Kanchipuram
gbmurugan1977@gmail.com

Abstract: In this paper the marked graph of cases of assembling plan is analyzed using sign incidence matrix and converted into digraphs in three methods. The converted digraphs are analyzed for graph theoretic properties

1.1 Introduction: In this paper **we** take the Petri net model which is also marked graphs present in [7].First we analyze them using the algorithm given in [3,4,5].Then we convert them into digraphs by the methods given in [8].The resulting digraphs are analyzed for graph theoretic properties.

1.2 Basic Definitions:

Definition 1.2.1: Petri Net: A Petri Net is a directed bipartite graph composed of four parts, a set of places P, a set of transitions T, an input function I, an output function O. These two functions connects places and transitions. A Petri Net N is denoted by N = {P, T, I, O, M_o} Where M_o is the initial marking (no of tokens present in each place in the beginning)[1,2].

Definition 1.2.2: Siphon and Trap: A subset of places denoted as S in Petri Net N is called a siphon if *S C S *, i,e every transition having an output place in S has an input place in S. where
*S denotes the set of input places for all transitions.
S* denotes the set of output places for all transitions.
A non-empty subset of places Q in a Petri Net N is called a trap if Q * C *Q i,e every transition having an input place in Q has an output place in Q.[3,4,5].

Definition: 1.2.3: A Marked graph is a Petri net C = (P, T, I, O) such that for each $p_i \in P, |I(p_i)| = |\{ t_j / p_i \in O(t_j)\}| = 1$ and $|O(p_i)| = |\{ t_j / p_i \in I(t_j)\}| = 1$. [3,4,5]

1.3 Enumeration of Siphon and Trap Subsets of Places of Marked Graphs: Here the algorithm is presented to find all subsets of places which are both siphon and trap for marked graphs given in .To apply the Algorithm the sign incidence matrix is required, and that is also defined[3,4,5].

Definition 1.3.1: Sign Incidence Matrix: For a Petri net N with n-transitions and m-places, the sign incidence matrix A = [aij] is an n x m matrix whose entry is given as follows.

a_{ij} = + if place j is an output place of transition i.
a_{ij} = - if it is an input place of transition i.
a_{ij} = ± if it is both input and output places of transition i (I.e. transition i and place j form a self loop)
a_{ij} = o otherwise.[3,4,5].

Definition 1.3.2: Addition: The addition denoted by $\oplus$ is a commutative binary operation on the set of four elements. B = {+,-, o, ±} defined as follows.

$+\oplus - = \pm$

$x\oplus x = x$, For every $x \in B$

$\pm\oplus x = \pm$, For every $x \in B$

$o\oplus x = x$, For every $x \in B$ [3,4,5].

Theorem: 1.3.3: A subset of k-places Z = $\{p_1, p_2 \ldots\ldots p_k)$ in a marked graph N is both siphon and trap if and only if the addition of k-column vectors of the sign incidence matrix of N, $A_1\oplus A_2\oplus\ldots\ldots\oplus A_k$ contains either zero entry or ± entry where $A_j$denote the column vector corresponding to place P_j, j = 1,2,....k. [3,4,5]

Definition: 1.3.4: A + entry is said to be neutralized by adding a—entry to get a ± entry.

1.4 Algorithm for Finding Siphon and Trap using Sign Incidence Matrix:

Input: Sign incidence matrix A of order m x n.

Step 1: Select A_j, the first column in the sign incidence matrix A, whose corresponding 'place is denoted as $PLACE_j$.

Set recursion level r to 1

Set $V_{j\,r} = A_j$

Set $PLACE_{jr} = PLACE_j$

Step 2: If V_{jr} has a ± entry at i^{th} row then $PLACE_j$ is a self loop with transition t_j. Go to step 5.

Step 3: If $V_{i\,j}$ has a+ entry in the kth row find a column in A, which contains a - entry at the kth row.

(a) If no such column in A\exists, Go to step 5.

(b) If such A, exists add it to $V_{j\,r}$ to obtain $V_{j(r+1),} = V_{j\,r} \oplus A_s$ containing a ± entry at k^{th} row. Then $PLACE_{j(r+1)} = PLACE_{jr} \cup PLACE_s$.

(c) Repeat this step for all possible neutralizing columns A_s. This gives a new set of $V_{j(r+1)}$'s and $PLACE_{j(r+!)}$'s.

Step 4: Increment r by 1. Repeat step 3 until there are no more + entries in each

$V_{jr} = A_1 \oplus A_2 \oplus \ldots A_{jr}$ or no neutralizing column can be defined.

Step 5: Any V_{jr} without + entries and without-entries (i.e., all the entries are either zero or ±) represents siphon and trap. i.e., the places in $PLACE_{jr}$ form both siphon and trap.

Step 6:

Delete A_j

j=j+1

Go to step 1.

Output: All sets which are both siphon and trap.[3,4,5]

1.5 Basic Definitions of Graph Theory

Definition:1.5.1A digraph D consists of a non-empty finite set V (D) of elements called vertices, and finite family A (D) of ordered pairs of elements of V (D) called arcs. V (D) is called the vertex set and A (D) the arc family of D.[6].

Definition:1.5.2 Euler Digraph: In a digraph G a closed directed walk which traverses every edge of G exactly once is called a directed Euler line. A digraph containing a directed Euler line is called Euler digraph.[6].

Theorem: 1.5.3 A digraph G is an Euler digraph if and only if G is connected and is balanced i.e. $d^-(v) = d^+(v)$ for every vertex v in G.[6].

Methods to Convert Petri Nets into Digraphs: A Petri net can be converted into a digraph in three ways.

Method 1: Here the transitions are changed in to vertices and places in to edges and connections as in the marked graph.
Method 2: Here the transitions are changed into edges and places into vertices.
Method 3: Here both transitions and place are changed in to vertices and arcs between them as edges.

1.7 Enumerating the Set of Places which are both Siphons and Traps for the Marked Graphs: Consider the following marked graph given in [7]

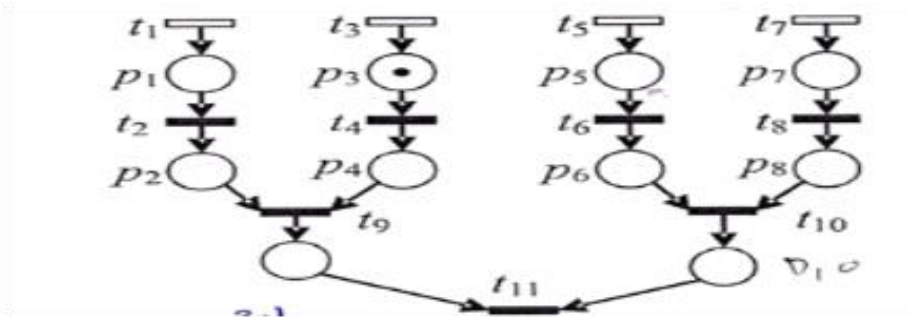


Figure 1: Marked Graph of Cases of Assembling Plan

The sign incidence matrix for the above marked graph is given by

	P1	P2	P3	P4	P5	P6	P7	P8	P9	P10
t1	-	0	0	0	0	0	0	0	0	0
t2	-	+	0	0	0	0	0	0	0	0
t3	0	0	-	0	0	0	0	0	0	0
t4	0	0	-	+	0	0	0	0	0	0
t5	0	0	0	0	-	0	0	0	0	0
t6	0	0	0	0	-	+	0	0	0	0
t7	0	0	0	0	0	0	-	0	0	0
t8	0	0	0	0	0	0	-	+	0	0
t9	0	-	0	-	0	0	0	0	+	0
t10	0	0	0	0	0	-	0	-	0	+
t11	0	0	0	0	0	0	0	0	-	-

$$V_{11} = A_1 = \begin{bmatrix} - \\ - \\ 0 \\ 0 \\ 0 \\ 0 \\ 0 \\ 0 \\ 0 \\ 0 \\ 0 \end{bmatrix}$$

V_{11} has no + in 1 st row we can't proceed further
Place $_{11}$ = { P_1}

$$V_{21} = A_2 = \begin{bmatrix} 0 \\ + \\ 0 \\ 0 \\ 0 \\ 0 \\ 0 \\ 0 \\ - \\ 0 \\ 0 \end{bmatrix}$$

Place $_{21}$ = { P_2}
∴ V_{21} has a + in IInd row
The neutralizing column is A_1

$$V_{21}^{(1)} = V_{21} \oplus A_1$$

$$= \begin{bmatrix} 0 \\ + \\ 0 \\ 0 \\ 0 \\ 0 \\ 0 \\ 0 \\ - \\ 0 \\ 0 \end{bmatrix} \oplus \begin{bmatrix} - \\ - \\ 0 \\ 0 \\ 0 \\ 0 \\ 0 \\ 0 \\ 0 \\ 0 \\ 0 \end{bmatrix} = \begin{bmatrix} - \\ \pm \\ - \\ 0 \\ 0 \\ 0 \\ 0 \\ 0 \\ - \\ 0 \\ 0 \end{bmatrix}$$

Since V_2 has no + no neutralizing column.
Proceeding in the similar manner we find no set of places which are both siphon and trap.

1.8 Conversion of Marked Graph into Digraphs: The above marked graph is converted into digraphs by the three methods given in [8].They are shown below.

Method 1

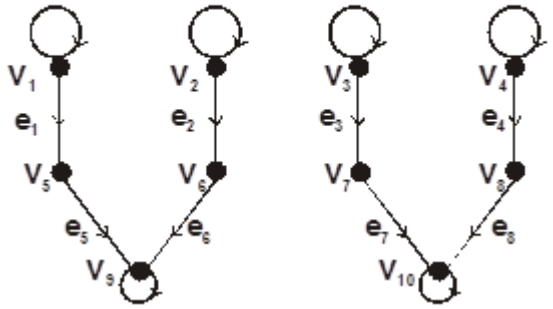


Figure 2

Method 2

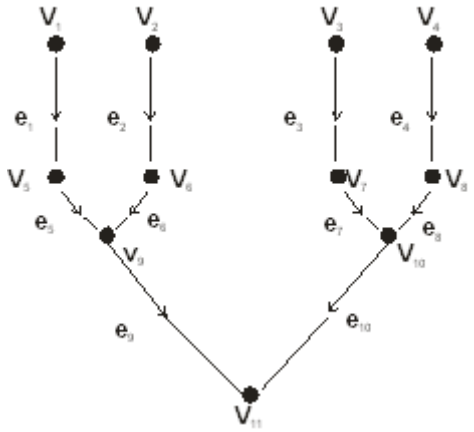


Figure 3

Method 3

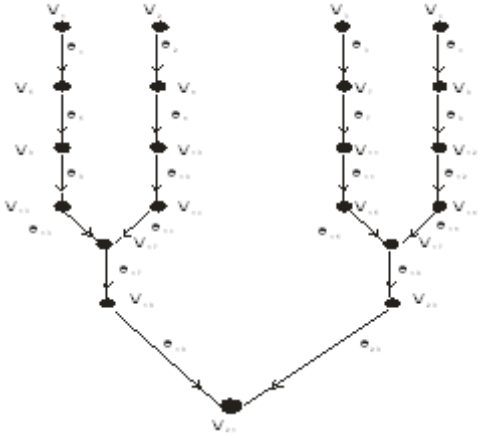


Figure 4

The converted digraphs in Figure 2, 3, 4 are analyzed for graph theoretic properties and the results are tabulated.

1.9 Analysis of the Digraphs of the Marked Graph

S. No	Digraph Figure number	Number of vertices	Number of Edges	Directed Euler Graph	Chromatic number	No of Directed Circuits
1	2	10	8	No	2	0
2	3	11	10	No	2	0
3	4	21	16	No	3	0

Conclusion: From the above analysis the marked graph taken does not have any set of places that are both siphon and trap. Also the converted digraphs are not Euler digraphs. The graph theoretic properties of the digraphs are discused.Smiliar work done by the same author is given in [9, 10]

References:

1. J L Peterson, Petri nets, Computing Survey Vol 9, No 3, September 1977, Department of Computer Sciences, The University of Texas, Austin, Texas 78712.
2. Murata T:Petrinets: Properties, Analysis and Applications, Proceedings of IEEE,Vol.77, No.4,pp.541-580(1989)
3. Ervin R.Boer and Tadao Murata, Generating Basis Siphons and Traps of Petri Nets using the Sign Incidence Matrix, IEEE Transaction on Circuits and System-I. Fundamental Theory and Application, Vol.41, No.4,April 1994
4. K.Thirusangu and K.Rangarajan, Marked Graphs and Euler Graphs, Microelectron.Reliab., Vol.37, No.2.pp. 225-235,1997
5. K.Thirusangu and K.Rangarajan, Marked Graphs and Hamiltonian Graphs, Microelectron.Reliab., Vol.37, No.8.pp. 1243-1250,1997
6. NarasingDeo,Graph Theory with applications to Engineering and Computer Science (Prentice Hall India) 2011.
7. H. Sioud, Z. Achour , A. Sava and N. Rezg, Deadlock freeness supervisor for marked graph, Bulletin of the polish academy of sciences(vol. 57, No. 3, 2009).
8. Sunita Kumawat,A Graph Theoretic Approach: Petri Net,International Journal of Mathematical Sciences and Applications,Vol 1,No.3,September 2011.
9. Balaji P &Rangarajan K &.Tamil mozhi M, Analysis of Marked Graphs of Two Machine System Processing Two Part Types Using Sign Incidence Matrix, Paper presented to the National conference NCISE 2014,AVIT Chennai, India,18 & 19 December 2014
10. Balaji P. and Rangarajan K, Marked Graph of Automated Manufacturing Cell with three Machines three Robots and two Part Types and its Conversion into Digraph, Transylvanian Review, Special Issue ,Vol XXIV, No. 9, Special Issue, 2016

***

ANALYSIS OF MARKED GRAPH WITH EQUIVALENT CRITICAL PLACE USING SIGN INCIDENCE MATRIX AND ITS CONVERSION INTO DIGRAPHS

P Balaji
Assistant Professor, Department of Mathematics,
Sri Chandrasekara Saraswathi Viswa Maha Vidyalaya,,Kanchipuram, pbr1002007@yahoo.com
I Davidraj
M.Phil Scholar, Department of Mathematics,
Sri Chandrasekara Saraswathi Viswa Maha Vidyalaya, Kanchipuram, idavidrajsinnaci@gmail.com

Abstract: In this paper the marked graph with equivalent critical place is analyzed using sign incidence matrix and converted into digraphs in three methods. The converted digraphs are analyzed for graph theoretic properties.

1.1 Introduction: In this paper **we** take the Petri net model which is also marked graph present in [6].First we analyze it using the algorithm given in .[3,4,5].Then we convert them into digraphs by the methods given in [7].The resulting digraphs are analyzed for graph theoretic properties.

1.2 Basic Definitions:

Definition 1.2.1: Petri Net: A Petri Net is a directed bipartite graph composed of four parts, a set of places P, a set of transitions T, an input function I, an output function O.These two functions connects places and transitions. A Petri Net N is denoted by N = {P, T, I, O, M_o} Where M_o is the initial marking (no of tokens present in each place in the beginning).[1,2]

Definition 1.2.2: Siphon and Trap: A subset of places denoted as S in Petri Net N is called a siphon if *S C S *, i,e every transition having an output place in S has an input place in S. where
*S denotes the set of input places for all transitions.
S* denotes the set of output places for all transitions.

A non-empty subset of places Q in a Petri Net N is called a trap if Q * C *Q i,e every transition having an input place in Q has an output place in Q. [3,4,5]

Definition: 1.2.3 Marked Graph: A Marked graph is a Petri net in which each place as exactly one input transition and one output transition. [3,4,5]

1.3 Enumeration of Siphon and Trap Subsets of Places of Marked Graphs: Here the algorithm is presented to find all subsets of places which are both siphon and trap for marked graphs given in .To apply the Algorithm the sign incidence matrix is required, and that is also defined. [3,4,5]

Definition 1.3.1: Sign Incidence Matrix: For a Petri net N with n-transitions and m-places, the sign incidence matrix A = [aij] is an n x m matrix whose entry is given as follows.

a_{ij} = + if place j is an output place of transition i.
a_{ij} = - if it is an input place of transition i.
a_{ij} = ± if it is both input and output places of transition i (I.e. transition i and place j form a self loop)
a_{ij} = o otherwise. [3,4,5]

Definition 1.3.2: Addition: The addition denoted by ⊕ is a commutative binary operation on the set of four elements. B = {+,-, o, ±} defined as follows.

$+\oplus - = \pm$
$x\oplus x = x$, For every $x \in B$
$\pm\oplus x = \pm$, For every $x \in B$
$o\oplus x = x$, For every $x \in B$..[3,4,5]

Theorem: 1.3.3: A subset of k-places Z = {p_1, p_2 ..... p_k) in a marked graph N is both siphon and trap if and only if the addition of k-column vectors of the sign incidence matrix of N, $A_1\oplus A_2\oplus.....\oplus A_k$ contains either zero entry or ± entry where A_j denote the column vector corresponding to place P_j, j = 1,2,....k. . .[3,4,5]

Definition: 1.3.4: A + entry is said to be neutralized by adding a—entry to get a ± entry. .[3,4,5]

1.4 Algorithm for Finding Siphon and Trap using Sign Incidence Matrix:
Input: Sign incidence matrix A of order m x n.
Step 1: Select A_j, the first column in the sign incidence matrix A, whose corresponding 'place is denoted as $PLACE_j$.
Set recursion level r to 1
Set $V_{j\,r} = A_j$
Set $PLACE_{jr} = PLACE_j$
Step 2: If V_{jr} has a ± entry at i^{th} row then $PLACE_j$ is a self loop with transition t_j. Go to step 5.
Step 3: If $V_{i\,j}$ has a+ entry in the kth row find a column in A, which contains a - entry at the kth row.
(a) If no such column in A \exists, Go to step 5.
(b) If such A, exists add it to $V_{j\,r}$ to obtain $V_{j(r+1),} = V_{j\,r} \oplus A_s$ containing a ± entry at k^{th} row. Then $PLACE_{j(r+1)} = PLACE_{jr} \cup PLACE_s$.
(c) Repeat this step for all possible neutralizing columns A_s. This gives a new set of $V_{j(r+1)}$'s and $PLACE_{j(r+!)}$'s.
Step 4: Increment r by 1. Repeat step 3 until there are no more + entries in each
$V_{jr} = A_1 \oplus A_2 \oplus ...A_{jr}$ or no neutralizing column can be defined.
Step 5: Any V_{jr} without + entries and without-entries (i.e., all the entries are either zero or ±) represents siphon and trap. i.e., the places in $PLACE_{jr}$ form both siphon and trap.
Step 6:
Delete A_j
j=j+1
Go to step 1.
Output: All sets which are both siphon and trap. [3,4,5]

1.5 Basic Definitions of Graph Theory:
Definition: 1.5.1A digraph D consists of a non-empty finite set V (D) of elements called vertices, and finite family A (D) of ordered pairs of elements of V (D) called arcs. V (D) is called the vertex set and A (D) the arc family of D. [10]

Definition: 1.5.2 Euler Digraph: In a digraph G a closed directed walk which traverses every edge of G exactly once is called a directed Euler line. A digraph containing a directed Euler line is called Euler digraph.[10]

Theorem: 1.5.3 A digraph G is an Euler digraph if and only if G is connected and is balanced i.e. $d^-(v) = d^+(v)$ for every vertex v in G. [10]

1.6 Enumerating the Set of Places which are both Siphons and Traps for the Marked Graph
Consider the following marked graph given in [6]

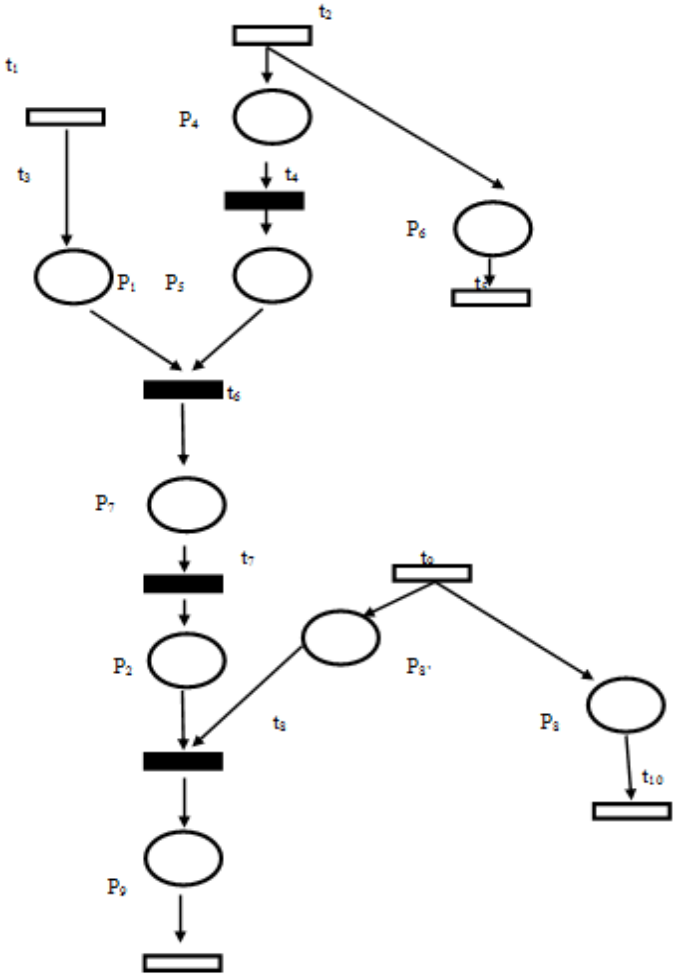


Figure 1: Marked Graph with Equivalent Critical Place

The sign incidence matrix for the above marked graph is given by

$$A= \begin{array}{c} \\ t1 \\ t2 \\ t3 \\ t4 \\ t5 \\ t6 \\ t7 \\ t8 \\ t9 \\ t10 \end{array} \begin{array}{c} \begin{array}{ccccccccc} p1 & p2 & p3 & p4 & p5 & p6 & p7 & p8 & p9 \end{array} \\ \begin{pmatrix} + & 0 & 0 & 0 & 0 & 0 & 0 & 0 & 0 \\ 0 & 0 & + & + & 0 & 0 & 0 & 0 & 0 \\ 0 & 0 & - & 0 & 0 & 0 & 0 & 0 & 0 \\ 0 & - & 0 & + & 0 & 0 & 0 & 0 & 0 \\ - & 0 & 0 & - & + & 0 & 0 & 0 & 0 \\ 0 & 0 & 0 & 0 & - & + & 0 & 0 & 0 \\ 0 & 0 & 0 & 0 & 0 & - & - & 0 & + \\ 0 & 0 & 0 & 0 & 0 & 0 & + & + & 0 \\ 0 & 0 & 0 & 0 & 0 & 0 & 0 & - & 0 \\ 0 & 0 & 0 & 0 & 0 & 0 & 0 & 0 & - \end{pmatrix} \end{array}$$

Applying Algorithm 1.4 [3,4,5]

$$A_1 = \begin{bmatrix} + \\ 0 \\ 0 \\ 0 \\ - \\ 0 \\ 0 \\ 0 \\ 0 \\ 0 \end{bmatrix} \qquad \text{Place}_1 = \{p_1\}$$

For v=1

$$V_{11} = \begin{bmatrix} + \\ 0 \\ 0 \\ 0 \\ - \\ 0 \\ 0 \\ 0 \\ 0 \\ 0 \end{bmatrix} \qquad \text{Place}_{11} = \{p_1\}$$

V_{11} has a (+) in Ist Row But in Ist row no (-) .Therefore no neutralizing column. Similarly for A_2,A_3 no neutralizing column.

$$A_4 = \begin{bmatrix} 0 \\ 0 \\ 0 \\ + \\ - \\ 0 \\ 0 \\ 0 \\ 0 \\ 0 \end{bmatrix} \qquad V_{41} \text{ has a + in } 4^{th} \text{ row.Neutralizing column is } A_2$$

$V_{42}^{(1)} = V_{41} + A_2$

$$= \begin{bmatrix}0\\0\\0\\+\\-\\0\\0\\0\\0\\0\end{bmatrix} + \begin{bmatrix}0\\+\\-\\0\\0\\0\\0\\0\\0\\0\end{bmatrix} = \begin{bmatrix}0\\+\\0\\\pm\\-\\0\\0\\0\\0\\0\end{bmatrix}$$

Place $_{42}^{(1)} = \{p_4, p_2\}$

$v_{42}^{(1)}$ has + in 2nd row
But no – in IInd row
∴ no Naturalizing column.

Proceeding in the above manner we get no set of places which are both siphon and trap.

1.7 Methods to Convert Petri Net into Digraphs and Conversion of above Marked Graph into Digraph: A Petri net can be converted into a digraph in three ways. [7]

Method 1: Here the transitions are changed in to vertices and places in to edges and connections as in the marked graph.

Method 2: Here the transitions are changed into edges and places into vertices.

Method 3: Here both transitions and place are changed in to vertices and arcs between them as edges.

Now we convert the marked graph in Figure 1 into digraphs by the above three methods. The following digraph given in Figure 2 is obtained by method I.[7]

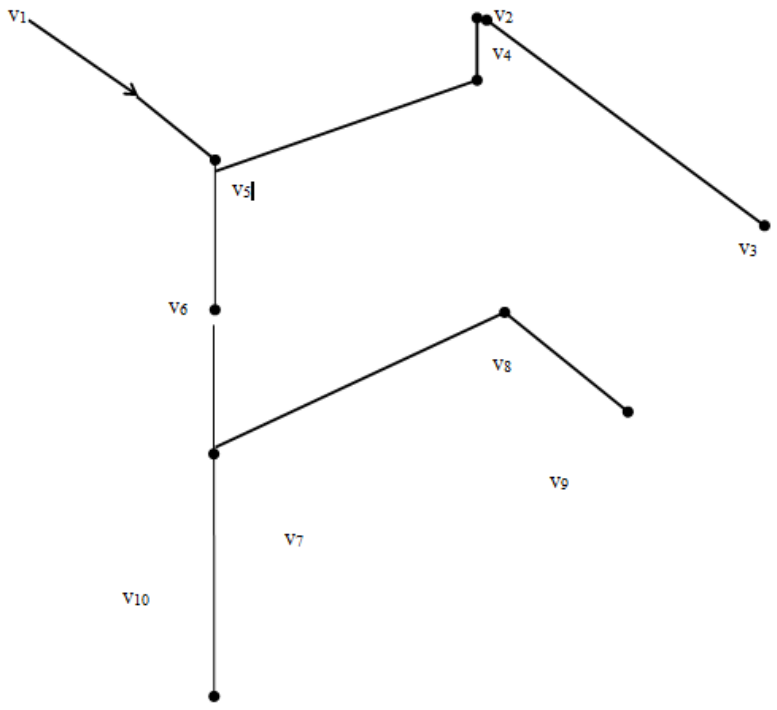


Figure 2: Digraph of the marked graph given in Figure 1(Method-I)

The following digraph given in Figure 3 is obtained by method II.[7]

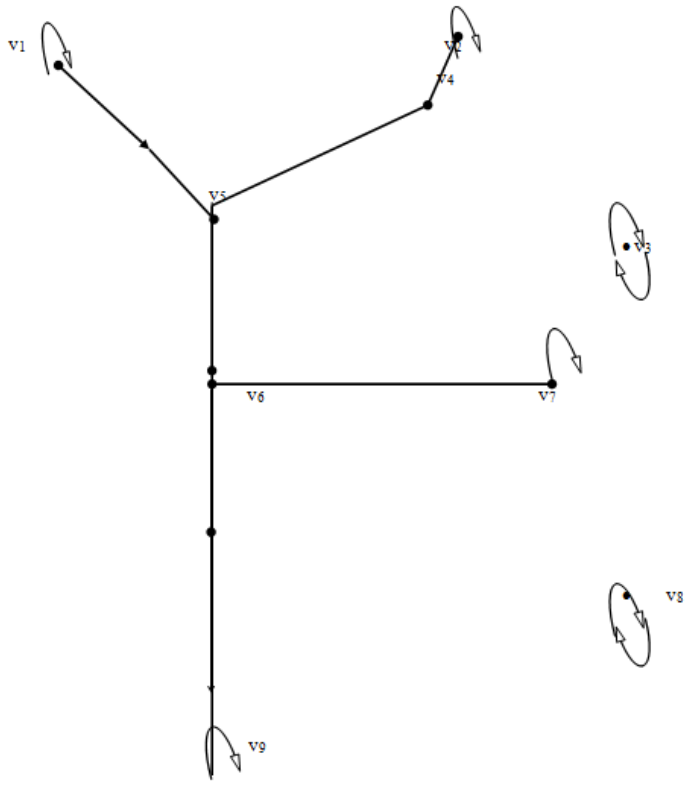


Figure 3: Digraph of the marked graph given in Figure3.1 (Method-II)

The following digraph given in Figure 4 is obtained by method III.[7]

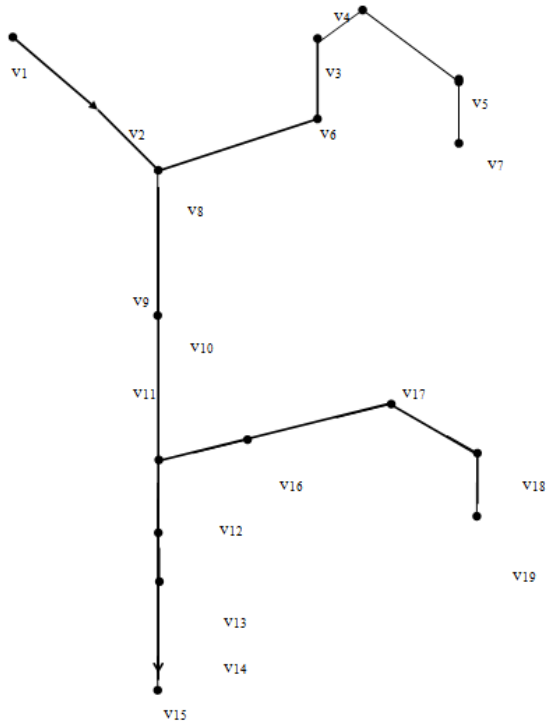


Figure 4: Digraph of the marked graph given in Figure1 (Method-III)

1.8 Analysis of the Above Three Digraphs

S. No	Digraph Figure number	Number of vertices	Number of Edges	Directed Euler Graph	Chromatic number	No of Directed Circuits
1	2	10	9	No	3	0
2	3	9	7	No	2	0
3	4	18	12	No	3	0

Conclusion: In this paper the marked graph with equivalent critical place is taken and analyzed for set of places which are both siphon and trap. Then the marked graph is converted into diagraphs by three methods. For one marked graph three diagraphs are obtained none of them are Euler or Hamiltonian diagraphs the graph of theoretic properties of the directed graph are analyzed and reported. The similar papers are referred in [8, 9]

References:

1. J L Peterson, Petri nets, Computing Survey Vol 9, No 3, September 1977, Department of Computer Sciences, The University of Texas, Austin, Texas 78712.
2. Murata T:Petrinets: Properties, Analysis and Applications, Proceedings of IEEE,Vol.77, No.4,pp.541-580(1989)
3. Ervin R.Boer and Tadao Murata, Generating Basis Siphons and Traps of Petri Nets using the Sign Incidence Matrix, IEEE Transaction on Circuits and System-I. Fundamental Theory and Application, Vol.41, No.4,April 1994
4. K.Thirusangu and K.Rangarajan, Marked Graphs and Euler Graphs, Microelectron.Reliab., Vol.37, No.2.pp. 225-235,1997
5. K.Thirusangu and K.Rangarajan, Marked Graphs and Hamiltonian Graphs, Microelectron.Reliab., Vol.37, No.8.pp. 1243-1250,1997.
6. H.Sioud,Z.Achour,A.Sava,N.Rezg,"Deadlock Freeness Supervisor for Marked graph"Bulletin of Polish academy of sciences, Vol 57,n03,pp 281-288 (2009)
7. Sunita Kumawat,A Graph Theoretic Approach: Petri Net,International Journal of Mathematical Sciences and Applications,Vol 1,No.3,September 2011.
8. P Balaji and Rangarajan K, Analysis of Marked graph of Basic control systems and kanban control systems using sign incidence matrix, Journal of Chemicals and Pharmaceutical sciences, Special issue-9, Article no 38, April 2015.
9. Balaji P & Rangarajan K &.Tamil mozhi M, Marked Graph of an Four Work Station Automated Manufacturing System and its conversion into Euler Digraph ,Paper presented to the National Conference NCCC2015, Anna University, Tirunelveli region,Tamilnadu, India on May 4th and 5th 2015.
10. Narasing Deo,Graph Theory with applications to Engineering and Computer Science (Prentice Hall India) 2011.

***

DIGRAPHS OF THE MARKED GRAPHS OF A MACHINE THAT PROCESS ONE JOB AT A TIME AND BASIC SCHEMA OF A PRODUCTION STATE

P Balaji
Assistant Professor of Mathematics,
Sri ChandraSekarendra Saraswathi Viswa Maha Viidyalaya(Deemed University), Kanchipuram, India
pbr1002007@yahoo.com
M Devarajulu
M.Phil Scholar, Department of Mathematics,
Sri Chandrasekara Saraswathi Viswa Maha Vidyalaya, Kanchipuram

Abstract: In this paper the marked graphs of Machine that process one job at a time, Basic Schema of a Production state are converted into digraph by two methods. The resulting digraphs except one are not Euler digraphs. In a previous paper the same marked graphs are analysed and the sets of places which form both siphon and trap using a Algorithm found out..For the two marked graphs no sets of places are siphon and traps.

Keywords: : Petri Nets, Marked Graphs, Flexible Manufacturing Systems, Machine that process one job at a time, Basic Schema of a Production state, Sign Incidence Matrix, digraphs, Euler Digraphs.

Introduction: A Petri net is a powerful modeling formulation in a computer science, system engineering and many others disciplines. A Petri net combines a well-defined mathematical theory with a graphical representation of the dynamic behavior of the system the theoretic aspects of Petri net allows precise modeling and analysis of system behavior while the graphical representation of Petri net enables visualization of the modeled system state change. Because of this Petri net has been used to model various kinds of dynamic event driven system like computer networks, communication system, manufacturing plant etc.

Petri Nets are introduced in [1,2] Generating Basis Siphons and traps of Petri Nets using the Sign Incidence Matrix is in [3] The analysis of marked graphs using sign Incidence matrix is given [3,4,5]. For different FMS/AMS finding the set of places which are both siphon and trap by using the algorithm given in [3,4,5] is shown in [,8,9,10,11,12].In [11] we took the marked graph models of one basic stock control system and three kanban control system given in [6] and analyzed it using sign incidence matrix. By the analysis we got a few set of places which are both siphon and trap. In this paper we Convert two of the marked graphs found in [6] in to a digraph by changing transitions into vertices and places into edges. We found that the resulting digraph is not an Euler digraph. So further investigation is not possible according to [4].But in [12] the same authors found out one marked graph of a AMS conversion gives an Euler Digraph and analysis as per [4] was possible.

The rest of the paper is organized as follows. Section I contains basic definitions. Section II contains the marked graph models of and the set of places which are both siphon and trap found out using the Algorithm given in [3,4]. It also contains the digraphs converted from the marked graphs as given in [7]. Section III contains Conclusions and References.

1. Basic Definition:

Definition 1.1: A PN is a bipartite graph, where nodes are classified as places and transitions (graphically pictured as circles and bars, respectively), and directed arcs connect only nodes of different

type. Places are endowed with integer variables called tokens. A marked PN is a 5-tuple N = (P, T, F, W, M_0), where P is a finite set of places, T is a finite set of transitions, with $P \cap T = \emptyset$, $F \subset (P \times T) \cup (T \times P)$ is the incidence or flow relation (each element of F corresponds to an arc in the PN), W : F —> N \ {o} is the arc weight function, and M_0: P —> N is the initial marking (a marking M : P —> N defines the distribution of tokens in places), where N is the set of natural numbers.

Definition1.2: **Marked Graph:** A Marked graph is a Petri net in which each place as exactly one input transition and one output transition.

Definition 1.3: Flexible Manufacturing System: A Flexible manufacturing system (FMS) is an integrated computer controlled configuration of machine tools and automated material handling devices that simultaneously process medium sized volumes of a variety of part types. Flexible manufacturing system is a discrete event dynamical system in which the work pieces Of various job classes enter the system asynchronously and are Concurrently, sharing the limited resources , viz.,workstations,robots,MHS,buffrers and so on

Definition 1.4: A subset of places denoted as S in Petri Net N is called a siphon if $*S \subseteq S*$, i.e every transition having an output place in S has a input place in S. A nonempty subset of places Q in a Petri Net N is called a trap if $Q* \subseteq *Q$ i.e every transition having an input place in Q has an output place in Q.

Definition 1.5: Digraph A directed graph G consists of a set of vertices $V = \{v_1, v_2, ...\}$ and a set of edged $E=\{e_1, e_2, ...\}$ and a mapping ψ that maps every edge onto some ordered pair of vertices (V_i, V_j)

Definition1.6: Euler Digraph: In a digraph G a closed directed walk which traverses every edge of G exactly once is called a directed Euler line. A digraph containing a directed Euler line is called directed Euler digraph.

Theorem 1.7: A digraph G is an Euler digraph if and only if G is connected and is balanced i.e. $d^-(v) = d^+(v)$ for every vertex v in G

2. Discussion: In this section we present the marked graph model of the machine that processes one job at a time and basic schema of a production stage (2 models).We convert the marked graph in to digraph in two ways as given in [7].

Method 1: Here we change transitions in to vertices and places in to edges and connect as in the marked graph.

Method 2: Here we change both transitions and places in to vertices and arcs between them as edges.

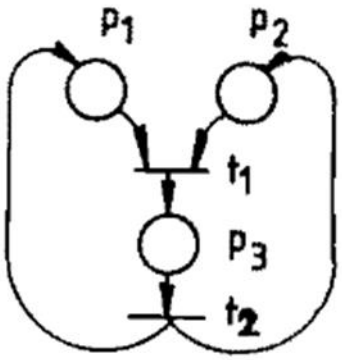


Figure 1: Petri Net model of a machine that processes one job at a time

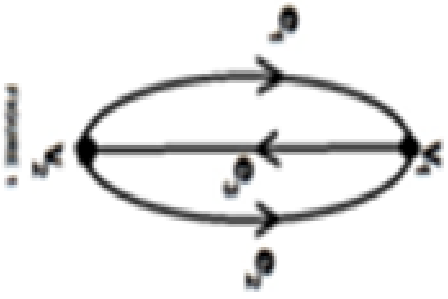


Figure 2: Digraph of the above marked graph (method 1)

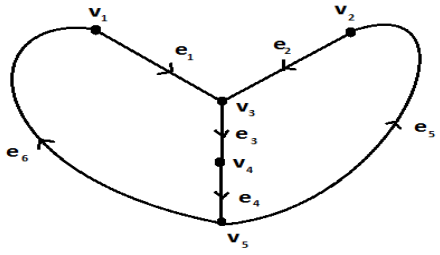


Figure 3: Digraph of the Above Marked Graph (method 2)

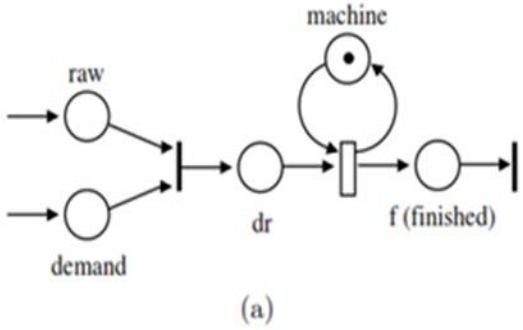


Figure 4: Marked graph of Basic Schema of a Production Stage

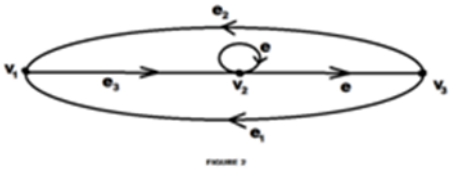


Figure 5: Digraph of the Above Marked Graph (Method 1)

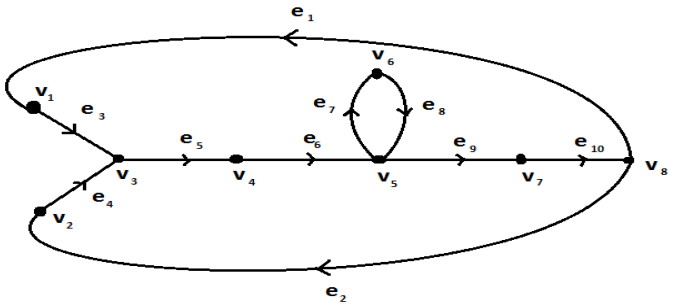


Figure 6: Digraph of the Above Marked Graph (Method 2)

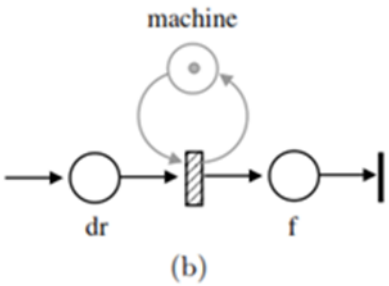


Figure 7: Marked graph of Basic Schema of A Production Stage (Another form)

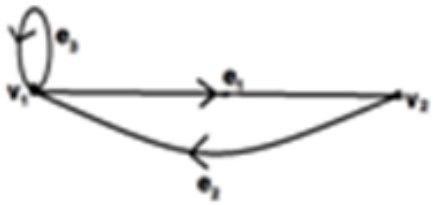


Figure 8: Digraph of the Above Marked Graph (Method 1)

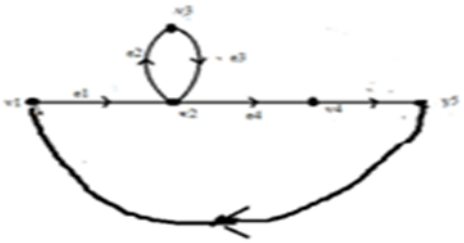


Figure 9: Digraph of the Above Marked Graph (Method 2)

None of the above 6 graphs are Euler/Hamiltonian digraphs.

3. Conclusion: In this paper we take marked graphs of Machine that process one job at a time, Basic Schema of a Production stage and convert them in to digraphs by using the methods given in [7] in two

ways. First changing the transitions into vertices and places into edges.Then we convert in to the digraph by changing both transitions and places in to vertices and arc between them as edges. The resulting digraphs are not Euler digraphs. Therefore further Analysis according to [4] is not possible.

References:

1. J L Peterson, Petri nets, Computing Survey Vol 9, No 3,September 1977, Department of Computer Sciences, The University of Texas, Austin, Texas 78712
2. Murata T:Petrinets: Properties, Analysis and Applications, Proceedings of IEEE,Vol.77, No.4,pp.541-580(1989)
3. Ervin R.Boer and Tadao Murata, Generating Basis Siphons and Traps of Petri Nets using the Sign Incidence Matrix, IEEE Transaction on Circuits and System-I. Fundamental Theory and Application, Vol.41, No.4,April 1994
4. K.Thirusangu and K.Rangarajan, Marked Graphs and Euler Graphs, Microelectron.Reliab., Vol.37, No.2.pp. 225-235,1997
5. K.Thirusangu and K.Rangarajan, Marked Graphs and Hamiltonian Graphs, Microelectron.Reliab., Vol.37, No.8.pp. 1243-1250,1997
6. L.Recalde , M.Silva, J.Ezpeleta and E.Teruel , Petri nets and Manufacturing Systems: An example – driver tour . Dep . informatica e ingeneria de sistemas , centro politencio superior de ingenioros, universidaded De zaragoza, maria de luna 3 , E – 50012 , spain .
7. Sunita Kumawat,A Graph Theoretic Approach: Petri Net,International Journal of Mathematical Sciences and Applications,Vol 1,No.3,September 2011.
8. Balaji P & Rangarajan & K.Tamil mozhi M, Analysis of Marked Graphs of Flexible Manufacturing System using Sign Incidence Matrix, Paper presented to the International conference on Mathematics and its Applications, University of College of Engineering, Villupuram, India , 15-17 December 2014,
9. Balaji P & Rangarajan K &.Tamil mozhi M, Analysis of Marked Graphs of Two Machine System Processing Two Part Types Using Sign Incidence Matrix, Paper presented to the National conference NCISE 2014,AVIT Chennai, India,18 & 19 December 2014
10. Balaji P & Rangarajan K &.Tamil mozhi M, Marked Graph of an Four Work Station Automated Manufacturing System Sign Incidence Matrix, Applied Mechanics and Materials,Vol 813-814(2015).pp 1121-1125.
11. Balaji P & Rangarajan K, Marked Graphs of Basic Stock Control System and Kanban Control System and their Conversion into Digraphs,International Journal of Applied Engineering Research, ISSN 0973-4562 Vol. 10 No.80 (2015)
12. Balaji P & Rangarajan K, Analysis of Marked graph of Basic control systems and kanban control systems using sign incidence matrix, Journal of Chemicals and Pharmaceutical sciences, Special issue-9, Article no 38, April 2015.
13. Narasing Deo,Graph Theory with applications to Engineering and Computer Science (Prentice Hall India) 2011.
14. Marked Graph of Automated Manufacturing Cell with three Machines three Robots and two Part Types and its Conversion into Digraph, Balaji P. and Rangarajan K. Transylvanian Review ,Special Issue ,Vol XXIV, No. 9, Special Issue, 2016.
15. Balaji P, Rangarajan K, (2016)," Siphon and Trap Analysis of Buffer of a Flexible Manufacturing System with Three Machines and two Jobs using Sign Incidence Matrix and its digraphs", International Journal of Chemical Sciences,volume 14,no 4. pp3057-3063
16. Balaji P, Rangarajan K, (2017) "Marked Graphs of Independent Kanban Control System and Independent Extended Kanban Control System and their Conversion into Digraphs", Global Journal of Pure and Applied Mathematics, Volume 13, Number 1.pp 1-4.

***

ANALYSES OF DIGRAPHS OF NON-DEAD LOCK FREE FMS AND MACHINING STATION WITH FOUR MACHINES AND TWO ROBOTS

P Balaji
Assistant Professor of Mathematics,
Sri ChandraSekarendra Saraswathi Viswa Maha Viidyalaya, Kanchipuram, India
pbr1002007@yahoo.com,
M Dinesh
M.Phil Scholar, Department of Mathematics,
Sri Chandrasekara Saraswathi Viswa Maha Vidyalaya, Kanchipuram
vijidinesh4891@gmail.com

Abstract: In this paper two Petri net models of two different FMS are taken and converted into digraph. Interestingly both of them are found to be Euler digraphs. Further the graph theoretic properties of digraphs are analysed.

Keywords: Petri Nets, FMS, Digraph, Euler Digraph.

Introduction: A Petri net is a powerful modeling formulation in a computer science, system engineering and many others disciplines. A Petri net combines a well-defined mathematical theory with a graphical representation of the dynamic behavior of the system the theoretic aspects of Petri net allows precise modeling and analysis of system behavior while the graphical representation of Petri net enables visualization of the modeled system state change. Because of this Petri net has been used to model various kinds of dynamic event driven system like computer networks, communication system, manufacturing plant etc.

Petri net are introduced in [1,2] conversion of Petri nets into digraphs are given in [4].We take two Petri net models of two different FMS s from [3] and convert them into digraphs. Interestingly both of them are Euler digraphs. Other graph theoretic properties of the two digraphs are analysed according to [7].

Definition 1.1: A PN is a bipartite graph, where nodes are classified as places and transitions (graphically pictured as circles and bars, respectively), and directed arcs connect only nodes of different type. Places are endowed with integer variables called tokens. A marked PN is a 5-tuple N = (P, T, F, W, M_o), where P is a finite set of places, T is a finite set of transitions, with $P \cap T = \emptyset$,$F \subset (PxT) U (T x P)$ is the incidence or flow relation (each element of F corresponds to an arc in the PN), W : F —> N \ {o} is the arc weight function, and M_o: P —> N is the initial marking (a marking M : P —> N defines the distribution of tokens in places), where N is the set of natural numbers.[1,2]

Definition 1.3: Flexible Manufacturing System: A Flexible manufacturing system (FMS) is an integrated computer controlled configuration of machine tools and automated material handling devices that simultaneously process medium sized volumes of a variety of part types.Flexible manufacturing system is a discrete event dynamical system in which the work pieces Of various job classes enter the system asynchronously and are Concurrently, sharing the limited resources , viz.,workstations,robots,MHS,buffrs and so on.

Definition 1.4: Diagraph A directed graph G consists of a set of vertices V = $\{v_1,v_2,....\}$ and a set of edged E=$\{e_1,e_2,....\}$ and a mapping ψ that maps every edge onto some ordered pair of vertices (V_i,V_j).[7]

Definition 1.5: Euler Digraph: In a digraph G a closed directed walk which traverses every edge of G exactly once is called a directed Euler line. A digraph containing a directed Euler line is called directed Euler digraph..[7]

Theorem 1.6: A digraph G is an Euler digraph if and only if G is connected and is balanced i.e. $d^-(v) = d^+(v)$ for every vertex v in G.[7]

3. Conversion of Petri net models of a non-deadlock free FMS and a FMS with Four Machines and Two Robots:

3.1: In this sub section we take the Petri net model of non deadlock free FMS from [3] and the Petri net obtained by adding a control place Fig-1.First we consider the Petri net without the control place added. We convert this Petri net into a digraph by the method given in [4].That is by changing transitions into vertices and places into edges. The result is as shown in Fig-2.Interstingly the digraph so obtained is Euler digraph by theorem1.6 as $d(v^+) = d(v^-)$ for each vertex.

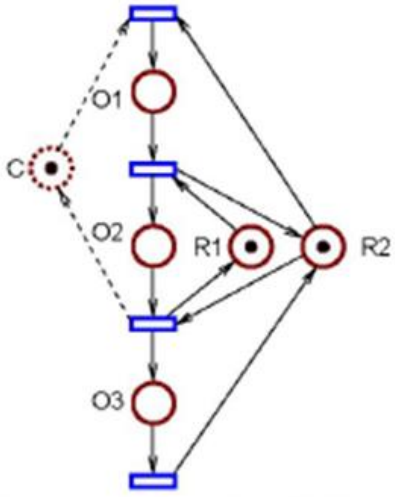


Fig 1

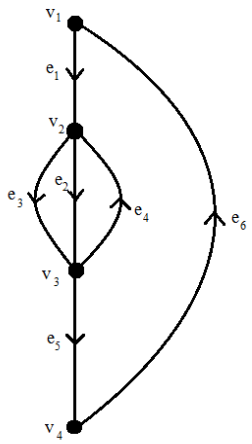


Fig 2

Next we consider the Petri net with the control place added. We convert this Petri net into a digraph by the method given in [4].That is by changing transitions into vertices and places into edges. The result is given in Fig-3.This digraph is also an Euler digraph by theorem 1.6.

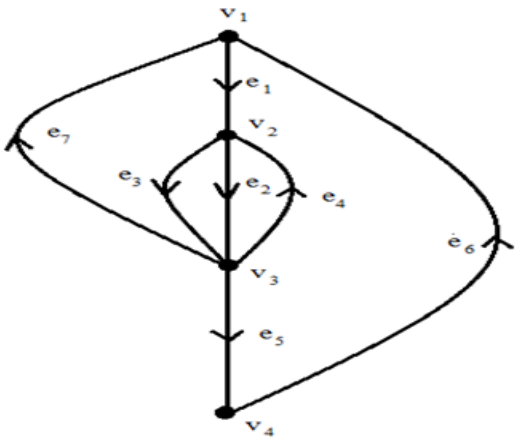


Fig 3

3.2: In this sub-section we take the Petri net model of the machining station with four machines and two robots and convert it into dir\graph by the method given in [4].In Fig- 4 the FMS is given. In Fig- 5 the Petri net model is given. In Fig-6 the converted Digraph is given which is also an Euler digraph by theorem 1.6.

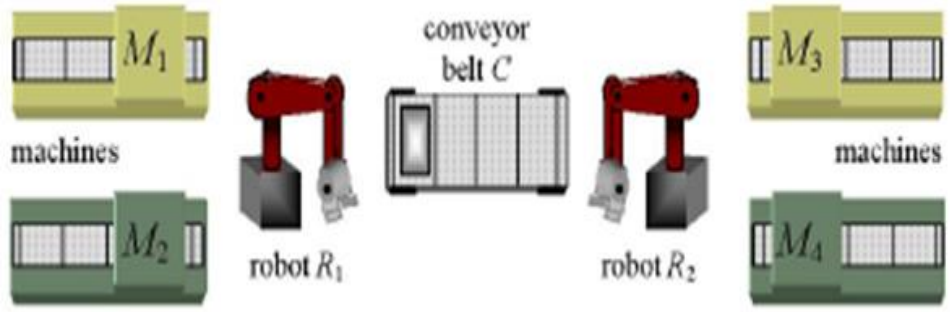


Fig 4

In this sub-section we take the Petri net model of the machining station with four machines and two robots and convert it into dir\graph by the method given in [4].In Fig- 4 the FMS is given. In Fig- 5 the Petri net model is given. In Fig-6 the converted Digraph is given which is also an Euler digraph by theorem 1.6.

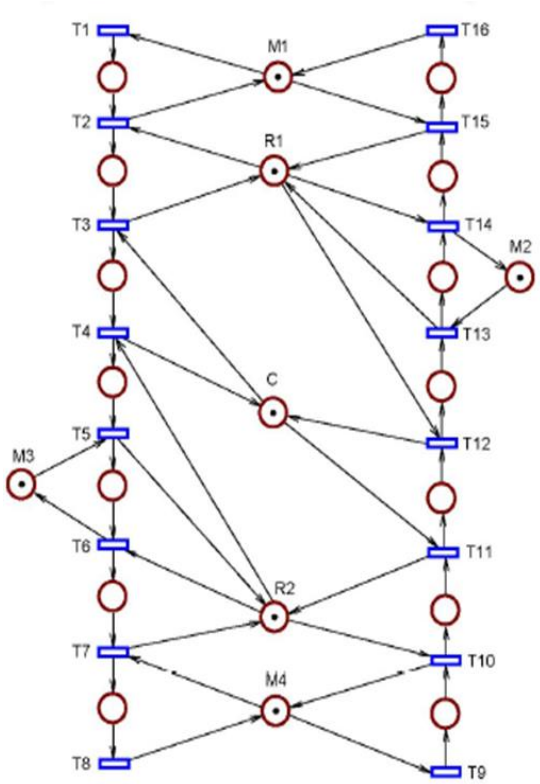


Fig 5

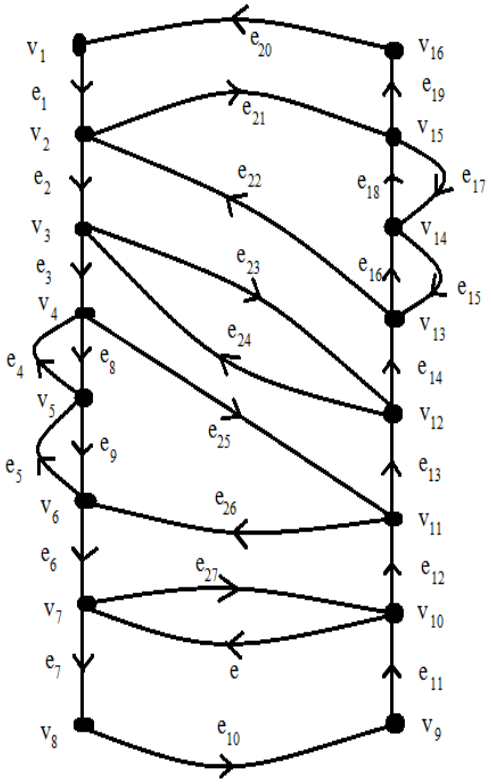


Fig 6

3.3: In this sub-section we take the AB- model of the machining station with four machines and two robots and convert it into dir\graph by the method given in [4]. In Fig- 7 the Petri net model is given. In Fig-8 the converted Digraph is given which is not an Euler digraph by theorem 1.6 as $d^-(v_2) = 2$,but $d^+(v_2)=4$.

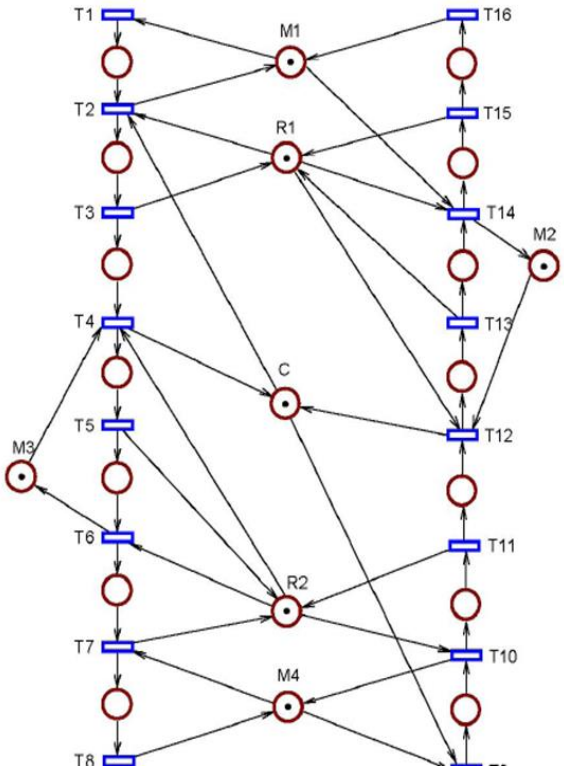


Fig 7

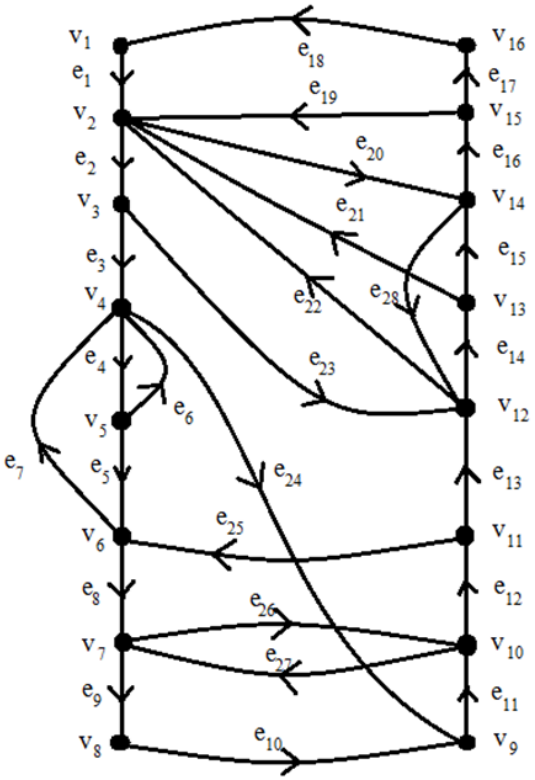


Fig 8

Conclusion: In this paper we have taken three Petri net models of non-deadlock free FMS and a FMS with Four machines and two robots and converted them into Digraphs by the method suggested in [4].We found that except the last one all are Euler digraphs. In [5] and [6] one also the same conversion according to [4] applied and [5] the result was Euler digraph and in [6] it was not.

References:

1. J L Peterson, Petri nets Computing Survey Vol. 9 No -3, September 1977, Department of Computer Sciences, The University of Texas, Austin, Texas 78712
2. Murata T: Petri nets: Properties, Analysis and Applications, Proceedings of IEEE, Vol. 77, No.4, pp. 541-580(1989).
3. Luigi Piroddi ,Luca Ferrarini,A modular approach for deadlock avoidance in FMS,Proceedings on IEE conferences on decision and control,(Dec-2015)
4. Sunita Kumawat,A Graph Theoretic Approach: Petri Net,International Journal of Mathematical Sciences and Applications,Vol 1,No.3,September 2011.
5. Balaji P & Rangarajan K &.Tamil mozhi M, Marked Graph of an Four Work Station Automated Manufacturing System and its conversion into Euler Digraph ,Paper presented to the National Conference NCCC2015, Anna University, Tirunelveli region, Tamilnadu, India on May 4th and 5th 2015
6. Balaji P & Rangarajan K, Marked Graphs of Basic Stock Control System and Kanban Control System and their Conversion into Digraphs,International Journal of Applied Engineering Research, ISSN 0973-4562 Vol. 10 No.80 (2015).
7. Narasing Deo, Graph Theory with applications to Engineering and Computer Science (Prentice Hall India) 2011.

***

ANALYSIS OF MARKED GRAPH OF CASES OF SEVERAL DEPENDANT CRITICAL PLACES USING SIGN INCIDENCE MATRIX AND ITS CONVERSION INTO DIGRAPHS

P Balaji
Assistant Professor, Department of Mathematics Sri Chandrasekara Saraswathi Viswa Maha Vidyalaya,,Kanchipuram.
pbr1002007@yahoo.com
S.Arumugam
M.Phil Scholar, Department of Mathematics Sri Chandrasekara Saraswathi Viswa Maha Vidyalaya, Kanchipuram, arukmkr@gmail.com

Abstract: In this paper the marked graph of cases of cases of several dependant critical places is analyzed using sign incidence matrix and converted into digraphs in three methods. The converted digraphs are analyzed for graph theoretic properties.

1.1 Introduction: In this paper **we** take the Petri net model which is also marked graphs present in [7].First we analyze them using the algorithm given in [3,4,5].Then we convert them into digraphs by the methods given in [8].The resulting digraphs are analyzed for graph theoretic properties.

1. 2 Basic Definitions:

Definition 1.2.1: Petri Net: A Petri Net is a directed bipartite graph composed of four parts, a set of places P, a set of transitions T, an input function I, an output function O. These two functions connects places and transitions. A Petri Net N is denoted by N = {P, T, I, O, M_o} Where M_o is the initial marking (no of tokens present in each place in the beginning)[1,2].

Definition 1.2.2: Siphon and Trap: A subset of places denoted as S in Petri Net N is called a siphon if *S C S *, i,e every transition having an output place in S has an input place in S. where
*S denotes the set of input places for all transitions.
S* denotes the set of output places for all transitions.

A non-empty subset of places Q in a Petri Net N is called a trap if Q * C *Q i,e every transition having an input place in Q has an output place in Q.[3,4,5].

Definition: 1.2.3: A Marked graph is a Petri net C = (P, T, I, O) such that for each $p_i \in P, |I(p_i)| = |\{ t_j / p_i \in O(t_j)\}| = 1$ and $|O(p_i)| = |\{ t_j / p_i \in I(t_j)\}| = 1$. [3,4,5]

1.3 Enumeration of Siphon and Trap Subsets of Places of Marked Graphs: Here the algorithm is presented to find all subsets of places which are both siphon and trap for marked graphs given in .To apply the Algorithm the sign incidence matrix is required, and that is also defined[3,4,5].

Definition 1.3.1: Sign Incidence Matrix: For a Petri net N with n-transitions and m-places, the sign incidence matrix A = [aij] is an n x m matrix whose entry is given as follows.

a_{ij} = + if place j is an output place of transition i.
a_{ij} = - if it is an input place of transition i.
a_{ij} = ± if it is both input and output places of transition i (I.e. transition i and place j form a self loop)
a_{ij} = o otherwise.[3,4,5].

Definition 1.3.2: Addition: The addition denoted by $\oplus$ is a commutative binary operation on the set of four elements. B = {+,-, o, ±} defined as follows.

$+\oplus - = \pm$

$x\oplus x = x$, For every $x \in B$

$\pm\oplus x = \pm$, For every $x \in B$

$o\oplus x = x$, For every $x \in B$ [3,4,5].

Theorem: 1.3.3: A subset of k-places Z = $\{p_1, p_2 \ldots\ldots p_k)$ in a marked graph N is both siphon and trap if and only if the addition of k-column vectors of the sign incidence matrix of N, $A_1\oplus A_2\oplus\ldots\ldots\oplus A_k$ contains either zero entry or ± entry where $A_j$denote the column vector corresponding to place P_j, j = 1,2,....k. [3,4,5]

Definition: 1.3.4: A + entry is said to be neutralized by adding a—entry to get a ± entry.

1.4 Algorithm for Finding Siphon and Trap using Sign Incidence Matrix:

Input: Sign incidence matrix A of order m x n.

Step 1: Select A_j, the first column in the sign incidence matrix A, whose corresponding 'place is denoted as $PLACE_j$.

Set recursion level r to 1

Set $V_{j\,r} = A_j$

Set $PLACE_{jr} = PLACE_j$

Step 2: If V_{jr} has a ± entry at i^{th} row then $PLACE_j$ is a self loop with transition t_j. Go to step 5.

Step 3: If $V_{i\,j}$ has a+ entry in the kth row find a column in A, which contains a - entry at the kth row.

(a) If no such column in A\exists, Go to step 5.

(b) If such A, exists add it to $V_{j\,r}$ to obtain $V_{j(r+1),} = V_{j\,r} \oplus A_s$ containing a ± entry at k^{th} row. Then $PLACE_{j(r+1)} = PLACE_{jr} \cup PLACE_s$.

(c) Repeat this step for all possible neutralizing columns A_s. This gives a new set of $V_{j(r+1)}$'s and $PLACE_{j(r+!)}$'s.

Step 4: Increment r by 1. Repeat step 3 until there are no more + entries in each

$V_{jr} = A_1 \oplus A_2 \oplus \ldots A_{jr}$ or no neutralizing column can be defined.

Step 5: Any V_{jr} without + entries and without-entries (i.e., all the entries are either zero or ±) represents siphon and trap. i.e., the places in $PLACE_{jr}$ form both siphon and trap.

Step 6:

Delete A_j

j=j+1

Go to step 1.

Output: All sets which are both siphon and trap.[3,4,5]

1.5 Basic Definitions of Graph Theory:

Definition:1.5.1A digraph D consists of a non-empty finite set V (D) of elements called vertices, and finite family A (D) of ordered pairs of elements of V (D) called arcs. V (D) is called the vertex set and A (D) the arc family of D.[6].

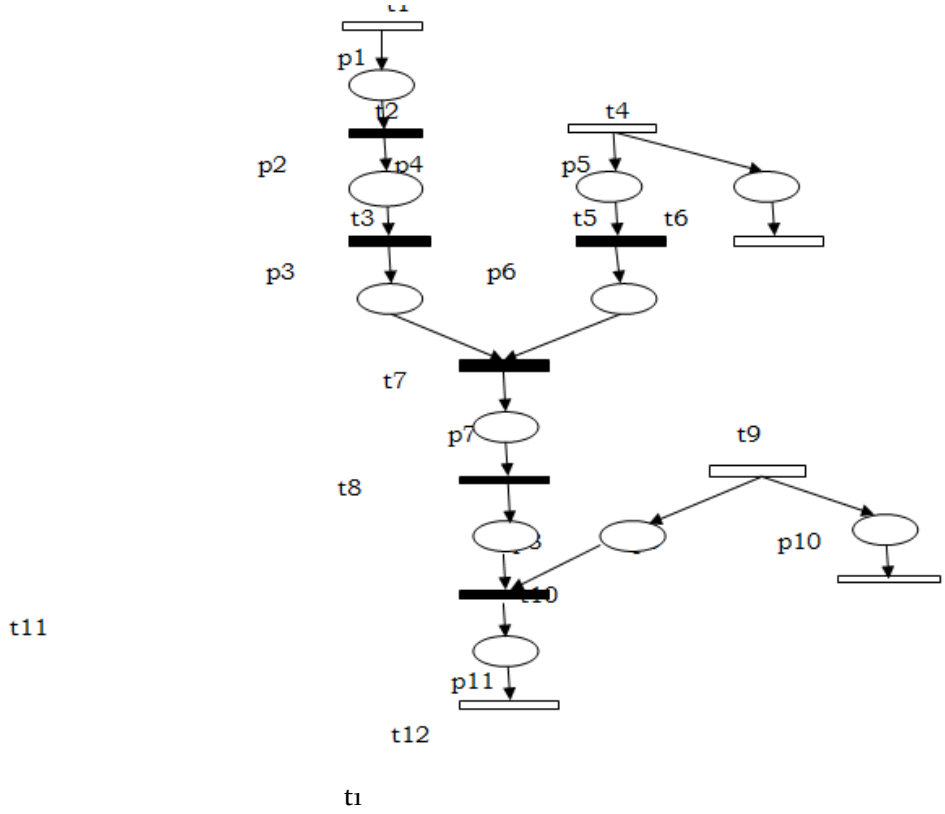
Definition:1.5.2 Euler Digraph: In a digraph G a closed directed walk which traverses every edge of G exactly once is called a directed Euler line. A digraph containing a directed Euler line is called Euler digraph.[6].

Theorem: 1.5.3 A digraph G is an Euler digraph if and only if G is connected and is balanced i.e. $d^-(v) = d^+(v)$ for every vertex v in G.[6].

1.6 Methods to Convert Petri Nets into Digraphs: A Petri net can be converted into a digraph in three ways.

Method 1: Here the transitions are changed in to vertices and places in to edges and connections as in the marked graph.
Method 2: Here the transitions are changed into edges and places into vertices.
Method 3: Here both transitions and place are changed in to vertices and arcs between them as edges.

1.7 Enumerating the Set of Places which are both Siphons and Traps for the Marked Graphs: Consider the following marked graph given in [7]



t1

Its sign incidence matrix is given by

$$A = \begin{array}{c} \\ t1 \\ t2 \\ t3 \\ t4 \\ t5 \\ t6 \\ t7 \\ t8 \\ t9 \\ t10 \\ t11 \\ t12 \end{array} \begin{array}{c} \begin{array}{cccccccccc} P_1 & P_2 & P_3 & P_4 & P_5 & P_6 & P_7 & P_8 & P_9 & P_{10} & P_{11} \end{array} \\ \begin{bmatrix} + & 0 & 0 & 0 & 0 & 0 & 0 & 0 & 0 & 0 & 0 \\ - & + & 0 & 0 & 0 & 0 & 0 & 0 & 0 & 0 & 0 \\ 0 & - & + & 0 & 0 & 0 & 0 & 0 & 0 & 0 & 0 \\ 0 & 0 & 0 & + & 0 & + & 0 & 0 & 0 & 0 & 0 \\ 0 & 0 & 0 & - & + & 0 & 0 & 0 & 0 & 0 & 0 \\ 0 & 0 & 0 & 0 & 0 & - & 0 & 0 & 0 & 0 & 0 \\ 0 & 0 & - & 0 & - & 0 & + & 0 & 0 & 0 & 0 \\ 0 & 0 & 0 & 0 & 0 & 0 & - & 0 & + & 0 & 0 \\ 0 & 0 & 0 & 0 & 0 & 0 & 0 & - & - & + & 0 \\ 0 & 0 & 0 & 0 & 0 & 0 & 0 & + & 0 & 0 & + \\ 0 & 0 & 0 & 0 & 0 & 0 & 0 & 0 & 0 & 0 & - \\ 0 & 0 & 0 & 0 & 0 & 0 & 0 & 0 & 0 & - & 0 \end{bmatrix} \end{array}$$

Applying the algorithm

$$A_1 = \begin{bmatrix} + \\ - \\ 0 \\ 0 \\ 0 \\ 0 \\ 0 \\ 0 \\ 0 \\ 0 \\ 0 \\ 0 \end{bmatrix} = v_{11}$$

V_{11} has a (+) in first row but no (-) in first row in the matrix :. No neutralizing columns.

$$A_2 = \begin{bmatrix} 0 \\ + \\ - \\ 0 \\ 0 \\ 0 \\ 0 \\ 0 \\ 0 \\ 0 \\ 0 \\ 0 \end{bmatrix} = v_{21}$$

V_{21} has a (+) in second row place $_{21}=p_2$ No(-) A_1.

$$V_{21}' = V_{21} \oplus A_1 = \begin{bmatrix} 0 \\ + \\ - \\ 0 \\ 0 \\ 0 \\ 0 \\ 0 \\ 0 \\ 0 \\ 0 \\ 0 \end{bmatrix} \oplus \begin{bmatrix} + \\ - \\ 0 \\ 0 \\ 0 \\ 0 \\ 0 \\ 0 \\ 0 \\ 0 \\ 0 \\ 0 \end{bmatrix} = \begin{bmatrix} + \\ \pm \\ - \\ 0 \\ 0 \\ 0 \\ 0 \\ 0 \\ 0 \\ 0 \\ 0 \\ 0 \end{bmatrix}$$

$$\text{place}_{21} = \{P_2, P_1$$

V21 has a (+) in first row but no (-) in first row:. No neutralizing columns.

$$A_3 = \begin{bmatrix} 0 \\ 0 \\ + \\ 0 \\ 0 \\ 0 \\ - \\ 0 \\ 0 \\ 0 \\ 0 \end{bmatrix} = V_{31}$$

V_{31} has a (+) in third row no (-) in A_2
place $_{31}=p_3$ No(-) A_1.

$$V'_{31}=V_{31} \oplus A_2 = \begin{bmatrix} 0 \\ + \\ 0 \\ 0 \\ 0 \\ - \\ 0 \\ 0 \\ 0 \\ 0 \\ 0 \\ 0 \end{bmatrix} \oplus \begin{bmatrix} 0 \\ + \\ - \\ 0 \\ 0 \\ 0 \\ 0 \\ 0 \\ 0 \\ 0 \\ 0 \\ 0 \end{bmatrix} = \begin{bmatrix} 0 \\ + \\ - \\ 0 \\ 0 \\ - \\ 0 \\ 0 \\ 0 \\ 0 \\ 0 \\ 0 \end{bmatrix}$$

$\text{place}_{31} = \{P_3, P_2$

V31 has a (+) in first row but no (-) in first row :.

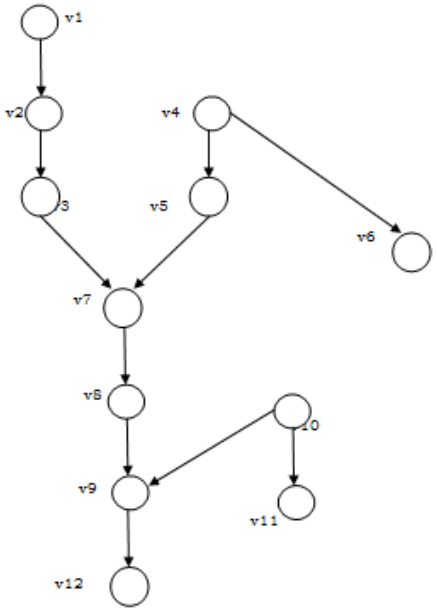
$$V'_{32}=V'_{31} \oplus A_1 = \begin{bmatrix} 0 \\ + \\ - \\ 0 \\ 0 \\ - \\ 0 \\ 0 \\ 0 \\ 0 \\ 0 \end{bmatrix} \oplus \begin{bmatrix} + \\ - \\ 0 \\ 0 \\ 0 \\ 0 \\ 0 \\ 0 \\ 0 \\ 0 \\ 0 \end{bmatrix} = \begin{bmatrix} + \\ \pm \\ - \\ 0 \\ 0 \\ 0 \\ 0 \\ 0 \\ 0 \\ 0 \\ 0 \end{bmatrix}$$

$place_{32} = \{P_3, P_2, P_1$

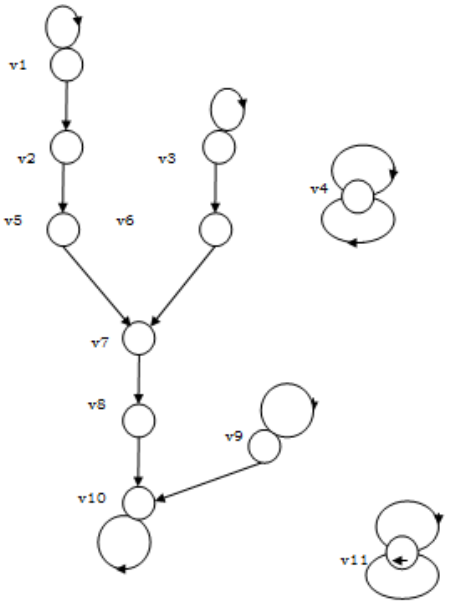
V32 has a (+) in first row but no (-) in first row :. No neutralizing columns.

Proceeding in this manner we find that there are no places which are both siphon and trap

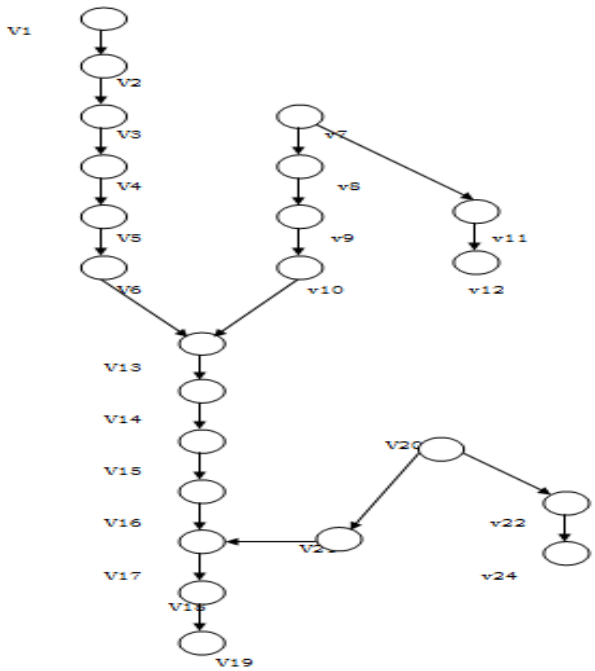
1.8 Conversion of marked Graph into Digraphs: The above marked graph is converted into digraphs by the three methods given in [8].They are shown below



Method 1



Method 2



Method 3

The converted digraphs in Figure 2, 3, 4 are analyzed for graph theoretic properties and the results are tabulated.

1.9: Analysis of the digraphs of the Marked Graph

S. no	Digraph Figure number	Number of vertices	Number of Edges	Directed Euler Graph	Chromatic number	No of Directed Circuits
1	2	12	8	No	2	0
2	3	11	10	No	2	0
3	4	24	16	No	3	0

Conclusion: From the above analysis the marked graph taken does not have any set of places that are both siphon and trap. Also the converted digraphs are not Euler digraphs. The graph theoretic properties of the digraphs are discused.Smiliar work done by the same author is given in [9, 10]

References:

1. J L Peterson, Petri nets, Computing Survey Vol 9, No 3, September 1977, Department of Computer Sciences, The University of Texas, Austin, Texas 78712.
2. Murata T:Petrinets: Properties, Analysis and Applications, Proceedings of IEEE,Vol.77, No.4,pp.541-580(1989)
3. Ervin R.Boer and Tadao Murata, Generating Basis Siphons and Traps of Petri Nets using the Sign Incidence Matrix, IEEE Transaction on Circuits and System-I. Fundamental Theory and Application, Vol.41, No.4,April 1994
4. K.Thirusangu and K.Rangarajan, Marked Graphs and Euler Graphs, Microelectron.Reliab., Vol.37, No.2.pp. 225-235,1997
5. K.Thirusangu and K.Rangarajan, Marked Graphs and Hamiltonian Graphs, Microelectron.Reliab., Vol.37, No.8.pp. 1243-1250,1997
6. NarasingDeo,Graph Theory with applications to Engineering and Computer Science (Prentice Hall India) 2011.
7. H. Sioud, Z. Achour , A. Sava and N. Rezg, Deadlock freeness supervisor for marked graph, Bulletin of the polish academy of sciences(vol. 57, No. 3, 2009).
8. Sunita Kumawat,A Graph Theoretic Approach: Petri Net,International Journal of Mathematical Sciences and Applications,Vol 1,No.3,September 2011.
9. Balaji P &Rangarajan K &.Tamil mozhi M, Analysis of Marked Graphs of Two Machine System Processing Two Part Types Using Sign Incidence Matrix, Paper presented to the National conference NCISE 2014,AVIT Chennai, India,18 & 19 December 2014
10. Balaji P. and Rangarajan K, Marked Graph of Automated Manufacturing Cell with three Machines three Robots and two Part Types and its Conversion into Digraph, Transylvanian Review, Special Issue ,Vol XXIV, No. 9, Special Issue, 2016

***

ANALYSIS OF DIGRAPH OF FLEXIBLE MANUFACTURING CELL WITH FOUR MACHINES AND THREE ROBOTS

P Balaji
Assistant Professor, Department of Mathematics,
Sri Chandrasekara Saraswathi Viswa Maha Vidyalaya, Kanchipuram, pbr1002007@yahoo.com
V Elumalai
M.Phil Scholar, Department of Mathematics,
Sri Chandrasekara Saraswathi Viswa Maha Vidyalaya, Kanchipuram, velumalai711@gmail.com

Abstract: In this work we take the Petri net model of a Flexible Manufacturing Cell along with two other Petri nets and convert them into digraph by changing both the transitions and places into vertices and arcs between them into edges and resulting digraph are not Euler digraph which prevents further analysis.

Keywords: Petri Nets, Flexible Manufacturing Cell, Digraph, Euler Digraph.

1. Introduction: A Petri net is a powerful modeling tool in a computer science, system engineering and many others areas. It combines a well-defined mathematical theory together with a graphical representation of the dynamic behavior of the system. The theoretic aspects of Petri net permits perfect modeling and analysis of system behavior while the graphical representation of net visualizes of the modeled system state change.

Petri net are defined in [1, 2] Changing Petri nets into digraphs are given in [4].We take three Petri net models FMC s from [3] and convert them into digraphs using the method suggested in .[4Actually none of them are Euler digraphs.

Definition 1.1: A marked Petri net is a 5-tuple N = (P, T, F, W, M_o), where P is a finite set of places, T is a finite set of transitions, with P∩T = ∅,F⊂(PxT)U (T x P) is the incidence or flow relation (each element of F corresponds to an arc in the PN), W : F —> N \ {0} is the arc weight function, and M_o: P —> N is the initial marking (a marking M : P —> N defines the distribution of tokens in places), where N is the set of natural numbers.[1,2]

Definition 1.2: Flexible Manufacturing System: A Flexible manufacturing system (FMS) is an integrated computer controlled configuration of machine tools and automated material handling devices that simultaneously process medium sized volumes of a variety of part types. Flexible manufacturing system is a discrete event dynamical system in which the work pieces Of various job classes enter the system asynchronously and are Concurrently, sharing the limited resources , viz.,workstations,robots,MHS,buffrs and so on.[3]

Definition 1.3: Diagraph A directed graph G consists of a set of vertices V = {v_1,v_2,....} and a set of edged E={e_1,e_2,....} and a mapping ψ that maps every edge onto some ordered pair of vertices (V_i,V_j).[11]

Definition1.4: Euler Digraph: In a digraph G a closed directed walk which traverses every edge of G exactly once is called a directed Euler line. A digraph containing a directed Euler line is called directed Euler digraph..[11]

Theorem 1.5: A digraph G is an Euler digraph if and only if G is connected and is balanced i.e. $d^-(v) = d^+(v)$ for every vertex v in G.[11]

2. Conversion of Petri Net Models into Digrpahs:

2.1 Petri Net Model (N,M_0): In this sub section we analyze the Petri net model given in [3].We convert the above Petri net into digraph by changing both places and transitions into vertices and arcs between them as edges as given in [4].

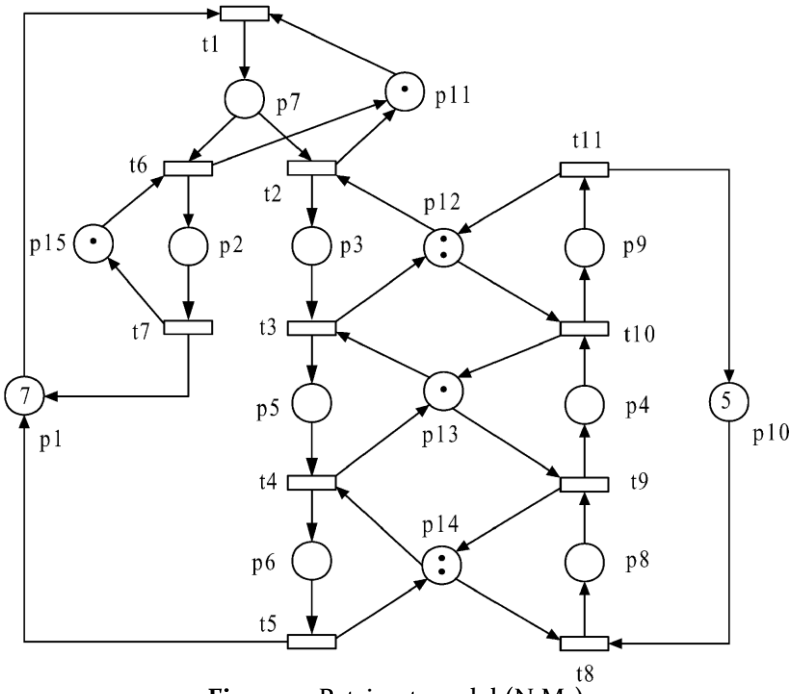


Figure 1: Petri net model ($N.M_0$)

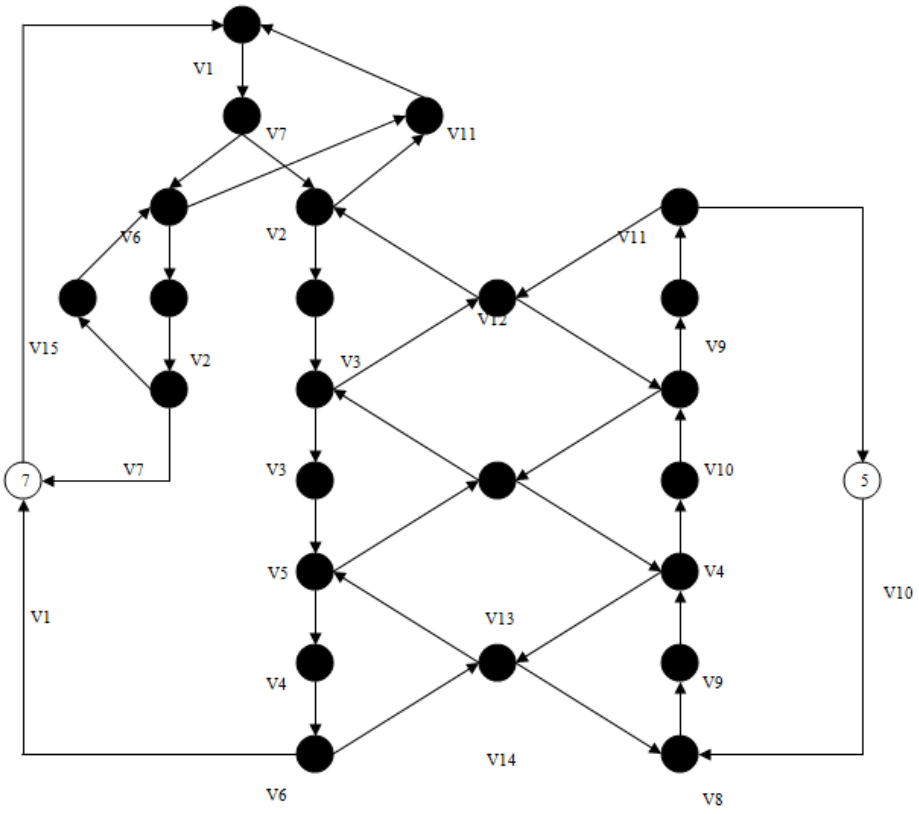


Figure 2: Digraph of Petri Net Model ($N.M_0$)(Figure-1)

Since $d^+(V_1) = 2, d^-(V_1) = 1$, The above digraph is not Euler digraph by theorem 1.5

2.2 Petri Model of (N,M_0) Added with Two Control Places: In this sub-section we take the Petri net model of Figure-1 added with 2 control places given in Figure-3 and convert it in to digraphs as suggested in [4] as we did previously, we get figuree-4.

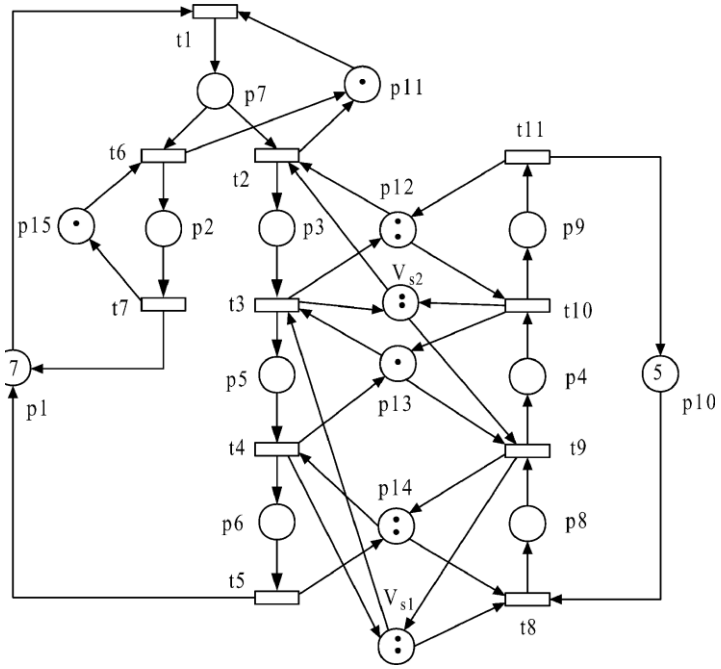


Figure 3: Petri Model of (N,M_0) Added With Two Control Places

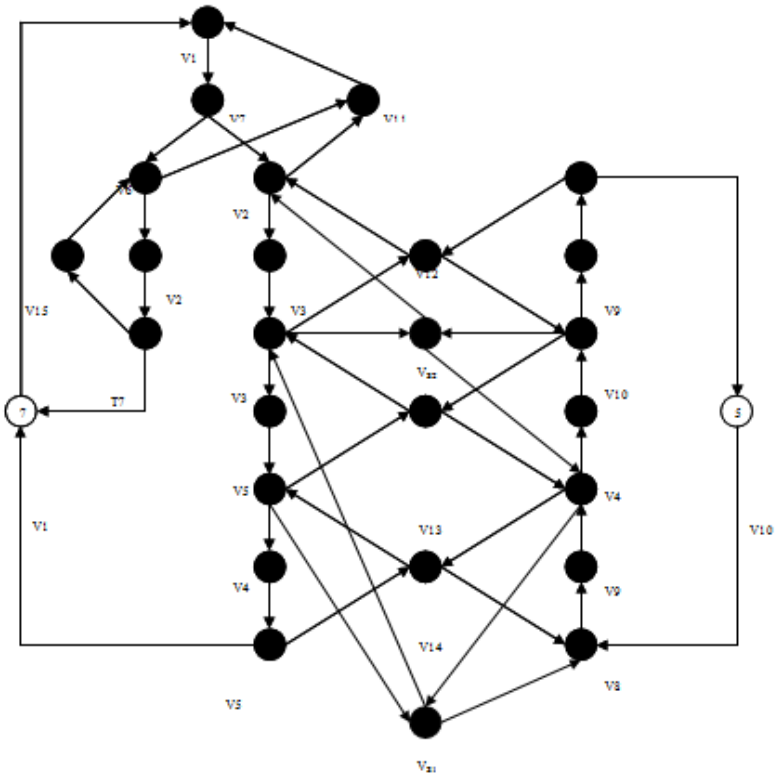


Figure 4: Digraph of Petri Model of (N,M_0) Added With Two Control Places

Since $d^+(V_1) = 2, d^-(V_1) = 1$, The above digraph is not Euler digraph by theorem 1.5

2.3 Petri Net Model of Flexible Manufacturing Cell: Consider the following Flexible Manufacturing Cell with four machines and three robots. We convert this in to digraph as above.

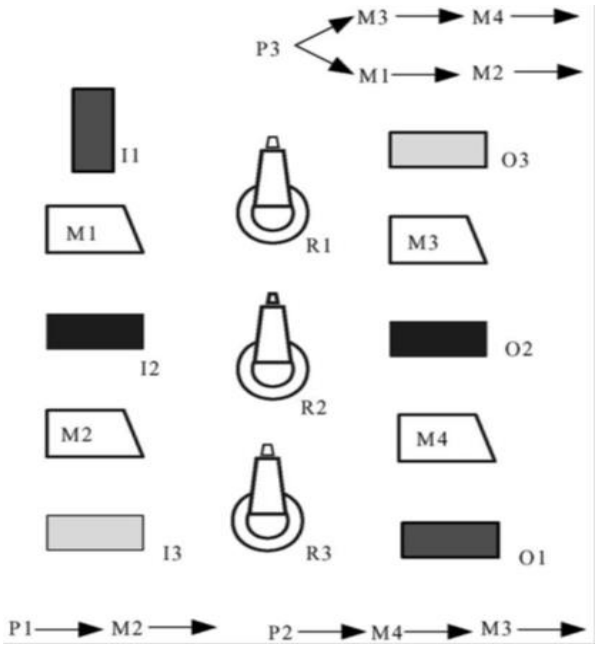


Figure 5: Flexible Manufacturing Cell

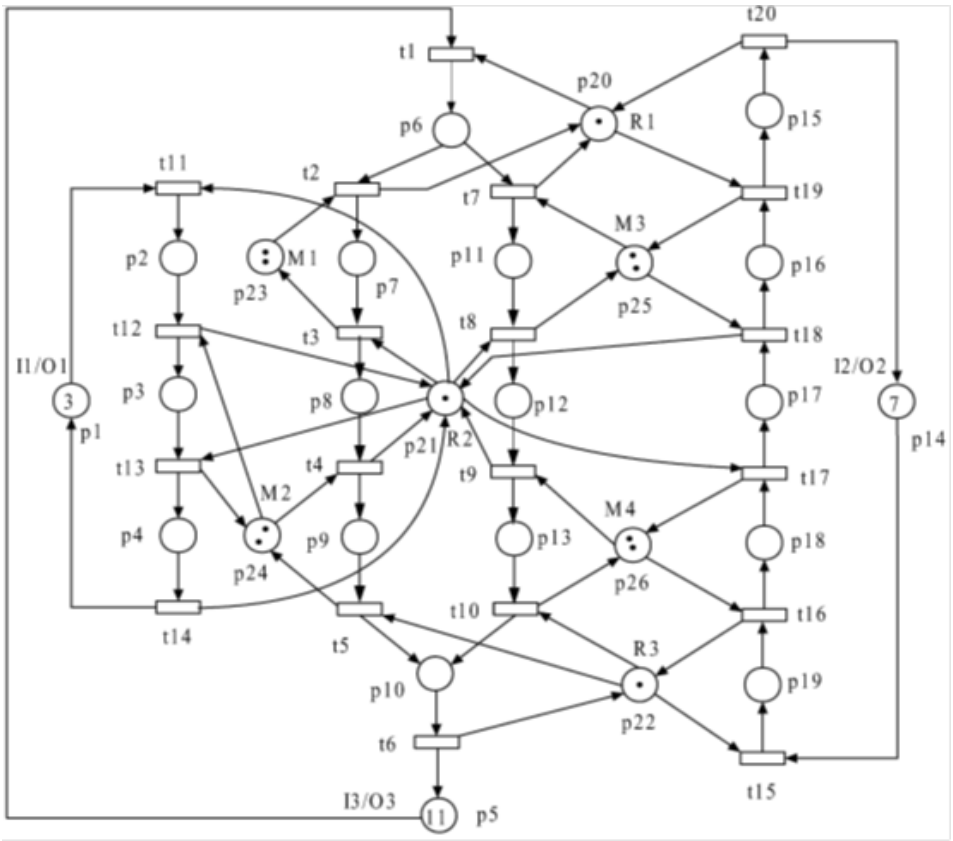


Figure 6: Petri Net Model of Flexible Manufacturing Cell

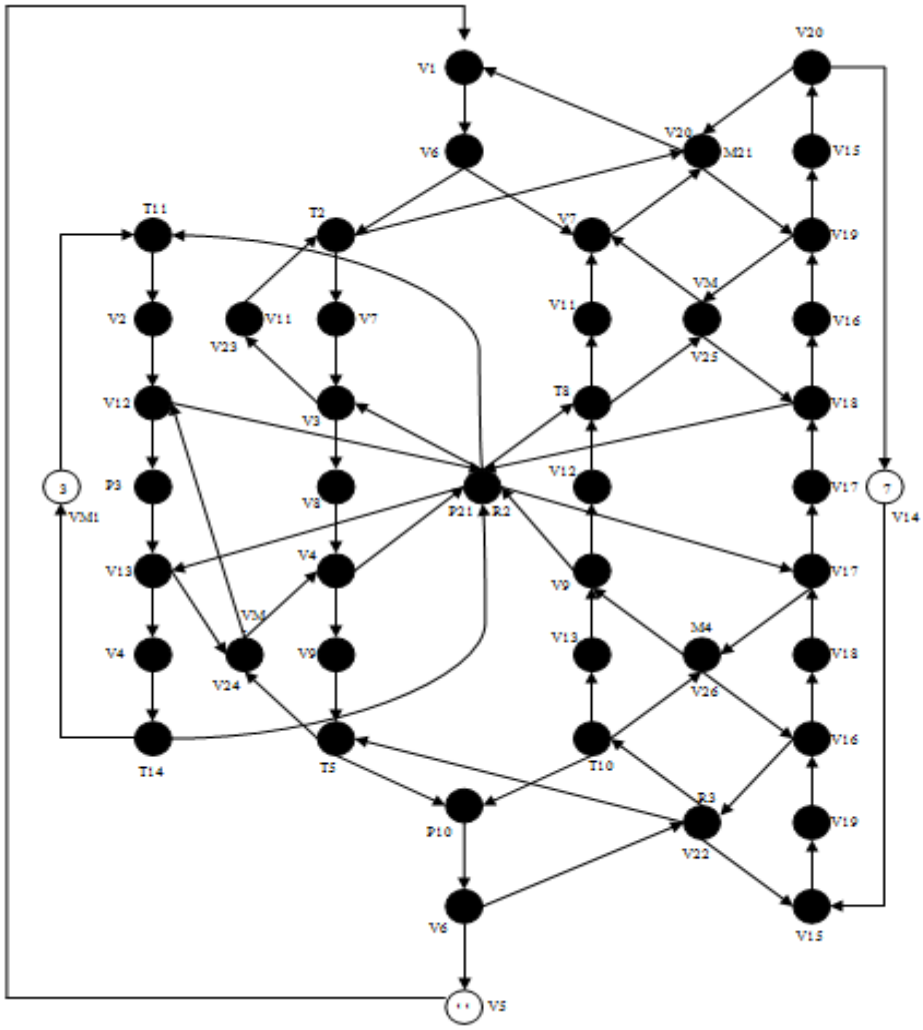


Figure 7: Digraph of Petri Net Model of Flexible Manufacturing Cell

Since $d^+(V_1) = 2, d^-(V_1) = 1$, The above digraph is not Euler digraph by theorem 1.5

3. Conclusion: In this paper we have taken three Petri net models from [3].and converted them into digraphs by using the methods suggested in [4]..None of the digraphs are Euler digraphs which prevents further discussion according to [5][6].The authors have done similar work in the references from[7] to [10].

References:

1. J L Peterson, Petri nets Computing Survey Vol. 9 No -3, September 1977, Department of Computer Sciences, The University of Texas, Austin, Texas 78712
2. Murata T: Petri nets: Properties, Analysis and Applications, Proceedings of IEEE, Vol. 77, No.4, pp. 541-580(1989).
3. ZhiWu Li,MengChu Zhou,Elementary Siphons of Petri Nets and their Application to Deadlock Prevention in Flexible Manufacturing Sytems.IEEE transaction on Sytems,Man,And Cybernetics,Vol 34,No 1,2004.
4. Sunita Kumawat,A Graph Theoretic Approach: Petri Net,International Journal of Mathematical Sciences and Applications,Vol 1,No.3,September 2011.
5. K.Thirusangu and K.Rangarajan, Marked Graphs and Euler Graphs, Microelectron.Reliab., Vol.37, No.2.(1997),pp. 225-235.

6. K.Thirusangu and K.Rangarajan, Marked Graphs and Hamiltonian Graphs, Microelectron.Reliab., Vol.37, No.8.(1997),pp.1243-1250.
7. Balaji P & Rangarajan K &.Tamil mozhi M, Marked Graph of an Four Work Station Automated Manufacturing System and its conversion into Euler Digraph ,Paper presented to the National Conference NCCC2015, Anna University, Tirunelveli region, Tamilnadu, India on May 4th and 5th 2015
8. Balaji P & Rangarajan K, Marked Graphs of Basic Stock Control System and Kanban Control System and their Conversion into Digraphs,International Journal of Applied Engineering Research, ISSN 0973-4562 Vol. 10 No.80 (2015).
9. Marked Graph of Automated Manufacturing Cell with three Machines three Robots and two Part Types and its Conversion into Digraph, Balaji P. and Rangarajan K. Transylvanian Review, Special Issue ,Vol XXIV, No. 9, Special Issue, 2016.
10. Balaji P & Rangarajan K &.Tamil mozhi M, Analysis of Marked Graphs of Two Machine System Processing Two Part Types Using Sign Incidence Matrix, Paper presented to the National conference NCISE 2014,AVIT Chennai, India,18 & 19 December 2014.
11. Narasing Deo, Graph Theory with applications to Engineering and Computer Science (Prentice Hall India) 2011.

***

ANNIHILATOR IDEALS OF PRE A*-ALGEBRA

Vijayabarathi.S
Assistant Professor of Mathematics, SCSVMV, Kanchipuram, Tamilnadu

Abstract: The concept of Zero of a Pre A*-algebra is introduced and annihilator ideals of Pre A*-algebra is developed. Some properties of annihilator ideals of Pre A*-algebra and dense ideals of Pre A*-algebra have been studied. A set of equivalent conditions are obtained for every ideals of pre A*-algebra to become an annihilator ideal.

Keywords: Pre A*-Algebra, Zero of a Pre A*-Algebra, Annihilator Ideals, Dense Ideal.

Introduction: In 2000, J.Venkateswara Rao[5] introduced the concept Pre A*-algebra $(A,\wedge,\vee,(-)^{\tilde{}})$ analogous to C-algebra as a reduct of A*- algebra, studied their sub direct representations, obtained the results that **2**= {0, 1} and **3**= {0, 1, 2} are the sub directly irreducible Pre-A*-Algebras and every Pre-A*-algebra can be imbedded in $\mathbf{3}^X$ for some set X**.** Boolean algebra depends on two-element logic. C-algebra, Ada, A*- algebra and our Pre A*-algebra are regular extensions of Boolean logic to 3 truth-values, where the third truth-value stands for an undefined truth-value.. Venkateswara Rao, Srinivasa Rao, defined [7] partial ordering on a Pre A* -algebra A and derived necessary conditions to become a lattice, defined [7] congruence relation on Pre A*-Algebra and studied the properties, defined[7] ternary operation on Pre-A* algebra and studied the properties and established Cayley's Theorem on Centre of a Pre A*-Algebra, studied [7] Decomposition of Pre A*-algebra. A.Satyanarayana, et al [6] formulate the definitions of ideal, prime ideal, maximal ideal of Pre A*-algebra and studied the properties. In this paper , Zero of a Pre A*-algebra is introduced and annihilator ideals of Pre A*-algebra is developed and investigate it. Some properties of annihilator ideals and dense ideals of Pre A*-algebra have been studied. A set of equivalent conditions are obtained for every ideals of pre A*-algebra to become an annihilator ideal.

1. Preliminaries:

Definition 1.1 [5]: An algebra $(A,\wedge,\vee,(-)^{\tilde{}})$ where A is non-empty set with $1,\wedge,\vee$ are binary operations and $(-)^{\tilde{}}$ is a unary operation satisfying

(a) $x^{\tilde{}\tilde{}}=x, \quad \forall x\in A$

(b) $x\wedge x=x, \quad \forall x\in A$

(c) $x\wedge y=y\wedge x, \quad \forall x,y\in A$

(d) $(x\wedge y)^{\tilde{}}=x^{\tilde{}}\vee y^{\tilde{}}, \quad \forall x,y\in A$

(e) $x\wedge(y\wedge z)=(x\wedge y)\wedge z, \quad \forall x,y,z\in A$

(f) $x\wedge(y\vee z)=(x\wedge y)\vee(x\wedge z), \quad \forall x,y,z\in A$

(g) $x\wedge y=x\wedge(x^{\tilde{}}\vee y), \quad \forall x,y\in A.$

is called a Pre A*-algebra.

Example 1.2. [5]:

3 = {0, 1, 2} with operations $\wedge,\vee,(-)^{\tilde{}}$ defined below is a Pre A*-algebra.

$\wedge$	0	1	2
0	0	0	2
1	0	1	2
2	2	2	2

$\vee$	0	1	2
0	0	1	2
1	1	1	2
2	2	2	2

x	$x^{\tilde{}}$
0	1
1	0
2	2

Note 1.3.: The elements 0, 1, 2 in the above example satisfy the following laws:
(a) $2^{\sim} = 2$ (b) $1 \wedge x = x$ for all $x \in 3$
(c) $0 \vee x = x$, $\forall\ x \in \mathbf{3}$ (d) $2 \wedge x = 2 \vee x = 2$, $\forall\ x \in \mathbf{3}$.

Example 1.4 [5]: 2 = {0, 1} with operations $\wedge, \vee, (-)^{\sim}$ defined below is a Pre A*-algebra.

Note 1.5.[5]:
(i)$(\mathbf{2}, \wedge, \vee, (-)^{\sim})$ is a Boolean algebra. So every Boolean algebra is a Pre A* algebra
(ii) The identities 1.1(a) and 1.1(d) imply that the varieties of Pre A*-algebras satisfies all the dual statements of 1.1

Lemma 1.6: Every Pre A*-algebra with 1 satisfies the following laws
(a) $x \vee 1 = x \vee x^{\sim}$ (b) $x \wedge 0 = x \wedge x^{\sim}$

Lemma 1.7.[5]: Every Pre A*-algebra with 1 satisfies the following laws.
(a) $x \wedge (x^{\sim} \vee x) = x \vee (x^{\sim} \wedge x) = x$
(b) $(x \vee x^{\sim}) \wedge y = (x \wedge y) \vee (x^{\sim} \wedge y)$
(c) $(x \vee y) \wedge z = (x \wedge z) \vee (x^{\sim} \wedge y \wedge z)$

Definition 1.8.[5]: Let A be a Pre A*-algebra. An element $x \in A$ is called central element of A if $x \vee x^{\sim} = 1$ and the set $\{x \in A / x \vee x^{\sim} = 1\}$ of all central elements of A is called the centre of A and it is denoted by $B(A)$.
Note that if A is a Pre A*- algebra with 1, then $1, 0 \in B(A)$. If the centre of a Pre A*- algebra coincides with {0,1} then we say that A has trivial centre.

Theorem 1.9.[5]: Let A be a Pre A*-algebra with 1, then $B(A)$ is a Boolean algebra with the induced operations $\wedge, \vee, (-)^{\sim}$

Theorem 1.10.[5]: Let A is a Pre A*-algebra with 1. Then A has trivial centre if and only if $A = \overline{A}_0$, for some Pre A*-algebra A_0.

Lemma 1.11.[5]: Let A be a Pre A*-algebra with 1 ,
(a) If $y \in B(A)$ then $x \wedge x^{\sim} \wedge y = x \wedge x^{\sim}$, $\forall x \in A$
(b) If $x, y \in B(A)$ then $x \wedge (x \vee y) = x \vee (x \wedge y) = x$

Lemma 1.12[5]: Let A be a Pre A*algebra with 1, 0 and let $x, y \in A$
(a) If $x \vee y = 0$, then $x = y = 0$ (b) If $x \vee y = 1$, then $x \vee x^{\sim} = 1$

Theorem 1.13[5]: Let A be a Pre A*-algebra with 1 and $x, y \in A$, if $x \wedge y = 0$, $x \vee y = 1$, then $y = x^{\sim}$

Lemma 1.15[6]: Let A be a Pre A*-algebra and $p \in A$. Then $\{x \wedge p / x \in A\}$ is the smallest ideal containing p.

Lemma 1.16[6]: Let A be a Pre A*-algebra and $p, y \in A$.Then $y \in \langle p \rangle \Leftrightarrow y = y \wedge p$.

Definition 1.17[6]: A nonempty subset U of a Pre A*- algebra A is said to be a ideal of A if the following hold

$a,b \in U \Rightarrow a \vee b \in U$
$a \in U \Rightarrow x \wedge a \in U$ for each x∈A

2. Zero of a Pre A*-Algebra:
Definition 2.1: Let S be a subset of Pre A*-algebra A. An element z of S is called as a Zero of S for $\wedge$ if $z \wedge s = z \quad \forall s \in S$.

For each $x \in A, x \wedge x^{\sim} \in I$ for all ideals I of A.
The class of all ideals of a Pre A*-algebra is closed under arbitrary intersections
$I_0 = \bigcap I_j$ where I_j is the set of all ideals of Pre A*-algebra. Therefore I_0 is the smallest ideal of Pre A*-algebra and $I_0 = \{x \wedge x^{\sim} / x \in A\}$.
In fact, in the following any zero for $\wedge$ must be of the form $x \wedge x^{\sim}$ for some $x \in A$.

Example2.2: $A = \{0,1,2\}$ $I_1 = \{0,2\}, I_0 = \{2\}, I_2 = \{0,1,2\}$ are the ideals of A. $I_0 = \bigcap I_j$; j=0,1,2. where $I_0 = \{2\}$ is the smallest ideal.

Theorem 2.3: Let A be a Pre A*-algebra with 1,
a. Let S ={0,1} be a non empty subset of A and if $y \in B(A)$ then $x \wedge x^{\sim} \wedge y = x \wedge x^{\sim}, \forall x \in S$.
b. If S= { 2}, $y \in A$ then $x \wedge x^{\sim} \wedge y = x \wedge x^{\sim}$ then $x \wedge x^{\sim}$ is a zero of S.
Proof:
a. If $y \in B(A)$ then $x \wedge x^{\sim} \wedge y = o \wedge y = 0 = x \wedge x^{\sim}, \forall x \in S$
b. If S = {2}, $y \in A$ then $x \wedge x^{\sim} \wedge y = 2 \wedge y = 2 = x \wedge x^{\sim} \ \forall x \in S$ .Then $x \wedge x^{\sim}$ is a zero of S.

3. Annihilator Ideals:
Definition 3.1: For any non- empty subset M of a Pre A*-algebra A, define M* as follows:
$M^* = \{x \in A / x \wedge m$ is a zero, $\forall m \in M\}$
M* is called the annihilator of M. It is obvious that $I_0^* = A \& A^* = I_0$. If S={ a }, then we write (a)* for ({ a })*.

Lemma 3.2: For any non-empty subset M of a Pre A*-algebra A, M* is an ideal in A.
Proof: Clearly $I_0 \subseteq M^*$ and hence $M^* \neq \phi$.
Let $x, y \in M^*$.Then $x \wedge m, y \wedge m$ are zeros $\forall m \in M$ .For any $c \in M$ we have
$c \wedge (x \vee y) = (c \wedge x) \vee (c \wedge y)$ is a zero. $\Rightarrow x \vee y \in M^*$
Again let $x \in A$ and $a \in M^*$.Then $x \wedge a$ is zero $\forall m \in M$ .For any $c \in M$, we get
$(x \wedge a) \wedge c = x \wedge (a \wedge c)$ is a zero $\Rightarrow x \wedge a \in M^* \Rightarrow$ M* is an ideal of Pre A*-algebra.

Definition 3.3: An ideal I of a Pre A*-algebra A is called an annihilator ideal if $I = I^{**}$ or equivalently $I = S^*$ for some non-empty subset S of A .It is oblivious that S* is an annihilator ideal in A.

Example 3.4: Consider the three element Pre A*-algebra $A = \{0,1,2\}$ with the operations given by

$\wedge$	0	1	2
0	0	0	2

$\vee$	0	1	2
0	0	1	2

x	$x^{\sim}$
0	1

1	0	1	2	1	1	1	2	1	0
2	2	2	2	2	2	2	2	2	2

Now consider the Pre A*-algebra $F = A_1 \times A_2 = \{e_1, e_2, e_3, e_4, e_5, e_6, e_7, e_8, e_9\}$ where

$e_1 = (1,2); e_2 = (0,2); e_3 = (2,1); e_4 = (2,0); e_5 = (2,2); e_6 = (1,1); e_7 = (0,0); e_8 = (1,0) \& e_9 = (0,1)$
Then clearly $I_0 = \{e_2, e_4, e_5, e_7\}$. Consider $I = \{e_1, e_2, e_4, e_5, e_7, e_8\}$ Then $I^* = \{e_2, e_3, e_4, e_5, e_7, e_9\}$
$I^{**} = \{e_1, e_2, e_4, e_5, e_7, e_8\}$ $I^{**} = I$
$\therefore I$ is an annihilator ideal of F.

4. Support of M:

Definition 4.1: Let A be a Pre A*-algebra. Support of M is the set of all prime ideals of A and it is denoted by M_p.

Theorem 4.2: Let M be a subset of Pre A*-algebra A. Then prime ideal P is in the support of M iff M_p is zero.

Proof: If P is in the support of M . This implies M_p is the collection of all prime ideals of M. By the definition of annihilator ideals , $I_0^* = A$ and $A^* = I_0$ where $I_0 = \{x \wedge \tilde{x} / x \in A\}$. $\therefore$ M_P is zero. Suppose M_P is zero then M* is the collection of prime ideals. This implies that Prime ideal P is in the support of M.

5. Dense Ideal:

Definition 5.1: An ideal I of a pre A*-algebra is called a dense ideal if $I^* = I_0$ Otherwise I is called a non-dense ideal.

Note5.2: It is clear that a dense ideal cannot be an annihilator ideal in Pre A*-algebra.

Theorem 5.3: Let A be a Pre A*-algebra in which every proper ideal is non-dense. Then the following conditions are equivalent.

a) Every ideal is an annihilator ideal.
b) Every prime ideal is an annihilator ideal.
c) Every prime ideal is minimal
d) Every prime ideal is maximal only if $x_0 \in B(A), x \in A$ then $x_0 \wedge x = x \& \tilde{x_0} \vee x = 1$

Proof: $(i) \Rightarrow (ii)$ It is obvious.

$(ii) \Rightarrow (iii)$ Assume that every prime ideal is an annihilator ideal. Let P be a prime ideal of A
Then $P^{**} = P$ .Suppose P is not a minimal prime ideal, then there exist $Q \subseteq P$. Let $a \in P^*. \because x \in P$ we get $a \wedge x$ is a zero. Hence $a \wedge x \in Q$ .Since Q is prime & $x \notin Q$ $\Rightarrow a \in Q \subset P \Rightarrow a \in P$ $\therefore P^* \subseteq P$. $P^* = P^* \cap P = I_0$ Contradiction to P is non-dense. Therefore P is a minimal prime ideal of A

$(iii) \Rightarrow (iv)$ For any ideal of a Pre A*-algebra A $I = \bigcap \{P / P$ is a prime ideal of A and $I \subseteq P\}$

We know that every maximal ideal is prime. By (ii) Every prime ideal is an annihilator ideal. And therefore every prime ideal is maximal only if $x_0 \in B(A), x \in A$ then $x_0 \wedge x = x$ & $x_0^{\sim} \vee x = 1$

$(iv) \Rightarrow (i)$ Every prime ideal is maximal only if $x_0 \in B(A), x \in A$ then $x_0 \wedge x = x$ & $x_0^{\sim} \vee x = 1$

Then $x_0 \wedge x = x \Rightarrow x$ is zero. $\forall x \in A \Rightarrow x$ belongs to an annihilator ideal .Therefore every ideal is an annihilator ideal.

References:

1. Manes E.G: The Equational Theory of Disjoint Alternatives, personal communication to Prof.N.V.Subrahmanyam(1989)
2. Manes E.G: Ada and the Equational Theory of If-Then-Else, Algebra Universalis30(1993), 373-394.
3. Fernando Guzman and Craig C.Squir: The Algebra of Conditional logic, Algebra Universalis 27(1990), 88-110
4. KoteswaraRao.P, A*-Algebra an If-Then-Else structures(thesis) 1994, Nagarjuna University, A.P., India
5. VenkateswaraRao.J., On A*-Algebras(Thesis) 2000, Nagarjuna University, A.P., India
6. A.Satyanarayana, J.Venkateswara Rao, Prime and Maximal Ideals of Pre A*- algebra, Trends in Applied Sciences Research, 6(2): 108-120, 2011.
7. K.Srinivasa Rao, Structural Compatibility of Pre A*-algebra with Boolean algebra: A novel approach, Ph.D Thesis , 2009, Acharya Nagarjuna University , A.P., India.

***

International Journal of Mathematical Archive-9(4), 2018, 45-48
Available online through www.ijma.info ISSN 2229 – 5046

LAPLACE EXPANSION IN RHOTRIX

VIJAYABARATHI.S*

Assistant professor of Mathematics,
Sri Chandrasekharendra Saraswathi Viswa Mahavidyalaya, Enathur, Kancheepuram, India.

(Received On: 25-02-18; Revised & Accepted On: 19-03-18)

ABSTRACT

L*aplace expansion of rhotrix matrices has been defined and the results* $\Delta R_1 = \Delta R_3 = \Delta C_1 = \Delta C_3$ *in the third order and in the fifth order* $\Delta R_1 = \Delta C_1$ & $\Delta R_5 = \Delta C_5$ *have been proved.*

Keywords: *Laplace expansion, cofactors, determinants, NE-elements.*

1. PRELIMINARY

Definition [2]1.1:

Rhotrix is defined as $R = \left\{ \left\langle \begin{matrix} & a & \\ b & c & d \\ & e & \end{matrix} \right\rangle : a,b,c,d,e \in R \right\}$ R is of dimension 3.This is a rhomboidal arrangement.

Entry c in R is the heart of R and denoted by h(R).This is analogous to concepts in Matrix Theory.

Multiplication of Rhotrix matrices [2]1.2:

$$A \circ B = \left\langle \begin{matrix} & a & \\ b & h(A) & d \\ & e & \end{matrix} \right\rangle \circ \left\langle \begin{matrix} & f & \\ g & h(B) & i \\ & j & \end{matrix} \right\rangle = \left\langle \begin{matrix} & af+dg & \\ bf+eg & h(A)h(B) & ai+dj \\ & bi+ej & \end{matrix} \right\rangle$$

Cardinality is $\frac{1}{2}\left(n^2+1\right)$

Right triangular Rhotrix1.3:

All the entries to the left of the main diagonal in R are zero.

Left triangular Rhotrix1.4:
All the entries to the right of the main diagonal in R are zero.

Upper triangular Rhotrix1.5:
All the entries to the below the horizontal diagonal in R are zero.

Lower triangular Rhotrix1.6:
All the entries to the above the horizontal diagonal in R are zero

Corresponding Author: Vijayabarathi.S*, Assistant professor of Mathematics,
Sri Chandrasekharendra Saraswathi Viswa Mahavidyalaya, Enathur, Kancheepuram, India.

2. LAPLACE EXPANSION

Determinants of the Rhotrix 2.1: $|A| = \left| \left\langle \begin{matrix} & a & \\ c & h(A) & d \\ & b & \end{matrix} \right\rangle \right|$ is called the determinant of the rhotrix of the third order. The diagonals from top to bottom which contains the element $a.h(A),b$ called the leading or principal diagonal.

Cofactors: 2.2: The sign of an element in the ith row and j^{th} column is $(-1)^{i+j}$. But in Rhotrix if i+j is odd, null entries will be there.

$$A = \left\langle \begin{matrix} & a & \\ c & h(A) & d \\ & b & \end{matrix} \right\rangle$$

Co-factors of $a = h(A) \times b$

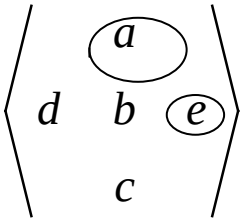
Co-factors of $d = h(A) \times c$

Co-factors of $c = h(A) \times d$

Co-factors of $b = h(A) \times a$

Co-factors of $h(A) = (a \times b) - (c \times d)$

If the order of rhotrix increases then convert this into coupled (ordinary) matrix and find the del value of that matrix.



The elements a and e are called as North –East elements (NE-elements)

Similarly the elements e and c are called as East-South elements (ES-elements).

The elements c and d are called as South-west elements (NE-elements) and the elements d and a are called as West-North elements (WN-elements).

Laplace Expansion 2.3:
A determinant can be expanded in terms of North –East elements (row) as follows:
Multiply each element of the NE in terms of which we intend expanding the del, by its cofactor then add up all these terms.

Expanding NE-Row

$$\Delta = a[h(A) \times b] + d[h(A) \times c]$$

Expanding by NW-column

$$\Delta = a[h(A) \times b] + c[h(A) \times d]$$

Thus Δ is the sum of the products of the elements of any NE-row(or column) by their corresponding cofactors

Let the rhotrix be $\left\langle \begin{matrix} & a & \\ d & b & e \\ & c & \end{matrix} \right\rangle$

$$\Delta_{NE} = \Delta_{R_1} = abc - deb .$$

$$\Delta_{NW} = \Delta_{C_1} = abc - dbe$$

© 2018, IJMA. All Rights Reserved

$$\Delta_{WS} = \Delta_{R_3} = -deb + abc$$
$$\Delta_{ES} = \Delta_{C_3} = abc - deb$$
$$\Delta_{R_1} = \Delta_{C_1} = \Delta_{R_3} = \Delta_{C_3}$$

Let the rhotrix be

$$\left\langle \begin{array}{ccccc} & & a & & \\ & m & b & n & \\ f & g & c & h & l \\ & p & d & q & \\ & & e & & \end{array} \right\rangle$$

$$\Delta_{NE} = \Delta_{R_1} = abcde - abqpd - ahcge + ahqgp - nbmde + nbqfd + nhmge - nhqfg + lbmpd - lbcfd - lhmgp + lhcfg$$

$$\Delta_{NW} = \Delta_{C_1} = abcde - abqpd - ahcge + ahqgp - nbmde + nbqfd + nhmge - nhqfg + lbmpd - lbcfd - lhmgp + lhcfg$$

$$\Rightarrow \Delta_{R_1} = \Delta_{C_1}$$

$$\Delta_{WS} = \Delta_{R_5} = fnbdq - nhgqf - flbcd + flhgc - pabdq + phgqa + plbmd - plhmg + eabcd - heagc + enhmg$$

$$\Delta_{SE} = \Delta_{C_5} = fnbdq - nhgqf - flbcd + flhgc - pabdq + phgqa + plbmd - plhmg + eabcd - heagc + enhmg$$

$$\Rightarrow \Delta_{R_5} = \Delta_{C_5}$$

These results have been supported by numerical judgment.

- The Laplace Expansion of the rhotrix $A = \left\langle \begin{array}{ccc} & 5 & \\ 3 & 4 & 8 \\ & 6 & \end{array} \right\rangle$

Cofactors of 5=24
Cofactors of 8=12
Cofactors of 3=32
Cofactors of 6=20
Cofactors of 4=6
NE-elements (R_1)
$\Delta R_1 = 5(24) + 8(12) = 216$
NW- elements(C_1)
$\Delta C_1 = 5(24) + 3(32) = 216$
WS-elements (R_3)
$\Delta R_3 = 3(32) + 6(20) = 216$
ES-elements (C_3)
$\Delta C_3 = 8(12) + 6(20) = 216$

$$\therefore \Delta R_1 = \Delta R_3 = \Delta C_1 = \Delta C_3$$

Note 2.4: In the third order Rhotrix, the above problems leads to the conclusion that $\Delta R_1 = \Delta R_3 = \Delta C_1 = \Delta C_3$.

© 2018, IJMA. All Rights Reserved

The Laplace expansion of $\left\langle \begin{matrix} & & 2 & & \\ & 3 & 6 & 4 & \\ 1 & 4 & 5 & 25 & 6 \\ & 7 & 17 & 3 & \\ & & 8 & & \end{matrix} \right\rangle$

Expansion of NE- elements (R_1)

$$\Delta R_1 = 2(38) + 4(-42) + 6(32) = 100$$

Expansion of NW- elements (C_1)

$$\Delta C_1 = 2(38) + 3(20) + 1(-36) = 100$$

Expansion of ES- elements (C_5)

$$\Delta C_5 = 6(32) + 3(-20) + 8(-4) = 100$$

Expansion of WS- elements (R_5)

$$\Delta R_5 = 1(-36) + 7(24) + 8(-4) = 100$$

$$\therefore \Delta R_1 = \Delta C_1 \ \& \ \Delta R_5 = \Delta C_5$$

REFERENCES

1. Ajibade.A.O: The concept of rhotrix in mathematical enrichment. Int. J. Math. Educ. Sci.Technol.34, 175-179 (2003).
2. Abdul Mohammed, Musa Balarabe: Rhtrix linear transformation, Advances in Linear Algebra & Matrix Theory 2012, 2, 43-47.
3. S.M Tudunkaya: Rhotix polynomial and polynomial rhotrices in Pure and Applied Mathematics Journal, 2013, 2(1): 38-41.
4. P.L Sharma, Satish Kumar; On Factorization of a special type of Vandermonde Rhotix in Application and applied Mathematics, an international journal, 2016, 11(1): 317-338.

Source of support: Nil, Conflict of interest: None Declared.

[Copy right © 2018. This is an Open Access article distributed under the terms of the International Journal of Mathematical Archive (IJMA), which permits unrestricted use, distribution, and reproduction in any medium, provided the original work is properly cited.]

SOLVING INTEGER PROGRAMMING PROBLEMS USING MATLAB

K.Pramila
Assistant Professor of Mathematics,
Sri Chandrasekarenda Saraswathi Viswa Maha Vidyalaya, Kanchipuram

Abstract: MATLAB stands for matrix laboratory. MATLAB is a high-performance language for technical computing. It integrates computation, visualization, and programming in an easy-to-use environment where problems and solutions are expressed in familiar mathematical notation. Integer Programming Problems like transportation, assignment, travelling salesman problem, capital budgeting, production scheduling occurs quite frequently in business and industry. Each commodity takes integer values or binary integer values. Hence there is a need of integer programming in our real life. Algorithms available for obtaining optimal solution in the traditional methods are time consuming. As the MATLAB software is a matrix-based language, it is a powerful tool to solve such type of problems. This paper deals with solving integer programming and binary integer programming problems using MATLAB and numerical examples are given for illustration.

Keywords: Integer Programming Problems, MATLAB, Intlinprog.

1. Introduction: An integer programming problem is a mathematical programming problem in which $S \subseteq Z^n \subseteq R^n$ where Z^n is the set of all n-dimensional integer vectors (i.e. all the components of x are restricted to integer values). A mixed integer programming problem is a mathematical programming problem in which at least one, but not all, of the components of $x \in S$ are required to be integers. The Mathematical formulation of integer linear programming (ILP) is

Max (or Min) $Z= \sum_{j=1}^{n} C_j X_j$

Subject to $\sum_{j=1}^{n} C_{ij} X_j \leq b_i$, i=1,2, m

$0 \leq X_j \leq 1$, X_j integer, j=1,2.....n

If the variables in an IP is restricted to take values in {0,1} then the IP is called a Binary Integer Program (BIP)

There are two widely used methods for generating the special constraints that will force the optimum point of the relaxed LP problem towards the desired integer solution:

(i) Cutting plane (ii) . Branch-and-bound

MATLAB is widely used in all areas of applied mathematics, in education, research and in the industry. It has literally hundreds of built-in functions for a wide variety of computations and many toolboxes designed for specific research disciplines, including statistics, optimization, solution of partial differential equations, data analysis. The matrix-based MATLAB language is the world's most natural way to express computational mathematics. Built-in graphics make it easy to visualize and gain insights from data. As a result, linear programming problems which involve large data can also be solved using MATLAB. The command intlinprog solves integer programming problems. This paper deals with solving integer programming and binary integer programming problems using MATLAB.

2. Integer Programming, Binary Integer Programming Problem using MATLAB: MATLAB accepts only minimization problem in LPP. So whenever you want to solve maximization problem first convert it in to minimization one. Let us see how to find the solution of integer programming problems using MATLAB. To solve integer programing problem, branch and bound technique is a lengthy procedure and also consuming. But in MATLAB it is not so, using a command and the input values, solution will be displayed immediately in the command window. We can also solve binary integer programming and mixed integer programming using MATLAB.

The command 'intlinprog' solves integer programming problems in MATLAB.

x = intlinprog(f, intcon A, b) solves min f* x such that the components of x in intcon are integers and A * x ≤ b.

x = intlinprog(f, intcon, A, b, Aeq, beq) solves the problem above while additionally satisfying the equality constraints Aeq * x = beq.

Set A = [ ] and b = [ ] if no inequalities exist.

x = intlinprog(f, intcon,A, b, Aeq, beq, lb, ub) defines a set of lower and upper bounds on the decision variables x, so that the solution is always in the range lb ≤ x ≥ub. Set Aeq = [ ] and beq = [ ] if no equalities exist.

x= bintprog(f,A,b,Aeq,beq,lb,ub) solves binary integer programming problem (i.e) linear programming problem in which the decision variables are binary integers. Binary integer programming problem can also be solved by 'intprog" by setting the lower bound as 'o' and upper bound as '1' of the binary variable.

The following lists the values of exitflag and the corresponding reasons intlinprog stopped.

Value	Description	Value	Description
2	intlinprog stopped prematurely, integer feasible point found	-1	intlinprog stopped by an output function or plot function
1	intlinprog converged to the solution x	-2	No feasible point found
0	intlinprog stopped prematurely, no integer feasible point found.	-3	Root LP problem is unbounded

Description of the output terms

Relative gap: Relative difference between upper (U) and lower (L) bounds of the objective function that intlinprog calculates in its branch- and-bound algorithm.

Relativegap = (U - L) / (abs(U) + 1). If intcon = [ ], relativegap = [ ].

Absolute gap: Difference between upper and lower bounds of the objective function that intlinprog calculates in its branch and bound algorithm.If intcon = [ ], absolute gap = [ ].

Numfeaspoints: Number of integer feasible points found. If the initial relaxed problem is infeasible, numfeaspoints = [ ].

Numnodes: Number of nodes in branch-and-bound algorithm. If the solution was found during pre-processing or during the initial cuts, numnodes = 0

3. Numerical Examples:

3.1. Diet Problem (Integer Programming Problem): An ideal diet would meet or exceed basic nutritional requirements, be inexpensive, have variety, and be "pleasing to the palate". How can we find such a diet? Suppose the only foods in the world are as follows:

After consulting with nutritionists, we decree that a satisfactory diet has at least 2000 kcal of energy, 55 g of protein, and 800 mg of calcium (vitamins and iron are supplied by pills). While some of us would be happy to subsist on 10 servings of pork and beans, we have decided to impose variety by having a limit on the number of servings/day for each of our six foods. What is the least cost satisfactory diet? Formulate this as linear programming problem in which the numbers of servings are integers.

Food	Serving Size	Energy (kcal)	Protein (g)	Calcium (mg)	Price (cents/serving)	Limit (servings/day)
Oatmeal	28g	110	4	2	3	4
Chicken	100g	205	32	12	24	3
Eggs	2 Large	160	13	54	13	2
Whole Milk	237cc	160	8	285	9	8
Cherry Pie	170g	420	4	22	20	2
Pork& Beans	260g	260	14	80	19	2

Solution: Let us label the foods as 1, 2, ... 6, and let X_i represent the number of servings of food' i ' in the diet.Our objective is to minimize cost, which can be written as

Min Z= $3X_1 + 24X_2 + 13X_3 + 9X_4 + 20X_5 + 19X_6$.

The diet must have at least 2000 kcal of energy, hence

$110X_1 + 205X_2 + 160X_3 + 160X_4 + 420X_5 + 260X_6 \geq 2000$, similarly

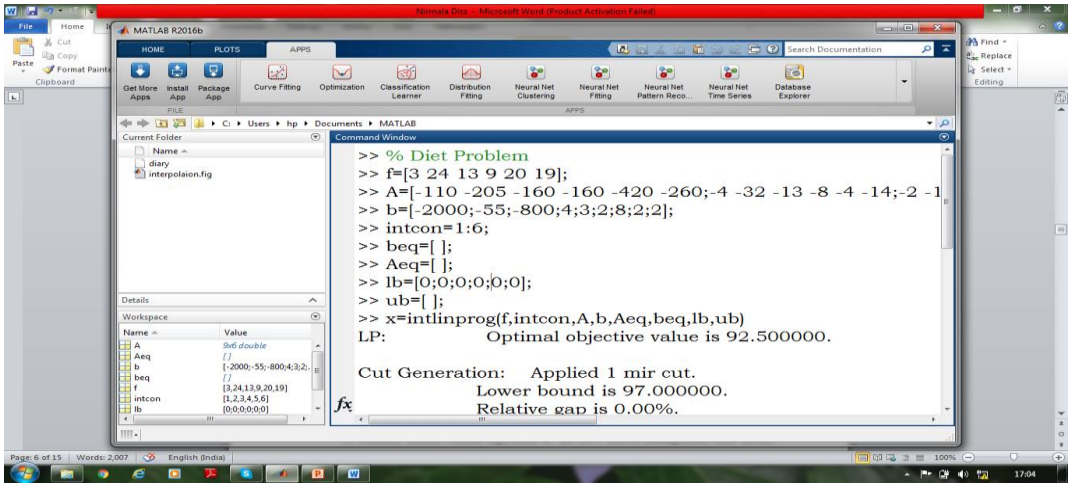
$4X_1 + 32X_2 + 13X_3 + 8X_4 + 4X_5 + 14X_6 \geq 55$

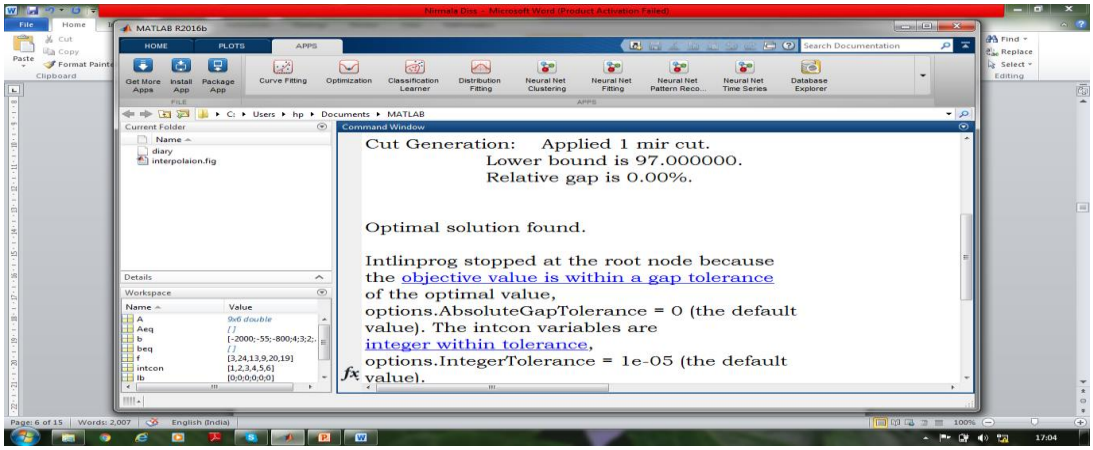
$2X_1 + 12X_2 + 54X_3 + 285X_4 + 22X_5 + 80X_6 \geq 800$

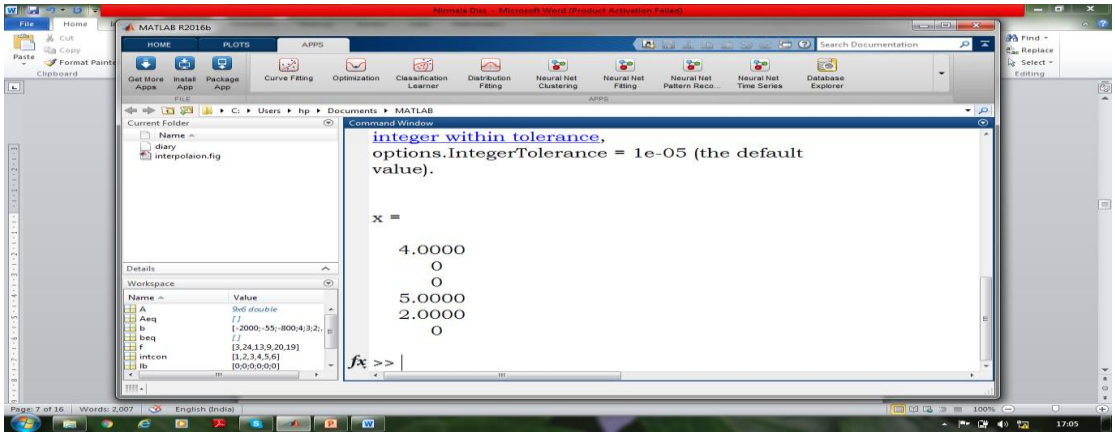
There is a limitation in number of servings, thus

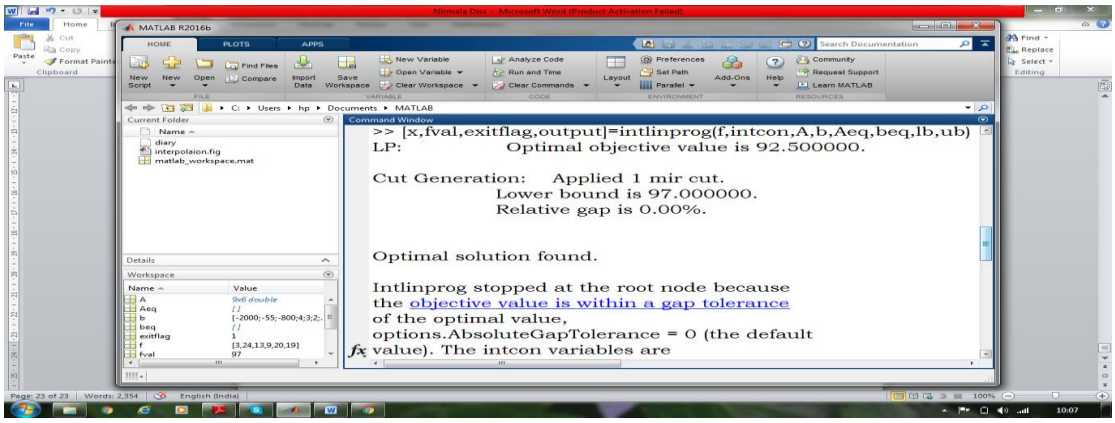
$X_1 \leq 4$, $X_2 \leq 3$, $X_3 \leq 2$, $X_4 \leq 8$, $X_5 \leq 2$, $X_6 \leq 2$

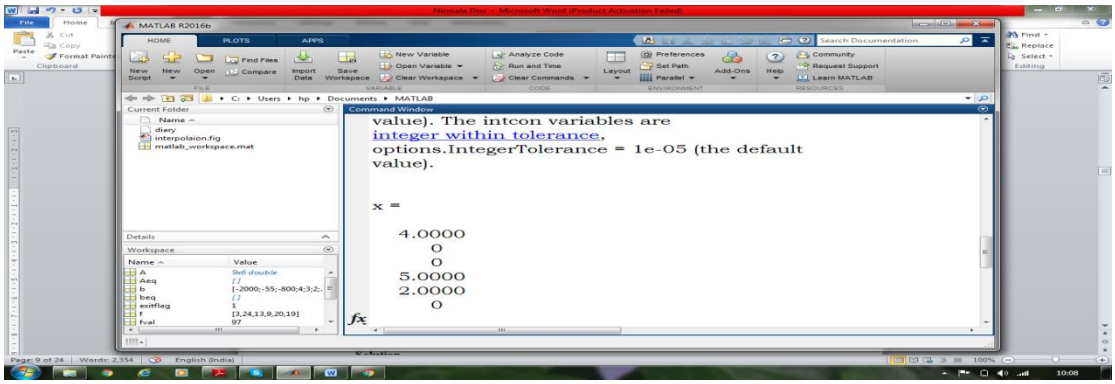
$X_i \geq 0$, are integers i= 1,2.....6.

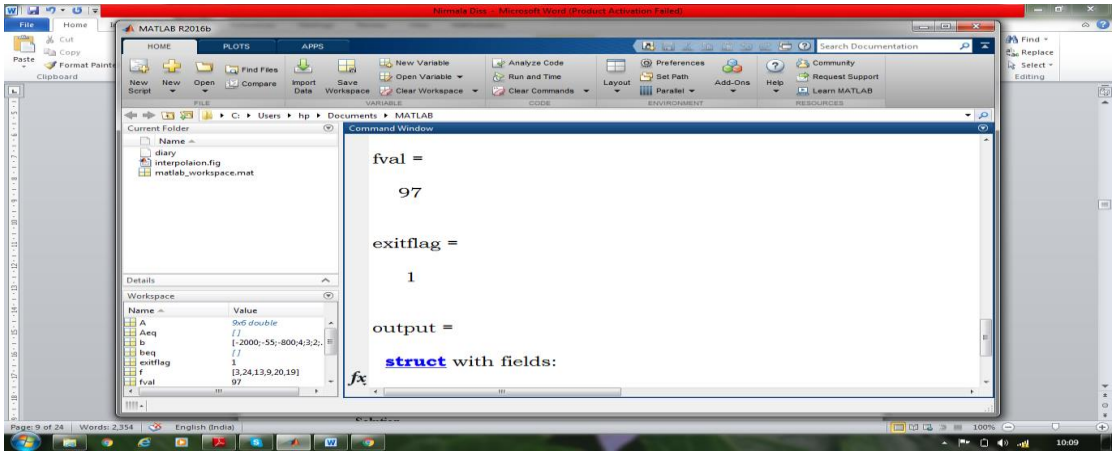


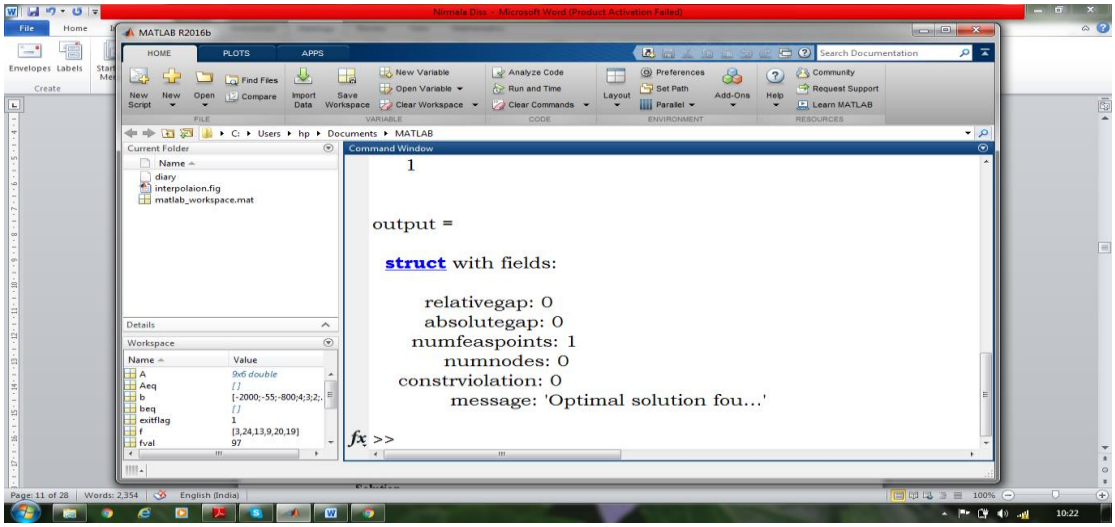



integer within tolerance,
options.IntegerTolerance = 1e-05 (the default
value).
x =
4.0000
0
0
5.0000
2.0000
0


>> [x,fval,exitflag,output]=intlinprog(f,intcon,A,b,Aeq,beq,lb,ub)
LP: Optimal objective value is 92.500000.
Cut Generation: Applied 1 mir cut.
Lower bound is 97.000000.
Relative gap is 0.00%.
Optimal solution found.
Intlinprog stopped at the root node because
the objective value is within a gap tolerance
of the optimal value,
options.AbsoluteGapTolerance = 0 (the default
value). The intcon variables are


value). The intcon variables are
integer within tolerance,
options.IntegerTolerance = 1e-05 (the default
value).
x =
4.0000
0
0
5.0000
2.0000
0


fval =
97
exitflag =
1
output =
struct with fields:



Result:
Least Cost of satisfactory Diet is 97 cents
Number of Servings of Oatmeal = 4
Number of Servings of Chicken = 0
Number of Servings of Eggs = 0
Number of Servings of Milk = 5
Number of Servings of Cherry Pie = 2
Number of Servings of Pork & Beans = 0

3.2 Binary Integer Programming Problem:
Assignment Problem: A law firm maintains a large staff of young attorneys who hold the title of junior partner. The firm concerned with the effective utilization of this personnel resources, seeks some objective means of making lawyer-to-client assignments. On March 1, four new clients seeking legal assistance came to the firm. While the current staff is overloads and identifies four junior partners who, although busy, could possibly be assigned to the cases. Each young lawyer can handle at most one new client. Furthermore each lawyer differs in skills and specialty interests. Seeking to maximize the overall effectiveness of the new client assignment, the firm draws up the following table, in which he rates the estimated effectiveness (of a scale of 1 to 9) of each lawyer on each new case

Lawyer	Divorce	Corporate Merger	Embezzlement	Exhibitionism
Adam	6	2	8	5
Brook	9	3	5	8
Carter	4	8	3	4
Darwin	6	7	6	4

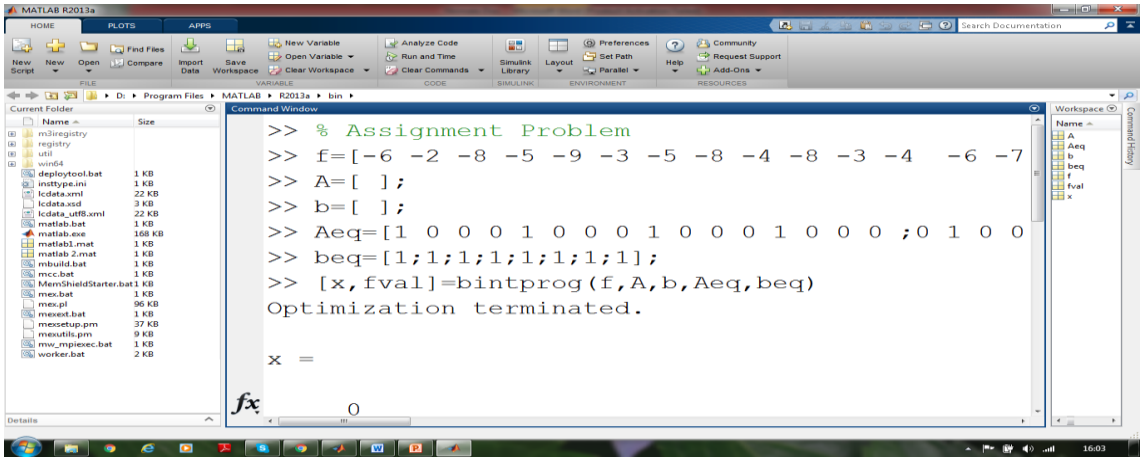
Solution:
Decision variables:

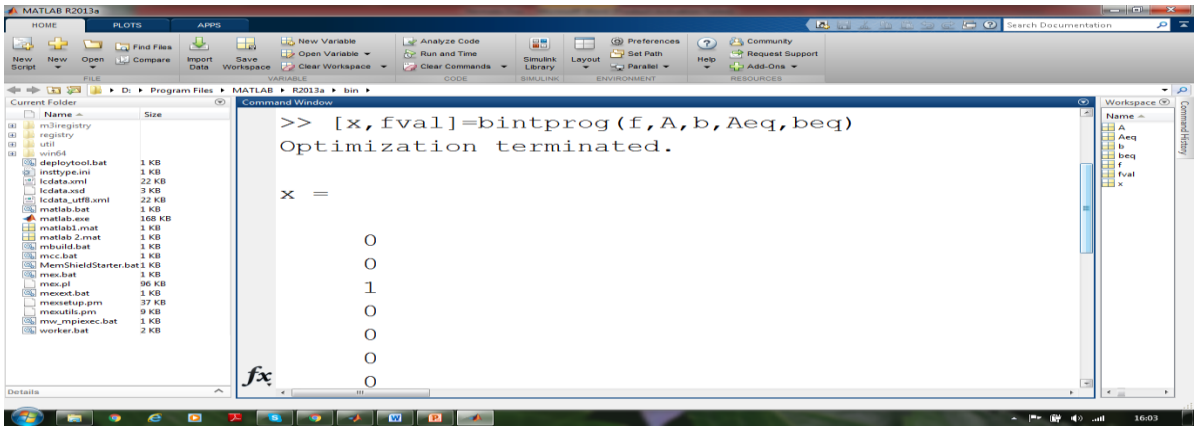
Let $X_{ij} = \begin{cases} 1 \text{ if attorney i is assigned to case j} \\ 0 \text{ otherwise} \end{cases}$

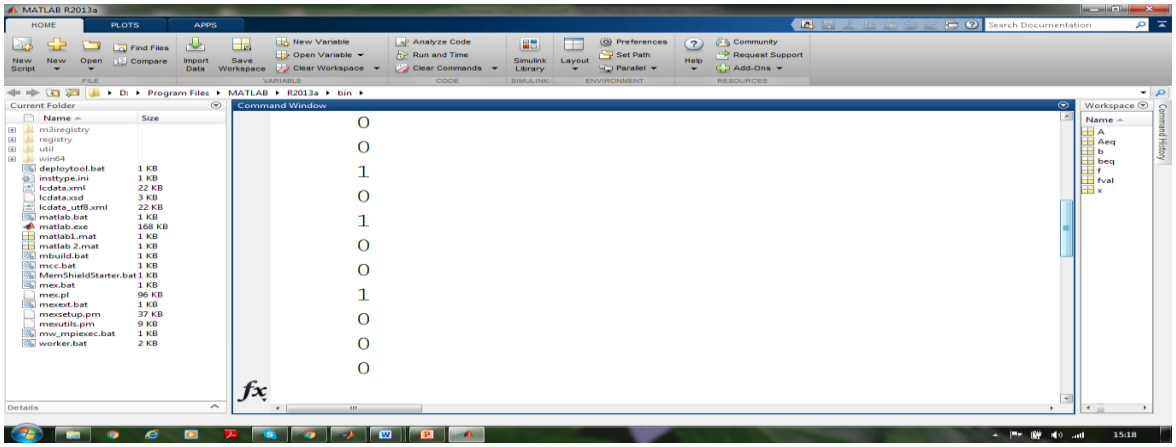
Where : i = 1, 2, 3, 4 stands for Adam, Brook, Carter, and Darwin respectively j = 1, 2, 3, 4 stands for divorce, merger, embezzlement, and exhibitionism respectively.
The LP formulation will be as follows:
Max Z = $6 X_{11} + 2 X_{12} + 8 X_{13} + 5 X_{14} + 9 X_{21} + 3 X_{22} + 5 X_{23} + 8 X_{24} + 4 X_{31} + 8 X_{32} + 3 X_{33} + 4 X_{34} + 6 X_{41} + 7 X_{42} + 6 X_{43} + 4 X_{44}$

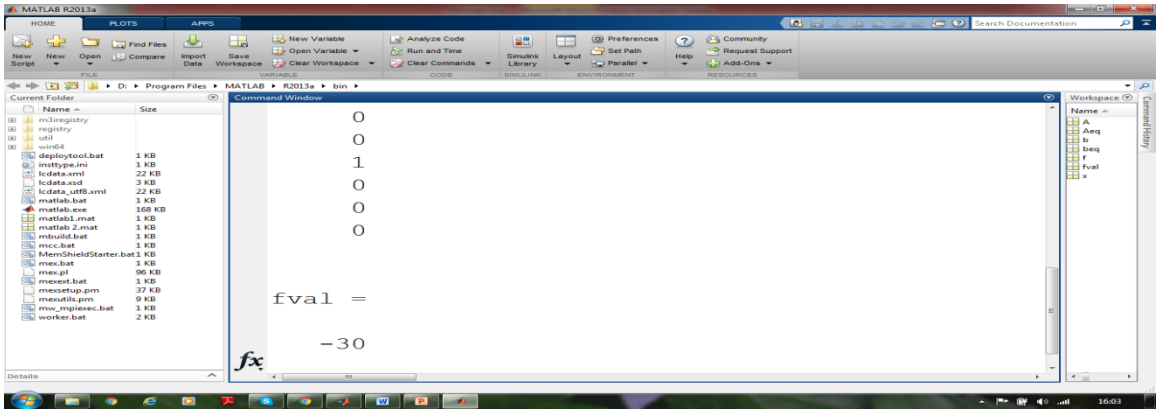
Such that

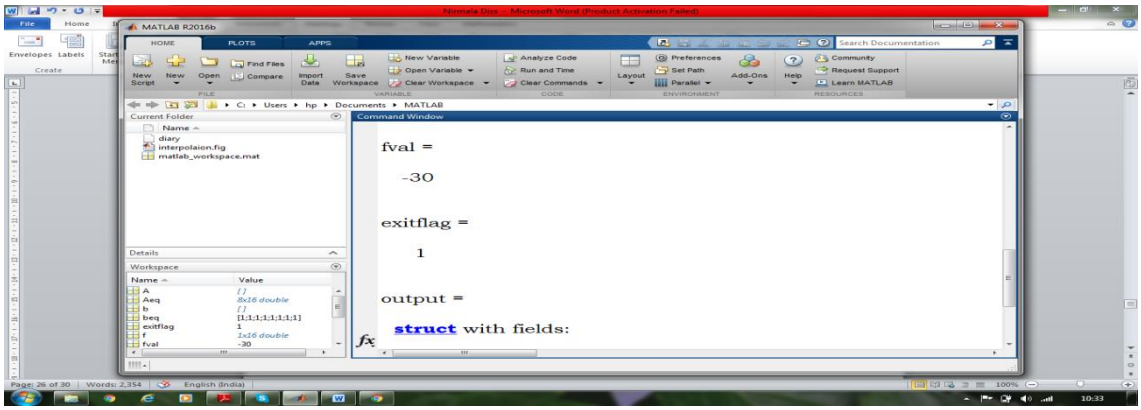
$X_{11} + X_{21} + X_{31} + X_{41} = 1$ (divorce case)
$X_{12} + X_{22} + X_{32} + X_{42} = 1$ (merger)
$X_{13} + X_{23} + X_{33} + X_{43} = 1$ (embezzlement)
$X_{14} + X_{24} + X_{34} + X_{44} = 1$ (exhibitionism)
$X_{11} + X_{12} + X_{13} + X_{14} = 1$ (Adam)
$X_{21} + X_{22} + X_{23} + X_{24} = 1$ (Brook)
$X_{31} + X_{32} + X_{33} + X_{34} = 1$ (Carter)
$X_{41} + X_{42} + X_{43} + X_{44} = 1$ (Darwin)
$X_i \geq 0$, binary integers

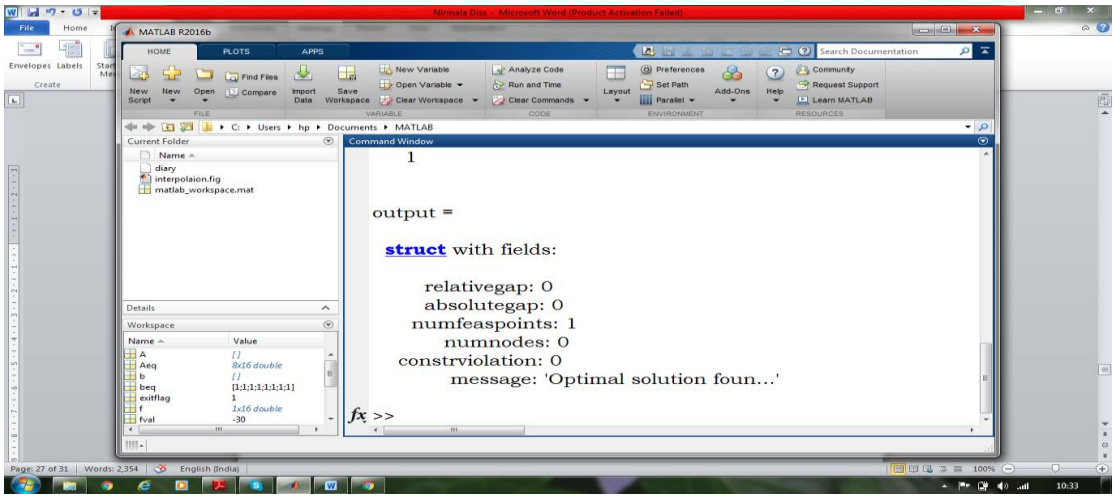












Result:
Adam is assigned for embezzlement case
Brook is assigned for exhibitionism case
Carter is assigned for Merger case
Darwin is assigned for divorce case

Conclusion: MATLAB is globally used in all important fields of applied mathematics and in management science. It has variety of uses in several computations and tool boxes are created for unique research departments, includes statistics optimization, solution of partial differential equations, data analysis. Using MATLAB we can solve more difficult problems that can occur in our day to day life.

In this paper, integer programming and binary integer programming problems are solved using MATLAB in an easy way.

References:

1. Integer Programming and Submodular Optimization, Debasis Mishra, Planning Unit, Indian Statistical Institute.
2. Integer Programming and Combinatorial Optimization, MIT, Open Education Consortium.
3. Integer Programming, Chapter 9, wwwhome.math.utwente.nl
4. An Integer Programming Proof of Cook's theorem of NP-completeness, Benjamin Letham, Operations Research Center, Massachusetts Institute of Technology, Cambridge, September 2011.
5. Integer Programming Duality, Chapter 11, www.mi.fu-berlin.de.
6. Mixed Integer Linear Programming Formulation Techniques, Juan Pablo Vielma_ Sloan School of Management, Massachusetts Institute of Technology, Cambridge, Massachusetts.
7. Recognizing Unbounded Integer Programs, R.H.Bryd eyal., Operations Research, Volume 35,No.1, 1987.
8. Integer Programming, Chapter 11, College of Management, NCTU, Spring 2009.
9. A Brief Introduction to MATLAB, M.Gerritsen, Linear Algebra with Applications to Engineering Computation, 2006.

***

COST EFFECTIVE AND VERY COST EFFECTIVE BIPARTITION OF FEW FAMILIES OF GRAPH

K.Pramila
Assistant Professor of Mathematics,
Sri Chandrasekarendra Saraswathi Viswa Mahavidyalaya, Enathur
P.Sebasti Suganya
M.Phil Scholar, Sri Chandrasekarendra Saraswathi Viswa Mahavidyalaya, Enathur

Abstract: Cost effective domination is derived from the study of unfriendly partitions of graphs. In this paper, the concept of cost effective and very cost effective is extended to subdivision and complement of graphs, and few families of graphs.

Keywords: cost effective, very cost effective, Bipartition.

1. Introduction: The concept of cost effective partition was first introduced by Cowan and Emerson [1] in the year 1990 in the name of unfriendly partition. Favaron [2] has studied unfriendly partition in the name of global offensive alliances in graphs. The concept of unfriendly partition was changed as satisfactory partition by Gerber [3] in 1998. The cost effective partition on graphs was introduced by Hedetnimei [4] in 2012. The term 'cost effective' was become familiar and then unfriendly partition was renamed as cost effective. The very cost effective bipartitions in graphs was introduced by Haynes and Vasylieva I [5] in 2015.

In terms of an application, we assume that maintaining edges in a network has an associated cost, and thus they should be used effectively. We assume that an edge between a vertex in a set S and a vertex in V \ S is being used effectively, while an edge between two vertices in S is not necessarily being used cost effectively. Thus, a vertex is considered to be cost effective if at least as many edges incident to it are being used cost effectively as not.

Also, (very) cost effective partitions are motivated by business applications. For example, a company that offers service to both customers and employees would want to be certain to make more money than it is spending. Let the edges inside S represent services that employees are using (internal cost), and let edges between S and V \ S represent income from customers paying the company for services. If the company allows employees to use the services it offers for free or at a discounted price, then the company needs to have more edges between S and V \ S to be able to make a profit. Thus, for each vertex, v ∈ S it would be necessary for v to have at least as many neighbors in V \ S as in S in order for the company to make money.

1.1 Preliminaries:

Definition 1.1.1: A vertex in a set $v \in S$ is said to be cost effective if it is adjacent to at least as many vertices in $V \setminus S$ as it in S, that is, $|N(v) \cap S| \leq |N(v) \cap (V \setminus S)|$. A set is cost effective if every vertex $v \in S$ is cost effective.

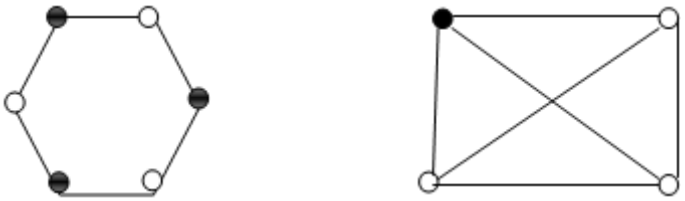


Fig 1.1.1: C_6 *and* K_4 is Cost Effective

Definition 1.1.2: A vertex in a set $v \in S$ is said to be very cost effective if it is adjacent to more vertices as in $V \setminus S$ than in S, that is, $|N(v) \cap S| < |N(v) \cap (V \setminus S)|$. A set is very cost effective if every vertex $v \in S$ is very cost effective.

Definition 1.1.3: A bipartition π = {S, V \ S} is called cost effective if (i) for every vertex i ∈ S, |N(i) ∩ (V \ S)| ≥ |N(i) ∩ S|, and (ii) for every vertex j ∈ V \ S, |N(j) ∩ S| ≥|N(j)∩(V \S)|. Thus, given a cost effective partition π = {S, V \S}, every vertex in S is cost effective with respect to the set S, and every vertex in V \ S is cost effective with respect to the set V \ S.

Definition 1.1.4: A bipartition π = {S, V \ S} of the vertices V of a graph G = (V, E) is very cost effective if (i) for every vertex u ∈ S, |N[u] ∩ (V \ S)| ≥ |N[u] ∩ S|, and (ii) for every vertex v ∈ V \S, |N[v]∩S| ≥ |N[v]∩(V \S)|. Equivalently, every vertex in S is very cost effective with respect to S, and every vertex in V \ S is very cost effective with respect to V \ S. A graph G is called very cost effective if it has a very cost effective bipartition. A bipartition $\pi = \{S, V \setminus S\}$ is called very cost effective if both the sets are very cost effective sets.

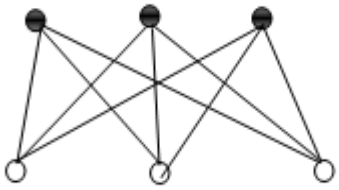


Fig 1.1.2: $K_{3,3}$ **is very cost effective**

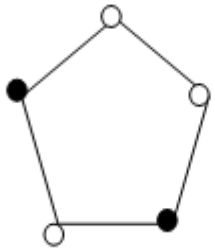


Fig 1.1.3: C_5 **is not very cost effective**

In 1.1.2, the darkened vertices are cost effective and very cost effective but in figure 1.1.3, the darkened vertices are cost effective but not very cost effective.

Definition 1.1.5: A wheel graph is a graph formed by connecting a single vertex to all vertices of a cycle. The wheel graph is denoted as W_n. It has n vertices and $2(n-1)$ edges. In other words, the wheel graph is the graph join of $C_n + K_1$.

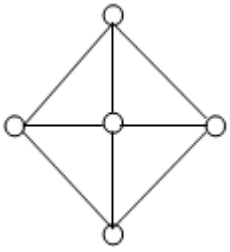


Fig 1.1.4: Wheel Graph $W_{1,4}$.

Definition 1.1.6: A shell graph is a graph formed by cycle C_n with $(n-3)$ chords sharing a common point called apex. The shell graph is denoted by $C(n, n-3)$.

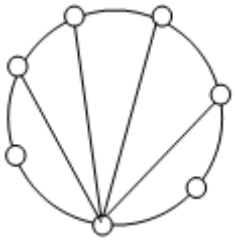


Fig 1.1.5: Shell Graph $C(7,4)$.

Definition 1.1.7: Let G be a graph, then complement of G is denoted by $\overline{G}$, if $\overline{G}$ have the same vertex set of G and two vertices are adjacent in G are not adjacent in $\overline{G}$.



Fig 1.1.6: Complement Graph $\overline{C_6}$

Definition 1.1.8: A subdivision of graph $S(G)$ is a graph resulting from a subdivision of edges of G. Subdivision of some edge e with end points (u,v) yields a graph containing one new vertex w and with an edge set replacing the e by two new edges (u,w) and (w,v).



Fig 1.1.7: Subdivision of Graph

Subdivision of Few Graphs:

Graph	Graph G		Subdivision of G	
	No. of vertices	No. of edges	No. of vertices	No. of edges
P_n	n	$n-1$	$2n-1$	$2(n-1)$
C_n	n	n	$2n$	$2n$
W_n	n	$2(n-1)$	$3n-2$	$4(n-1)$
$S_{1,n}$	n	$n-1$	$2n-1$	$2(n-1)$
K_n	n	$\frac{n(n-1)}{2}$	$\frac{n(n+1)}{2}$	$n(n-1)$

2. Basic Results:

Theorem 2.1: (T. W. Haynes, S. T. Hedetnimei & McCoy, 2012)
Every finite connected graph G of order $n \geq 2$ is unfriendly (cost effective) partition.

Corollary 2.1: (T. W. Haynes, S. T. Hedetnimei & McCoy, 2012)

Let S be cost effective set of G. If every vertex in S has odd degree, then S is a very cost effective set of G.

Theorem 2.2: (Inna Vasylieva & T. W. Haynes, 2013)
The following classes of graphs are very cost effective:

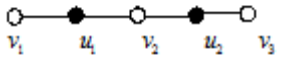
1. Connected bipartite graphs $G=(X,Y,E)$ of order $n\geq 2$,
2. Complete graphs K_{2k} of even order,
3. The corona GoK_1, where G is a nontrivial connected graph ,
4. The wheel $W_{1,k}$ for $k\neq 4$.

Theorem 2.3: (Inna Vasylieva & T. W. Haynes, 2013)
No cycle of C_{2k+1} of odd order is very cost effective

3. Cost Effective and Very Cost Effective Bipartition

Theorem 3.1: If path graph is cost effective and very cost effective for an even order, then subdivision of path graph is also cost effective and very cost effective.

Proof: Let G be a graph having n vertices and $n-1$ edges and H be subdivision of graph G. Consider the bipartition $\pi_G=\{X,Y\}$ such that X has odd order vertices and Y has even order vertices .Let $\{v_1,v_2,....,v_n\}$ be the vertices in X and $\{u_1,u_2,....,u_n\}$ be vertices in Y. Consider $v\in X$, such that v has more adjacency in Y than in X and consider $u\in Y$,where u has more adjacency in X than in Y. Hence G is cost effective and very cost effective. Consider another bipartition $\pi_H=\{S,T\}$ such that S has vertices of G and T has subdivided vertices. Then the vertices in S has more adjacency in T than in S, and vice-versa. Hence, H is cost effective and very cost effective.



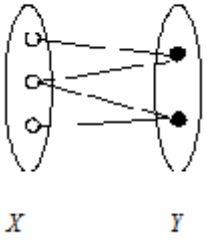


Fig 3.1: Illustration for Subdivision of Path P_3.

Theorem 3.2: The complement of path graph is cost effective and very cost effective.

Proof: Let G be a graph with n vertices is cost effective and very cost effective. Let H be complement $\overline{G}$ of graph G. By definition of complement graph, the vertices adjacent in G are not adjacent in H .Consider the partition $\pi_H=\{S,T\}$ such that X and Y has vertex set with adjacency in G but not in H. Check for adjacency in complement graph. Let v_i be the vertex in X and u_i be the vertex in Y. Consider $v\in X$, it has more adjacency in Y, and $u\in Y$, it has more adjacency in X than in Y. Hence H is cost effective and very cost effective. v_1

v_3

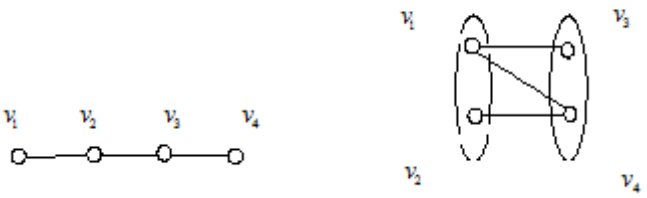


Fig 3.2: Illustration for $\overline{P_4}$.

Theorem 3.3: The complement of odd order path graph is cost effective but not very cost effective.
Proof: Let G be a graph with n vertices is cost effective and very cost effective. Let H be complement $\overline{G}$ of graph G.
Consider a bipartition $\pi = (X, Y)$ such that X and Y are vertex set with adjacency in G but not adjacency in H. Let $\{v_1, v_2, ..., v_n\}$ be set of vertices in X and $\{u_1, u_2, ..., u_n\}$ be set of vertices in Y. Consider $v \in X$, v has adjacency, at least as many vertices in Y. Also consider $u \in Y$, then u has more adjacency in X. Since X satisfies only the condition of cost effective, H is cost effective but not very cost effective.

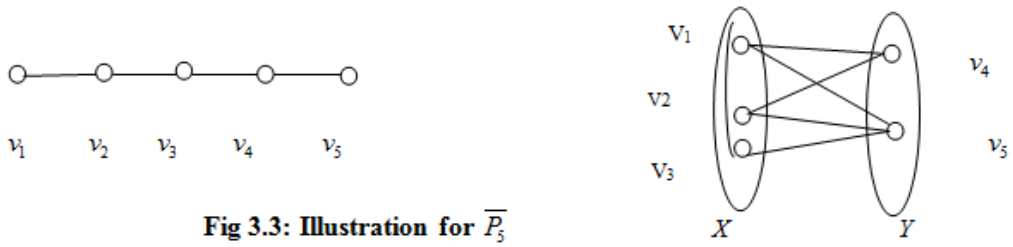


Fig 3.3: Illustration for $\overline{P_5}$

Theorem 3.4: All book graphs are cost effective and very cost effective.
Proof: Consider a bipartition $\pi = (X, Y)$ such that X has set of vertices with even order, represented by u_i and Y has the set of vertices with odd order, represented by v_i, where $i = 1, 2, 3, ..., n$. Consider a vertex $u \in X$, it has more adjacency in Y than in X and $v \in Y$ has more adjacency in X than in Y. (i.e) Every vertex in X is cost effective and very cost effective with respect to X and every vertex in Y is cost effective and very cost effective with respect to Y. Hence book graphs are cost effective and very cost effective.

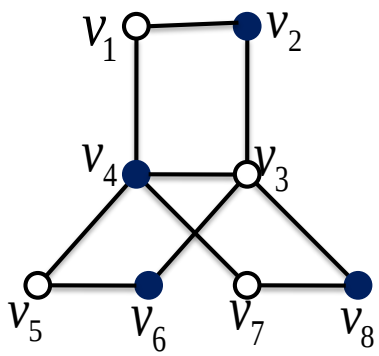


Fig 3.4: Illustration for Book Graph

Theorem 3.5: If C is a cycle of even order, then the shell graph $C(n, n-3)$ is cost effective and very cost effective.

Proof: Let G be a shell graph. Let us label the vertices as $v_1, v_2, .., v_n$. Consider a bipartition $\pi = \{X, Y\}$ such that X has even order vertices and Y has odd order vertices. Consider a vertex $v_i \in X$, i=2,4...n then it has more adjacency with Y. Consider a vertex $v_j \in Y$ for j=1,3,5...n-1 then it has more adjacency with X. Hence G is cost effective and very cost effective.

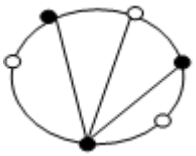


Fig 3.5: Illustration for Shell Graph

Theorem 3.6: If cycle is odd order, then $C(n, n-3)$ is cost effective but not very cost effective.

Proof: Let G be a shell graph. Let us label the vertices as $v_1, v_2, .., v_n$. Consider a bipartition $\pi = \{X, Y\}$ such that X has even order vertices and Y has odd order vertices. Consider a vertex $v_i \in X$, i=2,4...n. One of vertex v_i has equal number of adjacency in X as well as in Y. Also for $v_j \in Y$ j=1,3,5...n-1 one of the vertex has equal number of adjacency in both sets. Hence the graph G is cost effective but not very cost effective.

Theorem 3.7: The complement of wheel graph is cost effective and very cost effective for even order but not very cost effective for odd order.

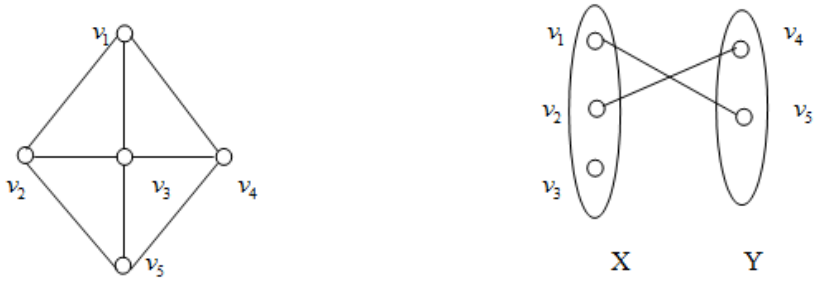


Fig 3.6: Illustration for $\overline{W_{1,4}}$.

Proof: In $\overline{W_{1,4}}$, the vertices are partitioned into two sets such as X and Y such that X has vertices v_1, v_2, v_3 and the set Y has vertices v_4, v_5. Consider a vertex v_1, such that it has more adjacency with Y than in X and consider a vertex in Y such that it has more adjacency in X than in Y. Hence the wheel graph is cost effective and very cost effective for even order. For odd order, the adjacency condition is not satisfied for very cost effective. Hence for wheel $\overline{W_{1,n}}$ for odd order n is cost effective but not very cost effective.

Conclusion: Cost effective and very cost effective bipartition is extended to few families of graph. We found that subdivision and the complement of path graph is cost effective and very cost effective, the complement of odd order path is cost effective but not very cost effective. Cost effectiveness of shell graph, book graph, etc., were also found.

References:

1. Cowan, R. and Emerson. W, . Proportional Coloring of Graphs, unpublished, 1990.
2. Favaron, O, Fricke, G. H. Goddard, W., Hedetnimei, S.M., Hedetnimei, S. T., Kristiansen , P. Laskar, R.C. and Skaggs, R.D, Offensive Alliances in Graphs, Discuss. Math. Graph Theory, Vol.24 (2004), PP.263-275.
3. Gerber,M.,U.and Kobler,D, Partitioning a Graph to Satisfy All Vertices, Tech. Rept. Swiss Federal Inst. Tech., Lausanne, 1998.
4. Hedetnimei, S. M. Hedetnimei,S. T. and McRae, A. A.,Cost Effective Sets in Graphs,. Manuscript, August, 2012.
5. Haynes T. W., Hedetnimei S. T. and Vasylieva I., Very Cost Effective Bipartition in Graphs, Cong. Number. Vol.12 (2015), PP 155-160.
6. Haynes, T. W. Hedetnimei, S. M. , Hedetnimei, S. T. ,MacCoy T. L., and Rodriguez, K. L.,Bounds on Cost Effective Domination Numbers, 2016,PP 1-11.
7. Haynes, T. W. Hedetnimei, S. M. , Hedetnimei, S. T. ,MacCoy T. L. and Vasylieva, . Cost Effective Dominations in Graphs, Cong. Number .Vol 211(2012), PP 197-209.
8. Haynes T. W., Hedetnimei S. T. and Slater P. J., Fundamentals of Dominations in Graphs, Marcel Dekker, Inc., New York, 1998.
9. Vasylieva, I., Haynes, T. W., Robert A. Beeler, Very Cost Effective Partitions in Graphs, 2013.

***

APPLICATION OF GRAPH THEORY IN TRAFFIC CONTROL PROBLEM

K.Pramila
Assistant Professor of Mathematics, Sri Chandrasekarendra Saraswathi Viswa Mahavidyalaya, Enathur
D.Ramya
M.Phil Scholar, Sri Chandrasekarendra Saraswathi Viswa Mahavidyalaya, Enathur

Abstract: One of the major drawbacks of the growing population is the equivalent growth of road vehicles. The increasing number of vehicles on road causes a serious problem that is traffic congestion. Since traffic signals are used to control large number of junctions, the achievement of good control performance at signal controlled road junctions is now of great importance. A traffic control problem at an intersection can be efficiently modeled as a graph. This paper deals with application of clique matrix, circular graph which is used to study the most efficient route or the traffic control system to direct the traffic flow to its maximum capacity using the minimum number of edges. This result has got application in traffic control problems at an arbitrary intersection so as to minimize the waiting time of the traffic participants by locating the sensors in order to collect traffic data.

Keywords: Compatible Graph, Circular Arc Graph, Traffic Stream.

1. Introduction: In the present era of the globalized world, graph theory has gained much attention to almost all the areas of science and other disciplines due to its direct applications of the real life problems. Graph theory is an important mathematical tool that allows users to solve their problem by constructing it into a graph. Many problems of practical interests can be represented by graphs. One of the main uses of traffic theory is the development of traffic models which can be used for estimation, prediction, and control related tasks for the automobile traffic process. Here we discuss about application of graph theory in efficient traffic management.

1.1 Preliminaries:

Definition 1.1.1: A ***clique*** in an undirected graph G = (V, E) is a subset of the vertex set C⊆V, such that for every two vertices in C, there exists an edge connecting the two. This is equivalent to saying that the subgraph induced by C is complete.

Definition 1.1.2: A ***maximum clique*** is a clique of the largest possible size in a given graph. The ***clique number*** ω(*G*) of a graph*G* is the number of vertices in a maximum clique in*G*. Intersection number of *G* is the smallest number of cliques that together cover all edges of *G*.

Definition 1.1.3: ***Circular arc graph*** is the intersection graph of a family of arcs on a circle. We say that these arcs are a circular arc representation of the graph.

Definition 1.1.4: A clique of graph G is a ***maximal clique*** of G if it is not properly contained in another clique of G.

1.2 Previous Work: Darshankumar Dave, Nityangini Jhala [1] solved the problem of phasing of traffic lights at a junction such that traffic signals which can be used more efficiently to avoid long time waiting at junctions and congestions using the concept of circular arc graphs.Shakera Tanveer [2] gives the application of connectivity (vertex or edge) in traffic management problems in an efficient way by minimizing the waiting time of the traffic participants and the cost to locate the sensors at an appropriate place so as to have the traffic data and discussed four and seven traffic streams.Niky Baruah and Arun Kumar Baruah [3] showed cut-set of a graph can be used to study the most efficient route or

the traffic control system to direct the traffic flow to its maximum capacity using the minimum number of edges.

2. Traffic Management: The most common problem of huge cities throughout the world is traffic congestion. New roads and highways are constructed in most of the urban areas to accommodate the growing number of vehicles. This increase in the number of vehicles in urban cities has led to the increase in time losses of traffic participants, ecological and noise pollution and also increases the number of traffic accidents. Traffic congestion has become one of the major obstacles for the development of many urban areas, affecting millions of people.

Constructing new roads may improve the situation, but it is very costly and in many cases it is impossible due to the existing structures. The only way to control the traffic flow in such a situation is to use the current road network more efficiently. A methodology of handling city traffic in a very efficient way by proper traffic management instead of modifying the road infrastructure is reducing the time that the vehicle stays on the road which helps in reducing its effect on the environment.

In this paper, graph theoretic model of a traffic control problem at an intersection is used for its solution. The resulting compatibility graph of the intersection and its connectivity, circular arc graph are used to study the most efficient route or the traffic control system to direct the traffic flow to its maximum capacity using the minimum number of edges or the minimum number of vertices.

Vehicles in the lane prepare themselves for certain move as they move through, turn right or turn left. The vehicles that perform those move forms a flow component called traffic stream. To study about the traffic problem in the intersection a mathematical model is to be formed using the graph where the set of edges represents the communication link between the nodes. In this traffic control system the traffic streams which can move simultaneously at an intersection without any conflict will be joined by an edge and the traffic streams which cannot move together will not be connected. The graph thus obtained is a connected graph known as compatibility graph. Also it is very important to install traffic lights at a intersection in such a way that traffic flows smoothly and efficiently.

Efficient controlling of the timing patterns of traffic lights is based on the capacity of each incoming lane. Each signal is connected to its neighboring signal and the activation depends upon the average time a vehicle takes to cross the distance between the two traffic lights. The phasing of lights should be such that when the green lights are on for two streams, they should be compatible. Certain traffic streams may be termed compatible if their simultaneous flow would not result in any accidents. Consider that the total time for the completion of green and red lights during one cycle is two minutes. The graph G is formed only whose vertex set consist of the traffic streams and two vertices of G joined by an edge if, and only if, the corresponding streams are compatible. Also once the interruption to the continuous traffic flow is minimized the traffic flow may be effective.

3.1:Traffic Control Problem With Five Streams: Let us consider a traffic control problem with four leg intersection and five streamsa,b,c,d and e.

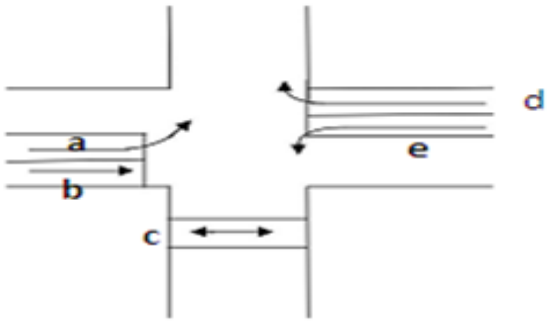


Fig 3.1: Traffic Intersection with Five Traffic Streams

The traffic streams may be termed as compatible whose simultaneous flow would not result in any accident. For instance, in Figure 3..1, streams *a* and *b* are compatible, whereas *a* and *d* are not.Corresponding compatible graph of Figure 3.1 is given below.

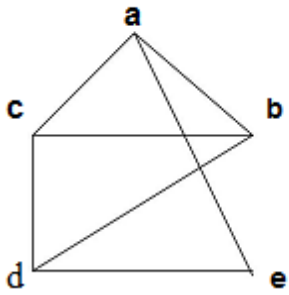


Fig 3.2: Compatible Graph G

Here a circle and its perimeter corresponds to the total cycle period, namely 120 seconds and also the duration when a given traffic stream gets a green light corresponds to an arc of this circle. Hence, two such arcs of the circle can overlap only if the corresponding streams are compatible. The resulting circular arc graph may not be the compatibility graph because we do not demand that two arcs intersect whenever corresponds to compatible flows. (There may be two compatible streams but they need not get a green light at the same time). However, the intersection graph *H* of this circular arc graph will be a spanning sub graph of the compatibility graph.

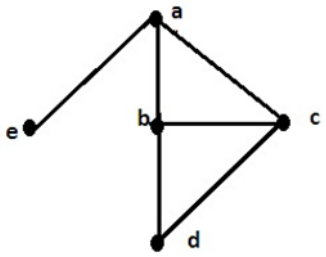


Fig 3.3: Graph J (Intersection graph)

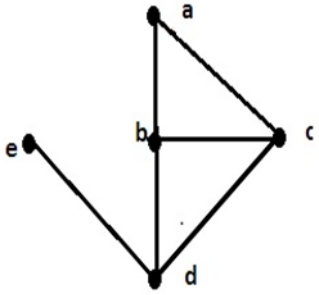


Fig 3.4: Graph H (Intersection graph)

Here, we have to take all spanning subgraphs of G into account and select from them the spanning sub graph that have the maximal cliques. The proper groups H and J for this example are depicted in Figure 3..3 &Figure 3.4..

The performance of the phasing may be calculated by minimizing the total red light time for a traffic cycle that is the total waiting time for all the traffic streams during a cycle. For the sake of concreteness, suppose that at the starting time, all lights are red.

The maximal clique of H are K_1 ={a,b,c}, ,K_2= {b,c, d} and K_3={d,e}. Each clique K_i, $1 \leq i \leq 3$, corresponds to the phase when all streams in that clique receive green light.

In phase I, traffic streams a,b and c receive a green light; in phase II, c, b and d receive a green light. Consider for each phase K_i a duration d_i. We have to determine d_i's(≥ 0) so that the total waiting time is minimum. Also consider the minimum green light time for any stream is 20 seconds. Traffic stream 'a' gets a red light when the phase K_2 receive a green light.

Hence a's total red light time is $d_2 + d_3$. Therefore the total red light time of all streams b,c,d and e are d_3, d_3, d_1 and d_1+d_2 .Therefore the total red light time of all streams in one cycle is

$$\text{Min } Z= 2\, d_2+2\, d_1+3\, d_3.$$

subject to $d_i \geq 0$, $1 \leq i \leq 3$, and $d_1 \geq 20$, $d_2 \geq 20$,
$d_3 \geq 20$, $d_1 + d_2 \geq 20$, $d_2 + d_3 \geq 20$, $d_1 + d_2 + d_3 = 120$.
The optimal solution to this problem is $d_1=80$, $d_2=20$ and $d_3=20$ and

Min z =260 seconds. The phasing that corresponds to this least value would be the best phasing of the traffic lights.

3.2 Traffic Control Problem With Six Streams: Let us consider a traffic control problem with six streams a, b, c, d, e and f.

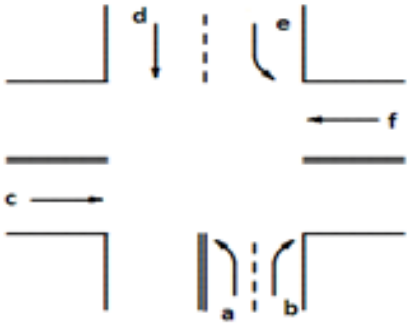


Fig 3.5: Traffic Intersection with Six Traffic Streams

In the above six streams *a* and *b* are compatible, whereas a and *f* are not.
Corresponding compatible graph is given below :

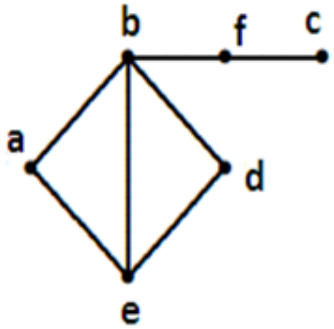


Figure 3.6: Compatible Graph G

Consider all spanning subgraphs of G into account and select from them the spanning sub graph that have the maximal cliques. The proper groups H for this example is depicted in Figure 3.7.

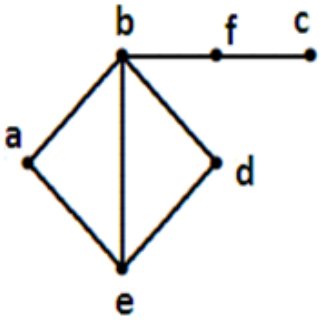


Figure 3.7: Graph H (Intersection graph)

For the sake of concreteness, suppose that at the starting time, all lights are red.
The maximal clique of H is K_1 ={a,b,e}, K_2= {b,d,e}, K_3= {b,f} and , K_4={f,c}.
Each clique K_i, $1 \le i \le 4$, corresponds to the phase when all streams in that clique receive green light. In phase I, traffic streams a,b and e receive a green light; in phase II b,d and e receive a green light. Consider for each phase K_i a duration d_i. The minimum green light time for any stream is 20 seconds. Traffic stream a gets a red light when the phase K_2 receive a green light.

Hence a's total red light time is $d_2 + d_3 + d_4$.

Therefore the total red light time of all streams b,e,d,f and c are d_4, $d_3 + d_4$, $d_1 + d_3 + d_4$, $d_1 + d_2$ and $d_1 + d_2 + d_3$. The phasing that corresponds to this least value would be the best phasing of the traffic lights.

Therefore the total red light time of all streams in one cycle is $Z=3d_1+3d_2+4d_3+4d_4$.
LPP is Minimize $Z=3d_1+3d_2+4d_3+4d_4$
Subject to $d_i \ge 0$, $1 \le i \le 4$, and $d_1 \ge 20$,
$d_2 \ge 20$, $d_4 \ge 20$, $d_1 + d_2 \ge 20$,
$d_3 + d_4 \ge 20$, $d_1 + d_3 + d_4 \ge 20$, $d_2 + d_3 + d_4 \ge 20$, $d_1 + d_2 + d_3 \ge 20$,
$d_1 + d_2 + d_3 + d_4 = 120$.
The optimal solution to this problem is $d_1=80$, $d_2=20$ $d_3=0$ and $d_4=20$ and
Min Z =380 seconds.The phasing that corresponds to this least value would be the best phasing of the traffic lights.

Conclusion: The problem of phasing of traffic lights at junction of five and six traffic streams has been solved by the LPP method such that the traffic signals could be used more proficiently to evade the long waiting time at junctions and overcrowding.

References:

1. Darshankumar Dave, Nityangini Jhala, Application of Graph Theory in Traffic Management, International Journal of Engineering and Innovative Technology, Vol 3, Issue 12 (2014), PP 124-126.
2. Shakera Tanveer, Application of Graph Theory in Representing and Modelling Traffic Control Problems, International Journal of Mathematics and Computer Applications Research ,Vol. 6, Issue 3 (2016) , PP:29-34.
3. Baruah, N., Baruah, A. K., On a Traffic Control Problem Using Cut-Set of Graph, International Journal of Advanced Networking and Applications, Vol. 3(4) (2012), 1240-1244.
4. Gazis, D. C., 2002, Traffic Theory, Kluwer Academic Publishers, London.
5. Guberinic, S., Senborn, G., Lazic, B., Optimal Traffic Control Urban Intersection, CRC Press, 2008.
6. Baruah, N., Baruah, A. K., 2012, Minimum Cut Maximum Flow of Traffic in a Traffic Control Problem, International Journal of Mathematical Archive-4(1), (2013), PP:171-175.
7. Raunak Singh Saluja, Purva Joshi, Archit Kashyap, Application of Graph Theory in Traffic Management, The International Journal of Computer Science & Applications (TIJCSA), Volume 2, No . 03, (2013) .
8. Baruah, A. K., and Baruah, N, Clique Matrix of a Graph in Traffic Control Problems, International Journal of Computer Applications ,Volume 53, No.6(2012).

***

OPTIC MATH OF LINEAR PROGRAMMING PROBLEM AND GRAPHICAL METHOD USING THE OPEN SOURCE SOFTWARE



J.Sengamalaselvi
Assistant Professor , Department of Mathematics,
Sri Chandra Sekharendra Saraswathi Viswa Mahavidyalaya Kanchipuram,Tamilnadu
T.Latha
Assistant Professor, Department of Mathematics,
Sri Kanchi Krishna Arts and Science college, Kilambi, Kanchipuram
T.Venugopal
Professor of Mathematics, Research, and Director of Publications, Dean(arts & Humanties)
Sri Chandra Sekharendra Saraswathi Viswa Mahavidyalaya Kanchipuram,Tamilnadu

Abstract: The Government of India has recognized the importance of ICT in education with the latest initiatives being the distribution of computers to the Government schools. The endeavor is not merely to facilitate learning with the use of ICT but also to make students comfortable with them. The National Curriculum Framework (2005) appreciated that the psychological impact of ICT's and the potential they offer for global sharing of knowledge cannot be denied. ICT should be used to enhance learning in all parts of the curriculum and interdisciplinary and cross-disciplinary thinking. Opportunities for professional development in the area are given to the teacher so that they can efficiently perform the role of facilitators, thus allowing students to learn independently. A Meta survey conducted by UNESCO on the use of ICT in education reported that India actively promotes the use of ICT in education both in formal and in the non-formal education sectors. This varies from the use of radio to facilitate the green revolution, to satellite based one way and interactive television for rural development in some of the most backward districts to one and distance learning models. At present the use of newer computer and internet based ICT resources on education along with broadcast ICT, is being explored. This paper discuss the optic math of linear programming problem and graphical method using the open source software Geogebra.

Introduction: Operations research is a new branch of Mathematics dealing in the optimization problems in real-life situations. It is also a quantitative technique to deal many management problems. In this discipline, we study cost minimization of various inventory problems, the minimization of transportation costs of sending goods from various warehouses to different centres, the profit maximization or cost minimization in linear programming models, the assignment of different persons to different jobs so that total time taken to perform the jobs is minimized (called Assignment problem), the congestion problem in traffic places, airline counters, supermarkets, to find out the waiting time of customers in the queue, the project completion time with limited resources and many other similar problems. We now study the origin of OR, some of the definitions of OR, modeling OR problems, their applications and their limitations.

1. Linear Programming Problem:

1.1 Simplex Method: The simplex method is a technique of solving linear programming problems by obtaining a feasible solution and, by iterative procedure, improving this solution until the optimal solution reached. The computational routine for the simplex method is based on matrix algebra and consists of obtaining an inverse matrix in order to solve a set of simultaneous linear equations.

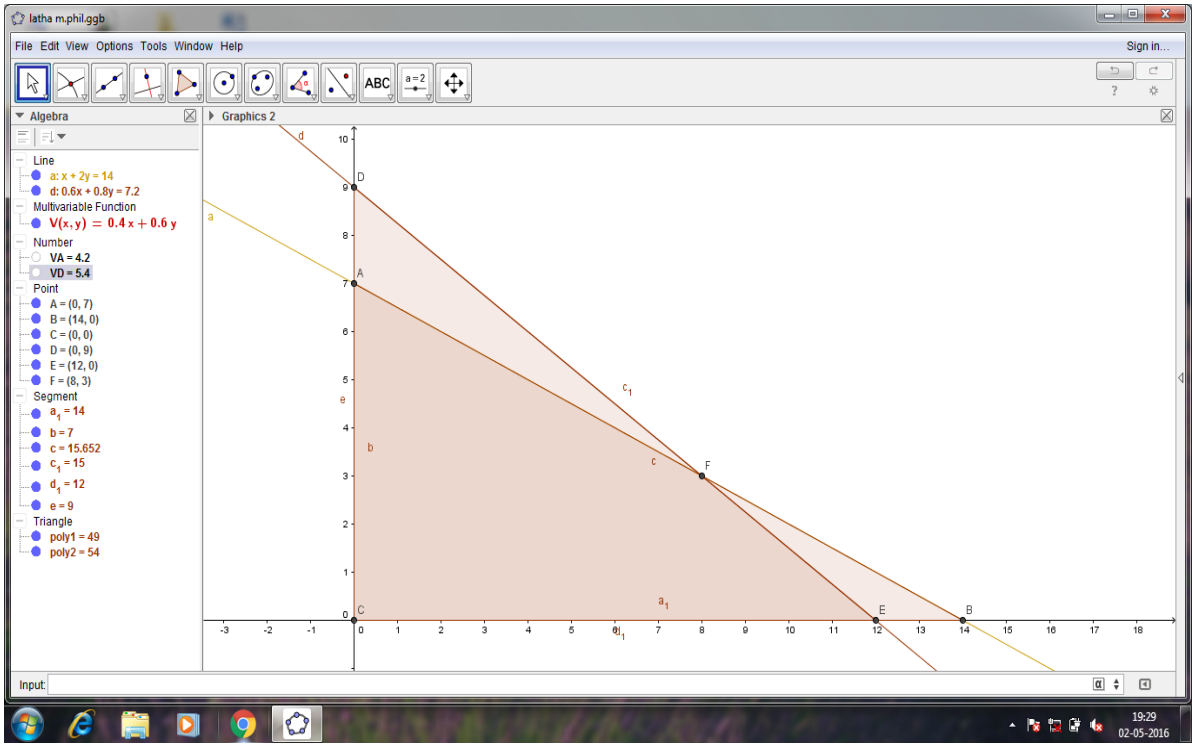
Given a linear programming problem (LPP) to solve it by simplex method we have to convert the inequality constraints into equality constraints. If an inequality is of the form ≤ , by adding a positive variable, referred to as slack variable, to the L.H.S. of the equality we convert into equalty. In order that the maximum value of the linear function is unaffected, slack variables are introduced into the objective function with zero coefficients.

If an inequality constraints is of the form ≥ , a positive variable is subtracted from the LHS of the constraint into an equality. Such a variable is called a surplus variable. For this variable also we attack zero co-efficient in the objective function.

1. Solve the following linear programming problem by simplex method.

- **Max z =0.4x+0.6y**

Subject to x+2y≤14,
0.6x+0.8y≤7.2,
x , y≥0

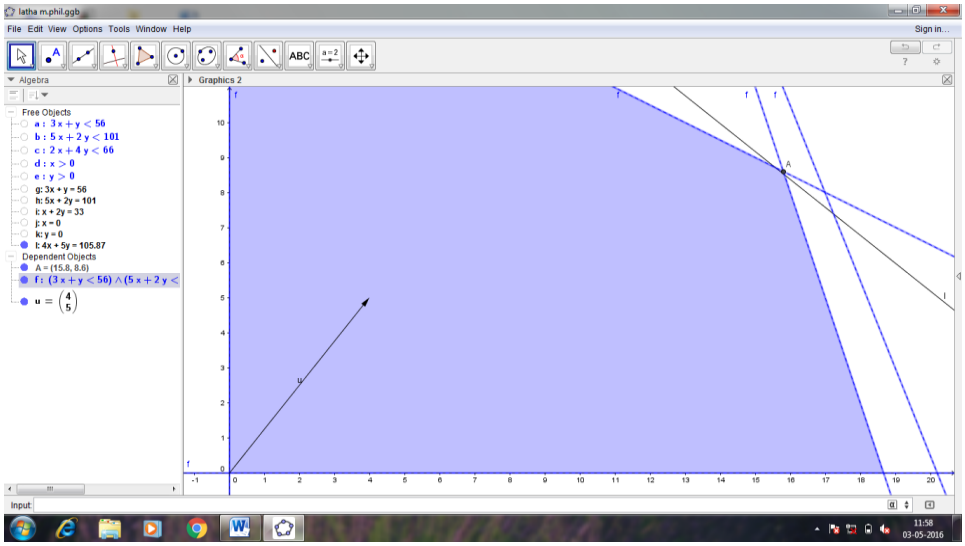


Answer:
x=8, y= 3
Maximize z=5.4

2. Solve the following linear programming problem by simplex method.

- **Max z=4x+5y**

Subject to 3x+y≤56
5x+2y≤101
2x+4y≤66
x, y≥0



Answer:
x=15.8, y=8.6
Maximize z=105.87

2. Graphical Method:

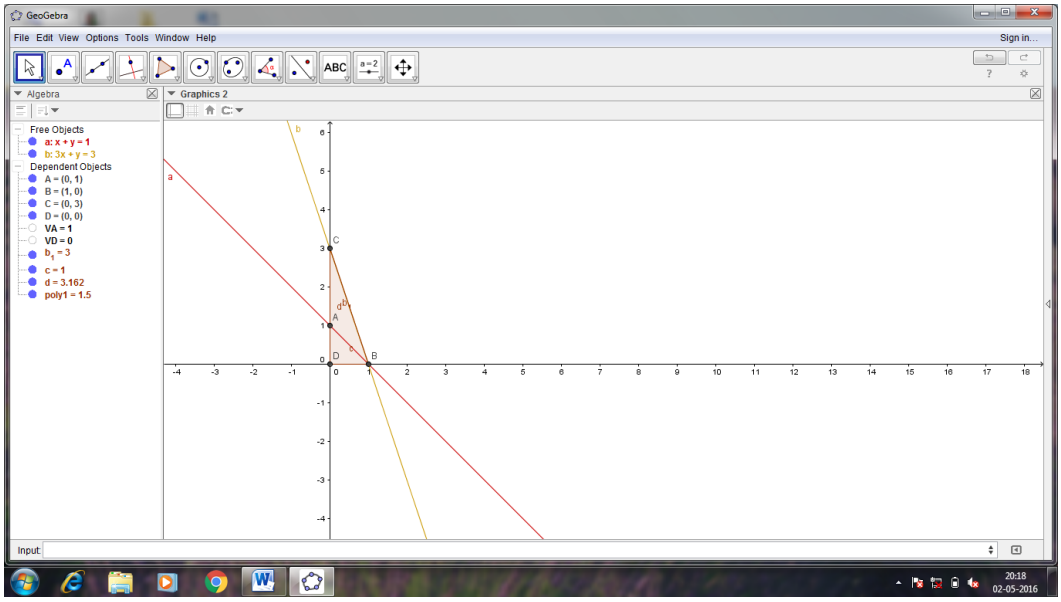
2.1. Solution by Graphical Method: To determine the optimal solution to a linear programming problem by graphical method the following procedure is to be adopted.

Step I: Take inequality constraints as equalities. Draw the graph of these constraints. The graph of each constraint is a straight line and join these points. Generally, the points where the straight line meets x_1 and x_2 axes are chosen to draw the straight line.

Step II: Determine the feasible region. The unknown corners can be determined either from the graph or by solving the constraints equation corresponding to each corner.

Step III: Determine the values of the objective function at the corners. In the case of maximization problem the maximum value of objective function and the corresponding vertex determine the optimal solution. In the case of minimization problem the minimum value of objective function and corresponding vertex determine the optimal solution.

1. Mark the feasible regions represented by constraint in equations x+y≤1, 3x+y≥3, x, y≥o of a linear optimizing function z=x+y

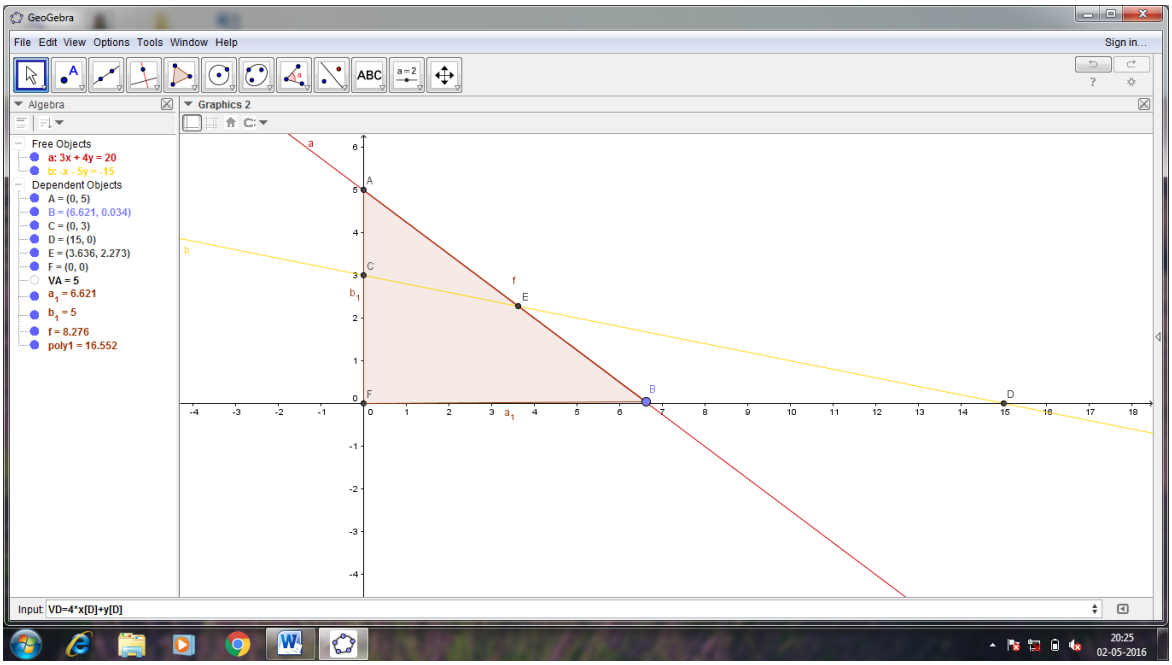


Answer:
x=1, y=0
Maximize z=0

3. Big 'M' Method:
3.1. Charnes' Penalty Method: We have introduced the Simplex technique to solve LPP with all the constraints '≤' type. In such cases we introduce only a slack variable in each constraint to convert the inequalities to the equalities and to obtain a basic feasible solution. However, the introduction of such slack variables should not alter the optimal value of the objective function. To satisfy this criterion we take the coefficients of these slack variables in the objective function as zeros. We have given the physical meaning of the slack variables.

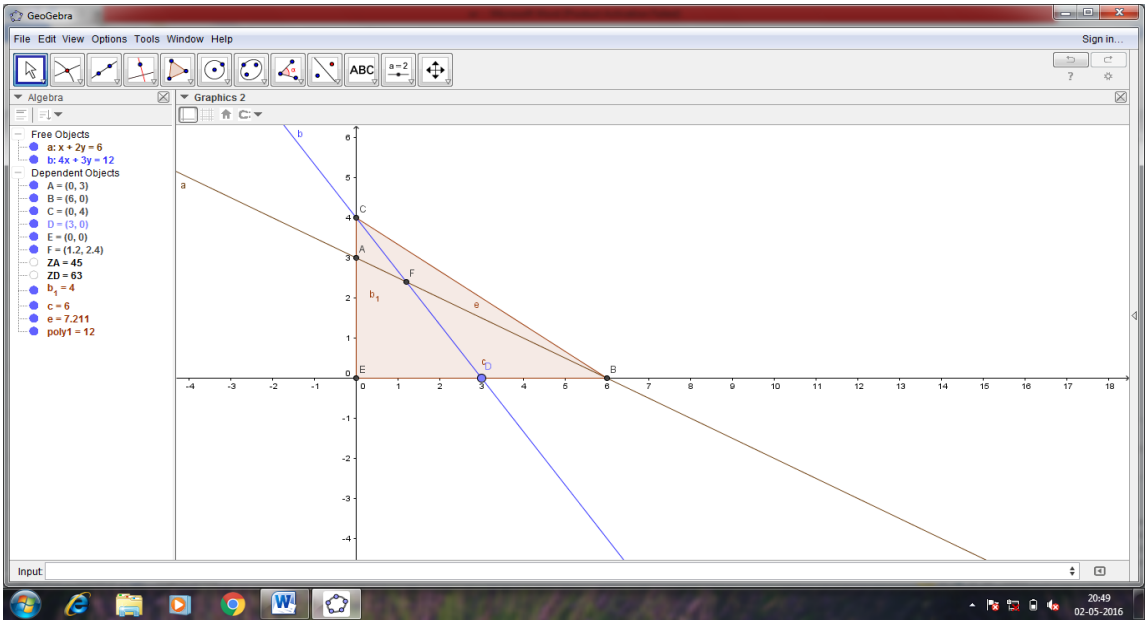
All Linear programming problems may not always be expressed with the constraints of type '≤' such that there exists a basic feasible solution. There may be constraints of the type '≥' which may not be possible to convert into the type '≤' so that there is a basic feasible solution. In such cases we first convert the inequality constraints into equality constraints by introducing surplus variables. However, ths will not provide the basic feasible initial solution. To overcome this difficulty we adopt a method called 'Big M' method. We introduce artificial variable into each constraint of the type '≥' or '=' and adopt a method called 'Big M' method to solve such LPP.

1. Minimise z = 4x+y subject to
3x+4y≥20, -x-5y≤-15, x, y≥0



Answer:
x=3.636, y= 2.273
Minimum z=5

4. Two Phase Method
1. Solve the linear programming problems:
Maximise z= 21x+15y subject to the constrain's
x-2y≥-6, 4x+3y≤12 , x,y≥0



Answer:

x=1.2, y= 2.4

Maximize z=63

5. Dual Simplex Method

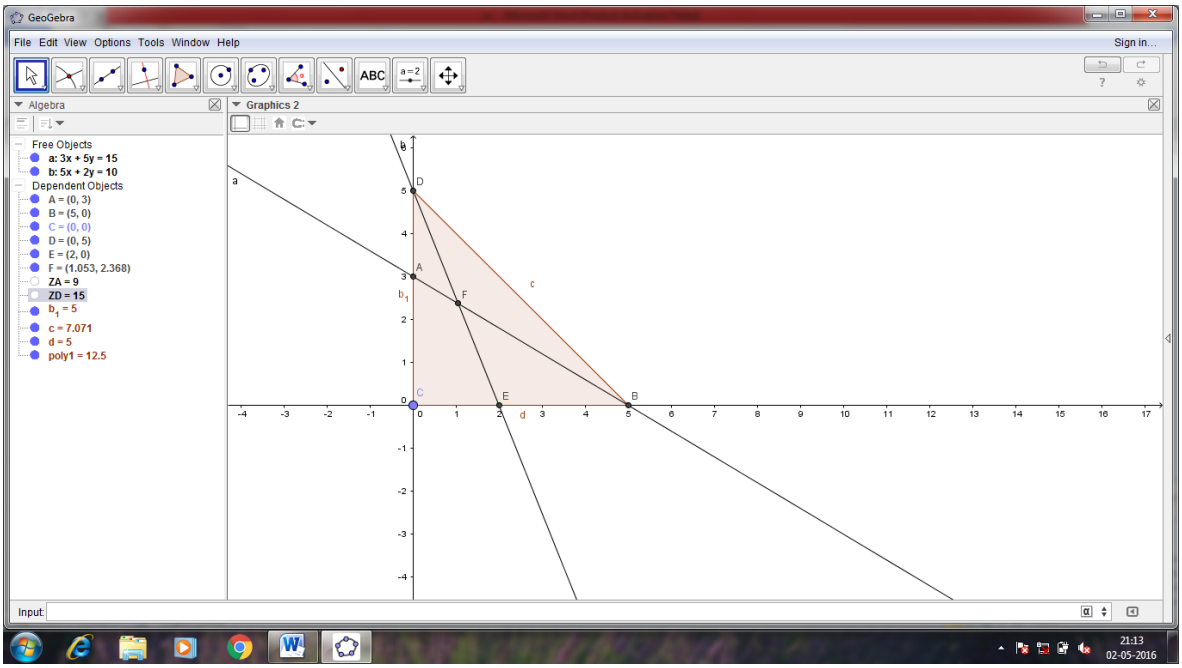
1. Solve the following LPP, using Dual Simplex method.

Max z=5x+3y

Subject to 3x+5y≤15,

5x+2y≤10,

x,y≥0



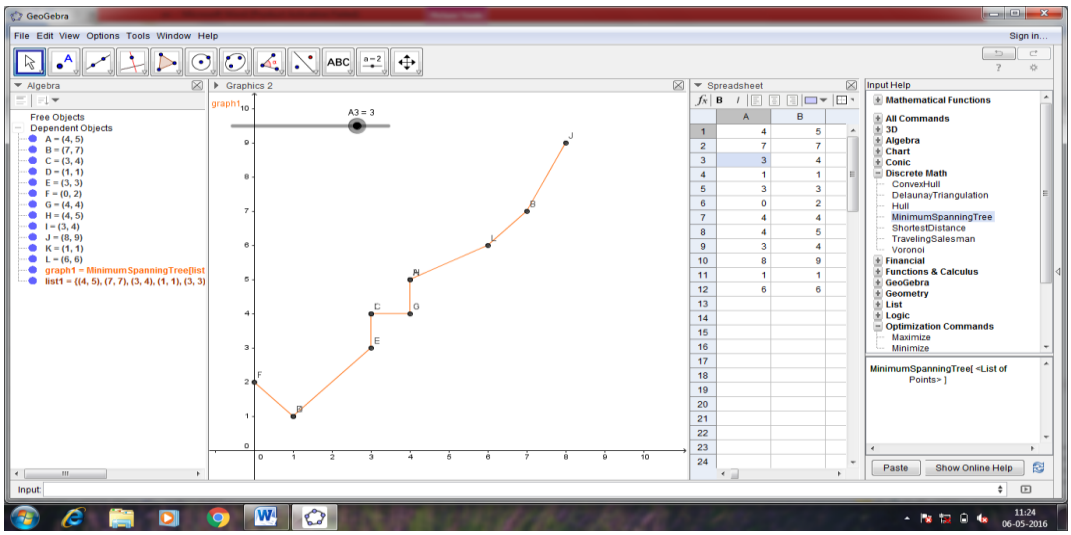
Answer:

x=1.053, y= 2.368

Maximize z=15

6. Minimal spanning tree:

Draw a minimum spanning tree A={4,7,3,1,3,0,4,4,3,8,1,6} & B={5,7,,4,1,3,2,4,5,4,9,1,6}



Conclusion: The use of ICT in teaching Mathematics can make the Teaching process more effective as well as enhance the Capability of student in understanding basic concepts. The Geogebra software used by the students help them to solve the problem efficiently and this software saves time.

References:

1. Alias, 2000 Alias, M. (2000), Spatial visualization ability and civil engineering problem solving. University of suorey,Guildford, united kingdom.
2. Almeqdali, 2005 Almeqdalai, F. (2005), the effect of using The geometer's sketchpad (GSP) on Jordanian student's Understanding some geometrical concepts, International Journal for mathematics teaching and learning, from http://www/cimt.plymouth.ac.uk/journal/almeqdadi.pdf.
3. Battisa, 1999 Battisa, M. (1999), Geometry Results from the Third International Mathematics and science study. Teaching Children Mathematics, 5(6), (pp.367-373). Reston, VA: NCTM.
4. J.Sengamalaselvi, T.Venugopal Implementation Of Information And Communication Technology in The Three Dimensional Graphical Representation By Using The Open Source Mathematics Software Geogebra" in the International Journal of Business Intelligence & innovations (3) 141-149 ,2016 .
5. J.Sengamalaselvi, T.Venugopal "Implementation of Information and Communication Technology in Statistics by using the Open source Software Geogebra" in the International Journal of Scientific Research 5 (7) 2016.382-385.
6. T.Latha J.Sengamalaselvi, T.Venugopal "Enactmentation of ICT in continuous and Discrete Distributions by the open source software Geogebra in the International Journal of Mathematical Archive7(10), 2016,1-11.
7. J.Sengamalaselvi, T.Venugopal " Impact of Information and Communication Technology in Teaching Mathematics with Geogebra and winplot open source Mathematics software" in the Global journal of Pure and Applied Mathematics 12(3) 2016 pp-28-33.
8. J.Sengamalaselvi, T.Venugopal " Impact of Visual Math Among Higher Education Using Open Source Software" in the International journal of current research and Review, 2017, pp 120-124.
9. J.Sengamalaselvi, T.Venugopal " Role of Geogebra in the Hard Spots of Higher Education Through Optic Math" in the International journal of current research and Review 2(10) 2017.
10. J.Sengamalaselvi, T.Venugopal " A Study On The Impact Of ICT At The Higher Secondary Level Using Geogebra" in the International Journal of Pure and Applied Mathematics ,2017 .pp:191-198

VISUAL MATH OF SECONDARY MATHEMATICS EDUCATION IN THE AREA OF GEOMETRY USING GEOGEBRA

J.Sengamalaselvi
Assistant Professor, Department of Mathematics,
Sri ChandraSekharendra Saraswathi Viswa Mahavidyalaya, Kanchipuram, Tamilnadu
V.Nalini
Research Scholar, Department of Mathematics,
Sri ChandraSekharendra Saraswathi Viswa Mahavidyalaya, Kanchipuram, Tamilnadu
T.Venugopal
Professor of Mathematics, Research, and Director of Publications, Dean (Arts & Humanities)
Sri ChandraSekharendra Saraswathi Viswa Mahavidyalaya, Kanchipuram, Tamilnadu.

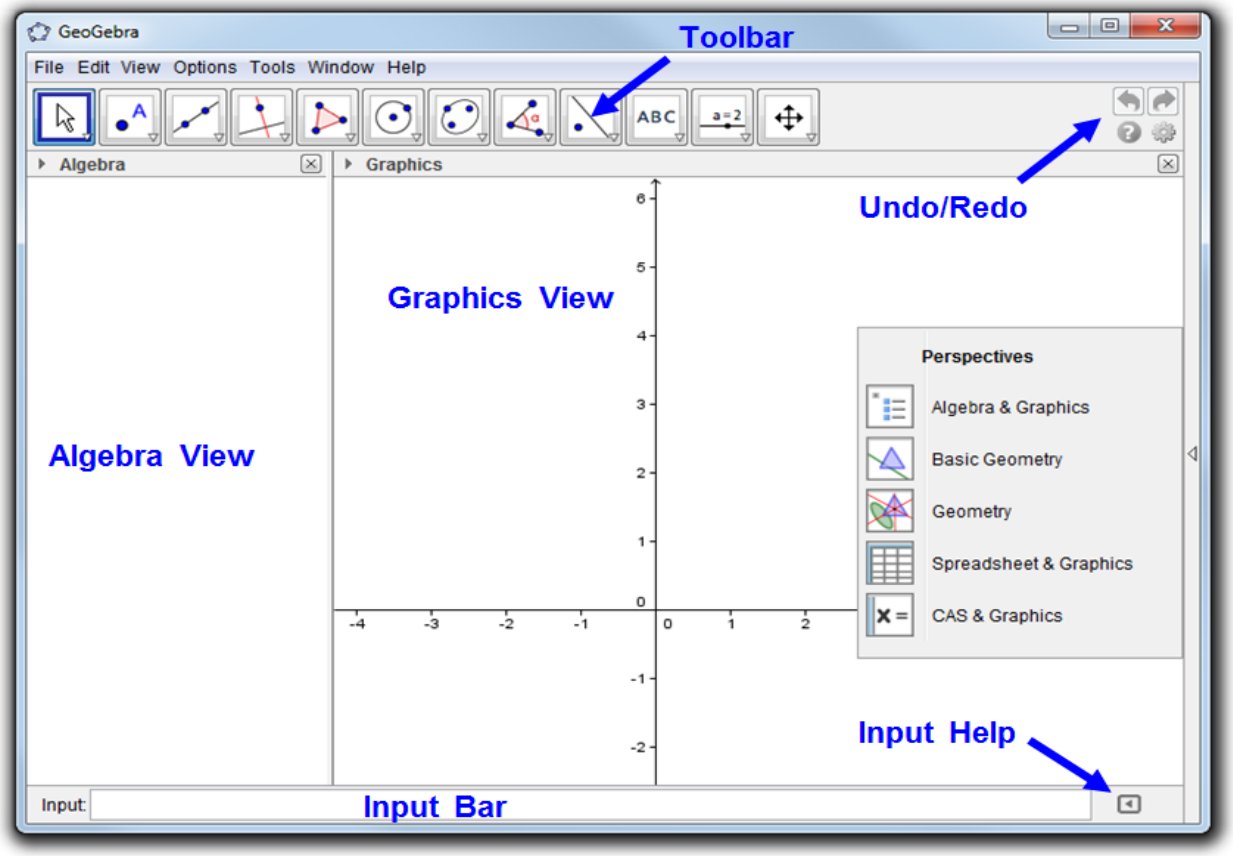
Abstract: Information and Communication Technology (ICT) is an important instrument, which can transfer the present isolated, teacher-centered, book-centered learning environment into a rich student-centered environment. It is a new teaching-learning process, aims at transferring the old traditional paradigm of learning to the new paradigm of learning and of course teaching. In this sense, UNESCO is giving a high priority to the use of ICT for more equitable and pluralistic development in education, this research work pivoted aiming to expand the knowledge base about the issues pertaining in the implementation of ICT tool Geogebra in education which mainly centered on interactive learning environment. Based on the literature gap , the paper highlights in the area of Mathematics, particularly in the field of Geometries for Secondary Mathematics Education. The issues related to graphical representation diagrams are addressed with the help of Geogebra (i.e. open source software), which can be downloaded by students without any cost.

Keywords: Geogebra, Geometry, Secondary Mathematics Education, Visual Math.

Introduction: Geo Gebra is an interactive Mathematics software package incorporating geometry, algebra, and calculus, each of which can be used separately. In the context of a developing country like India, open source (Public domain) software like Geogebra is most important since it can be downloaded without costs by anyone with internet access.

Geo Gebra is the best example of Mathematical software were geometric figures can be manipulated and algebraic operations can be conducted not only by teachers, but at times by students working independently of the teacher.

Geogebra is not computer supported rather computer created mathematics. The problem identification, definitions, thesis and proofs are created with the help of computer. The Main aim is to present how experimental mathematics can be adapted to teaching mathematics.



1. Construction of Quadrilaterals:

1.1. Construct a quadrilateral ABCD with AB=4cm, BC=6cm, CD=5.6cm, DA=5cm, and AC=8cm.Find also its area.

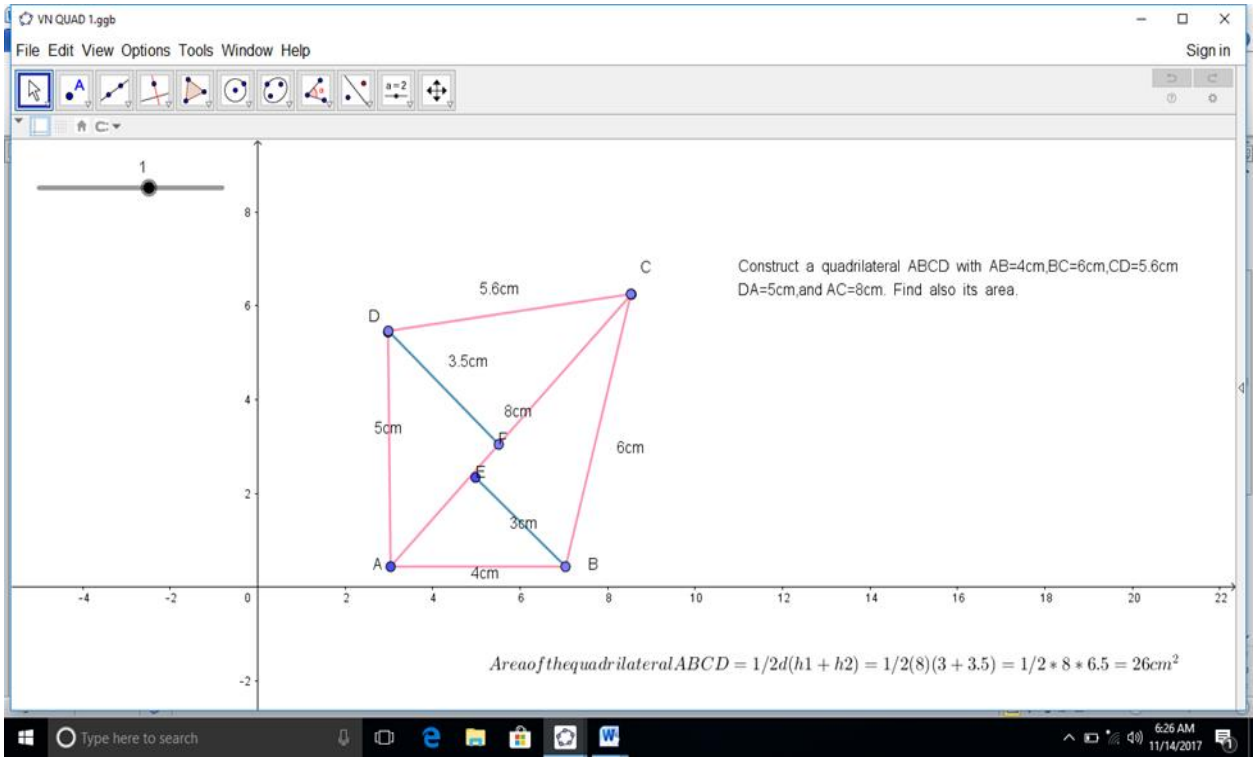


Figure 1.1: Construction of a Quadrilateral with 4 Sides & 1 Diagonal.

Area of the Quadrilateral ABCD=1/2d(h1+h2)=1/2(8)(3+3.5)=1/2*8*6.5=26cm2.

1.2. Construct a quadrilateral ABCD with AB=6.5cm , AD=5cm, CD=5cm,∠BAC=40◦ and ∠A BC=50◦ And also find its area.

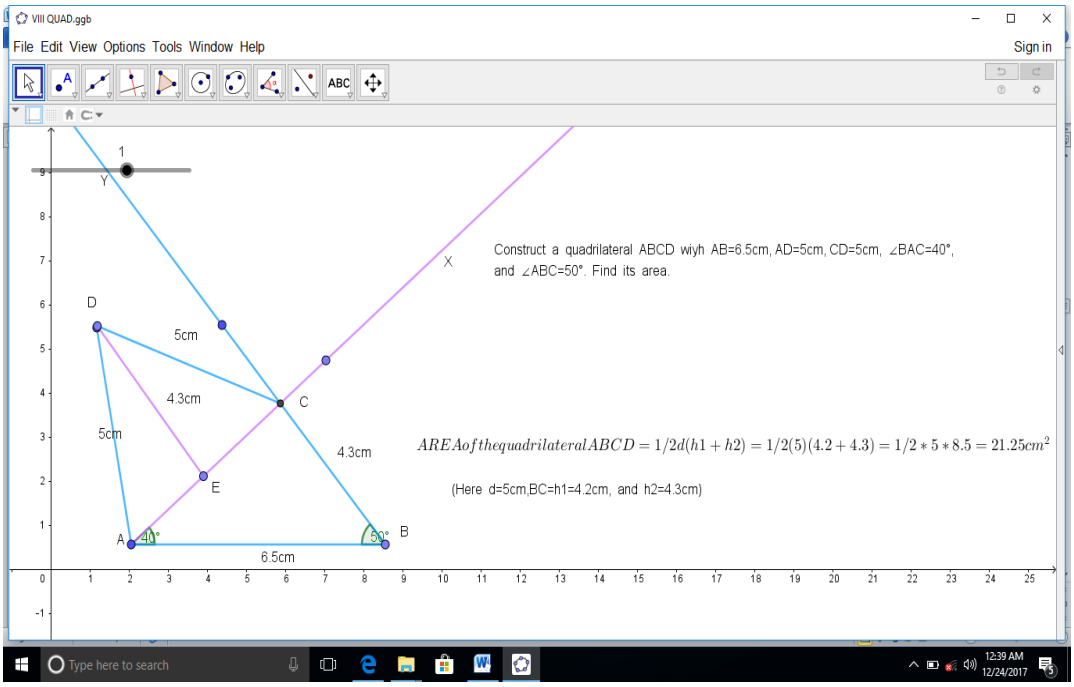


Figure 2.1: Construction of an Isosceles Trapezium.

Area of the trapezium ABCD=1/2h(a=b)=1/2(5.6)(11+7)=1/2*5.6*18=50.4cm2

3. Construction of Parallelograms:

3.1. Construct a parallelogram ABCD with AC=9cm, BD=7cm, and ∠AOB=120◦ where AC and BD intersect at 'O' and find its area.

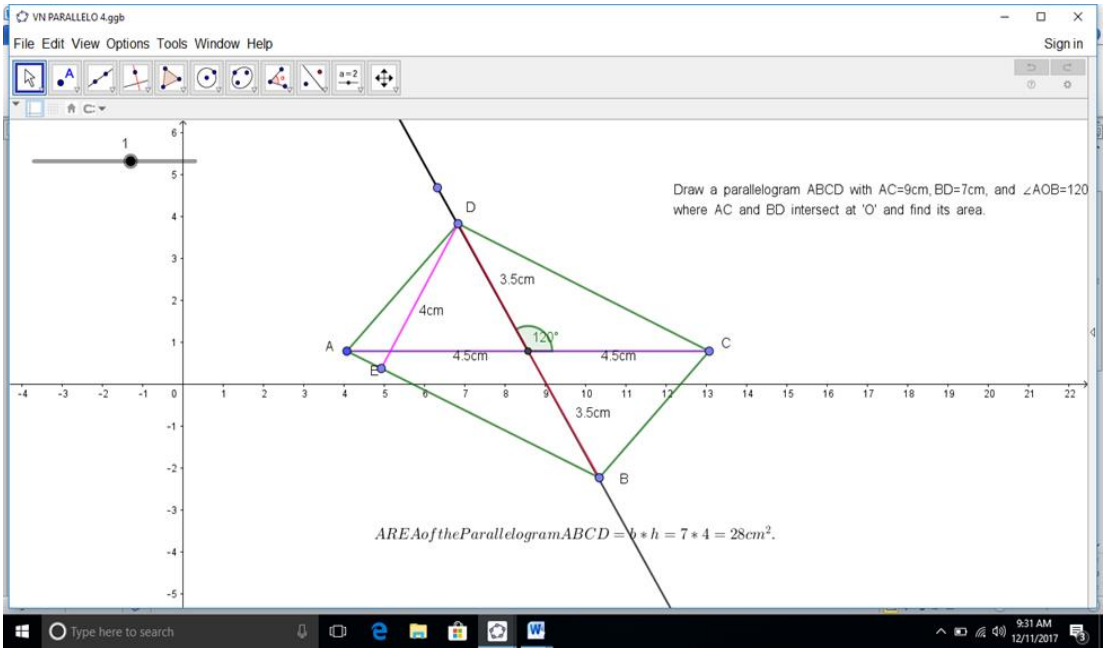


Figure 3.1: construction of a parallelogram ABCD with 2 diagonals & 1 included angle

Area of the parallelogram ABCD=b*h=7*4=28cm2.

4. Construction of Rhombus:

4. Construct a rhombus ABCD with AC=7.5cm, and ∠A=100◦. Find its area.

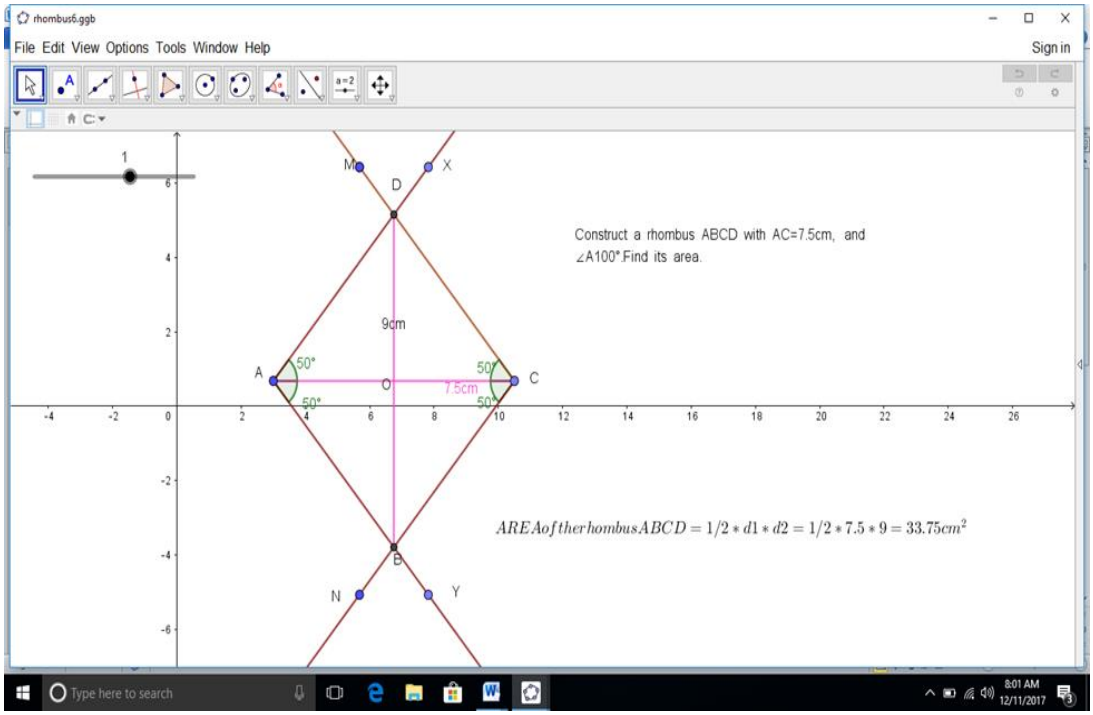
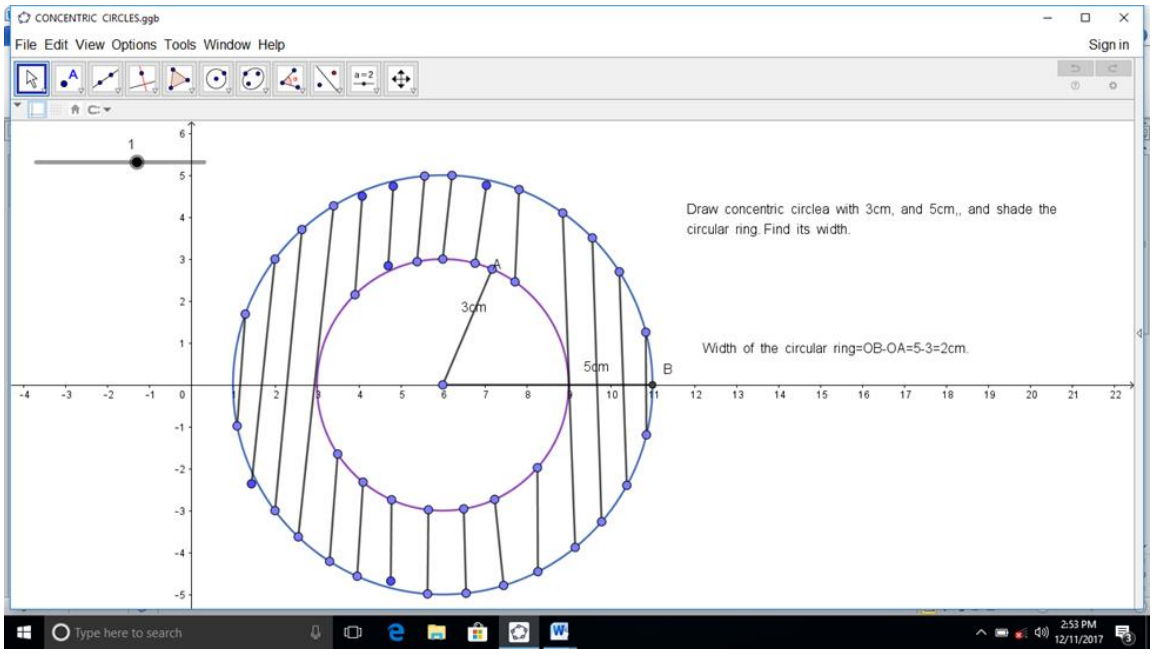


Figure 3.3.4d: Construction of rhombus with 1 diagonal & 1 angle.
Area of the Rhombus ABCD=1/2*d1*d2=1/2*7.5*9=33.75cm2.

4. Construction Of Concentric Circles When The Radii Are Given:

4.1 Draw concentric circles with radii 3cm and 5cm and shade the circular Ring. Find its width.



Width of the circular ring=OB-OA=5-3=2cm.

Conclusion:

- In the conventional method the students are able to only imagine the pictures. There is no scope for seeing the plotting, angle, etc. from a different point of view. So it is difficult for them to have a clear vision of the picture. Whereas in the Geogebra method the students are able to visualize the pictures clearly and understand it better. The graphical representation helps in are easy understanding.
- The society which adopts new technological inventions will grow very fast. At present there is a tremendous change in computer and information technology. So this is a proper time for the switch over to the new methodology in the teaching field. Moreover, the students will easily adopt and have access to this new technology rather than the teaching faculty. This will help the students to keep in pace with the latest technologies as well as the other pupil who live in the other part of this world. The age old traditional teaching cannot be easily dislodged or evaded, but at the same time we should not ignore implementing new methodology in teaching learning process. The author strongly believes that this new technology will rule our classrooms in the near future.

References:

1. Alias, 2000 Alias, M. (2000), Spatial visualization ability and civil engineering problem solving. University of suorey,Guildford, united kingdom.
2. Almeqdali, 2005 Almeqdalai, F. (2005), the effect of using The geometer's sketchpad (GSP) on Jordanian student's Understanding some geometrical concepts, International Journal for mathematics teaching and learning, from http://www/cimt.plymouth.ac.uk/journal/almeqdadi.pdf.
3. Battisa, 1999 Battisa, M. (1999), Geometry Results from the Third International Mathematics and science study. Teaching Children Mathematics, 5(6), (pp.367-373). Reston, VA: NCTM.
4. J.Sengamalaselvi, T.Venugopal Implementation Of Information And Communication Technology in The Three Dimensional Graphical Representation By Using The Open Source Mathematics Software Geogebra" in the International Journal of Business Intelligence & innovations (3) 141-149 ,2016 .
5. J.Sengamalaselvi, T.Venugopal "Implementation of Information and Communication Technology in Statistics by using the Open source Software Geogebra" in the International Journal of Scientific Research 5 (7) 2016.382-385.
6. T.Latha J.Sengamalaselvi, T.Venugopal "Enactmentation of ICT in continuous and Discrete Distributions by the open source software Geogebra in the International Journal of Mathematical Archive7(10), 2016,1-11.
7. J.Sengamalaselvi, T.Venugopal " Impact of Information and Communication Technology in Teaching Mathematics with Geogebra and winplot open source Mathematics software" in the Global journal of Pure and Applied Mathematics 12(3) 2016 pp-28-33.
8. J.Sengamalaselvi, T.Venugopal " Impact of Visual Math Among Higher Education Using Open Source Software" in the International journal of current research and Review, 2017, pp 120-124.
9. J.Sengamalaselvi, T.Venugopal " Role of Geogebra in the Hard Spots of Higher Education Through Optic Math" in the International journal of current research and Review 2(10) 2017.
10. J.Sengamalaselvi, T.Venugopal " A Study On The Impact Of ICT At The Higher Secondary Level Using Geogebra" in the International Journal of Pure and Applied Mathematics ,2017 .pp:191-198

***

AN ANALYTICAL METHOD FOR FINDING CRITICAL PATH IN A FUZZY PROJECT NETWORK

J.Sengamalaselvi
Assistant Professor, Dept. of Mathematics,
Sri Chandrasekharendra Saraswathi Viswa Maha Vidyalaya Enathur, kanchipuram,Tamil Nadu – 631561
K.Murugesan
M.Phil Reasearch Scholar, Dept. of Mathematics,
Sri Chandrasekharendra Saraswathi Viswa Maha Vidyalaya Enathur, kanchipuram,Tamil Nadu – 631561

Abstract: Critical Path method (CPM) techniques have become widely recognized as valuable tools for the planning and scheduling of large projects the aim of this paper is to present and analytical method for measuring the criticality in a fuzzy project network where the duration time of each activity is represented by a trapezoidal fuzzy number. In this paper, we use a ne defuzzification formula for trapezoidal fuzzy number and apply to the float time (slack time) for each activity in the fuzzy project network to find the critical path. The defuzzification formula used for critical path cannot be applied to the trapezoidal fuzzy number having equal elements because that trapezoidal fuzzy number is a crisp number. The proposed method can overcome the drawback of existing fuzzy CPM method. We use examples to compare our proposed method with the existing method. The comparison reveal method proposed in this paper is more effective in determining the activity criticalities and finding the critical path.

Keywords: Fuzzy Number, Defuzzification, Fuzzy CPM Method.

1.1 Introduction: The critical path is the one form the start of the project of the project to finish of project where the slack times are all zero. The purpose of the critical path method (CPM) is to identify critical activities on the critical path so that resources may be concentrated on these activities in order to reduce project length time.

Besides, CPM has proved very valuable in evaluating project performance and identifying bottlenecks thus. CPM is a vital tool for the planning and control of complex project.

According to the critical path, the decision-maker can control the time and the cost of the project and improve the efficiency of resource allocation to ensure the project quality CPM has been used in business management The activity duration time often is an factory production etc,[1,2] is an uncertain value so that the result of classical CPM computation cannot properly match the real world situation.

In this paper, we used a new used a new defuzzification formula for trapezoidal fuzzy number and applied to the float time (slack time) for each activity in the fuzzy project network to find the critical path. The defuzzification formula used for critical path can not be applied to the trapezoidal fuzzy number having equal numbers because that trapezoidal fuzzy numbers is a crisp number. The proposed method can overcome the drawback of the existing fuzzy CPM method [6]. In trapezoidal fuzzy number having equal numbers is used as a trapezoidal number and obtained defuzzified value for it to find critical path but that type of fuzzy number is a crisps number. We used example to compose our proposed method with the existing method [6]. The comparison reveals that the method proposed in this paper is more effective in determining the activity criticalities and finding the critical path.

1.2 Fuzzy Concept: A fuzzy set can be mathematically constructed by assigning to each possible individual in the universe of discourse a value representing its grade of member in the fuzzy set [10,11].

This grade corresponds to the individual's similarity to the concept represented by the fuzzy set. The fuzzy number A is fuzzy set whose membership function $\mu_{\bar{A}}(x)$ satisfies the following condition [12]:

a) $\mu_A(x)$ is piecewise Continuous:

b) $\mu_A(x)$ is a convex fuzzy subsets;

c) $\mu_A(x)$ is the normality of a fuzzy subset, implying that for at least once element x_0 x the membership grade must be 1 ie) $\mu_{\bar{A}}(x_0)=1$

Definition 1.1 Membership Function: The characteristic function of a crisp set assigns a value of either 1 or 0 to each individual in the universal set, theory discriminating between members and non members of the crisp set under consideration. This function can be generalized such that the values assigned to the elements of the Universal set fall within a specified range and indicate that membership grade of these elements in the set in question. large values denoted higher degrees of set membership. Such a function is called a membership function, and the set defined by it a fuzzy set.

Definition 1.2 Critical Paths: An activity is said to be critical if there is no "leeway" in determining its start and finish times. A noncritical activity allows some scheduling slack, so that the start time of the activity can be advanced or delayed within limits without affecting the complaints date of the entire project.

Definition 1.3 Triangular Fuzzy Numbers: A fuzzy number with membership function in the form

$$\mu_A(x) = \begin{cases} \dfrac{(x-a)}{(b-a)} & \text{if } a \le x \le b \\ \dfrac{(d-x)}{(d-c)} & \text{if } c \le x \le d \\ 0 & \text{if otherwise} \end{cases} \qquad (1.1)$$

is called a triangular fuzzy number A = (a, b, c)

Definition 1.4 Trapezoidal Fuzzy Numbers: A fuzzy number with membership function in the form

$$\mu_A(x) = \begin{cases} \dfrac{(x-a)}{(b-a)}, & a \le x < b \\ 1, & b \le x < c \\ \dfrac{(d-x)}{(d-c)}, & c \le x \le d \\ 0, & \text{otherwise} \end{cases} \qquad (1.2)$$

is called a trapezoidal fuzzy number A = (a, b, c,d)

Theorem 2.1: Let A = (a, b, c) be a triangular fuzzy number. The centroid $(A)=\dfrac{a+b+c}{3}$

Proof: From the definition of the centroid method by using figure 1,
We may writte the following:

Centroid $$(A) = \frac{\int_a^b \frac{x-a}{b-a} x dx + \int_b^c \frac{c-x}{c-b} x dx}{\int_a^b \frac{x-a}{b-a} dx + \int_b^c \frac{c-x}{c-b} dx}$$

$$= \frac{\frac{(c-b)\int_a^b (x-a)\,x dx + (b-a)\int_b^c (c-x)\,x dx}{(b-a)(c-b)}}{\frac{(c-b)\int_a^b (x-a)\,dx + (b-a)\int_b^c (c-x)\,dx}{(b-a)(c-b)}}$$

$$= \frac{(c-b)\int_a^b (x-a)\,x dx + (b-a)\int_b^c (c-x)\,x dx}{(c-b)\int_a^b (x-a)\,dx + (b-a)\int_b^c (c-x)\,dx}$$

$$= \frac{1}{3}\left\{\frac{(c-b)\left[2b^3 + a^3 - 3ab^2\right] + (b-a)\left[2b^3 + c^3 - 3cb^2\right]}{(c-b)[b-a]^2 + (b-a)(b-c)^2}\right\}$$

Multiply by $[b-a]^2$ and $[b-c]^2$

$$= \frac{1}{3}\left\{\frac{(c-b)(b-a)^2\left[2b^3 + a^3 - 3ab^2\right] + (b-a)(b-c)^2\left[2b^3 + c^3 - 3cb^2\right]}{(c-b)[b-a]^2 + (b-a)(b-c)^2}\right\}$$

$$= \frac{2b^3 + a^3 - 3ab^2 + 2b^3 + c^3 - 3cb^2}{3}$$

We can simplify these equations we get $(A) = \frac{a+b+c}{3}$

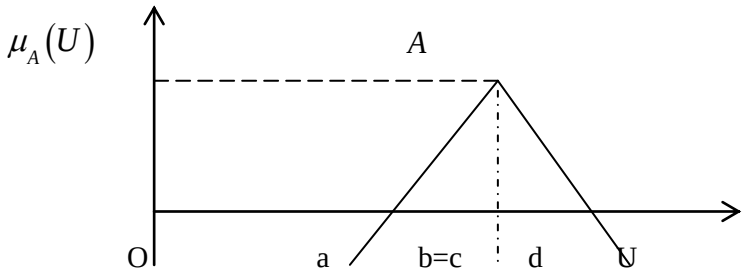


Fig. 1: Membership Function Curve of Triangular Fuzzy Number A

For Example:

Let B_1 and B_2 two trapezoidal fuzzy numbers

$B_1 = (16, 20, 22, 24)$ and $B_2 = (3, 4, 5, 6)$ then,

$B_1 \oplus B_2 = (16, 20, 22, 24) \oplus (3, 4, 5, 6) = (19, 24, 27, 30)$

$B_1 \ominus B_2 = (16, 20, 22, 24) \ominus (3, 4, 5, 6) = (10, 15, 18, 21)$

1.3. Calculating Fuzzy Time Values and Critical Path in A Fuzzy Project Network: A fuzzy project network is an a cyclic digraph, when the vertices represent events, and the direct edges represent the

activities, to be performed in a project formally, A fuzzy project network is represented by $N=(V,A,T)$. Let $V=\{V_1,V_2.....V_n\}$ be a set of vertices, where V_1 and V_n are the start and final events of the project. And each V_i belongs to some path from V_1 to V_n let $A\subset V\times V$ be the set of directed edge $a_{ij}=(V_i,V_j)$ that represented the activities to be performed in the project.

Activity a_{ij} is then represented by one and one, arrow with a tail event V_i and a head event for each activity a_{ij} a fuzzy number $t_{ij}\in T$ is defined, where t_{ij} is the fuzzy time required for the completion of a_{ij}

A critical path is a longest path from V_1 to V_n and an activity a_{ij} on a critical path is called a critical activity. Let E_i and L_i be the earliest fuzzy event time and the latest fuzzy event time for event *i*, respectively. Let E_j and L_j earliest event time for event i, event *j* respectively. Let $D_j=\{i/i\in V and\ a_{ij}\in A\}$ be a set of events obtained from event $j\in V$ and $i<j$ we then obtain E_j using the following equations.

$$E_j=\underset{i\in D_j}{Max}\left[E_i+t_{ij}\right] and\ E_j=L_i=0 \qquad (1.3)$$

Similarly,

Let $H_i=\{j/j\in V and\ a_{ij}\in A\}$ and be a set of events obtained from event $i\in V$ and $i<j$. we obtain using the following equations.

$$L_i=\underset{j\in H_i}{Min}\left[L_j-t_{ij}\right] and\ L_n=E_n$$

The interval $[E_i,L_j]$ is the time during which must be completed. When the earliest fuzzy event time and latest fuzzy event time have been obtained, we calculate the total float of each activity. For activity *i- j* in a fuzzy project network,

The total float T_{ij} of the activity i- *j* can be computed as follows.

$$T_{ij}=L_j-E_i-t_{ij} \qquad (1.4)$$

Hence we can obtain the earliest fuzzy event time and latest fuzzy event time and the total float of every activity by using

$$E_j=\underset{i\in D_j}{Max}\left[E_i+t_{ij}\right] and\ E_j=L_i=0$$

We defuzzify the total float of each activity by equation $A=\frac{a+b+c}{3}$ or

$A=\frac{\left[c^2+d^2+cd\right]-\left[a^2+b^2+ab\right]}{3(c+d)-(b+a)}$ and find the critical path such that the sum of the total floats of the activities in the path is zero

1.4. Example: Figure 2 shows the network representation of a fuzzy project network table 1 compares the original defuzzified value and proposed defuzzified value for the total float of each activity in the fuzzy project network.

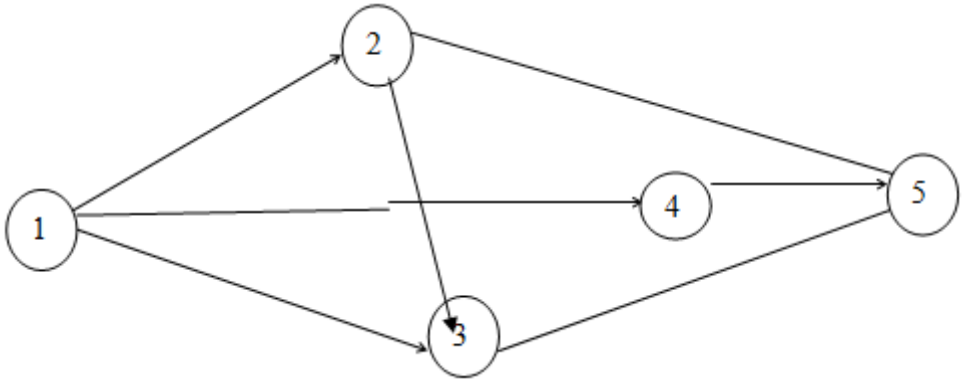


Fig 2: Fuzzy Project Network –I

Table 1: Defuzzifical Values of Slack Time for Fuzzy Project-I

Activity	Fuzzy Activiy time	Slack time (a,b,c,d)	Origional Defuzzified value a+b+c+d/4	Proposed deffuzified value using equation (2.4)
1-2	(10,15,15,20)	(-160, 60,60,160)	$\frac{-160-60+60+160}{4}=0$	0
1-3	(30,40,40,50)	(-130,-35,75,170)	$\frac{-130-35+75+170}{4}=20$	20
2-3	(30,40,50,60)	(-160,-60,60,160)	$\frac{-160-60+60+160}{4}=0$	0
1-4	(15,20,25,30)	(-110,-20,95,185)	$\frac{-110-20+95+185}{4}=37.5$	37.5
2-5	(60,100,150,180)	(-100,-10,100,190)	$\frac{-100-10+100+190}{4}=45$	45
3-5	(60,100,150,180)	(-160,-60,60,160)	$\frac{-160-60+60+160}{4}=0$	0
4-5	(60,100,150,180)	(-110,-20, 95+185)	$\frac{-110-20+95+185}{4}=37.5$	37.5

The path in fuzzy project network –I are 1-2-3-5, 1-2-5, 1-3-5, 1-4-5
The critical path for fuzzy project network- I is 1-2-3-5.

Conclusion: A new analytical method for finding critical path in a fuzzy project network has been proposed. We have used a new defuzzification formula for trapezoidal fuzzy number and applied to the float time for each activity in the fuzzy project network to find the critical path. We have shown examples to compare our proposed method with the exacting method the comparison reveal that the method proposed in this paper has shown more effective in determining the activity criticalities and finding the critical path.

References:

1. Ahuja. H.N., Dozzi. S.P, and Abourizk. S. M Project Management Network Wiley, 1994
2. Chanas, S.and Mon. D.L , kamburowski, J.(1981). The use of fuzzy variable in PERT. Fuzzy Sets and systems. 5(1),11-19.

3. Dubois and Prade. H Possibility theory : An Approach to computerized `Processing of Uncertainty. New York 1988
4. Chen, S.P. and Hsueh, Y.J.(2008). A simple approach to fuzzy critical path analysis in project networks, Applied Mathematical Mathematical Modelling, 32(7), 1289-1297.
5. Dubois, D., Fargier, H. and Galvagnon, V.(2003) on latest startimg times and float in activity network with ill-known dueations, European Journal of Operation Research, 147(2), 266-280.
6. Gazdik, I.(1983). Fuzzy network planning-FNET,IEEE Transactions on Reliability, 32(3),304-313.
7. Kaufmann, A. and Gupta, M.M.(1988). Fuzzy Mathematical Science. Elsevier, Amsterdam.
8. Kuafmann, A. and Gupta, M.M. (1985). Introduction to fuzzy
9. Kumar, A and kaur, P (2010). A New method for fuzzy critical path analysis in project networks with a new representation of triangular fuzzy numbers, Application and Applied Mathematics, 5(10), 1442-1466.
10. Mc Cahon, C.S. and Lee, E.S.(1988). Project network analysis with Application, 15(10),829-838.
11. Zadeh. L.A, Toward a generalized theory of Uncentrainty (GTU)- Outline Information Science, (2005)1-40
12. Yuan.B, Fuzzy sets and fuzzy logic: Theory and Applications Prentice- Hall, International Inc., 1995

***

RESEARCHERID
THOMSON REUTERS

[Selvi * *et al.*, 7(6): June, 2018]
IC™ Value: 3.00

ISSN: 2277-9655
Impact Factor: 5.164
CODEN: IJESS7

IJESRT

INTERNATIONAL JOURNAL OF ENGINEERING SCIENCES & RESEARCH TECHNOLOGY

VISUAL GRAPH OF HIGHER SECONDARY MATHEMATICS EDUCATION USING THE OPEN SOURCE SOFTWARE GEOGEBRA

J. Sengamala Selvi
Assistant Professor, Sri Chandrasekharendra Saraswathi Viswa Mahavidyalaya, Enathur, kanchipuram, Tamilnadu, India

DOI: 10.5281/zenodo.1297380

ABSTRACT

ICT popularly known, involve in the most general since the use of technology in managing and processing information. ICT provides "anytime, anywhere" access to reliable information. It paves the way for construction of knowledge by any individual. A belief promoted in the research literature (Fasieyitan, Libii and Hirchbuhl 1996) and amongst the administration is that university/college education can make imaginative or innovative use of ICT to enrich the learning environment and support student learning. It can be used to make students' facet knowledge public and help them develop math cognitive skills to become more reflective and self regulated learners. A shift from teacher-centered instruction to learner-centered instruction is needed to enable students to acquire the new millennium knowledge and skills. The shift will take place in changing from a focus on teaching to a focus on learning (sanclhots, Ringstaff and Dwyer 1977). This paper prominence the execution of Visual graph of Higher secondary Mathematics Education.

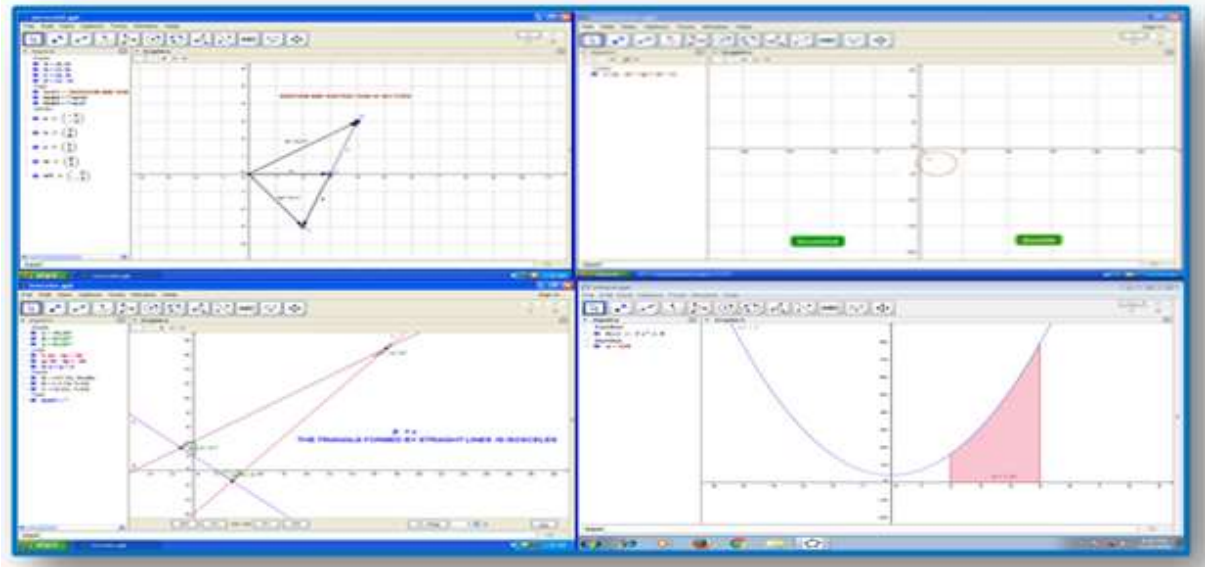
Keywords: Geogebra, Higher secondary Mathematics, ICT, Visual Graph.

I. INTRODUCTION

Geogebra is free dynamic Mathematical software designed to work on different operating systems. It is an Interactive geometry System. It has flexible user interface. It is open source software. Geogebra was translated to more than 25 languages. It won European and German educational software award. It can be downloaded without any cost with the help of internet access. Geogebra will be a supporting Tool to promote the education level. In Geogebra there is a possibility to find the area of conics, complex root of a polynomial, derivative of a function and definite integral values over the interval, determinant of the matrix and to solve the set of equations and It is used to calculate the limit of the function. It offers commands, functions and events to do the task easily.

Geogebra equips the higher secondary students with enough knowledge and skills and increase their ability in problem solving in Mathematics Geogebra is the most powerful Open source Mathematics software. While learning Mathematics with Geogebra, students can overcome obstacles and achieve their learning objectives. This type of new methodology definitely encourages the students to develop and expand their knowledge in Mathematics concepts. All level students can easily understand the Mathematics problem easily. It will help to remove the fear of Mathematics. The visual display of data clarifies the students doubt in Mathematics.

ISSN: 2277-9655
Impact Factor: 5.164
CODEN: IJESS7



1. Solve by graphically : x+2y=4 : 2x+4y=8

Input

x+2y=4

X	-2	0	2
Y	3	2	1

2x+4y=8

X	-4	0	4
Y	4	2	0

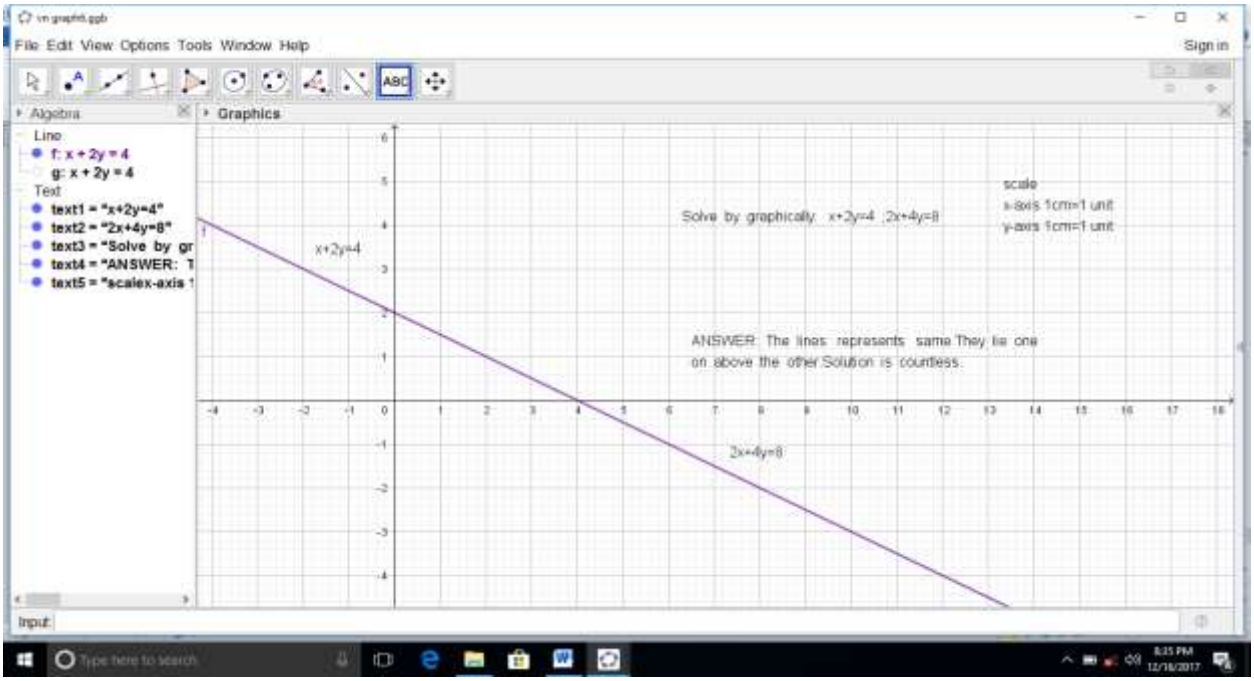


Figure: 1 Graph of same straight lines.

ISSN: 2277-9655
Impact Factor: 5.164
CODEN: IJESS7

Answer: The lines represents same straight lines. Solution is Countless.

2. Solve by graphically: x-3y=6 ; x-3y=-9

Input

x-3y =6

X	-3	0	3
Y	-3	-2	-1

x-3y= -9

X	-3	0	3
Y	2	3	4

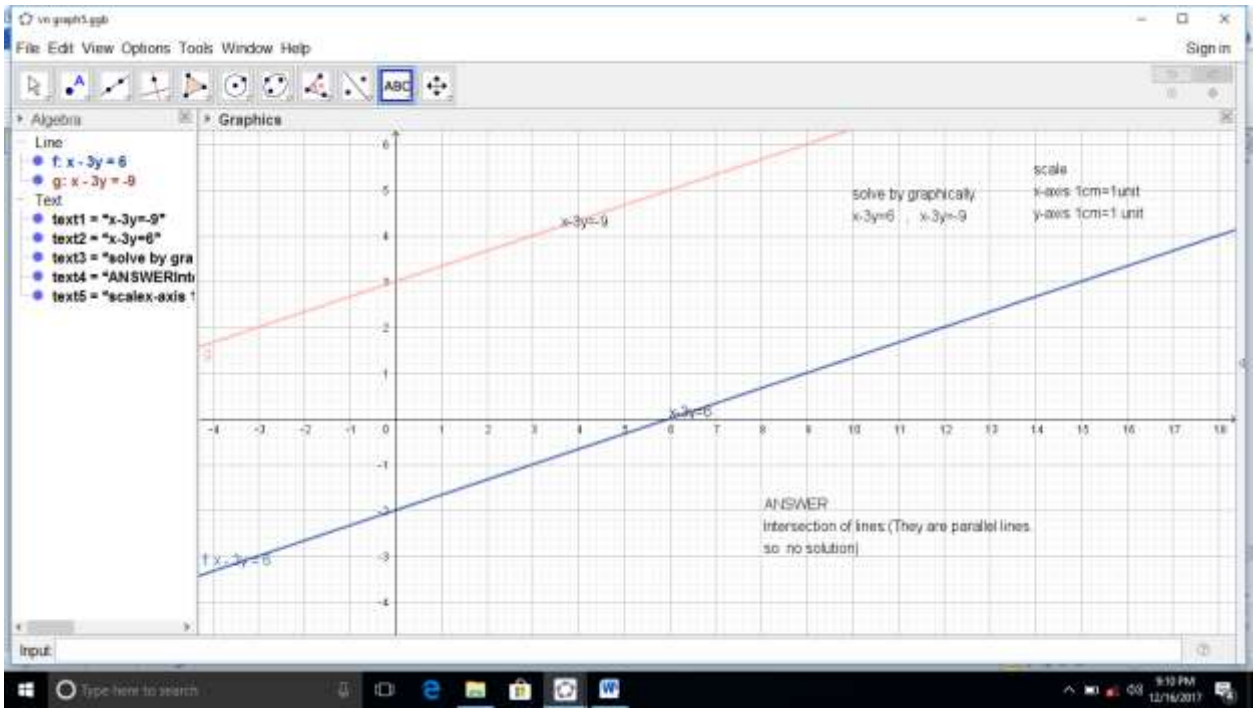


Figure: 2 Graph of parallel lines.

Ans : The straight lines are parallel. So there is no solution.

3. Solve by graphically: 2x-y=1 : x+2y=8

Input

2x-y=1

X	-1	0	1
Y	-3	-1	1

X+2y=8

X	-2	0	2
Y	5	4	3

ISSN: 2277-9655
Impact Factor: 5.164
CODEN: IJESS7

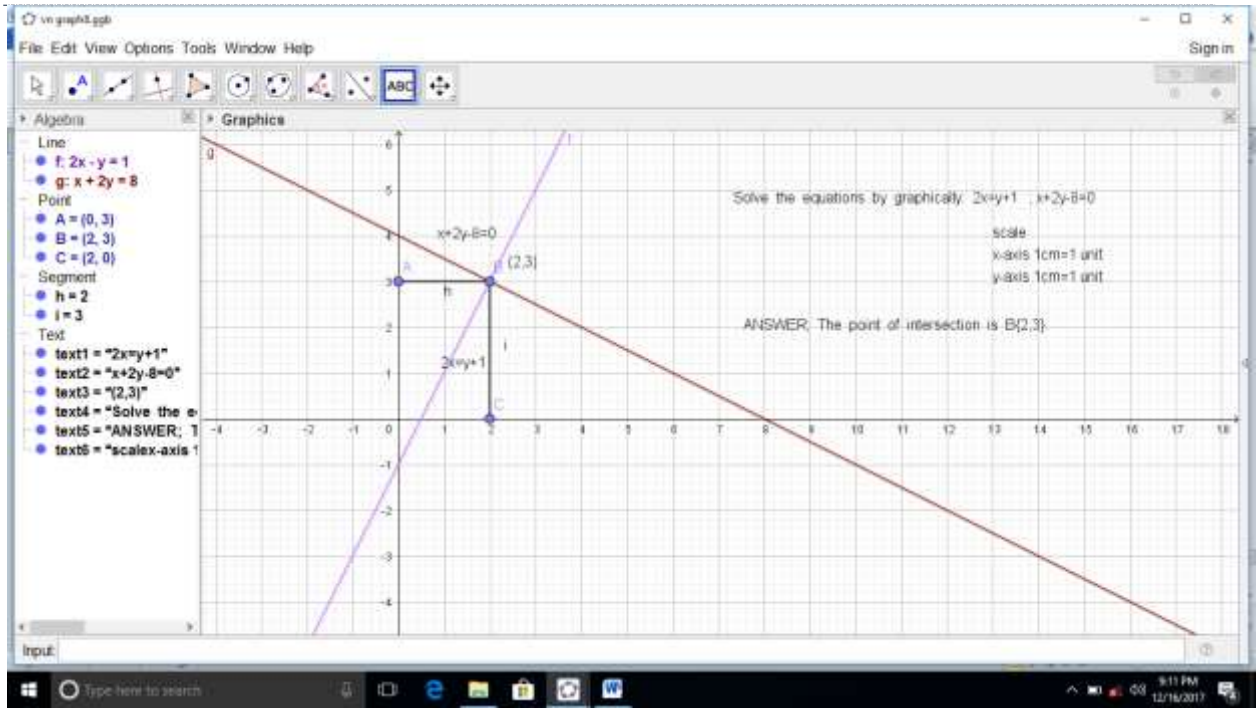


Figure: 3 Graph of intersecting lines

Answer: Point of Intersection is (2,3).
So the only solution is {2,3}.

4. Amudha walks at a speed of 3km/hr. Draw a linear graph to show the relationship between the time and distance.

Input

Time in hours (x)	0	1	2	3	4	5
Distance in km (y)	0	3	6	9	12	15

Plot the points (0,0), (1,3), (2,,6), (3,9), (4,12), (5,15).
Join all the points.

ISSN: 2277-9655
Impact Factor: 5.164
CODEN: IJESS7

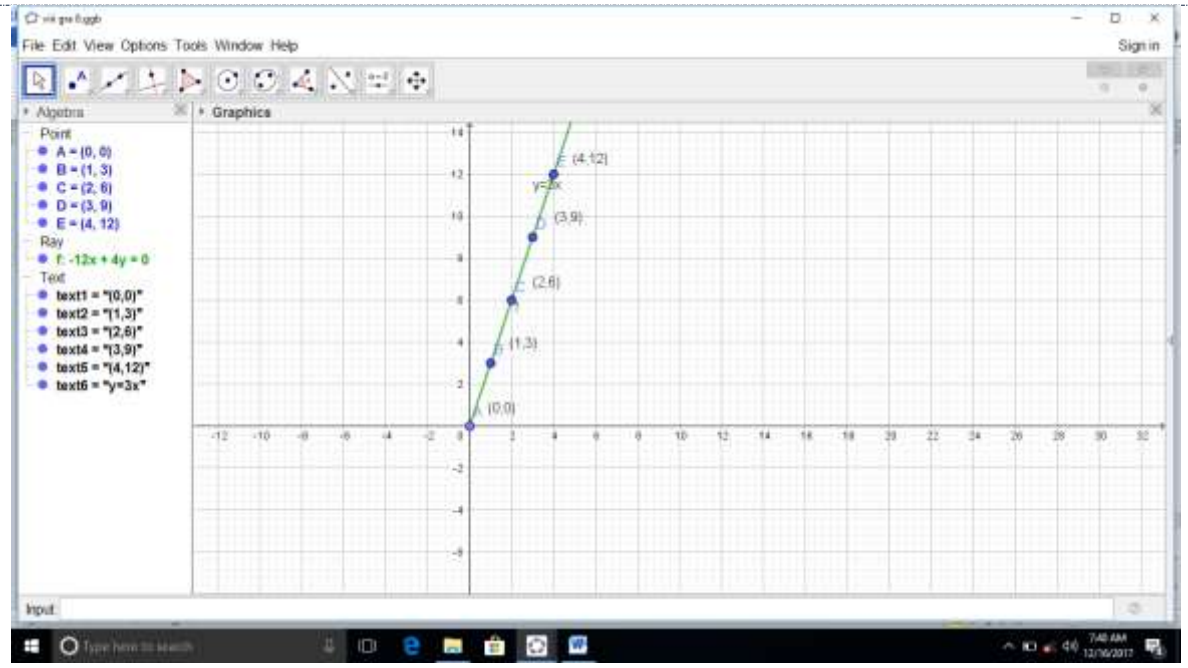


Figure : 4 Linear graph.

Answer:
It is a straight line. Distance=Speed*Time. Relationship is y=3x.

II. CONCLUSION

Accessing to technology is an effective way to stimulate the student's interest in Mathematics. The world's favorite software Geogebra is excellent Mathematical software. It will be an effective tool to change the student's attitude positively towards the learning of mathematics. The youngsters can easily solve mathematical problem with the help of this technology. With the help of this Geogebra the students can explore critical topics like vector algebra; complex numbers. In order to bring the clarity in 3dimensional construction, Geometry, Graph. Geogebra provides the visualization technique. This technique enables the higher secondary students to eliminate memorization of Mathematical concepts in 2 and 3dimensional. Viewing 3-dimension mathematical figure, animating mathematical figure, finding the angle, finding the area, finding the slope helps the students to understand the mathematical concepts clearly. In conventional method, the students can build only the memory palace. But in the case of conventional with ICT the students can view the Mathematics figure visually and easily develop their learning skill.

REFERENCES

[1] Adolphus, Telima andAderonmu, temitopeS.B.Comparative analysis of problem solving ability among JSS mathematics students using Computer – assisted instruction blended with problem solving approach (CAI-PS) Versus traditional teaching approach(TTP) in teaching basic statistics, American Journal of Scientific and Industrial Research.
[2] Alacapınar, F. G. (2003). The effect of traditional education and education via computer on the students' gain, Eurasian Journal of Educational Research, 10, 40-45.
[3] Albayrak, R. (2003). Öğrencilerinb ağıntıkavramınınol uşmasındag örülensıkıntılarve giderilmeönerileri. Yayınl anmamışYüksekLisansTezi, DokuzEylül Üniversitesi Eğitim BilimleriEnstitüsü, İzmir. Alkan, C. (1998).
[4] Alias, 2000 Alias, M. (2000), Spatial visualization ability and civil engineering problem solving. University of suorey,Guildford, united kingdom.
[5] Almeqdali, 2005 Almeqdalai, F. (2005), the effect of using The geometer's sketchpad (GSP) on Jordanian student's Understanding some geometrical concepts, International Journal for Mathematics teaching and learning, from http://www/cimt.plymouth.ac.uk/journal/almeqdadi.pdf.
[6] Akinsola, M. K., &Animasahun, I. A. (2007). The effect of simulation-games environment on Student's achievement in and attitudes to mathematics in secondary schools. The Turkish Online

ISSN: 2277-9655
Impact Factor: 5.164
CODEN: IJESS7

Journal of6 (3), 113-119.
[7] Aktümen, M., &Kaçar, A. (2008). Bilgisayarce birisistem lerininmatem atiğeyönelik tutumaetkisi, HacettepeÜniversitesiEğitimFakültesiDergisi, 35, 13-26.
[8] Battisa, 1999 Battisa, M. (1999), Geometry Results from the Third International Mathematics and science study. Teaching Children Mathematics, 5(6), (pp.367-373). Reston, VA: NCTM..

CITE AN ARTICLE

Selvi, J. S. (2018). VISUAL GRAPH OF HIGHER SECONDARY MATHEMATICS EDUCATION USING THE OPEN SOURCE SOFTWARE GEOGEBRA. *INTERNATIONAL JOURNAL OF ENGINEERING SCIENCES & RESEARCH TECHNOLOGY*, *7*(6), 406-411.

EXHIBITING RAILWAY JUNCTIONS AS STEINER POINTS

V.K. Radhakrishnan
Assistant Professor of Mathematics
Sri Chandrasekharendra Saraswathi Viswa Mahavidyalaya, Enathur, Kanchipuram

Abstract: In the problem of finding minimum spanning tree, to reduce the sum of the lengths of all the edges, we introduce some new points or vertices, these points are called Steiner points which makes the graph a Steiner Tree. The main purpose of adding these new vertices to the graph G is to ensure the reachability of each vertex is minimum. In this article, we apply the theory of Steiner points to Railway Junction.

Keywords: Tree, Steiner Points, Steiner Tree, Railway Junction.

Introduction: Steiner tree problem, or minimum Steiner tree problem, named after Jakob Steiner, is playing a major role for a class of problems in combinatorial optimization. Steiner tree problems can be designed in many ways, they all require an optimal interconnect for a given set of objects and an objective function. Given an undirected graph with non-negative edge weights and a subset of vertices, the Steiner tree problem in graphs finds a tree of minimum weight that contains all vertices, but may include additional vertices.

The Steiner tree problem in graphs perceived as a generalization of two well-known combinatorial optimization problems: the shortest path problem and the minimum spanning tree problem. If a Steiner tree problem in graphs contains exactly two terminals, it reduces to finding a shortest path. If, on the other hand, all vertices are terminals, the Steiner tree problem in graphs is equivalent to the minimum spanning tree. The Steiner tree problem has many applications, in finding an optimal way to build roads and railways to connect a set of cities, in circuit theory and so on.

Consider the following graph with 3 vertices, we are looking to find minimum spanning tree that connects all the three vertices:

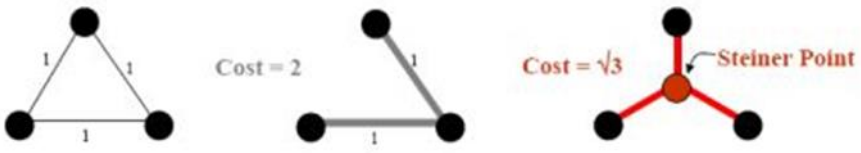


Fig. 1: Steiner Point

On the left side, we are given an equilateral triangle with length 1. The minimum spanning tree for this triangle must include any of the two edges and hence the length will be 2, as given in the middle. Though the Steiner tree adds one more point to the graph, called Steiner point: the point in the middle of the triangle as in the right side. With this extra Steiner point, now the total cost becomes $\sqrt{3}$ (1.732 approx.) based on the fact that the angle in the middle is 120 degree. Thus Steiner tree further optimise the MST problems by adding additional points to the given network.

Theorem 1: (a) No two edges of an ST can meet at an angle less than 120'. (b) An ST has no crossing edges. (c) Each Steiner point of an ST is of degree exactly three.

Theorem 2: A Steiner tree for a graph with n points contains at most $n - 2$ Steiner points.
Proof: Suppose that an ST has k Steiner points. Then it has $n + k - 1$ edges. Since each Steiner point has three edges and each terminal at least one, the number of edges must be at least $(3k + n)/2$; the division by 2 accounts for the fact that each edge is counted at two vertices. It follows that:
$n + k - 1 \geq (3k + n)/2$ (or) $n - 2 \geq k$

Definition: In a graph G, a Steiner tree (ST) with the maximum $n - 2$ Steiner points is called full Steiner tree (FST).

Corollary 1: Each terminal is of degree one in an FST

Corollary 2: For n ≥ 4 there exists at least two Steiner points in an FST which are adjacent to two terminals.

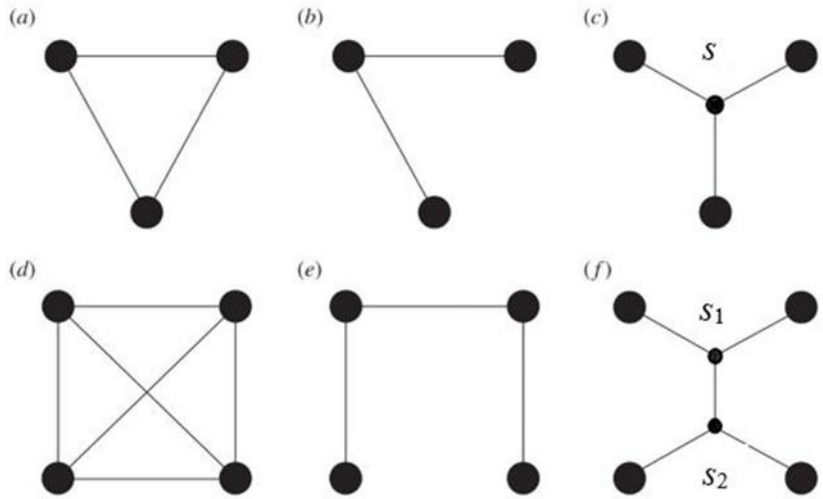


Fig. 2: Steiner Points for K_3 and K_4 Graphs

The above is the example of Steiner tree for the complete graph K_3 and K_4 graphs. Here, (a, d) are complete graphs with 3 vertices and 4 vertices respectively, (b, e) represents the minimum spanning trees of the graph, and (c, f) represents the Steiner trees of the respective graphs. The vertices s, s_1 and s_2 are called Steiner points.

In this article, we are exhibiting the connection between the Steiner points and the railway junction by showing two examples. The first example has a Steiner tree with one Steiner point, while the other has a Steiner tree with two Steiner point.

Railway Junction: A railway junction refers to a railway station situated on or close to a junction where lines to multiple destinations depart, having minimum with three incoming lines.

Problem of A Railway Junction: We express the railway stations in the form of graph as below for the clear representation of the Steiner points.

Steiner point is used in the Railway signals for the development of railway signals network, and in the signal diversions. The designed structure shows the connection between the stations from Chennai Central railway station is routed via Basin Bridge. We can identify that Basin Bridge station is acting as a Steiner point for the graph.

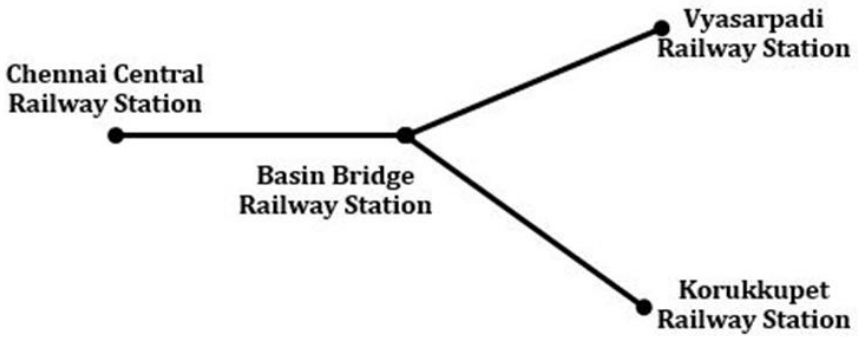


Fig. 3: Graphical Representation of the Railway Map of Basin Bridge Junction

The significant point is that the train comes from Thiruvallur via Vyasarpadi could not reach Central station without crossing Basin Bridge and the same for the train which comes from Ponneri via Korukkupet could not reach Central without crossing Basin Bridge. As in the definition of Steiner tree, the Steiner point Basin Bridge minimizes the distance between the stations and it helps reaching the other. The following is another example with two Steiner point:

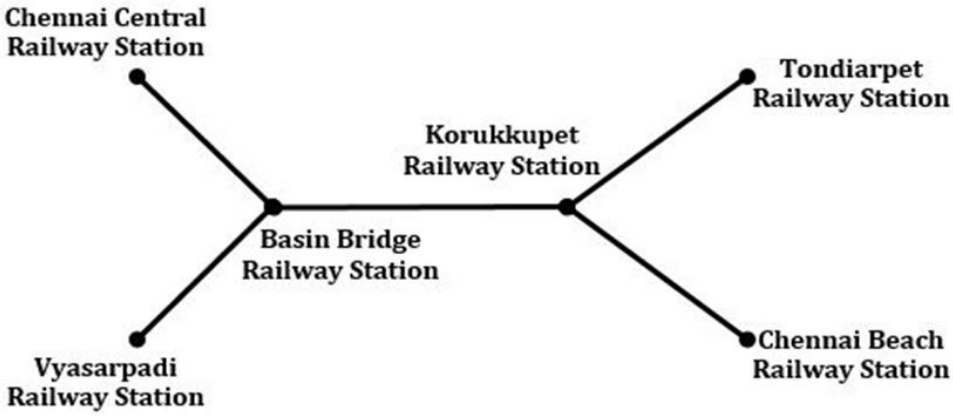


Fig. 4: Graphical representation of the railway map of Basin Bridge and Korukkupet Junction

From Fig. 4, the railways stations Vyasarpadi, Chennai Central can be reached through Basin Bridge and the stations Chennai Beach, Tondiarpet can be reached Korukkupet. Here, the stations Basin Bridge and Korukkupet are functioning as Steiner points so as to connect the places with minimum distance. Trains can reach the destination Tondiarpet from Chennai Central after crossing two Steiner points Basin Bridge (s_1) and Korukkupet (s_2).

Conclusion: In this article we have presented Steiner points and Steiner tree and highlighted the importance of Steiner point running in the railway routes. This shows that all the railway junctions possesses Steiner points, removal of which makes the link between the stations a disconnected one.

References:

1. Bondy, John Adrian, and Uppaluri Siva Ramachandra Murty. Graph theory with applications. Vol. 290. London: Macmillan, 1976.
2. Berge, Claude. "La theorie des graphes." Paris, France (1958).
3. Bern, Marshall W., and Ronald L. Graham. "The shortest-network problem." *Scientific American* 260.1 (1989): 84-89.
4. Chlebík, Miroslav, and Janka Chlebíková. "The Steiner tree problem on graphs: Inapproximability results." Theoretical Computer Science 406.3 (2008): 207-214.

***

OBJECT ORIENTED APPROACH TO TRAVELLING SALESMAN PROBLEM

V.K. Radhakrishnan
Assistant Professor, Department of Mathematics
Sri Chandrasekharendra Saraswathi Viswa Mahavidhyalaya
Enathur, Kanchipuram, Tamilnadu, India

J. Senthilkumar
Research Scholar, Department of Mathematics
Sri Chandrasekharendra Saraswathi Viswa Mahavidhyalaya
Enathur, Kanchipuram, Tamilnadu, India

Abstract: Travelling salesman problem, often considered as a problem related to managerial decision helps the management in sending their salesman to different granaries with minimum cost. In this article, the concept of object oriented programming is introduced in travelling salesman problem and then solved for different entries.

Keywords: Assignment Problem, Travelling Salesman Problem, Object Oriented Language, C++.

Introduction: A salesperson generally visits a range of cities starting from his command centre. Assuming the distance between the cities, or the time taken to travel among the cities, or the cost spent to visit the cities are known, the problem of finding the minimal distance or time or cost, if the salesman starting from his head office with a condition that he has to visit all the cities comes under his influence exactly once and reaching back where he started (head office) is called Travelling Salesman Problem (TSP).

A TSP is a special case of Assignment problem with the following additional constraints: (a) the salesman must visit every city exactly once except the starting city, (b) the salesman should start from a city, basically the headquarters, and return to the same place, (c) going from any city to the same directly is not allowed. Here, conditions (a) and (b) are called route conditions.

This problem can be formulated as, there are n cities and ways between all of them are known weights. The target is to find the shortest likely way which passes through all cities only once, start and end in the same place, simply a shortest possible round trip. Actually, the real problem is not only to find the shortest round trip which exists and also which optimises the trip. In table 1, we have listed the possible ways of visiting places up to a maximum of ten cities. With this, we are giving it to the reader to imagine the complexity occurs for the firm that has more than 20 cities. Considerably this leads to a huge computation to solve it in a real time.

Table 1: Number of Permutations for TSP

Number of Points	Number of Possible Ways
4	24
5	120
6	720
7	5 040
8	40 320
9	3 62 880
10	36 28 800

These difficulties can be domineered with the help of computer and with an appropriate program which follows the algorithm and the conditions listed above. In this article, we are implementing object oriented approach to solve the travelling salesman problem.

Object Oriented Programming: Object oriented programming is a method of implementing programs which are organized as a collections of objects, which may contain data in the form of fields (attributes), and code, in the form of procedures (methods). In object oriented program, the computed codes are designed by making them out of objects that relate with each other. An object is just like a box which contains data and functions operates on the data. There are diverse OOP languages, and the most popular one among all are class-based, objects are instances of classes. Objects are the building blocks for the execution of the program while classes are basic elements for defining the object oriented program. Some of the significant object oriented languages include Java, C++, C#, Python, PHP etc.

C++ Program for Travelling Salesman Problem:

```
#include<iostream.h>
#include<conio.h>
int array[30][30],finish[30],n,cost=0;
void takeInput()
{
   int i,j;
   cout<<"\nEnter the number of villages: ";
   cin>>n;
   cout<<"\nEnter the Cost Matrix\n";
   for(i=0;i < n;i++)
   {
 cout<<"Enter Elements of Row: "<<i+1<<"\n";
          for( j=0;j < n;j++)
             cin>>array[i][j];
          finish[i]=0;
   }
   cout<<"\nThe cost list is:";
   for( i=0;i < n;i++)
   {
          cout<<"\n";
          for(j=0;j < n;j++)
             cout<<"\t"<<array[i][j];
   }
}
int least(int c)
{
   int i,nc=999;
   int min=999,kmin;
   for(i=0;i < n;i++)
   {
          if((array[c][i]!=0)&&(finish[i]==0))
             if(array[c][i]+array[i][c] < min)
             {
                    min=array[i][0]+array[c][i];
                    kmin=array[c][i];
                    nc=i;
             }
   }
   if(min!=999)
```

```
            cost+=kmin;
    return nc;
}
void mincost(int city)
{
    int i,ncity;
    finish[city]=1;
    cout<<city+1<<"--->";
    ncity=least(city);
    if(ncity==999)
    {
            ncity=0;
            cout<<ncity+1;
            cost+=array[city][ncity];
            return;
    }
    mincost(ncity);
}
int main()
{
    clrscr();
    takeInput();
    cout<<"\nThe Path is:\n";
    mincost(0);
    cout<<"\nMinimum cost is "<<cost;
    return 0;
}
```

Output:

```
Enter the number of villages: 5

Enter the Cost Matrix
Enter Elements of Row: 1
0 3 6 2 3
Enter Elements of Row: 2
3 0 5 2 3
Enter Elements of Row: 3
6 5 0 6 4
Enter Elements of Row: 4
2 2 6 0 6
Enter Elements of Row: 5
3 3 4 6 0

The cost list is:
        0       3       6       2       3
        3       0       5       2       3
        6       5       0       6       4
        2       2       6       0       6
        3       3       4       6       0
The Path is:
1--->4--->2--->5--->3--->1
Minimum cost is 17
```

Fig. 1: Program Output

Conclusion: This article addresses the complexity of travelling salesman problem if the number of cities is just about immense. Also we are suggesting object oriented approach to solve the same and found the solution for a simple problem.

References

1. J K Sharma, "Operations Research-Theory and Applications", Macmillan India Ltd, New Delhi, 2003. A.K.Bhunia and Shri L Sahoo, "Advanced Operations Research", Asian Books Private Ltd, New Delhi, 2011.
2. P.K. Gupta and Man Mohan, "Problems in Operations Research (Methods & Solutions)", Sultan Chand & Sons, New Delhi, 2006.
3. Grady Booch, "Object Oriented Analysis and Design", Addison-Wisley Professional. 2 editions, USA,1993.
4. Peretz Shovel, "Functional and Object Oriented Analysis and Design" (an integrated methodology). Idea Group Publishing (an imprint of Idea Group Inc.). United States of America, 2006.
5. Taghrid, I., Mohamed G., Iman S., 2009. Solving Transportation Problem Using Object Oriented Model.IJCSNS International Journal of Computer Science and Network Security, VOL.9 No.2

***

MAT JOURNALS

Journal of Statistics and Mathematical Engineering
Volume 4 Issue 1

Nurse Scheduling Problem using Linear Programming Problemfor Day-wise Schedule

***V.K. Radhakrishnan*[1], *B. Shanmugam*[2]**
[1]Assistant Professor, [2]Research Scholar
[1,2]Department of Mathematics
Sri ChandrasekharendraSaraswathiViswaMahavidhyalaya
Enathur, Kanchipuram, Tamilnadu, INDIA

Abstract

Nurse Scheduling Problem is a branch of Operations Research, helps the hospital management to construct time/day schedule for the staff nurses so as to maintain the discipline of the hospital and minimising the cost as well. This article identifies the problem of nurses who are available in the hospital according to day wise schedule and solving the same by dual simplex method.

Keywords: *nurse scheduling problem, day-wise schedule, linear programming problem, dual simplex method*

INTRODUCTION

Operations Research is a science intended to provide quantitative tools to decision-making procedures. It comprises a set of mathematical optimization and simulation models, such as linear and nonlinear programming, combinatory optimization, theory of queues, dynamic programming, sequencing and scheduling etc. Nurse Scheduling Problem is a multi-objective problem which optimises the cost for the hospital management and also suggests the minimal number of nurses to be available to maintain the hospital patients. Systematic approach in allocating the nurse must need to ensure continuous and suitable level of patient care services while maintaining the statutory requirements as well as internal policies. This problem becomes a complex one when adding factors such as patient admission, nurse qualifications or license to practice, type of diseases and unforeseen accidents. The personal needs of the nurses such as vacation or work shift preferences add a new dimension to the scheduling problem. The need to balance all the various dimension of the problem makes nurse scheduling a particularly intimidatingphysical task.

There are various grades of nurses ranging from registered to junior staff nurse. Some of the nurses might be trained to manage certain medical conditions or skilled in certain area such as intensive care. Due to the varied trainings and specializations, certain type of nurses has to be staffed forwards requiring those skills. These varied conditions make physical nurse scheduling to consume a substantial extent of time. Even when the schedule has been planned manually, it does not necessarily guarantee the fairness of distribution of work such as the number of night shifts or weekend shifts. While the nurses indicated their preferences, the planner might not have taken all these into consideration resulting in poorly designed schedules. These schedules have to be modified by the nurses swapping duties or working under unwanted conditions. Occasionally, the plans did not attempt to efficiently utilize the manpower properly.

Page 1-7 © MAT Journals 2018. All Rights Reserved

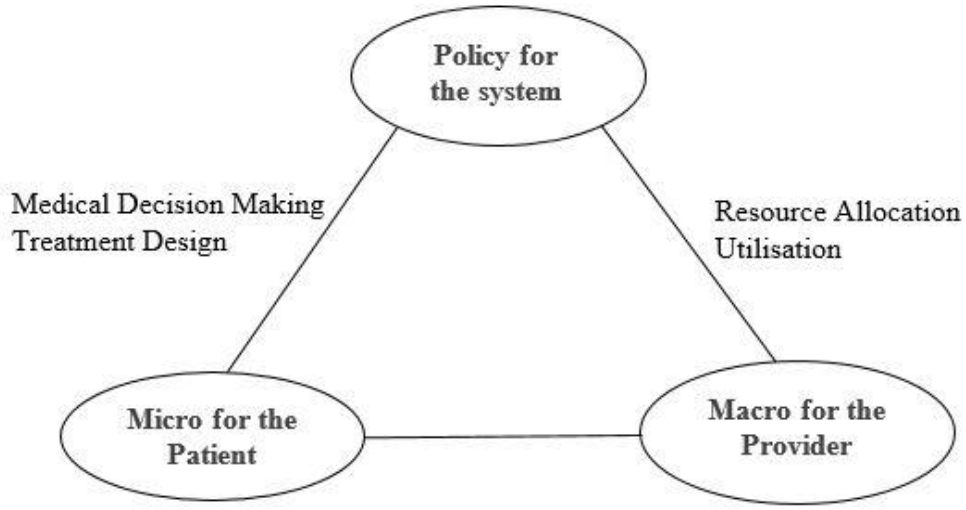


Fig. 1 *Operations in Health Management*

LINEAR PROGRAMMING

Linear programming techniques are considered as mathematics based decision-making tool. Such technique requires two fundamental types, one is objective function and the subject to the availability of the resources, called as constraints. In a Linear Programming problem, the objective function, often expressed as *Z*, is formulated to determine the maximum profit or minimizing the cost with a given set of rules or constraints such as business policies, resource availability, maintenance schedule, transportation distance or time and capacity.

PROBLEM DEFINITION

Consider a hospital that is open seven days a week. Every nurse must work for five consecutive days, and given takes two days off, repeating this pattern indefinitely. How can we minimize the number of nurses that staff the hospital? Based on previous experience, the number of nurses needed on a particular day in one of the hospitals at Chennai, is given as follows.

Table 1 *Nurse Requirement Day-wise*

Variables	x_1	x_2	x_3	x_4	x_5	x_6	x_7
Day	Sunday	Monday	Tueday	Wednesday	Thursday	Friday	Saturday
No. of nurses	100	200	150	250	90	160	300

MODEL

Let x_i be the number of people working on day *i*. The condition here is, nurses will work for 5 days consecutively and will take 2 days leave.

Let x_1 be the number of nurses starts their duty on Sunday and works till Thursday, and x_2, x_3, x_4, x_5, x_6 and x_7 are the number ofnurses starts their duty accordingly and works for 5 days respectively from Monday to Saturday and they take 2 days leave.

The demand for the number of nurses in the hospital as per the given table: Sunday – 100, Monday – 200, Tuesday – 150, Wednesday – 250, Thursday – 90, Friday – 160 and Saturday – 300.

Our objective is to find,

$$\boldsymbol{x_1 + x_2 + x_3 + x_4 + x_5 + x_6 + x_7}$$

Consider the constraint for Sunday staffing level of 100.Those who start their shift on Sunday (x_1), they will work for consecutively 5 days, that is, Sunday to Thursday. Those, who start their shift on

Page 1-7 © MAT Journals 2018. All Rights Reserved

Monday (x_2), they will work for consecutively 5 days, that is, Monday to Friday. Similarly, those who start their shift on Tuesday (x_3), they will work Tuesday to Saturday and so on. We can formulate the following table, representing the term W – Working and H – Holiday:

Table 2 *Nurse Working Schedule*

Shift	x_1	x_2	x_3	x_4	x_5	x_6	x_7
Sunday	W	W	W	W	W	H	H
Monday	H	W	W	W	W	W	H
Tuesday	H	H	W	W	W	W	W
Wednesday	W	H	H	W	W	W	W
Thursday	W	W	H	H	W	W	W
Friday	W	W	W	H	H	W	W
Saturday	W	W	W	W	H	H	W

Similar arguments give a total formulation of Min $Z = x_1 + x_2 + x_3 + x_4 + x_5 + x_6 + x_7$
Subject to constraints

$$x_1 + x_4 + x_5 + x_6 + x_7 \geq 100$$
$$x_1 + x_2 + x_5 + x_6 + x_7 \geq 200$$
$$x_1 + x_2 + x_3 + x_6 + x_7 \geq 150$$
$$x_1 + x_2 + x_3 + x_4 + x_5 \geq 250$$
$$x_2 + x_3 + x_4 + x_5 + x_6 \geq 160$$
$$x_1 + x_2 + x_3 + x_4 + x_5 \geq 90$$
$$x_3 + x_4 + x_5 + x_6 + x_7 \geq 300$$
$$x_1 + x_2 + x_3 + x_4 + x_5 + x_6 + x_7 \geq 0;\ x_i \geq 0 \text{ for all } i$$

Initial Dual Simplex Method

	x_1	x_2	x_3	x_4	x_5	x_6	x_7	θ
R_1	1	0	0	1	1	1	1	100
R_2	1	1	0	0	1	1	1	200
R_3	1	1	1	0	0	1	1	150
R_4	1	1	1	1	0	0	1	250
R_5	0	1	1	1	1	1	0	160
R_6	1	1	1	1	1	0	0	90
R_7	0	0	1	1	1	1	1	300
R_8	1	1	1	1	1	1	1	1

Page 1-7 © MAT Journals 2018. All Rights Reserved

A =

TRANSPORT MATRIX

1	1	1	1	0	1	0	1
0	1	1	1	1	1	0	1
0	0	1	1	1	1	1	1
1	0	0	1	1	1	1	1
1	1	0	0	1	1	1	1
1	1	1	0	1	0	1	1
1	1	1	1	0	0	1	1
100	200	150	250	160	90	300	1

AT =

Subject to the constraints

$$Y_1+Y_2+ Y_3+ Y_4+0Y_5+Y_6+0Y_7\leq 1$$
$$0Y_1+Y_2+Y_3+Y_4+Y_5+Y_6+0Y_7\leq 1$$
$$0Y_1+0Y_2+Y_3+Y_4+Y_5+Y_6+Y_7\leq 1$$
$$Y_1+0Y_2+0Y_3+Y_4+Y_5+Y_6+Y_7\leq 1$$
$$Y_1+Y_2+0Y_3+0Y_4+ Y_5+Y_6+Y_7\leq 1$$
$$Y_1+Y_2+ Y_3+0Y_4+ Y_5+0Y_6+ Y_7\leq 1$$
$$Y_1+Y_2+ Y_3+ Y_4+0Y_5+0Y_6+ Y_7\leq 1$$

Maximize Equation

$$100Y_1+200Y_2+150\ Y_3+250\ Y_4+160Y_5+90Y_6+300\ Y_7\leq P$$

Subject to the constraints,

$$-100Y1-200Y2-150Y_3-250Y_4-160Y_5-90Y_6-300Y_7+P=0$$
$$Y_1+Y_2+ Y_3+ Y_4+0Y_5+Y_6+0Y_7+X_1+0X_2+0X_3+0X_4+0X_5+0X_6+0X_7=1$$
$$0Y_1+Y_2+ Y_3+ Y_4+Y_5+Y_6+0Y_7+0X_1+X_2+0X_3+0X_4+0X_5+0X_6+0X_7=1$$
$$0Y_1+0Y_2+ Y_3+ Y_4+Y_5+Y_6+Y_7+0X_1+0X_2+X_3+0X_4+0X_5+0X_6+0X_7=1$$
$$Y_1+0Y_2+0\ Y_3+ Y_4+Y_5+Y_6+Y_7+0X_1+0X_2+0X_3+X_4+0X_5+0X_6+0X_7=1$$
$$Y_1+Y_2+ 0Y_3+ 0Y_4+Y_5+Y_6+Y_7+0X_1+0X_2+0X_3+0X_4+X_5+0X_6+0X_7=1$$
$$Y_1+Y_2+ Y_3+0Y_4+0Y_5+Y_6+Y_7+0X_1+0X_2+0X_3+0X_4+0X_5+X_6+0X_7=1$$
$$Y_1+Y_2+ Y_3+ Y_4+0Y_5+0Y_6+Y_7+0X_1+0X_2+0X_3+0X_4+0X_5+0X_6+X_7=1$$

Page 1-7 © MAT Journals 2018. All Rights Reserved

FIRST ITERATION

	Y1	Y2	Y3	Y4	Y5	Y6	**Y7**	X_1	X2	X3	X4	X5	X_6	X7	P	θ
R1	1	1	1	1	0	1	**0**	1	0	0	0	0	0	0	0	1= -
R2	0	1	1	1	1	1	**0**	0	1	0	0	0	0	0	0	1= -
R3	0	0	1	1	1	1	**1**	0	0	1	0	0	0	0	0	1= 1
R4	**1**	**0**	**0**	**1**	**1**	**1**	**1**	**0**	**0**	**0**	**1**	**0**	**0**	**0**	**0**	**1= 1**
R5	1	1	0	0	1	1	**1**	0	0	0	0	1	0	0	0	1= 1
R6	1	1	1	0	1	0	**1**	0	0	0	0	0	1	0	0	1=- 1
R7	1	1	1	1	0	0	**1**	0	0	0	0	0	0	1	0	1= 1
R8	-100	-200	-150	-250	-160	-90	**-300**	0	0	0	0	0	0	0	1	0

SECOND ITERATION

	Y1	**Y2**	Y3	Y4	Y5	Y6	Y7	X_1	X2	X3	X4	X5	X_6	X7	P	θ
R1	1	**1**	1	1	0	1	0	1	0	0	0	0	0	0	0	1 = 1
R2	0	**1**	1	1	1	1	0	0	1	0	0	0	0	0	0	1 = 1
R3	-1	**0**	1	0	0	0	0	0	0	1	-1	0	0	0	0	0 = -
R4	1	**0**	0	1	1	1	1	0	0	0	1	0	0	0	0	1 = -
R5	**0**	**1**	**0**	**-1**	**0**	**0**	**0**	**0**	**0**	**0**	**-1**	**1**	**0**	**0**	**0**	**0= 0**
R6	0	**1**	1	-1	0	-1	0	0	0	0	-1	0	1	0	0	0 = 0
R7	0	**1**	1	0	-1	-1	0	0	0	0	-1	0	0	1	0	0 = 0
R8	200	**-200**	-150	50	140	210	0	0	0	0	300	0	0	0	1	300

THIRD ITERATION

	Y1	Y2	**Y3**	Y4	Y5	Y6	Y7	X_1	X2	X3	X4	X5	X_6	X7	P	Θ
R1	1	0	**1**	2	0	1	0	1	0	0	1	-1	0	0	0	1 = 1
R2	0	0	**1**	2	1	1	0	0	1	0	1	-1	0	0	0	1 = 1
R3	-1	0	**1**	0	0	0	0	0	0	1	-1	0	0	0	0	0 = 0
R4	1	0	**0**	1	1	1	1	0	0	0	1	0	0	0	0	1 = -
R5	0	1	**0**	-1	0	0	0	0	0	0	-1	1	0	0	0	0 = -
R6	0	0	**1**	0	0	-1	0	0	0	0	0	-1	1	0	0	0 = 0
R7	**0**	**0**	**1**	**1**	**-1**	**-1**	**0**	**0**	**0**	**0**	**0**	**-1**	**0**	**1**	**0**	**0 = 0**
R8	200	0	**-150**	-150	140	210	0	0	0	0	100	200	0	0	1	300

Page 1-7 © MAT Journals 2018. All Rights Reserved

FOURTH ITERATION

	Y1	Y2	Y3	Y4	**Y5**	Y6	Y7	X_1	X2	X3	X4	X5	X_6	X7	P	Θ
R1	1	0	0	1	**1**	0	0	1	0	0	1	0	0	-1	0	1 = 1
R2	0	0	0	1	**0**	0	0	0	1	0	1	0	0	-1	0	1 = -
R3	**-1**	**0**	**0**	**-1**	**1**	**1**	**0**	**0**	**0**	**1**	**-1**	**1**	**0**	**-1**	**0**	**0 = 0**
R4	1	0	0	1	**1**	1	1	0	0	0	1	0	0	0	0	1 = 1
R5	0	1	0	-1	**0**	0	0	0	0	0	-1	1	0	0	0	0 = 0
R6	0	0	0	-1	**1**	0	0	0	0	0	0	0	1	-1	0	0 = -
R7	0	0	1	1	**-1**	-1	0	0	0	0	0	-1	0	1	0	0 = 0
R8	200	0	0	0	**-10**	60	0	0	0	0	100	50	0	150	1	300

FIFTH ITERATION

	Y1	Y2	Y3	**Y4**	Y5	Y6	Y7	X_1	X2	X3	X4	X5	X_6	X7	P	Θ
R1	**2**	**0**	**0**	**2**	**0**	**-1**	**0**	**1**	**0**	**-1**	**2**	**-1**	**0**	**0**	**0**	**1 = 1/2**
R2	0	0	0	**1**	0	0	0	0	1	0	1	0	0	-1	0	1 = 1
R3	-1	0	0	**-1**	1	1	0	0	0	1	-1	1	0	-1	0	0 = -
R4	2	0	0	**2**	0	0	1	0	0	-1	2	-1	0	1	0	1 = 1/2
R5	0	1	0	**-1**	0	0	0	0	0	0	-1	1	0	0	0	0 = 0
R6	1	0	0	**0**	0	-1	0	0	0	-1	1	-1	1	0	0	0 = -
R7	-1	0	1	**0**	0	0	0	0	0	1	-1	0	0	0	0	0 = -
R8	190	0	0	**-10**	0	70	0	0	0	10	90	60	0	140	1	300

SIXTH ITERATION

	Y1	Y2	Y3	**Y4**	Y5	Y6	Y7	X_1	X2	X3	X4	X5	X_6	X7	P	Θ
R1	**1**	**0**	**0**	**1**	**0**	**-1/2**	**0**	**1/2**	**0**	**-1/2**	**1**	**-1/2**	**0**	**0**	**0**	**1/2**
R2	0	0	0	**1**	0	0	0	0	1	0	1	0	0	-1	0	1 = 1
R3	-1	0	0	**-1**	1	1	0	0	0	1	-1	1	0	-1	0	0 = -
R4	2	0	0	**2**	0	0	1	0	0	-1	2	-1	0	1	0	1 = 1/2
R5	0	1	0	**-1**	0	0	0	0	0	0	-1	1	0	0	0	0 = 0
R6	1	0	0	**0**	0	-1	0	0	0	-1	1	-1	1	0	0	0 = -
R7	-1	0	1	**0**	0	0	0	0	0	1	-1	0	0	0	0	0 = -
R8	190	0	0	**-10**	0	70	0	0	0	10	90	60	0	140	1	300

SEVENTH ITERATION

	Y1	Y2	Y3	Y4	Y5	Y6	Y7	X_1	X2	X3	X4	X5	X_6	X7	P	Θ
R1	1	0	0	1	0	-1/2	0	1/2	0	-1/2	1	-1/2	0	0	0	1/2
R2	-1	0	0	0	0	1/2	0	-1/2	1	1/2	0	1/2	0	-1	0	1/2
R3	0	0	0	0	1	1/2	0	1/2	0	1/2	0	1/2	0	-1	0	1/2
R4	0	0	0	0	0	1	1	1	0	0	0	0	0	1	0	0
R5	1	1	0	0	0	-1/2	0	1/2	0	-1/2	0	1/2	0	0	0	1/2
R6	1	0	0	0	0	-1	0	0	0	-1	1	-1	1	0	0	0
R7	-1	0	1	0	0	0	0	0	0	1	-1	0	0	0	0	0
R8	200	0	0	0	0	65	0	5	0	5	100	55	0	140	1	300

Page 1-7 © MAT Journals 2018. All Rights Reserved

Solution: $x_1 = 5$, $x_2 = 0$, $x_3 = 5$, $x_4 = 100$, $x_5 = 55$, $x_6 = 0$, $x_7 = 140$. Hence, $Z = x_1 + x_2 + x_3 + x_4 + x_5 + x_6 + x_7 = 5+0+5+100+55+0+140 = 305$.

Using Dual Simplex method, we found the solution for the linear programming problem framed with the data of nurse requirements as 305. This suggests that the demand for the requirement of nurses for each is 305.

CONCLUSION

In this paper we modelled a nurse scheduling problem, day-wise, into a linear programming problem and solved it by dual simplex method. This way we can suggest the management to maintain the minimal number of nurses for the hospital and help them in minimising their cost.

REFERENCES

1. Berrada, I., J. Ferland, P. Michelon. 1996. A multi-objective approach to nurse scheduling with both hard and soft constraints. Socio- Econom. Planning Sci. 30(3) 183–193.
2. De Grano, M.L, Medeiros, D.G and Eitel, D.(2009). Accommodating individual preferences in nurse scheduling via auctions and optimization, Health Care Management Science,12: 228 – 242
3. Ernst, A.T., Jiang, H., Krishnamoorthy, M. and Sier, D. (2004). Staff scheduling and rostering: A review of applications, methods and models, European Journal of Operational Research, 153: 3 – 27
4. Jaumard, B., F. Semet, T. Vovor. 1998. A generalized linear programming model for nurse scheduling. European Journal of Operational Research 107(1) 1-18.
5. Okada, M. 1992. An approach to the generalised nurse scheduling problem – generation of a declarative program to represent institution-specific knowledge. Computers and Biomedical Research 25.

Page 1-7 © MAT Journals 2018. All Rights Reserved

KEKULE INDICES OF CIRCUMCORONENE

A.Dhanalakshmi
Assistant Professor, Department of Mathematics
Sri ChandrasekharendraSaraswathiViswaMahavidyalaya,Kanchipuram,Tamilnadu
C.Sivakumar
M.Phil.,Scholar, Department of Mathematics
Sri ChandrasekharendraSaraswathiViswaMahavidyalaya,Kanchipuram,Tamilnadu

Abstract: The valence structures of Polycyclic Aromatic Hydrocarbon systems have been characterized by an index K, called the Kekule Index, which relates a set of molecular orbitals to orbitals localized on pairs of adjacent carbons. The localized orbitals can be associated with valence bond structures in a simple and unique way. The Kekule Index orders different valence structures in a series which should qualitatively indicate relative importance of the individual structures. The approach can be extended also to excited formal structures as discussed for CircumCoronene. Application of such analyses to a number of alternate polycyclic conjugated systems confirms to systems constructed from rings of various sizes.

Keywords: Conjugated Hydrocarbon, Kekule Index, Benzene, Circumcoronene.

1. Introduction: A representation of an object giving information only about the number of elements composing it and their connectivity is named as topological representation of an object. A topological representation of a molecule is called molecular graph. A molecular graph is a collection of points representing the atoms in the molecule and set of lines representing the covalent bonds. These points are named vertices and the lines are named edges in graph theory language. The advantage of topological indices is in that they may be used directly as simple numerical descriptors in a comparison with physical, chemical or biological parameters of molecules in Quantitative Structure Property Relationships (**QSPR**) and in Quantitative Structure Activity Relationships (**QSAR**). One of the most widely known topological descriptor is the **Kekule Index.**

Gutman I [1], he provides the basics of chemical Graph Theory Notes In [2], Damir Verkicevic, Nenod Trinajstic have obtained the Wiener index of Benzenoid graphs. Mojtaba Shamsipur, Bahram Hemmateenejad, et.al.[3] computed the highly Correlating Distance Connectivity-Based Topological Indices of some molecules. . K. Lavanya Lakshmi,[4] has calculated the highly correlating topological indices for some polyacenes. In this paper we have calculated the kekule indices of some circumcoronene.

2. Kekule Index: The most used molecular graph descriptors in establishing Quantitative structure-property relationships (QSPRS) and Quantitative structure-activity relationships (QSARS) are topological indices. Molecular descriptors are normally chosen based on their ability to give good results in statistical models. In this chapter, we calculated a set of five new indices (Kekule Indices) K, K_1 K_2, K_3 and K_4.

2.1 Kekule Index: The Kekule Index of a graph G = (V, E) is defined as

$$K(G) = \sum_{e=uv \in E(G)} W(e)$$

where **W(e)** = **|i-j|,** i, j are the degrees of the vertices u and v in G.

2.2 K_1 Index: The K_1 Index of a graph G = (V, E) is defined as

$$K_1(G) = \sqrt{\sum_{e=uv \in E(G)} W(e)}$$

where **W(e)** = **|i-j|²** i, j are the degrees of the vertices u and v in G.

2.3 K_2 Index: The K_2 Index of a graph G = (V, E) is defined as

$$K_2(G) = \sum_{v \in V(G)} W(v)$$

where **W(v) = sum of the degrees of the neighbouring vertices in G.**

2.4 K_3 Index: The K_3 Index of a graph G = (V, E) is defined as

$$K_3(G) = \sum_{v \in V(G)} W(v)$$

where **W(v) = product of the degrees of the neighbouring vertices in G.**

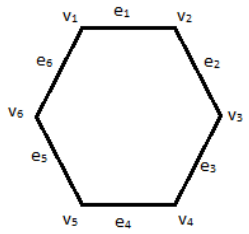
2.5 K_4 Index: The K_4 Index of a graph G = (V, E) is defined as

$$K_4(G) = \sum_{v \in V(G)} W(v)$$

where **W(v) = max{d(v,v_i)/ $v_i \in$ V(G)}.**

where **d(v,v_i) is the maximum distance between v and v_i.**

3. Kekule Indices of Benzene: [C_6H_6]:



Total number of vertices in benzene is 6
Total number of Edges in benzene is 6

3.1 Calculation of K Index:
3.1.1 Kekule Index : The Kekule Index of a graph G = (V, E) is defined as

$$K(G) = \sum_{e=uv \in E(G)} W(e)$$

where W(e) = |i-j|, i, j are the degrees of the vertices u and v in G.

To find $W(e_1)$:
v_1 and v_2 are the vertices of the edge 'e_1'.
The degree of the vertex 'v_1' is 2, i.e. i = 2
The degree of the vertex 'v_2' is 2, i.e. j = 2
Then $W(e_1)$ is the modulous value of the difference between i and j. i.e. $W(e_1) = |i-j| = |2-2| = 0$
In the same way, we can find the remaining values from $W(e_2)$ to $W(e_6)$.
$W(e_1) = |2-2| = 0$ $W(e_2) = |2-2| = 0$ $W(e_3) = |2-2| = 0$
$W(e_4) = |2-2| = 0$ $W(e_5) = |2-2| = 0$ $W(e_6) = |2-2| = 0$

$K(G) = \sum_{e=uv \in E(G)} W(e)$

K(G) = 0

3.1.2. Calculation of K_1 Index:
K_1 Index : The K_1 Index of a graph G = (V, E) is defined as

$$K_1(G) = \sqrt{\sum_{e=uv \in E(G)} W(e)}$$

where $W(e) = |i-j|^2$ i, j are the degrees of the vertices u and v in G.

To find $W(e_1)$:
v_1 and v_2 are the vertices of the edge 'e_1'.
The degree of the vertex 'v_1' is 2, i.e. i = 2
The degree of the vertex 'v_2' is 2, i.e. j = 2
Then $W(e_1)$ is the square of the modulous value of the difference between i and j.
i.e. $W(e_1) = |i-j|^2 = |2-2|^2 = 0$
In the same way, we can find the remaining values from $W(e_2)$ to $W(e_6)$.
$W(e_1) = |2-2|^2 = 0$ $W(e_2) = |2-2|^2 = 0$ $W(e_3) = |2-2|^2 = 0$
$W(e_4) = |2-2|^2 = 0$ $W(e_5) = |2-2|^2 = 0$ $W(e_6) = |2-2|^2 = 0$

3.1.3. Calculation of K_2 Index: K_2 Index : The K_2 Index of a graph G = (V, E) is defined as

$$K_2(G) = \sum_{v \in V(G)} W(v)$$

where W(v) = sum of the degrees of the neighbouring vertices in G.
To find $W(v_1)$:
'v_6' and 'v_2' are the neighbouring vertices of 'v_1'
The degree of the vertex 'v_6' is 2.
The degree of the vertex 'v_2' is 2.
Then the value of $W(v_1)$ is the sum of those degrees. i.e. $W(v_1) = 2 + 2 = 4$
In the same way, we can find all the values from $W(v_2)$ to $W(v_6)$
$W(v_1) = 2 + 2 = 4$ $W(v_2) = 2 + 2 = 4$ $W(v_3) = 2 + 2 = 4$
$W(v_4) = 2 + 2 = 4$ $W(v_5) = 2 + 2 = 4$ $W(v_6) = 2 + 2 = 4$
$K_2(G) = \sum_{e=uv \in E(G)} W(e)$

K_2(G) = 24

3.1.4. Calculation of K_3 Index: K_3 Index : The K_3 Index of a graph G = (V, E) is defined as

$$K_3(G) = \sum_{v \in V(G)} W(v)$$

where W(v) = product of the degrees of the neighbouring vertices in G.
To find $W(v_1)$:
'v_6' and 'v_2' are the neighbouring vertices of 'v_1'
The degree of the vertex 'v_6' is 2.
The degree of the vertex 'v_2' is 2.
Then the value of $W(v_1)$ is the product of those degrees. i.e. $W(v_1) = 2 * 2 = 4$
In the same way, we can find all the values from $W(v_2)$ to $W(v_6)$
$W(v_1) = 2 * 2 = 4$ $W(v_2) = 2 * 2 = 4$ $W(v_3) = 2 * 2 = 4$
$W(v_4) = 2 * 2 = 4$ $W(v_5) = 2 * 2 = 4$ $W(v_6) = 2 * 2 = 4$
$K_3(G) = \sum_{e=uv \in E(G)} W(e)$

$K_3(G) = 24$

3.1.5. Calculation of K_4 Index: K_4 Index : The K_4 Index of a graph G = (V, E) is defined as

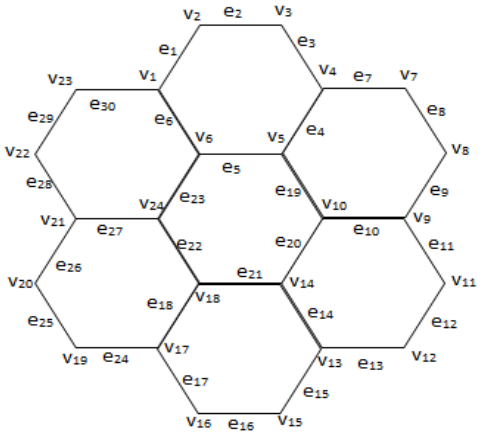
$$K_4(G) = \sum_{v \in V(G)} W(v)$$

where $W(v) = \max\{d(v,v_i)/\ v_i \in V(G)\}$.
where $d(v,v_i)$ is the maximum distance between v and v_i.

To find $W(v_1)$:
The distances of 'v_1' to all the remaining vertices v_2, v_3, v_4, v_5 and v_6 are respectively 1, 2, 3, 2 and 1. Then $W(v_1)$ is the maximum of all distances. i.e. $W(v_1) = \max\{d(v_1,v_i)\} = 3$
Similarly, we can find all the values from $W(v_2)$ to $W(v_6)$.
$W(v_1) = 3$ $W(v_2) = 3$ $W(v_3) = 3$
$W(v_4) = 3$ $W(v_5) = 3$ $W(v_6) = 3$
$K_4(G) = \sum_{e=uv \in E(G)} W(e)$

$K_4(G) = 18$

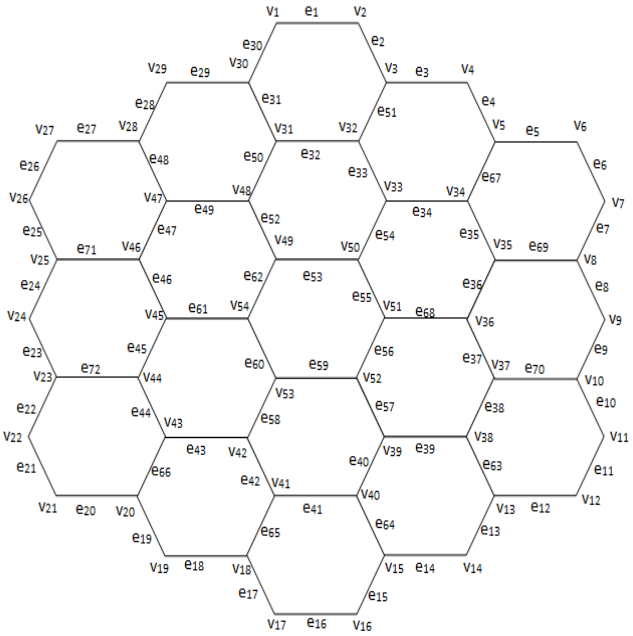
3.2 Kekule Indices of Coronene: [$C_{24}H_{12}$]
Coronene (also known as superbenzene) is a polycyclic aromatic hydrocarbon (PAH) comprising six peri-fused benzene rings. Its Chemical formula is $C_{24}H_{12}$.



Chemical graph of coronene ($C_{24}H_{12}$)

Total number of vertices in coronene is 24
Total number of edges in coronene is 30

3.3 Kekule Indices Of Circum Coronene: [$C_{54}H_{18}$]
Total number of vertices in Circumcoronene is 54
Total number of edges in Circumcoronene is 72



Chemical Structure of Circumcoronene ($C_{54}H_{18}$)

We calculated the Kekule Indices of coronene and circumcorone in this paper and tabulated below:

Table-1

S. No.	Chemical Structures	K	K_1	K_2	K_3	K_4
1	Benzene	0	0	24	24	18
2	Coronene	12	$2\sqrt{3}$	156	306	150
3	Circumcoronene	24	$2\sqrt{6}$	396	918	522

Conclusion: The main aim of this dissertation is to present the importance of graph Theoretical ideas in various areas of Science & Engineering for researches that we used the Kekule Index concepts for the research. An overview is presented especially to project the idea of Topological Indices. Researchers may get some information related to graph theory in various field especially in chemistry and can get some ideas related to Kekule Indices to their field of research.

References:

1. Gutman I, 1999. Graph Theory Notes, Newyork, 27, 9-15
2. Damir Verkicevic, Nenod Trinajstic, 2004. Wiener index of Benzenoid graphs, Bulletin of Chemists and Technologists of Macedonia, 23(2), 113-129.
3. Mojtaba Shamsipur, Bahram Hemmateenejad, Morteza Akhond, 2004. Highly Correlating Distance Connectivity-Based Topological Indices, Bull. Korean Chem. Soc. Vol.25, No.2, 253-259.
4. K. Lavanya Lakshmi, A highly correlated topological index for polyacenes, Journal of Experimental Sciences 2012, 3(4): 18-21
5. Prabhakara Rao N, Lavanya Lakshmi K, 2008. On the computation of PI, Sz and S indices of tetragonal systems, Acta Ciencia Indica, Vol.XXXIV M, No.4, 1753-1766.
6. Prabhakara Rao N, Lavanya Lakshmi K, Laxmi Prasanna A, 2007. On the Wiener index of product Of Path graphs, proceedings of national conference on discrete mathematics and its applications, NCDMA, Thiagarajar college of engineering, Madurai, p(30)-p(37).

***

COMPUTATIONAL METHOD OF AN INCOMPRESSIBLE VISCOUS COUETTEE FLOW BY MEANS OF CRANK NICOLSON TECHNIQUE AND THOMAS ALGORITHM

A. Dhanalakshmi
Assistant Professor Department of Mathematics
Sri ChandrasekharendraSaraswathiViswaMahavidyalaya,Kanchipuram,Tamilnadu
S.Thamarai Lakshmi
M.Phil Scholar, Department of Mathematics
Sri ChandrasekharendraSaraswathiViswaMahavidyalaya,Kanchipuram,Tamilnadu

Abstract: Computational fluid dynamics is an advanced tool used to solve the critical fluid dynamics problems by applying numerical methods and with the help of computational techniques. In this paper, the main Discretization method in computational fluid dynamics namely, Finite difference method is discussed. A physical problem of incompressible, viscous couettee flow is proposed for the solution by means of Crank Nicolson implicit technique.
A system of partial differential equations of the physical problem is reduced to a tri-diagonal matrix using crank Nicolson technique. Further, Thomas algorithm is used to solve these set of equations which are represented in matrix form. The first time step values are calculated using back substitution method. A coding is developed using JAVA language to generate tri-diagonal matrix and to solve the first time step values which are calculated using Crank Nicolson technique.

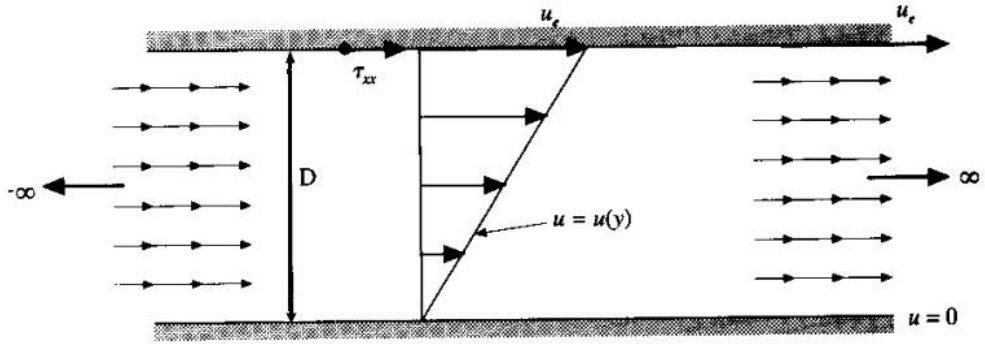
Keywords: ViscousCouttee, Fluid Dynamics, Thomas Algorith, Crank Nicolson Technique.

Introduction: In[1],the two-dimensional Navier–Stokes equations for incompressible flow between two parallel plates in relative motion to each other using the Crank Nicolson method are disscussed. Considering the two dimensional initial conditions ,the iterative solution converges to the Couette flow solution.

The Physical Problem: Consider the viscous flow between two parallel plates separated by the vertical distance *D,* as sketched in following figure. The upper plate is moving at the velocity U_e, and the lower plate is stationary; i.e., its velocity is *u* = 0. The flow field between the two plates is driven exclusively by the shear stress exerted on the fluid by the moving upper plate, resulting in a velocity profile across the flow, *u* = *u(v),* as sketched in Fig 1
The governing equation for this flow is the x -momentum equation, given by

$$\rho\frac{Du}{Dt}=-\frac{\partial p}{\partial x}+\frac{\partial \tau_{xx}}{\partial x}+\frac{\partial \tau_{yx}}{\partial y}+\frac{\partial \tau_{zx}}{\partial z}+\rho fx$$

And also the y-momentum equation is given by, $\rho\frac{Dv}{Dt}=\frac{\partial p}{\partial y}+\frac{\partial \tau_{xy}}{\partial x}+\frac{\partial \tau_{yy}}{\partial y}+\frac{\partial \tau_{zy}}{\partial z}+\rho f_y$



For Couette flow, there are no pressure gradients in either the x or y direction.

$$\rho u\frac{\partial u}{\partial x}+\rho v\frac{\partial u}{\partial y}=-\frac{\partial p}{\partial x}+\frac{\partial \tau_{xx}}{\partial x}+\frac{\partial \tau_{yx}}{\partial y}$$

Combining both x and y directions we get

$$\rho\frac{Dv}{Dt}=\frac{\partial p}{\partial y}+\frac{\partial \tau_{xy}}{\partial x}+\frac{\partial \tau_{yy}}{\partial y}+\frac{\partial \tau_{zy}}{\partial z}+\rho f_y \qquad (1)$$

On simplifying , we get the equation in the form of $\frac{u}{u_e}=\frac{y}{D}$

which is the analytical solution for the velocity profile for incompressible Couette flow.

Initial Conditions: Let us imagine that a velocity profile which is not linear, i.e., a different velocity profile than the exact solution given by Eq. (5). Specifically, let us assume a velocity profile defined as

$$u=\begin{cases}0 & \text{for } 0\le y<D\\ u_e & \text{for } y=D\end{cases}$$

This will be identified as our *initial* profile. We will consider this to be the initial condition at time t = o. We will set up a time-marching solution for the flow field, starting from this initial condition.

Crank Nicolson technique

Following the Crank-Nicolson technique, the finite-difference representation of Eq.(3))is

$$u_j^{n+1}=u_j^n+\frac{\Delta t}{2(\Delta y)^2R_{eD}}(u_{j+1}^{n+1}+u_{j+1}^n-2u_j^{n+1}-2u_j^n+u_{j-1}^{n+1}+u_{j-1}^n)$$

Grouping all terms at time level $n+1$ on the left-hand side and factoring both sides appropriately it becomes,

$$\left[-\frac{\Delta t}{2(\Delta y)^2R_{eD}}\right]u_{j-1}^{n+1}+\left[1+\frac{\Delta t}{(\Delta y)^2R_{eD}}\right]u_j^{n+1}+\left[-\frac{\Delta t}{2(\Delta y)^2R_{eD}}\right]u_{j+1}^{n+1}=\left[1-\frac{\Delta t}{(\Delta y)^2R_{eD}}\right]u_j^n+\frac{\Delta t}{2(\Delta y)^2R_{eD}}\left(u_{j+1}^n+u_{j-1}^n\right)$$

which is of the form

$$Au_{j-1}^{n+1}+Bu_j^{n+1}+Au_{j+1}^{n+1}=K_j \qquad (3.9)$$

Where $A=-\frac{\Delta t}{2(\Delta y)^2R_{eD}}$ $B=1+\frac{\Delta t}{(\Delta y)^2R_{eD}}$

$$K_j=\left(1-\frac{\Delta t}{(\Delta y)^2R_{eD}}\right)u_j^n+\frac{\Delta t}{2(\Delta y)^2R_{eD}}(u_{j+1}^n+u_{j-1}^n)$$

Equation (3.9) is solved on a grid such as that sketched in following figure. The vertical distance across the duct is divided into *N* equal increments of length Δy by distributing *N* + 1 grid points over the height *D,*

that is, $\Delta y=\frac{D}{N}$ (2)

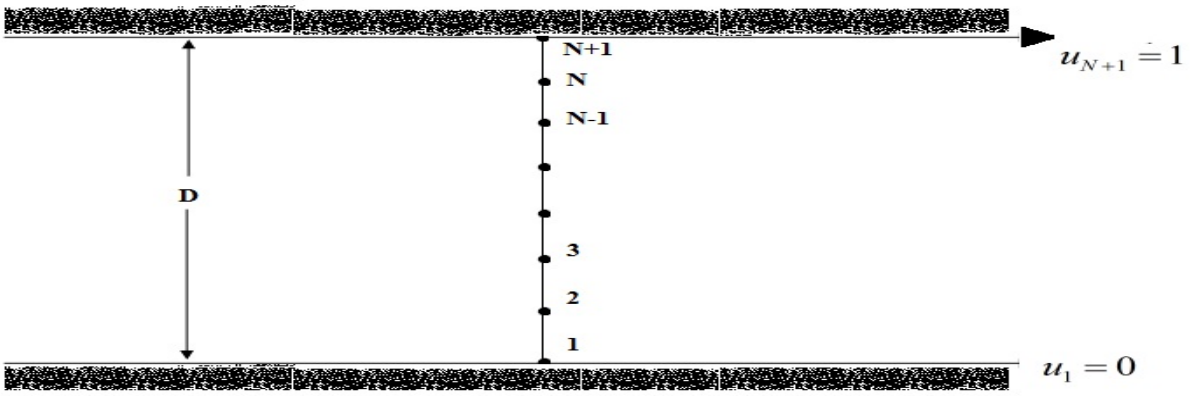


Fig 3.3: Labeling of Points for the Grid

From the boundary conditions, u and u_{N+1} are known:

$u_1 = 0 \quad u_{N+1} = 1$

Hence, the system of equations represented by Eq. (3.9) represents *N-1*equations with *N-1* unknowns, namely $u_2, u_3 ..... u_N$. We can write this system in more detail as follows. The first equation is $Au_1^{n+1} + Bu_2^{n+1} + Au_3^{n+1} = K_2$

However, $u_1 = 0$. Thus the above equation becomes $Bu_2^{n+1} + Au_3^{n+1} = K_2$

The last equation in the system represented by Eq. (3.9) is

$$Au_{N-1}^{n+1} + Bu_N^{n+1} + Au_{N+1}^{n+1} = K_N \qquad (3)$$

However, $u_{N+1} = 1$. Thus, Eq. (3.11) becomes

$$Au_N^{n+1} + Bu_N^{n+1} = K_N - Au_e \qquad (4)$$

With this, the system of equations represented by Eq. (4) can be written, in matrix form, as

$$\begin{pmatrix} B & A & 0 & 0 & 0 & 0 & 0 & 0 & 0 \\ A & B & A & 0 & 0 & 0 & 0 & 0 & 0 \\ 0 & A & B & A & 0 & 0 & 0 & 0 & 0 \\ 0 & 0 & A & B & A & 0 & 0 & 0 & 0 \\ & & & \cdots & & & & & \\ & & & & \cdots & & & & \\ & & & & & \cdots & & & \\ 0 & 0 & 0 & 0 & 0 & 0 & A & B & A \\ 0 & 0 & 0 & 0 & 0 & 0 & 0 & A & B \end{pmatrix} \begin{pmatrix} u_2^{n+1} \\ u_3^{n+1} \\ u_4^{n+1} \\ u_5^{n+1} \\ . \\ . \\ . \\ u_{N-1}^{n+1} \\ u_N^{n+1} \end{pmatrix} = \begin{pmatrix} K_2 \\ K_3 \\ K_4 \\ K_5 \\ . \\ . \\ . \\ K_{N-1} \\ K_N - Au_e \end{pmatrix} \qquad (5)$$

Clearly, the system represented by Eq. (5) is in tridiagonal form. It can be solved using Thomas' algorithm.

After applying Thomas' algorithm to the system of equations represented by Eq. (5), we have the solution for $u_2^{n+1}, u_3^{n+1}, ..., u_n^{n+1}$. These are the values of the velocities at the time step $n+1$. The whole process is then repeated for a number of time steps until the velocity profile converges to a steady state.

For our specific solution, we choose to use 21 grid points across the flow, $N+1 = 21$. Since y is non-

dimensional, it varies from 0 to 1; hence $\Delta y = \frac{1}{20}$

The Crank-Nicolson technique is *unconditionally stable; i.e.,* it is stable for *all* values of Δt . This is the main advantage of an implicit method. That is, stability considerations tell us that we can use as large a value of Δt .

$$\frac{\alpha \Delta t}{(\Delta x)^2} \leq \frac{1}{2}$$

For our present implicit method, we will calculate Δt as

$\Delta t = E\,\mathrm{Re}_D (\Delta y)^2$

where *E is* a parameter. Since the Crank Nicolson technique is unconditionally stable, we could choose *E* to be *any* value. But We take*E* is varied from 1 to 4000.

The definition of *E* given by implicit Crank Nicolson method, namely,

$$E = \frac{\Delta t}{\mathrm{Re}_D (\Delta y)^2} \qquad (5)$$

We now simplify the coefficients that appear in Eq.(5) for our Couttee flow.

For the first time step n = 1. We choose $E = 1$ and $\mathrm{Re}_D = 5000$. Also, since we are using 21 grid points across the flow, $\Delta y = \frac{1}{20} = 0.05$. With these values, we have for Δt from Eq. (5),

$$\Delta t = E\,\mathrm{Re}_D \left(\Delta y^2\right) = 1(5000)(0.05)^2 = 12.5$$

$$A = -\frac{E}{2} = -0.51 \quad B = 2$$

These are the values of *A* and *B* that appear in the following system of equations

We now invoke Thomas' algorithm. We get,

$$2u_2^{n+1} - 0.5u_3^{n+1} = K_2$$

From initial conditions $u_1^n = u_2^n = u_3^n = 0$, we have

$$K_2 = (1-E)u_2^n + \frac{E}{2}\left(u_3^n + u_1^n\right) = 0$$

So Eq. (3.18) becomes

$$2u_2^{n+1} - 0.5u_3^{n+1} = 0$$

The second line in Eq. (3.15) is

$$-0.5u_2^{n+1} + 2u_3^{n+1} - 0.5u_4^{n+1} = K_3$$

where, since $u_2^n = u_3^n = u_4^n = 0$,

$$K_3 = (1-E)u_3^n + \frac{E}{2}\left(u_4^n + u_2^n\right) = 0$$

it becomes,

$$-0.5u_2^{n+1} + 2u_3^{n+1} - 0.5u_4^{n+1} = 0$$

Converting tridiagonal to bi-diagonal matrix by applying the Thomas algorithm

$$d_i' = d_i - \frac{b_i a_{i-1}}{d_{i-1}'} \qquad (6)$$

when applied to Eq. (6) becomes

$$d_3' = d_3 - \frac{b_3 a_2}{d_2'}$$

From the coefficients in Eq.(6) , we have $d_3 = 2$, $b_3 = -0.5$, $a_2 = -0.5$, and $d_2' = 2$. We have,

$$d_3' = 2 - \frac{-0.5(-0.5)}{2} = 1.875$$

Similarly, from Thomas algorithm,

$$c_i' = c_i - \frac{c_{i-1}' b_i}{d_{i-1}'}$$

when applied to Eq. (6) becomes

$$c_3' = c_3 - \frac{c_2' b_2}{d_2'}$$

From the values of d_3' and c_3' obtained above, the new, bi-diagonal form of Eq. (6)ecomes

$$1.875u_3^{n+1} - 0.5u_4^{n+1} = 0$$

Let us proceed to the third line ,

$$-0.5u_3^{n+1} + 2u_4^{n+1} - 0.5u_5^{n+1} = K_4$$

Since $u_3^n = u_4^n = u_5^n = 0$ then $K_4 = 0$, and it becomes,

$$-0.5u_3^{n+1} + 2u_4^{n+1} - 0.5u_5^{n+1} = 0$$

It Can be put in bi-diagonal form as follows, $d_4' = d_4 - \frac{b_4 a_3}{d_3'}$

The values in Eq. (3.24) are obtained from the coefficients in Eqs.(6) as follows: $d_4 = 2$, $b_4 = -0.5$, $a_3 = -0.5$ and $d_3' = 1.875$. Hence

$$d_4' = 2 - \frac{-0.5(-0.5)}{1.875} = 1.867 \qquad c_4' = c_4 - \frac{c_3' b_4}{d_3'}$$

Then we have $c_4 = 0$, $c_3' = 0$, $b_4 = -0.5$ and $d_3' = 1.875$. Thus, $c_4' = 0$

From the values of d_4' and c_4' obtained above, the new, bi-diagonal form of Eq.

$$1.867u_4^{n+1} - 0.5u_5^{n+1} = 0$$

For the remaining bi-diagonalization of the system given by Eq., the coefficients turn out to be exactly the same (to three significant figures) as calculated above, except for the last line in Eq. This last line corresponds to the equation

$$-0.5u_{19}^{n+1} + 2u_{20}^{n+1} = K_{20} - (-0.5)u_e \qquad (7)$$

where, from Eq.,

$$K_{20} = (1 - \mathrm{E})u_{20}^n + \frac{E}{2}\left(u_{21}^n + u_{19}^n\right) \qquad (8)$$

From the initial conditions, we have $u_{19}^n = 0$, $u_{20}^n = 0$ and $u_{21}^n = 1$. Hence, from Eq. (8),

$$K_{20} = 0.5$$

and Eq. (7) becomes,

$$-0.5u_{19}^{n+1} + 2u_{20}^{n+1} = 1.0$$

the above values are written as

$$d_{20}' = d_{20} - \frac{b_{20} a_{19}}{d_{19}'}$$

where $d_{20} = 2$, $b_{20} = -0.5$, $a_{19} = -0.5$ and $d_{19}' = 1.866$. Thus

$$d_{20}' = 2 - \frac{-0.5(-0.5)}{1.866} = 1.866$$

From Eq. (9) ,we have

$$c_{20}^{'} = c_{20} - \frac{c_{19}^{'} b_{20}}{d_{19}^{'}}$$

where in Eq. $c_{20} = 1.0$, $c_{19}^{'} = 0$, $b_{20} = -0.5$ and $d_{19}^{'} = 1.866$. Thus, from Eq. , we have

$c_{20}^{'} = 1.0$

With this, Eq. (7) becomes, in upper bi-diagonal form, $1.866 u_{20}^{n+1} = 1.0$

To solve for the velocities u_j^{n+1}, $j = 2$ to 20,. Obviously, u_{20}^{n+1} can be obtained directly from Eq. as

$$u_{20}^{n+1} = \frac{1.0}{1.866} = 0.536$$

this result is *exactly the* same that is obtained for all diagonal elements,

$$u_m = \frac{c_m^{'}}{d_m^{'}}$$

Now by again Thomas algorithm,

$$u_i = \frac{c_i^{'} - a_i u_{i+1}}{d_i^{'}} \qquad (3.32)$$

For $j = 19$,

$$u_{19}^{n+1} = \frac{c_{19}^{'} - a_{19} u_{20}}{d_{19}^{'}} \qquad (3.33)$$

In Eq. (3.33), we have $c_{19}^{'} = 0$, $a_{19} = -0.5$, $u_{20} = 0.536$ and $d_{19}^{'} = 1.866$. Thus, from Eq. (3.33),

$$u_{19}^{n+1} = \frac{0 - (-0.5)(0.536)}{1.866} = 0.144$$

The remaining velocities, $u_{18}, u_{17}, ..., u_2$ are calculated in the back substitution method.

The numbers for $b_j, d_j^{'}, \mathrm{a}_j,$. and $c_j^{'}$ are found in this same manner along with the corresponding calculated velocities u_j. $u_{19} = 0.144$. whereas the subscript $j = 19$ is used in our present calculation.

The velocities calculated in the above for all j= 1, 2, ..., 21 represent the velocity profile in the unsteady Couette flow after time t reaches 21. The above calculations are subsequently carried out for a number of time steps until the velocity profile reaches a steady state.

From the above numerical experiment associated with increasing the value of Δt , we can make the following conclusion regarding the behavior of the Crank-Nicolson implicit method as applied to the present problem: By simply increasing the value of Δt (that is, increasing e), we first see a reduction in the number of time steps required to obtain a steady-state; this is consistent with the practical advantage of using an implicit method. However, for a large-enough value of in Δt (the present results, for E>5), the trend reverses itself, and as E increases further, more (not less) time steps are required to obtain the steady state. When we reach this condition, the practical value of using an implicit method is lost. In other words, there is some optimum value of E which leads to the most efficient implementation of the Crank Nicolson method. For the present results, that optimum value of E is about 1.

Conclusion: The main discretization method in CFD namely, finite difference method was discussed. An incompressible, viscous Couettee flow problem was solved using Implicit finite difference technique namely, Crank Nicolson technique. Crank Nicolson technique is used to reduce the simplified partial differential equation of the incompressible Couettee flow to a tridiagonal system of linear, simultaneous, algebraic equations.

Then the tri-diagonal system of equations is reduced to the upper bi-diagonal system of equations by means of Thomas algorithm. The solution for the first time step of the given system of equations

are determined easily using the backward substitution method.

"Java coding" was developed to find the first time step values of the given incompressible, viscousCouette flow problem and also developed the Java coding for generating a tri diagonal matrix. The output of two programs are executed and compared with the values found are same.

References:

1. Anderson, John D., Jr.: Computational Fluid Dynamics-The Basics with Applications, McGraw-Hill, New York, 1995.
2. Anderson, John D., Jr.: Hypersonic and High Temperature Gas Dynamics, McGraw-Hill, New York, 1989.
3. Anil W. Date: Introduction to Computational Fluid Dynamics, Cambridge University Press, New York, 2005.
4. Algorithmic Trends in Computational Fluid Dynamics, Springer-Verlag Inc., New York, 1993.
5. Anderson, John D., Jr.: The History of Aerodynamics, and Its Impact on Flying Machines, Cambridge University Press, New York ,1998.

***

Evolutionary Analysis for Optimization Model with the Design of Job Shop Scheduling

K. Bharathi, Department of Mathematics, Sri Chandrasekharendra Saraswathi Viswa Mahavidyalaya, Kanchipuram, India.

E-mail:03bharathi@gmail.com

C. Vijayalakshmi, SAS, Mathematics Division, Vellore Institute of Technology, Chennai, India. E-mail:vijayalakshmi.c@vit.ac.in

Abstract--- A job-shop scheduling is a highly NP-hard type of multi solution optimal problem which is considered as a hard form so as to get an optimal result. The use of a new Evolutionary algorithm is derived from natural genetic represented algorithms to get an optimal solution. The Job shop scheduling was one oft hard optimal type problem with the criterions as to minimize the total make span and to get a reasonable time of completion of each job. A graph based structure effective coding, such as each job operating schedule is Graphical tree shaped which is formed as the structure of the initial solution space. By applying the natural based algorithm and evolutionary operators the optimal criteria is reached.

Keywords--- Job-Shop Scheduling, Evolutionary Algorithms, Genetic Representation, Graphical Tree Shaped, Coding, Make Span.

Subject Classification--- 65K Mathematical Programming, Optimization and Variational Techniques.

I. Introduction

The scheduling presses in the production area are to decide an optimal sequence of the jobs in a order which is termed NP-hard combinatorial problems. That is this type of is named as job-shop scheduling which due to input data space the problem of JSSP takes more time indirect search methods, for problems of any size such complexity is termed as computational optimal problems.

The concept based Multi Objective Optimization models are designed and its distinction from the traditional multi objective problem is discussed. Novel Evolutionary Algorithms are developed for real time applications. The proposed Evolutionary Algorithms are compared with the existing algorithms based on the computational time and the quality of the representations.

The collection of optimization techniques which is functioning based on metaphors of biological processes term evolutionary algorithm (EA). A multi-objective optimization problem (MOOP) has several incompatible objectives with a set of many optimal solutions. A developed set of solutions as population, evolutionary algorithms in multi-objective optimisation (EAMOOP) are able to estimate the Pareto optimal position.

The scheduling process in the production area is to decide an optimal sequence of the jobs in an order is termed NP-hard combinatorial models. That is this type modelled design is named as Job Shop Scheduling due to input data space of JobShop Scheduling takes more time in direct search methods, for models of any size such complexity is termed as computational optimizations designed. A Multi Objective Optimization Problem has several incompatible objectives with a set of many optimal solutions.

A developed set of solutions as population, Evolutionary Algorithms in Multi Objective Optimization are able to estimate the Pareto optimal position. Scheduling has an important role in many fields such as to develop efficiency in production of the manufacturing system. The classification of scheduling is defined as one operating machine; many operating machines such can be defined as Flow shop scheduling and Job shop scheduling. The optimal scheduling as to be attained by the formulation of the mathematical model of multi objective type and solution methods has been applied. The mathematical formulation of this type of process is harder using normal methods there is a turn over to the algorithms proposing such as Tabu search, simulating analysis, bottleneck shifting, genetic algorithms, artificial respired system, swarm analysis and machine learning algorithms.

Received: 5 Feb 2018/Accepted: 15 Mar 2018

II. Job Shop Scheduling Problem

A part of work which is down in a defined order is stated as a Job. The given jobs should be performed in place called shops. A scheduled order of the work in processing order is named as scheduling. The jobs are as a defined finite set where all the jobs have different operations on a series of defined finite number of machines. The machines can handle only one operation at a prescribed amount of time. The operations should be down on the set of machines till the end without an interpretation. The parameters of the JSSP is as 'M' is the Number of machines; N is the Number of jobs; where the jth operation of the ith job is denoted as $O_{i,j}$; The processing time of each operator is as $T_{i,j}$; Starting time of the operators as S_{ij}; The completion time each operations is$C_{i,j}$; End time of each job CT_i and the maximum completion time of all the job as C_{max}.

III. Graphical Tree Shaped solutions space in Evolutionary Algorithm for JSSP

Step 1:A special encoding type of tree graph with node values assigned as follows to enrich the solution space for JSSP are made. Nodes at the first level of the tree are position of machines, the second level is assigned as the operational time and the pendent nodes are completion time of the corresponding jobs.

Step 2: An equally likely method of solution selection are used to produce population initially if the Graphical tree shaped structure can be formed.

Step 3: The operators like crossover and mutation are introduced in Evolutionary algorithms to generate a solution Space.

Step 4: An evaluating system is set up to assess all generate a solution and to select fit enough solutions for the next generation.

Step 5: Step 2 to step 4 is repeated till the optimal criteria is reached.

IV. Graphical Tree Shaped solutions space in Evolutionary Algorithm for JSSP– Example

The table 1 is an example with five machines and three jobs should be down in a following operating sequence.

Table 1: The Operating Sequences

J	O	M1	M2	M3	M4	M5
J1	O11	1	8	3	7	5
	O21	3	5	2	6	4
	O31	6	7	1	4	3
J2	O12	1	4	5	3	8
	O22	2	8	4	9	3
	O32	9	5	1	2	4
J3	O13	1	8	9	3	2
	O23	5	9	2	5	3

STEP 1: Solution encoded as a Graphical tree shaped structure

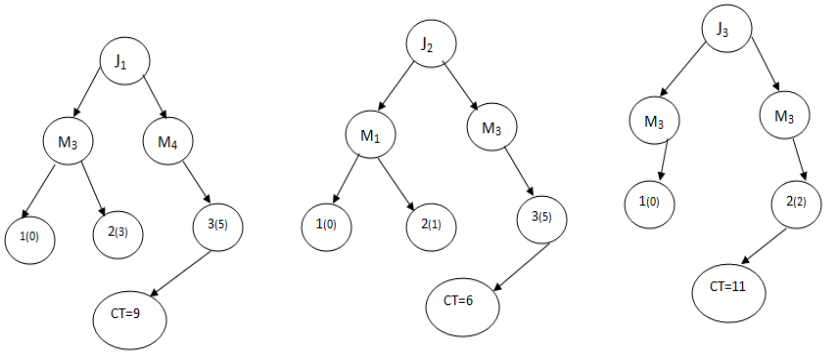


Fig. 1: Solution Graph

ISSN 1943-023X
Received: 5 Feb 2018/Accepted: 15 Mar 2018

STEP 2: From table 1 the solutions are selected and encoded as tree shaped graph with the completion time of the constraint with C_{max} = 11 and with C_{max} = 13as shown in the fig 2 and fig 3 respectively.

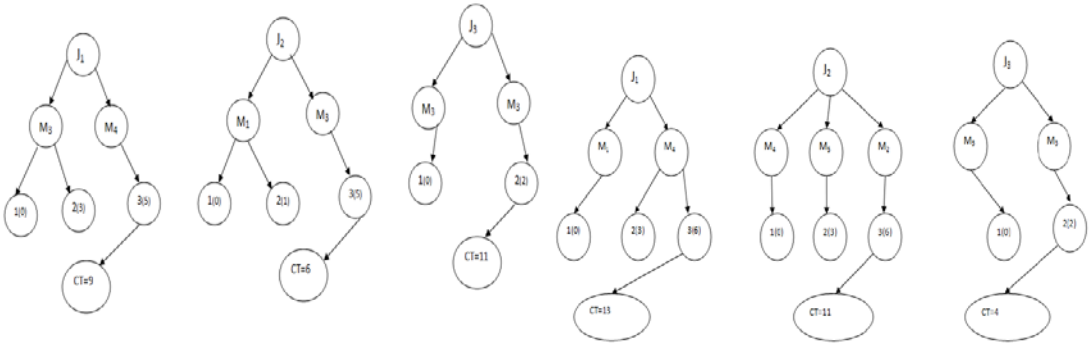


Fig. 2: Parent 1 Fig. 3: Parent 2

STEP 3: The algorithm flows as create the child in the population after generation of parent space of solution as applying crossover at single point and child's are given with child 1 having C_{max}=11 and child 2 having C_{max}=13.

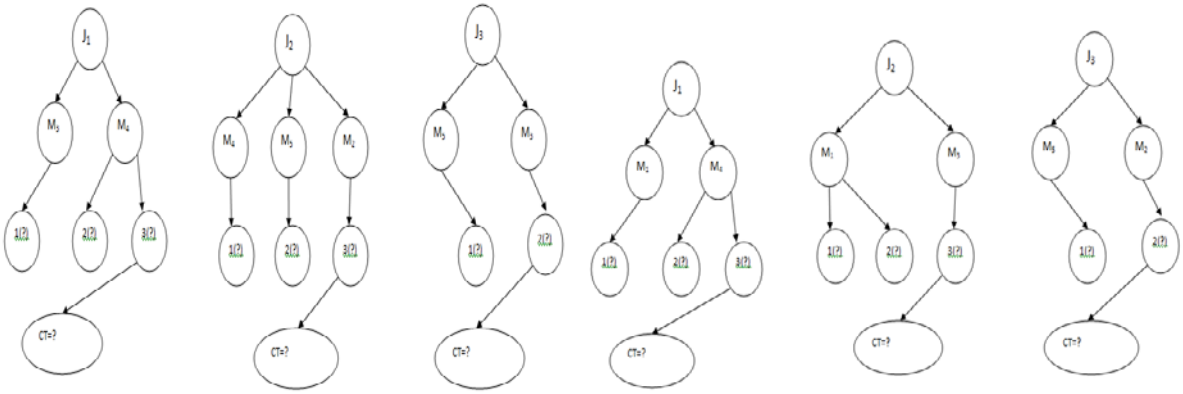


Fig. 4 Fig. 5

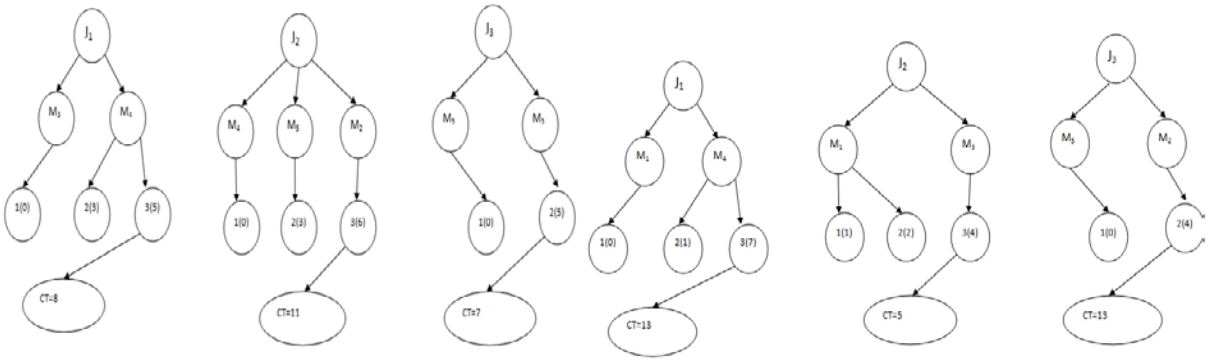


Fig. 6: Child 1 Fig. 7: Child 2

STEP 4: The child solutions after crossover where implied to application of mutation. Mutation is developed as by giving a little change to the jobs and machines with has largest CT and O respectively in the solution space. This operation act as shown infig.8 and fig.9.

ISSN 1943-023X
Received: 5 Feb 2018/Accepted: 15 Mar 2018

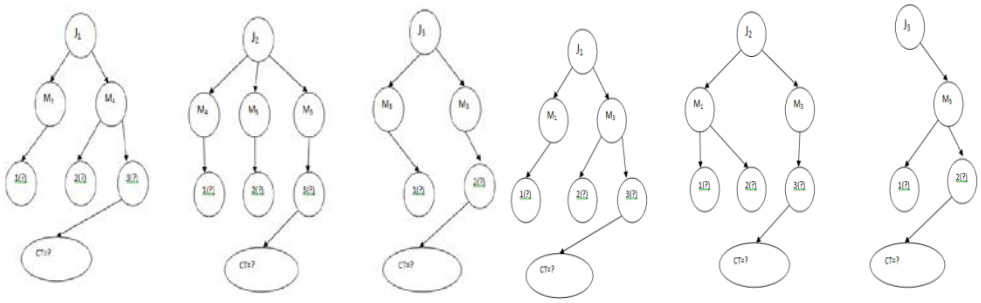


Fig. 8 Fig. 9

STEP 5: The Graphical tree shaped structure solutions of the resulting solution space representation after the different operators applied is shown in the fig.10 and fig.11 with maximum completion times as C_{max}=8 and C_{max}=5.

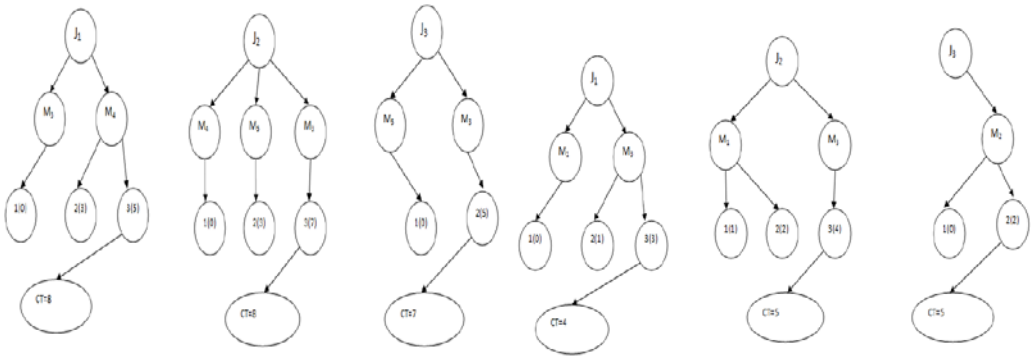


Fig. 10 Fig. 11

A Graphical tree shaped structure solution space with Evolutionary algorithm is derived from natural genetic represented algorithms to get an optimal solution. The Job shop scheduling is defined as a multi objective optimizations problem with the criterions as to minimize the total make span and to get a reasonable time of completion of each job.

V. Comparison of Algorithms

Algorithms	**CT_1**	**CT_2**	**CT_3**	**C_{max}**
Shifting bottleneck	**10**	**11**	**13**	**13**
Genetic algorithm	**9**	**11**	**8**	**11**
Artificial immune system	**9**	**9**	**11**	**11**
Graphical tree shaped- Evolutionary algorithm	**4**	**5**	**5**	**5**

VI. Conclusion

The Application of a Graphical tree shaped solution space in Evolutionary algorithm encoding is derived from natural genetic represented algorithms to get an optimal solution. One of the NP hard division of scheduling problem with multi objective criterions which is named as Job shop scheduling is stated. A Graphical tree shaped effective coding, such as each job operating schedule is Graphical tree shaped which is formed as the structure of the initial solution space. By applying the natural based algorithm and evolutionary operators the optimal criteria is reached. The resulting solution where compared with the existing algorithms.

References

[1] Mohammadi, A., Omidvar, M.N., Li, X. and Deb, K. Integrating user preferences and decomposition methods for many-objective optimization. *IEEE Congress on Evolutionary Computation (CEC),* 2014, 421-428.

Received: 5 Feb 2018/Accepted: 15 Mar 2018

[2] Deb, K. and Jain, H. An evolutionary many-objective optimization algorithm using reference-point-based non dominated sorting approach, part I: Solving problems with box constraints. *IEEE Trans. Evolutionary Computation* **18** (4) (2014) 577-601.

[3] Singh, H.K., Isaacs, A. and Ray, T. A Pareto corner search evolutionary algorithm and dimensionality reduction in many-objective optimization problems. *IEEE Transactions on Evolutionary Computation* **15** (4) (2011) 539-556.

[4] Liu, H.L., Gu, F. and Zhang, Q. Decomposition of a multi objective optimization problem into a number of simple multi objective sub problems. *IEEE Transactions on Evolutionary Computation* **18** (3) (2014) 450-455.

[5] Cheng, J., Yen, G.G. and Zhang, G. A many-objective evolutionary algorithm with enhanced mating and environmental selections. *IEEE Transactions on Evolutionary Computation* **19** (4) (2015) 592-605.

[6] Bharathi, K. and Vijaylakshmi, C. Optimization for flexible job shop scheduling by evolutionary representation. *Ann Pure Appl Math.*, **1** (7) (2014) 29-34.

[7] Bharathi, K. and Vijayalakshmi, C. Implementation of Multi-objective Job Scheduling Algorithms with Evolutionary Representation. International Journal of Applied Engineering Research. *International Journal of Applied Engineering Research* **9** (23) (2014) 19075-19081.

[8] Asafuddoula, M., Ray, T. and Sarker, R. A decomposition-based evolutionary algorithm for many objective optimization. *IEEE Transactions on Evolutionary Computation* **19** (3) (2015) 445-460.

[9] Li, M., Yang, S. and Liu, X. Diversity comparison of Pareto front approximations in many-objective optimization. *IEEE Transactions on Cybernetics* **44** (12) (2014) 2568-2584.

[10] Cheng, R., Olhofer, M. and Jin, Y. Reference vector based a posterior preference articulation for evolutionary multi objective optimization. *IEEE Congress on Evolutionary Computation (CEC),* 2015, 939-946

[11] Cheng, R., Jin, Y., Narukawa, K. and Sendhoff, B. A multi objective evolutionary algorithm using Gaussian process-based inverse modeling. *IEEE Transactions on Evolutionary Computation* **19** (6) (2015) 838-856.

[12] Bandyopadhyay, S. and Mukherjee, A. An algorithm for many-objective optimization with reduced objective computations: A study in differential evolution. *IEEE transactions on Evolutionary Computation* **19** (3) (2015) 400-413.

[13] Zhang, X., Tian, Y. and Jin, Y. A knee point-driven evolutionary algorithm for many-objective optimization. *IEEE Transactions on Evolutionary Computation* **19** (6) (2015) 761-776.

[14] Zhang, X., Tian, Y., Cheng, R. and Jin, Y. An efficient approach to non dominated sorting for evolutionary multi objective optimization. *IEEE Transactions on Evolutionary Computation* **19** (2) (2015) 201-213.

[15] Yuan, Y., Xu, H., Wang, B., Zhang, B. and Yao, X. Balancing convergence and diversity in decomposition-based many-objective optimizers. *IEEE Transactions on Evolutionary Computation* **20** (2) (2016) 180-198.

Received: 5 Feb 2018/Accepted: 15 Mar 2018

DESIGN AND REVIEW OF OPTIMIZATION USING EVOLUTIONARY ALGORITHMS

K.Bharathi
Department of Mathematics,
Sri Chandrasekharendra Saraswathi Viswa Mahavidyalaya, Kanchipuram.
03bharathi@gmail.com
C.Vijayalakshmi
SAS, Mathematics Division, VIT, Chennai
vijayalakshmi.c@vit.ac.in

Abstract: The applications of Evolutionary Algorithms in Multi Objective Optimization are currently receiving growing interest from researchers with various backgrounds. Most research in this area has understandably concentrated on the selection stage of Evolutionary Algorithms, due to the need to integrate victories performance measures with the inherently scalar way in which Evolutionary Algorithms reward individual performance. In this review work, current multi objective evolutionary approaches are discussed, ranging from the conventional analytical aggregation of the different objectives into a single function to a number of population based approaches.

Keywords: Algorithms, Evolutionary Algorithm, Multi-Objective Optimization Problem, Pareto Evolutionary Model, Travelling Salesman Model.

1. Introduction: Evolutionary algorithms (EAs) are the machine learning approaches from natural collection in the biological world. EAs vary from more established optimization techniques, where EAs involve a set of solutions called population. The iterations of an EA involve an aggressive selection that includes feasible solutions. The set of solutions where operated by using one are more operations to get a best optimal solution. If we have more than one criterion to be optimized with several conditions said to be constraint equation such a problem is named as Multi-objective optimization.

A computational model is a mathematical object representing a collection of questions that might be able to solve by a computer. It can be viewed as an infinite collection of instances together with solution for every instance. The calculations are to be done by taking a set of data as input, using the input values the operating machine can proceeds with its calculations and gives an acceptable solution set as output data. A finite sequence of states of a real values discretely distributed in time, the real values as an abstract computational model having a restricted rate of performance of the operations, a restricted number of digit places to form a number and a restricted storage capacity.

2. Evolutionary Models:

2.1 Pareto Evolutionary Models: Liu et al. (2014) have in detailed study about multiple optimality condition present in the model of structures of antenna model to get a feasible solution. By applying the evolutionary based iterative process for this multi criteria system running time of the modelled objectives present in the antenna were inter linked with the machine based stimulated values. Li, Zhang, Kwong, Li and Wang (2014) investigate the multi criterion decision model with Morkov condition applied in the technique of policy proceeded. They have applied an algorithm of evolutionary gradient conditions acted as a joint process so as to solve the modelled problem.

2.2 Multi Objective Models using Evolutionary Algorithms: Li, Deb, Zhang and Kwong (2015) designed an algorithm so as to balance the convergence and diversity points present in multi objective model evolutionary based approaches. The designed model of algorithm was applied on a multi criteria based with more than fifteen objective functions to be optimized simultaneously. The model balance the

point of convergence and diversity in the optimal value when compared with the existing classical methods to solve a multi objective optimization model. The results was compared with the traditional methods.

Mohammadi et al. (2014) proposed an algorithm of evolutionary preformed application with user method. This designed model of process was used in multi criteria optimality algorithms. Many real world modelled problems was communicated and the results were analyses. The implied algorithm was compared with existing models. Li, Kwong, Zhang and Deb (2015) addressed the sub problems present in multi optimal methods using inter relative preferences with involved solutions of the divisions. In all generated population solutions the methodology of the inter relative preferences was applied to get an optimality. By applying the proposed algorithm diversity of the solution is minimized with increased in solution convergence. The output was compare with empirical methods.

Wang et al. (2015) proposed a novel of two arch algorithms based on multi objective evolutionary approaches for multi model objective function. The design of two arch processes selects the different norms of pareto and indicator based operation models. Many benchmark problems was evaluated using two arch algorithm and the results were compared the traditional methods. Wang et al. (2016) applied constraint property to the sub problems decomposed from the evolutionary multi modelled optimization. The new applied constraints were evaluated by applying operators of evolutionary process and decomposed solution is derived. The new model was tested with the numerical examples with comparison.

Cheng, Olhofer and Jin (2015) proposed a articulation of reference based vector performance to the selected set of solutions from the pareto front approach. Here the selection of solution was done by the logical constraints created by the decision making process. By applying this method the convergence of the optimal results for the multi objective model was achieved. Bandyopadhyay and Mukherjee (2015) designed a new algorithm based on differential multi objective evolutionary models applications with additional technique. The process of checking convergence of optimality in every position of the flow is vital part. Many benchmark problems was evaluated using algorithm based on differential multi objective evolutionary models and the results were compared the traditional methods.

Cheng, Jin, Narukawa and Sendhoff (2015) modelled an non dominated solution in search of multi mode representation using construct process involving gaussian methods. An inverse model of gaussian process creates the new solution set for optimality. The proposed method run in an robust performance and give the optimality. The modelled algorithm was compared with existing models.

Zhang et al. (2018) proposed an innovative method of platform tension leg programming for multi modelled optimization techniques. The real world designed model of multi objective optimality process was developed and applied the proposed programming method. The results of applying innovating platform tension leg programming method was efficient enough by attaining the optimality criteria of the multi modelled process. This method reduces the dynamic model error values obtained in the classical methods. The proposed model was sufficient enough to attained the minimized total weight platform for the multi objective model.

Biswas et al. (2018) introduced an evolutionary modelled application of windfarm layout as a multi objective optimization method. Here the objectives are to minimize the maximum power out released by the wind in the layout and to minimize the structure of windfarm. The designed model applying evolutionary approach an efficient solution was obtained. Ramli et al. (2018) designed a multi objective model of solar energy power system and wind energy system to be optimized. By applying a self adaptive evolutionary differential method of algorithm to the proposed method an set of feasibility was obtained. The modelled problem was based on real world application of jobs with machines.

2.3 Travelling Salesman Model: Mohammadpour and Yadollahi (2014) worked based on two approaches of scheduling the salesman in appropriate places with many conditions involved. The

approaches was to fix the cites and visited of the salesman designed. By this method the multi valued variable was transformed to single objective model and genetic operators was introduced to attain optimality. The proposed model was tested with examples and compared. Nodehi et al. (2016) proposed a revised generation evolutionary services algorithm to solve a travelling salesman model. The model of heuristic approaches the nearest optimized solution to the complex model. The design of the algorithm was tested with numerical example.

Odili and Mohmad Kahar (2016) introduced a meta heuristic model of african buffalo optimality condition applied algorithm for travelling salesman approaches. The behavior of buffalo in forest was used as a inter linked step in the process of algorithm. Applying this methodology many real model of travelling salesman was solved.

Ponraj and Amalanathan (2014) and Bolan˜os et al. (2016) presented a changed genetic algorithm for the multi modelled travelling salesman. The refined selection of initial set population generating was implemented to the process. The proposed model was applied for many benchmark methods and compared with the existing algorithm.

Huang et al. (2014) describes an optimization process applied with graphics processing unit improved model to generate a good schedule for travelling salesman. The developed method was used to solve practical applied models and solutions were compared.

3. Conclusion: A multi-objective optimization problem has many complicated objectives with a set of Pareto optimal solutions. The way developed by set of solutions as population, evolutionary algorithms in multi- objective optimisation where estimates the Pareto optimal position. Here we deal with a general overview of Evolutionary algorithms to Multi objective optimizations in the past sixteen years. We have discussed the algorithms, methodology used, applied field and significant work where briefly given. Also the most delegate existing study trends were discussed, and provided the advantages present in using EAs in the different fields.

References:

1. Ahmed, M. M., Khan, A. R., Ahmed, F. and Uddin, M. S. (2016), 'Incessant allocation method for solving transportation problems', *American Journal of Operations Research* **6**(03), 236.
2. Bandyopadhyay, S. and Mukherjee, A. (2015), 'An algorithm for many-objective optimization with reduced objective computations: A study in differential evolution', *IEEE transactions on Evolutionary Computation* **19**(3), 400–413.
3. Bechikh, S., Elarbi, M. and Said, L. B. (2017), Many-objective optimization using evolutionary algorithms: a survey, *in* 'Recent Advances in Evolutionary Multi-objective Optimization', Springer, pp. 105–137.
4. Bharathi, K and Vijayalakshmi, C., 2014. Implementation of Multi-objective Job Scheduling Algorithms with Evolutionary Representation. International Journal of Applied Engineering Research, 9(23), 19075-19081.
5. Bharathi, K and Vijayalakshmi, C., 2016. Optimization of Multi-objective Transportation Problem Using Evolutionary Algorithms. Global Journal of Pure and Applied Mathematics, 12(2), 1387-1396.
6. Bharathi, K and Vijayalakshmi, C., 2016. A Framework for the Design and Analysis of an Evolutionary Algorithm for Multi Travelling Salesman Problem. Indian Journal of Science and Technology, 9(48), 1-4.
7. Biswas, P. P., Suganthan, P. and Amaratunga, G. A. (2018), 'Decomposition based multi-objective evolutionary algorithm for windfarm layout optimization', *Renewable Energy* **115**, 326–337.
8. Bolaños, R. et al. (2016), 'A population-based algorithm for the multi travelling salesman problem', *International Journal of Industrial Engineering Computations* **7**(2), 245–256.
9. Branco, R. M., Coelho, A. S. and Mayerle, S. F. (2016), 'Hybrid genetic algorithms: solutions in realistic dynamic and setup dependent job-shop scheduling problems', *International Journal of Production Management and Engineering* **4**(2), 75–85.

10. Brands, T. and Van Berkum, E. C. (2014), 'Performance of a genetic algorithm for solving the multi-objective, multimodel transportation network design problem', *International journal of transportation* **2**(1), 1–20.
11. Centobelli, P., Converso, G., Murino, T. and Santillo, L. (2016), 'Flow shop scheduling algorithm to optimize warehouse activities', *International Journal of Industrial Engineering Computations* **7**(1), 49–66.
12. Chakroborty, S. and Hasan, M. B. (2016), 'A chronicle of analyzing stochasticity in multi period transportation problems for uncertainty', *International Journal of Computer Applications* **133**(8), 5–9.
13. Cheng, J., Yen, G. G. and Zhang, G. (2015), 'A many-objective evolutionary algorithm with enhanced mating and environmental selections', *IEEE Transactions on Evolutionary Computation* **19**(4), 592–605.
14. Cheng, R., Jin, Y., Narukawa, K. and Sendhoff, B. (2015), 'A multiobjective evolutionary algorithm using gaussian process-based inverse modeling', *IEEE Transactions on Evolutionary Computation* **19**(6), 838–856.
15. Cheng, R., Olhofer, M. and Jin, Y. (2015), Reference vector based a posteriori preference articulation for evolutionary multiobjective optimization, *in* 'Evolutionary Computation (CEC), 2015 IEEE Congress on', IEEE, pp. 939–946.
16. Deb, K. and Jain, H. (2014), 'An evolutionary many-objective optimization algorithm using reference-point-based nondominated sorting approach, part i: Solving problems with box constraints.', *IEEE Trans. Evolutionary Computation* **18**(4), 577–601.
17. Elarbi, M., Bechikh, S., Said, L. B. and Datta, R. (2017), Multi-objective optimization: Classical and evolutionary approaches, *in* 'Recent Advances in Evolutionary Multi- objective Optimization', Springer, pp. 1–30.
18. Jorapur, V. S., Puranik, V. S., Deshpande, A. S. and Sharma, M. (2016), 'A promising initial population based genetic algorithm for job shop scheduling problem', *Journal of Software Engineering and Applications* **9**(05), 208.
19. Kapsoulis, D., Tsiakas, K., Trompoukis, X., Asouti, V. and Giannakoglou, K. (2018), 'Evolutionary multi-objective optimization assisted by metamodels, kernel pca and multi-criteria decision making techniques with applications in aerodynamics', *Applied Soft Computing* **64**, 1–13.
20. Khan, A. R., Vilcu, A., Uddin, M. S. and Ungureanu, F. (2015), 'A competent algorithm to find the initial basic feasible solution of cost minimization transportation problem', *Buletinul Institutului Politehnic Din Iasi, Romania, Sec¸tia Automatica si Calculatoare* pp. 71–83.

***

SOME RELATIONS ON A RIGHT NEAR IDEMPOTENT SEMIGROUP

T.N.Kavitha
Assistant Professor of Mathematics, SCSVMV, Kanchipuram, Tamilnadu
A.Jayalakshmi
Professor of Mathematics(Retd), Kanchipuram, Tamilnadu

Abstract: In a previous paper we introduced a near idempotent semigroup and studied its structure through the relations λ, ρ and δ. In this paper, we introduce a new pair of relations λ_r and ρ_r on a near idempotent semigroup. The relation λ_r is not an equivalence relation on a near idempotent semigroup S. It is easy to check that λ_r is not in general, reflexive on a near idempotent semigroup. We prove that $\lambda_r$is reflexive on a near idempotent semigroup S if and only if $xy = xy^2$ for all x, y in S. This prompted us to define a right near idempotent element and a right near idempotent semigroup.λ_r is a right congruence and $\rho_r$is a left congruence on a right near idempotent semigroup S. We prove that a near idempotent semigroup S is a right near idempotent semigroup if and only if $\rho_r = \rho$ on S.In a right near idempotent semigroupS , Every λ_r (ρ_r) - class is a subsemigroup of S.

Keywords: Equivalence Relations, Inflation, Left Zero Semigroup, Near Idempotent Semigroup, Right Near Idempotent Semigroup.

1. Introduction: In a previous paper we introduced a near idempotent semigroup[2] and studied its structure through the relations λ, ρ and δ. In this paper, we define the relations λ_r and ρ_r on a near idempotent semigroup. We prove that λ_r is not in general,reflexive on a near idempotent semigroupand hence not an equivalence relation and we find necessary and sufficient condition for λ_r to be reflexive on near idempotent semigroup and this led to the definition of right near idempotent semigroup.

1.1 Definition [2]: Let S be a semigroup and 'a' an element of S. 'a' is said to be a near – idempotent element of S if $xa^2y = xay$ for all x, y in S.

1.2 Definition [2]: A semigroup S is called a near idempotent semigroup if every element of S is near idempotent element of S.

2. Relations on a Near Idempotent Semigroup:

2.1 Definition [2]: Let S be a near- idempotent semigroup and a and b, elements of S. We define the relations λ and ρ on S as follows:

a λ b if and only if $xaby = xay$ and $xbay = xby$ for all $x, y \in S$

a ρ b if and only if $xaby = xby$ and $xbay = xay$ for all $x, y \in S$.

Both λ and ρ turn out to be equivalence relations on S. It is easy to check that λ is a right congruence and ρ is a left congruence relation on S.

2.2 Definition: Let S be a near idempotent semigroup. For a, b ∈ S, we define

1. a λ_rb if and only if $xab = xa$ and $xba = xb$ for all $x \in S$
2. a ρ_rb if and only if $xab = xb$ and $xba = xa$ for all $x \in S$

It is easy to prove the following lemmas

2.3 Lemma: Let S be a near idempotent semigroup. The relation $\lambda_r$on S defined in 2.2 is symmetric and transitive on S.

2.4 Lemma: Let S be a near idempotent semigroup. Let λ_r be defined on S as above.
Let $a \in S$. If a λ_rb for some $b \in S$, then a λ_ra

2.5 Remark: Lemma 2.4 simply means that if an element a of a near – idempotent semigroup S is λ_r - related to some element of S, then it is λ_r - related to itself.

In what follows, we find necessary and sufficient conditions under which an element of a near idempotent semigroup S is related to itself under λ_r.

2.6 Lemma: Let S be a near idempotent semigroup and $a \in S$. Then $a\lambda_r a$ if and only if $xa = xa^2$ for all x in S.

The following lemma gives a necessary and sufficient condition for the relation $\lambda_r$to be reflexive on a near idempotent semigroup S.

2.7 Lemma: The relation λ_r is reflexive on a near idempotent semigroup S if and only if $xy = xy^2$ for all x, y in S.
From lemma 2.3 and 2.7, we get

2.8 Remark: Let S be a near idempotent semigroup satisfying the identity $xy = xy^2$ for all x, y in S. Then λ_r is an equivalence relation on S

The above leads us to the definition of a right near idempotent element and a right near idempotent semigroup.

3. Right Near Idempotent Semigroup:
3.1 Definition: Let S be a semigroup and a an element of S. a is said to be a right near – idempotent element of S if $xa^2 = xa$ for all x in S.

3.2 Definition (RNIS): A semigroup S is called a right near idempotent semigroup if every element of S is right near idempotent element of S.

3.3 Remark: It is easy to see that a Right Near Idempotent Semigroup is a Near Idempotent seomigroup but a Near Idempotent semigroup is not necessarily a Right Idempotent semigroup.

4. The Relations $\lambda_r$andρ_r on A Right Near Idempotent Semigroup: We now define the relations $\lambda_r$and ρ_r on a right near idempotent semigroup as follows

4.1 Definition: Let S be a right near- idempotent semigroup and a and b, elements of S. We define the relations $\lambda_r$andρ_r on S as follows:
$a\lambda_r b$ if and only if $xab = xa$ and $xba = xb$ for all $x \in S$.

$a\rho_r b$ if and only if $xab = xb$ and $xba = xa$ for all $x \in S$.
The above relations$\lambda_r$and ρ_r are equivalence relations on a right near idempotent semigroup S. It is easy to verify that λ_r is a right congruence and $\rho_r$is a left congruence on a right near idempotent semigroup S.

4.2 Lemma: λ_r is a right congruence and $\rho_r$is a left congruence on a right near idempotent semigroup S.
Proof: Let $a\ \lambda_r\ b$ where $a, b \in S$.
We claim that for any $c \in S$, $ac\ \lambda_r bc$.
$a\ \lambda_r\ b \Rightarrow xab = xa$ and $xba = xb$ for all $x \in S$
Then for all $x \in S$, we have
$xacbc = xacbc = xabcbc = x\,a\,(bc)^2 = xabc$ (by the definition of S)
$= xabc = xac$
and
$xbc\,ac = x\,b\,cac = x\,bacac = xb\,(ac)^2 = x\,b\,ac$ (by the definition of S)

$= x\,ba\,c = xbc$

leading to $ac\ \lambda_r bc$ for all $c \in S$
Hence λ_r is a right congruence on S.
Similarly, ρ_r is a left congruence relation on S.
In what follows, we prove that a near idempotent semigroup in which $\rho = \rho_r$ is a right near idempotent semigroup.

4.3 Lemma: $\rho_r \subset \rho$ in a near idempotent semigroup.[by definition 2.1 and 2.2]
Proof: Let S be a near idempotent semigroup. Let $a, b \in S$.
$a\ \rho_r\ b \Rightarrow xab = xb$ and $xba = xa$ for all $x \in S$
$\Rightarrow xaby = xby$ and $xbay = xay$ for all x, y in $S \Rightarrow a\ \rho\ b$

4.4 Lemma: Let $\rho_r = \rho$ in a near idempotent semigroup S. Then S is a right near idempotent semigroup.
Proof: Let S be a near idempotent semigroup in which $\rho_r = \rho$.
Let $a \in S$. Then $xay = xa^2y$ for all x, y ,$a \in S$. This means that $a\ \rho\ a^2$. By the hypothesis of the theorem, $\rho_r = \rho$, so that $a\ \rho_r\ a^2$.
Hence for all x in S, $x\,a^3 = x\,a\,a^2 = x\,a^2$ and $x\,a^3 = x\,a^2\,a = x\,a$, so that $xa^2 = xa^3 = xa$ for all x, a in S.
Thus S is a right near idempotent semigroup.

4.5 Lemma: In a right near idempotent semigroup S, ρ and ρ_r are identical.
Proof: Let $a, b \in S$ such that $a\ \rho\ b$
Then $xaby = xby$ and $xbay = xay$ for all x, y in S. Replace y by b
Hence $xab^2 = xb^2$ for all x so that we get $xab = xb$ for all x in S. -------(1)
Also $xbay = xay$ for all x, y in S. Replacing y by a
We get $xba^2 = xa^2$, so that $xba = xa$ for all x in S. ----(2)
from (1) and (2) we get $xab = xbxba = xa$ for all x in S.
Therefore $a\ \rho_r b$
Therefore $\rho \subset \rho_r$ .....(3)
Conversely, $a\ \rho_r b$ implies that for all x in S, $xab = xbxba = xa$, which, in turn,
implies that $xaby = xbyxbay = xay$ for all x, y in S.
Thus $a\ \rho\ b$
Hence we get $\rho_r \subset \rho$ .....(4)
From (3) and (4) we get $\rho = \rho_r$ in a right near idempotent semigroup S.
By lemma 4.5 and lemma 4.4, we get

4.6 Theorem: A near idempotent semigroup S is a right near idempotent semigroup if and only if $\rho_r = \rho$ on S.

4.7 Lemma: In a right near idempotent semigroupS , Every $\lambda_r(\rho_r)$ - class is a subsemigroup of S.
Proof: Let S be a right near – idempotent semigroup Consider the relation λ_r on right near idempotent semigroup S.
For $a, b \in R$
$a\ \lambda_r\ b$ if and only if $xab = xa$ and $xba = xb$ for all $x \in S$.
Consider an equivalence class λ_{r_a} where $a \in S$
We claim that λ_{r_a} is a subsemigroupof S.
Let $u,v \in \lambda_{r_a}$
$a\ \lambda_r\ u$ and $a\ \lambda_r\ v$
Also by transitivity $u\lambda_r\ v$
For all $x \in S$
$xuv\,a = xu.\,va = xuv$
and
$xauv = xau.v = xav = xa$

Hence $uv\lambda_r a$, so that $uv \in \lambda_{r_a}$

Thus λ_{r_a} is a subsemigroupof S.

Also xuv = xu and xvu = xv for all x in S, and hence for all x in λ_{r_a}.

Thus for x, y, z $\in \lambda_{r_a}$

xyz =xy

Thus λ_{r_a} is a semigroup satisfying the identity xyz = xy

In the following example we exhibit λ_r classes of a right near idempotent semigroup.

4.8 Example: Consider the set S = {1, 2, 3, 4 } under the operation $a * b = a^b \pmod 2$
The multiplication table given below shows that S is a semigroup.

*	1	2	3	4
1	1	1	1	1
2	2	2	2	2
3	1	1	1	1
4	2	2	2	2

Here in this example the elements 1 and 2 are idempotent elements, so that they are right near idempotent elements as well.
$x.3^2 = x.1 = x.3$ (from the table)
Therefore 3 is a right near idempotent element
$x.4^2 = x.2 = x.4$ (from the table)
Therefore 4 is a right near idempotent element.
Also,
x.1.2 = x.1 & x.2.1 = x.2 for all x in S. Therefore $1 \lambda_r 2$
x.1.3 = x.1 & x.3.1 = x.1 = x.3 for all x in S. Therefore $1\lambda_r 3$
x.1.4 = x.1 & x.4.1 = x.2 = x.4 for all x in S. Therefore $1\lambda_r 4$
x.2.3 = x.2 & x.3.2 = x.1 = x.3 for all x in S. Therefore $2\lambda_r 3$
x.2.4 = x.2 & x.4.2 = x.2 = x.4 for all x in S. Therefore $2\lambda_r 4$
x.3.4 = x.1 = x.3 & x.4.3 = x.2 = x.4 for all x in S. Therefore $3\lambda_r 4$
Thus all the elements of this right near idempotent semigroupare λ_r- related to each other and hence belong to the same λ_r -class.
These elements satisfies the identity xyz =xy for all x, y, z in S

Remark: A. Jayalakshmi has discussed a semigroup S, satisfy the relation xyz = xy for all x, y, z in S in her doctoral thesis[1].

4. Conclusion: Near- idempotencyand Right near- idempotency are both generalizations of idempotency. We have dealt with right near idempotent semigroup in this paper.We have defined new relations in the Right near idempotent semigroup, and obtained characterizations for right near idempotent semigroup as follows

1. A near idempotent semigroupS is a right near idempotent semigroup if and only if $\lambda_r$is reflexive on S.
2. A near idempotent semigroupS is a right near idempotent semigroup if and only if $\rho_r = \rho$ on S.

References:

1. Jayalakshmi, A., "Some Studies in Algebraic Semigroups and Associated Structures", Doctoral Thesis, Bangalore University, 1981.
2. T.N. Kavitha, A. Jayalakshmi, On near – idempotent semigroups, vol 5, no 5, International Journal of Mathematical Archive, May 2014.

3. Clifford, A.H. and Preston, G.B., "The Algebraic Theory of Semigroups", Vol. I, Providence, 1961
4. Kimura, N.,The Structure of Idempotent Semigroups (I), Pacific J. of Math. (1958).
5. Mc Lean, D.,IdempotentSemigroups, Am. Math. Mon. 61 (1954).

***

APPLICATION OF NEURO-FUZZY CONTROLLER IN FINDING THE QUALITY OF JAGGERY

M. Uma Priya
M.Phil Scholar, SCSVMV, Kanchipuram, Tamilnadu
T.N. Kavitha
Assistant Professor of Mathematics, SCSVMV, Kanchipuram, Tamilnadu

Abstract: The Aim of our paper is to find the quality of jaggery using Neuro-fuzzy controller. In this journal, we have to study about Application of Hybrid Approach for determining the quality of jaggery by manufacturing system using Neuro-fuzzy. And also, the quality of jaggery is determined by considering various factors which have an advanced Neuro-fuzzy process controller is developed and its control technique is compared with the existing Automatic fuzzy PID PH controller. The Neuro-fuzzy model is developed by using the sample data of Ph of juice, milk of lime and other quality testing parameters collected from the process expert in the jaggery industry.

Keywords: Neuro-Fuzzy Controller, Automatic Fuzzy PID PH Controller, Hybrid Approach, Linguistic Sample.

1. Introduction: Sugarcane is versatile crop being a rich source of food like sucrose, jaggery and syrups**.** The process of making granular jaggery is similar up to concentration. But it does not best in jaggery quality. All the jaggery industries use conventional control techniques, which found fall short of providing effective means of controlling the processes when the process is complicated. With the rising demand for better and better quality and productivity, there is a need to automate the manufacturing processes. Many processes are complex, non-linear, stochastic and even ill defined in some cases. However, it is fact that, once trained or experienced human, can successfully control various complex systems without having to depend on mathematical models. This facts, lead us to the need of developing intelligent monitoring and control schemes.

Jaggery and sugar are two common sweeteners used throughout the world. It is for sweeten foods and beverages. Cane sugar is simply known as sucrose, which is sweetening agent for food manufacture. Sucrose a basic foodstuff, supply approximately 40-60% of all energy from foods. Sucrose is a disaccharide that it is made up of two simple sugars namely glucose and fructose.

The extraction of sucrose from sugar cane is a complex process. In India most of the jaggery mills follows traditional method of manufacturing jaggery which lack in monitoring and in process control techniques. The modern process control techniques have to be implemented to produce large quality of jaggery with superior quality. The conventional method of juice extraction suffers from drawback of PH control of juice, control of limewater, sulphur-dioxide, impurities in juice, dextrons means bacterial content, control of temperature, pressure, and flow of juice etc which affects the quality of juice.

Neuro-fuzzy controller is the advanced process control technique which is used to control the sugarcane process effectively. Improper control of factors not only affects the quality of Jaggery but also leads to abnormal condition of sugar plant. so, abnormal events is considered as the important risk assessment in process industries. Thus the operator is forced to focus through large amount of interrelated data to identify the causes, which leads to poor quality of jaggery. This requires integration and analysis of large amount numerical and abstract data. So, a knowledge based on artificial intelligence system is more appropriate for such situations.

Fuzzy and Neural networks separately and works together plays an increasingly important role in understanding human cognition and to simulate human decision making under uncertain and imprecise

environments. They learn from experience with numerical and linguistic sample data. Learning from samples involves construction of a system from knowledge of collection of input-output pairs.

2. Problem Description and Analysis: India is the largest producer of sugarcane. But, it does not best rank in jaggery quality. We cannot equalize the international standards due to failure in implementing advanced process in control techniques. The main problem in sugarcane process industry while processing is improper control of PH of cane juice, milk of lime, sulphur-di-oxide , presence of impurities in cane juice, grain size of jaggery, suspended matters and colour of the syrup etc., affects the quality of jaggery. There are other non-technical factors like soil, nutrients, cane varieties climate, Trash, sucrose and non-sucrose content, nature of juice etc., which also affects the quality of jaggery.

The above problem can be solved by advanced control techniques like Neuro-fuzzy controller along with Simulink model. The quality of jaggery manufactured should meet the international standard International commission for uniform Methods of jaggery Analysis, which is a world wide body that brings together the activities of the National Committees for jaggery Analysis in more than thirty member's countries.

3. Factors Affecting the Jaggery Quality: Nature of Juice

1. Presence of non-sucrose in cane.
2. pH of juice.
3. Excess or deficient supply of lime water and Sulphur-di-oxide
4. Brix of lime and juice.
5. Adequate or deficiency of nutrients in soil.
6. Colour of the juice.
7. Temperature and flow control of juice.
8. Delay in harvesting and crushing.
9. Loss of sucrose in cane.
10. pH of soil.
11. Grade and grain size of jiggery.
12. Conventional process control methods.
13. Bacterial contents in juice.

4. Parameters Used to Measure the Quality of Jaggery: There are several parameters to be measured based on which the quality of the sugar can be tested, graded and confirmed whether it has to be accepted or not. Some of the parameters to be measured are

1. Grade of the sugar as per ISS

(a) L 31 M 31 S 31
(b) L 30 M 30 S 30
(c) L 29 M 29 S 29

2. Grade of the jaggery as per ICUMSA

(a) 100 - Standard
(b) Between 80 to 90 - Good Quality
(c) Between 40 to 70 - Superior Quality
(d) Between 100 to 125 - Accepted Level
(e) Greater than 125 - Inferior Quality

3. Colour of the jaggery

(a) Dark Brown - Superior Quality
(b) Dull Brown - Good
(c) Yellowish Brown - Inferior

4. Presence of Sulphur

(a) 0 to 16 ppm - Accepted
(b) 0 - Good
(c) > 16 ppm - Inferior

6. Presence of Lead - Nil

7. Presence of Ash
(a) 0 to 0.05% - Accepted
(b) > 0.05% - Inferior
(c) 0 - Good
8. Presence of Moisture
(a) 0 to 0.04% - Accepted
(b) 0 - Good
(c) > 0.05% - Inferior
9. Presence of Dextron
(a) 0 to 100 ppm - Accepted
(b) 0 ppm - Very Good
(c) > 100 ppm - Inferior
10. Presence of Sediments
(a) 0 to 100 ppm - Accepted
(b) 0 ppm - Very Good
(c) > 100 ppm - Inferior

5. Solution Methodology: The modeling tool such as Fuzzy logic and Neutral network is adopted to solve the problem. Fuzzy logic was invented by LOFTIZADEH. Fuzzy logic is a generalization of classical logic in which there is a smooth transition from true to false. Fuzzy uses numeric computation between 0 to 1 to facilitate approximate reasoning. The basics of fuzzy logic are derived from the fuzzy set theory. The fuzzy set is defined in such a way to dichotomize the individuals in some given universe of discourse in two groups as members (those that certainly belongs to the set) and nonmembers (those that certainly not belong to the set).A fuzzy set A is X is characterized by a membership function (MF) $\mu_A(x)$, which associates a real number with each element in X in the interval [0,1] (with the value of μ_A (x) representing the grade of membership of X in A). Thus the fuzzy set A on a universe of discourse X is defined as $A = \{(x, \mu A (x))/x \in X \}$.

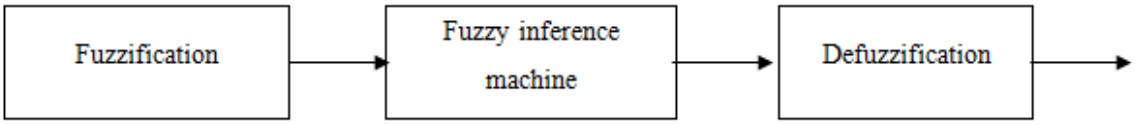
The MF is a curve that maps each element to its membership value between 0 and 1. There are various types of membership functions. They are of triangular type, trapezoidal, Gaussioan generalized bell shaped, S-Shape, X-Shape and Sigmoidal shaped functions.

A fuzzy set can be defined mathematically by assigning each possible individual in the universe of discourse, a value representing its grade of membership in fuzzy set. The individuals may belong to the fuzzy sets to a greater or lesser degree as indicated by a larger or smaller membership grade. These membership grades are very often represented by real number values ranging in the closed interval between 0 and 1.

Fuzzy logic belongs to the class of knowledge-based system. Fuzzy logic can mimic experts. Fuzzy systems are knowledge based software environments constructed from a collection of linguistic If-Then rules. Fuzzy systems realize non-linear mapping and hence they are recognize as alternative control schemes for dynamic, non-linear and complex process.The past few years have witnessed a rapid growth in the number and variety of application of fuzzy logic. The application ranges from consumer products, refrigerators, washing machines, microwave ovens, medical instrumentations, decision support systems and in industries. To understand the reasons for the growing use of fuzzy logic it is necessary first to clarify the meaning of fuzzy. The basic concept underlying fuzzy logic is that of a linguistic variable (i.e.) a variable whose values are words rather than numbers. Another basic concept in fuzzy logic, which plays a central role in most of its applications, is that of a fuzzy IF-THEN rule.

In rule based fuzzy logic, machinery is provided by calculus of fuzzy rules. The calculus of fuzzy rules serves as a basis for what might be called the fussy dependency and command language (FDCL).
In most of the applications of fuzzy logic, a fuzzy logic solution is in reality a translation of a human solution in to fuzzy dependency and command language. Fuzzy logic is viewed as soft computing. Unlike, the traditional hard computing and soft impression of the real world. The guiding principle of

soft computing is to exploit the tolerance for impression, uncertainty and partial truth to achieve (a) traceability (b) robustness and (c) low solution cost.
Among various combinations of methodologies in soft computing, the one that has highest visibility at this juncture is that of fuzzy logic and neuro-computing leading to so called neuro fuzzy systems.



6. Fuzzification: The fuzzification component maps an observed input space into suitable linguistic value which can be viewed as labels of fuzzy set.

7. Fuzzy Inference Machine: The fuzzy inference machine consists of two conceptual parts.

a. A rule base which contains a selection of fuzzy rules. "If-Then" rules are used to relate fuzzy variables.
b. A database defining the membership functions used in the fuzzy rules, normalizing the input and out universe of discourse and performing the fuzzy partition of input and out spaces. A reasoning mechanism, which performs the inference procedure upon the rules and given conditions to derive a reasonable output. A simple fuzzy rule has the form if x is A, y is B, where A and B are the input and out linguistic variables defined by fuzzy sets on the universe of discourse X and Y respectively. In the if part A is called the consequence. The rule can be represented as a fuzzy relation as $R = A \rightarrow B$, where R is the fuzzy relationship defined on the Cartesian product universe X*Y. A and B are the antecedent part and the consequent part respectively. These relations may be obtained from sources such as human expert knowledge and experience, commonsense and engineering intuitive knowledge about the system under development, general principles and laws governing the system, by using pattern recognition classification, clustering and learning techniques. The process to obtain the inference result from the observed data is predominantly used max-min compositional technique.

8. Defuzzification: It converts the aggregated fuzzy set to a non-fuzzy output value by taking the average of the area bounded by the membership function curve.

9. Overview of Artificial Neural Network: In present years artificial neural network is attracted by Researchers, as well as industrial practitioners. An artificial neural network is popular in powerful pattern recognition and flexible non-linear modeling capabilities. Neural networks offer great promise for process control. Advanced manufacturing systems are becoming more complex and dynamic for traditional ruled based decision support systems. Neural network technology application is gathering momentum in all aspects of manufacturing processes. Since decision making process in an advanced manufacturing systems environment is becoming increasingly difficult and overwhelming to humans, Artificial intelligence is widely adopted to assist human efforts. Artificial intelligence is useful in all aspects of manufacturing processes. Expert systems is the common type in Artificial intelligence. Still, expert system are less effective in the ever changing, complex and open system environment of today's manufacturing system.

The type of Artificial intelligence capable of responding to the rapid changes and ill structured nature of the automated manufacturing environment has to be able to learn, adapt to changes, recognize trends and mimic human thoughts. It must be able to recognize patterns and relationships among prevailing factors which are not apparent to human experts. Neural net ability to recognize patterns and trends in an historic database is one of the reasons that the technology is effectively used in manufacturing processes.

10. Design of Neural Network: The design issues of neural networks are so complex. Designing of network consists of

(a) Arranging neurons in various layers.
(b) Deciding the type of connection among neurons for different layers as well as among neurons with in a layer.
(c) Deciding a way neuron receives input and produces output.
(d) Determining the strength of connections with in the network by allowing the network, the approximate values of connection weights by using a training data set.

11. Constructing A New Neuro-Fuzzy Model: A new application of Neuro-fuzzy system to the processing of jaggery is developed. The first step in constructing a model is to observe the real sugarcane processing system and the interaction among its various components and system behavior. The second step in model building is construction of a conceptual model by collection of various data's and the structure of the system. The third step is the translation of the operation model in to computer recognizable format. While building a model there is a need for continuous verification and validation by comparing the real system to the conceptual model and repeated modification is done to improve its accuracy.

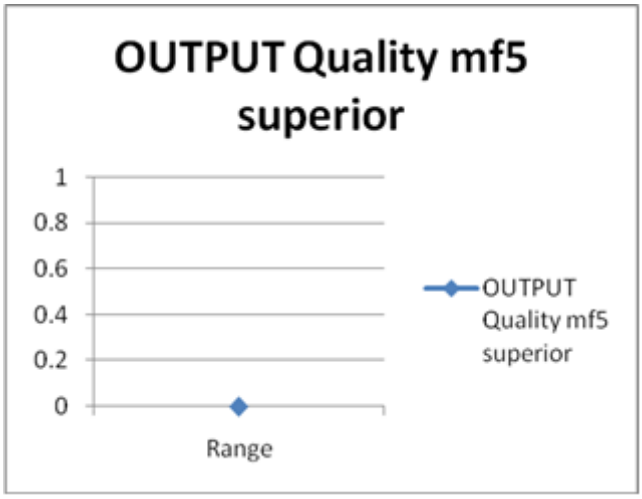
Three fuzzy models of type mamdani are developed by mapping an input data vector into a scalar output using fuzzy logic. In first model pH of crushed juice is taken as input and lime water to be added to juice is taken as output and the mapping between these data which are non-linear mapping are performed using fuzzification, fuzzy inference and defuzzification components found in fuzzy logic. Similarly in the second model pH of juice after treatment of lime water is taken as input and sulphurdioxide to be added to juice is taken as out and the data are mapped in a similar manner and in the third fuzzy model the parameters which is used to test the quality of jaggery is taken as input and the quality of jaggery is taken as out and the data are mapped in a non-linear manner.

Similarly the fuzzy logic tool box is highly impressive in all respects. It makes fuzzy logic and effective tool for conception and design of intelligent system. The fuzzy logic toolbox is a collection of functions built with numeric computing environment. It provides tool to create and edit fuzzy inference systems. The fuzzy system can be integrated with simulink and the model can be simulated. The fuzzy models can be created using graphical tools or by using command line functions.

12. To Determine The Quality of Jaggery: The input and out membership functions label and its corresponding range is given in Table 1.1

Table 1.1: Input and Output Membership Functions Label

LABLE	Parameter	Membership functions	Membership functions label	Range
	Grain	mf1	fine	0-0.25
		mf2	standard	0.25-1
		mf3	extracourse	1-1.5
INPUT	Colour	mf1	purewhite	40-60
		mf2	white	60-90
		mf3	stand	90-100
		mf4	accept	100-125
INPUT		mf5	unacceptable	125-150
	ash	mf1	acceptable	0-0.05
		mf2	unacceptable	0.05-0.15
	moisture	mf1	acceptable	0-0.04
		mf2	unacceptable	0.04-0.08
	Dextron	mf1	acceptable	0-100
		mf2	unacceptable	100-200
OUTPUT	Quality	mf1	highly-inferior	0-30
		mf2	inferior	30-60
		mf3	average	60-75
		mf4	good	75-85
		mf5	superior	85-100



Results and Conclusion: In this journal the quality of jaggery is determined by considering various factors which have an impact on quality using Neuro fuzzy approach and an advanced Neuro-fuzzy process controller is developed and its control technique is compared with the existing Automatic fuzzy PID pH controller. It has been observed that poor control technique fails to sense the pH of juice accurately and it leads to excess or less addition of lime water and sulphur- di-oxide which fails to achieve the desired pH value of juice. It was also observed that low pH or high pH of juice not only affects the final quality of the product but also affects the entire operation of sugar plant due to transient conditions of the plant. The collected online process data of critical process variables are trained by neural network by setting target values till the desired values is achieved. Once the Neural network is trained a fuzzy model is created using If-Then rules. By combining Neural network and fuzzy logic a Neuro-fuzzy controller is developed which is an advanced process controller that overcomes the drawbacks of existing fuzzy PID controller.

The result in fig.1.1 shows that these input parameters have serious impact on jaggery in terms of jaggery quality. Though there are several other quality parameters which are not mentioned in this model due to its complexity nature, grain size and colour are considered to be the most important parameters in fixing the quality of jaggery.

References:

1. Zadeh, L.A., Fuzzy Sets, Info. and Control, 8, 1965.
2. Atanassov. K.T, Fuzzy sets and systems, 20(1),(1986), 87– 96.
3. Ganesh. M., On Fuzzy Sets and Their Applications, (1997) (Unpublished notes)
4. Ganesh.M., introduction to fuzzy sets and fuzzy logic., Rajasthan., (2006).
5. Kannan.G.,fuzzy logic and fuzzy decision making., Tamilnadu., (2008).
6. Kickert, W.J.M., Fuzzy Theories on Decision Making, Martinus-Nijhoff, 1978.
7. Zimmermann, H.J., Fuzzy Set Theory and its Application, Kluwer-Nijhoff, Boston, 1985.

***

Volume 5, No.5, May 2018

Journal of Global Research in Mathematical Archives

ISSN 2320 – 5822

RESEARCH PAPER

Available online at http://www.jgrma.info

A SPECIAL CASE OF NEAR – IDEMPOTENT SEMIGROUPS

T.N.Kavitha,
A.Jayalakshmi, Professor of mathematics(Retd)
SCSVMV University, Enathur, kanchipuram- 631 561- Tamil Nadu- India.

***Abstract*:** In a previous paper we introduced a near idempotent semigroup and studied its structure through the relations λ, ρ and δ. In this paper, we introduce a new pair of relations λ_r and ρ_r on a near idempotent semigroup. In general λ_r and ρ_r are not reflexive relations on a near idempotent semigroup and hence not equivalence relations. We study the special case when λ_r becomes reflexive on a near idempotent semigroup. This gives rise to a special case of a near idempotent semigroup, namely, a right near idempotent semigroup.
***Key words*:** Near idempotent semigroup, right near idempotent semigroup, reflexive relations, equivalence relations.

1. INTRODUCTION

A near idempotent semigroup is a semigroup S[3] is a semigroup whose elements satisfy the identity $xyz = xy^2z$ for all $x, y, z \in S$. We studied the structure of a near idempotent semigroup be defining equivalence relations λ, ρ, δ and ξ on S. In this paper we defined λ_r and ρ_r on near idempotent semigroup S. It is easy to check that λ_r is not in general, reflexive on a near idempotent semigroup. In fact, S may contains an element a such that $a \not\lambda_r a$. we prove that for $a \in S$, $a \lambda_r a$ if and only if $xa = xa^2$ for all $x \in S$. It follows that λ_r is reflexive on a near idempotent semigroup S if and only if $xy = xy^2$ for all x, y in S. This leads us to the definition of a right near idempotent semigroup as a semigroup in which $xy = xy^2$ for all $x, y \in S$. It is easy to see that a right near idempotent semigroup is a near idempotent semigroup but a near idempotent semigroup need not be a right near idempotent semigroup.

2. λ_r (ρ_r) ON A NEAR IDEMPOTENT SEMIGROUP

We define the relations λ_r and ρ_r respectively on a near idempotent semigroup as follows

2.1 Definition

Let S be a near idempotent semigroup. For $a, b \in S$, we define

1. $a \lambda_r b$ if and only if $xab = xa$ and $xba = xb$ for all $x \in S$
2. $a \rho_r b$ if and only if $xab = xb$ and $xba = xa$ for all $x \in S$

2.2 Lemma

Let S be a near idempotent semigroup. The relation λ_r on S defined in 2.1 is symmetric and transitive on S.

PROOF

Let S be a near idempotent semigroup. For a, b in S,
$a \lambda_r b$ if and only if $xab = xa$ and $xba = xb$ for all $x \in S$.
1. λ_r is symmetric.
By definition, it is obvious.

© JGRMA 2018, All Rights Reserved

2. λ_r is transitive
Let a, b, c $\in$ S such that
Let a λ_r b and b λ_r c.
Then for all x $\in$ S
xab = xa, xba = xb
and
xbc = xb, xcb = xc
We have, for all x in S,
xa = xab = xa bc = x(ab) c = xac
xc = xcb = xc ba = xcb a = xca whereby λ_r is transitive

In the following example, S is a near idempotent semigroup in which that λ_r is not reflexive.

2.3 Example

Let 1 = $\begin{bmatrix} 0 & 0 \\ 0 & 0 \end{bmatrix}$, 2 = $\begin{bmatrix} 1 & 0 \\ 0 & 0 \end{bmatrix}$, 3 = $\begin{bmatrix} 0 & 1 \\ 0 & 0 \end{bmatrix}$, 4 = $\begin{bmatrix} 1 & 1 \\ 0 & 0 \end{bmatrix}$
the elements of $M_2(Z_2)$ under matrix multiplication modulo 2. The following multiplication table shows that these elements form a semigroup.

x	1	2	3	4
1	1	1	1	1
2	1	2	3	4
3	1	1	1	1
4	1	2	3	4

It is easy to see that 1, 2 and 4 are idempotent elements and hence are near idempotent elements as well.
For x=1 and 3, x.3 = 1, so that x.3.y = 1.y = 1 for all y in the above semigroup. This shows that x.3.y = $x.3^2$.y for all y when x=1 or 3.
For x = 2 or 4, x.3 = 3, so that x.3.y = 3.y =1 for all y. $x.3^2$.y = x.1.y = 1 for all y. Thus x.3.y = $x.3^2$.y for x=2 or 4 also.
Hence x.3.y = $x.3^2$.y for all x, y in the semigroup. Hence S is a near idempotent semigroup.
From the multiplication table, it is clear that 2.3 =3 and 2.3^2 = 2.1 = 1
so that $2.3 \neq 2.3^2$
Thus there exist x such that x.3 $\neq$ $x.3^2$ which implies that 3 $\not\lambda_r$ 3.
Hence λ_r is not reflexive.

2.4 Remark

In the above example , we proved that 3 $\not\lambda_r$ 3. In fact, we can easily see that
3 is not λ_r related to any of the elements in the above semigroup
2.3.1 = 2.1 = 1, 2.3 = 3, so that 2.3.1 $\neq$ 2.3, which implies 3 $\not\lambda_r$ 1
2. 3.2 = 2.1 = 1, 2.3 = 3, so that 2.3.2 $\neq$ 2.3, which implies 3 $\not\lambda_r$ 2
2.3.4 = 2.1 =1, 2.3 = 3, so that 2.3.4 $\neq$ 2.3, which implies 3 $\not\lambda_r$ 4
We will soon see that this situation is not special to this example alone but to every near idempotent semigroup.
Thus, in a near idempotent semigroup, an element which is not related by λ_r to itself, is not related by λ_r to any other element of the near idempotent semigroup. The following lemma brings out this point very clearly.

2.5 Lemma

© JGRMA 2018, All Rights Reserved

Let S be a near idempotent semigroup. Let λ_r be defined on S as above.
Let $a \in S$. If $a \lambda_r b$ for some $b \in S$, then $a \lambda_r a$

Proof

Let $a \in S$
Suppose $a \lambda_r b$ for some $b \in S$
$xab = xa$ and $xba = xb$ for all $x \in S$
$xa = xa^2 b = xa\, ab = xa^2$ for all $x \in S$
Hence $a \lambda_r a$

2.6 Remark

Lemma 2.5 simply means that if an element a of a near – idempotent semigroup S is λ_r - related to some element of S, then it is λ_r - related to itself.

In what follows, we find necessary and sufficient conditions under which an element of a near idempotent semigroup S is related to itself under λ_r.

2.7 Lemma

Let S be a near idempotent semigroup and $a \in S$. Then $a \lambda_r a$ if and only if $xa = xa^2$ for all x in S.

Proof

Suppose $a \lambda_r a$ for $a \in S$.
Then $xa^2 = xa$ for all $x \in S$
Conversely, suppose that $xa^2 = xa$.
It is obvious that $a \lambda_r a$

The following lemma gives a necessary and sufficient condition for the relation λ_r to be reflexive on a near idempotent semigroup S.

2.8 Lemma

The relation λ_r is reflexive on a near idempotent semigroup S if and only if $xy = xy^2$ for all x, y in S.

Proof

Suppose λ_r is reflexive on a near idempotent semigroup S
$y \lambda_r y$ for all $y \in S$.
Therefore $xy^2 = xy$ for all $x, y \in S$
The Converse part is true by lemma 2.8.

2.9 Remark
Let S be a near idempotent semigroup satisfying the identity $xy = xy^2$ for all x, y in S. Then λ_r is an equivalence relation on S

The above remark leads us to the definition of a right near idempotent element and a right near idempotent semigroup.

3. RIGHT NEAR IDEMPOTENT SEMIGROUP

© JGRMA 2018, All Rights Reserved

3.1 Definition

Let S be a semigroup and a an element of S. a is said to be a right near – idempotent element of S if $xa^2 = xa$ for all x in S.

3.2 Definition

A semigroup S is called a right near – idempotent semigroup if every element of S is a right near – idempotent element.
Alternatively, a semigroup S is a right near idempotent semigroup if $xy = xy^2$ for all x, y ∈ S.

3.3 Remark

It is easy to see that every right near idempotent element a is a near idempotent element , since $xa = xa^2$ for all x ∈ S implies $xay = xa^2y$ for all x, y ∈ S.
But the converse is not true.
By a similar argument a right near idempotent semigroup is a near idempotent semigroup but a near idempotent semigroup need not be a right near idempotent semigroup.

3.4 Example

(1). The semigroup S of example 2.3 is a near idempotent semigroup, but it is not right near idempotent semigroup.

(2). The subsemigroup A = { 1, 3 } is a right near idempotent subsemigroup of S.

·	1	3
1	1	1
3	1	1

x.1.3 = x.1 for all x in A since 1.3 = 1
x.3.1 = x.1 = 1 = x.3 for all x in A from the table.
Therefore $1 \lambda_r 3$ in A

3.5 Remark

In example 2.3,
S is a near idempotent semigroup.
$2.3 = 3$ and $2.3^2 = 2.1 = 1$ This implies that $3 \not\lambda_r 3$ in the near idempotent semigroup S.
Since x.3 = x.1, x.3.y = x.1.y
i.e, $1 \lambda 3$
λ - classes are {1, 3 }, {2}, {4}.
x.1.2 = x.1 since 1.2 = 1, and x.2.1 = x.2
x.1 = x.1 ,since 1.2 = 1 and $x.1 \neq x.2$ for x in S, here 2.1 = 1
therefore $2 \not\lambda_r 1$
x.1.4 = x.1 and x.4.1 = x.4
x.1 = x.1 and $x.1 \neq x.4$ for all x in S, here 1.4 = 1 and 4.1 = 1
therefore $1 \not\lambda_r 4$
hence xa need not be equal to xa^2 for all x, a ∈ S. Hence there may be elements in S such that $a \not\lambda_r a$.

© JGRMA 2018, All Rights Reserved

The above discussions show that a near idempotent semigroup S need not be a right near idempotent semigroup. But S may contain a right near idempotent semigroup under certain conditions.

In fact, if there exists an element a in S which is λ_r - related to some element of S, then S contains a right near idempotent semigroup.

3.6 Theorem

In a near idempotent semigroup S, the right near idempotent elements form a right near idempotent subsemigroup of S.

Proof

Let S be a near idempotent semigroup and let $a \in S$.
Let $K_a = \{ x \in S \mid x \ \lambda_r \ a\}$ be non - empty. Then K_a is a right near idempotent subsemigroup of S.
Let $b, c \in K_a$.
$xba = xb, xab = xa$ for all $x \in S$
$xca = xc, xac = xa$ for all $x \in S$
$x\ bc\ a = (xb)\ ca = xbc$ for all $x \in S$
$xabc = x\ ab\ c = x\ ac = xa$ for all $x \in S$
hence $bc\ \lambda_r\ a$
therefore $bc \in K_a$
Thus K_a is a subsemigroup of S.

Also $b \in K_a \Rightarrow b\ \lambda_r\ a$
$\Rightarrow b\ \lambda_r\ b$ by lemma 2.8
$\Rightarrow xb^2 = xb$ for all $x \in S$ by 3.1
and hence $xb^2 = xb$ for all $x \in K_a$
Thus K_a is an right near idempotent subsemigroup of S.

3.7 Example

S = { 2, 6, 8, 12 }, under the operation $a * b = (\frac{ab}{2}) \pmod 6$ is a right near idempotent semigroup.

The semigroup S has the following multiplication table.

*	2	6	8	12
2	2	6	2	6
6	6	6	6	6
8	2	6	2	6
12	6	6	6	6

Since 2 and 6 are idempotent elements, $x*2^2 = x*2$, $x*6^2 = x*6$ for every x in S. But 8 and 12 are not idempotent elements and hence we check them for right near idempotency.
$8^2 = 2$
From the table it is clear that $x*8 = x*2 = x*8^2$ for all x in S.
$12^2 = 6$
$x*12^2 = x*6 = x*12$
Thus $x*y = x*y^2$ for all $x, y \in S$, so that S is a RNIS.

4. CONCLUSION

Near- idempotency is a kind of generalization of idempotency. Right near- idempotency is yet another generalization of idempotency which we have dealt with, in this paper.

© JGRMA 2018, All Rights Reserved

REFERENCES

[1] Clifford, A.H. and Preston, G.B., "The Algebraic Theory of Semigroups", Vol. I, Providence, 1961
[2] Jayalakshmi, A., "Some Studies in Algebraic Semigroups and Associated Structures", Doctoral Thesis, Bangalore University, 1981.
[3] T.N. Kavitha, A. Jayalakshmi, On near – idempotent semigroups, vol 5, no 5, International Journal of Mathematical Archive, May 2014
[4] Kimura, N.,The Structure of Idempotent Semigroups (I), Pacific J. of Math. (1958).
[5] Mc Lean, D.,Idempotent Semigroups, Am. Math. Mon. 61 (1954).

© JGRMA 2018, All Rights Reserved

A STUDY ON HIGHER ORDER TRIANGULAR SUM NUMBERS OF POLYHEDRAL AND GRACEFUL GRAPHS

A.Gayathri

Dept. of Mathematics, SCSVMV (Deemed University), Kanchipuram, India

Abstract: In this paper we will prove that the polyhedral graphs and graceful graphs admits some higher order triangular sum numbers. We will derive the path of graceful graphs edge based on the node count and order of triangular sum numbers. We will also come to know about the graceful graphs edge values '*sequence type'* based on some higher order of triangular sum numbers.

Keywords: Polyhedral Graphs, Graceful Graphs, Triangular Sum Numbers, Edge, Node, 3-Vertexconnected Planar Graphs.

1. Introduction: In graph theory, a graceful labeling of a graph with m-edges is a labeling of its vertices with some subset of the integers between o and m inclusive, such that no of two vertices share a label, and such that each edge is uniquely identified by the positive, or absolute difference between its end points. A graph which admits a graceful labeling is called a graceful graph. In geometric graph theory, a branch of mathematics, a polyhedral graph is the undirected graph formed from the vertices and edges of a convex polyhedron. Alternatively, in purely graph- theoretic terms, the polyhedral graphs are the 3-vertex-connected planar graphs. In the upcoming topics we will study on higher order triangular sum numbers and how it can be used in Polyhedral and Graceful graphs.

Definition.1.1: A triangular sum numbers is a number obtained by adding all positive integers less than or equal to a given integer n. If the nth triangular sum numbers is denoted by T_n. Then $T_n = 1/2[n(n+1)]$. The triangular sum numbers are 1,3,6,10,15,21,28,36,45,55,66,78,91,105,120,...n.

Definition.1.2: A second order triangular sum numbers is a number obtained by adding all the squares of positive integers less than or equal to a given positive integer n. If the nth second order triangular sum numbers is denoted by S_n. Then $S_n=1/6[(n)(n+1)(2n+1)]$. The second order triangular sum numbers are 1,5,14,30,55,91,140,204,285,385,506,650,.....n.

Definition.1.3: A third order triangular sum numbers is a number obtained by adding all the cubes of positive integers less than or equal to a given positive integer n. If the nth third order triangular sum numbers is denoted by T_n, Then $T_n = 1/4[(n)^2(n+1)^2]$. The third order triangular sum numbers are 1,9,36,100,225,441,784,1296,2025, 3025,4356,6084,11025,.....n.

Definition.1.4: A fourth order triangular sum numbers is a numbers obtained by adding all the fourth powers of positive integers less than or equal to a given positive integer n. If the nth fourth order triangular sum numbers is denoted by F_n. Then $F_n = 1/30[(n)(n+1)(2n+1)(3n^2+3n-1)]$. The fourth order triangular sum numbers are 1,17,98,354,979,2275,4676,8772,15333,25333,39974.....n.

Definition.1.5: A fifth order triangular sum numbers is a numbers obtained by adding all the fifth powers of positive integers less than or equal to a given positive integer n. If the nth fifth order triangular sum numbers is denoted by F_n, Then $F_n = 1/12[(n)^2(n+1)^2(2n^2+2n-1)]$. The fifth order triangular sum numbers are 1,33,276,1300,4425,12201,29008,61776,120825,220825,.....n.

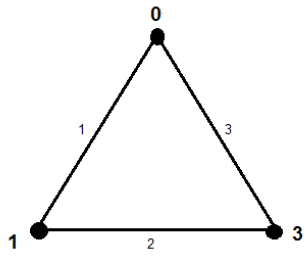
Definition.1.6: A sixth order triangular sum numbers is a numbers obtained by adding all the sixth powers of positive integers less than or equal to a given positive integer n. If the nth fifth order triangular

sum numbers is denoted by S_n, Then $S_n = 1/42[(n)(n+1)(2n+1)(3n^4+6n^3-3n+1)]$. The sixth order triangular sum numbers are 1,65,794,4890,20515,67171,184820,446964, 978405,.....n.

This concept was introduced by Hegde and Shankaran [6].Motivated by the concept of higher order triangular sum labeling, Murugesan [7], some higher order triangular sum labeling of graphs.

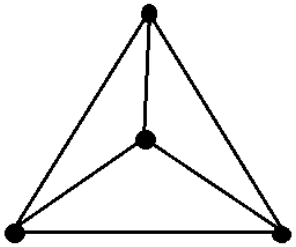
2. Characterization of Graceful and Polyhedral Graphs:

2.1. Graceful Graphs: In graph theory, a graceful labeling of a graph with 'e' edges is a labeling of its vertices with some subset of the integers between o and *e* inclusive, such that no of two vertices share a label, and such that each edge is uniquely identified by the positive, or absolute difference between its end points. A graph which admits a graceful labeling is called a "*Graceful graph"*. The name graceful labeling is due to Solomon W. Golomb [1].



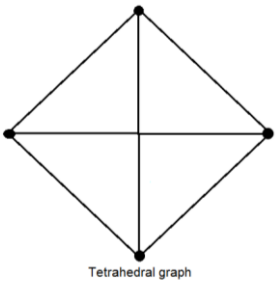
K_3graph

2.2. Polyhedral Graphs: An n-polyhedral graph (sometimes called a c-net) is a 3-connected simple planar graph on n nodes. Every convex polyhedron can be represented in the plane or on the surface of a sphere bya 3-connected planar graph. Conversely, by a theorem of Steinitz as restated by Grunbaum [2], every 3-connected planar graph can be realized as a convex polyhedron (Duijvestijn and Federico [3]). "*Polyhedral graph"* are sometimes simply known as "polyhedra" (which is rather confusing since the term "polyhedron" more commonly refers to a solid with n-faces, not n-vertices).



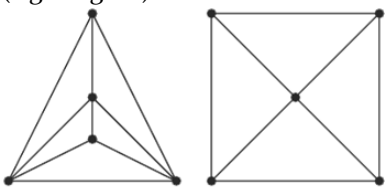
Polyhedral graph

2.3. Tetrahedral Graphs: The tetrahedral graph is the Platonic graph that is the unique polyhedral graph on four nodes which is also the complete graph K_4 and therefore also the wheel graph W_4. It is implemented in the wolfram language as graph data*"Tetrahedral Graph"*.



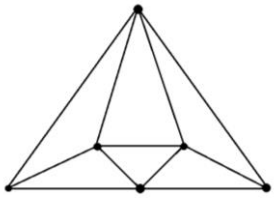
Tetrahedral graph

2.4. Pentahedral Graphs: A polyhedral graph on five nodes. There are two topologically distinct *Pentahedral graph* which, through duality, correspond to the skeletons of the square pyramid (left figure) and triangular di-pyramid (right figure).



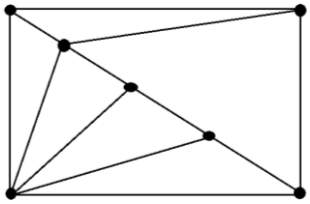
Pentahedral graphs

2.5. Hexahedral Graphs: A *Hexahedral graph* is a polyhedral graph on six vertices. There are seven distinct hexahedral graphs which, through duality, correspond to seven convex hexahedra.



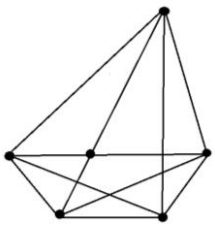
Hexahedral graph

2.6. Heptahedral Graphs: A polyhedral graph on seven nodes. There are 34 nonisomorphic *Heptahedral graph*, as firstenumerated by Kirkman [5], Federico [4], Duijvestijn and Federico [3].



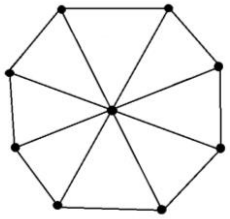
Heptahedral graph

2.7. Octahedral Graphs: The octahedral graph is the 6-node 12-edge Platonic graph having the connectivity of the octahedron. It is isomorphic to the circulant graph Ci_6 (1,2). It is implemented in the Wolfram Language as Graph data *Octahedral graph*. It has chromatic polynomial. Confusingly, the term octahedral graph is also used to refer to a polyhedral graph on eight nodes.



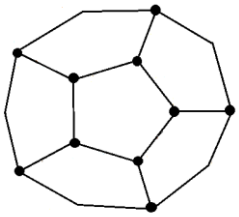
Octahedral graph

2.8. Nonahedral Graph: A polyhedral graph having nine vertices. There are 2606 nonisomorphic nonahedral graphs, as first enumerated by Federico [4], Duijvestijn and Federico [3]). Named *Nonahedral graph* include the Fritsch graph, Soifer graph, and 9-wheel graph W_9. Other nonahedral graphs include the skeletons of Johnson solids 3, 8, 10, and 63, the (2,7)-fan graph, and the (3,3)-prism graph.



Nonahedral graph

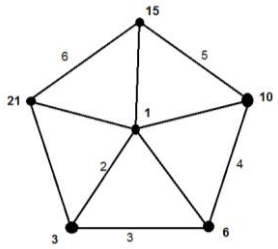
2.9. Decahedral Graph: A polyhedral graph having 10 vertices. There are 32300 non-isomorphic *Decahedral graph*, as first enumerated by Duijvestijn and Federico [3].



Decahedral graph

3. Proposed Results: Here we prove that Polyhedral and Graceful graphs admit Some higher order triangular sum numbers.

Example 3.1: Labeling Graph With Triangular Sum Numbers



Hexahedral graph

Results:

Triangular Sum Numbers As Polyhedralgraph: The triangular sum numbers are placed in each node of any polyhedral graph in a random node order. The so obtained graph is a three connected planner graph with n-nodes.Hence polyhedral graph admits triangular sum numbers.

Triangular Sum Numbers As Graceful Graph: From the above observations made, we can say that the Polyhedral graph formed by labeling the nodes and edges with the triangular sum numbers and their node differences respectively form a gracefully numbered graph. Hence we can say that the Graceful graph also admits triangular sum numbers.

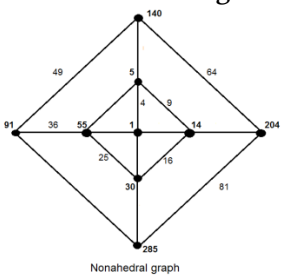
Graceful Graph Node Differences: When the absolute differences between the nodes are taken and the edges are labeled, the obtained node differences are 'Natural numbers' for Triangular sum numbers. The below results has been derived based on number of nodes and node values.

Value of (n)thnode - Value of (n-1)thnode = (No of connecting node)order of triangular sum numbers
FigureHexahedral graph (above), The last two nodes are 15, 21. No of nodes-6 and 1-order.

Valueof(n)thnode -Valueof(n-1)thnode= (Noofconnectingnode)$^{\text{orderoftriangular sum numbers}}$

21 – 15 = (6)1 6 = 6...Hence proved.

Example.3.2: Labeling Graph With Second Order Triangular Sum Numbers:



Nonahedral graph

Results:

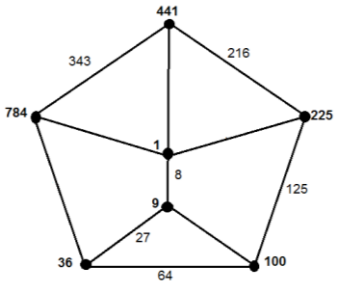
Second Order Triangular Sum Numbers As Polyhedral Graph: The second order triangular sum numbers are placed in each node of any polyhedral graph in a random node order. The so obtained graph is a three connected planner graph with n-nodes. Hence polyhedral graph admits second order triangular sum numbers.

Second Order Triangular Sum Numbers As Graceful Graph: When the absolute differences between the nodes are taken and the edges are labeled, it forms a gracefully numbered graph. Hence we can say that Graceful graph also admits second order triangular sum numbers.

Graceful Graph Node Differences: Also the obtained node differences are 'Square of natural numbers' for Second order triangular sum numbers. The below results has been derived based on number of nodes and node values.

Figure Nonahedral graph (above),The last two nodes are 204, 285. No of nodes-9 and 2-order.
Value of (n)thnode - Value of (n-1)thnode = (No of connecting node) order of triangular sum numbers
285 – 204 = (9)2
81 = 81....Hence proved.

Example.3.3: Labeling Graphs with Third Order Triangular Sum Numbers



Heptahedral graph

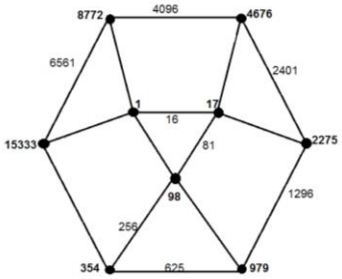
Results:

Third Order Triangular Sum Numbers As Polyhedral Graph: The third order triangular sum numbers are placed in each node of any polyhedral graph in a random node order. The so obtained graph is a three connected planner graph with n-nodes. Hence polyhedral graph admits third order triangular sum numbers.

Third Order Triangular Sum Numbers As Graceful Graph: From the above observations made, we can say that the Polyhedral graph formed by labeling the nodes and edges with the third order triangular numbers and their node differences respectively form a gracefully numbered graph. Hence we can say that the Graceful graph also admits Third order triangular sum numbers.

Graceful graph node differences: When the absolute differences between the nodes are taken and the edges are labeled, the obtained node differences are 'Cubic of natural numbers' for Third order triangular sum numbers.
Figure Heptahedral graph, The first two nodes are 1, 9. No of connecting nodes-2 and 3-order Value of (n)thnode - Value of (n-1)thnode = (No of connecting node) order of triangular sum numbers
9 – 1 = (2)3
8 = 8....Hence proved.

Example.3.4: Labeling Graphs with Fourth Order Triangular Sum Numbers



Nonahedral graph

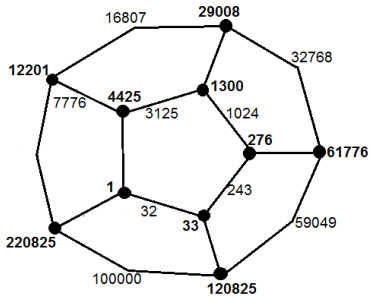
Results:
Fourth Order Triangular Sum Numbers As Polyhedral Graph: The fourth order triangular sum numbers are placed in each node of any polyhedral graph in a random node order. The so obtained graph is a three connected planner graph with n-nodes. Hence polyhedral graph admits fourth order triangular sum numbers.

Fourth Order Triangular Sum Numbers As Graceful Graph: When the absolute differences between thenodesaretakenandtheedgesarelabeled,itformsa gracefullynumberedgraph.Hence wecan say that Graceful graph also admits fourth order triangular sumnumbers.

Graceful graph node differences:Also the obtained node differences are 'fourth power of natural numbers' for fourth order triangular sum numbers. The below results has been derived based on number of nodes and node values.

Figure Nonahedral graph,The last two nodes are 8772, 15333. No of nodes-9 and 4-order
Value of (n)thnode - Value of (n-1)thnode = (No of connecting node) order of triangular sum numbers
15333 - 8772 = (9)4
6561 = 6561.....Hence proved.

Example.3.5:
Labeling Graphs with Fifth Order Triangular Sum Numbers



Decahedral graph

Results:

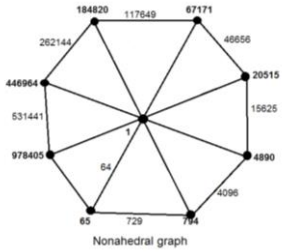
Fifth Order Triangular Sum Numbers As Polyhedral Graph: The fifth order triangular sum numbers are placed in each node of any polyhedral graph in a random node order. The so obtained graph is a three connected planner graph with n-nodes. Hence polyhedral graph admits fifth order triangular sum numbers.

Fifth Order Triangular Sum Numbers As Graceful Graph: From the above observations made, we can say that the Polyhedral graph formed by labeling the nodes and edges with the fifth order triangular sum numbers and their node differences respectively form a gracefully numbered graph. Hence we can say that the Graceful graph also admits fifth order triangular sum numbers.

Graceful Graph Node Differences: When the absolute differences between the nodes are taken and the edges are labeled, the obtained node differences are 'fifth power of natural numbers' for fifth order triangular sum numbers.

Figure Decahedral graph,the center of two nodes are 4425, 12201. No of connecting nodes-6 and 5-order.
Value of (n)thnode - Value of (n-1)thnode = (No of connecting node) order of triangular sum numbers
12201 – 4425 = (6)5
7776 = 7776
Hence proved.

Example.3.6:
Labeling Graphs with Sixth Order Triangular Sum Numbers



Results:

Sixth Order Triangular Sum Numbers As Polyhedral Graph: The sixth order triangular sum numbers are placed in each node of any polyhedral graph in a random node order. The so obtained graph is a three connected planner graph with n-nodes. Hence polyhedral graph admits sixth order triangular sum numbers.

Sixth Order Triangular Sum Numbers As Graceful Graph: When the absolute differences between the nodes are taken and the edges are labeled, it forms a gracefully numbered graph. Hence we can say that Graceful graph also admits sixth order triangular sum numbers.

Graceful Graph Node Differences: Also the obtained node differences are 'sixth power of natural numbers' for Sixth order triangular sum numbers.

The below results has been derived based on number of nodes and node values.
Figure Nonahedral graph. The last two nodes are 446964,978405. No of nodes-9 and 6-order
Value of (n)thnode - Value of (n-1)thnode = (No of connecting node) order of triangular sum numbers
978405 – 446964 = (9)6
531441 = 531441....Hence proved.

Conclusion: In this paper we have dealt plottingtriangular sum numbers on polyhedral and graceful graph and proved that these graphs admits those numbers.We have derived the path of graceful graphs edge based on the node count and some higher order triangular sum numbers using below formula .We

also have found the graceful graphs edge values 'Sequence type'as Natural, Square, Cube numbers etc...based on order of triangular sum numbers.
Formula: value of (n)thnode - value of (n-1)th node = (No of connecting node) order of triangular sum numbers

References:

1. Golomb.S.W "How to number a graph in graph theory and computing" (Ed. R. C. Read). New York: Academic press, pp. 23-37, 1972."The largest graceful subgraph of the complete graph." Amer. Math. 81, 499-501, 1974.
2. Grunbaum.B "Polytopalgraphs". In studies in graph theory, Part-2(Ed. D. R. Fulkerson). Washington, DC: Math. Assoc. Amer., pp. 201-224, 1975. Convex Polytopes, 2nd Ed. New York: Springer-Verlag, 2003.
3. Duijvestijn.A.J.W and Federico "List of 3-connected planar graphs with 6 to 22 edges".Unpublished computer tape. Enschede, Netherlands:Twente Univ. Technology, 1979."The number of polyhedral (3-connected planar) graphs", Math. Computer, vol. 37, 523-532,1981.
4. Federico.P.J. "Enumeration of polyhedra: The number of 9-Hedra". J. Combin. Th. 7, 155-161, 1969."The Number of Polyhedra".Philips Res. Rep. vol. 30, 220-231,1975.
5. Kirkman.T.P. "Application of the theory of the polyhedra to the Enumeration and Registration of Results". Proc. Roy. Soc. London vol.12, 341-380,1862-1863.
6. Hegde.S.M and Shankaran. P, On triangular sum labeling of graphs, in Labeling of discrete Structures and applications, Narosa publishing house, NewDelhi, 109-115, 2008.
7. Murugesan.S, Jayaraman.D and Shiama.J, Some higher order triangular sum labeling of graphs, International journal of computer Applications vol. 72(10), 2013.

***

A STUDY ON CLASS OF LATTICE ORDERED RECURSIVELY ENUMERABLE AND RECURSIVE LANGUAGES

D Tabhita
Ph.D Research Scholar, Dept. of Mathematics, SKSVMV, Kanchipuram
Lecturer, Andhra Loyola College, Vijayawada, Andhra Pradesh
dtabhita@ymail.com

Dr.K Srinivas Rao
Professor & Head, Dept. of Mathematics, SKSVMV, Kanchipuram
Lecturer, Andhra Loyola College, Vijayawada, Andhra Pradesh
raokonda@yahoo.com

Dr. P.Vijaya Vani
Faculty, Dept. of IBS, Acaharya Nagarjuna University
vijayavanipachala@gmail.com

Abstract: In this paper we recalled Turing Machines which are necessary for further study are noted. Languages accepted by Turing Machine called Recursively Enumerable Languages and their proper subclass called Recursive Languages are studied. We induced a relation on the Class of Recursively Enumerable Languages and Recursive Languages and tested for Lattice and Boolean structure. A Turing Operation is defined to carry the lattice order on Recursively Enumerable Languages and Recursive Languages and attempted to prove different algebraic forms.

Keywords: Turing Machines, Recursively Enumerable Languages, Recursive Languages

A Turing Machine (TM) is a machine $M = (Q, \Sigma, \Gamma, \delta, q_0, B, F)$ where Q is a non-empty finite set, called the set of states of M.
Γ is a finite set, called the set of allowable tape symbols of M.
B is a designated symbol of Γ, called the blank symbol.
Σ is a finite set, called the input alphabet of M.
$\delta : Q \times \Gamma \rightarrow Q \times \Gamma \times \{L, R\}$ is a partial function called the next move function of M, where L and R are reserved symbols denoting Left and Right direction moves respectively.
q_0 is a fixed element of Q called the initial state of M F is a subset of Q called the set of final states of M The Turing machine Model

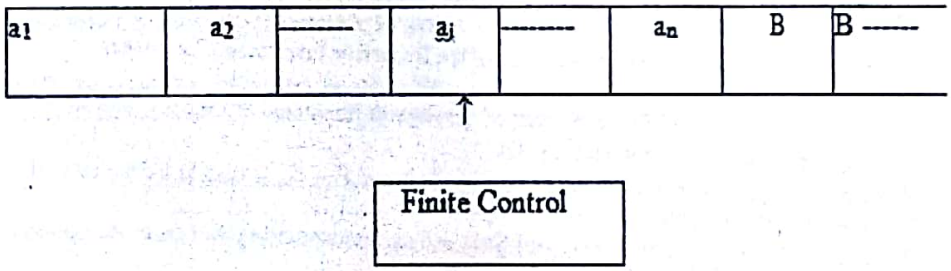


Figure 1

A formal basic model depicted above has a finite control, an input tape that is divided into cells and a tape head that scans one cell of the tape at a time. The tape has a leftmost cell but is infinite to the right. Each cell of the tape may hold exactly one tape symbol, which are finite in number. Initially the n leftmost cells, for some finite $n \geq 0$ hold the input, which is a string of symbols $a_1, a_2, a_3, \ldots\ldots\ldots a_n$.

A subset of the tape symbols is called the input symbols. The remaining infinity of cell each hold the blank indicated by B which is a special tape symbol that is not an input symbol.

263
Scanned by CamScanner

In one move the Turing Machine, depending upon the symbol scanned by the tape head and the state of the finite control:

1) changes state
2) prints a symbol on the tape cell scanned, replacing what was written there and
3) Moves its head left or right one cell.

We assume that Q and Γ are disjoint.

An Instantaneous Description (I D) of the Turing Machine M is given by $\alpha_1 q \alpha_2$. Here $q \in Q$, is the current state of M ; $\alpha_1\alpha_2$ is a string in Γ^* ,that is, the contents of the tape up to the rightmost nonblank symbol or the symbol to the left of the head, whichever is rightmost.

We note that the blank B may occur in $\alpha_1\alpha_2$.

The tape head is assumed to be scanning the leftmost symbol of α_2 or if $\alpha_2 = \varepsilon$, the head is scanning a blank.

We define a move of M as follows:
Let $x_1 x_2 \ldots\ldots x_{i-1} q x_i \ldots\ldots x_n$ be an ID.
(a) Suppose $\delta(q, x_i) = (p, y, L)$ where x_i is taken to be B if $i - 1 = n$
If $i = 1$, then there is no next ID, as the tape head is not allowed to fall off the left end of the tape.
If $i > 1$, then we write
$x_1 x_2 \ldots\ldots x_{i-1} q x_i \ldots\ldots x_n \vdash_M x_1 x_2 \ldots\ldots x_{i-2} p x_{i-1} y x_{i+1} \ldots\ldots x_n$ ----------(1)
(b) Suppose $\delta(q, x_i) = (p, y, R)$ where x_i is taken to be B if $i-1 = n$. If $i \geq 1$, then we write
$x_1 x_2 \ldots\ldots x_{i-1} q x_i \ldots\ldots x_n \vdash_M x_1 x_2 \ldots\ldots x_{i-1} y p x_{i+1} \ldots\ldots x_n$ ----------(2) In each case of (a) and (b) the equations (1) and (2) shows the move.

If two ID's are related by $\vdash_M$ or simply $\vdash$, we say that the second results from the first by one move. If one ID_2 results from ID_1 by some finite number of moves including zero moves, then we write ID1 $\vdash^*$ ID_2.

The language accepted by a Turing Machine $M = (Q, \Sigma, \Gamma, \delta, q_0, B, F)$, is the set $L(M) = \{w / w \text{ in } \Sigma^* \text{ and } q_0 w \vdash^* \alpha_1 p \alpha_2 \text{ for some p in F and } \alpha_1\alpha_2 \in \Gamma\}$.

A language is said to be Recursively Enumerable (RE) if it is accepted by a Turing Machine.
A Turing Machine is said to halt if it has no next move after the input is accepted. Note that for words not accepted, TM will never halt.

A subclass of the Recursively Enumerable languages, called the Recursive Languages, are those languages accepted by at least one Turing Machine that halts on all inputs.

Recursive Languages are a proper subclass of the Recursive Enumerable languages.

A Transition diagram for TM is a directed graph with the states as vertices, and directed labeled arcs from a vertex q to a vertex p with a label (x, y, D),
if $\delta(q, x) = (p, y, D)$ where x and y are tape symbols and $D \in \{L, R\}$ stands for a direction
(L for left and R for right).
We present the start state with the word Start and an arrow entering that state. Accepting states are indicated by double circles.

We present a TM that accepts the language $\{a^n b^n / n \geq 1\}$
as $M = (Q, \Sigma, \Gamma, \delta, q_0, B, F)$ where $Q = \{q_0, q_1, q_2, q_3, q_4\}$; $\Gamma = \{a, b, x, y, B\}$;
$\Sigma = \{a, b\}$; and $F = \{q_4\}$ and δ given in the following table and it is shown as diagram form as follows :

State	A	B	x	Y	B
q_0	(q_1, x, R)	-	-	(q_3, y, R)	-

Scanned by CamScanner

q_1	(q_1, a, R)	(q_2, y, L)	-	(q_1, y, R)	-
q_2	(q_2, a, L)	-	(q_0, x, R)	(q_2, y, L)	-
q_3	-	-	-	(q_3, y, R)	(q_4, B, R)
q_4	-	-	-	-	-

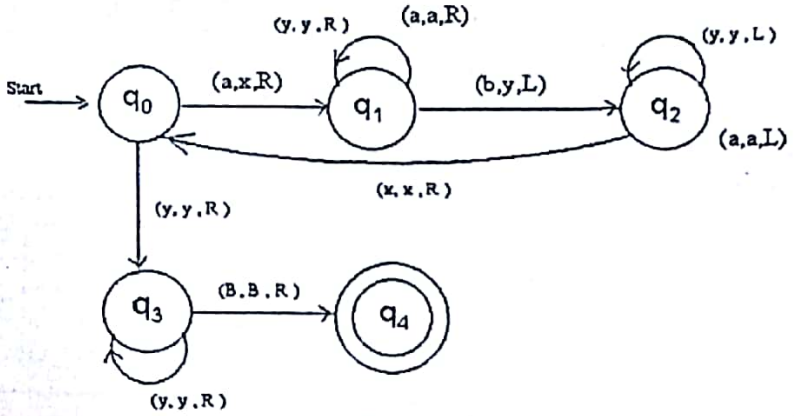
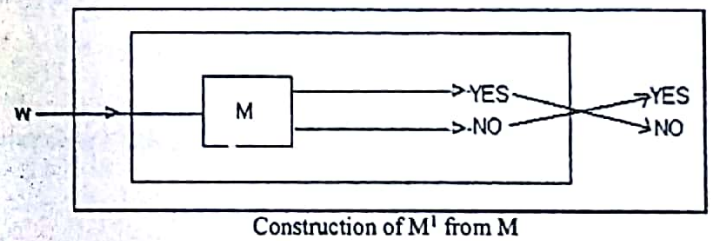


Figure 2

The Complement of a recursive language is recursive.

Proof. Let L be a recursive language and M a Turing machine that halts on all inputs and accepts L. Now we construct a new Turing machine M^1 from M so that if M enters a final state on input w then M^1 halts without accepting. If M halts without accepting, then M^1 enters a final state. Since one of these two events occurs, so M^1 is Turing Machine. Clearly $L(M^1)$ is the complement of L and thus the complement of L is recursive language.



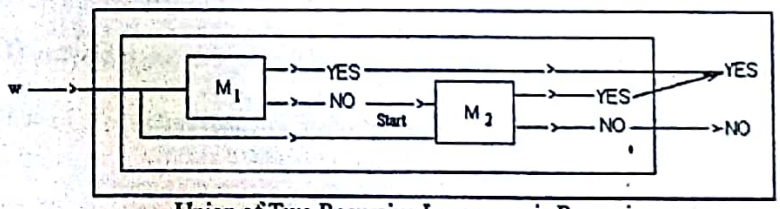
Construction of M^1 from M

Figure 3

Thus recursive languages are closed under complementation.

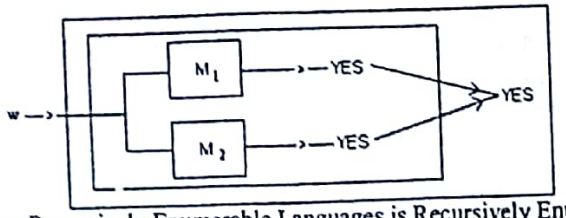
The Complement of a recursively enumerable language is not recursively enumerable.

The Union of two recursive languages is recursive.
Also the Union of two recursively enumerable languages is recursively enumerable.



Union of Two Recursive Languages is Recursive

Scanned by CamScanner

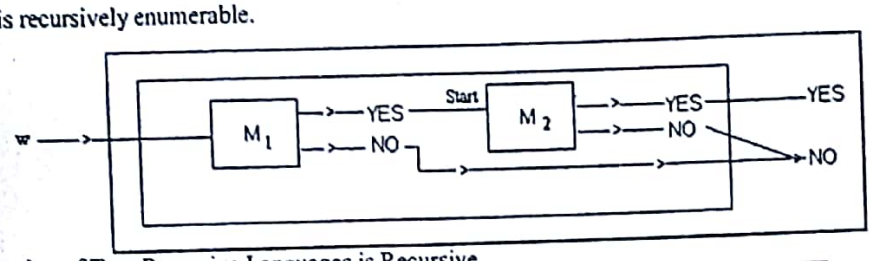


Union of Two Recursively Enumerable Languages is Recursively Enumerable

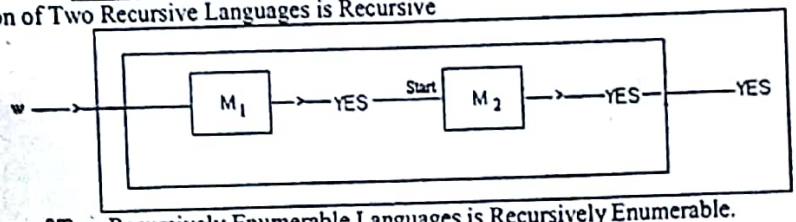
Construction of $M = M_1 \cup M_2$

Figure 4

The intersection of two recursive languages is recursive. Also the intersection of two recursively enumerable languages is recursively enumerable.



Intersection of Two Recursive Languages is Recursive



Intersection of Two Recursively Enumerable Languages is Recursively Enumerable.

Construction of $M = M_1 \cap M_2$

Figure 2.5

Turing Machine does not accept any input imply $L = \phi$ clearly $L = \phi$ is not recursively enumerable and so not recursive.

$L = \varepsilon$, $L = B$ are recursively enumerable and also recursive.

SECTION 2:

Notation 2.1: We write $Ł_{RE}$ for the class of Recursively Enumerable languages and $Ł_R$ for the class of Recursive languages.

Definition 2.2: Let $Ł_{RE}$ be the class of Recursively Enumerable languages. Define a relation "$\leq$" on $Ł_{RE}$ by $L_1 \leq L_2$ if $L_1 \subseteq L_2$. Also let $Ł_R$ be the class of Recursive languages. Define a relation "$\leq$" on $Ł_R$ by $L_1 \leq L_2$ if $L_1 \subseteq L_2$

Proposition 2.3: If $Ł_{RE}$ be the class of Recursively Enumerable languages then $(Ł_{RE}, \leq)$ is a partially ordered language.

Proof: For any $L_1 \in Ł_{RE}$ we have by the definition of "is" contained in $L_1 \subseteq L_2 \Rightarrow L_1 \leq L_2$

Thus '$\leq$' is reflexive.

Suppose $L_1 \leq L_2$ and $L_2 \leq L_1$

$\Rightarrow L_1 \subseteq L_2$ and $L_2 \subseteq L_1$

Now by the definition of equality in languages Since $L_1 \subseteq L_2$ and $L_2 \subseteq L_1$ imply $L_1 = L_2$

Thus '$\leq$' is antisymmetric.

Suppose $L_1 \leq L_2$ and $L_2 \leq L$

$\Rightarrow L_1 \subseteq L_2$ and $L_2 \subseteq L_3$

Now $L_1 \subseteq L_2 \subseteq L_3 \Rightarrow L_1 \subseteq L_3 \Rightarrow L_1 \leq L_3$ Thus '$\leq$' is transitive.

Scanned by CamScanner

Therefore ($Ł_{RE}$, $\leq$) is a partially ordered set.

Corollary 2.4: If $Ł_R$ be the class of Recursive languages then ($Ł_R$, $\leq$) is a partially ordered set.

Theorem 2.5: Let $Ł_{RE}$ be the class of Recursively Enumerable languages. Then the Poset. $Ł_{RE}$ is a lattice in which $L_1 \vee L_2 = L_1 \cup L_2$ and $L_1 \wedge L_2 = L_1 \cap L_2$.

Proof: Now we show that $Ł_{RE}$ is a lattice.

Claim 1: l. u. b. $\{ L_1 , L_2 \} = L_1 \vee L_2 = L_1 \cup L_2$

Let $L = L_1 \cup L_2$

By definition of union on sets $L_1 \subseteq L$ and $L_2 \subseteq L$

$\Rightarrow L_1 \leq L$ and $L_2 \leq L$

Suppose there exists $L_\bullet$ such that $L_1 \leq L_\bullet$ and $L_2 \leq L_\bullet$

$\Rightarrow L_1 \subseteq L_\bullet$ and $L_2 \subseteq L_\bullet$

$\Rightarrow L_1 \cup L_\bullet = L_\bullet$ and $L_2 \cup L_\bullet = L_\bullet$

Consider $L_\bullet = L_1 \cup L_\bullet$

$= L_1 \cup (L_2 \cup L_\bullet)$

$= (L_1 \cup L_2) \cup L_\bullet$

$\Rightarrow L_1 \cup L_2 \subseteq L_\bullet$

$\Rightarrow L \subseteq L_\bullet$

$\Rightarrow L \leq L_\bullet$

Thus, l. u. b. $\{L_1, L_2\} = L_1 \vee L_2 = L_1 \cup L_2 = L$

Claim 2: g. l. b. $\{L_1, L_2\} = L_1 \wedge L_2 = L_1 \cap L_2$ Let $L = L_1 \cap L_2$

By definition of intersection on sets $L \subseteq L_1$ and $L \subseteq L_2$

$\Rightarrow L \leq L_1$ and $L \leq L_2$

Suppose there exists $L_\bullet$ such that $L_\bullet \leq L_1$ and $L_\bullet \leq L_2$

$\Rightarrow L_\bullet \subseteq L_1$ and $L_\bullet \subseteq L_2$

$\Rightarrow L_\bullet = L_\bullet \cap L_1$ and $L_\bullet = L_\bullet \cup L_2$

Consider $L_\bullet = L_\bullet \cap L_2$

$= (L_\bullet \cap L_1) \cap L_2$

$= L_\bullet \cap (L_1 \cap L_2)$

$\Rightarrow L_\bullet \subseteq L_1 \cap L_2$

$\Rightarrow L_\bullet \subseteq L$

$\Rightarrow L_\bullet \leq L$

Thus g. l. b. $\{ L_1 , L_2 \} = L_1 \wedge L_2 = L_1 \cap L_2 = L$

Hence $Ł_{RE}$ is a lattice in which $L_1 \vee L_2 = L_1 \cup L_2$ and $L_1 \wedge L_2 = L_1 \cap L_2$.

Corollary 2.6: Let $Ł_R$ be the class of Recursive languages. Then the poset $Ł_R$ is a lattice in which $L_1 \vee L_2 = L_1 \cup L_2$ and $L_1 \wedge L_2 = L_1 \cap L_2$.

Theorem 2.7: Let $Ł_{RE}$ be the class of Recursively Enumerable languages. Then the lattice $Ł_{RE}$ is distributive.

Proof: Now we show that the lattice $Ł_{RE}$ is a distributive lattice.

Claim : $L_1 \wedge (L_2 \vee L_3) = (L_1 \wedge L_2) \vee (L_1 \wedge L_3)$

Consider $L_1 \wedge (L_2 \vee L_3) = L_1 \cap (L_2 \vee L_3)$

$= L_1 \cap (L_2 \cup L_3)$

$= (L_1 \cap L_2) \cup (L_1 \cap L_3)$

$= (L_1 \wedge L_2) \cup (L_1 \wedge L_3)$

$= (L_1 \wedge L_2) \vee (L_1 \wedge L_3)$

Therefore $L_1 \wedge (L_2 \vee L_3) = (L_1 \wedge L_2) \vee (L_1 \wedge L_3)$ Thus $Ł_{RE}$ is a distributive lattice.

The proof is complete.

Corollary 2.8: Let $Ł_R$ be the class of Recursive languages. Then the lattice $Ł_R$ is distributive.

Note 2.9: For $Ł_{RE}$, the class of Recursively Enumerable languages over a fixed Γ , $B \in Ł_{RE}$ is the minimal

Scanned by CamScanner

element of $Ł_{RE}$ and $\Gamma^* \in Ł_{RE}$ is the maximal element of $Ł_{RE}$ as $L \leq \Sigma^*$ for all $L \in Ł_{RE}$.

Note 2.10: For $Ł_R$, the class of Recursive languages over a fixed Γ, $B \in Ł_R$ is the minimal element of $Ł_R$ and $(\Sigma \cup B)^* \in Ł_R$ is the maximal element of $Ł_R$.

Note 2.11: Since $Ł_{RE}$ is not closed under complementation, so $Ł_{RE}$ is not a complemented distributive lattice. So it is not a Boolean Algebra.

Theorem 2.12: Let $Ł_R$ be the class of Recursive languages. Then $Ł_R$ is a distributive lattice in which $L_1 \vee L_2 = L_1 \cup L_2$ and $L_1 \wedge L_2 = L_1 \cap L_2$. This distributive lattice $Ł_R$ is complemented where the complement of $L \in Ł_R$ is the element $(\Sigma \cup B)^* - L$. In other words, $Ł_R$ is a Boolean Algebra, which is denoted by $B(Ł_R)$.

Proof: Let $Ł_R$ is a distributive lattice in which $L_1 \vee L_2 = L_1 \cup L_2$ and $L_1 \wedge L_2 = L_1 \cap L_2$. In order to show that this distributive lattice $Ł_R$ is complemented it is enough to check that the complement of every element L in $Ł_R$ is the element $(\Sigma \cup B)^* - L$.

Claim 1: $L \vee \bar{L} = (\Sigma \cup B)^*$

Consider $L \vee \bar{L} = L \cup \bar{L}$

$= L \cup ((\Sigma \cup B)^* - L)$

$= (L \cup (\Sigma \cup B)^*) - (L \cup L)$

$= (L \cup (\Sigma \cup B)^*) - L$

$= L + (\Sigma \cup B)^* - L$

$= (\Sigma \cup B)^*$

Therefore $\bar{L} = (\Sigma \cup B)^* - L$ is a complement of L.

Hence $Ł_R$ is a complemented distributive lattice. So $Ł_R$ is a Boolean Algebra.

Theorem 2.13: Let $Ł_R$ be the class of Recursive languages. Then $Ł_R$ is a distributive lattice in which $L_1 \vee L_2 = L_1 \cup L_2$ and $L_1 \wedge L_2 = L_1 \cap L_2$. This distributive lattice $Ł_R$ is relatively complemented. That is, $Ł_R$ is a Generalized Boolean Algebra.

Proof: Let $Ł_R$ be the class of Recursive languages. We have $Ł_R$ is a distributive lattice $Ł_R$ in which $L_1 \vee L_2 = L_1 \cup L_2$ and $L_1 \wedge L_2 = L_1 \cap L_2$. In order to show that this distributive lattice $Ł_R$ is complemented it is enough to check that for any triplet of its elements

L_1, L_2, L $(L_1 \leq L \leq L_2)$

$L \wedge L_* = L_1$ and $L \vee L_* = L_2$ for some L_* in $[L_1, L_2]$

Put $L_* = (L_1 \vee \bar{L}) \wedge L_2 = L_1 \vee (\bar{L} \wedge L_2)$

Consider $L \wedge L_*$

$L \wedge L_* = L \wedge ((L_1 \vee \bar{L}) \wedge L_2)$

$= L \wedge (L_1 \vee \bar{L})$

$= (L \wedge L_1) \vee (L \wedge \bar{L})$

$= L \wedge L_1$

$= L_1$

Also $L \vee L_* = L \vee (L_1 \vee (\bar{L} \wedge L_2))$

$= L \vee (\bar{L} \wedge L_2)$

$= (L \vee \bar{L}) \wedge (L \vee L_2)$

$= (\Sigma \cup B)^* \wedge L_2$

$= L_2$

Hence $Ł_R$ is relatively complemented distributive lattice. Clearly $Ł_R$ is a bounded below (Since B is the least element).

Therefore, $Ł_R$ is relatively complemented distributive lattice bounded below. Hence $Ł_R$ is a Generalized Boolean Algebra.

SECTION 3:

Definition 3.1: A binary operation $*$ on $[B, \Gamma^*]$ is said to be Turing operation if it satisfies:

(a) For all $L \in [B, \Gamma^*]$, $\Gamma * L = L$

(b) $L_1 * L_2 \leq L_3 * L_4$ whenever $L_1 \leq L_3$ and $L_2 \leq L_4$ that is., $*$ is L_1non decreasing.

(c) For any $L_1, L_2, L_3 \in [B, \Gamma^*]$, $(L_1 * L_2) * L_3 = L_1 * (L_2 * L_3)$ that is, $*$ is associative.

Scanned by CamScanner

(d) For any $L_1, L_2 \in [B, \Gamma^*]$, $L_1 * L_2 = L_2 * L_1$ i.e., $*$ is commutative.

Definition 3.2: A lattice ordered Turing machine (LTM) is a machine
$M = (Q, \sum, \Gamma, \delta, I, B, F, *)$ where
Q is a nonempty finite set called the set of states of M.
$\sum$ is a finite set, called the input alphabet of M.
Γ is a finite set called the set of allowable tape symbols of M.
B is a designated symbol of Γ called the blank symbol.
$\delta : Q \times \Gamma \times Q \times \Gamma \times \{L, R\} \rightarrow [B, \Gamma^*]$ is a function called the fuzzy transition function of M, where l and R are reserved symbols denoting Left and Right direction moves respectively.
$I: Q \rightarrow [B, \Gamma^*]$ is a fuzzy subset of Q called the fuzzy initial state set of M.
$F: Q \rightarrow [B, \Gamma^*]$ is a fuzzy subset of Q called the fuzzy final state set of M.

Definition 3.3: An instantaneous Description (I.D) of the lattice ordered Turing machine M is given by $\delta(q, a, p, b, D)$. Here $q \in Q$ is the current state of M; a is the tape symbol being scanned, p is the next state after a is scanned, b is the rewritten tape symbol and $D = \{L, R\}$ stands for a direction (L for left and R for right).

Definition 3.4: A move from ID, I_1 to another ID, I_2 denoted by $\vdash_M$. $\vdash_M$ is defined as $x, y \in \Gamma^*$, $a, b, c \in \Gamma$ and $p, q \in Q$.

$$I_1 \vdash_M I_2 = \begin{cases} \delta(q, a, p, b, R) \text{ if } I_1 = x\ q\ a\ y,\ I_2 = x\ b\ p\ y \\ \delta(q, a, p, b, L) \text{ if } I_1 = x\ c\ q\ a\ y,\ I_2 = x\ p\ c\ p\ y \\ \delta(q, B, p, b, L) \text{ if } I_1 = x\ q,\ I_2 = x\ b\ p \\ \delta(q, B, p, b, L) \text{ if } I_1 = x\ c\ q,\ I_2 = x\ p\ c\ b \\ B \text{ otherwise} \end{cases}$$

Definition 3.5: A lattice ordered Turing Machine is said to halt if it enters a state q,scanning a symbol a and there is no move i.e., $\delta(q, a, p, b, D) = B$ for any $p \in Q$, $b \in \Gamma$ and $D \in \{L,R\}$. We also say that $\delta(q, a)$ is not defined if $\delta(q, a, p, b, D) = B$ for any $p \in Q$, $b \in \Gamma$ and $D \in \{L,R\}$.

Definition 3.6: The Language accepted by a lattice ordered Turing Machine LTM, $M = (Q, \sum, \Gamma, \delta, I, B, F, *)$ denoted by L(M) is the set
$L(M) = \{s / s \in \sum^* \text{ and } (I(Q)s \vdash^* x\ p\ y) * F(p) : P \in Q, x\ y \in \Gamma^*\}$ and is called ℓ-languages.

Definition 3.7: Two lattice ordered Turing Machines LTM's M_1 and M_2 are said to be equivalent if they accept same ℓ-languages. That is, $L(M_1) = L(M_2)$.

Definition 3.8: A ℓ-language L(M) is said to be ℓ- recursively enumerable language if it is accepted by some lattice ordered Turing machine that is, L = L(M). Furthermore, if for any input $s \in \sum^*$, the lattice ordered. Turing machine M always halts that is, M halts on input s then we say L(M) is a ℓ- recursive language.

Theorem 3.9: Both ℓ- recursively enumerable languages and ℓ- recursive languages are closed under union, concatenation and kleene closure.
Proof: Claim:1: Union of ℓ- recursive languages is ℓ- recursive.
Let L_1 be $L(M_1)$ for LTM $M_1 = (Q_1, \sum_1, \Gamma_1, \delta, I_1, B, F_1, *)$ and
Let L_2 be $L(M_2)$ for LTM, $M_2 = (Q_2, \sum_2, \Gamma_2, \delta, I_2, B, F_2, *)$
$\delta(I, \varepsilon, \{q_1, q_2\}, \varepsilon, D) = \{I_1, I_2\}$, $q_1 \in Q_1, q_2 \in Q_2$.
$\delta(\{f_1, f_2\}, \varepsilon, F, \varepsilon, D) = \{F_1, F_2\}, f_1 \in Q_1, f_2 \in Q_2$.
So $L_1 \cup L_2$ is also ℓ- recursive.
Thus Union of ℓ- recursive languages is a ℓ- recursive language.
Claim 2: Union of ℓ- recursive languages is ℓ- recursive.
Let L_1 be $L(M_1)$ for LTM $M_1 = (Q_1, \sum_1, \Gamma_1, \delta, I_1, B, F_1, *)$ and
Let L_2 be $L(M_2)$ for LTM $M_2 = (Q_2, \sum_2, \Gamma_2, \delta, I_2, B, F_2, *)$
If ℓ_1, ℓ_2 are ℓ- recursive languages L_1 and L_2
then $\ell_1\ \ell_2$ denotes $L_1(M)\ L_2(M) = L_1\ L_2 = L(M)$ for LTM
$M = (Q, \sum, \Gamma_1 \cup \Gamma_2, \delta, I, B, F, *)$, where $Q = Q_1 \cup Q_2 \cup \{q_0, f_0\}$.

269
Scanned by CamScanner

If ℓ_1 and ℓ_2 are ℓ- recursive expressions denoting ℓ- recursive languages L_1 and L_2 then $\ell_1 \ell_2$ denotes $L_1(M)\, L_2(M) = L_1 L_2 = L(M)$ for LTM $M = (Q, \sum, \Gamma_1 \cup \Gamma_2, \delta, I_1, B, F_2, \bullet)$, where δ is $\delta(q, a, p, b, D) = \delta_1(q, a, p, ab, D)$ for q, p in Q_1-F_1 and a, b in $\sum_1 \cup \{\varepsilon\}$ so L_1L_2 is also ℓ- recursive.
Thus concatenation of ℓ- recursive languages is ℓ- recursive.
Hence ℓ- recursive languages are closed under Concatenation.
Claim 3: Kleene Closure of ℓ- recursive languages is ℓ- recursive.
Let L_1 be $L(M_1)$ for LTM $M_1 = (Q_1, \sum_1, \Gamma_1, \delta, I_1, B, F_1, \bullet)$
If ℓ_1 is a ℓ- recursive expression denoting ℓ- recursive language L_1 then ℓ_1^* denotes $L_1^* = L = L(M)$ for LTM, $M = (Q_1 \cup \{q_0, \tilde{q}_0\}, \sum_1, \Gamma_1, \delta, I_1, B, F_1, \bullet)$,
where $I: Q \to [B, \Gamma_1^*]$, $F: Q \to [B, \Gamma_1^*]$, and δ is given by
$\delta(I, \varepsilon, D) = \delta(F_1, \varepsilon, D) = \{I_1, F_1\}$
$\delta(q, a, p, b, D) = \delta_1(q, a, p, b, D)$ for q in Q_1-F_1 & a, b in $\sum_1 \cup \{\varepsilon\}$.
So $L = L_1^*$ is ℓ- recursive.
Thus kleen closure of is ℓ- recursive languages is ℓ- recursive.

Theorem 3.10: The class of ℓ- recursive languages is not closed under complementation.
Proof: Let L be L (M) for LTM $M = (Q, \sum, \Gamma, \delta, I, B, F, \bullet)$ and let $L \subseteq \Gamma^*$.
In a contrary way, we shall assume that the class of ℓ- recursive languages is closed under complementation.
Then construct LTM $M = (Q^1, \sum^1, \Gamma^1, \delta^1, I^1, B, F^1, \bullet)$ where $F^1 = Q - F$ where $F: Q \to [B, \Gamma^*]$ and since $[\emptyset, \Gamma^*]$ is a universal interval $F^1 = \emptyset$. Therefore, $\emptyset \to [B, \Gamma^*]$ is not defined and F^1 is not a fuzzy final state set. Therefore, M^1 is not a lattice ordered finite automaton.
Thus the class of ℓ- recursive languages is not closed under complementation. The proof is complete.

Corollary 3.11: The class of ℓ- recursive languages is not closed under intersection.
Proof: Since closure under intersection follow from closure under union and complementation, ℓ- recursive languages are not closed under intersection.

Theorem 3.12: Let Ł be the class of ℓ- recursive languages. Then the lattice Ł is distributive.
Proof: Let the lattice Ł be the class of ℓ- recursive languages. Now we shall show that Ł is a distributive lattice.
Claim: That is, $L_1 \wedge (L_2 \vee L_3) = (L_1 \wedge L_2) \vee (L_1 \wedge L_3)$

$$\begin{aligned} \text{Consider} \quad L_1 \wedge (L_2 \vee L_3) &= L_1 \cap (L_2 \vee L_3) \\ &= L_1 \cap (L_2 \cup L_3) \\ &= (L_1 \cap L_2) \cup (L_1 \cap L_3) \\ &= (L_1 \wedge L_2) \cup (L_1 \wedge L_3) \\ &= (L_1 \wedge L_2) \vee (L_1 \wedge L_3) \end{aligned}$$

Therefore $L_1 \wedge (L_2 \vee L_3) = (L_1 \wedge L_2) \vee (L_1 \wedge L_3)$
Thus ℓ- recursive language is a distributive lattice.
The proof is complete.

Theorem 3.13: Let Ł be the class of ℓ- recursive languages. Then the distributive lattice Ł is not a complemented distributive lattice and not a generalized Boolean algebra.
Proof: Let Ł be the class of ℓ- recursive languages.
Now we shall show that the distributive lattice Ł is not a complemented distributive lattice and not a generalized Boolean algebra.
By 3.10 and 3.11 ℓ- recursive languages Ł is not a complemented distributive lattice and follows Ł is not a generalized Boolean Algebra.

References:

1. Pedro Garcia, Jose Ruiz; Right and left locally testable languages; Theoretical Computer Science 246 (2000) 253-264
2. Pedro Garcia, Jose Ruiz, Manuel Vazquez De Parga; Bilateral locally testable languages; Theoretical Computer Science 299 (2003) 775 – 783
3. Jean-Eric Pin; Open problems about regular languages,; https://hal.archives-ouvertes.fr/hal-01614375v2
4. A.N. Trahtman; The Existence of Synchronizing Word and Cerny Conjecture For Some Finite Automata;

Scanned by CamScanner

pg. no. 1-9.
5. Howard Straubing; Forest Categories; pg. no.1-30
6. Márton Makrai; Finite State Language Models; Diploma Thesis; pg. no. 1-28
7. Alair Pereira Do Lago and Imre Simon; Free Burnside Semigroups; Theoret. Informatics Appl. 35 (2001) 579-595
8. S. Eilenberg; Automata, Languages and Machines. Vol A, Academic Press ,1974.
9. Mike Stannett; The Theory of X-Machines - Part 1; Technical Report CS-05-09; pg. no. 1-11.
10. Benoit Razet; Finite Eilenberg Machines; pg. no. 1-11
11. Adolfo Ballester-Bolinches, Jean-Eric Pin, Xaro Soler-Escriva; Formation of finite monoids and formal languages: Eilenbergs variety theorem revisited. pg. no. 1-24
12. Dominique Perrin and Jean- Eric Pin; Semigroups and automata on infinite words; pg. no. 1-28
13. Christian Glaßer; Counting with Counter free Automata; Electronic Colloquium on Computational Complexity, Report No. 11 (2004); pg. no. 1-22
14. Fabrice Chevalier, Deepak D'Souza, Pavithra Prabhakar; Counter-free input-determined timed automata; pg. no. 1-16
15. Kamal Lodaya; Logic As Regular Behaviour; pg. no. 1-18
16. Wolfgang Thomas; A Combinatorial Approach to the Theory of –Automata; Information And Control 48, 261-283 (1981)
17. Fabrice Chevalier, Deepak D'Souza, M. Raj Mohan, Pavithra Prabhakar; Automata and logics over signals; pg. no. 1-30
18. A. N. Trahtman; An Algorithm to Verify Local Threshold Testability of Deterministic Finite Automata; pg. no. 1-8.
19. Michael A. Harrison; On the Error Correcting Capacity of Finite Automata; Information -And Control 8, 430-450 (1965)
20. Marie-Pierre Beal, Jean Senellart ; On the bound of the synchronization delay of a local automaton; Theoretical Computer Science 205 (1998) 297-306
21. Stojan Bogdanovi, Balazs Imreh, Miroslav Ciric and Tatjana Petkovi; Directable Automata And Their Generalizations: A Survey; Novi Sad J. Math. Vol. 29, No. 2 (1999), 29–69
22. Ivan M. Havel; The Theory of Regular Events II; KYBERNETIKA ČISLO 6, ROČNIK 5/1969; pg. no. 521-542
23. Giovanni Pighizzini; Two-Way Finite Automata: Old and Recent Results; pg. no. 1-18
24. Sumaiya Faizyab; Comparative Study of Two-way Finite Automata and Turing machine; International Journal of Advanced Research in Computer Engineering & Technology (IJARCET) Volume 2, Issue 6, June 2013; pg no. 2205-2207
25. Patrick C. Fischer, Arnold L. Rosenberg, Multitape One-Way Nonwriting Automata; Journal Of Computer And System Sciences: 2, 88-101 (1968)
26. Markus Holzer, Martin Kutrib, Andreas Malcher; Complexity of multi-head finite automata: Origins and directions; Theoretical Computer Science 412 (2011) 83–96
27. Oscar H. Ibarra; Reversal-Bounded Multicounter Machines and Their Decision Problems; Journal of the Assoclauon for Computing Machmery, Vol 25 No 1, January 1978, pp 116-133
28. M. P. Schutzenberger; Une Theorie Algebricque du codage- Seminaire Dubreil 1956. Pg 1-24
29. Jitender Kumar And K. V. Krishna; Syntactic Semigroup Problem For The Semigroup Reducts Of Affine Near-Semirings Over Brandt Semigroups; pg. no. 1-9
30. Imre Simon; The Product of Rational Languages; pg. no. 1-15
31. Thomas Colcombet; Green's Relations and their Use in Automata Theory; pg. no. 1-21
32. Ondrej Klima and Libor Polak ; Biautomata for k-Piecewise Testable Languages;; pg. no. 1-18
33. Friedrich Martin Schneider, Daniel Borchmann; Topological Entropy of Formal Languages; February 19, 2018; pg. no. 1-24
34. Yo-Sub Han, Kai Salomaa, Derick Wood; Nondeterministic State Complexity of Basic Operations for Prefix-Free Regular Languages; Fundameta Informaticae 90 (2009) 93-106
35. Guo-Qiang- Zhang; Automata, Boolean Matrices, and Ultimate Periodicity; Information and Computation 152, 138-154 (1999).
36. Songfa You, Yijun Feng, Ming Cao, Yaping Wei; An Application of Linear Automata to Near Rings; Applied Mathematics, 2012, 3, 1614-1618.
37. John E. Hopcroft and Jeffery D. Ullman - Introduction to Automata Theory, Languages and Computation; Narosa Publishing House. 1979.
38. Gunter Pilz ; Near Rings, 1983

Scanned by CamScanner

Software Approach to Minimize Boolean Function as 'n' Distinct Functions

A. Kanchana, Research Scholar, Sri Chandra Sekharendra Saraswathi Viswa Mahavidyalaya, Kanchipuram, Tamilnadu.

Assistant Professor, Department of Mathematics, Rajalakshmi Institute of Technology, Kuttambkkam, Chennai.

E-mail:Kanchana.anbazhagan@gmail.com

K. Srinivasa Rao, Department of Mathematics, Sri Chandra Sekharendra Saraswathi Viswa Maha Vidyalaya, Kanchipuram, Tamilnadu.

Abstract--- Minimized Boolean function is used in the world of digital life. Several methods were implemented before to minimize Boolean function. Every method overcome the drawbacks of previous methods. This paper also explains a new method to minimize the boolean function which is comparatively better than the previous methods by time constraints. This can be done with the help of Java Scripts

Keywords--- Boolean Function, Boolean Law, Combining Possible Equations, Java Scripts.

AMS Subject Classification (2000)--- 03G05, 06E30, 94C10.

I. Introduction

Several methods were implemented to reduce the Boolean function. Huntington introduced the Boolean laws in 1904to reduce the expression. The above method cannot be implemented if the variable is greater than four. Then, Maurice Karnaugh in 1953 introduced a method called K- Map [4] which is a pictorial form of truth table. Here also, the method cannot be implemented if the variable is greater than six. Later, a new approach of minimized Boolean function in tabular form is explained by W. V. Quine [5] in 1956. But then the tabular column becomes lengthier for more number of variables and making it difficult to implemented by both students and faculty members.

Out of all the above mentioned methods, Q. M. method is the computer based method which has many advantages over the first two methods. In recent days, many methods are being developed to minimize the Boolean function.

An internet based implementation [6] is used with the help of the Java applet. It runs only till four variables and can be extended to more variables in the given conclusion. Also, in the above method only one expression can be found at a time for a single Boolean function.

In 2016 [7], a D. C K-map method was imposed to minimize the Boolean function. This method takes less time and space than Q. M. method, but the drawbacks are that it requires additional map to compute the final expression and it is not computerized.

Considering all the constraints, we have found out a new method [8] to minimize the Boolean function. This method is also a tabular method. In this method, many minimized Boolean function can be found at a single instant. The disadvantage is that, the additional tables should be used when the variables are more in number, hence making it difficult to pair. To overcome this disadvantage, we develop a Java scripts programme to minimize the Boolean function up to 15 variables

II. Boolean Law

This section explains the Booleanlaw and small introduction about the JavaScripts which we have used in later text.

The Boolean law we have used here is $x + x' = 1$.

III. Java Script

The programming control can be provided by JavaScript in a web browser. Hereit is used as a tool to minimize the Boolean Function.

Received: 15 May 2018/Accepted: 20 June 2018

IV. Distinct Minimized Algorithm

The algorithm explains clearly in paper[8]with an example of two, three and four variables.

Considering a Boolean function and then constructing of a new table by numbering each terms of the above function. Next table is framed by pairing each of the rows using the algebraic rule $x + x' = 1$. The table will be framed until such pairing does not occur.

V. Java Script to Minimize Boolean Functions

The following Java Scripts programme gives minimized Boolean function up to fifteen variables

Structure of the Program

```
'use strict';
// A $( document ).ready() block.
$( document ).ready(function() {
   const variableName =
['x','y','z','w','a','b','c','d','e','f','g','h','i','j','k','l','m','n','o','p','q','r','s','t','u','v'];
   // set values for the dropdown menu
   let $select = $(".truthtableRange");
   for (let i=1;i<=15;i++){
      $select.append($('<option></option>').val(i).html(i))
   }
   // set values for the dropdown menu
   $select = $(".sequenceRange");
   for (let i=1;i<=100;i++){
      $select.append($('<option></option>').val(i).html(i))
   }
   $('button#truthTableGenerator').click(function() {
      console.log('Inside click');
      let numberRange = $(".truthtableRange").val();
      let sequenceRange = $(".sequenceRange").val();
      let arrayData = generateRandomNumberArray(numberRange,sequenceRange);
      $('textarea#truthtable').val(arrayData.join("\n"));
   });
   $('button#simplifyTable').click(function() {
      let truthTable = $('textarea#truthtable').val();
      if (!truthTable) {
         return false;
      }
      //send to server and process response
      let variableLength = (""+(truthTable.split(/\n/)[0])).split("").length;
      let data = [];
      let modifiedHeaderRow, headerRow;
      headerRow = variableName.slice(0,variableLength);
      modifiedHeaderRow = variableName.slice(0,variableLength);
      modifiedHeaderRow.unshift("Num","Function");
      data.push(modifiedHeaderRow);
      $.each(truthTable.split(/\n/), function(i, line){
        if(line && line.length){
            let finalLine = [];
            finalLine.push(data.length);
            finalLine.push(getFunctionForTable(line,headerRow));
            finalLine = finalLine.concat(line.split(""));
            data.push(finalLine);
        }
      });
```

ISSN 1943-023X
Received: 15 May 2018/Accepted: 20 June 2018

```
            // empty the table
            $('.table-div').empty();
            // add the first table
            convertArrayToTable($('.table-div'), data);
            // get the first simplified table
            let firstData = compareArrayRowsForOneDifference(data
            // remove duplicates
            firstData = removeDuplicates(firstData);
            // add the data to page
            convertArrayToTable($('.table-div'), firstData);
            // get the second simplified table
            let secData = compareArrayRowsForOneDifference(firstData)
            secData = removeDuplicates(secData);
            // add the data to page
            convertArrayToTable($('.table-div'), secData);
            // get the third simplified table
            let thirdData = compareArrayRowsForOneDifference(secData)
            thirdData = removeDuplicates(thirdData);
            // add the data to page
            Convert Array To Table($('.table-div'), third Data);
        });});
function removeDuplicates(arrayData){
                let newArr = []
                let arrKey = []
                newArr.push(arrayData[0]);
                for (let i = 1; i < arrayData.length ; i++ ){
                        if(arrKey.indexOf(arrayData[i][1]) == -1){
                                arrKey.push(arrayData[i][1]);
                                newArr.push(arrayData[i]);
            }}
          return newArr;
        }
function compareArrayRowsForOneDifference(arrayData){
            // new output array
            let newData = [];
            let newLine = [];
            newData[0] = arrayData[0];
            for (var k = 1, outlen = arrayData.length; k < outlen; k++) {
                    let firstArray = arrayData[k];
                    for (var i = k, len = arrayData.length; i < len; i++) {
                            newLine = [];
                            let diffCount = 0;
                            let secondArray = arrayData[i];
                            console.log("firstArray ",firstArray);
                            console.log("secondArray ",secondArray);
                for(var j = 2; j < firstArray.length; j++) {
                  if(firstArray[j] > secondArray[j] || firstArray[j] < secondArray[j]) {
                      newLine[j] = "-";
                      diffCount++;
                  }else{
                      newLine[j] = firstArray[j];
                  }}
                            if(diffCount == 1){
                                    newLine[0] =  "("+firstArray[0]+","+secondArray[0]+")";
```


Received: 15 May 2018/Accepted: 20 June 2018

```
                                                newLine[0] = newLine[0].replace('),(', ',').replace('((', '(').replace('))',
')')
                                                //reassemble everything before position diffIndex, and everything after
                                                newLine[1] =
getFunctionForTableWithHypen(newLine.slice(2),arrayData[0].slice(2));
                                                newData.push(newLine);
                                        }
                                        // stop the loop for the last index
                                        if(i+1 >= arrayData.length){
                                                break;
                                        }
                                }
                        }
                        return newData;
}
        function convert Array To Table (table Obj, data){
                let table = arrayToTable(data, {
                        thead: true,
                        attrs: {class: 'boolean'}
                })
                tableObj.append(table);
        }
        function getFunctionForTableWithHypen(dataArray,headerRow){
                let finalArray = [];
                for (let i = 0; i < headerRow.length ; i++ ){
                        var data = "";
                        switch(dataArray[i]){
                                case "0":
                                        data = headerRow[i]+'\';
                                        break;
                                case "1":
                                        data = headerRow[i];
                                        break;
                                case "-":
                                        data = "";
                                        break;
                        }
                        finalArray.push(data);
                }
                return finalArray.join("");
        }
        function getFunctionForTable(lineData,headerRow){
                let finalArray = [];
                let dataArray = lineData.split("");
                for (let i = 0; i < headerRow.length ; i++ ){
                        finalArray.push( dataArray[i] == 1 ? headerRow[i] : headerRow[i]+'\');
                }
                return finalArray.join("");
        }
        function generateRandomNumber(numberRange) {
                let text = "";
                const possible = "0101010101010101010101010010100101010";
                for (var i = 0; i < numberRange; i++)
                  text += possible.charAt(Math.floor(Math.random() * possible.length));
                return text;
        }
```

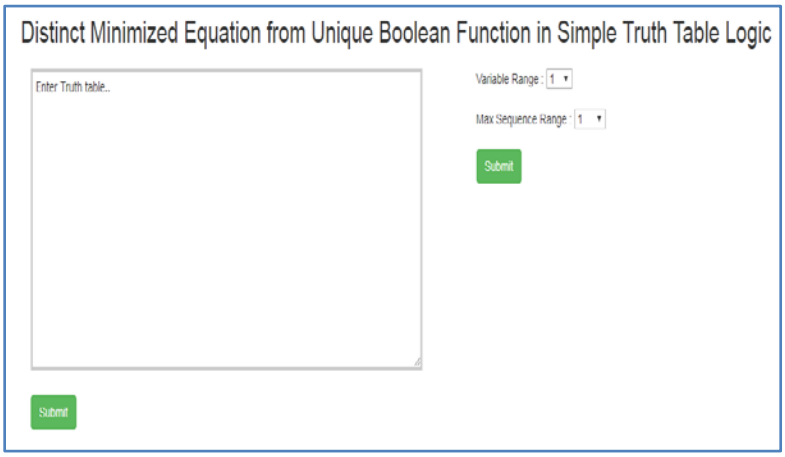
```
function checkLength(randomnumber, numberRange){
   return (randomnumber+").length == numberRange ? true : false;
}
function generateRandomNumberArray(numberRange,sequenceRange){
   let arr = []
   let loopCount = 0;
   while(loopCount <= 99 && arr.length < sequenceRange){
         loopCount++;
      const randomnumber = generateRandomNumber(numberRange);
      if(checkLength(randomnumber, numberRange) && arr.indexOf(randomnumber) == -1){
         arr[arr.length] = randomnumber;
      }
   };
   console.log("arr ",arr);
   return arr;
}
```

The above program can be viewed in

https://s3.amazonaws.com/kanchana-boolean/index.html.

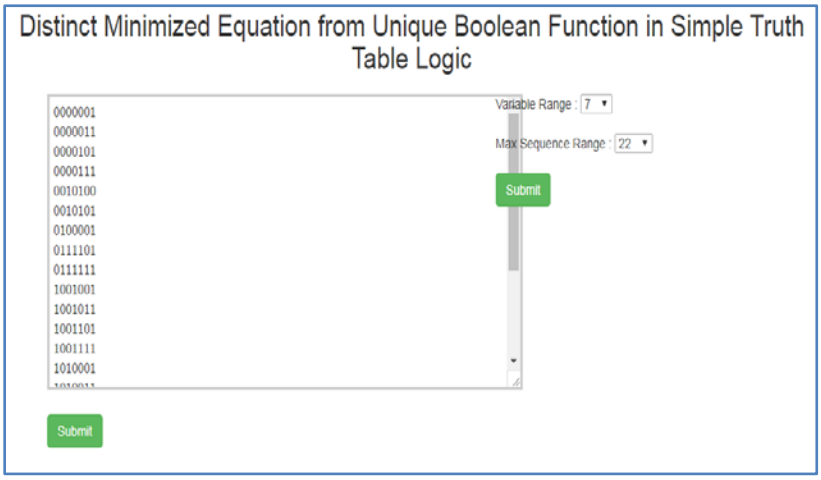
VI. Description of Program with Examples

The table below will be the outlook of the above program if we click the above mentioned link



Consider the example in paper [7],

1. Variable range and maxiumum sequence range is fixed, then truth table value is entered.



Received: 15 May 2018/Accepted: 20 June 2018

2. Submit button is pressed in the bottom of the table.

Num	Function	x	y	z	w	a	b	c
1	x'y'z'w'a'b'c	0	0	0	0	0	0	1
2	x'y'z'w'a'bc	0	0	0	0	0	1	1
3	x'y'z'w'ab'c	0	0	0	0	1	0	1
4	x'y'z'w'abc	0	0	0	0	1	1	1
5	x'y'zw'ab'c'	0	0	1	0	1	0	0
6	x'y'zw'ab'c	0	0	1	0	1	0	1
7	x'yz'w'a'b'c	0	1	0	0	0	0	1
8	x'yzwab'c	0	1	1	1	1	0	1
9	x'yzwabc	0	1	1	1	1	1	1
10	xy'z'wa'b'c	1	0	0	1	0	0	1
11	xy'z'wa'bc	1	0	0	1	0	1	1
12	xy'z'wab'c	1	0	0	1	1	0	1
13	xy'z'wabc	1	0	0	1	1	1	1
14	xy'zw'a'b'c	1	0	1	0	0	0	1
15	xy'zw'a'bc	1	0	1	0	0	1	1
16	xy'zw'ab'c	1	0	1	0	1	0	1
17	xyz'w'a'b'c'	1	1	0	0	0	0	0
18	xyz'w'a'b'c	1	1	0	0	0	0	1
19	xyz'w'a'bc	1	1	0	0	0	1	1
20	xyzwab'c'	1	1	1	1	1	0	0
21	xyzwab'c	1	1	1	1	1	0	1
22	xyzwabc	1	1	1	1	1	1	1

Num	Function	x	y	z	w	a	b	c
(1,2)	x'y'z'w'a'c	0	0	0	0	0	-	1
(1,3)	x'y'z'w'b'c	0	0	0	0	-	0	1
(1,7)	x'z'w'a'b'c	0	-	0	0	0	0	1
(2,4)	x'y'z'w'bc	0	0	0	0	-	1	1
(3,4)	x'y'z'w'ac	0	0	0	0	1	-	1
(3,6)	x'y'w'ab'c	0	0	-	0	1	0	1
(5,6)	x'y'zw'ab'	0	0	1	0	1	0	-
(6,16)	y'zw'ab'c	-	0	1	0	1	0	1
(7,18)	yz'w'a'b'c	-	1	0	0	0	0	1
(8,9)	x'yzwac	0	1	1	1	1	-	1
(8,21)	yzwab'c	-	1	1	1	1	0	1
(9,22)	yzwabc	-	1	1	1	1	1	1
(10,11)	xy'z'wa'c	1	0	0	1	0	-	1

Show

ISSN 1943-023X
Received: 15 May 2018/Accepted: 20 June 2018

(10,12)	xy'z'wb'c	1	0	0	1	-	0	1
(11,13)	xy'z'wbc	1	0	0	1	-	1	1
(12,13)	xy'z'wac	1	0	0	1	1	-	1
(14,15)	xy'zw'a'c	1	0	1	0	0	-	1
(14,16)	xy'zw'b'c	1	0	1	0	-	0	1
(17,18)	xyz'w'a'b'	1	1	0	0	0	0	-
(18,19)	xyz'w'a'c	1	1	0	0	0	-	1
(20,21)	xyzwab'	1	1	1	1	1	0	-
(21,22)	xyzwac	1	1	1	1	1	-	1

Num	Function	x	y	z	w	a	b	c
(1,2,3,4)	x'y'z'w'c	0	0	0	0	-	-	1
(8,21,9,22)	yzwac	-	1	1	1	1	-	1
(10,11,12,13)	xy'z'wc	1	0	0	1	-	-	1

3. The equation can be framed by combining the numbers such that the each numbers occur only once,

(1,2,3,4)+(8,21,9,22)+(10,11,12,13)+(5,6)+(7,18)+(14,15)+16+17+19+20

(1, 2, 3, 4)+(8,21,9,22)+(10,11,12,13)+(17,18)+(5,6)+7+(14,15)+16+19+20

Similarly we can frame many combinations.

IV)The above numbers are written in terms of variables to get the final equations,

$$x'y'z'w'c + yzwac + xy'z'wc + x'y'zw'ab' + yz'w'a'b'c + xy'zw'a'c + xy'zw'ab'c + xyz'w'a'b'c' + xyz'w'a'bc + xyzwab'c'$$

$$x'y'z'w'c + yzwac + xy'z'wc + xyz'w'a'b' + xy'zw'a'c + x'y'zw'ab' + xy'zw'ab'c + xyz'w'a'bc + x'yz'w'a'b'c + xyzwab'c'$$

VII. Time Efficiency

In paper [7] it is clearly mentioned that DC- K- Map method is more efficient than the QM method. But this method is more efficient than the DC- K- Map method. In DC- K- Map method the size requirement of n variable is 2^n , but for this method the space requirement is 2^n –(the minterms assigned the value zero). Hence it takes less space than the DC- K- Map method.

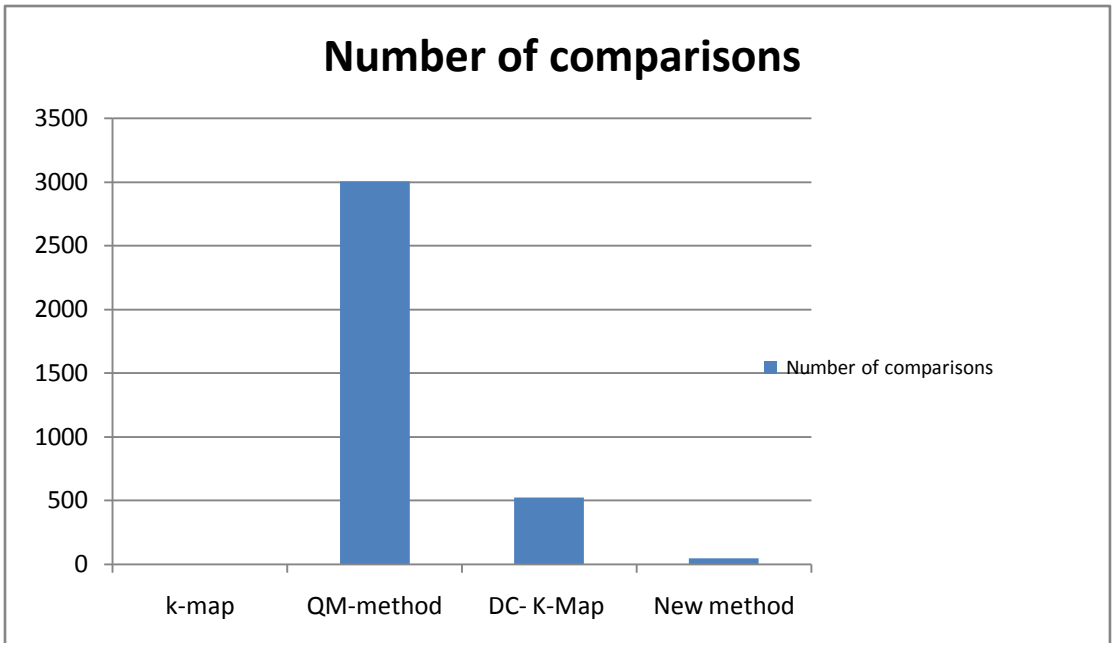
For seven variables QM method takes 3003 comparisons and DC- K- Map method takes 520 comparisons but this method can takes only number of (number of minterms-1) (number of minterms-2)/2 comparisons. Hence this method is more easier and user friendly than the previous methods.

VIII. Graphical Representation

The following table gives the comparison of above results,

Method	K- Map	QM-method	DC-K-Map	New method
Number of Comparisons (11 variables)	Not valid	3003	520	(11-1)(11-2)/2=(10*9)/2 =90/2=45

ISSN 1943-023X
Received: 15 May 2018/Accepted: 20 June 2018



IX. Conclusion

In this paper, a new method to minimize the Boolean function is found which is implemented in a Java Scripts using up to fifteen variables to achieve the result fast. This method is easier than the previous methods. It can also frame many equations in a single time which is useful to all digital designers. This can be accessed at **https://s3.amazonaws.com/kanchana-boolean/index.html.**

References

[1] Claude, E.S. Symbolic Analysis of Relay and Switching Circuits. *Transactions American Institute of Electrical Engineers* **57** (6) (1938) 713-723.

[2] Boole, G. *An Investigation of the Laws of Thoughts*. New York: Dover Publications, 1954.

[3] Mohan Ranga Rao, R. An Innovative Procedure to Minimize Boolean Function. *International Journal of Advanced Engineering Sciences and Technologies* **3** (1) (2011) 12-14.

[4] Bob, H. and Bob, B. *Karnaugh Maps*. Southern Polytechnic State University, 2001.

[5] Quine, W.V. *The Problem of Simplifying Truth Tables.* The American Mathematical Monthly **59** (8) (1952) 521-531.

[6] Sebestian, P.T. WWW-Based Boolean Function Minimization. *International Journal of Applied Mathematics and Computer Sciences and Technologies* **13** (4) (2003) 577-583.

[7] Visvam, D.A.K. Static Structure Simplification of Boolean function for 'N' Variables-A Novel Approach. *Journal of Micro Electronics* **1** (4) (2016) 160-167.

[8] Kanchana, A. and Srinivasa Rao, K. Distinct Minimized Equation from Unique Boolean Functionin Simple Truth Table Logic. *International Journal of Pure and Applied Mathematics* **116** (23) (2017) 115-120.

Received: 15 May 2018/Accepted: 20 June 2018

International Journal of Pure and Applied Mathematics
Volume 119 No. 9 2018, 89-100
ISSN: 1311-8080 (printed version); ISSN: 1314-3395 (on-line version)
url: http://www.ijpam.eu
Special Issue

ijpam.eu

Reducing the Variables in Boolean Function Using Fuzzy Cognitive Map to Create a Circuit

A.Kanchana[1] K. Srinivasa Rao [2]
[1]Research Scholar
Sri Chandrasekharendra saraswathi viswa mahavidyalaya
Kanchipuram, Tamilnadu
[1] Assistant Professor of Mathematics
Rajalakshmi Institute of Technology
Kuttambkkam, Chennai. E-mail:Kanchana.anbazhagan@gmail.com
[2] Sri Chandrasekharendra saraswathi viswa mahavidyalaya
Kanchipuram, Tamilnadu.

October 26, 2017

Abstract

In this paper, we used the fuzzy cognitive map to reduce the variables in a Boolean function and it is used to create a circuit for cost reduction. An example is given for above justification.
AMS Subject Classification (2000) - 06E30, 94C10

Key Words: Refrigerator, Performance of the variable, Fuzzy cognitive map, Boolean function, Switch circuit.

1 Introduction

The concept of Boolean function is introduced by George Boole in 1854. In 1938[1], Claude Shannon introduce the Booles concept which is applied in creation of circuit, field of Computer Science

etc.
Many methods were used to minimize the Boolean function which is also explained in the paper [9] and [10]. None of the method is imposed to delete the variable so that the Boolean function is minimized.
The minimized Boolean functions are solved in [3], so that the input is obtained from the output. Several methods are used to minimize a Boolean function, which is useful to create a circuit to reduce the cost which is explained in [4]. In the paper [5], we introduced a new technique so that we can find more than one minimized function in single Boolean function which is helpful in several practical situations.
But without the minimization we have to use the circuit in some problems like we have solved in Paper [2]. In such case, how to reduce the cost?
This paper gives the solution for above problem by using the technique of Fuzzy Cognitive Map. The above method can be used for any number of variables. Hence we have taken the problem of refrigerator which involves eleven important parts (11 variables) to work in a good condition.

2 Material And Methods

In this section we concentrate on Fuzzy Cognitive Map, Boolean function, Truth table and simple Boolean Laws which will be useful in later text.

Fuzzy Cognitive Map

Networks of complex system can be solved by Fuzzy Cognitive Map [8]. It was introduced by Bart Kosko. A fuzzy relational matrix is created with the help of below equation given by,

$$R_{ij} = (r_{ij}) \tag{1}$$

In r_{ij} stands for the impact of one variable on another with membership values.

Boolean function

If $x_1, x_2...X_n$ are Boolean variables, $f : x_1, x_2...X_n \to 0, 1$ is called Boolean function of degree n.

Boolean Expression
A Boolean expression in n Boolean variables $x_1, x_2...X_n$ is a finite string of symbols formed recursively

3 Fuzzy Cognitive Map

The algorithm of Fuzzy Cognitive Map model is designed to the variables have both positive as well as negative impact on each other. Here, the motive of the work is Good Working Condition of Refrigerator So we add this as one of the variable. Before going to the problem, we have to fix the Linguistic term with membership value. Since the parts of the refrigerator is having the positive impacts on working condition of the refrigerator. Hence we always fix it in a positive mode.

Table 1: Table - 1

Linguistic Term	Membership Value
Very High(VH)	100
High(H)	80
Medium(M)	60
Low(L)	40
Very Low(VL)	20

From Table 1, it is clear that the values are represented between [0,100] because of the software (Java Programmed applet) but usually it is represented in the interval [0, 1].

Now we frame the problem by defining the variables below,

- V_1- Frosted evaporator coil.
- V_2- Faulty evaporator fan
- V_3- Out of order defrost system
- V_4- Faulty compressor
- V_5- In sufficient refrigerant level

- V_6- Dirt insulated condenser coils
- V_7-Defective condenser fan
- V_8- Defective start relay
- V_9- Defective start capacitor
- V_{10}- Faulty thermistor
- V_{11}- Good working condition of refrigerator

Now we are explaining the variables below.

V1. Frosted evaporator coil:
There are evaporator coils and circulating fan in the freezer zone of the refrigerator.

V2. Faulty evaporator fan:
The fan circulates the cool air from the freezer to other compartments inside refrigerator.

V3. Out of order defrost system:
In any frost free refrigerator there is a defrost system which controls the cooling and defrost cycle.

V4. Faulty compressor:
A compressor is the heart of the refrigerator cycle. When it does not work properly then the entire cooling process does not even start.

V5. In sufficient refrigerant level:
If compressor is the heart, the refrigerant is the blood of the cooling cycle.

V6. Dirt insulated condenser coils:
When high pressure hot refrigerant condenses in the condenser, lot of heat is dissipated during this conversion.

V7. Defective condenser fan:
It forces hot air out of the refrigerator.

V8. Defective start relay:
A start relay is a small device located near compressor. It helps compressor in starting up.

V10. Faulty thermistor:
A thermistor is a sensor that control the air temperature inside refrigerator and controls the start and stop of cooling cycle.

V11- Good working condition of refrigerator

This variable is very important which is affected by all other variables. Now we define the relational matrix as follows,In the Table 2, we are going to enter the impact values of each other in the Java Program Applet and we are assuming that all the variable is having positive impact on each other.

Table 2: Table- 2

Impact Values	V1	V2	V3	V4	V5	V6	V7	V8	V9	V10	V11
V1	-	H	L	L	-	-	-	-	-	-	M
V2	L	-	VL	-	-	-	-	-	-	L	M
V3	L	L	-	-	-	-	-	-	-	L	M
V4	H	M	VH	-	VH	H	H	VH	H	H	VH
V5	L	L	L	-	-	-	-	-	-	L	H
V6	-	-	-	L	-	-	H	-	-	-	M
V7	-	-	-	-	L	VH	-	-	-	-	L
V8	L	-	-	VH	-	-	-	-	-	-	L
V9	L	-	-	VH	H	-	-	-	-	L	H
V10	-	-	-	-	VH	-	-	-	H	-	L
V11	-	-	-	-	-	-	-	-	-	-	-

4 Results

After, fixing the above relational matrix we start our iterations with different cases and from that we are going to identify the important variables require to run the refrigerator. In each case I stands for input values and O stands for output values.

Table 3: 7 Iterations

	V1	V2	V3	V4	V5	V6	V7	V8	V9	V10	V11
I	100	40	40	40	40	40	40	40	40	40	40
O	47	47	47	46	46	45	45	46	46	46	46

In the Table 3 to Table 12, we are giving importance to each variable in each case. And in each case, V11 shows that working

Table 4: 7 Iterations

	V1	V2	V3	V4	V5	V6	V7	V8	V9	V10	V11
I	40	100	40	40	40	40	40	40	40	40	40
O	42	42	42	41	42	40	40	41	42	42	42

Table 5: 6 Iterations

	V1	V2	V3	V4	V5	V6	V7	V8	V9	V10	V11
I	40	40	100	40	40	40	40	40	40	40	40
O	43	43	43	42	43	41	41	42	43	43	43

Table 6: 6 Iterations

	V1	V2	V3	V4	V5	V6	V7	V8	V9	V10	V11
I	40	40	40	100	40	40	40	40	40	40	40
O	60	60	60	61	60	62	62	61	60	60	60

Table 7: 6 Iterations

	V1	V2	V3	V4	V5	V6	V7	V8	V9	V10	V11
I	40	40	40	40	100	40	40	40	40	40	40
O	42	42	42	41	42	40	40	41	42	42	42

Table 8: 8 Iterations

	V1	V2	V3	V4	V5	V6	V7	V8	V9	V10	V11
I	40	40	40	40	40	100	40	40	40	40	40
O	43	43	43	43	43	44	44	43	43	43	43

Table 9: 8 Iterations

	V1	V2	V3	V4	V5	V6	V7	V8	V9	V10	V11
I	40	40	40	40	40	40	100	40	40	40	40
O	42	42	42	42	42	43	43	42	42	41	42

Table 10: 5 Iterations

	V1	V2	V3	V4	V5	V6	V7	V8	V9	V10	V11
I	40	40	40	40	40	40	40	100	40	40	40
O	45	45	45	46	45	47	47	46	45	45	45

Table 11: 5 Iterations

	V1	V2	V3	V4	V5	V6	V7	V8	V9	V10	V11
I	40	40	40	40	40	40	40	40	100	40	40
O	47	47	47	48	48	48	48	48	48	47	47

Table 12: 6 Iterations

	V1	V2	V3	V4	V5	V6	V7	V8	V9	V10	V11
I	40	40	40	40	40	40	40	40	40	100	40
O	47	47	47	47	48	46	46	47	48	48	47

Table 13: 8 Iterations

	V1	V2	V3	V4	V5	V6	V7	V8	V9	V10	V11
I	40	40	40	100	40	40	40	40	100	100	40
O	76	76	76	77	77	77	77	77	77	76	76

Table 14: 8 Iterations

	V1	V2	V3	V4	V5	V6	V7	V8	V9	V10	V11
I	100	100	100	40	100	100	100	100	40	40	40
O	64	64	64	63	63	63	63	63	63	64	64

condition of Refrigerator. In Table 6, Table 11 and Table 12, we are giving importance to the variables V4, V9 and V10 by fixing the value as 100 respectively and we obtain the corresponding V11 values are more than 47. So in the next Table 13 we are taking the corresponding variables as 100 and remaining variables as 40. From this V11 taking the value 76 implies the good working condition of refrigerator. In the reverse way, If we take other seven variables 100 in Table 14, we are getting the working percentage as 64. So we create the circuit for above three variables.

5 Circuit Creation For Above Variables

Now, we create a circuit for three important variables V4(Compressor), V9(Defective start capacitor), V10(Faulty thermistor). First, if the compressor is not working properly we define it has to be 0 otherwise 1. Second, if the defective start capacitor is not working properly we define it has to be 0 otherwise 1. At last, if the Faulty thermistor is not working properly we define it has to be 0 otherwise 1. The sensor is fixed for above three parts in the above conditions.

5.1 Output 1

In the above three things, if any one of the thing is not working properly then the following Boolean function will occur,

$$f_1 = v_4 v_9 v_{10} + \bar{v}_4 v v_{10} + v_4 \bar{v}_9 v_{10} + v_4 v_9 \bar{v}_{10} \tag{2}$$

5.2 Logic Gates, Switch Circuit and PLC circuit

The corresponding [7] logic gate circuit for f1 is given in Figure 1. The switch circuit for above logic gate circuit is given in Figure 2 and the Programming Logic Circuit is used to fix the sensor for the variables is explained in Figure 3.

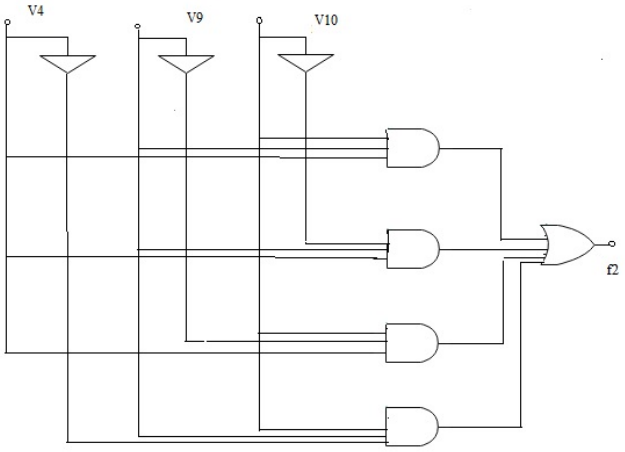


Figure 1: figure 1

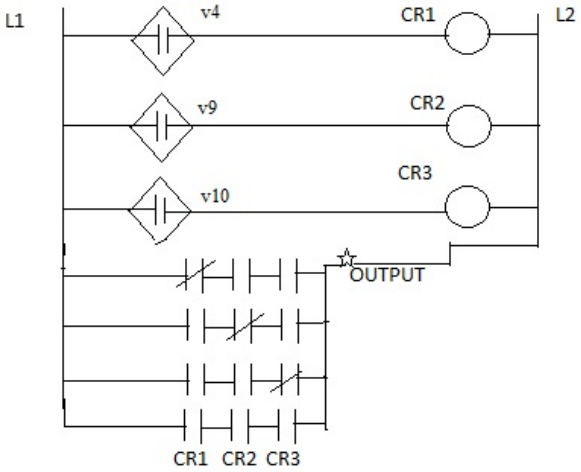


Figure 2: figure 2

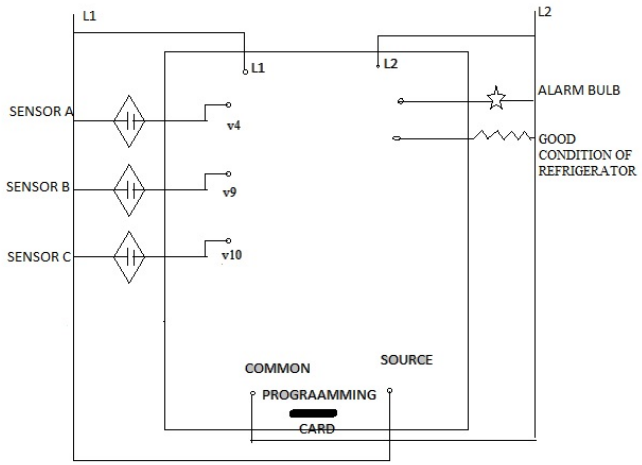


Figure 3: figure 3

6 Application

We can use the above concept in several applications in electrical field. We have chosen the application as refrigerator because it is used as many purpose like home, shops, medical equipment's, medicines etc. It reduces the cost of repairing electrical equipment and we identify the fault immediately with the help of sensors.

7 Conclusion

We used the Fuzzy Cognitive Map to reduce the variable in Boolean function and the sensor circuit to identify the problem in the electrical equipment.

References

[1] Shannon C.E. (1938): A Symbolic analysis of relay and switching circuits.-Trans. AIEE.

[2] Kanchana A., Srinivasa Rao .K, Indentifying the problem in Motorcycle using Boolean function ,International Journal of Information Research and Review, Volume 03, Issue 11(2016), PP:3160-3167.

[3] Kanchana A., Srinivasa Rao .K : Solution of system of Boolean function to give the input of the circuit, Journal of Chemical and Pharmaceutical Sciences, Volume 9 Issue 4(2016).

[4] Kanchana A., Srinivasa Rao .K , Minimizing Cost problem Solved by Boolean function using Switch circuit, Global Journal of Pure and Applied Mathematics, Volume 13, Issue 1(2017),PP:287-290.

[5] Kanchana A., Srinivasa Rao .K (2017), Distinct Minimized Equation from Unique Boolean Function in Simple Truth Table Logic, Presented in the International Conference on Contemporary Approaches in Mathematics and Emerging Engineering Trends ,2017, Book of Proceedings,PP: 84- 88 Aarupadai Veedu Institute of Technology, Vinayakka Mission University

[6] Boole G. (1954): An investigation of the Laws of Thought.- New York: Dover Publications.

[7] Kenneth H. Rosen, Discrete Mathematics and its Applications, McGrew Hill Publications.

[8] Holsworth, switching circuit and Logic Design .

[9] uillermo Ochoa de Aspuru, java applet software for Fuzzy Cognitive Maps, www.ochoadeaspuru.com/fuzcogmap/index.php.

[10] Visvam Devadoss Ambeth Kumar and S. Gokul Amuthan static structure simplification of Boolean function for N variables A novel approach, Journal of Microelectronics, Volume 01, Issue 4(2016), PP: 160-167

[11] Sebestian P. Tomaszewski, Ilgaz U. Celik, George E. Antoniou, WWW- Base Boolean Function Minimization, International journal of applied Mathematics and Computer science, Volume 13,Issue 4(2003), PP:577-583.

ISSN: 2350-0328

International Journal of AdvancedResearch in Science, Engineering and Technology

Vol. 5, Issue 10 , October 2018

Condition for Double Line Graph – Using FUZZY GRAPH

A.R.Shoba, Hemanath S, R.Malathi

M.Phil Scholar, SCSVMV, Kanchipuram.
3r[d] year, CSE, Sastra University, Tanjore.
Asst Prof of Mathematics, SCSVMV, Kanchipuram.

ABSTRACT: In this paper, we will be learning some new concepts of notions of fuzzy graph, union, intersection of two fuzzy graphs and a few properties relating to finite union and intersection of fuzzy graphs are established here. We are also going to find the conditions for complete graph.

KEY WORDS*:* Finite intersection, Finite union, fuzzy graph, notions of fuzzy graph.

I. INTRODUCTION

There are many theories like theory of probability, theory of fuzzy sets, theory of intuitionistic fuzzy sets, theory of rough sets, etc. which can be considered as mathematical tools to deal with uncertainties. But all these theories have their own inherent difficulties. The theory of probabilities can deal only with possibilities. The most appropriate theory to deal with uncertainties is the theory of fuzzy sets, developed by Zadeh in 1965. But it has an inherent difficulty to set the membership function in each particular cases. Also the theory of intuitionistic fuzzy set is more generalized concept than the theory of fuzzy set, but also there have same difficulties. Thereafter many researchers have applied this concept on different branches of mathematics, like group theory decision making problems, relations topology etc[5].

In 1736, Euler first introduced the concept of graph theory. The theory of graph is extremely useful tool for solving combinatorial problems in different areas such as geometry, algebra, number theory, topology, operation research, optimization and computer science, etc.. In 1975, Rosenfeld introduced the concept of fuzzy graphs. Thereafter many researchers have generalized the different notions of graph theory using the notions of fuzzy sets

In this paper, our aim is to introduce the notion of fuzzy graph and then a few operations, like union, intersection.

II. PRELIMINARIES

Definition: 1.1

Let V be a nonempty finite set and σ: V $\rightarrow$[0; 1].
Again, let μ: V x V $\rightarrow$ [0; 1] such that $\mu \leq (x; y)\ \sigma(x) \wedge \sigma(y) \quad \forall (x; y) \in V \times V$
Then the pair G := (σ; μ) is called a fuzzy graph over the set V

Here σ and μ are respectively called fuzzy vertex and fuzzy edge of the fuzzy graph (σ; μ).

A fuzzy graph G := (σ; μ) over the set V is called strong fuzzy graph if

$$\mu(x; y) = \sigma(x) \Lambda \sigma(y) \quad \forall (x; y) \in V \times V.$$

Definition: 1.2

Let H := (ρ; υ) and G := (σ; μ) be two fuzzy graphs over the set V .Then H is called the fuzzy subgraph of the fuzzy graph of G if

ISSN: 2350-0328
International Journal of AdvancedResearch in Science, Engineering and Technology
Vol. 5, Issue 10 , October 2018

$\rho(x) \leq \sigma(x)$ and $\upsilon(x; y) \leq \mu(x; y)$ $\forall$ x; y $\in$ V:

Definition: 1.3

Let $G_1 := (\sigma_1; \mu_1)$ and $G_2 := (\sigma_2; \mu_2)$ be two fuzzy graphs over the set V .

Then the union of G_1 and G_2 is another fuzzy graph $G_3 := (\sigma_3; \mu_3)$ over the set V,
where $\sigma_3(x) = \sigma_1 \vee \sigma_2$ and $\mu_3 = \mu_1 \vee \mu_2$;
i:e: $\sigma_3(x) = \max\{\sigma_1(x); \sigma_2(x)\}$ $\forall$ x $\in$ V
and $\mu_3(x;y) = \max\{\mu_1(x; y); \mu_2(x; y)\}$ $\forall$ x; y $\in$ V

Definition: 1.4

Let $G_1 := (\sigma_1; \mu_1)$ and $G_2 := (\sigma_2; \mu_2)$ be two fuzzy graphs over the set V .
Then the intersection of G_1 and G_2 is another fuzzy graph
$G_3 := (\sigma_3; \mu_3)$ over the set V , where

$\sigma_3 = \sigma_1 \wedge \sigma_2$ and $\mu_3 = \mu_1 \wedge \mu_2$;

i:e: $\sigma_3(x) = \min\{\sigma_1(x); \sigma_2(x)\}$ $\forall$ x $\in$ V

and $\mu_3(x; y) = \min\{\mu_1(x; y); \mu_2(x; y)\}$ $\forall$ x; y $\in$ V

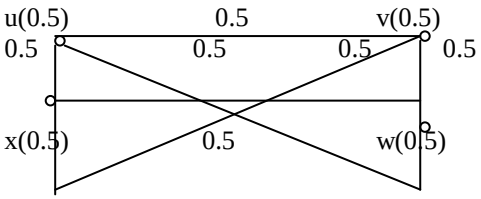
Let U be an initial universal set and E be a set of parameters. Let IU
denotes the collection of all fuzzy subsets of U and A $\subseteq$E.

Definition: 1.5

The complement of a fuzzy graph G : (σ,μ) is also a fuzzy graph and denoted as
$G^c : (\sigma , \mu^c)$
where $\sigma^c = \sigma$ and $\mu^c(x, y) = \sigma(x) \wedge \sigma(y) - \mu(x, y)$ $\forall$ x, y $\in$ V [4]

Definition: 1.6

A fuzzy graph G:(μ, ρ) is complete graph if $\rho(u, v) = \mu(u) \wedge \mu(v)$ $\forall$ u, v $\in$ V
Example of the complete graph**:**[3]



Definition: 1.7

Let V be a nonempty finite set and σ: V $\rightarrow$[0; 1].
Again, let μ: V x V $\rightarrow$ [0; 1] such that

$\mu(x; y) = \min\{ \sigma(x) ,\sigma(y) \}$ $\forall$(x; y) $\in$ V x V

Then the triplet G := (V, σ ,μ) is called a fuzzy graph over the set V.
Here V and μ are respectively called fuzzy vertex and fuzzy edge of the fuzzy graph (σ; μ).

ISSN: 2350-0328
International Journal of AdvancedResearch in Science, Engineering and Technology
Vol. 5, Issue 10 , October 2018

Definition 1.8

Let V be a nonempty finite set and σ: V →[0; 1]. C:[0,1]→[0,1]

Again, let μ: V x V → [0; 1] such that
$\mu^c(x; y) = 1 - [\min\{ \sigma(x) ,\sigma(y) \}]$ $\forall(x; y) \in V \times V$

Definition 1.9

Let V be a nonempty finite set and σ: V →[0; 1].
Again, letυ: V x V → [0; 1] such that
$\upsilon(x; y) = \max\{ \sigma(x) ,\sigma(y) \}$ $\forall(x; y) \in V \times V$

Then the triplet G := (V, σ ,υ) is called a fuzzy graph over the set V. Here V and υ are respectively called fuzzy vertex and fuzzy edge of the fuzzy graph (σ; υ).

Definition 1.10

Let V be a nonempty finite set and σ : V →[0; 1] & C:[0,1]→[0,1]
Again, let υ: V x V → [0; 1] such that $\upsilon^c(x; y) = 1 - [\max\{ \sigma(x) ,\sigma(y) \}]$ $\forall(x; y) \in V \times V$
Example

Consider V = $\{x_1, x_2, x_3\}$ and
E = $\{e_1, e_2, e_3\}$
Here $G_{E,V}$ is described by the below table 1

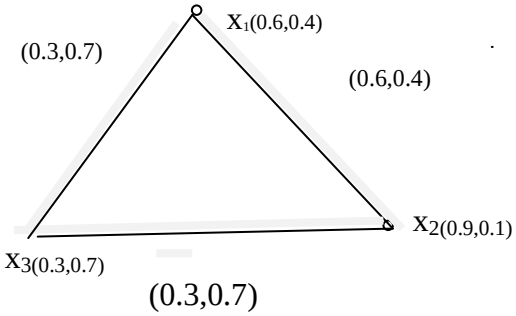
$\forall (x_i, x_j) \in V \times V \setminus \{(x_1, x_2), (x_1, x_3), (x_2, x_3)\}$ and for all e ∈ E

TABLE I

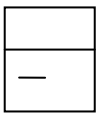
σ (μ,μ^c)	x_1	x_2	x_3
e_1	0.5,0.5	0.2,0.8	0.3,0.7
e_2	0.8,0.2	0.7,0.3	0.4,0.6
e_3	0.6,0.4	0.9,0.1	0.3,0.7

minμ,maxμ^c	(x_1,x_2)	(x_1,x_3)	(x_2,x_3)
e_1	0.2,0.8	0.3,0.7	0.2,0.8
e_2	0.7,0.3	0.4,0.6	0.4,0.6
e_3	0.6,0.4	0.3,0.7	0.3,0.7

ISSN: 2350-0328
International Journal of AdvancedResearch in Science, Engineering and Technology
Vol. 5, Issue 10 , October 2018

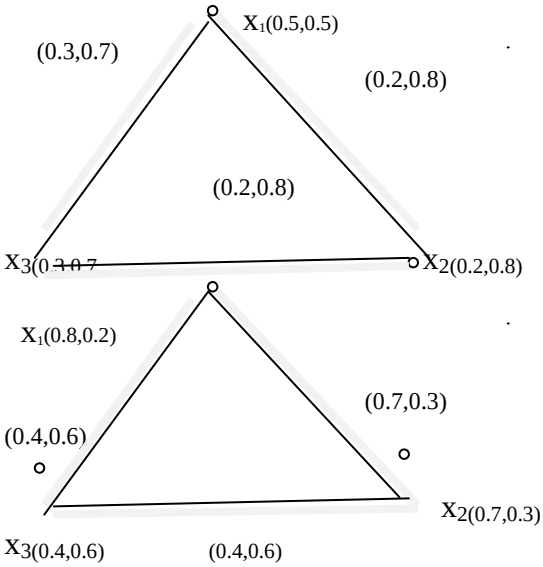


corresponding to e_3



max

min



corresponding to e_1

corresponding to e_2

III. CONCLUSION

In this paper, we have discussed about the notions of fuzzy graph, union and intersection of two fuzzy graphs and also conveyed few properties relating to finite union and intersection of fuzzy graphs. We have also found the conditions for double line complete graph.

IV. RESULT

If $0 < \sigma < 1$ then graph of $\{\min(\mu), \max(\mu^c)\}$ is a double line complete graph.

ISSN: 2350-0328

International Journal of AdvancedResearch in Science, Engineering and Technology

Vol. 5, Issue 10 , October 2018

REFERENCES

[1] A. Rosenfeld, Fuzzy graphs, Fuzzy sets and their Applications ,(L.A. Zadeh, K. S.Fu, M.Shimura, Eds) Academic Press, New York (1975) 77-95

[2] B. Dinda, T. K. Samanta, Relations on intuitionistic fuzzy soft sets, General Mathematics. Notes 1(2) (2010), 74-83.

[3] Beena G Kittur, Eigen Values of Complete Fuzzy Graphs,International Journal of Fuzzy Mathematics and System ISSN 2248-9940 Volume 2, Number 3 (2012), pp. 293-296.

[4] N. Sathyaseelan,Dr.E. Chandrasekaran, Self Weak complimentary fuzzy graphsInternational Journal of Engineering Research and Applications(IJERA) ISSN:2248-9622 www.ijera.com vol.2,Issue 4, July-August 2012, pp.1627-1633

[5] Sumit Mohinta and T.K. Samanta (An introduction to fuzzy soft graph) mathematica moravica vol. 19-2 (2015), 35-48

JECET; September 2018 - November 2018; Section C; Vol.7. No.4, 315-320. E-ISSN: 2278–179X
[DOI: 10.24214/jecet.C.7.4.31520]



Journal of Environmental Science, Computer Science and Engineering & Technology
An International Peer Review E-3 Journal of Sciences and Technology
Available online at www.jecet.org
Section C: Engineering & Technology
Research Article

Condition for Complete Graph – Using Fuzzy Graph

A.R.Shoba and R.Malathi

M.Phil Scholar, SCSVMV

Asst.Prof.of Mathematics, SCSVMV

Received: 00 October 2018; **Revised:** 11 November 2018; **Accepted:** 16 November 2018

Abstract: In this paper, we will be learning some new concepts of notions of fuzzy graph, union, intersection of two fuzzy graphs and a few properties relating to finite union and intersection of fuzzy graphs are established here. We are also going to find the conditions for complete graph.

Key words:Finite union, fuzzy graph, notions of fuzzy graph.

I.INTRODUCTION

There are many theories like theory of probability, theory of fuzzy sets, theory of intuitionistic fuzzy sets, theory of rough sets, etc. which can be considered as mathematical tools to deal with uncertainties. But all these theories have their own inherent difficulties. The theory of probabilities can deal only with possibilities. The most appropriate theory to deal with uncertainties is the theory of fuzzy sets, developed by Zadeh[1]in 1965. But it has an inherent difficulty to set the membership function in each particular cases. Also the theory of intuitionistic fuzzy set is more generalized concept than the theory of fuzzy set, but also there have same difficulties [2-4]. Thereafter many researchers have applied this concept on different branches of mathematics, like group theory decision making problems, relations topology etc. [5].

In 1736, Euler first introduced the concept of graph theory. The theory of graph is extremely useful tool for solving combinatorial problems in different areas such as geometry, algebra, number theory, topology, operation research, optimization and computer science, etc.. In 1975, Rosenfeld introduced the concept of

fuzzy graphs. Thereafter many researchers have generalized the different notions of graph theory using the notions of fuzzy sets

In this paper, our aim is to introduce the notion of fuzzy graph and then a few operations, like union, intersection.

II. PRELIMINARIES

Definition: 1.1:

Let V be a nonempty finite set and $\sigma: V \rightarrow [0; 1]$.

Again, let $\mu: V \times V \rightarrow [0; 1]$ such that

$\mu \leq (x; y)\ \sigma(x) \wedge \sigma(y) \quad \forall (x; y) \in V \times V$

Then the pair $G: = (\sigma; \mu)$ is called a fuzzy graph over the set V

Here σ and μ are respectively called fuzzy vertex and fuzzy edge of the fuzzy graph $(\sigma; \mu)$.

A fuzzy graph $G: = (\sigma; \mu)$ over the set V is called strong fuzzy graph if

$\mu(x; y) = \sigma(x) \Lambda\ \sigma(y) \quad \forall (x; y) \in V \times V.$

Definition: 1.2:

Let $H: = (\rho; \upsilon)$ and $G: = (\sigma; \mu)$ be two fuzzy graphs over the set V .Then H is called the fuzzy subgraph of the fuzzy graph of G if

$\rho(x) \leq \sigma(x)$ and $\upsilon(x; y) \leq \mu(x; y)\ \forall\ x; y \in V$:

Definition: 1.3:

Let $G_1 := (\sigma_1; \mu_1)$ and $G_2 := (\sigma_2; \mu_2)$ be two fuzzy graphs over the set V .

Then the union of G_1 and G_2 is another fuzzy graph $G_3 := (\sigma_3; \mu_3)$ over the set V,

where $\sigma_3(x) = \sigma_1 \vee \sigma_2$ and $\mu_3 = \mu_1 \vee \mu_2$;

i:e: $\sigma_3(x) = \max\{\sigma_1(x); \sigma_2(x)\} \quad \forall\ x \in V$

and

$\mu_3(x;y) = \max\{\mu_1(x; y); \mu_2(x; y)\}$

$\forall\ x; y \in V$

Definition: 1.4:

Let $G_1 := (\sigma_1; \mu_1)$ and $G_2 := (\sigma_2; \mu_2)$ be two fuzzy graphs over the set V .

Then the intersection of G_1 and G_2 is another fuzzy graph

$G_3 := (\sigma_3; \mu_3)$ over the set V, where

$\sigma_3 = \sigma_1 \wedge \sigma_2$ and $\mu_3 = \mu_1 \wedge \mu_2$;

i:e: $\sigma_3(x) = \min\{\sigma_1(x); \sigma_2(x)\}$ $\forall$ x $\in$ V

and $\mu_3(x; y) = \min\{\mu_1(x; y); \mu_2(x; y)\}$ $\forall$ x; y $\in$ V

Let U be an initial universal set and E be a set of parameters.

Let IU denotes the collection of all fuzzy subsets of U and A $\subseteq$E.

Definition: 1.5:

The complement of a fuzzy graph G: (σ,μ) is also a fuzzy graph and denoted as

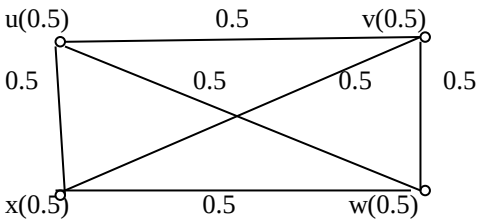
G^c: (σ , μ^c)

Where $\sigma^c = \sigma$ and $\mu^c(x, y) = \sigma(x) \wedge \sigma(y) - \mu(x, y)$ $\forall$ x, y $\in$ V [4]

Definition: 1.6:

A fuzzy graph G:(μ, ρ) is complete graph if ρ (u, v) = μ(u) $\wedge$ μ(v) $\forall$ u, v $\in$ V

Example of the complete graph**:**[3]



Definition 1.7:

Let V be a nonempty finite set and σ: V $\rightarrow$[0; 1].

Again, let μ: V x V $\rightarrow$ [0; 1] such that

$\mu(x; y) = \min\{ \sigma(x) ,\sigma(y) \}$ $\forall(x; y) \in V \times V$

Then the triplet G: = (V, σ ,μ) is called a fuzzy graph over the set V.

Here V and μ are respectively called fuzzy vertex and fuzzy edge of the fuzzy graph (σ; μ).

Definition 1.8:

Let V be a nonempty finite set and σ: V →[0; 1]. C:[0,1]→[0,1]

Again, let μ: V x V → [0; 1] such that

$\mu^c(x; y) = 1 - [\min\{ \sigma(x) ,\sigma(y) \}]$ $\forall(x; y) \in V \times V$

Definition 1.9:

Let V be a nonempty finite set and σ: V →[0; 1]

Again, let υ: V x V → [0; 1] such that

$\upsilon(x; y) = \max\{ \sigma(x) ,\sigma(y) \}$ $\forall(x; y) \in V \times V$

Then the triplet G := (V, σ ,υ) is called a fuzzy graph over the set V. Here V and υ are respectively called fuzzy vertex and fuzzy edge of the fuzzy graph (σ; υ).

Definition 1.10*:*

Let V be a nonempty finite set and

σ:V →[0; 1] &C:[0,1]→[0,1]

Again, let υ: V x V → [0; 1] such that

$\upsilon^c(x; y) = 1 - [\max\{ \sigma(x) ,\sigma(y) \}]$ $\forall(x; y) \in V \times V$

Example

Consider $V = \{x_1, x_2, x_3\}$ and

$E = \{e_1, e_2, e_3\}$

Here $G_{E,V}$is described by the below table 1

$\forall (x_i, x_j) \in V \times V \setminus \{(x_1, x_2), (x_1, x_3), (x_2, x_3)\}$ and for all $e \in E$

TABLE I

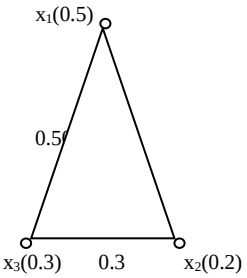
Maximum

σ	x_1	x_2	x_3
e_1	0.5	0.2	0.3
e_2	0.8	0.7	0.4
e_3	0.6	0.9	0.3

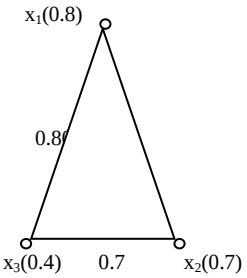
υ	(x_1,x_2)	(x_1,x_3)	(x_2,x_3)
e_1	0.5	0.5	0.3
e_2	0.8	0.8	0.7
e_3	0.9	0.6	0.9

υ^c	(x_1,x_2)	(x_1,x_3)	(x_2,x_3)
e_1	0.5	0.5	0.7
e_2	0.2	0.2	0.3
e_3	0.1	0.4	0.1

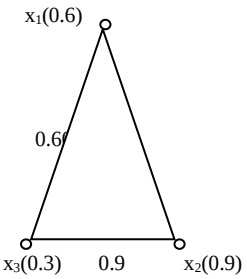
Graph of υ



Corresponding to e_1

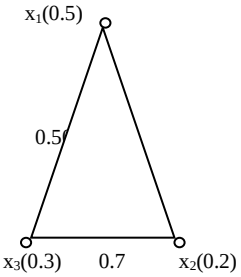


Corresponding to e_2

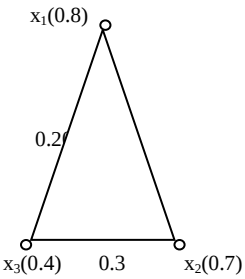


Corresponding to e_3

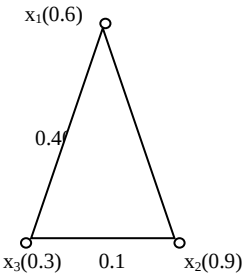
Graph of υ^C



Corresponding to e_1



Corresponding to e_2



Corresponding to e_3

III CONCLUSION

In this paper, we have discussed about the notions of fuzzy graph, union and intersection of two fuzzy graphs and also conveyed few properties relating to finite union and intersection of fuzzy graphs. And we also found the conditions for complete graph using fuzzy graphs.

IV RESULT

If $0 < \sigma < 1$, then graph of υ and υ^{c} is a complete graph**.**

REFERENCES

1. A. Rosenfeld, Fuzzy graphs, Fuzzy sets and their Applications ,(L. A. Zadeh, K. S.Fu, M.Shimura, Eds) Academic Press, New York ,1975, 77-95
2. B. Dinda, T. K. Samanta, Relations on intuitionistic fuzzy soft sets, General Mathematics Notes,2010, 1(2), 74-83.
3. Beena G Kittur, Eigen Values of Complete Fuzzy Graphs,International Journal of Fuzzy Mathematics and System ISSN 2248-9940 , 2012, 2, 3 ,293-296.
4. N. Sathyaseelan,Dr.E. Chandrasekaran, Self-Weak complimentary fuzzy graphsInternationalJournal of Engineering Research and Applications(IJERA) ISSN:2248-9622 www.ijera.com2012, 2,1627-1633
5. SumitMohinta and T.K. Samanta (An introduction to fuzzy soft graph) mathematica moravica, 2015, 19-2, 35-48.

*** Corresponding Author: R.Malathi**

Asst.Prof.of Mathematics, SCSVMV

RESEARCHERID
THOMSON REUTERS

[Selvi * *et al.*, 7(6): June, 2018]
IC™ Value: 3.00

ISSN: 2277-9655
Impact Factor: 5.164
CODEN: IJESS7

IJESRT

INTERNATIONAL JOURNAL OF ENGINEERING SCIENCES & RESEARCH TECHNOLOGY

VISUAL GRAPH OF HIGHER SECONDARY MATHEMATICS EDUCATION USING THE OPEN SOURCE SOFTWARE GEOGEBRA

J. Sengamala Selvi
Assistant Professor, Sri Chandrasekharendra Saraswathi Viswa Mahavidyalaya, Enathur, kanchipuram, Tamilnadu, India

DOI: 10.5281/zenodo.1297380

ABSTRACT

ICT popularly known, involve in the most general since the use of technology in managing and processing information. ICT provides "anytime, anywhere" access to reliable information. It paves the way for construction of knowledge by any individual. A belief promoted in the research literature (Fasieyitan, Libii and Hirchbuhl 1996) and amongst the administration is that university/college education can make imaginative or innovative use of ICT to enrich the learning environment and support student learning. It can be used to make students' facet knowledge public and help them develop math cognitive skills to become more reflective and self regulated learners. A shift from teacher-centered instruction to learner-centered instruction is needed to enable students to acquire the new millennium knowledge and skills. The shift will take place in changing from a focus on teaching to a focus on learning (sanclhots, Ringstaff and Dwyer 1977). This paper prominence the execution of Visual graph of Higher secondary Mathematics Education.

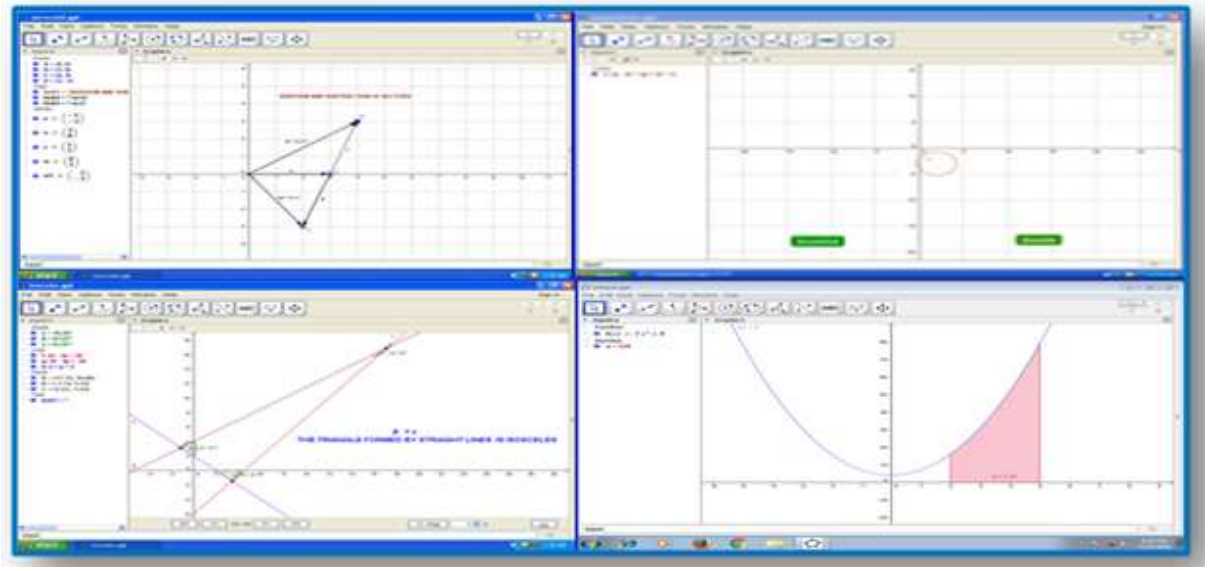
Keywords: Geogebra, Higher secondary Mathematics, ICT, Visual Graph.

I. INTRODUCTION

Geogebra is free dynamic Mathematical software designed to work on different operating systems. It is an Interactive geometry System. It has flexible user interface. It is open source software. Geogebra was translated to more than 25 languages. It won European and German educational software award. It can be downloaded without any cost with the help of internet access. Geogebra will be a supporting Tool to promote the education level. In Geogebra there is a possibility to find the area of conics, complex root of a polynomial, derivative of a function and definite integral values over the interval, determinant of the matrix and to solve the set of equations and It is used to calculate the limit of the function. It offers commands, functions and events to do the task easily.

Geogebra equips the higher secondary students with enough knowledge and skills and increase their ability in problem solving in Mathematics Geogebra is the most powerful Open source Mathematics software. While learning Mathematics with Geogebra, students can overcome obstacles and achieve their learning objectives. This type of new methodology definitely encourages the students to develop and expand their knowledge in Mathematics concepts. All level students can easily understand the Mathematics problem easily. It will help to remove the fear of Mathematics. The visual display of data clarifies the students doubt in Mathematics.

ISSN: 2277-9655
Impact Factor: 5.164
CODEN: IJESS7



1. Solve by graphically : x+2y=4 : 2x+4y=8

Input

x+2y=4

X	-2	0	2
Y	3	2	1

2x+4y=8

X	-4	0	4
Y	4	2	0

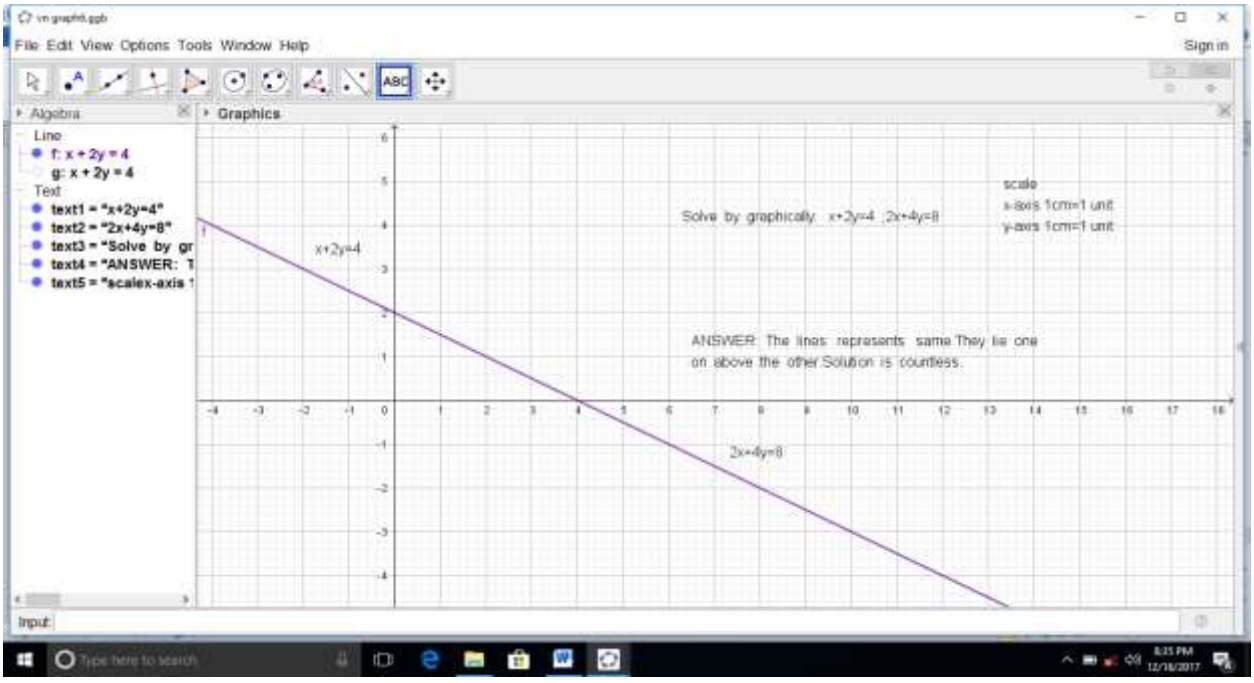


Figure: 1 Graph of same straight lines.

ISSN: 2277-9655
Impact Factor: 5.164
CODEN: IJESS7

Answer: The lines represents same straight lines. Solution is Countless.

2. Solve by graphically: x-3y=6 ; x-3y=-9

Input

x-3y =6

X	-3	0	3
Y	-3	-2	-1

x-3y= -9

X	-3	0	3
Y	2	3	4

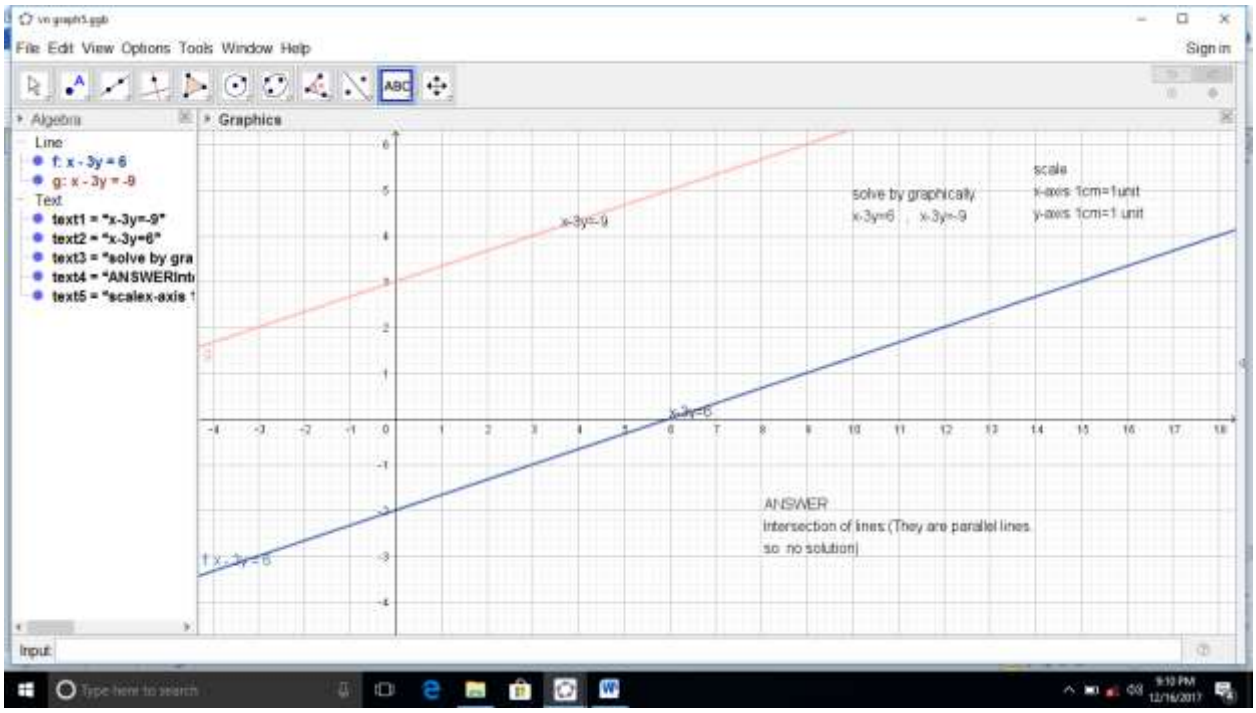


Figure: 2 Graph of parallel lines.

Ans : The straight lines are parallel. So there is no solution.

3. Solve by graphically: 2x-y=1 : x+2y=8

Input

2x-y=1

X	-1	0	1
Y	-3	-1	1

X+2y=8

X	-2	0	2
Y	5	4	3

ISSN: 2277-9655
Impact Factor: 5.164
CODEN: IJESS7

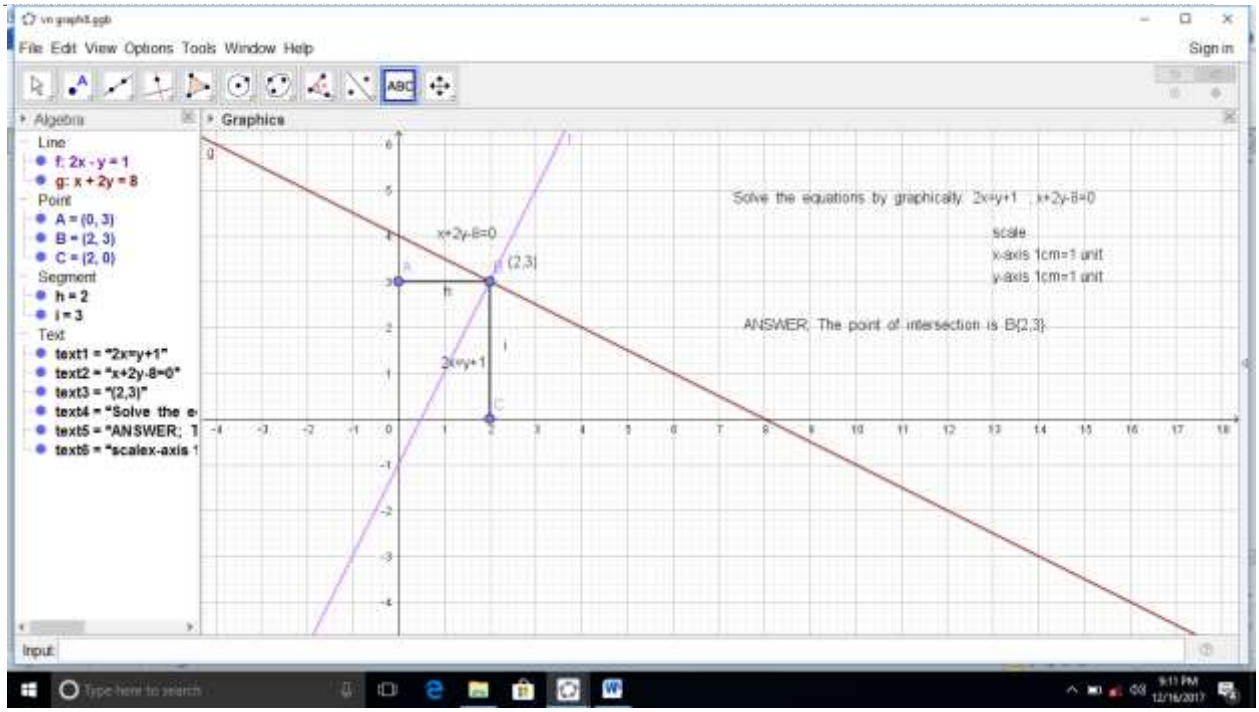


Figure: 3 Graph of intersecting lines

Answer: Point of Intersection is (2,3).
So the only solution is {2,3}.

4. Amudha walks at a speed of 3km/hr. Draw a linear graph to show the relationship between the time and distance.

Input

Time in hours (x)	0	1	2	3	4	5
Distance in km (y)	0	3	6	9	12	15

Plot the points (0,0), (1,3), (2,,6), (3,9), (4,12), (5,15).
Join all the points.

ISSN: 2277-9655
Impact Factor: 5.164
CODEN: IJESS7

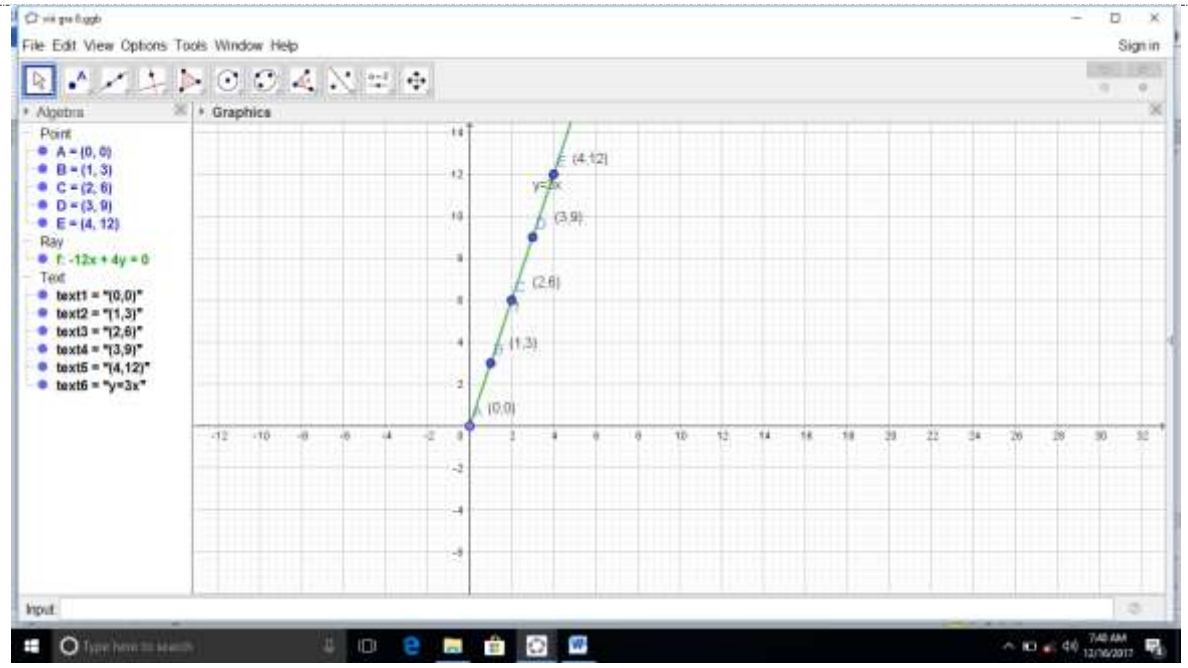


Figure : 4 Linear graph.

Answer:
It is a straight line. Distance=Speed*Time. Relationship is y=3x.

II. CONCLUSION

Accessing to technology is an effective way to stimulate the student's interest in Mathematics. The world's favorite software Geogebra is excellent Mathematical software. It will be an effective tool to change the student's attitude positively towards the learning of mathematics. The youngsters can easily solve mathematical problem with the help of this technology. With the help of this Geogebra the students can explore critical topics like vector algebra; complex numbers. In order to bring the clarity in 3dimensional construction, Geometry, Graph. Geogebra provides the visualization technique. This technique enables the higher secondary students to eliminate memorization of Mathematical concepts in 2 and 3dimensional. Viewing 3-dimension mathematical figure, animating mathematical figure, finding the angle, finding the area, finding the slope helps the students to understand the mathematical concepts clearly. In conventional method, the students can build only the memory palace. But in the case of conventional with ICT the students can view the Mathematics figure visually and easily develop their learning skill.

REFERENCES

[1] Adolphus, Telima andAderonmu, temitopeS.B.Comparative analysis of problem solving ability among JSS mathematics students using Computer – assisted instruction blended with problem solving approach (CAI-PS) Versus traditional teaching approach(TTP) in teaching basic statistics, American Journal of Scientific and Industrial Research.
[2] Alacapınar, F. G. (2003). The effect of traditional education and education via computer on the students' gain, Eurasian Journal of Educational Research, 10, 40-45.
[3] Albayrak, R. (2003). Öğrencilerinb ağıntıkavramınınol uşmasındag örülensıkıntılarve giderilmeönerileri. Yayınl anmamışYüksekLisansTezi, DokuzEylül Üniversitesi Eğitim BilimleriEnstitüsü, İzmir. Alkan, C. (1998).
[4] Alias, 2000 Alias, M. (2000), Spatial visualization ability and civil engineering problem solving. University of suorey,Guildford, united kingdom.
[5] Almeqdali, 2005 Almeqdalai, F. (2005), the effect of using The geometer's sketchpad (GSP) on Jordanian student's Understanding some geometrical concepts, International Journal for Mathematics teaching and learning, from http://www/cimt.plymouth.ac.uk/journal/almeqdadi.pdf.
[6] Akinsola, M. K., &Animasahun, I. A. (2007). The effect of simulation-games environment on Student's achievement in and attitudes to mathematics in secondary schools. The Turkish Online

ISSN: 2277-9655
Impact Factor: 5.164
CODEN: IJESS7

Journal of6 (3), 113-119.
[7] Aktümen, M., &Kaçar, A. (2008). Bilgisayarce birisistem lerininmatem atiğeyönelik tutumaetkisi, HacettepeÜniversitesiEğitimFakültesiDergisi, 35, 13-26.
[8] Battisa, 1999 Battisa, M. (1999), Geometry Results from the Third International Mathematics and science study. Teaching Children Mathematics, 5(6), (pp.367-373). Reston, VA: NCTM..

CITE AN ARTICLE

Selvi, J. S. (2018). VISUAL GRAPH OF HIGHER SECONDARY MATHEMATICS EDUCATION USING THE OPEN SOURCE SOFTWARE GEOGEBRA. *INTERNATIONAL JOURNAL OF ENGINEERING SCIENCES & RESEARCH TECHNOLOGY*, *7*(6), 406-411.

International Journal of Engineering & Technology, 7 (4.10) (2018) 602-604

International Journal of Engineering & Technology

Website: www.sciencepubco.com/index.php/IJET

Research paper



A Comparative Study of Experimental and Theoretical Ultrasonic Velocity of Binary Liquid Mixtures Using Mathematical Methods

A. Gayathri[1], T. Venugopal[1], K. Venkatramanan[2,*]

[1]Dept. of Mathematics, SCSVMV (Deemed University), Kanchipuram, India
[2]Dept. of Physics, SCSVMV (Deemed University), Kanchipuram, India
**Corresponding author E-mail: kv@kanchiuniv.ac.in*

Abstract

A comparative study of ultrasonic velocities of binary liquid mixtures such as O-cresol+carbon tetrachloride, anisicaldehyde+methylacetate, anisicaldehyde+ethylacetate, having industrial applications are analysed at temperature 303K for different concentrations [0 to 1%]. In the present study experimental values are taken from literature and there values are compared with theoretical values obtained by various mathematical equations such as Nomoto's relation, VandealVangeal formula, Impedance relation, Rao's specific relation. Thus, the present study reveals the nature of interaction between component molecules in the mixtures and enables us to identify a suitable mathematical model for predicting the ultrasonic velocity various binary liquid mixtures.

Keywords: *Binary liquids; Impedance relation; Nomoto's relation; Rao Specific relation; Ultrasonic velocity; Vand-deal and Van-Geal.*

1. Introduction

In recent years, there has been a continuous improvement in the experimental investigation of excess thermodynamic properties of liquid mixtures. Particularly, ultrasonic study of liquid mixtures has gained much importance in assessing the nature of molecular interactions present in the mixtures. Experimental and theoretical ultrasonic velocity studies in liquids and polymer solutions have been the subject of research in recent years. The experimental ultrasonic velocity values of O-Cresol with carbon tetrachloride, anisicaldehyde + methylacetate, anisicaldehyde + ethylacetate are compared with their theoretical values obtained by using various mathematical methods like Nomotto's Relation, Vandeal and Vangeal Relation, Impedance Relation and Rao's specific sound velocity. The most accurate mathematical method is identified using Average Percentage Error (APE).

2. Methods and Materials

The binary mixtures are prepared by dissolving O-Cresol with Carbon tetrachloride, anisicaldehyde with methylacetate and anisicaldehyde with ethylacetate to get desired concentrations. Magnetic stirrer [REMI make] was used for this purpose at a rate of 1000 rpm. Density values are measured using specific gravity method. The mass of the liquid was measured using a K-ROY make Electronic balance, with an accuracy of ±0.001gm. The ultrasonic velocity measurements are performed using Mittal make single frequency ultrasonic interferometer at 2 MHz (F-81 model) (uncertainty ± 0.01m/s).

3. Results and Discussion

3.1. Evaluation of Ultrasonic velocity

In recent years, measurement of ultrasonic velocity found extensive application in determining the physicochemical behavior of liquid mixtures. Theoretical evaluation of ultrasound velocity gives a better understanding of molecular arrangement in liquids [1-3]. In the present study, the experimental ultrasonic velocity values of O-Cresol with carbon tetrachloride, anisicaldehyde + methylacetate, anisicaldehyde + ethylacetateare compared with their theoretical ultrasonic velocities by Nomotto's relation (U_{Nom}), Vandeal Vangeal (U_{IMR}) relation, Impedance relation (U_{IR}) and Rao's specific sound velocity relation (U_R) as given below.

Nomotto's relation

On assuming the additivity of molar sound velocity (R) and no volume change on mixing, Nomotto established the following relation for a liquid mixture.

$$U_{NOM} = \left[\frac{X_1 R_1 + X_2 R_2}{X_1 V_1 + X_2 V_2} \right]^3 \quad (1)$$

Where, R is molar sound velocity, X_1 and X_2 are the mole fractions of 1st and 2nd components of the liquid mixture and V is molar volume. The molar sound velocity can be determined using the formula

Copyright © 2018 Authors. This is an open access article distributed under the Creative Commons Attribution License, which permits unrestricted use, distribution, and reproduction in any medium, provided the original work is properly cited.

$$R_1 = (M_1/d_1)U_1^{1/3} \quad (2)$$

$$R_2 = (M_2/d_2)U_2^{1/3} \quad (3)$$

where, M_1 and M_2 are the effective molecular weight of the 1st and 2nd components, d_1 and d_2 are the densities of the 1st and 2nd components and U_1 and U_2 are the ultrasonic velocities of the 1st and 2nd components.

Van Deal and Van Geal ideal mixing relation

Van Deal and Van Geal proposed the following expression for the estimation of sound velocity U_{IMR} in an ideal mixture using the sound velocities in the pure components.

$$U_{IMR} = \left[\frac{1}{(X_1M_1 + X_2M_{21})^{1/2}}\right]\left[\frac{1}{\left(\frac{X_1}{M_1U_1^2} + \frac{X_2}{M_2U_2^2}\right)^{1/2}}\right] \quad (4)$$

where, X_1 and X_2 are the mole fractions of 1st and 2nd components of the liquid mixture, M_1 and M_2 are the effective molecular weight of the 1st and 2nd components, d_1 and d_2 are the densities of the 1st and 2nd components and U_1 and U_2 are the ultrasonic velocities of the 1st and 2nd components.

Impedance relation

Impedance relation is given by

$$U = \frac{\sum X_i Z_i}{\sum X_i d_i} \quad (5)$$

Where, X_i, Z_i and d_i and $Z_i = U_i\, d_i$ are the mole fractions of the liquid mixture, specific acoustical impedance of the liquid mixture and density of liquid mixture.

Rao's specific relation

The Rao's Specific Sound velocity relation for determination of ultrasonic velocity in binary liquid mixture can be given as

$$U = \left(\sum X_i r_i d_i\right)^3 \quad (6)$$

Where, r_i is the Rao's specific sound velocity and Z_i is the acoustical impedance. Rao's specific sound velocity can be calculated using the relation

$$r_i = U_i^{1/3} / d_i \quad (7)$$

3.2 Average Percentage Error

The average percentage error of deviation is calculated by the following formula

$$APE = \frac{1}{n}\sum\left[\left(\frac{U_{exp} - U_{cal}}{U_{exp}}\right)\right] * 100 \quad (8)$$

The experimentally measured ultrasonic velocity and the estimated ultrasonic velocity from various mathematical models like Nomotto, Vandeal Vangeal, Impedance Relation and Rao's Specific Velocity Method for the binary liquid mixture O-Cresol with Carbon tetrachloride at five different concentrations at 303K are presented in the Table 1. From Table 1, it is observed that the experimental values of ultrasonic velocity increases with increase in concentration. The molecular association is responsible for this increasing trend. Similar trend is observed in Nomotto relation method, Impedance relation and Rao's specific velocity method. The ultrasound velocities obtained from Nomotto's relation method and Rao's specific sound velocity values are almost same [4-6]. The limitations and approximations incorporated in these theories are responsible for the deviations of theoretical values from experimental values. Table 2 shows the variation of percentage of deviation with respect to the composition of O-Cresol with Carbon tetrachloride at 303 K. In this system, it is understood that the percentage of deviation is more in Impedance relation (IMP) than Rao's specific relation (RAO) than Van-Deal and Vang-Geal (VV) than Nomotto's relation. i.e, IMP>RAO>VV>NOM. In Nomotto's relation only negligible deviation to experimental values is observed when compared to other methods. The experimentally measured ultrasonic velocity and the estimated ultrasonic velocity from various mathematical models for the binary liquid mixture anisic aldehyde (AA) +methyl acetate (MA) at five different concentrations at 303K are presented in the Table 2. From Table 3, it is observed that the experimental values of ultrasonic velocity increases with increase in concentration. The molecular association is responsible for this increasing trend. Similar trend is observed in Nomotto's relation method, Impedance relation and Rao's specific velocity method. The ultrasound velocities obtained from Nomotto's relation method and Rao's specific sound velocity values are almost same.

Table 1: Experimental and mathematical values of ultrasound velocity for O-cresol with Carbon tetrachloride

Conc (%)	EXP	NOM	VV	RAO	IMP
0.0154	971	1190	1150	1183	1151
0.0341	958	1289	1248	1282	1249
0.0571	996	1347	1312	1342	1312
0.1239	1116	1412	1390	1409	1390
0.175	1171	1432	1416	1430	1416
0.2482	1294	1447	1436	1446	1436
0.3614	1321	1460	1453	1459	1453
0.5601	1403	1470	1466	1469	1466

Table 2: Average percentage values of O-cresol with Carbon tetrachloride

Conc(%)	EXP	%NOM	%VV	%RAO	%IMP
0.0154	971	-22.55	-18.49	-21.80	-18.51
0.0341	958	-34.58	-30.3	-33.84	-30.33
0.0571	996	-35.22	-31.67	-34.63	-31.70
0.0861	1081	-28.13	-25.49	-27.71	-25.52
0.1239	1116	-26.49	-24.51	-26.18	-24.53
0.2482	1294	-11.8	-10.98	-11.72	-10.99
0.3614	1321	-10.48	-9.94	-10.40	-9.95
0.5601	1403	-4.77	-4.53	-4.73	-4.53
APE		-21.8	-19.7	-21.5	-19.6

Table 3: Experimental and mathematical values of ultrasound velocity for anisic aldehyde (AA) + methyl acetate (MA)

Conc(%)	EXP	NOM	VV	RAO	IMP
0.0685	1157	1145	1103	1171	1142
0.1420	1200	1186	1104	1230	1179
0.2210	1240	1227	1108	1285	1218
0.3062	1281	1269	1118	1338	1259
0.3984	1322	1312	1134	1387	1301
0.4983	1361	1357	1160	1432	1345
0.6071	1403	1402	1200	1471	1391
0.7259	1445	1448	1263	1502	1440

Table 4, illustrates the variation of percentage of deviation for binary mixture anisic aldehyde (AA) +methyl acetate (MA) at 303K. It is understood that percentage deviation is RAO>NOM>IMP>VV. In Van-Deal and Van Geal relation only negligible deviation to experimental values is observed when compared to other methods. The experimentally measured ultrasonic velocity and the estimated ultrasonic velocity from various mathematical models for the binary liquid mixture anisic aldehyde

(AA) + methyl acetate (MA) at five different concentrations at 303K are presented in the Table 5. Table 6, illustrates the variation of percentage of deviation for binary mixture anisic aldehyde (AA) + ethylacetate (EA) at 303K. It is clear that the variation of percentage of deviation which is RAO>IMP>NOM>VV. In Van-Deal and Van-Geal relation only negligible deviation to experimental values is observed when compared to other methods.

Table 4: Average percentage values of anisic aldehyde (AA) + methyl acetate (MA)

Conc(%)	EXP	%NOM	%VV	%RAO	%IMP
0.0685	1157	-0.95	-4.61	1.24	-1.26
0.1420	1200	-1.14	-7.99	2.54	-1.68
0.2210	1240	-1.04	-10.64	3.64	-1.76
0.3062	1281	-0.87	-12.71	4.46	-1.70
0.3984	1322	-0.74	-14.21	4.90	-1.60
0.4983	1361	-0.33	-14.74	5.20	-1.16
0.6071	1403	-0.10	-14.43	4.81	-0.84
0.7259	1445	-0.19	-12.60	3.97	-0.37
0.8563	1496	-0.04	-8.82	2.12	-0.37
AVG		-0.6	-11.2	3.65	-1.2

Table 5: Experimental and mathematical values of ultrasound velocity for anisaldehyde (AA) + ethyl acetate (EA)

Conc(%)	EXP	NOM	VV	RAO	IMP
0.0832	1170	1160	1128	1184	1165
0.1695	1215	1199	1138	1243	1208
0.2592	1259	1239	1153	1298	1251
0.3524	1303	1279	1172	1350	1293
0.4494	1342	1321	1198	1397	1335
0.5504	1381	1364	1232	1440	1377
0.6557	1421	1407	1277	1476	1419
0.7655	1462	1451	1337	1506	1461
0.8802	1503	1497	1421	1528	1502

Table 6: Average percentage values of anisic aldehyde (AA) + ethyl acetate (EA)

Conc(%)	EXP	%NOM	%VV	%RAO	%IMP
0.0832	1170	-0.85	-3.54	1.24	-0.422
0.1695	1215	-1.30	-6.27	2.31	-0.562
0.2592	1259	-1.63	-8.45	3.06	-0.688
0.3524	1303	-1.77	-10.01	3.60	-0.726
0.4494	1342	-1.55	-10.74	4.10	-0.498
0.5504	1381	-1.26	-10.81	4.22	-0.275
0.6557	1421	-0.99	-10.16	3.84	-0.147
0.7655	1462	-0.70	-8.50	2.99	-0.076
0.8802	1503	-0.41	-5.43	1.67	-0.072
AVG		-1.2	-8.2	3	-0.39

4. Conclusion

The experimental ultrasonic velocity values of binary liquid mixtures such as O-Cresol with carbon tetrachloride, anisicaldehyde+methylacetate, anisicaldehyde+ethylacetateare compared with their theoretical ultrasonic velocity values for different concentrations at a temperature 303K. From these it may be concluded that the binary mixtures anisicaldehyde + methylacetate, anisicaldehyde + ethylacetateshowed Vandeal & Vangeal relation as the best suitable method for calculating the speed of ultrasound waves in the liquid systems.

5. References

[1] Siddharthan N & Jayakumar S (2015), Experimental and theoretical studies of ultrasonic velocity in binary liquid mixtures of toluene with benzene and carbon tetra chloride. *Indian Journal of Science* 13, 145–154.

[2] Sandhya Sri P, Zareena Begum B & Rambabu C (2013), Theoretical evaluation of ultrasonic velocities in binary liquid mixtures of Anisic aldehyde with some Esters at different temperatures using different theories and models. *Journal of Thermodynamics and Catalysis* 4, 1–8.

[3] Vadamalar R, Mani D & Balakrishnan R (2011), Ultrasonic study of binary liquid mixtures of Methyl methacrylate with Alcohols. *Research Journal of Chemical Sciences* 1, 79-82.

[4] Gayathri A & Venugopal T (2015), Analysis of speed of acoustic waves in binary liquid system through mathematical and experimental methods. *Indian Journal of Science* 13, 1-4.

[5] Gayathri A & Venugopal T (2015), A comparative analysis of ultrasound velocity in binary liquid systems of PPG by mathematical and experimental methods. *Physics Procedia* 70, 241–244.

[6] Venkatramanan K & Arumugam V (2009), Miscibility studies of blends of PPG and PEG using viscosity technique. *AIP Conference Proceedings* 1004, 235-240.

IOP Conf. Series: Materials Science and Engineering **390** (2018) 012038 doi:10.1088/1757-899X/390/1/012038

A study on Thermodynamic, Acoustic and Elastic properties of aqueous solutions of Hydroxyethyl Cellulose

R Padmanaban, A Gayathri and K Venkatramanan

Faculty of Science, Sri Chandrasekharendra Saraswathi Viswa Mahavidyalaya, Enathur, Kanchipuram – 631561, India

E-mail :kv.scsvmv@gmail.com

Abstract. Hydroxyethyl cellulose is a thickening and gelling derived from cellulose. It is broadly used in household products, cosmetics and cleaning solutions. Hydroxyethyl cellulose is frequently used with hydrophobic drugs in capsule formulations, to improve the drugs dissolution in the gastrointestinal fluids. Ultrasonic technique is one of the basic non-destructive methods for evaluation of materials and structures. A significant part of every ultrasonic inspection is the way in which the ultrasonic energy is transferred between the transducer and the tested object. In the present investigation, we have tried to compute the activation energy, ultrasound investigations, elastic property (bulk modulus) and molecular interaction properties of aqueous solutions of Hydroxyethyl cellulose at different concentrations (0.05%, 0.10%, 0.15%, 0.20%, 0.25%, 0.30%, 0.35%, 0.40%, 0.45% and 5%) for different temperatures (303K, 308K, 313K, 318K) by determining the relative viscosity.

1. Introduction

Ultrasonic technique has been engaged as commendable tool for non-destructive testing and imaging. Although the relationship between material properties and acoustic parameters has been studied for a long period of time [1-5].In the recent years, the usage of ultrasound sound waves are escalated, because of the advantage it offers to synthetic chemistry. This includes time consumption in reaction, saving energy, higher yield, milder conditions and higher purity of the product. For analyzing the molecular interaction properties, ultrasonic method has the added advantage of being less costly with efficiency comparable to other methods [6-8]. The molecular interaction parameters such as free volume, internal pressure, attenuation, compressibility, acoustic impedance and scattering provide us a clear picture of structural changes in cellulose derivate polymers and biological substances [9].When ultrasound waves are propagated in polymeric materials, acoustic waves are influenced by the polymer structure and molecular relaxation process [10]. Activation energy is an important thermodynamic property and used to describe the minimum energy that must be available for initiating a chemical process. For analyzing the properties and interactions taking place in polymer-polymer systems, knowledge of rheological properties is essential and viscometry is one of the efficient techniques for studying the properties [11]. Most commonly, the elastic property of the polymer solution particles has been accessed using atomic force microscopy (AFM). In this approach, it is calculated by theoretical method. In the present investigation, we have tried to compute the activation energy of aqueous solutions of Hydroxyethyl cellulose at different concentrations (0.05%, 0.10%, 0.15%, 0.20%, 0.25%, 0.30%, 0.35%, 0.40%, 0.45% and 5%) for different temperatures (303K, 308K, 313K, 318K) by determining the relative viscosity and ultrasound velocity and density studies were taken for the above

Content from this work may be used under the terms of the Creative Commons Attribution 3.0 licence. Any further distribution of this work must maintain attribution to the author(s) and the title of the work, journal citation and DOI.
Published under licence by IOP Publishing Ltd

concentrations at 303K for aqueous solutions of Hydroxyethyl cellulose. From these experimental values, the acoustical parameters such as adiabatic compressibility, intermolecular free length and internal pressure etc were calculated and effect of solute solvent interaction were analysed. From adiabatic compressibility values, the elastic property (bulk modulus) was calculated for the above concentrations. The important reason for choosing this material is it has variety of applications in household cleaning products, soaps, and shampoos and the detailed literatures showed that no measurements have been previously reported for the mixtures reported in this paper.

2. Experimental Details

The cellulose derived polymer Hydroxyethyl cellulose (HEC – SPECTRA Grade) was purchased from Sri Ganapathy Trading Company, Kanchipuram. The polymer HEC is dissolved in double distilled water and the polymer solutions are prepared for various concentrations (0.05%, 0.10%, 0.15%, 0.20%, 0.25%, 0.30%, 0.35%, 0.40%, 0.45% and 5%). A magnetic stirrer (REMI make) operating at a rate of 1000 rpm is used for preparing the polymer solutions. BROOKFIELD Viscometer (USA) is used to determine the relative viscosity of the prepared polymer solutions at different concentrations at 303K, 308K, 313K & 318K. The viscometer was connected to an electronically controlled thermostat having a thermal stability of ± 0.05K for taking measurements at different temperatures. Pyknometric method is employed to determine the density of the solutions. A K-ROY electronic balance having an accuracy of ±0.001gm is used to measure the mass of the liquid. A digital ultrasonic velocity meter (VCT-70A model, VI MICROSYSTEMS) is used to measure the ultrasonic velocity. The measurements were taken at a frequency of 2 MHz (accuracy ± 0.1m/s). The ultrasound velocity measurements are taken at 303K by circulating water from a thermostat having a thermal stability of ± 0.05 K.

3. Results and Discussions

3.1. Determination of Activation Energy

Viscosity studies are performed for aqueous solutions of Hydroxyethyl cellulose for different concentrations at different temperatures as mentioned above. Fig. 1 shows the variation of relative viscosity against concentration for aqueous solutions of Hydroxyethyl cellulose at different temperatures.

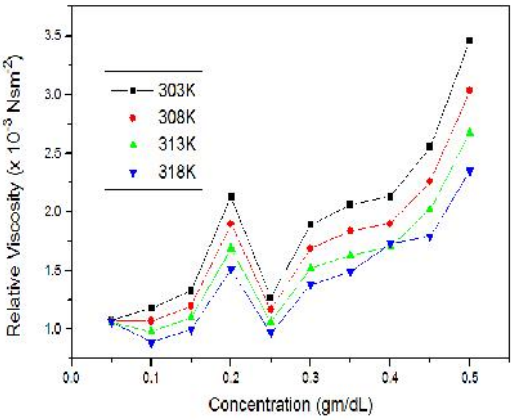


Figure 1. Variation of Relative Viscosity against concentration of aqueous solutions of HEC

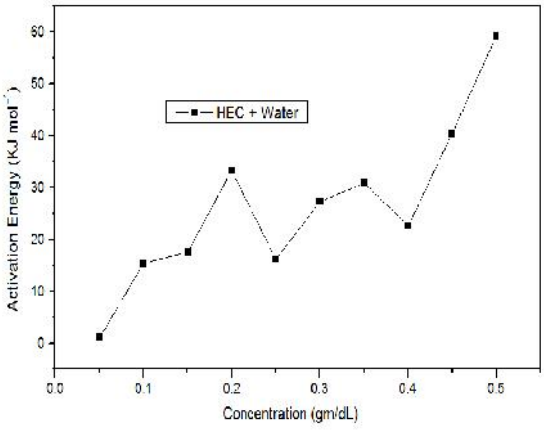


Figure 2. Variation of Activation Energy against concentration of aqueous solutions of HEC

In this system, the relative viscosity shows a non-linear variation with increase in concentration and temperature. The nonlinear variation of viscosity with concentration of HEC indicates presence of intermolecular interaction within the system. The decreasing trend of viscosity indicates that water is a

poor solvent for HEC. Arrhenius expression is valid for pure solvents and also for dilute polymer solutions. According to Venkatramanan et al. [12],

$$\eta = A\, e^{Q/R}$$

Where Q is the apparent activation energy of flow and A is the pre-exponential term with an activation entropy significance.

The logarithm of this equation leads to a straight-line type given by

$$\ln \eta = \ln A + (Q / R)\frac{1}{T}$$

The graph is drawn between lnη against 1/ T. The slope of these straight lines gives the value for activation energy. The variation of activation energy (Q) with concentration (C) of aqueous solutions of HEC is shown in Fig. 2.

In this system, it is observed that there is a sudden decrease in the activation energy for 0.2% and 0.35% concentration. In most cases, activation energy for the viscous flow of polymer solution increases continuously with increasing polymer concentration, except in particular cases of critical mixtures [13]. The reason being the activation energy for the viscous flow of polymer solutions in poor solvent decreases with polymer concentration at high dilution and this is ascribed to the temperature dependence of the limiting viscosity number [14, 15].

The experimentally observed values of density and ultrasonic velocity of the above systems are presented in Table 1. It is observed that the density and ultrasonic velocity values are non-linear. The pronounced increase or decrease in these parameters with composition of mixtures indicates the presence of interactions between the components of molecules [16].

Table 1. Values of density and ultrasonic velocity of aqueous solutions of HEC

Concentration (w/v)	Density (kg/m^3)	Ultrasonic Velocity (m/s)
0.05	995.6609	1493.675
0.10	995.8627	1493.762
0.15	995.9636	1493.159
0.20	996.3673	1494.364
0.25	996.0645	1493.762
0.30	996.8718	1494.967
0.35	996.2663	1494.967
0.40	996.5691	1494.967
0.45	996.7709	1493.762
0.50	997.1745	1494.967

3.2. Determination of Molecular Interaction Parameters

Normally a decrease in adiabatic compressibility indicates closed packing and decreased ionic repulsion. The variation of adiabatic compressibility for aqueous solutions of HEC with concentration is shown [Fig. 3].It is observed that there is a non-linear variation with increase in concentration of HEC. The actual deviation depends on the resultant effect. The observed decrease or increase in adiabatic compressibility with composition is an evidence of significant interaction between the component molecules in the binary mixtures. This shows the complex formation and molecular dissociation. It also indicates weakening of hydrogen bond at this molar concentration [17].Intermolecular free length shows a similar behavior as reflected by adiabatic compressibility. Free length varies nonlinearly with increasing concentration of HEC at lower concentration which suggests that there is a significant interaction between solute and solvent molecules due to which structural arrangement is also affected [Fig. 4].Free volume refers to the void space between the molecules, i.e., the volume present as holes because of irregular packing of the molecules. It may be defined as the average volume in which the central molecule can move inside the hypothetical cell freely without

affected by the repulsion of surrounding molecules. The free volume plot follows reverse trend of viscosity. Therefore viscosity rather than velocity determines the free volume of our system. The free volume reduces when the internal pressure increases [6]. In the present case, free volume for aqueous solutions of HEC is maximum at 0.05% and minimum at 0.50% [Fig. 5] and this variation is found to be nonlinear. The reverse trend of free volume with internal pressure is clearly shown in Fig.5.

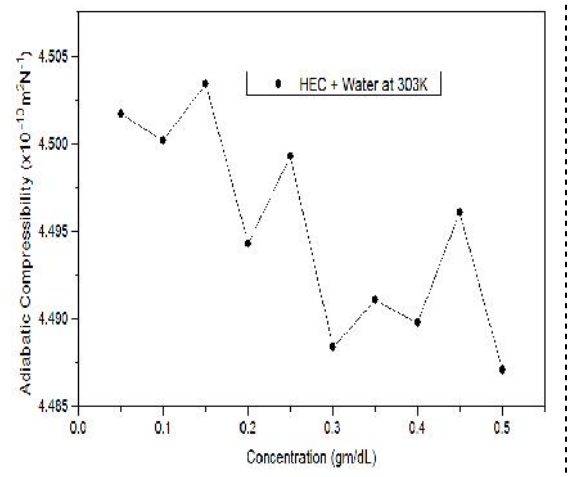


Figure 3. Variation of Adiabatic compressibility against concentration of aqueous solutions of HEC

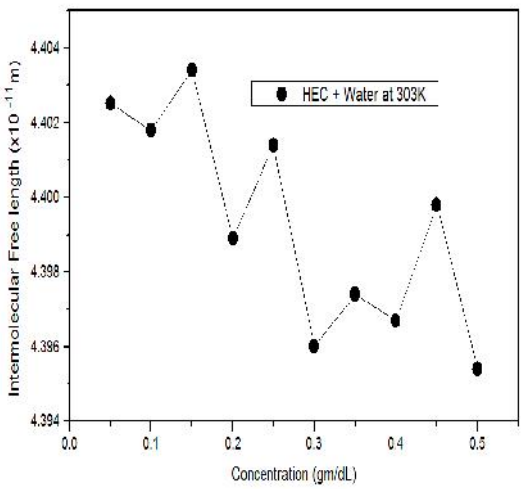


Figure 4. Variation of Intermolecular free length against concentration of aqueous solutions of HEC

The internal pressure of a liquid reflects the molecular interaction. Internal pressure studies show a nonlinear variation with increase in concentration of HEC and thus it is the evidence for the existence of significant interaction between the solvent – polymer molecules. Internal pressure shows dip at 0.25% concentration, whereas the free volume shows peak at corresponding concentration. This shows the complex formation and molecular dissociation. It also indicates weakening of hydrogen bond at this molar concentration.In the present study the classical absorption coefficient has been calculated for Aqueous HEC at different concentrations of 0.05%, 0.10%, 0.15%, 0.20% 0.25%, 0.30%, 0.35%, 0.40%, 0.45% and 0.50% at 303 K and it is shown in Fig 6.A non-linear variation is observed. The values of viscous relaxation time, specific acoustical impedance, relative association, Rao's constant and Wada's constant are reported in Table 2.

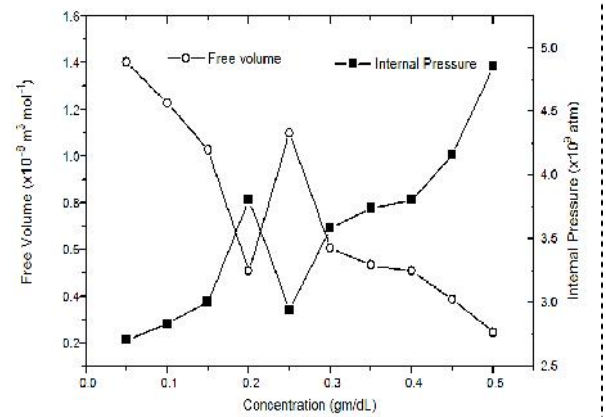


Figure 5. Variation of Free volume and Internal pressure against concentration of aqueous solutions of HEC

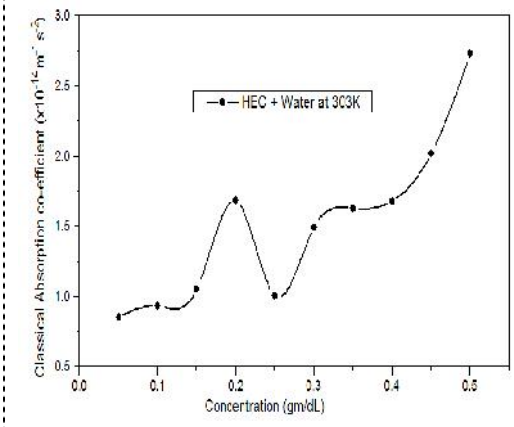


Figure 6. Variation of Classical absorption co-efficient against concentration of aqueous solutions of HEC

Table 2. Values of Molecular Interaction Parameters

Concentration (w/v)	Specific Acoustical Impedance (x 10^6 kg m^{-2} s^{-1})	Relaxation Time (x10^{-12} sec)	Relative Association	Rao's Constant (X 10^{-4} $[m^3mol\text{-}1][ms^{-1}]^{1/3}$)	Wada's Constant (X 10^2 m^3 mol^{-1} $[Nm^{-2}]^{1/7}$)
0.05	1.4871	0.6482	0.9996	2.0168	3.8817
0.10	1.4875	0.7080	0.9999	2.0164	3.8826
0.15	1.4871	0.7986	1.0001	2.0160	3.8826
0.20	1.4889	1.2764	1.0002	2.0157	3.8853
0.25	1.4878	0.7618	1.0001	2.0160	3.8835
0.30	1.4902	1.1310	1.0006	2.0149	3.8880
0.35	1.4893	1.2335	1.0000	2.0162	3.8853
0.40	1.4889	1.2751	1.0003	2.0156	3.8866
0.45	1.4889	1.5286	1.0008	2.0146	3.8866
0.50	1.4907	2.0700	1.0009	2.0143	3.8893

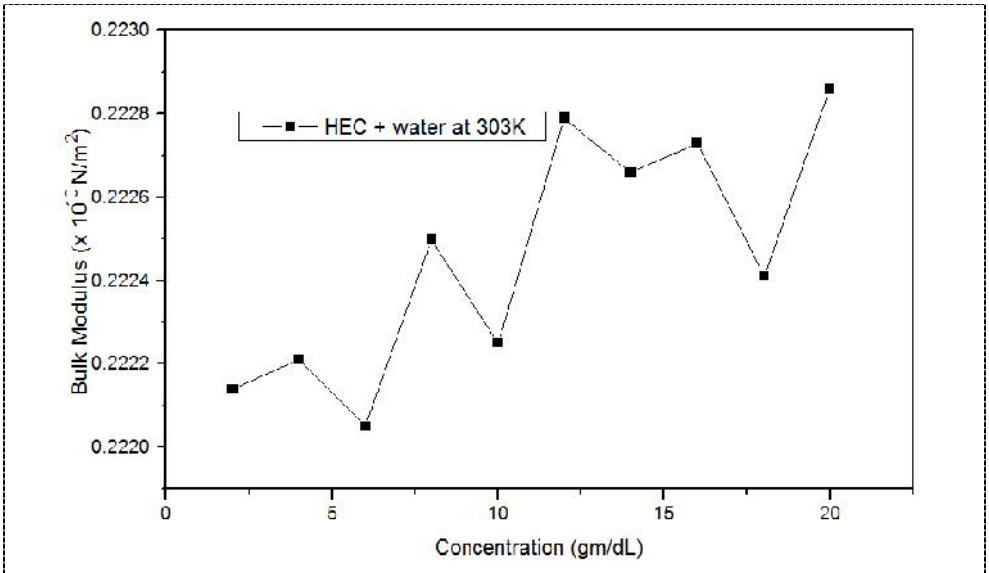


Figure 7. Variation of Bulk modulus against concentration of aqueous solutions of HEC

The relaxation time depends upon the size and shape of the rotating molecular entities in the solution. From Table 2, it is observed that the viscous relaxation time shows non-linear variation with increase in concentration throughout the system. This nonlinear variation with increase in concentration is due to the existence of significant molecular interaction between the solute and solvent molecules [18]. Specific acoustic impedance is defined as impedance offered to the sound wave by the components of mixture. Mathematically it is directly proportional to ultrasonic velocity and inversely proportional to adiabatic compressibility. The non-linear decrease of impedance with concentration shows that the

molecular interaction of aqueous solutions of HEC is dissociative [17]. Relative association is influenced by two factors (i) breaking up of the associated solvent molecules on addition of solute and (ii) the solvation of solute molecules. The former leads to decrease and latter leads to increase in relative association. In the present system, the Relative Association is minimum at 0.05% concentration and maximum at 0.50% concentration. Rao's constant and Wada's constant also show a non-linear variation with increase in concentration.

3.3 Determination of Bulk modulus

The variation of bulk modulus with different concentration of HEC in binary mixture with water at room temperature is plotted in Fig. 7, which shows the non-linear variation with increase in concentration of HEC. Bulk modulus determines how compressible a fluid is. In other words, it tells us how the density of a liquid changes when the liquid is subjected to pressure. Higher the values of Bulk modulus indicate that it is difficult to compress the fluid [19].

4. Conclusion

The nonlinear variation of ultrasonic velocity and other thermo acoustical parameters with increase in concentration of HEC in water provides useful information about the nature of intermolecular forces existing in the mixture. The observed complex formation in the binary liquid mixture may be due to the formation of hydrogen bonding and the tendency of solute-solvent interaction. This complex formation is very much important in solid pesticides in water-based sprays for agriculture formulations.

Acknowledgments

The authors acknowledge the financial support of SCSVMV University, Enathur, Kanchipuram for carrying out this research work.

References

[1] SumanGahalyan, Manju Rani, and SanjeevMaken (2016)*J. Mol. Liq.***219** 1107
[2] Kushare S K, Terdale S S, Dagade D H and Patil K J (2007) *J. Chem. Thermodyn.***39** 1125
[3] Amalendu Pal, Harsh Kumar, RituMaan and Harish Kumar Sharma (2014)*Thermochim. Acta* **590** 127
[4] Yadava S S andNeetuYadav (2010) *J. Mol. Liq.***157** 6
[5] Krzysztof Klimaszewski, EwaStronka-Lewkowska, KatarzynaAbramczyk and Adam Bald (2015) *J. Chem. Thermodyn.***89** 212
[6] Venkatramanan K, Padmanaban R and Arumugam V (2015)*Phys. Procedia***70** 1052
[7] BushraNaseem, Mahreen Khan and Muhammad Asghar Jamal (2016) *J. Mol. Liq.* 220 581
[8] Kulkarni S S and Khadke U V (2016) *Indian J. Mater. Sci.* **2016** 1
[9] Punitha S, Uvarani R, Panneerselvam A and Nithiyanantham S (2014) *J. Saudi Chem. Soc.***18** 657
[10] Kannappan V, Santhi B S and Reuban Jonathan D (2014) *Indian J. Chem.***53A** 688
[11] Al-Furhood J A, Alsewailem F D and Almutabaqani L A (2014) *Eur. Chem. Bull.***3** 93
[12] Venkatramanan K and Arumugam V (2006) *Int. J. Thermophys.***27** 66
[13] Debye P, Chu B and Woermann D (1963) *J. Polym. Sci.A Polym. Chem.***1** 249
[14] Padmanaban R and Venkatramanan K (2015) *AIP Conf. Proc.***1675** 020019
[15] Reisuke Okada and Hiroshi Tanzawa (1965) *J. Polym.Sci. A***3** 4294
[16] Ravichandran S (2011) *Res. J. Chem. Sci.***1** 12
[17] PriyankaShamkuwar and Chimankar O P (2014) *Int. J. Sci. Res. Phy. Appl. Sci.***1** 14
[18] Venkatramanan K, Padmanaban R and Kavitha B (2016) *Adv. Sci. Lett.***22** 3948
[19] Monupal and Suthar B (2016) *AIP Conf. Proc.***1728** 020003

IOP Conf. Series: Materials Science and Engineering **390** (2018) 012116 doi:10.1088/1757-899X/390/1/012116

A comparative study of experimental and theoretical refractive index of binary liquid mixtures using mathematical methods

A Gayathri, T Venugopal, R Padmanaban, K Venkatramanan and R Vijayalakshmi

Faculty of Science, Sri Chandrasekharendra Saraswathi Viswa Mahavidyalaya, Enathur, Kanchipuram – 631561, India

E-mail :kv@kanchiuniv.ac.in

Abstract. A comparative study of refractive index of binary liquid mixtures such as Cyclohexane+O-xylene, PEG200+Water, PPG400+toluene having industrial applications are analysed at temperature 303K for different concentrations [0 to 1%]. In the present study experimental values are taken from literature and there values are compared with theoretical values obtained by various mathematical equations such as Lorentz – Lorenz relation, Gladstone- Dale equation, Weiner's relation, Heller's (H) equation, Arago-Biot equation. Thus the present study reveals the nature of interaction between component molecules in the mixtures and enables us to identify a suitable mathematical model for predicting the refractive index of various binary liquid mixtures.

1. Introduction

The general applicability of refractive index in chemical analysis and industry are revealed in literature survey. Many researchers have been studied the theoretical refractive index measurements by the refractive index mixing rules [1-4]. The generally used theoretical rules are Arago-biot, GladstoneDale, Lorentz-Lorentz, Weiner, Heller, Newton and Eyring-John. The validity of the mixing rules has been tested by several researchers and pointed out the importance of mixing rules [1-5]. In the present study, we report the experimental and theoretical refractive index of binary mixtures such as Cyclohexane+O-xylene, PEG200+Water, PPG400+toluene and from these the validity of the mixing rules have been analyzed.

2. Methods and Materials

The binary mixtures are prepared by dissolving Cyclohexane+O-xylene, PEG200+water, PPG400+toluene to get desired concentrations. Magnetic stirrer [REMI make] was used for this purpose at a rate of 1000 rpm. Refractive index values are measured using thermostatically controlled Abbe Refractometer having accuracy less than 0.0001 units. Density values are measured using specific gravity method. The mass of the liquid is measured using a K-ROY make electronic balance, with an accuracy of ±0.001gm.

3. Results and Discussions

In the present study, refractive index is determined for aqueous mixtures of Cyclohexane+O-xylene, PEG200+water, PPG400+toluene for different concentrations (0 to 1%) at a temperature 303K. The

Content from this work may be used under the terms of the Creative Commons Attribution 3.0 licence. Any further distribution of this work must maintain attribution to the author(s) and the title of the work, journal citation and DOI.
Published under licence by IOP Publishing Ltd

experimental refractive index values of these mixtures are compared with theoretical refractive indices by mathematical models like Lorentz-Lorenz equation, Gladstone-Dale equation, Newton's equation, Arago-Biot(AB) equation, Heller equation and Weiner equation which are listed below.

Lorentz-Lorentz (L-L)

Lorentz-Lorenz (L-L) relation for refractive index is based on the change in the molecular interaction with volume fraction:

$[(n_m^2 - 1)/(n_m^2 + 2)](1/\rho_m) = \phi_1(n_1^2 - 1/n_1^2 + 2) + \phi_2(n_2^2 - 1/n_2^2 + 2)$

where, $\phi_1 = w_1/\rho_1$ and $\phi_2 = w_2/\rho_2$, w_1 and w_2 are the weight fractions of the pure components 1 and 2 respectively, and, ρ_m, ρ_1 and ρ_2 are the density of the mixture, and densities of the pure components 1 and 2 respectively and n_m, n_1 and n_2 are the refractive index of the mixture, refractive indices of the pure components 1 and 2 respectively.

Galdstone-Dale relation (G-D)

The Gladstone-Dale relation is used for optical analysis (the determination of composition from optical measurements), or to calculate the density of a liquid for use in fluid dynamics. The relation has also been used to calculate refractive index. Gladstone-Dale (G-D) equation for predicting the refractive index of a binary liquid mixture is as follows

$$(n_m - 1) = \phi_1(n_1 - 1) + \phi_2(n_2 - 1)$$

Where, n_m, n_1 and n_2 are the refractive index of the mixture, refractive indices of the pure components 1 and 2 respectively.

Weiner's relation (W)

Weiner's (W) relation may be represented as

$$(n_m^2 - n_1^2)/(n_m^2 + 2n_1^2) = [(n_2^2 - n_1^2)/(n_2^2 + 2n_1^2)]\phi_2$$

where, $\phi_2 = w_2/\rho_2$ and, w_2 is the weight fraction of the pure component and ρ_2 is the density of the pure component 2 and n_m, n_1 and n_2 are the refractive index of the mixture, refractive indices of the pure components 1 and 2 respectively.

Heller's equation (H)

Heller's (H) equation is given by

$$(n_m - n_1)/n_1 = 3/2[(m^2 - 1)/(m^2 + 2)]\phi_2$$

where, $m = n_2/n_1$, $\phi_2 = w_2/\rho_2$, w_2 is the weight fraction of the pure component 2 and ρ_2 is the density of the pure component 2 and n_m, n_1 and n_2 are the refractive index of the mixture, refractive indices of the pure components 1 and 2 respectively.

Arago-Biot (A-B)

Arago-Biot (A-B), assuming volume additively, proposed the following relation for refractive index of binary liquid mixtures

$$n_m = \phi_1 n_1 + \phi_2 n_2$$

where, $\phi_1 = w_1/\rho_1$ and $\phi_2 = w_2/\rho_2$, w_1 and w_2 are the weight fractions of the pure components 1 and 2 respectively, and, ρ_m, ρ_1 and ρ_2 are the density of the mixture, and densities of the pure components 1 and 2 respectively and n_m, n_1 and n_2 are the refractive index of the mixture, refractive indices of the pure components 1 and 2 respectively.

Newton (N)

Newton (N) gave the following equation

$$(n_m^2 - 1) = \phi_1(n_1^2 - 1) + \phi_2(n_2^2 - 1)$$

where, $\phi_1 = w_1/\rho_1$ and $\phi_2 = w_2/\rho_2$, w_1 and w_2 are the weight fractions of the pure components 1 and 2 respectively, and, ρ_m, ρ_1 and ρ_2 are the density of the mixture, and densities of the pure components 1

and 2 respectively and n_m, n_1 and n_2 are the refractive index of the mixture, refractive indices of the pure components 1 and 2 respectively.

Average percentage error

The percentage of deviation is calculated by the following equation

$$APE = 1/n \sum[(R.I._{\exp} - R.I._{cal}) / R.I._{\exp}] * 100$$

Where n is the number of data used, R.I.exp is the experimental refractive index and R.I.cal is the theoretical refractive index. The experimentally measured refractive index and the estimated refractive index from various mathematical models for the binary liquid mixture Cyclohexane+O-Xylene at different concentrations at 303K are presented in the Table 1.

Table 1. Experimental and mathematical values of Refractive index Cyclohexane + O-Xylene

Conc(%)	EXP	A-B	G-D	L-L	W	H
0.0000	1.4200	1.4200	1.4200	1.4200	1.4200	1.4200
0.0908	1.4333	1.4423	1.4409	1.4265	1.4287	1.4284
0.1835	1.4422	1.4604	1.4606	1.4335	1.4373	1.4368
0.2781	1.4495	1.4851	1.4793	1.4413	1.4458	1.4452
0.3747	1.4556	1.4976	1.4968	1.4499	1.4544	1.4536
0.4734	1.4606	1.5232	1.5127	1.4589	1.4631	1.4622
0.5742	1.4654	1.5345	1.5261	1.4651	1.4715	1.4705
0.6772	1.4702	1.5487	1.5387	1.4733	1.4799	1.4790
0.7824	1.4792	1.5509	1.5496	1.4787	1.4880	1.4872
0.8900	1.4919	1.5673	1.5598	1.4880	1.4966	1.4959
1.0000	1.4950	1.5780	1.5685	1.4950	1.5048	1.5043

Table 2. Average percentage values of Cyclohexane + O-Xylene

Conc(%)	EXP	%A-B	%G-D	%L-L	%W	%H
0.0908	1.4333	-0.6279	-0.5302	0.4744	0.32093	0.3418
0.1835	1.4422	-1.2619	-1.2758	0.60324	0.33975	0.3744
0.2781	1.4495	-2.4560	-2.0558	0.56571	0.2552	0.2966
0.3747	1.4556	-2.8854	-2.8304	0.39159	0.0824	0.1374
0.4734	1.4606	-4.2859	-3.5670	0.11639	-0.1711	-0.1095
0.5742	1.4654	-4.7154	-4.1422	0.02047	-0.4162	-0.3480
0.6772	1.4702	-5.3394	-4.6592	-0.2108	-0.6597	-0.5985
0.7824	1.4792	-4.8472	-4.7593	0.03380	-0.5949	-0.5408
0.89	1.4919	-5.0539	-4.5512	0.26141	-0.3150	-0.2681
1	1.495	-5.5518	-4.9163	0.0000	-0.6555	-0.6220
AVG		-3.3659	-3.0261	0.20510	-0.1649	-0.1215

From Table 1, it is observed that the experimental values of refractive index increases with increase in concentration. Arago-Biot relation, Weiner relations, Glad-stone relations shows good agreement with theoretical values of binary liquid mixture Cyclohexane + O-Xylene. The limitations and approximations incorporated in these theories are responsible for the deviations of theoretical values from experimental values.
For the binary liquid mixture Cyclohexane+O-Xylene at 303K the average percentage values are given in Table 2 Further from the table 2 the deviations are more in Lorentz-Lorenz relation. At all concentrations the values obtained from Glad-Stone relations and Arago-Biot relations are found to be nearer. Exactly **Lorentz-Lorenz** relations performs the best of all methods.
The experimentally measured refractive index and the estimated refractive index from various mathematical models for the binary liquid mixture PEG200+Water at different concentrations at 303K are presented in the Table 3.

Table 3. Experimental and mathematical values of Refractive index PEG 200 + Water

Conc(%)	EXP	A-B	G-D	L-L	W	H
2	1.341	1.3458	1.3416	1.3418	1.3397	1.3383
4	1.343	1.3454	1.3418	1.3419	1.3399	1.3385
6	1.346	1.3457	1.3419	1.342	1.3401	1.3387
8	1.348	1.3456	1.342	1.3421	1.3403	1.3389
10	1.350	1.3455	1.3422	1.3422	1.3405	1.3391

Table 4. Average percentage values of PEG 200 + Water

Conc(%)	%EXP	%A-B	%G-D	%L-L	%W	%H
2	1.341	-0.3579	-0.0444	-0.0597	0.0969	0.2013
4	1.343	-0.1787	0.0894	0.0819	0.2308	0.3350
6	1.346	0.0223	0.3046	0.2972	0.4383	0.5423
8	1.348	0.1780	0.4451	0.4377	0.5712	0.6751
10	1.350	0.3333	0.5778	0.5778	0.7037	0.8074
AVG		-0.0006	0.2744	0.2670	0.4082	0.5122

From Table 3, it is observed that the experimental values of refractive index vary with increase in concentration. In Gladstone values the refractive indices first decreases and suddenly increases and further decreases with increase in concentration. It shows that Arago-Biot relation, L-L relations, Glad-stone relations shows good agreement with theoretical values.
Average percentage values for binary liquid mixture PEG 200 + Water is given in Table 4 Further in the Table 4 the deviations are more in Heller's relation. At all concentrations the values obtained from L-L realtions and Arago-Biot relations are found to be nearer. Particularly Arago-Biot relations perform the best of all methods.
The experimentally measured refractive index and the estimated refractive index from the various mathematical models like Arago-Biot, Gladstone-Dale, Lorentz-lorenz, Weiner equation, Heller

equation for the binary liquid mixture of PPG 400 + toluene at five different concentrations at 303K are summarized in the Table 5.

Table 5. Experimental and mathematical values of Refractive index PPG 400 + toluene

Conc(%)	EXP	A-B	G-D	L-L	W	H
2	1.494	1.4935	1.4939	1.4942	1.4947	1.4944
4	1.493	1.4945	1.4937	1.4945	1.4944	1.4942
6	1.492	1.4955	1.4935	1.4947	1.4942	1.494
8	1.49	1.4965	1.4933	1.4949	1.494	1.4938
10	1.489	1.4975	1.4932	1.4951	1.4938	1.4935

From Table 5 it is observed that the experimental values of refractive index decreases with increase in concentration.Whereas the Arago-Biot relation increases with increase in concentration. This table reveals that Arago-Biot relation, L-L relations, Glad-stone relations shows good agreement with theoretical values. The limitations and approximations incorporated in these theories are responsible for the deviations of theoretical values from experimental values.
For the binary liquid mixture PPG 400 + Toluene at 303K the average percentage values are given in Table 6. Also from the Table 6 the deviations are more in Glad-Stone relation. At all concentrations the values obtained from L-L realtions and Arago-Biot relations are found to be nearer. Altogether Arago-Biot relations perform the best of all methods.

Table 6. Average percentage values of PPG 400 + toluene at 303K

Conc(%)	%EXP	%A-B	%G-D	%L-L	%W	%H
2	1.494	0.0335	0.0067	-0.0134	-0.0469	-0.0268
4	1.493	-0.1005	-0.0469	-0.1005	-0.0938	-0.0804
6	1.492	-0.2346	-0.1005	-0.1810	-0.1475	-0.1341
8	1.49	-0.4362	-0.2215	-0.3289	-0.2685	-0.2550
10	1.489	-0.5709	-0.2821	-0.4097	-0.3224	-0.3022
AVG		-0.2617	-0.1289	-0.2067	-0.1758	-0.1597

4. Conclusion

In this present study the experimental refractive index of binary liquid mixtures such as Cyclohexane + O-xylene, PEG200 + water, PPG400 + toluene are compared with their theoretical refractive index for different concentrations at a temperature 303K. From these it may be concluded that the binary mixtures PEG200 + water, PPG400 + toluene showed Arago-Biot relation as the best suitable method for calculating the refractive index in the liquid systems.

Acknowledgments

The authors acknowledge the financial support of SCSVMV, Enathur, Kanchipuram for carrying out this research work.

References

[1] Gayathri A and Venugopal T (2016) *International Journal of Mathematics Trends and Technology* **34** 126
[2] Narendra K, Krishnamurthy P and Srinivasu Ch (2011) *Asian Journal of applied sciences* **4** 535
[3] Dyaneshwar S and Wankhede (2011) *International Journal of Chemistry research* **2** 23
[4] Padmanaban R, Venkatramanan K, Girivel S, Kasthuri K, Usharani A, Gayathri A and Roy Vellaichamy (2017) *Springer Proceedings in Physics* **189** 709
[5] Azhagiri S, Jayakumar S, Padmanaban R, Gunasekaran S and Srinivasan S (2009) *Journal of Solution Chemistry* **38** 441